

A Collection of 48 Published Papers

Derek Steele

Ph.D.

1969

Royal Holloway and Bedford New College

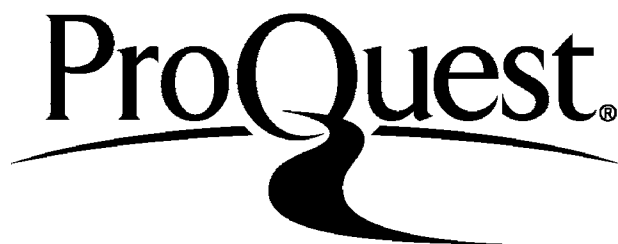
ProQuest Number: 10107275

All rights reserved

INFORMATION TO ALL USERS

The quality of this reproduction is dependent upon the quality of the copy submitted.

In the unlikely event that the author did not send a complete manuscript and there are missing pages, these will be noted. Also, if material had to be removed a note will indicate the deletion.



ProQuest 10107275

Published by ProQuest LLC(2016). Copyright of the Dissertation is held by the Author.

All rights reserved.

This work is protected against unauthorized copying under Title 17, United States Code  
Microform Edition © ProQuest LLC.

ProQuest LLC  
789 East Eisenhower Parkway  
P.O. Box 1346  
Ann Arbor, MI 48106-1346

A thesis submitted by Dr. Derek Steale for the  
degree of D.Sc. of the University of London.

April 1969

R. H. C. LIBRARY	
CLASS	T C D C
No.	S T e
ACC. No.	90,102
*ATE ACQ	Jan. '70

## Introduction

This collection of 48 publications is divided into four groups which may be labelled -

1. Original papers on the vibrational spectra of aromatic systems. These comprise A1 to A25.
2. Studies of empirical inter-nuclear potential functions B1-6.
3. Vibrational analyses as an aid to structural analysis C1-14.
4. Instrumentation and techniques D1-3.

1. As is seen from the distribution of papers amongst the groups, most effort has been devoted to a study of aromatic systems, primarily of fluoro-aromatics. The latter offer special unique and advantageous properties for vibrational studies. The objectives of this work and the extent to which they have so far been realised may be summarised as follows.

(i) - the establishing of the pattern of fundamental vibrational frequencies. Much effort has been devoted to showing that the assignments for the various molecular species are consistent with one another. (A6, A8, A9, A19, A22 etc.). In this context three extremely useful and general rules have been established (A2, A9, A22). All are strictly applicable only to isotopically related systems but have been shown to be remarkably well upheld when the systems compared differ by non isotopic substitution. The 'Inequality Rule' was first proposed by the writer and D.H. Whiffen (A2). The second rule, the 'Sum Rule', is a well established rule for isotopic systems, but has been shown (A9) to be

R.H.C.  
LIBRARY



very useful outside of its normal realm of applicability as a consequence of linear gradation of bond properties with isotopic substitution. An adaptation of the 'Redlich-Teller Product Rule' has also been usefully employed in deciding between alternative proposed assignments (A22).

In addition to the fluoro-benzene systems  $C_6H_{6-n}F_n$  a number of substituted nitrogen heterocyclic systems have been investigated. (A13, A18-20). It is anticipated that these studies will soon permit a more detailed analysis of important naturally occurring systems - for example it is hoped to establish the role of  $\pi\pi$  electron interactions in purine pyrimidine base pairing. Again the rules have allowed internal consistency checks to be applied.

Two types of polycyclic aromatic systems have been examined. Vibrational evidence for conformational changes accompanying phase changes for biphenyl and its perfluoro analogue has proved extremely unsatisfactory (A8, A16, A23). The cause of this is now being examined by computational analysis of the effects of changes in the dihedral angle on the modes. Strong evidence has been found for co-planarity or near co-planarity - of the two rings in crystalline  $C_{12}F_{10}$ . The major axes of the molecules are aligned in the crystal (A16). The vibrational spectra of azulene is of interest in view of the non-aromaticity of the system and the fact that it is a homologue of naphthalene. Calculation of the vibrational frequencies has been of considerable value in understanding the spectra (A15, A17).

(ii) - establishing the quadratic force fields. Force fields for both  $C_6H_6$  and  $C_6F_6$  (A3) have been proposed which unfortunately are not unique. Nevertheless transference of the force constants to other aromatic systems has resulted in good agreement of calculated with observed spectra (A4, A11, A13, A15, A18, A19, A23). Assumptions about transferability of fields between members of the series  $C_6H_{6-n}X_n$  are leading to resolution of the problems associated with indeterminacy and multiplicity of force constant solutions (A21 and current work).

(iii) Once the frequency patterns are established it is natural to seek an understanding of the intensities. The experimental difficulties are considerable and the factors determining intensities are as yet poorly understood. The early measurements on  $C_6F_6$  (A1) have been extended (A25) and the results interpreted in terms of  $\pi$  electron rehybridisations accompanying angular deformations involving the CF bond. The theory of derivation of transition moments from band contours of symmetric top molecules has been derived (A25). Earlier intensity investigations included studies of  $p.C_6H_4F_2$ ,  $p.C_6D_4F_2$  and  $p.C_6H_2F_4$  (A5). Intensity theory and measurements were reviewed in 1964 (A14).

## 2. Empirical Inter-nuclear Potential Functions.

The properties of Lippincott's potential function have been examined and its range of applications extended to the study of excited states (E2), of higher order spectroscopic parameters (E6), and of the nature of electronically excited states (E5). The latter work demonstrated that the

Birge Spomer extrapolation may lead to low as well as high values for bond dissociation energies. A method has been proposed and examined for construction of realistic potential curves in the absence of electronic state perturbations (B3). A critical review of potential functions in common use has been made and criteria for the reliability of functions established (B4).

### 3. Analytical Applications of Vibrational Spectroscopy.

This group comprises a wide range of analytical applications - each designed to investigate some specific problem, usually posed by a colleague of a discipline other than spectroscopy. The scope of techniques involved and the aims are therefore wide.

(i) Equatorial and axial hydrogens in fluorocyclohexanes were shown to be distinguishable by their CH stretching frequencies under conditions of high resolution. The range of frequencies is extremely narrow (about  $10 \text{ cm.}^{-1}$ ) but it allowed the conformations of a number of fluorocyclohexanes to be determined. The normal olefinic = CH stretching frequency is enhanced by the vicinity of fluorine atoms (C1).

(ii) The similarity of the spectra of ferrocene and magnesium dicyclopentadienyl strongly suggested similar structures (C2). Prior to this work it was believed that the magnesium compound existed as an ionic compound. A study of the intensities of the low frequency modes confirmed the covalent sandwich structure.

(iii) The spectra of sulphur dicyanide were shown to be inconsistent with the isocyanide structure. The intensities of the overlapping CN modes were interpreted as indicating an angle between the CN bonds close to  $140^\circ$  (C3). For reasons not understood this value is far too high as has been shown by microwave studies.

(iv) Features of the spectrum of diboron tetrafluoride were suggested to be compatible with free rotation about the BB bond. The appropriate permutation point group was derived and shown to be isomorphous with  $D_{4h}$  (C4).

(v) The infra-red and Raman spectra of thioborolans have shown that the ring is of  $C_2$  symmetry (puckered ring confirmation) (C10). Assignments were assisted by calculations using highly approximate force fields (C5, C10).

(vi) The structure of the acetyl chloride antimony penta-chloride complex has been shown to be  $CH_3CO^+SbCl_6^-$  (C14). A comparison of the vibrational fundamentals of  $CH_3CO^+$  with  $CH_3CN$  and  $CD_3CO^+$  with  $CD_3CN$  has been made.

(vii) Intensity enhancements have permitted the study of complexing between boron trihalides and benzene. The interaction appears to be through the  $\pi$  electron system of the aromatic ring (C8).

(viii) Spectral investigations have also been made on

- (a) boron tribromide and boron tri-iodide (C6).
- (b) cyclo-octatetraene iron tricarbonyl (C7).
- (c) some heterocyclic tin compounds (C9).

- (d) the complex between  $PI_3$  and  $BI_3$  (C11).
- (e) orthophosphoric acid in non-aqueous solvents (C12).
- (f) the dimethylamino grouping (C13). This publication is soon to be followed by a series of papers in which the structures of compounds containing the  $N(CH_3)_2$  group attached to an aromatic ring are examined.

4. Instrumentation and Techniques.

Radiofrequency excited arcs were shown to be useful long wavelength sources for Raman spectroscopy (D1). The use of these arcs was rendered obsolete by the advent of the laser. Polythene has been examined as a matrix material for use not only in the far infra-red region, but also in the conventional NaCl/KBr regions (D2). A note has been published on the manufacture of high density polythene cells which are reliably vacuum tight (D3).

- A1 Infra-red Absorption Intensities of Hexa-fluorobenzene.  
D. Steele and D.H. Whiffen; J. Chem. Physics, 29, 1194 (1958).
- A2 Vibrational Frequencies of Hexa-fluorobenzene.  
D. Steele and D.H. Whiffen; Trans. Far. Soc., 55, 369 (1959).
- A3 The Force Field of Hexa-fluorobenzene.  
D. Steele and D.H. Whiffen; Trans. Far. Soc., 56, 5 (1960).
- A4 The Force Fields of the I.R. Active Classes of 1,4-Difluorobenzene  
and 1,2,4,5 Tetra-fluorobenzene.  
D. Steele and D.H. Whiffen; Trans. Far. Soc., 56, 8 (1960).
- A5 The Infra-red Absorption Intensities in 1,4 Difluorobenzene and  
1,2,4,5 Tetra-fluorobenzene.  
D. Steele and D.H. Whiffen; Trans. Far. Soc., 56, 177 (1960).
- A6 The Vibrational Frequencies of Penta-fluorobenzene.  
D. Steele and D.H. Whiffen; Spectrochim. Acta., 16, 368 (1960).
- A7 The Vibrational Spectra of Penta-deutero fluorobenzene.  
D. Steele, E.R. Lippincott and J. Xavier; Spectrochim. Acta., 33,  
1242 (1960).
- A8 The Crystal and Solution Vibrational Spectra of Biphenyl.  
D. Steele and E.R. Lippincott; J. Mol. Spect., 6, 238 (1961).
- A9 The Vibrational Spectra of Tetra-fluorobenzenes.  
D. Steele; Spectrochim. Acta., 18, 915 (1962).
- A10 The Far Infra-red Spectra of p-difluoro-benzene.  
D. Steele, W. Kynaston and H.A. Gebbie; Spectrochim. Acta.,  
19, 785 (1963).

- A11 The In-Plane Frequencies and Atomic Displacements for  $C_6F_5H$ ,  $C_6F_5D$  and the Model Compounds  $C_6F_5X$  (X - mass 35.5, 80 and 127).  
D.A. Long and D. Steele; *Spectrochim Acta.*, 19, 1947 (1963).
- A12 The Vibrational Spectra and Assignments for  $C_6F_5Cl$ ,  $C_6F_5Br$  and  $C_6F_5I$ .  
D.A. Long and D. Steele; *Spectrochim. Acta.*, 19, 1955 (1963).
- A13 Spectroscopic and Thermodynamic Properties of Pyridine Compounds VI. Force Constants and Atomic Displacements for Penta-fluoropyridine.  
D.A. Long and D. Steele; *Spectrochim Acta.*, 19, 1791 (1963).
- A14 The Absolute Intensities of Infra-red Absorption Bands.  
D. Steele; *Quarterly Review of the Chemical Society (London)*, 18 (1964).
- A15 The Out-of-Plane Vibrations of Azulene.  
D. Steele; *J. Mol. Spect.* 15, 333 (1965).
- A16 The Vibrational Spectrum and Geometrical configuration of Decafluoro-biphenyl.  
D. Steele, T.R. Nanney and E.R. Lippincott, *Spectrochim. Acta.*, 22, 849 (1966).
- A17 The In-plane Vibrations of Azulene.  
D. Steele, *Spectrochim. Acta.*, 22, 1275 (1966).
- A18 The Vibrational Spectra of Substituted Nitrogen Heterocyclic Systems. Part I. 1, 3,5 trifluoro-pyrimidine.  
R.T. Bailey and D. Steele. *Spectrochimica Acta* 23A, 2989 (1967).

- A19 The Vibrational Spectra of Substituted Nitrogen Heterocyclic Systems. Part II. 2,6 difluoro-pyridine.  
R.T. Bailey and D. Steele. Spectrochimica Acta 23A, 2997 (1967).
- A20 The Vibrational Spectra of Substituted Nitrogen Heterocyclic Systems. Part III. 1,3,5 trichloro-pyrimidine.  
R.T. Bailey and D. Steele. Spectrochimica Acta. 25A, 219 (1969).
- A21 The Force Field for the Out-of-Plane Vibrations of Halogenated Aromatic Molecules.  
K. Radcliffe and D. Steele, Spectrochimica Acta. 25A, 597 (1969)
- A22 The Vibrational Spectra of Mono and Para Disubstituted Halogenobenzenes. P.N. Gates, K. Radcliffe and D. Steele, Spectrochimica Acta, 25A, 507 (1969)
- A23 Some Further Observations on the Vibrational Spectrum of Decafluorobiphenyl. D. Steele, Spectrochimica Acta.
- A24 Studies in Vibrational Absorption Intensities I. The Determination of Vibrational Transition Moments for Symmetric Top Molecules from P and R Branch Maxima. D. Steele and W. Wheatley, J. Mol. Spectroscopy,
- A25 Studies in Vibrational Absorption Intensities II Vibronic Effects in Hexafluoro-benzene and Benzene. D. Steele and W. Wheatley, J. Mol. Spectroscopy.
- B1 Dissociation Energies of Diatomic Molecules.  
E.R. Lippincott, R. Schroeder and D. Steele; J. Chem. Phys., 34, 1448 (1961).



- B2 A general Relation between Potential Energy and Internuclear Distance for Diatomic Molecules III Excited States.  
E.R. Lippincott, D. Steele and P. Caldwell; J. Chem. Phys.,
- B3 The Construction of Reliable Internuclear Potential Curves from Equilibrium Bond Lengths and Vibrational Frequencies.  
D. Steele and E.R. Lippincott; J. Chem. Phys., 35, 2065 (1961).
- B4 A comparative Study of Empirical Internuclear Potential Functions.  
D. Steele, E.R. Lippincott and J.T. Vanderslice; Rev. Mod. Phys., 34, 239 (1962).
- B5 On the Dissociation Products of  $C_2$ .  
D. Steele; Spectrochim. Acta., 19, 411 (1963).
- B6 Calculations of Higher Order Spectroscopic Parameters Using Empirical Potential Functions.  
J.M. Stutman, E.R. Lippincott and D. Steele; J. Chem. Phys., 39, 564 (1963).
- C1 Carbon-hydrogen Stretching Vibrations in Fluorocyclohexanes.  
D. Steele and D.H. Whiffen; Tetrahedron, 3, 181 (1958).
- C2 The Vibrational Spectra and Structure of Bis-cyclopenta-dienyl magnesium.  
E.R. Lippincott, J. Xavier and D. Steele; J. Am. Chem. Soc., 83, 2262 (1961).

- C3 Vibrational Spectra, Assignments and Configuration of Sulphur Dicyanide. D.A. Long and D. Steele; *Spectrochim. Acta.*, 19, 1731, (1963).
- C4 The Vibrational Spectra and Structure of Diboron Tetra-fluoride. A. Finch, I. Hyams and D. Steele; *Spectrochim Acta.*, 21, 1423 (1965).
- C5 Vibrational Spectra of Some Heterocyclic Boron Compounds. Part 1. Computations. A. Finch and D. Steele; *Trans. Far. Soc.*, 60, 2125, (1964).
- C6 The Far Infra-red Spectra of Boron Tribromide and Boron Tri-iodide A. Finch, I.J. Hyams and D. Steele; *Trans. Far. Soc.*, 61, 203 (1965).
- C7 The vibrational Spectra and Structure of cyclo-octatetraene Iron Tri-carbonyl. E.T. Bailey, E.R. Lippincott and D. Steele, *J. Amer. Chem. Soc.*, 87, 5346 (1965).
- C8 Spectroscopic Evidence for Complex Formation between Benzene and Boron Tri-halides. A. Finch, P.N. Gates, and D. Steele, *Trans. Far. Soc.*, 61, 2623 (1965).
- C9 The Vibrational Spectra of Some Heterocyclic Tin Compounds. A. Finch, R.C. Poller and D. Steele, *Trans. Far. Soc.*, 61, 2628 (1965).
- C10 Vibrational Spectra of some Heterocyclic Boron Compounds. Part II. Thioborolans. A. Finch, J. Pearn and D. Steele, *Trans. Far. Soc.*, 62, 1688 (1966).

- C11 Phosphorous Halide - Boron Halide Complexes PART I. The Infra-red Spectrum of  $PI_3 \cdot BI_3$ . G.W. Chantry, A. Finch, P.N. Gates and D. Steele, J. Chem. Soc., A(1966) 896.
- C12 The Vibrational Spectrum of Ortho-Phosphoric Acid in Non-Aqueous Solvents. R. Levine, D.P. Powell and D. Steele, Spectrochim. Acta., 22, 2033 (1966).
- C13 The Vibrational Spectra of Compounds Containing the Dimethylamino Grouping. Part 1. Dimethylamine and tetra-kis-dimethylamino diboron. A. Finch, I.J. Hyams and D. Steele. J. Mol. Spectroscopy, 16, 103 (1965).
- C14 The Infra-red Spectra of  $(CH_3CO^+)$  and  $(CD_3CO^+)$  Ions. P.N. Gates and D. Steele. Journal of Molecular Structure 1, 349 (1967).
- D1 A High Intensity Red Source for Raman Spectroscopy. F.X. Powell, E.R. Lippincott and D. Steele; Spectrochim. Acta., 17, 880 (1961).
- D2 The Use of Pressed Polythene Discs in Infra-red Spectroscopy. B. Smethurst and D. Steele; Spectrochim Acta., 20, 242 (1964).
- D3 The Fabrication of Vacuum Tight High Density Polythene Cells. S. Ashdown, T. Crowdy and D. Steele, Laboratory Practice, Aug. 1966.

## Infrared Absorption Intensities of Hexafluorobenzene

D. STEELE AND D. H. WHIFFEN

*The Chemistry Department, The University,  
Birmingham 15, England*

(Received June 23, 1958)

NOW that hexafluorobenzene is available<sup>1</sup> it seemed desirable that the intensities in its infrared absorption spectrum should be measured. The molecule has four active fundamentals, namely, the three in-plane  $e_{1g}$  modes and the out-of-plane  $a_{2u}$  mode. These have been assigned the values 1529, 1018+1003, 315, and 215  $\text{cm}^{-1}$ , respectively, by Delbouille.<sup>2</sup> These frequencies are supported by a complete assignment by the present authors which will be presented elsewhere. The 1018 and 1003 bands are interpreted as a Fermi resonance doublet and are taken together for intensity measurement.

The intensities in the vapor phase of the higher bands were measured on a 2500 line per inch grating under conditions analogous to those for benzene itself<sup>3</sup> and the results are given in Table I. Only a qualitative value is available for the band at 315  $\text{cm}^{-1}$ , namely, that it is about  $\frac{1}{4}$  times the strength of the band at 1529  $\text{cm}^{-1}$ . Force constants were chosen as far as possible to keep the interaction constants similar to those in benzene<sup>4</sup>; in the nomenclature of Crawford and Miller<sup>5</sup> the values chosen were  $\Gamma_4=0.991$ ;  $\Lambda_4=3.701$ ;  $\Omega_4=7.509$ ;  $\mu_4=0.122$ ;  $\tau_4=0.197$ ;  $\xi_4=0.998 \times 10^6$  dyne/cm. This set of force constants predicts the calculated frequencies of Table I and was used to calculate the normal modes.

In the absence of exact measurements for the band at 315  $\text{cm}^{-1}$  some further condition must be imposed before the dipole moment gradients can be derived. For benzene it was found experimentally<sup>3</sup> that the carbon stretching motion did not produce appreciable dipole moment provided the C—H links remained unchanged in direction. It is not unreasonable to assume that the corresponding result is true for hexafluorobenzene, i.e., that

$$\partial\mu/\partial S_{19} = 3^{\frac{1}{2}} \cdot 2^{-1} \rho \partial\mu/\partial S_{18}.$$

The relative sign ambiguity can be settled by invoking the approximate value of the 315- $\text{cm}^{-1}$  band intensity. The alternative solutions predict 8 and 54 compared

TABLE I.

Frequency		Intensity
Observed	Calculated	Observed
1531	1531	$27.2 \pm 2.0 \times 10^{-7} \text{ cm}^2 \text{ molecule}^{-1} \text{ sec}^{-1} \text{ ln}$
1020 1002	1006	$20.3 \pm 1.5 \times 10^{-7} \text{ cm}^2 \text{ molecule}^{-1} \text{ sec}^{-1} \text{ ln}$
315	312	$c.7 \times 10^{-7} \text{ cm}^2 \text{ molecule}^{-1} \text{ sec}^{-1} \text{ ln}$

with the observed  $c.7$  in  $10^{-7} \text{ cm}^2 \text{ molecule}^{-1} \text{ sec}^{-1} \text{ ln}$  units. Only the former is acceptable and the solution is  $\partial\mu/\partial S_{18} = \pm 2.2$ ,  $\partial\mu/\partial S_{19} = \pm 1.7$ ,  $\partial\mu/\partial S_{20} = \mp 8.7D/A$ . Referred to individual C—F links the bond stretching moment gradient,  $\partial\mu/\partial\Delta r = 5.0D/A$  and the in-plane bending moment gradient,  $\partial\mu/\partial\beta = 1.6D$ . The relative signs are such that if the fluorine is at the negative end of the bending dipole, then it behaves as if it carries a negative charge as regards the stretching gradient. The value of the stretching gradient is high, being one electron within experimental error, but it is not out of line with other fluorine containing bonds which have been reviewed by McKean.<sup>6</sup> The bending moment is reasonable and the relative signs are those to be expected. It seems improbable that an alternative force field or an accurate measurement of the band at 315  $\text{cm}^{-1}$  would alter the values quoted significantly.

We wish to thank Dr. J. C. Tatlow and his colleagues for the hexafluorobenzene and Dr. L. Bovey and Mr. A. M. Deane for the measurements at 315  $\text{cm}^{-1}$ . We must also acknowledge the receipt of a University Appeal Scholarship.

<sup>1</sup> Godsell, Stacey, and Tatlow, *Nature* **178**, 199 (1956).

<sup>2</sup> L. Delbouille, *J. Chem. Phys.* **25**, 182 (1956).

<sup>3</sup> H. Spedding and D. H. Whiffen, *Proc. Roy. Soc. (London)* **A238**, 245 (1956).

<sup>4</sup> D. H. Whiffen, *Phil. Trans. Roy. Soc. A* **248**, 131 (1955).

<sup>5</sup> B. L. Crawford and F. A. Miller, *J. Chem. Phys.* **17**, 249 (1949).

<sup>6</sup> D. C. McKean, *J. Chem. Phys.* **24**, 1002 (1956).

Offprinted from the *Transactions of the Faraday Society*,  
No. 435, Vol. 55, Part 3, March, 1959

## THE VIBRATIONAL FREQUENCIES OF HEXAFLUOROBENZENE

BY D. STEELE AND D. H. WHIFFEN

Chemistry Dept., The University, Edgbaston, Birmingham 15

Received 30th June, 1958

The infra-red and Raman spectra of hexafluorobenzene have been measured. The fundamental frequencies have been assigned the values shown in the final column of table 3.

Now that hexafluorobenzene can be prepared<sup>1</sup> in reasonable quantities it is clearly desirable to compare its vibrational frequencies and force constants with those of benzene.<sup>2, 3, 4</sup> When the present work had been started an assignment of the active fundamentals was published by Delbouille<sup>5</sup> who promises a further communication on the complete spectra. There are nine inactive fundamentals the determination of which will depend on a complete assignment of summation frequencies: this in turn requires a sample of very high purity. In view of some of these difficulties an independent investigation seemed highly desirable and the work has been continued. In the vibrational assignment of benzene much use was made of isotopic species but this approach is not feasible for hexafluorobenzene. However, pentafluorobenzene is now available<sup>6</sup> and the assignment of this material<sup>7</sup> is of some assistance in providing evidence for the hexafluorobenzene frequencies.

### EXPERIMENTAL

The infra-red spectra were measured in the vapour and the liquid phases using a Perkin-Elmer 21 spectrometer with a NaCl prism for general work, a Grubb-Parsons single-beam spectrometer with a KBr prism for work from 700-400  $\text{cm}^{-1}$  and a grating spectrometer<sup>8</sup> with a 2500 lines/in. replica grating to study special features. The spectrum below 400  $\text{cm}^{-1}$  was kindly measured by A. M. Deane and L. Bovey at Harwell using a CsBr prism.

A Hilger E 612 spectrograph was used for the Raman spectra of the liquid. The Hg 4358 Å line was used for excitation, other frequencies being removed with a filter solution<sup>9</sup> of Rhodamine GBN 500 and nitrobenzene in alcohol.

The hexafluorobenzene was prepared from polyfluorinated benzenes<sup>1</sup> and purified by preparative-scale vapour chromatography on a stationary phase of dinonylphthalate on kieselguhr. The frequencies are tabulated in table 1.

### DISCUSSION

The hexafluorobenzene molecule may be expected to consist of a flat regular hexagon of  $D_{6h}$  symmetry. This molecular geometry has been frequently discussed in connection with the benzene spectrum.<sup>10</sup> Here it suffices to repeat that there are twenty fundamental frequencies which are divided amongst the symmetry classes as indicated by

$$2a_{1g} + a_{2g} + 2b_{2g} + e_{1g} + 4e_{2g} + a_{2u} + 2b_{1u} + 2b_{2u} + 3e_{1u} + 2e_{2u}.$$

The selection rules for fundamentals allow the  $a_{1g}$  (polarized),  $e_{1g}$  and  $e_{2g}$  frequencies to appear in the Raman effect and the  $a_{2u}$  (parallel) and  $e_{1u}$  (perpendicular) in infra-red absorption. The remaining nine frequencies are forbidden in both spectra. The full summation selection rules have been given,<sup>11</sup> and for the present the simple summations leading to infra-red active vibrations are the most relevant and are indicated in table 2. Polarized Raman lines are permitted for all first overtones.

TABLE 1

Raman	infra-red		assignment
	vapour	liquid	
217? vw?	215*		$a_{2u}$ fundamental
264 dp m			$e_{2g}$ "
312 dp vw	315 vvs		$e_{1u}$ "
370 dp m		370 vw	$e_{1g}$ "
	420 m	416 m	$249 + 175 = 424$
		443 w	$264 + 175 = 439$
443 dp ms			$e_{2g}$ fundamental
465 vw?			$714 - 249 = 465$
	461 vvw	466 vvw	$264 + 208 = 472$
	489 vvw	482 vvw	?
499 p mw			$2 \times 249 = 498$
		514 vw	? $1157 - 640 = 517$
537 p w			$2 \times 264 = 528$
		553 m	$370 + 175 = 545$
559 p s			$a_{1g}$ fundamental
		569 w	$264 + 315 = 579$
		583 vw	$370 + 215 = 585$
		648 w	$443 + 208 = 651$
		717 w	$994 - 264 = 730$
			{ or $b_{2g}$ fundamental 714
737 p w			$2 \times 370 = 740$
		755 v w	$443 + 315 = 758$
		776 vw	$559 + 215 = 774$
		841 w	$249 + 595 = 844$
	849 w Q	?	$264 + 595 = 859$
	868 w	872 w	$559 + 315 = 874$
	883 w	885 w	$714 + 175 = 889$
		965 mw	$370 + 595 = 965$
	1002 vvvs	994 vvvs	{ $e_{1u}$ fundamental
	1020 vvvs	1019 vvvs	{ and $691 + 315 = 1006$
	1044 mwQ	1044 mw	$443 + 595 = 1038$
	1092 m	1086 m	$443 + 640 = 1083$
1157 dp m			$e_{2g}$ fundamental
		1160 mw	$1530 - 370 = 1160$
		1248 vw	? $b_{2u}$ fundamental 1253
	1259 w	1266 vw	$264 + 994 = 1258$
		1277 vw	$264 + 1019 = 1283$
1280 p w			$2 \times 640 = 1280$
	1297 w	1304 mw	$714 + 595 = 1309$
		1348 mw	$714 + 640 = 1353$
	1368 s	1365 s	$1157 + 208 = 1365$
		1402 vvw	$370 + 1019 = 1389$
1429 p w			$2 \times 714 = 1428$
	1439 vw	1442 w	$443 + 994 = 1437$
	1463 m	1470 m	$443 + 1019 = 1462$
	1486 w	1488 w	$1157 + 315 = 1472$
1490 p ms			$a_{1g}$ fundamental
	1513 w	1510 w	$264 + 1253 = 1517$
	1531 vvvs	1530 vvvs	$e_{1u}$ fundamental
	1547 m	1552 m	$559 + 994 = 1553$
	1560 m	1565 m	$249 + 1323 = 1572$
	1570 m	1575 m	$559 + 1019 = 1578$
	1601 m	1600 m	$264 + 1323 = 1587$
1655 dp m			$e_{2g}$ fundamental
	1685 w	1655 w	{ $691 + 994 = 1685$
		1693 w	{ $443 + 1253 = 1696$
	1699 w	1710 w	$691 + 1019 = 1710$
	1763 s	1765 s	$443 + 1323 = 1766$

Table 1 (continued.)

Raman	infra-red		assignment
	vapour	liquid	
	1802 m	1806 m	$\left\{ \begin{array}{l} 264 + 1530 = 1794 \\ 1157 + 640 = 1797 \\ 1489 + 315 = 1804 \end{array} \right.$
		1838 vw	
	1890 w	1897 m	
		1940 vw	$370 + 1530 = 1900$
	1980 w	1976 w	$?$
			$\left\{ \begin{array}{l} 1655 + 315 = 1970 \\ 443 + 1530 = 1973 \end{array} \right.$
		2040 vw	$714 + 1323 = 2037$
	2093 m	2087 m	$559 + 1530 = 2089$
	2160 w	2150 w	$1157 + 994 = 2151$
	2176 w	2173 w	$1157 + 1019 = 2176$
	2263 w	2261 w	$1655 + 595 = 2250$
	2410 vw	2408 w	$1157 + 1253 = 2410$
	2483 s	2480 s	$\left\{ \begin{array}{l} 1157 + 1323 = 2480 \\ 1490 + 994 = 2484 \end{array} \right.$
			$1490 + 1019 = 2509$
	2505 w	2500 w	$?$
		2580 vw	$?$
	2697 m	2686 m	$1157 + 1530 = 2687$
	2840 vw	2850 vw	$?$
	2900 m	2909 m	$1655 + 1253 = 2908$
	2976 m	2976 ms	$1655 + 1323 = 2978$
	3027 m	3024 ms	$1490 + 1530 = 3020$
	3160 m	3179 m	$1655 + 1530 = 3185$

s = strong, m = medium, w = weak, v = very, Q = prominent Q branch.  
 ?  $a_{2u}$  frequency. \* found by Plyler.<sup>5</sup>

TABLE 2.—INFRA-RED ACTIVE BINARY SUMMATIONS

	$a_{1g}$	$e_{2g}$	$a_{2g}$	$b_{2g}$	$e_{1g}$
$e_{1u}$	$e_{1u}$	$e_{1u}$	$e_{1u}$	ia	$a_{2u}$
$b_{1u}$	ia	$e_{1u}$	ia	$e_{1u}$	ia
$b_{2u}$	ia	$e_{1u}$	ia	ia	ia
$a_{2u}$	$a_{2u}$	ia	ia	ia	$e_{1u}$
$e_{2u}$	ia	$a_{2u}$	ia	$a_{2u}$	$e_{1u}$

The infra-red vapour band shapes are not of much value as all fundamentals above  $300\text{ cm}^{-1}$  are  $e_{1u}$  and all strong summation bands are also likely to be of this symmetry, though sharp vapour bands at  $1044$  and  $849\text{ cm}^{-1}$  are probably the Q branches of parallel bands. As a first guide to the frequencies to be expected, it was assumed that the force constants, except for the C—F stretch and C—F/C—C interaction, would be similar to related constants for benzene.<sup>12</sup> Therefore the frequencies of hexafluorobenzene were calculated using the force constants of benzene except for a C—F stretch of  $7.3 \times 10^5$  dynes/cm and a C—C/C—F interaction constant which lead to exact agreement for the  $a_{1g}$  class. The results are shown in table 3.

Since the Raman frequencies are necessarily liquid state values, in the succeeding discussion liquid infra-red frequencies will be quoted for both fundamentals and summation bands.

#### $a_{1g}$ FUNDAMENTALS

The two Raman lines which are strong and strongly polarized are at  $1490$  and  $559\text{ cm}^{-1}$  and there can be no doubt that these are the two  $a_{1g}$  fundamentals.

#### $e_{1g}$ AND $e_{2g}$ FUNDAMENTALS

There should be five depolarized Raman active fundamentals and comparison of tables 1 and 3 can leave no doubt that the two highest  $e_{2g}$  fundamentals are at

1655 and 1157  $\text{cm}^{-1}$ . The strongest intensity lines remaining are at 443, 370 and 264  $\text{cm}^{-1}$  and it seems unnecessary to postulate any of the weaker bands as fundamentals. Delbouille<sup>5</sup> found the 217  $\text{cm}^{-1}$  Raman shift to be of medium intensity: on the plates obtained in this work the line is so weak that its reality is in some doubt. Comparison with table 3 suggests the lowest of the three, 264  $\text{cm}^{-1}$ , is likely to be an  $e_{2g}$  frequency, but decision between the 443 and 370

TABLE 3

class	nature	approximate calculation	final assignment
$a_{1g}$	R p	1490, 559 *	1490, 559
$a_{2g}$	ia	580	691
$b_{2g}$	ia	773, 183	714, 249
$e_{1g}$	R dp	369	370
$e_{2g}$	R dp	1753, 1180, 414, 213	1655, 1157, 443, 264
$a_{2u}$	i-r	195	215
$b_{1u}$	ia	1585, 539	1323, 640
$b_{2u}$	ia	1265, 207	1253, 208
$e_{1u}$	i-r $\perp$	1610, 910, 254	1530, 1019-994, 315
$e_{2u}$	ia	612, 121	595, 175

\* these frequencies used to choose the C—F stretching and C—F/C—C interaction constants used in other classes.

$\text{cm}^{-1}$  as  $e_{2g}$  is more troublesome. The calculation favours 370  $\text{cm}^{-1}$  as the  $e_{1g}$  and this may be reliable since there is only one frequency in this class. It was hoped that the spectrum of pentafluorobenzene and 1 : 2 : 4 : 5-tetrafluorobenzene<sup>13</sup> would assist in this difficulty. One of the  $a_2$  modes of pentafluorobenzene and a  $b_{2g}$  mode of tetrafluorobenzene remain nearly unchanged from that of one of the degenerate decompositions for the  $e_{1g}$  frequency: they would be exactly the same for an isotopic substitution but may be affected by force constant changes. Table 4 shows this correlation for both assignments. On the basis of frequency alone it is not easy to decide, but the infra-red intensity of the  $\text{C}_6\text{F}_5\text{H}$  band at 435  $\text{cm}^{-1}$ , though not large, appears too strong for a forbidden fundamental. The 391  $\text{cm}^{-1}$  band of  $\text{C}_6\text{F}_5\text{H}$  is therefore preferred for the  $a_2$  frequency and this implies that 370  $\text{cm}^{-1}$  is the  $e_{1g}$  frequency of hexafluorobenzene.

TABLE 4

	$e_{1u}$ like frequencies	
	either	or
$\text{C}_6\text{F}_6$	370	443
$\text{C}_6\text{F}_5\text{H}$	391	435
$p\text{-C}_6\text{F}_4\text{H}_2$	417	417

 $e_{1u}$  FUNDAMENTALS

The infra-red intensities leave no doubt that the absorption at 1530 and 315  $\text{cm}^{-1}$  belong to  $e_{1u}$  fundamentals and that the pair of frequencies 994 and 1019  $\text{cm}^{-1}$  are connected with the third fundamental. It must be presumed that this band is double by virtue of strong Fermi interaction with an  $e_{1u}$  summation band.

 $a_{2u}$  FUNDAMENTAL

The  $a_{2u}$  infra-red active fundamental is certainly below 250  $\text{cm}^{-1}$  and has not been observed in the present work. Plyler is quoted by Debouille<sup>5</sup> as finding a strong band at 215  $\text{cm}^{-1}$  which must be the  $a_{2u}$  frequency.

The remaining fundamentals are inactive in both spectra and must be derived from summation bands. It is difficult to make a wholly satisfactory argument for their assignment.



THE HIGHER  $b_{1u}$  AND  $b_{2u}$  FUNDAMENTALS

Reference to table 3 shows that only two of the fundamentals forbidden in both spectra are expected to lie above  $1000\text{ cm}^{-1}$ , namely the higher  $b_{1u}$  and  $b_{2u}$  frequencies. Both combine with  $e_{2g}$  frequencies to give active summation bands and two of the stronger bands above  $2000\text{ cm}^{-1}$ , namely,  $2480\text{ cm}^{-1}$  ( $1157 + 1323 = 2480$ ) and  $2976\text{ cm}^{-1}$  ( $1655 + 1323 = 2978$ ) suggest one of these frequencies to be  $1323\text{ cm}^{-1}$ ; strong summation bands with the remaining  $e_{2g}$  frequencies appear at  $1600$  and  $1765\text{ cm}^{-1}$ . Less strong, but nevertheless clear, summation bands at  $2909$ ,  $2408$ ,  $1693$  and  $1510$  suggest themselves for summation bands between the  $e_{2g}$  frequencies and  $1253\text{ cm}^{-1}$ . It remains to decide which frequency belongs to which class. The requirement that only the  $b_{1u}$  frequency combines with the  $b_{2g}$  frequencies to give  $a_{2u}$  summation bands is of little help since all possible bands are too weak to show resolved rotational structure and the  $b_{2g}$  frequencies are not known with certainty. Weak bands occur at all four possible frequencies and three have alternative explanations; the fourth at  $2040\text{ cm}^{-1}$  ( $1323 + 714 = 2037$ ) is evidence which favours  $1323\text{ cm}^{-1}$  as the  $b_{1u}$  frequency. This assignment is supported by table 3 which suggests the  $b_{1u}$  frequency should be the higher. The calculated  $b_{2u}$  value,  $1265\text{ cm}^{-1}$  is in agreement with the suggested  $1253\text{ cm}^{-1}$ . A theorem discussed in the last section may be applied to the  $a_1$  class of  $\text{C}_6\text{F}_5\text{H}$  and to the  $\text{C}_6\text{F}_6$  classes which coalesce when the symmetry is only  $\text{C}_{2v}$ , namely,  $a_{1g}$ ,  $e_{2g}$ ,  $b_{1u}$ ,  $e_{1u}$ . The fifth frequency of the  $a_1$  class of  $\text{C}_6\text{F}_5\text{H}$  is undoubtedly  $1286\text{ cm}^{-1}$  and this should, according to the theorem, lie below the fourth  $\text{C}_6\text{F}_6$  frequency. This is true if the  $b_{1u}$  frequency is  $1323\text{ cm}^{-1}$  but not if it is  $1253\text{ cm}^{-1}$ . A similar argument may be applied by comparison with  $p\text{-C}_6\text{H}_2\text{F}_4$ . The spectra of this compound<sup>13</sup> gives the following inequalities for the  $\text{C}_6\text{F}_6$  frequencies  $1439 > b_{1u} > 1229$  and  $1277 > b_{2u} > 1164$ , which are also only in agreement if the  $b_{1u}$  is  $1323$ .

LOWER  $b_{1u}$  FUNDAMENTAL

Among the infra-red bands not interpretable using only the frequencies already assigned is a medium band at  $1086\text{ cm}^{-1}$  which appears to have perpendicular band contour appropriate to an  $e_{1u}$  level. With reasonable magnitudes for the missing frequencies the most plausible explanation is a summation of this  $b_{1u}$  frequency near  $640\text{ cm}^{-1}$  with  $443\text{ cm}^{-1}$ . One fundamental is almost certainly  $640\text{ cm}^{-1}$  as there is a polarized Raman line at  $1280\text{ cm}^{-1}$  which can only come from twice some fundamental. A band at  $1348\text{ cm}^{-1}$  is also interpreted with the use of this frequency.

LOWER  $b_{2u}$  FUNDAMENTAL

Another prominent band with  $e_{1u}$  contour is at  $1365\text{ cm}^{-1}$  for which the best explanation is  $1157$  ( $e_{2g}$ ) + lower  $b_{2u}$  frequency, with a less likely alternative being the sum of the higher  $b_{2g}$  and  $e_{2u}$  modes. The required value  $208\text{ cm}^{-1}$  is almost exactly the calculated  $207\text{ cm}^{-1}$ : it is also used to explain weak bands at  $648\text{ cm}^{-1}$  and  $466\text{ cm}^{-1}$ .

 $b_{2g}$  FUNDAMENTALS

The calculations suggest that the higher  $b_{2g}$  frequency will be the highest out-of-plane frequency. Its value is probably less than the  $738\text{ cm}^{-1}$ , the highest  $b_2$  frequency of  $\text{C}_6\text{F}_5\text{D}$ , but, by the theorem of the final section, above  $689\text{ cm}^{-1}$ , the second  $b_2$  frequency of  $\text{C}_6\text{F}_5\text{H}$ . A weak polarized Raman line at  $1429\text{ cm}^{-1}$  suggests that some fundamental lies at half this frequency, and the presumption is therefore strong that this is a  $b_{2g}$  fundamental at  $714\text{ cm}^{-1}$ . Although there are no allowed binary combinations between the  $b_{2g}$  class and any active fundamental, two weak bands at  $2040\text{ cm}^{-1}$  and  $1348\text{ cm}^{-1}$  find welcome explanation as  $714\text{ cm}^{-1} +$  the  $b_{1u}$  frequencies  $1323$  and  $640\text{ cm}^{-1}$ .

Another polarized Raman line lies at  $499\text{ cm}^{-1}$  and again half this value,  $249\text{ cm}^{-1}$ , is strongly suggested for some fundamental. This frequency is probably too high for the lower  $e_{2u}$  frequency and the only alternative is to place it as the lower  $b_{2g}$ . It can be used to explain weak bands at  $416$  and  $841\text{ cm}^{-1}$ .

#### $e_{2u}$ FUNDAMENTALS

Two spectral features still unexplained are the sharp  $Q$  branches at  $849$  and  $1044\text{ cm}^{-1}$  in the vapour assigned to  $a_{2u}$  summation modes. If the assignments already given are correct these can only arise with any plausibility from  $e_{2u} + e_{2g}$  binary combinations. There are none expected in these regions involving the lower  $e_{2u}$  frequency, but if the higher were  $595\text{ cm}^{-1}$  then they can be explained as  $595 + 264 = 859\text{ cm}^{-1}$  and  $595 + 443 = 1038\text{ cm}^{-1}$ . Infra-red bands at  $2261$ ,  $1304$  and  $965\text{ cm}^{-1}$  also suggest this frequency.

It is difficult to find any firm evidence for the value for the lower  $e_{2u}$  frequency, but a value of  $175\text{ cm}^{-1}$  receives some support from bands at  $1838$ ,  $885$ ,  $553$ ,  $443$  and  $416\text{ cm}^{-1}$ .

#### $a_{2g}$ FUNDAMENTAL

Using all the above assignments it is still not possible to find a second  $e_{1u}$  level near  $1006\text{ cm}^{-1}$  with which the fundamental mixes through Fermi resonance to provide two very strong absorption bands. A value of  $691\text{ cm}^{-1}$  for the  $a_{2g}$  frequency would provide this and be in agreement with the  $\text{C}_6\text{F}_5\text{H}$  and  $\text{C}_6\text{F}_5\text{D}$  frequencies which suggest the  $a_{2g}$  frequency to be between  $662$  and  $870\text{ cm}^{-1}$ .

#### UNASSIGNED BANDS

Table 1 shows a conspectus of these assignments and also a few difference bands. Several liquid bands, notably those at  $1160$  and  $1655\text{ cm}^{-1}$ , have been assigned as forbidden fundamentals appearing in the liquid state, but there are no corresponding vapour bands and nothing to suggest that the molecule has not a centre of symmetry.

The assignments given above differ slightly from the assignment of the active fundamentals by Delbouille.<sup>5</sup> Without a full description of his work it would be premature to argue the merits of the assignments, but the present set of fundamentals appear to give the most satisfactory interpretation of the present experimental findings, though it must be admitted that several points of doubt remain.

#### PLANARITY

If the molecule is slightly non-planar the most probable structure is that with three alternate fluorine atoms above the plane of the ring and three below, similar to that found by electron diffraction for  $\text{C}_6\text{Cl}_6$  and  $\text{C}_6\text{Br}_6$ .<sup>14</sup> This structure would have  $D_{3d}$  group symmetry and a close correspondence to the planar  $D_{6h}$  assumed above. The Raman spectrum would be virtually the same with two polarized and five depolarized active fundamental lines. There would be four extra infra-red active fundamentals being essentially those of the  $b_{1u}$  and  $e_{2u}$  classes of  $D_{6h}$  symmetry. There are no bands observable in the vapour at any of the corresponding frequencies and it must be concluded that hexafluorobenzene is planar in its equilibrium position.

#### SOME FREQUENCY INEQUALITY RULES FOR RELATED MOLECULES

Consider a molecule  $\text{R}-\text{X}$ , where  $\text{R}$  is a polyatomic radical and  $\text{X}$  is monatomic, with a symmetry class containing the  $\text{R}-\text{X}$  stretching mode and  $n$  internal modes of the complex radical  $\text{R}$ , but not the  $\text{R}-\text{X}$  deformation modes. If  $\text{X}$  is of zero mass the frequencies of  $\text{R}-\text{X}$  consist of infinity and the  $n$  frequencies of the radical  $\text{R}$ . As the mass of  $\text{X}$  increases all the frequencies decrease monotonically and the  $j$ th frequency of  $\text{R}$  must be higher than the  $(j + 1)$ th frequency of  $\text{R}-\text{X}$ ,

numbering from the highest downwards. Alternatively if the R—X stretching force constant is zero and the interaction force constants of X with the internal motions of R are unimportant, then the frequencies of R—X consist of the  $n$  frequencies of R and zero. As the force constant of R—X increases all the frequencies must rise so that the  $j$ th frequency of R lies below the  $j$ th frequency of R—X. Considering the two molecules R—X and R—Y the rules applied successively show

$$\nu_{j+1}(\text{R—X}) < \nu_j(\text{R}) < \nu_j(\text{R—Y}), \text{ even if } M_y > M_x.$$

This rule has been derived in terms of the stretching motion but applies equally to symmetry classes containing one R—X bend. It also applies to  $\text{R}'\text{X}_2$  molecules with only one X mode in each symmetry class. If there are two X modes in the class the analogous rule is  $\nu_{j+2}(\text{R—X}) < \nu_j(\text{R—Y})$  and if all three X motions are in the class  $\nu_{j+3}(\text{R—X}) < \nu_j(\text{R—Y})$ , etc. The applicability condition is that the internal force field of R is unchanged by the substitution of X for Y and that cross-terms in the potential energy between the substituent and the internal coordinates of the radical shall be unimportant. It is not necessary that the force constants for the motion of X and Y should be identical so that although applicable to isotopic molecules, such as deuterated sugars,<sup>15</sup> its validity should be wider. Table 5 shows a comparison of the spectra of  $\text{C}_6\text{F}_6$ ,  $\text{C}_6\text{F}_5\text{H}$  and  $\text{C}_6\text{F}_5\text{D}$  which illustrates the rule. The  $\text{C}_6\text{F}_5\text{H}$  and  $\text{C}_6\text{F}_5\text{D}$  assignment<sup>7</sup> is based largely on band shapes in the vapour. For the  $\text{C}_6\text{F}_6$  assignments for the purpose of table 5 only  $\text{C}_{2v}$  symmetry is assumed. It can be seen that without exception the  $j$ th frequency of  $\text{C}_6\text{F}_6$  in each class lies above the  $(j + 1)$ th frequency of  $\text{C}_6\text{F}_5\text{H}$  but that in the two highest frequencies of the  $b_2$  class the  $j$ th frequency of  $\text{C}_6\text{F}_5\text{D}$  lies below the  $j$ th of  $\text{C}_6\text{F}_6$  presumably as a result of changes in the force constants.

TABLE 5

	$\text{C}_6\text{F}_5\text{H}$	$\text{C}_6\text{F}_5\text{D}$	$\text{C}_6\text{F}_6$		$\text{C}_6\text{F}_5\text{H}$	$\text{C}_6\text{F}_5\text{D}$	$\text{C}_6\text{F}_6$		
$a_1$	3105	2315	1655	$b_2$	1648	1638	1655		
	1648	1638	1530		1535	1511	1530		
	1514	1503	1490		1268	1267	1253		
	1410	1400	1323		1182	1146	1157		
	1286	1277	1157		1138	1024	1011		
	1082	1067	1011		953	870	691		
	718	701	640		662	625	443		
	580	578	559		436	435	315		
	469	467	443		300	300	264		
	325	325	315		?	?	208		
	272	?	264						
	$a_2$	?	?		595	$b_1$	838	738	714
		391	?		370		689	670	595
171?		?	175	556	494		370		
				?	?		249		
				?	?		215		
				?	?		175		

We wish to thank Dr. J. C. Tatlow and his colleagues for assistance with the preparation of hexafluorobenzene and Dr. L. Bovey and Mr. A. M. Deane for the infra-red measurements below  $400 \text{ cm}^{-1}$ . D. S. wishes to acknowledge the receipt of a University Appeal scholarship.

<sup>1</sup> Godsell, Stacey and Tatlow, *Nature*, 1956, **178**, 199.

<sup>2</sup> Ingold *et al.*, *J. Chem. Soc.*, 1946, 223 *f*.

<sup>3</sup> Brodersen and Langseth, *Mat. Fys. Skr. Dansk. Vid. Selsk.*, 1956, **1**, no. 1.

<sup>4</sup> Mair and Hornig, *J. Chem. Physics*, 1949, **17**, 1236.

- <sup>5</sup> Delbouille, *J. Chem. Physics*, 1956, **25**, 182.
- <sup>6</sup> Stephens and Tatlow, *Chem. and Ind.*, 1957, 821.
- <sup>7</sup> Steele and Whiffen, to be published.
- <sup>8</sup> Spedding and Whiffen, *Proc. Roy. Soc. A*, 1956, **238**, 245.
- <sup>9</sup> Edsall and Wilson, *J. Chem. Physics*, 1938, 124.
- <sup>10</sup> Ingold *et al.*, *J. Chem. Soc.*, 1936, 912.
- <sup>11</sup> Bailey, Ingold, Poole and Wilson, *J. Chem. Soc.*, 1946, 222.
- <sup>12</sup> Whiffen, *Phil. Trans. Roy. Soc. A*, 1955, **248**, 131.
- <sup>13</sup> Nielsen, *J. Chem. Physics*, 1953, **21**, 1464.
- <sup>14</sup> Bastiansen and Hassel, *Acta Chem. Scand.*, 1947, **1**, 489.
- <sup>15</sup> Barker, Bourne, Moore, Stacey and Whiffen, *2nd Geneva Conf. Peaceful Uses of Atomic Energy*, 1958.

## THE FORCE FIELD OF HEXAFLUOROBENZENE

BY D. STEELE AND D. H. WHIFFEN  
Chemistry Dept., The University, Birmingham, 15

Received 14th September 1959

A force field is given in table 2 which reproduces the assigned frequencies of hexafluorobenzene and contains only small interaction constants when expressed in valency coordinates.

The recent assignment<sup>1</sup> of all the frequencies of hexafluorobenzene make it possible to derive a force field for this molecule. This was required for guidance on the force field of 1,4-difluorobenzene and 1,2,4,5-tetrafluorobenzene<sup>2</sup> and in connection with measurements of infra-red intensities.<sup>3, 4</sup> Consequently it was desirable to obtain a force-field fitting the assigned frequencies as closely as possible, even though some uncertainty remains regarding the inactive fundamentals.

### ASSIGNMENT

Full arguments were given previously for the assignment suggested by the present authors.<sup>1</sup> Almost simultaneously Delbouille<sup>5, 6</sup> published an independent assignment of the active fundamentals. A few comments can be made on the major differences. Price, Smart and Wilkinson<sup>7</sup> have measured the infra-red band at  $315\text{ cm}^{-1}$  and obtained a band contour which is consistent with it belonging to the  $e_{1u}$  class vibration. The two assignments agree in respect of the  $a_{1g}$  class and the disagreement in the  $e_{1g}$  and  $e_{2g}$  classes has been discussed previously.<sup>1</sup> The approximate calculations for inactive fundamentals of Delbouille<sup>6</sup> and the present authors<sup>1</sup> are not seriously inconsistent. Delbouille assigns to the inactive  $a_{2g}$  frequency a value of  $610\text{ cm}^{-1}$ ; the difficulty with this assignment is to find a cause for the splitting of the second  $e_{1u}$  band into two. Delbouille's suggested ternary combination is irrelevant as it is a difference band and therefore quite unable to borrow intensity from a fundamental at the same frequency. The present authors therefore see no reason to change their earlier assignment in the way preferred by Delbouille.

### FORCE FIELD

The  $a_{2g}$ ,  $e_{1g}$  and  $a_{2u}$  classes contain only one frequency each and the corresponding force constants are readily evaluated. The  $a_{1g}$ ,  $b_{2g}$ ,  $b_{1u}$ ,  $b_{2u}$  and  $e_{2u}$  classes each contain two frequencies. Since to each class there are three general force constants these are not uniquely determined. The possibilities may be expressed in graphical form as an ellipse by plotting two force constants with the third, preferably the interaction constant, as a running parameter. Any point on this ellipse represents force constants which lead exactly to the assigned frequencies. In the absence of further information from isotopic species, Coriolis coupling or centrifugal distortion, the choice between these points is arbitrary. A choice is, however, necessary for determining normal coordinates. For most molecules a simple valency force field is a good approximation to more accurate fields. With such a field, all interaction constants between valency coordinates are zero; that is, with the nomenclature used for benzene<sup>8, 9, 10</sup> all Latin interaction constants are zero. Consequently a choice of force constants has been made governed by the requirement that all Latin interaction constants shall be small. Where this proved to be an insufficient criterion

the force field in terms of symmetry coordinates (Greek force constants) was taken to be as close as possible to that for benzene.

The position with the larger  $e_{1u}$  and  $e_{2g}$  classes is more difficult. Starting with the original approximate constants, adjustments were made consistent with the above requirements until a satisfactory fit was obtained with the observed frequencies. For the  $e_{1u}$  class the calculated frequencies were 1531, 1006, 312  $\text{cm}^{-1}$  compared with the observed 1530, 1019-994, 315  $\text{cm}^{-1}$  and for the  $e_{2g}$  class the calculated 1653, 1160, 443, 263  $\text{cm}^{-1}$  are to be compared with the observed 1655, 1157, 443, 264  $\text{cm}^{-1}$ . With the symbols used previously for benzene and with  $R_0 = 1.40 \text{ \AA}$ ,  $r_0 = 1.29 \text{ \AA}$  the Greek constants<sup>8</sup> finally adopted are shown in table 1 and the corresponding Latin constants in table 2.

TABLE 1.—GREEK FORCE CONSTANTS IN mD/Å.

	in-plane		out-of-plane	
$\Omega_1$ 7.512	$\chi_3$	-0.180	$\Phi_1$	0.936
$\Omega_2$ 7.100			$\Phi_2$	0.447
$\Omega_3$ 7.400	$\mu_2$	0.235	$\Phi_3$	0.224
$\Omega_4$ 7.509	$\mu_3$	-0.248	$\Phi_4$	0.200
	$2^{\frac{1}{2}}\mu_4$	0.172		
$\Gamma_1$ 0.780			$\Theta_1$	0.319
$\Gamma_2$ 0.492	$\pi_3$	0.178	$\Theta_2$	0.321
$\Gamma_3$ 0.847				
$\Gamma_4$ 0.991	$\epsilon_1$	0.889	$\eta_1$	0.500
	$\epsilon_3$	0.444	$\eta_2$	-0.300
$A_1$ 7.400	$2^{\frac{1}{2}}\epsilon_4$	1.412		
$A_2$ 3.840				
$A_3$ 5.205	$\psi_2$	-0.764		
$2A_4$ 7.402	$\psi_3$	-0.420		
$\Sigma_2$ 0.748	$\tau_3$	-0.390		
$\Sigma_3$ 0.889	$\tau_4$	0.197		

For meaning of symbols, see ref. (8).

TABLE 2.—LATIN FORCE CONSTANTS IN mD/Å

	in-plane		out-of-plane	
$D$ 5.478	(5.553)	$\bar{i}_0$ -0.180 (-0.180)	$\bar{P}$ 0.230 (0.286)	
$\bar{d}_0$ 0.660	(0.633)		$\bar{p}_0$ 0.028 (0.012)	
$\bar{d}_m$ 0.071	(0.113)	$\bar{h}_0$ 0.708 (-)	$\bar{p}_m$ -0.019 (-0.022)	
$\bar{d}_p$ 0.459	(0.573)	$\bar{h}_m$ 0.001 (-)	$\bar{p}_p$ -0.048 (-0.017)	
		$\bar{h}_p$ -0.263 (-)		
$E$ 7.405	(5.093)		$\bar{Q}$ 0.080 (0.0290)	
$e_0$ 0.087	(0.025)	$\bar{j}_0$ 0.112 (0.043)	$\bar{q}_0$ -0.001 (-0.0100)	
$e_m$ -0.050	(0.008)	$\bar{j}_m$ -0.041 (-0.063)		
$e_p$ 0.032	(-0.040)	$\bar{j}_p$ -0.033 (0.043)	$\bar{i}_0$ 0.014 (0.014)	
			$\bar{i}_m$ 0.038 (0.000)	
$G$ 0.826	(0.864)	$\bar{k}$ -0.076 (-)		
$g_0$ 0.072	(0.012)	$\bar{k}_0$ 0.344 (-)		
$g_m$ -0.093	(-0.018)			
$g_p$ 0.002	(-0.019)	$\bar{n}_0$ -0.103 (-0.127)		
$\bar{F}$ 1.030	(1.031)	$\bar{l}_0$ 0.170 (-)		
$\bar{f}_0$ 0.141	(0.185)	$\bar{l}_m$ -0.054 (-)		

Values in parenthesis refer<sup>8</sup> to  $\text{C}_6\text{H}_6$ . For the meaning of the symbols, see ref. (8).

## DISCUSSION

Also given in table 2 are the corresponding values for benzene. A comparison of the interaction constants is relatively meaningless as small changes in the frequencies to be fitted or a variant choice of principal constants can affect these markedly. Also the  $h$ ,  $k$ ,  $l$  constants could be taken as zero for benzene as they scarcely affect the calculated frequencies since the C—H stretching frequencies are so much higher than all others that C—H interactions may be neglected. Such neglect is not feasible for C—F interactions. As regards the principal constants the C—C stretch  $\hat{D}$  and the C—C—C angle deformation  $\hat{F}$  are essentially the same in  $C_6H_6$  and  $C_6F_6$ . The C—F stretching force constant, associated with  $E$ , 7.4 mD/A is considerably larger than the C—H stretch, 5.1 mD/A. The in-plane C—F/C—H bending constants  $G$  and the out-of-plane equivalent  $\hat{P}$  are somewhat smaller for C—F than C—H. However, a fairer comparison is between the coefficients governing the angular displacements namely  $r_0^2 G$  which are 1.37 and 0.95 mD A and  $r_0^2 P$  which are 0.38 and 0.32 mD A for  $C_6F_6$  and  $C_6H_6$  respectively. These figures show that C—F deformation is more difficult than C—H. For the in-plane motion this may be due to repulsion between adjacent fluorine atoms.  $\hat{Q}$  appears to be much larger for  $C_6F_6$ , but since  $\hat{Q}$  is derived solely from the frequencies in the inactive  $b_{2g}$  and  $e_{2u}$  classes this may be the consequence of an error of assignment.

We wish to thank Prof. W. C. Price and his colleagues for their re-examination of the infra-red spectrum below  $400\text{ cm}^{-1}$ . D. S. wishes to acknowledge the receipt of a University Appeal Scholarship.

- <sup>1</sup> Steele and Whiffen, *Trans. Faraday Soc.*, 1959, **55**, 369.
- <sup>2</sup> Steele and Whiffen, *Trans. Faraday Soc.*, 1960, 56.
- <sup>3</sup> Steele and Whiffen, *J. Chem. Physics*, 1958, **29**, 1194.
- <sup>4</sup> Steele and Whiffen, *Trans. Faraday Soc.*, in press.
- <sup>5</sup> Delbouille, *J. Chem. Physics*, 1956, **25**, 182.
- <sup>6</sup> Delbouille, *Bull. Acad. roy. Belg.*, 1958 (V), **44**, 971.
- <sup>7</sup> Price, Smart and Wilkinson, personal communication.
- <sup>8</sup> Whiffen, *Phil. Trans. A*, 1955, **248**, 131.
- <sup>9</sup> Miller and Crawford, *J. Chem. Physics*, 1946, **14**, 282.
- <sup>10</sup> Crawford and Miller, *J. Chem. Physics*, 1949, **17**, 249.

PRINTED IN GREAT BRITAIN AT  
THE UNIVERSITY PRESS  
ABERDEEN



Offprinted from the *Transactions of the Faraday Society*,  
No. 445, Vol. 56, Part 1, January, 1960

THE FORCE FIELDS OF THE INFRA-RED ACTIVE CLASSES OF 1,4-  
DIFLUOROBENZENE AND 1,2,4,5-TETRAFLUOROBENZENE

# THE FORCE FIELDS OF THE INFRA-RED ACTIVE CLASSES OF 1,4-DIFLUOROBENZENE AND 1,2,4,5-TETRAFLUORO- BENZENE

BY D. STEELE AND D. H. WHIFFEN  
Chemistry Dept., The University, Birmingham, 15

*Received 14th September, 1959*

The infra-red active frequencies of  $p\text{-C}_6\text{H}_4\text{F}_2$ ,  $p\text{-C}_6\text{D}_4\text{F}_2$  and  $p\text{-C}_6\text{H}_2\text{F}_4$  have been calculated using force constants derived from  $\text{C}_6\text{F}_6$  and  $\text{C}_6\text{H}_6$  by transferring the valency force field in a logical manner. Good agreement with the observed frequencies is shown.

In connection with the interpretation of absolute intensity measurements it is necessary to know the normal coordinates of a molecule and this in turn requires a knowledge of its force field. The infra-red intensities of 1,4-difluorobenzene, 1,4-difluoro-2,3,5,6-tetradeuterobenzene and 1,2,4,5-tetrafluorobenzene have been measured and discussed in a companion paper.<sup>1</sup> The present paper concerns the force field of these molecules, the calculation of their infra-red active frequencies and a few comments on the vibrational assignments.

## THE FORCE FIELD

Details of the calculation of frequencies and normal coordinates by the Wilson FG matrix method<sup>2</sup> are well known. The three molecules have  $V_h$  symmetry and symmetry coordinates may be chosen in terms of valency coordinates as shown in table 1. The nomenclature generally follows that used by Whiffen<sup>3</sup> for benzene

TABLE 1.—DEFINITIONS OF SYMMETRY COORDINATES

$$\begin{array}{l}
 b_{1u} \\
 S_{18} = 2^{-1}(\Delta r_2 - \Delta r_3 - \Delta r_5 + \Delta r_6) \\
 S_{19} = 2^{-1}(\Delta R_1 - \Delta R_3 - \Delta R_4 + \Delta R_6) \\
 S_{20} = 2^{-1}R_0(\alpha_2 - \alpha_3 - \alpha_5 + \alpha_6) \\
 S_{21} = 2^{-1}r_x(\beta_2 + \beta_3 - \beta_5 - \beta_6) \\
 S_{22} = 2^{-1}(\Delta r_1 - \Delta r_4) \\
 \\
 b_{2u} \\
 S_{23} = 2^{-1}(\Delta r_2 + \Delta r_3 - \Delta r_5 - \Delta r_6) \\
 S_{24} = 2^{-1}(\Delta R_2 - \Delta R_5) \\
 S_{25} = 2^{-1}(\Delta R_1 + \Delta R_3 - \Delta R_4 - \Delta R_6) \\
 S_{26} = 2^{-1}r_x(\beta_2 - \beta_3 - \beta_5 + \beta_6) \\
 S_{27} = 2^{-1}r_y(\beta_1 - \beta_4) \\
 \\
 b_{3u} \\
 S_{28} = 2^{-1}r_x(\gamma_2 + \gamma_3 + \gamma_5 + \gamma_6) \\
 S_{29} = 2^{-1}R_0(\phi_1 - \phi_3 + \phi_4 - \phi_6) \\
 S_{30} = 2^{-1}r_y(\gamma_1 + \gamma_4)
 \end{array}$$

itself and is given for a molecule  $p\text{-C}_6\text{X}_4\text{Y}_2$  with the  $x$ -axis perpendicular to the ring and the  $z$ -axis passing through the Y atoms as recommended.<sup>4</sup>  $\rho_x$  is the ratio of the

C—X bond length  $r_x$  to the C—C length  $R_0$ , and  $\rho_y$  is similarly defined as  $r_y/R_0$ . The symmetry coordinates are numbered to accord with the approximate mode description<sup>5</sup> for  $C_6H_4F_2$ . The force field chosen was derived from that of benzene<sup>3</sup> and hexafluorobenzene.<sup>6</sup> Expressed in terms of valency coordinates (Latin constants) the principal terms for C—H/C—F stretching and bending were transferred unchanged as was that governing the ring angle bending,  $\alpha$ , which is 1.03 mD/A in both species. The C—C stretch is also virtually unchanged between  $C_6H_6$  and  $C_6F_6$  and a mean value was taken for the C(H)—C(F) stretch. Interaction constants are all small in the valency force field and in appropriate cases, e.g. C—H/C—F bending interactions, the geometric mean of the values for  $C_6H_6$  and  $C_6F_6$  was taken. The valency force field was converted to that appropriate to the symmetry coordinates by means of the definitions of table 1 and the internal relationships between the ring coordinates of a regular hexagon.<sup>3</sup> With these assumptions the F matrix is given by the numerical values of table 3. Solving the secular equation by iteration of the latent roots of the GF product matrix the calculated frequencies of table 4 were obtained and also the form of the normal coordinates.<sup>1</sup>

TABLE 2

$m_x$ ,  $m_y$  and  $m_c$  are the masses of atoms  $x$ ,  $y$  and carbon respectively.

G matrices. Coordinates taken in serial order.

$b_{1u}$

$m_x^{-1} + m_c^{-1}$	$-2^{-1}m_c^{-1}$	$3^{3/2} \cdot 2^{-1}m_c^{-1}$	$-3^{1/2} \cdot 4 \cdot \rho_x \cdot m_c^{-1}$	0
	$3 \cdot 2^{-1} \cdot m_c^{-1}$	$-3^{1/2} \cdot 2^{-1}m_c^{-1}$	$(3^{1/2} \cdot 2^{-1} + 3^{3/2} \cdot 4^{-1}\rho_x)m_c^{-1}$	$-2^{-1/2}m_c^{-1}$
		$17 \cdot 2^{-1}m_c^{-1}$	$-(2^{-1} + 3 \cdot 4^{-1} \cdot \rho_x)m_c^{-1}$	$-3^{1/2} \cdot 2^{-1/2}m_c^{-1}$
		SYMMETRICAL	$m_x^{-1} + (9 \cdot 8^{-1}\rho_x^2 + 3 \cdot 2^{-1}\rho_x + 1)m_c^{-1}$	$-3^{1/2} \cdot 2^{-3/2}\rho_x m_c^{-1}$
				$m_y^{-1} + m_c^{-1}$

$b_{2u}$

$m_x^{-1} + m_c^{-1}$	$-2^{-1/2}m_c^{-1}$	$-2^{-1}m_c^{-1}$	$3^{1/2} \cdot 4^{-1}\rho_x m_c^{-1}$	$3^{1/2} \cdot 2^{-3/2}\rho_y m_c^{-1}$
	$2 \cdot m_c^{-1}$	$-2^{-1/2}m_c^{-1}$	$-3^{1/2} \cdot 2^{-1/2}(2^{-1}\rho_x + 1)m_c^{-1}$	$-3^{1/2} \cdot 2^{-1}\rho_y m_c^{-1}$
		$5 \cdot 2^{-1}m_c^{-1}$	$3^{1/2} \cdot 2^{-1}(1 - 2^{-1}\rho_x)m_c^{-1}$	$-3^{1/2} \cdot 2^{-1/2}(1 + 2^{-1}\rho_y)m_c^{-1}$
		SYMMETRICAL	$m_x^{-1} + (3 \cdot 8^{-1}\rho_x^2 + 2^{-1}\rho_x + 1)m_c^{-1}$	$[3 \cdot 2^{-5/2}\rho_x\rho_y + 2^{-3/2}(\rho_x + \rho_y)]m_c^{-1}$
				$m_y^{-1} + (3 \cdot 4^{-1}\rho_y^2 + \rho_y + 1)m_c^{-1}$

$b_{3u}$

$m_x^{-1} + (1 + 2\rho_x + 3\rho_x^2)m_c^{-1}$	$-2 \cdot 3^{-1/2}\rho_x^{-1}m_x^{-1} + 2 \cdot 3^{-1/2}(3\rho_x - 2\rho_x\rho_y - \rho_x^{-1})m_c^{-1}$	$-2^{1/2}(\rho_x + \rho_y + 3\rho_x\rho_y)m_c^{-1}$
	$8 \cdot 3^{-1}\rho_y^{-2}m_y^{-1} + 4 \cdot 3^{-1}\rho_x^{-2}m_x^{-1} +$	$2^{3/2} \cdot 3^{-1/2}\rho_y^{-1}m_y^{-1} +$
SYMMETRICAL	$4 \cdot 3^{-1}(3 - 4\rho_y^{-1} + 2\rho_y^{-2} - 2\rho_x^{-1} + \rho_x^{-2})m_c^{-1}$	$2^{3/2} \cdot 3^{-1/2}(\rho_y^{-1} - 3\rho_y + 1 + \rho_y\rho_x^{-1})m_c^{-1}$
		$m_y^{-1} + (1 + 4\rho_y + 6\rho_y^2)m_c^{-1}$

TABLE 3.—F MATRICES. SYMMETRY COORDINATES TAKEN IN SERIAL ORDER. UNITS mD/Å. INITIAL TERMS REFER TO C<sub>6</sub>H<sub>4</sub>F<sub>2</sub> AND THOSE AFTER THE SEMICOLON TO C<sub>6</sub>H<sub>2</sub>F<sub>4</sub>.

$b_{1u}$				
5.116; 7.483	-0.658; 0.814	-0.380; -0.420	0; -0.113	0.021; 0.021
	7.737; 7.693	0.609; 0.585	-0.180; -0.175	1.200; 0
	SYMMETRICAL	1.020; 1.048	0; 0	0.565; 0
			0.913; 0.991	0; 0
				7.496; 5.133

$b_{2u}$				
5.150; 7.509	0; 0.874	0.203; 0.616	0; 0.113	0; 0
	6.207; 6.219	1.618; 1.660	0.225; 0.211	0.026; 0.020
	SYMMETRICAL	5.050; 5.046	-0.139; -0.123	0.041; 0.018
			0.853; 0.663	0.099; 0.099
				0.827; 0.883

$b_{3u}$		
0.259; 0.191	0.014 ; 0.014	0.000; 0.000
	0.0595; 0.0595	-0.020; -0.020
	SYMMETRICAL	0.182; 0.269

TABLE 4

	$p\text{-C}_6\text{H}_4\text{F}_2$		$p\text{-C}_6\text{D}_4\text{F}_2$		$p\text{-C}_6\text{H}_2\text{F}_4$	
	calc.	ass.	calc.	ass.	calc.	ass.
$b_{1u}$	3047	3065	2254	2277	3076	3088
	1543	1511	1466	1435	1475	1439
	1286	1225	1170	1125, 1139	1284	1222
	1028	1012	891	859	705	700
	772	737	709	685	334	ca. 330
$b_{2u}$	3074	—	2282	2310	1610	1534
	1431	1437	1342	1369?	1327	1277
	1301	1285	1285	1287	1193	1164
	1088	1085	815	802	855	853
	306	350	303	—	251	ca. 290
$b_{3u}$	850	833	701	729	971	869
	525	509	461	422	492	457
	168	ca. 186	166	—	189	ca. 200

## FREQUENCY ASSIGNMENT

## 1,4-DIFLUOROBENZENE

The complete assignments for 1,4-difluorobenzene<sup>7</sup> has been largely confirmed.<sup>5</sup> The change from 1183-1212 to 1285  $\text{cm}^{-1}$  suggested earlier<sup>5</sup> for vibration 25 is supported by the calculated value 1301  $\text{cm}^{-1}$ . Also a reinvestigation of the C—H stretching region shows a band with  $b_{1u}$  contour at 3067  $\text{cm}^{-1}$  which is very weak and fails to disclose the  $b_{2u}$  frequency.

## 1,4-DIFLUORO-2,3,5,6-TETRADEUTEROBENZENE

The assignment for 1,4-difluoro-2,3,5,6-tetradeuterobenzene<sup>1</sup> is based largely on band contours and is easily made. The pair of bands at 1125 and 1139  $\text{cm}^{-1}$  appear single in the vapour and are attributed to a  $b_{1u}$  fundamental and a combination band which interacts with it. The band at 1369  $\text{cm}^{-1}$  is very weak and is accompanied by another at 1388  $\text{cm}^{-1}$  and it is difficult to be sure of this assignment, especially in the absence of a knowledge of the spectrum of  $p\text{-C}_6\text{D}_3\text{HF}_2$  which is a known impurity.

## 1,2,4,5-TETRAFLUOROBENZENE

1,2,4,5-Tetrafluorobenzene has been assigned by Nielsen and coworkers.<sup>8</sup> Evidence from a comparison<sup>9</sup> with pentafluorobenzene has suggested that modifications in this assignment may be necessary. In particular, the lowest mode in each infra-red active in-plane class is probably too high in Nielsen's assignment<sup>8</sup> and this is confirmed by the present calculations. The assignment quoted in table 4 is discussed elsewhere<sup>9</sup> together with the spectrum of pentafluorobenzene.

## COMPARISON OF CALCULATED AND OBSERVED FREQUENCIES

The force constants of  $\text{C}_6\text{F}_6$  and  $\text{C}_6\text{H}_6$  are based on liquid state frequencies and also the comparison between frequencies observed in the liquid and calculated frequencies is given in table 4, for  $\text{C}_6\text{H}_4\text{F}_2$ ,  $\text{C}_6\text{D}_4\text{F}_2$  and  $\text{C}_6\text{H}_2\text{F}_4$ . The agreement is satisfactory throughout. It is thus clear that in the substituted benzenes a transference of valency force constants is reasonably valid and may be valuable in assisting the assignment.

## ADJUSTMENTS OF FORCE CONSTANTS

Since one of the objects of this work was to obtain normal coordinates for use in analysis of absolute intensities, attempts were made to obtain a force field agreeing even more closely with the observed frequencies. For the in-plane classes, no simple adjustment greatly improved the agreement and in view of the labour of

TABLE 5.—IMPROVED  $b_{3u}$  FORCE CONSTANTS.

0.229; 0.195	0.023; -0.004	-0.032; -0.032
	0.067; 0.062	-0.008; -0.042
	SYMMETRICAL	0.186; 0.239

evaluation of the classes with five frequencies on a desk calculator, the search was discontinued. The differences between liquid and vapour frequencies are unimportant. For the  $b_{3u}$  classes the labour is less and the normal coordinates were finally calculated with the force constant matrix of table 5 replacing that of table 3 and the agreement is shown in table 6. Since the intensities were measured in the vapour phase the observed frequencies for this state are quoted. The basis of the

TABLE 6.— $b_{3u}$  FREQUENCIES CALCULATED FROM IMPROVED F MATRIX OF TABLE 5 COMPARED WITH VAPOUR FREQUENCIES

$p\text{-C}_6\text{H}_4\text{F}_2$		$p\text{-C}_6\text{D}_4\text{F}_2$		$p\text{-C}_6\text{H}_2\text{F}_4$	
calc.	ass.	calc.	ass.	calc.	ass.
846	837	726	732	881	869
499	506	420	422	477	457
180	186?	180	—	199	—

adjustment was to calculate the change in the roots of the secular equation,  $\delta\lambda$ , for a given change of force field,  $\delta F$ , by the matrix expression

$$\mathbf{L}^\dagger \cdot \delta \mathbf{F} \cdot \mathbf{L} = \delta \lambda,$$

where the  $\mathbf{L}$  are the matrices appropriate to the unchanged  $\mathbf{F}$ . It is then relatively easy to suggest suitable changes  $\delta F$  and finally to recompute the frequencies and normal coordinates exactly.

D. S. wishes to acknowledge receipt of a University Appeal Scholarship.

- <sup>1</sup> Steele and Whiffen, *Trans. Faraday Soc.*, in press.
- <sup>2</sup> Wilson, Decius and Cross, *Molecular Vibrations* (McGraw-Hill, New York, 1955).
- <sup>3</sup> Whiffen, *Phil. Trans. A*, 1955, 248, 131.
- <sup>4</sup> Mullikan, *J. Chem. Physics*, 1955, 23, 1997.
- <sup>5</sup> Stojilkovic and Whiffen, *Spectrochim. Acta*, 1958, 12, 47.
- <sup>6</sup> Steele and Whiffen, *Trans. Faraday Soc.*, 1960, 56, 5.
- <sup>7</sup> Ferguson, Hudson, Nielsen and Smith, *J. Chem. Physics*, 1953, 21, 1457.
- <sup>8</sup> Ferguson, Hudson, Nielsen and Smith, *J. Chem. Physics*, 1953, 21, 1464.
- <sup>9</sup> Steele and Whiffen, *Spectrochim. Acta*, in press.

PRINTED IN GREAT BRITAIN AT  
THE UNIVERSITY PRESS  
ABERDEEN

## INFRA-RED ABSORPTION INTENSITIES IN 1,4-DIFLUOROBENZENE AND 1,2,4,5-TETRAFLUOROBENZENE

By D. STEELE AND D. H. WHIFFEN  
Chemistry Dept., The University, Birmingham 15

Received 12th October, 1959

The absolute infra-red absorption intensities of the bands above  $400\text{ cm}^{-1}$  have been measured in the vapour for 1,4-difluorobenzene, 1,4-difluorotetra-deuterobenzene and 1,2,4,5-tetrafluorobenzene. They are interpreted in terms of the dipole moment gradients of table 3. It is shown that the intensities are dominated by the motion of the fluorine atoms. The dipole moment gradients for hydrogen deformations are confirmed to have that sign which is equivalent to the H atom carrying a positive charge and to have similar magnitudes to those found in benzene itself.

In the interpretation of infra-red absorption frequencies it has been found that the directly observed frequencies can be transferred between molecules of related structure and, in favourable cases, the absorption intensities are likewise transferable. However, for molecules differing appreciably in geometrical structure, even though chemically related, a comparison of frequencies is not possible and the observations must be reduced to the form of force constants before valid comparisons can be made. Similarly intensity data must be converted to dipole moment gradients for comparison between molecules of different geometry. The fluorinated benzenes form a series for such comparison and the present work on the intensities of 1,4-difluorobenzene and 1,2,4,5-tetrafluorobenzene, follows earlier work on the extreme members of the series benzene<sup>1</sup> and hexafluorobenzene.<sup>2</sup>

### EXPERIMENTAL

The measurements were made on a grating spectrometer<sup>1</sup> (above  $950\text{ cm}^{-1}$ ), on a Perkin-Elmer 21 with a sodium chloride prism ( $650\text{--}1500\text{ cm}^{-1}$ ) or a Grubb-Parsons single-beam spectrometer with a potassium bromide prism ( $400\text{--}700\text{ cm}^{-1}$ ). Concordant results were obtained for the same band measured on different spectrometers. Small corrections were made for amplifier non-linearity on the single-beam spectrometers. Scattered light below  $700\text{ cm}^{-1}$  was removed with an alkali impurity potassium-bromide filter which eliminates radiation above  $1000\text{ cm}^{-1}$ .

Preliminary measurements of intensity against inert-gas pressure showed that the resolution and pressure broadening, with nitrogen as the inert gas, were such that the apparent intensity was independent of inert-gas pressure above 300 mm of Hg. The final measurements were made with added nitrogen to a total of 730 mm of Hg. The cell length was 10 cm and for the stronger bands the absorption was shown to be linearly dependent on the partial pressure of fluorohydrocarbon as measured on a glycol manometer. The absorption bands were plotted on a large scale and measured with a planimeter. For the present work, it was more important to measure as many bands of as many molecular species as possible than to obtain the highest accuracy and each band was studied at only a few pressures. In view of the many sources of minor errors, it cannot be claimed that the accuracy of any band intensity is necessarily better than 10% and may be worse on the weakest bands. For the  $b_{1u}$  classes of both 1,4-difluorobenzene and 1,4-difluorotetra-deuterobenzene all five fundamental bands are readily observed and the intensity sum rule<sup>3</sup> for isotopic species may be applied. The quantities  $\sum_j A_j/\nu_j^2$  appear to be 2% lower for the deuterated species and this is well within the errors of the experiment and the assumptions involved.

The 1,4-difluorobenzene was a commercial sample shown to be pure by vapour-phase chromatography and the 1,2,4,5-tetrafluorobenzene was prepared in the department and



its purity likewise checked. The 1,4-difluorotetradeuterobenzene was made from 1,4-difluorobenzene by the action of DCl, with AlCl<sub>3</sub> as catalyst, after the manner used by Bak<sup>4,5</sup> for related compounds. The progress of the reaction was followed by observing the infra-red spectrum and the exchange was stopped when bands attributed to C<sub>6</sub>HD<sub>3</sub>F<sub>2</sub>, other than those at 1206 and 892 cm<sup>-1</sup>, were no longer visible. A mass-spectroscopic examination of this product showed the isotopic purity to be 92.4%. Where the bands of the trideutero-compound did not overlap those of the tetradeutero compound a correction based on this figure was applied to the experimental intensities. Where the bands seriously overlapped it was assumed that the intensity, as well as the frequency, was insensitive to deuteration and the correction was accordingly omitted.

The results are quoted in table 2 of the next section and are expressed both as intensities integrated with respect to the frequency and in the cross-section form advocated by Crawford.<sup>6</sup> The bands are sufficiently narrow that  $\int_j \epsilon d\nu \approx \nu_j^{-1} \int_j \epsilon d\nu$  and the latter form has been used for convenience.

#### INTERPRETATION

##### GENERAL REMARKS

The force field and assignment used for interpreting the results has been discussed elsewhere.<sup>7</sup> The corresponding **L** matrices<sup>8</sup> which have been normalized to the calculated frequencies are given in table 1. An improved frequency fit and refined force constants and **L** matrices could doubtless have been obtained by a suitable programme on an electronic computer. Even such a programme would not remove the difficulty of obtaining reliable values for the smaller elements of the **L** matrices. The computed intensities are often sensitive to these elements which in turn are sensitive to small, off-diagonal force constants. The frequencies by contrast are insensitive to these terms. This difficulty arises most strongly with the C—H stretching frequencies above 3000 cm<sup>-1</sup>.

In many classes the C—F stretching motion governs the observed intensity and especially its sign and often the usual sign ambiguity is resolved by approximate calculations based on the results for benzene<sup>1</sup> and hexafluorobenzene.<sup>2</sup> These papers suggest dipole gradients of  $-5.0$  D/Å for C—F stretch;  $-0.45$  D/Å for C—H stretch; "effective" moments for C—H in-plane bending 0.31 D and out-of-plane bending 0.61 D with the H atom positive. The in-plane C—F deformation "effective moment" was shown to be 1.6 D which is close to the static dipole. The out-of-plane bending must be governed by a similar moment. The dipole moments produced on ring deformation were neglected in the preliminary, sign-determining calculations.

##### *b*<sub>1u</sub> CLASS OF C<sub>6</sub>H<sub>4</sub>F<sub>2</sub> AND C<sub>6</sub>H<sub>4</sub>F<sub>2</sub> AND C<sub>6</sub>D<sub>4</sub>F<sub>2</sub>

Table 2 shows the observed intensities and the corresponding dipole moment gradients with respect to the normal co-ordinates. Preliminary calculations show that with the **L** matrix signs as in table, 1 all the  $\partial\mu/\partial Q > |0.9|$  must clearly be taken with the positive sign and that the 859 cm<sup>-1</sup> band derivative should be taken as negative for C<sub>6</sub>D<sub>4</sub>F<sub>2</sub>. The C<sub>6</sub>H<sub>4</sub>F<sub>2</sub> band at 1012 cm<sup>-1</sup> is so weak that the sign of its derivative has little effect on derived quantities but the choice of a positive sign improves the agreement with the deuterio-compound. The signs for the C—H and C—D stretches only affect the values of  $\partial\mu/\partial S_{18}$  and both are taken to be negative on the grounds that the contribution of the C—F stretch is of this sign and this gives a more acceptable stretching gradient. Table 3 shows the dipole moment gradients with respect to the symmetry co ordinates obtained by solving the equations for C<sub>6</sub>H<sub>4</sub>F<sub>2</sub>. Also shown in table 2 are the calculated  $\partial\mu/\partial Q$  for C<sub>6</sub>D<sub>4</sub>F<sub>2</sub> using these values. The agreement with the observations is satisfactory.

##### THE *b*<sub>2u</sub> CLASS OF C<sub>6</sub>H<sub>4</sub>F<sub>2</sub> AND C<sub>6</sub>D<sub>4</sub>F<sub>2</sub>

The *b*<sub>2u</sub> class of C<sub>6</sub>H<sub>4</sub>F<sub>2</sub> does not include a C—F stretching motion and all the bands are quite weak. The C—H stretching band is hidden by that of the

TABLE 1.—**L** MATRIX ELEMENTS

		$C_6H_4F$					$C_6D_4F_2$					$C_6H_2F_4$				
$b_{1u}$ class		1543	1286	1028	772	2254	1466	1170	892	709	3076	1475	1284	705	334	
$\nu$		3047	1286	1028	772	2254	1466	1170	892	709	3076	1475	1284	705	334	
S18	1-034	0-071	0-031	0-000	-0-029	0-751	0-121	-0-022	-0-007	-0-023	-0-001	0-328	0-133	0-105	-0-004	
19	-0-064	0-281	0-042	-0-165	-0-113	-0-109	0-286	-0-120	-0-056	-0-069	-0-233	0-252	0-010	-0-044		
20	0-189	-0-003	0-407	0-652	-0-280	0-283	0-134	0-561	0-523	-0-108	0-659	0-319	-0-397	0-057		
21	-0-063	0-852	-0-617	0-314	0-104	-0-114	0-472	-0-305	0-392	-0-063	-0-306	0-414	0-121	0-215		
22	0-021	-0-220	-0-277	-0-032	-0-096	1-040	-0-293	-0-202	0-056	1-036	-0-011	0-041	-0-009	-0-001		
$b_{2u}$ class		1431	2301	1088	307	2282	1342	1285	815	303	1610	1327	1193	855	251	
$\nu$		3074	1431	2301	1088	2282	1342	1285	815	303	1610	1327	1193	855	251	
S23	1-036	-0-033	-0-014	0-018	0-000	0-075	-0-756	-0-047	0-013	0-001	0-255	-0-171	-0-166	0-118	0-000	
24	-0-072	-0-237	-0-239	0-218	0-017	-0-116	-0-146	-0-350	0-095	0-016	-0-204	0-286	-0-169	0-119	0-017	
25	-0-040	-0-160	0-424	0-007	0-030	-0-066	-0-311	0-326	0-016	0-030	-0-231	-0-269	0-260	0-123	0-005	
26	0-044	0-760	0-389	0-626	-0-033	0-081	0-297	0-412	0-602	0-197	-0-197	-0-207	0-190	-0-177	0-226	
27	0-057	0-359	-0-225	-0-161	0-239	0-104	0-441	-0-035	-0-061	0-728	0-534	0-534	0-533	0-271	-0-028	
$b_{3u}$ class		846	499	180		726	420	180		881	477	199				
$\nu$		846	499	180		726	420	180		881	477	199				
S28	1-133	-0-201	0-158			0-848	-0-331	0-154		-0-385	0-536	-0-256				
29	-1-291	0-800	0-370			-0-711	0-815	0-377		1-817	1-140	0-191				
30	-0-546	-0-741	0-143			-0-757	-0-523	0-140		1-260	-0-017	-0-182				

Units (a.m.u.)<sup>-1/2</sup>. For force constants and definition of symmetry coordinates see ref. (7). Frequencies are calculated frequencies in cm<sup>-1</sup>; normalization is made to these frequencies.

TABLE 2

<i>b<sub>1u</sub></i> class C <sub>6</sub> H <sub>4</sub> F <sub>2</sub>					
frequency	3065	1511	1225	1012	737
band area	0.17	10.77	8.35	0.036	2.85
cross-section	0.02	2.38	2.27	0.01	1.29
$\partial\mu/\partial Q$	(-) $0.28$	(+) $2.25$	(+) $1.98$	(+) $0.13$	(+) $1.16$
<i>b<sub>1u</sub></i> class C <sub>6</sub> D <sub>4</sub> F <sub>2</sub>					
frequency	2277	1435	1125-1139	859	685
band area	0.17	14.65	3.86	0.74	1.97
cross-section	0.02	3.40	1.14	0.29	0.96
$\partial\mu/\partial Q$ (obs.)	0.28	2.64	1.35	0.59	0.97
(calc.)	-0.51	+2.66	+1.34	-0.62	+0.91
<i>b<sub>2u</sub></i> class C <sub>6</sub> H <sub>4</sub> F <sub>2</sub>					
frequency	ca. 3074	1437	1285	1085	ca. 350
band area	0.1	0.2	0.052	0.51	—
cross-section	0.01	0.05	0.01	0.16	—
$\partial\mu/\partial Q$ (obs.)	0.22	0.31	0.16	0.49	—
(calc.)	-0.27	-0.15	-0.16	-0.49	+0.50
<i>b<sub>2u</sub></i> class C <sub>6</sub> D <sub>4</sub> F <sub>2</sub>					
frequency	2310	1390 or 1369	1287	802	ca. 303
band area	0.089	ca. 0.3 ca. 0.1	0.02	0.27	—
cross-section	0.01	ca. 0.07 ca. 0.02	0.01	0.11	—
$\partial\mu/\partial Q$ (obs.)	0.21	ca. 0.4 ca. 0.2	0.10	0.36	—
(calc.)	-0.20	+0.11	-0.03	-0.36	+0.50
<i>b<sub>3u</sub></i> class C <sub>6</sub> H <sub>4</sub> F <sub>2</sub>					
frequency	837	506	ca. 186		
band area	3.25	0.64	—		
cross-section	1.29	0.42	—		
$\partial\mu/\partial Q$ (obs.)	(+) $1.24$	(-) $0.55$	—		
(calc.)	—	—	+0.15+0.40 <i>p</i>		
<i>b<sub>3u</sub></i> class C <sub>6</sub> D <sub>4</sub> F <sub>2</sub>					
frequency	732	422	ca. 180		
band area	1.30	0.67	—		
cross-section	0.59	0.53	—		
$\partial\mu/\partial Q$ (obs.)	0.78	0.56	—		
(calc.)	+0.79+0.01 <i>p</i>	-0.63-0.02 <i>p</i>	+0.14+0.40 <i>p</i>		
		( <i>p</i> ~ -1.2 D/Å)			
<i>b<sub>1u</sub></i> class C <sub>6</sub> H <sub>2</sub> F <sub>4</sub>					
frequency	3088	1439	1222	700	ca. 330
band area	0.20	1.84	5.33	1.22	—
cross-section	0.02	0.43	1.46	0.58	—
$\partial\mu/\partial Q$ (obs.)	(-) $0.31$	(-) $0.93$	(-) $1.59$	(-) $0.76$	—
(calc.)	—	—	—	—	+0.19+0.51 <i>q</i>
<i>b<sub>2u</sub></i> class C <sub>6</sub> H <sub>2</sub> F <sub>4</sub>					
frequency	1534	1277	1164	853	ca. 290
band area	19.66	1.22	6.42	3.19	—
cross-section	4.27	0.32	1.84	1.24	—
$\partial\mu/\partial Q$ (obs.)	(-) $3.04$	(+) $0.76$	(+) $1.74$	(-) $1.23$	—
(calc.)	—	—	—	—	+0.01-0.25 <i>s</i>

TABLE 2 (contd.)

<i>b</i> <sub>3u</sub> class C <sub>6</sub> H <sub>2</sub> F <sub>4</sub>			
frequency	869	457	ca. 199
band area	3.80	0.13	—
cross-section	1.46	0.09	—
$\partial\mu/\partial Q$ (obs.)	(+)1.34	(-)0.24	—
(calc.)	—	—	-0.20-0.66 <i>t</i>

Units: frequencies in cm<sup>-1</sup>; band areas 10<sup>-7</sup> cm<sup>2</sup> molecule<sup>-1</sup> sec<sup>-1</sup>; cross-sections 10<sup>-4</sup> Å<sup>2</sup> = 10<sup>-20</sup> cm<sup>2</sup>;  $\partial\mu/\partial Q$  (a.m.u.)<sup>†</sup> D/Å.

*b*<sub>1u</sub> class and the band at 1437 cm<sup>-1</sup> is also confused by combination bands. For C<sub>6</sub>D<sub>4</sub>F<sub>2</sub> the C—D stretch is plain but the third band is too weak to measure and there is some uncertainty whether the second band is at 1369 cm<sup>-1</sup> in view of the very distorted band shape for this absorption. Also there is one missing band in each case below 400 cm<sup>-1</sup>.

TABLE 3.—DIPOLE MOMENT GRADIENTS WITH RESPECT TO SYMMETRY COORDINATES

	C <sub>6</sub> H <sub>4</sub> F <sub>2</sub>	C <sub>4</sub> H <sub>2</sub> F <sub>4</sub>
<i>b</i> <sub>1u</sub> class		
$\partial\mu/\partial S_{18}$	+0.02	-5.92-0.82 <i>q</i>
$\partial\mu/\partial S_{19}$	-0.55	-3.47-2.71 <i>q</i>
$\partial\mu/\partial S_{20}$	-0.60	+0.29+0.25 <i>q</i>
$\partial\mu/\partial S_{21}$	+0.46	+1.73 <i>q</i>
$\partial\mu/\partial S_{22}$	-9.15	-0.51-0.05 <i>q</i>
<i>b</i> <sub>2u</sub> class		
$\partial\mu/\partial S_{23}$	-0.23*	-9.56-0.28 <i>s</i>
$\partial\mu/\partial S_{24}$	+0.63	-0.68-1.08 <i>s</i>
$\partial\mu/\partial S_{25}$	+1.43	+1.36-0.17 <i>s</i>
$\partial\mu/\partial S_{26}$	-0.55	— <i>s</i>
$\partial\mu/\partial S_{27}$	+1.80	-0.59+0.01 <i>s</i>
<i>b</i> <sub>3u</sub> class		
$\partial\mu/\partial S_{28}$	+1.05+0.84 <i>p</i>	-0.16+1.27 <i>t</i>
$\partial\mu/\partial S_{29}$	-0.16+0.58 <i>p</i>	-0.12-0.58 <i>t</i>
$\partial\mu/\partial S_{30}$	+0.29+0.39 <i>p</i>	+1.20+1.23 <i>t</i>

Units D/Å ≡ 10<sup>-10</sup> e.s.u.

\* Figures in this column are of diminished reliability, see text.

There are thus five unknowns, the  $\partial\mu/\partial S$ , to be obtained from four clearly observed bands between the two isotopic species as well as the upper limits of four further bands. A wide variety of solutions are formally possible and given in table 3 is one solution which is reasonably consistent with that to be expected. The calculated  $\partial\mu/\partial Q$  in table 2 refer to these values.

#### *b*<sub>3u</sub> CLASS OF C<sub>6</sub>H<sub>4</sub>F<sub>2</sub> AND C<sub>6</sub>D<sub>4</sub>F<sub>2</sub>

For the out-of-plane *b*<sub>3u</sub> class the nature of the co-ordinates is such that each dipole gradient with respect to a symmetry co-ordinate contains appreciable admixture of C—F deformation. An experimental value of the C—F bending dipole gradient would depend very largely on the intensities of the lowest frequency bands below 200 cm<sup>-1</sup> which were not measured in this work. Consequently it seemed better to treat this quantity as a parameter (symbol *p*) and compute other features in terms of *p*. The expected value of *p* is ca. -1.2 D/Å and together with the expected "effective" moment of the C—H of 0.61 D/Å the signs of the

$\partial\mu/\partial Q$  can be predicted with some certainty. Numerical details are given in tables 2 and 3, where the  $\partial\mu/\partial S$  are exact solutions from the  $C_6H_4F_2$  observations. The predicted intensities of the observed bands of  $C_6D_4F_2$  are almost independent of  $p$  and if this were indeed  $-1.2 D/\text{\AA}$  the agreement is satisfactory. It is not reasonable to compute  $p$  by requiring exact agreement with the  $C_6D_4F_2$  observations since the errors in  $p$  would exceed its value.

#### $b_{1u}$ CLASS OF $C_6H_2F_4$

In this class the C—F stretching motion largely controls the intensities but there is appreciable contribution from the C—F bending dipole gradient. A satisfactory determination of this quantity would involve a measurement of the band expected near  $330\text{ cm}^{-1}$  and this is not available. The dipole gradient has been treated as a parameter (symbol  $q$ ) whose expected value is *ca.*  $-1.2 D/\text{\AA}$ . The numerical details are again shown in tables 2 and 3.

#### $b_{2u}$ CLASS OF $C_6H_2F_4$

In this class too the intensities are largely controlled by the C—F stretch with a contribution from the C—F bend whose dipole gradient may again be taken as a parameter (symbol  $s$ ) whose value is unknown in the absence of intensity measurements for the lowest frequency band. The details are in tables 2 and 3.

#### $b_{3u}$ CLASS OF $C_6H_2F_4$

This class may be treated in a manner analogous to the  $b_{3u}$  class for  $C_6H_4F_2$ . The sign to be taken for the dipole moment derivative with respect to the normal co-ordinate for the  $457\text{ cm}^{-1}$  band is somewhat uncertain inasmuch as the absolute value is so small. The negative sign chosen, as in table 2, is preferred as it gives a C—H bending dipole moment gradient closer to that observed in benzene and  $C_6H_4F_2$ . This leads to the dipole moment gradients with respect to the symmetry co-ordinates of table 3.

## DISCUSSION

It is often difficult to envisage dipole moment gradients with respect to the symmetry co-ordinates and it is customary to convert these to bond co-ordinates which are more easily visualized. For many molecules, including those with closed-ring systems, there are more bond co-ordinates than symmetry co-ordinates since there are relationships between certain bond co-ordinates, e.g. ring angles and sides. This leads to difficulties as to which elements are taken as unchanged in the formation of partial derivatives.

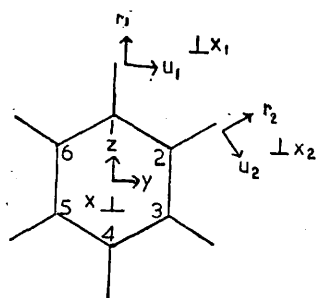


FIG. 1.

$C_6H_4F_2$ , H at 2,3,5,6.

$C_6H_2F_4$ , H at 1,4.

with the mass point.  $\partial\mu_y/\partial r_j$ , etc., are the resultants of  $\partial\mu/\partial r_j$ , etc., along the  $y$  direction. The  $\partial\mu/\partial r_j$  are readily calculated since

$$\partial\mu/\partial r_j = \sum_k (\partial\mu/\partial S_k) (\partial S_k/\partial r_j)$$

and the  $\partial S_k/\partial r_j$  are obtained from the definitions<sup>7</sup> of the  $S$ . These are such that the derivatives with respect to the substituent motions are fairly simple, namely:

$$\begin{aligned}\partial\mu_z/\partial r_1 &= 2^{-\frac{1}{2}}\partial\mu/\partial S_{22}; & \partial\mu_y/\partial u_1 &= -2^{-\frac{1}{2}}\partial\mu/\partial S_{27}; \\ \partial\mu_x/\partial x_1 &= 2\cdot 3^{-\frac{1}{2}}\rho_1^{-1}\partial\mu/\partial S_{29} + 2^{-\frac{1}{2}}\partial\mu/\partial S_{30} \\ \partial\mu_z/\partial r_2 &= 2^{-1}\partial\mu/\partial S_{18}; & \partial\mu_y/\partial r_2 &= 2^{-1}\partial\mu/\partial S_{23}; \\ \partial\mu_z/\partial u_2 &= -2^{-1}\partial\mu/\partial S_{21}; & \partial\mu_y/\partial u_2 &= -2^{-1}\partial\mu/\partial S_{26}; \\ \partial\mu_x/\partial x_2 &= 2^{-1}\partial\mu/\partial S_{28} - 3^{-\frac{1}{2}}\rho_2^{-1}\partial\mu/\partial S_{29},\end{aligned}$$

where  $\rho_1$  is the carbon substituent bond length divided by the ring C—C bond length for a substituent at position 1 and  $\rho_2$  the corresponding value for a substituent at position 2. For a fluorine substituent,  $\rho = 1\cdot 29/1\cdot 40 = 0\cdot 92$  and for hydrogen  $= 1\cdot 07/1\cdot 40 = 0\cdot 76$ .

#### C—F MOMENTS

The C—F bending moments all contribute largely to the intensities of the bands below  $400\text{ cm}^{-1}$  and no reliable values are obtained in this work.  $p$ ,  $q$ ,  $s$  and  $t$  are defined so that they are equal to  $r_{\text{C-F}}^{-1}(\partial\mu/\partial\theta)$ , where  $\theta$  is the angle of distortion of the C—F direction.  $\partial\mu/\partial\theta$  is approximately equal to the C—F dipole of *ca.*  $1\cdot 55\text{ D}$  (cf.  $\partial\mu/\partial\beta = 1\cdot 60$  in  $\text{C}_6\text{F}_6$ ) and since  $r_{\text{C-F}} = 1\cdot 29\text{ \AA}$ ,  $p$ ,  $q$ ,  $s$ ,  $t$  should each be  $-1\cdot 2\text{ D/\AA}$ . From the inaccurate value of  $\partial\mu/\partial S_{27}$  in  $\text{C}_6\text{H}_4\text{F}_2$  the equivalent quantity for this class is  $-1\cdot 3\text{ D/\AA}$ .

The C—F stretching gradients are determined with reasonable precision. For  $\text{C}_6\text{H}_4\text{F}_2$ ,  $\partial\mu_z/\partial r_1 = -6\cdot 5\text{ D/\AA}$ . For  $\text{C}_6\text{H}_2\text{F}_4$ ,  $\partial\mu_z/\partial r_2 = -2\cdot 96 - 0\cdot 41q \sim -2\cdot 47 = -4\cdot 9 \cos 60\text{ D/\AA}$ . Similarly  $\partial\mu_y/\partial r_2 = -4\cdot 78 - 0\cdot 14s \sim -4\cdot 61 = -5\cdot 3 \cos 30$ ,  $\text{D/\AA}$ . The last forms are given since the coefficients of the cosines are the values of  $\partial\mu/\partial r$  parallel to the bond which would give the same resolved moment in the  $z$  and  $y$  directions. These values are almost equal, showing  $\partial\mu/\partial r$  to lie nearly parallel to the bond direction with a value of  $-5\cdot 2\text{ D/\AA}$ . There is slight evidence of a reduction of  $\partial\mu/\partial r$  with increasing number of fluorine atoms present; the values obtained are  $\text{C}_6\text{H}_4\text{F}_2$   $6\cdot 5$ ;  $\text{C}_6\text{H}_2\text{F}_4$   $5\cdot 2$ ;  $\text{C}_6\text{F}_6$   $5\cdot 0\text{ D/\AA}$ . If each of these values is accurate to 10 % the trend would appear to be just significant.

#### C—H MOMENTS

All the C—H dipole moment derivatives are less than one-tenth of the C—F stretching derivative and they are consequently not obtained with much accuracy from classes containing a C—F stretch. The values of the C—H stretching derivative are  $\sim 0\cdot 0$  from the  $b_{1u}$  class of  $\text{C}_6\text{H}_4\text{F}_2$ ;  $\sim -0\cdot 1$  from the  $b_{2u}$  class and  $\sim -0\cdot 3\text{ D/\AA}$  from the  $b_{1u}$  class of  $\text{C}_6\text{H}_2\text{F}_4$  which can be compared with  $-0\cdot 45\text{ D/\AA}$  for benzene itself. These are calculated assuming the moment to lie along the C—H bond in  $\text{C}_6\text{H}_4\text{F}_2$  and are too inaccurate for any conclusion to be drawn on the correctness of this assumption.

Three values can also be obtained for the C—H in-plane bending gradient. Assuming this to be perpendicular to the C—H bond in  $\text{C}_6\text{H}_4\text{F}_2$  the values are  $+0\cdot 27$  from the  $b_{1u}$  class of  $\text{C}_6\text{H}_4\text{F}_2$ ;  $+0\cdot 55$  from the  $b_{2u}$  class; and  $+0\cdot 42\text{ D/\AA}$  from the  $b_{2u}$  class of  $\text{C}_6\text{H}_2\text{F}_4$ . These are consistent in approximate magnitude and in all cases the positive sign is confirmed. The magnitude can be compared with the benzene value<sup>1</sup>  $+0\cdot 31 r_0^{-1} = +0\cdot 29\text{ D/\AA}$ . The quantities quoted are  $\partial\mu/\partial u \equiv r_0^{-1}(\partial\mu/\partial\theta)$ , where  $\theta$  is the angle of twist of the bond.  $\partial\mu/\partial\theta$  is sometimes called the "effective" bond dipole but since the dipole moment is that of the whole molecule this nomenclature can be misleading.

Each of the out-of-plane classes leads to a value of  $\partial\mu/\partial z$  for hydrogen displacement which is surprisingly independent of the value assumed for  $\partial\mu/\partial z$  for

fluorine. The  $C_6H_4F_2$  case gives  $\partial\mu/\partial z = +0.65 - 0.01p \sim +0.66$  and  $C_6H_2F_4$  gives  $+0.66 + 0.01t \sim +0.67$  D/Å. The value found for benzene<sup>1</sup> was  $+0.58$  D/Å. There is thus no evidence for a major change in the C—H bending moment between these molecules.

### CONCLUSIONS

As might have been expected, there do not appear to be any gross changes of dipole moment gradients for hydrogen or fluorine motions along the series  $C_6H_6$ ,  $C_6H_4F_2$ ,  $C_6H_2F_4$ ,  $C_6F_6$ . The results furthermore confirm that the H atom behaves as if it carried a positive charge for both the in-plane and out-of-plane bending motions. Unfortunately, the C—F stretching gradient so dominates the in-plane intensities that this series of molecules is unsuitable for examining the constancy of the hydrogen moment gradients. There is some evidence that the C—F stretching gradient is reduced slightly by progressive fluorine substitution.

We should like to thank Prof. Tatlow and Messrs. Coe and Gething for the samples of  $C_6H_2F_4$  and for checking the purity of other materials and Dr. Majer for the mass-spectroscopic examination of the  $C_6D_4F_2$ . D. S. wishes to acknowledge the receipt of a University Appeal Scholarship.

<sup>1</sup> Spedding and Whiffen, *Proc. Roy. Soc. A*, 1956, **238**, 245.

<sup>2</sup> Steele and Whiffen, *J. Chem. Physics*, 1958, **29**, 1194.

<sup>3</sup> Crawford, *J. Chem. Physics*, 1952, **20**, 977.

<sup>4</sup> Bak, *J. Org. Chem.*, 1956, **21**, 797.

<sup>5</sup> Bak, Shoolery and Williams, *J. Mol. Spect.*, 1958, **2**, 525.

<sup>6</sup> Crawford, *J. Chem. Physics*, 1958, **29**, 1042.

<sup>7</sup> Steele and Whiffen, *Trans. Faraday Soc.*, 1959, 55,

<sup>8</sup> Wilson, Decius and Cross, *Molecular Vibrations* (McGraw Hill, New York, 1955).

## The vibration frequencies of pentafluorobenzene

D. STEELE and D. H. WHIFFEN

The Chemistry Department, The University, Birmingham 15, England

(Received 23 October 1959)

**Abstract**—The infra-red and Raman spectra of pentafluorobenzene and the infra-red spectrum of pentafluorodeuterobenzene have been measured. The values shown in Table 4 have been assigned as fundamental frequencies. A partial reassignment of 1:2:4:5-tetrafluorobenzene is also suggested.

### 1. Introduction

ASSIGNMENTS have been made for a number of fluorinated benzenes [1–5] in the past and now that pentafluorobenzene is readily available [6] a study of its spectra seemed desirable and it has already proved helpful in assigning the hexafluorobenzene spectra [5]. Pentafluorodeuterobenzene was also examined in the infra-red, but there was insufficient material for the determination of its Raman spectrum.

### 2. Experimental

The spectra were observed under conditions similar to those described for hexafluorobenzene [5]. The pentafluorobenzene was prepared [6] by dehydrofluorination of 1:2/4:5-tetrahydro-octafluorocyclohexane (b.p. 118°C) and purified by vapour phase chromatography.

The pentafluorobenzene was converted to pentafluorobromobenzene by the action of Br<sub>2</sub> in concentrated H<sub>2</sub>SO<sub>4</sub>, this was treated with Mg to form the Grignard reagent which was decomposed by D<sub>2</sub>O to form C<sub>6</sub>DF<sub>5</sub>. From the residual strength of the C—H out-of-plane deformation band at 837 cm<sup>-1</sup> it was estimated that the product contained less than 2 per cent of C<sub>6</sub>HF<sub>5</sub>.

The experimental observations are shown in tabular form in Tables 1 and 2. The infra-red spectra are to be published in the D.M.S. collection.

### 3. Assignment

C<sub>6</sub>HF<sub>5</sub> is expected to have a planar structure with C<sub>2v</sub> symmetry for which the *x*-axis is to be taken [7] perpendicular to the plane of the ring. Table 3 gives the relevant information for the basis of an assignment. Both theory [8] and experiment indicate three possible distinct band shapes in the infra-red vapour spectra and for the stronger bands these have provided valuable assistance in

- [1] J. R. NIELSEN, C. LIANG and D. C. SMITH, *Discussions Faraday Soc.* **9**, 177 (1950).  
 [2] E. E. FERGUSON, *J. Chem. Phys.* **21**, 886 (1953).  
 [3] E. E. FERGUSON, R. L. HUDSON, J. R. NIELSON and D. C. SMITH, *J. Chem. Phys.* **21**, 1457 (1953).  
 [4] E. E. FERGUSON, R. L. HUDSON, J. R. NIELSON and D. C. SMITH, *J. Chem. Phys.* **21**, 1464 (1953).  
 [5] D. STEELE and D. H. WHIFFEN, *Trans. Faraday Soc.* **55**, 369 (1959).  
 [6] R. STEPHENS and J. C. TATLOW, *Chem. & Ind. (London)* 821 (1957).  
 [7] R. S. MULLIKEN, *J. Chem. Phys.* **23**, 1997 (1955).  
 [8] R. M. BADGER and L. R. ZUMWALT, *J. Chem. Phys.* **6**, 711 (1938).



the assignment. Since Raman frequencies in this work are liquid state values, frequencies for this state will be quoted throughout the discussion.

#### $a_1$ class

Four frequencies, namely 3105, 1410, 718 and 578  $\text{cm}^{-1}$ , are immediately assigned to the  $a_1$  class on the basis of strong polarized Raman lines, while that at 718  $\text{cm}^{-1}$  is confirmed and 1286, 1075 and 325  $\text{cm}^{-1}$  may be added on the basis of strong infra-red bands with clear type-*B* shapes in the vapour. In most substituted benzene compounds there are two C—C stretching fundamentals near 1600  $\text{cm}^{-1}$  which are prominent in the Raman spectrum though often overlaying each other. The 1648  $\text{cm}^{-1}$  frequency is accordingly assigned in both the  $a_1$  and  $b_2$  classes. Of the frequencies near 1500  $\text{cm}^{-1}$  the lower, 1514  $\text{cm}^{-1}$ , is expected to be the  $a_1$ . Comparison with  $\text{C}_6\text{F}_6$  and its force constant treatment suggests that the three remaining fundamentals are below 550  $\text{cm}^{-1}$ . One is likely to be only slightly above the  $e_{2g}$  frequency of  $\text{C}_6\text{F}_6$  at 443  $\text{cm}^{-1}$  and since the normal mode is only slightly affected by the substitution of H for F, the Raman line will only be slightly polarized. Although observed as a depolarized Raman line the value 470  $\text{cm}^{-1}$  has been assigned to this frequency; 495  $\text{cm}^{-1}$  is a possible alternative value but the Raman line is very much weaker. Finally the weak Raman line at 272  $\text{cm}^{-1}$  is taken to indicate the lowest  $a_1$  fundamental since this is about the expected value.

Except for the highest fundamental, the  $\text{C}_6\text{DF}_5$   $a_1$  frequencies should be almost unchanged and this, together with the *B*-type vapour contours in most cases, makes the assignments of 1638, 1511, 1400, 1277, 1067, 701, 578, 467 and 325  $\text{cm}^{-1}$  almost inescapable. The lowest frequency is likely to be unchanged and the Redlich-Teller product rule may be applied as a guide to the highest frequency. The calculated ratio is 1.41 and the observed 1.43 if 2315  $\text{cm}^{-1}$  is the missing fundamental, whereas if 2215  $\text{cm}^{-1}$  were chosen the unacceptable product ratio 1.49 is obtained or if 2420  $\text{cm}^{-1}$  were chosen the ratio would be 1.36. The 2315  $\text{cm}^{-1}$  is also just the strongest although it would be unsafe to assign it on the grounds of intensity alone.

#### $b_2$ class

Following the argument for the  $a_1$  class the two highest  $b_2$  frequencies must be 1648 and 1540  $\text{cm}^{-1}$  and the arguments for assigning 436  $\text{cm}^{-1}$  as a  $b_2$  frequency have been given previously [5]. Type-*A* contours place the strong infra-red bands at 1182, 953 and 304  $\text{cm}^{-1}$  as  $b_2$  fundamentals. The bands at 1268, 1233 and 1138  $\text{cm}^{-1}$  also have type-*A* contours but only two further fundamentals are expected in this region. The existence of a medium intensity Raman line at 1138  $\text{cm}^{-1}$  supports the assignment of this frequency as a fundamental. Application of the inequality rules [5] suggest that the missing frequency is above the  $\text{C}_6\text{F}_6$  frequency at 1253  $\text{cm}^{-1}$  but below the *p*- $\text{C}_6\text{H}_2\text{F}_4$  frequency of 1277  $\text{cm}^{-1}$  [4]. Accordingly 1268  $\text{cm}^{-1}$  is favoured as the fundamental even though the 1233  $\text{cm}^{-1}$  band appears to be slightly stronger. There is a weak Raman line associated with a fairly strong infra-red absorption at 688  $\text{cm}^{-1}$  which may plausibly be assigned as a  $b_2$  even though overlapping bands make the vapour contour uncertain. This leaves one

Table 1. Infra-red and Raman frequencies of pentafluorobenzene

Infra-red		Raman	Interpretation
Vapour	Liquid		
—	—	171 vw dp	$a_2$ fundamental
—	—	217 w dp	$b_1$ fundamental
—	—	272 w	$a_1$ fundamental
304 A	—		$b_2$ fundamental
329 B	—	325 m dp	$a_1$ fundamental
415	—	391 m dp	$a_2$ fundamental
			$171 + 247 = 418; a_2 \times b_2 = b_1$
	436 w	435 m dp	$b_2$ fundamental
475	469 w	470 m dp?	$a_1$ fundamental
495		495 vw p	$2 \times 247 = 494; 2b_2 = a_1$
		522 w dp	$247 + 272 = 519; b_2 \times a_1 = b_2$
555 C	556 s	557 w dp	$b_1$ fundamental
	580 w	578 s p	$a_1$ fundamental
	599 vvw		$272 + 325 = 597; a_1 \times a_1 = a_1$
	657 vw	662 w p	$2 \times 325 = 650; 2a_1 = a_1$
674 C			$217 + 470 = 687; b_1 \times a_1 = b_1$
688	682 s	688 w dp	$b_2$ fundamental
697 C			$b_1$ fundamental
	710 m		$272 + 436 = 708; a_1 \times b_2 = b_2$
719 B	717 vvs	719 s p	$a_1$ fundamental
741			$272 + 470 = 742; a_1 \times a_1 = a_1$
	793 w	788 w	$325 + 470 = 795; a_1 \times a_1 = a_1$
837 C	838 vvs		$b_1$ fundamental
863			$171 + 697 = 868; a_2 \times b_1 = b_2$
879	879 w		$304 + 578 = 882; b_2 \times a_1 = b_2$
913	912 vw		$436 + 470 = 906; b_2 \times a_1 = b_2$
943 A	941 vs		$391 + 556 = 947; a_2 \times b_1 = b_2$
959 A	953 vvs		$b_2$ fundamental
980 A	980 m		$247 + 718 = 965; b_2 \times a_1 = b_2$
1015	1021 w		$436 + 578 = 1014; b_2 \times a_1 = b_2$
1049 B	1046 m		$470 + 578 = 1048; a_1 \times a_1 = a_1$
1079 B	1075 vvs	1078 vw	$a_1$ fundamental
1105	1100 vw	1112 vw p	$2 \times 556 = 1112; 2b_1 = a_1$
1142 A	1138 s	1139 m dp	$b_2$ fundamental
1178 A	1182 vvs	1189 vvw	$b_2$ fundamental
1228 A	1233 m		$391 + 838 = 1229; a_2 \times b_1 = b_2$
1275 A	1268 m		$b_2$ fundamental
1293 B	1286 s	1288 m dp?	$a_1$ fundamental
1323	1322 w	1317 vw p	$247 + 1075 = 1322; b_2 \times a_1 = b_2$
1352	1342 w		$272 + 1075 = 1347; a_1 \times a_1 = a_1$
1375 B	1370 m		$247 + 1138 = 1385; b_2 \times b_2 = a_1$
1414 B	1413 m	1410 ms p	$a_1$ fundamental
1448	1438 vw		$304 + 1138 = 1442; b_2 \times b_2 = a_1$
1468			$325 + 1138 = 1463; a_1 \times b_2 = b_2$
1492			$304 + 1182 = 1486; b_2 \times b_2 = a_1$
1504	1499 m		$436 + 1075 = 1511; b_2 \times a_1 = b_2$
1512	1514 vvs	1515 w	$a_1$ fundamental

The vibration frequencies of pentafluorobenzene

Table 1 (continued)

Infra-red		Raman	Interpretation	
Vapour	Liquid			
1535	1540 vvs	1648 ms dp	$b_2$ fundamental	
1563	1556 w		$272 + 1286 = 1558; a_1 \times a_1 = a_1$	
1620			$436 + 1182 = 1618; b_2 \times b_2 = a_1$	
1645	1647 vs		$a_1$ and $b_2$ fundamentals	
1656	1660 w		$578 + 1075 = 1653; a_1 \times a_1 = a_1$	
	1673 w		$2 \times 838 = 1676; 2b_1 = a_1$	
1715	1712 m		$578 + 1138 = 1716; a_1 \times b_2 = b_2$	
1754	1750 w		$470 + 1286 = 1756; a_1 \times a_1 = a_1$	
	1782 vw		$272 + 1514 = 1786; a_1 \times a_1 = a_1$	
	1811 vw		$304 + 1514 = 1818; b_2 \times a_1 = b_2$	
1836	1831 w		$325 + 1514 = 1839; a_1 \times a_1 = a_1$	
1855	1846 w		$436 + 1410 = 1846; b_2 \times a_1 = b_2$	
1895	1891 w		$718 + 1182 = 1900; a_1 \times b_2 = b_2$	
1921	1913 vvw		$272 + 1648 = 1920; a_1 \times a_1 = a_1$	
1949	1942 vvw		$436 + 1514 = 1950; b_2 \times a_1 = b_2$	
1989	1978 vw		$718 + 1268 = 1986; a_1 \times a_1 = a_1$	
2012	1998 w		$470 + 1540 = 2010; a_1 \times b_2 = b_2$	
2110	2094 w		$688 + 1410 = 2098; b_2 \times b_2 = b_2$	
2130	2113 w		$578 + 1540 = 2118; a_1 \times b_2 = b_2$	
2165	2146 vw		$2 \times 1075 = 2150; 2a_1 = a_1$	
	2210 vvw		$1075 + 1138 = 2213; a_1 \times b_2 = b_2$	
2225	2226 w		$718 + 1514 = 2232; a_1 \times a_1 = a_1$	
2259	2255 w		$1075 + 1182 = 2257; a_1 \times b_2 = b_2$	
2365	2345 w		$1075 + 1268 = 2343; a_1 \times b_2 = b_2$	
2440	2423 w		$1138 + 1286 = 2424; b_2 \times a_1 = b_2$	
2478	2467 w		$1182 + 1286 = 2468; b_2 \times a_1 = b_2$	
2495	2481 w		$1075 + 1410 = 2485; a_1 \times a_1 = a_1$	
2556	2548 w		$1268 + 1286 = 2554; b_2 \times a_1 = b_2$	
			2568 w	$2 \times 1286 = 2572; a_1 \times a_1 = a_1$
2591	2582 w			$1075 + 1514 = 2589; a_1 \times a_1 = a_1$
2616	2608 vvw			$1075 + 1540 = 2615; a_1 \times b_2 = b_2$
	2650 vvw			$1138 + 1514 = 2652; b_2 \times a_1 = b_2$
2680	2671 w			$1268 + 1410 = 2678; b_2 \times a_2 = b_{21}$
	2795 vvw		$1286 + 1514 = 2800; a_1 \times a_1 = a_1$	
2825	2826 vw		$1182 + 1648 = 2830; b_2 \times a_1$ or $b_2 = b_2$ or $a_1$	
	2875 vvw		—	
2937	2939 w		$1286 + 1648 = 2934; a_1 \times a_1$ or $b_2 = a_1$ or $b_2$	
3026	3023 vw		$2 \times 1514 = 3028; 2a_1 = a_1$	
3058	3065 w		$1410 + 1648 = 3058; a_1 \times a_1$ or $b_2 = a_1$ or $b_2$	
3102	3105 m	3097 w	$a_1$ fundamental	
3180	3184 w		$1540 + 1648 = 3188; b_2 \times a_1$ or $b_2 = b_2$ or $a_1$	
3295	3300 vw		$1648 + 1648 = 3296; a_1 \times b_2 = b_2$	

p = partially polarized, dp = depolarized, w = weak, m = medium, s = strong,  
v = very, A,B,C designate vapour band shapes, see Table 3.

Table 2. Infra-red frequencies of pentafluorodeuterobenzene

Vapour	Liquid	Interpretation
325		$a_1$ fundamental
420	435 m	$b_2$ fundamental
	467 m	$a_1$ fundamental
494 <i>C</i>	494 s	$b_1$ fundamental
	530 w	
	540 w	
	578 m	$a_1$ fundamental
	602 w	
631	625 s	$b_2$ fundamental
679 <i>C</i>	674 vs	$b_1$ fundamental
705 <i>B</i>	701 vs	$a_1$ fundamental
743 <i>C</i>	738 vs	$b_1$ fundamental
	753 m	
	762 w	
	778 w	
	783 w	
815	817 w	
	823 w	
838 <i>C</i>	835 w	$C_6HF_5$
873 <i>A</i>	870 vvs	$b_2$ fundamental
888	885 w	
	929 w	
936 <i>A</i>	938 w	
	942 w	
960	956 w	
	970 w	
1005	1005 vs	
1024 <i>A</i>	1018 vvs	$b_2$ fundamental
1046 <i>B</i>	1046 S	
1075 <i>B</i>	1067 vvs	$a_1$ fundamental
1133	1126 m	
	1146 m	
1157	1155 w	
1174	1175 m	$b_2$ fundamental
1225 <i>C?</i>	1218 w	
1267	1268 w	$b_2$ fundamental
1288 <i>B</i>	1277 vs	$a_1$ fundamental
	1306 vw	
1323 <i>B</i>	1319 w	
	1338 w	
1348	1344 vw	
	1351 vw	
	1372 w	
1383	1383 w	
1405 <i>B</i>	1400 vs	$a_1$ fundamental
1426	1423 w	
	1451 w	
1502	1503 ms	

The vibration frequencies of pentafluorobenzene

Table 2 (continued)

Vapour	Liquid	Interpretation
1515	1511 vs	$a_1$ fundamental
1527	1525 vs	$b_2$ fundamental
1537		
1547	1545 m	
1567		
1588	1579 m	
1608	w	
1644	1638 vs	$a_1$ and $b_2$ fundamentals
1679	1668 w	
1711	1698 m	
	etc.	
	2215 w	
	2270 w	
	2315 m	$a_1$ fundamental
	2420 m	
	etc.	

For explanation of symbols, see footnote to Table 1.

Table 3

Symmetry class	Number of fundamentals	Raman activity	Infra-red band shape
$a_1$	11	p	Type B, double peaks
$a_2$	3	dp	Forbidden
$b_1$	6	dp	Type C, PR sep. 13 $\text{cm}^{-1}$ , prominent Q-branch
$b_2$	10	dp	Type A, PR sep. 8 $\text{cm}^{-1}$ , medium Q-branch

missing fundamental at an even lower value. A value 247  $\text{cm}^{-1}$  is suggested on indirect evidence; it provides an explanation of the weak but undoubtedly polarized Raman line at 495  $\text{cm}^{-1}$  and also a weak infra-red band at 415  $\text{cm}^{-1}$ .

The  $\text{C}_6\text{F}_5\text{D}$   $b_2$  frequencies at 1638, 1525, 1268, 1018, 870, 625 and 435  $\text{cm}^{-1}$  are readily assigned by analogy and that at 1175  $\text{cm}^{-1}$  is the strongest infra-red band in this rather confused region where a fundamental must lie.

$b_1$  class

Strong bands with clear C-contours are at 838 and 556  $\text{cm}^{-1}$  for  $\text{C}_6\text{HF}_5$  and at 738, 674 and 494  $\text{cm}^{-1}$  for  $\text{C}_6\text{DF}_5$ . These figures show that there must be a  $\text{C}_6\text{HF}_5$  frequency slightly above 674  $\text{cm}^{-1}$ . The infra-red spectrum is confused in this region but there are two sharp Q-branches in the vapour at 674 and 697  $\text{cm}^{-1}$

which must belong to type-*C* bands additional to the central absorption at  $688\text{ cm}^{-1}$  attributed to a  $b_2$  fundamental. The higher is taken as the  $b_1$  fundamental since the  $\text{C}_6\text{HF}_5$  frequency is expected to be decidedly above the  $\text{C}_6\text{DF}_5$  figure. The remaining fundamentals are expected to be below  $350\text{ cm}^{-1}$ . The Raman frequency of  $217\text{ cm}^{-1}$  may belong to a fundamental of this class.

#### *a<sub>2</sub> class*

The  $a_2$  class frequencies should resemble the  $e_{1g}$  and  $b_{2g}$  frequencies of  $\text{C}_6\text{F}_6$  since these frequencies are not functions of the mass of substituents at positions 1 and 4. Arguments favouring  $391\text{ cm}^{-1}$  as one such frequency for  $\text{C}_6\text{HF}_5$  have previously been given [5]. The Raman frequency of  $171\text{ cm}^{-1}$  may belong to this class but no value is suggested for the highest frequency which should be about  $600\text{ cm}^{-1}$ . In the absence of a Raman spectrum there is no evidence for  $\text{C}_6\text{DF}_5$  frequencies which should be identical with those of  $\text{C}_6\text{HF}_5$ .

#### *Combination frequencies*

Also given in Table 1 are explanations for many other spectral features in terms of the assigned fundamentals. In some cases more than one explanation is available; the details are presented principally to show that no important feature is without any explanation. With nine unknown fundamentals it is unprofitable to attempt to explain the  $\text{C}_6\text{DF}_5$  combination bands.

### 4. Partial reassignment of 1:2:4:5-tetrafluorobenzene

It is necessary that the  $\text{C}_6\text{HF}_5$  frequencies should be intermediate between corresponding features of the tetrafluorobenzenes and hexafluorobenzene. 1:2:4:5-Tetrafluorobenzene has been fully examined and interpreted by NIELSEN and co-workers [4]. Work by the present writers reported elsewhere [9] on the intensities in the infra-red spectrum of this molecule have confirmed the experimental findings [4], but the earlier interpretation is not wholly consistent with the present work on  $\text{C}_6\text{HF}_5$ .

The  $p\text{-C}_6\text{H}_2\text{F}_4$  molecule is of  $V_h$  symmetry and the fundamentals divide as  $6a_g + 2a_u + 1b_{1g} + 3b_{2g} + 5b_{3g} + 5b_{1u} + 5b_{2u} + 3b_{3u}$  if the recommendation [7] is adopted that the  $z$ -axis passes through the H atoms and the  $x$ -axis be perpendicular to the ring. For direct comparison with reference [4], class subscripts 2 and 3 must be interchanged.

In the  $a_g$  class a frequency near  $1640\text{ cm}^{-1}$  is to be expected as in other benzene derivatives and it seems likely that the Raman line at  $1643\text{ cm}^{-1}$  arises from unresolved  $b_{2g}$  and  $a_g$  fundamentals and that the weak line at  $1335\text{ cm}^{-1}$  is to be attributed as the first overtone of the  $b_{2g}$  fundamental at  $669\text{ cm}^{-1}$ . Likewise it seems better to assign the  $832\text{ cm}^{-1}$  line as  $2 \times 417\text{ cm}^{-1}$  and to seek a low fundamental possibly at  $280\text{ cm}^{-1}$  where there is a weak Raman line. The remaining Raman assignments are satisfactory except that there is some doubt as to whether the lowest  $b_{3g}$  frequency is as low as  $202\text{ cm}^{-1}$ .

In the infra-red active classes it seems likely that there is one  $b_{1u}$  frequency

[9] D. STEELE and D. H. WHIFFEN, *Trans. Faraday Soc.* In press.

The vibration frequencies of pentafluorobenzene

below  $400\text{ cm}^{-1}$ , and if so the frequency  $963\text{ cm}^{-1}$  must be rejected as a fundamental;  $280 + 700 = 980\text{ cm}^{-1}$ ,  $a_g \times b_{1u} = b_{1u}$  provides an alternative explanation. Likewise the  $b_{2u}$  class is likely to have a frequency below  $400\text{ cm}^{-1}$  and the frequency  $755\text{ cm}^{-1}$  may be removed from the list of fundamentals. The infra-red spectra measured from  $400\text{--}150\text{ cm}^{-1}$  for all these highly fluorinated benzenes will be required to settle these points of doubt.

### 5. Comparison with related molecules

To examine the self consistency in the assignment of these molecules, Table 4 lists the fundamentals of  $\text{C}_6\text{HF}_5$  and  $\text{C}_6\text{DF}_5$  along with those of  $p\text{-C}_6\text{H}_2\text{F}_4$  and

Table 4

Symmetry class	$\text{C}_6\text{H}_2\text{F}_4$	$\text{C}_6\text{HF}_5$	$\text{C}_6\text{DF}_5$	$\text{C}_6\text{F}_6$	Symmetry class	$\text{C}_6\text{H}_2\text{F}_4$	$\text{C}_6\text{HF}_5$	$\text{C}_6\text{DF}_5$	$\text{C}_6\text{F}_6$	
$a_1$	3097	3105	2315	1655	$b_1$	871	838	738	714	
	3088	1648	1638	1530		869	697	674	595	
	1643	1514	1511	1490		669	556	494	370	
	1439	1410	1400	1323		461	?	?	249	
	1374	1286	1277	1157		295	217	?	215	
	1222	1075	1067	1011		240?	?	?	175	
	748	718	701	640		$b_2$	1643	1648	1638	1655
	700	578	578	559			1534	1540	1525	1530
	487	470	467	443			1277	1268	1268	1253
	?	325	325	315			1196	1182	1175	1157
280	272	?	264	1164	1138		1018	1011		
				1125	953		870	691		
$a_2$	ca. 600	?	?	595	853	688	625	443		
	417	391	?	370	635	436	435	315		
	140?	171	?	175	?	304	?	264		
					?	247	?	208		

$\text{C}_6\text{F}_6$ . For this purpose the frequencies of the latter molecules have been distributed as if the molecules possessed only  $C_{2v}$  symmetry.

With minor exceptions, which can be attributed to force constant changes, it can be seen that the  $\text{C}_6\text{H}_2\text{F}_4$  frequencies lie above the corresponding  $\text{C}_6\text{HF}_5$  frequencies which lie above the  $\text{C}_6\text{DF}_5$  frequencies which in turn exceed those of  $\text{C}_6\text{F}_6$ . Likewise the rule [5] requiring the  $(j + 1)$ th frequency of the lighter molecule to lie below the  $j$ th frequency of its neighbour is obeyed well. A single exception is the out-of-plane C—H deformation at  $869\text{ cm}^{-1}$  in  $\text{C}_6\text{H}_2\text{F}_4$  which is above the  $\text{C}_6\text{HF}_5$  value of  $838\text{ cm}^{-1}$ . Both assignments rest on clear band contours of very strong infra-red bands and the discrepancy must be attributed to a change of force constant.

*Acknowledgements*—We wish to thank Professor J. C. TATLOW and his colleagues for gifts of material and especially Dr. E. NIELD for assistance with the deuteration. We must thank the British Rayon Research Association for the loan of a Raman spectrometer and Mr. G. R. WILKINSON and Mr. C. SMART for the infra-red measurements below  $400\text{ cm}^{-1}$ . D. S. wishes to acknowledge the receipt of a University Appeal Scholarship.

## Vibrational Spectra of Penta-Deutero-Fluoro-Benzene

D. STEELE,\* E. R. LIPPINCOTT, AND J. XAVIER

Department of Chemistry, University of Maryland, College Park, Maryland

(Received April 11, 1960)

The infrared and Raman spectra of penta-deutero-fluoro-benzene have been measured and a set of assignments for the vibrational fundamentals is proposed. These are shown to be consistent with the present assignments of  $C_6H_5F$ ,  $C_6D_6$ , and  $C_6D_5H$  by application of the product and inequality rules.

### INTRODUCTION

IT HAS been shown that the vibrational spectra of biphenyl can be considered as due to two mono-substituted aromatic rings which vibrate almost independently.<sup>1,2</sup> By considering the mono-substituted group as a point mass the inequality rule of Whiffen and Steele<sup>3</sup> may be applied to the vibrational frequencies of biphenyl and those of any other mono-substituted benzene. This rule, which is an extension of Rayleigh's rule,<sup>4</sup> may be defined as follows. Consider two molecules, RX and RY, the mass of the substituent X being greater than that of the substituent Y. Then in any given symmetry class of RX containing "*a*" modes associated with the RX group the *j*th highest frequency lies between the *j*th and (*j*+*a*)th highest frequencies of the equivalent symmetry class of RY. The application of this rule to biphenyl has proved to be very useful and hence the extension of its use to biphenyl-*d*-10 seemed desirable.  $C_6D_5F$  was chosen as a compound suitable for comparison with the deuterated biphenyl because its moments of inertia are such as should give distinctive type band shapes, and the C-F stretching frequency is close to the inter-ring stretching frequency of biphenyl.

### EXPERIMENTAL

$C_6D_5F$  was prepared by a Friedel Crafts type reaction by bubbling DCl through fluoro-benzene in the presence of aluminum chloride catalyst.<sup>5</sup> The course of the reaction was studied by taking the infrared spectra of samples of the deuterated material. When the C-H stretching band was no longer visible and no further changes were observed to be occurring in the spectrum, the reaction was stopped and the isotopic purity of the product measured by mass spectroscopy. Due to coincidences of the high peaks with the mercury lines near mass number 100, the interpretation could not be made unambiguously, but suggested an isotopic purity

\* National Science Foundation Post-Doctoral Fellow.

<sup>1</sup> J. E. Katon and E. R. Lippincott, *Spectrochim. Acta* No. 9, 627 (1959).

<sup>2</sup> E. R. Lippincott and D. Steele, *J. Mol. Spectroscopy* (to be published).

<sup>3</sup> D. Steele and D. H. Whiffen, *Trans. Faraday Soc.* **55**, 369 (1959).

<sup>4</sup> Lord Rayleigh, *Theory of Sound* (The Macmillan Company, London, 1894), 2nd ed., Vol. 1, p. 110.

<sup>5</sup> B. Bak, J. N. Schoolery, and Y. A. Williams, *J. Mol. Spectroscopy* **2**, 525 (1958).

of about 97%. The very weak infrared absorptions in the C-H stretching region and in the C-H out-of-plane deformation region suggest that the purity is much higher than this.

The infrared spectra were run in the vapor and liquid phases on a Beckmann IR4 and a Perkin Elmer 12C from 5000 to 250  $cm^{-1}$  using LiF, NaCl, and CsBr optics.

Raman spectra and qualitative depolarization data were obtained using a two prism Huet spectrograph (aperture *f*/8) with a dispersion of 18 Å/mm at 4358 Å. Excitation was accomplished with a low-pressure water-cooled Toronto type arc using the 4358 Å Hg line with  $KNO_3$  and rhodamine dye as optical filters for radiations above and below this wavelength, respectively. Standard techniques were employed in the recording and the reading of the spectra. The observed Raman and infrared frequencies are listed in Table I, and the infrared spectra are illustrated in Figs. 1 and 2. For consistency the observed infrared frequencies in the liquid phase will be used throughout the text unless otherwise specified.

### GENERAL DISCUSSION

There is little doubt that  $C_6D_5F$  is planar. The vibrational spectra of most of the fluoro-benzenes have now been studied and no evidence of nonplanarity has been obtained, even for the fully fluorinated molecule.<sup>3</sup> Consequently the symmetry must be taken as  $C_{2v}$ , in which case the fundamental vibrations separate between the symmetry classes as  $11a_1+10b_2+6b_1+3a_2$ . In naming the symmetry classes the recommendations of Mulliken<sup>6</sup> have been followed taking the *x* axis as perpendicular to the plane of the ring and the *z* axis as colinear with the  $C_2$  axis. Using the data of Badger and Zumwalt,<sup>7</sup> the infrared band shapes of the active classes have been calculated taking the bond lengths as  $r_{CF}=1.29$  Å,  $r_{CC}=1.40$  Å, and  $r_{CH}=1.08$  Å. These are given in Table II along with the activities and Raman characteristics of the classes. In several cases in the infrared vapor spectrum, bands belonging to different symmetry classes are overlapping, and the calculated band contours proved very useful in identifying the component bands.

<sup>6</sup> R. Mulliken, *J. Chem. Phys.* **23**, 1997 (1955).

<sup>7</sup> R. M. Badger and L. R. Zumwalt, *J. Chem. Phys.* **6**, 711 (1938).



## 1243 VIBRATIONAL SPECTRA OF PENTA-DEUTERO-FLUORO-BENZENE

TABLE I. Observed vibrational spectra.

Raman	Vapor	Infrared	Liquid	Assignment
229 ms				$b_1$ fundamental
~350 vvw				$a_2$ fundamental
391 vvw			388 ms	$b_2$ fundamental
428 vw	427 C ms		438 s	$b_1$ fundamental
450 vvw				$2 \times 229$
505 m	504 A or B m		505 ms	$a_1$ fundamental
553 w	556 C s		563 s	$b_1$ fundamental
587 m			590 vvw	$b_2$ fundamental
618 m	622 m		627 ms	$b_1$ fundamental
639 m				1311-682
	662 vw		662 w	229+438
	678 A or B vvw			?
687 vvw			682 m	$a_2$ fundamental
721 vvw	717 C vvw			$b_1$ fundamental or 229+505
750 ms(p)	756 A s		753 s	$a_1$ fundamental
767 vw				$2 \times 388$
	808 B? ms		806 m	$b_2$ fundamental
820 ms(p)	818 A? w		817 m	$a_1$ fundamental
849 ms	844 vw		843 w	$b_2$ fundamental
860 ms				$2 \times 438$
885 ms(p)	878 A w		880 w	$a_1$ fundamental
	892 w		892 w	505+388
905 vw	916 C vw		922 w	590+350 or $C_6D_4HF$
956 s(p)	959 A vw		959 w	$a_1$ fundamental
976 w	980 B vvw		981 vvw	627+350
1031 vw	1034 B w		1035 m	$b_2$ fundamental
	1065 B vw		1071 vw	563+505 or 627+438
			1080 vvw	590+505
			1127 vw	$2 \times 563$
	1139 A vw		1139 vw	789+350
1155 m(p)	1163 A vs		1163 vs	$a_1$ fundamental
1186 vw	1201 A m		1193 ms	806+388
1215 vw	1228 A m		1222 ms	388+843 or 664+563
1244 vw			1244 vw	805+438
1283 vw	1281 vvw		1281 vvw	$b_2$ fundamental
			1289 vw	664+627
	1311 B w		1311 m	$b_2$ fundamental
1378 w	1391 A vs		1389 vs	$a_1$ fundamental
			1414 vvw	590+817 or 627+789
	1417 A w		1418 m	1035+388
	1423 w		1424 vw	789+627
1464 vw	1465 A w		1473 w	789+682 or 959+505
	1510 vw			
	1566 B s		1564 s	$b_2$ fundamental
1574 m	1577 A w		1578 vs	$a_1$ fundamental
	1617 A? w		1618 w	$2 \times 806$ or 1035+590 or 817+806
			1639 vw	825+817 or $2 \times 817$ or 843+789
			1660 vvw	1311+350 or 1163+505 or 843+817
	1680 w		1680 w	880+806 or 959+717 or $2 \times 843$
			1685 vvw	
	1729 w		1724 m	1035+682 or 843+880
	1797 C? w		1793 w	1035+753 or 1163+627 or 959+825
			1827 w	505+1311 or 1035+789
	1846 A w		1857 w	806+1035
	1929 w		1913 w	1564+350 or 1035+880
	1995 m		1985 m	1311+682 or 1163+817
2054 vw	2065 vw		2061 w	1281+789 or 1311+753
	2160 w		2140 w	1578+563 or 1311+843 or 1564+590
	2238 B vw			1389+843 or 1281+959
2295 ms(p)	2292 A ms	~2320 ms		$a_1$ fundamental
	2393	~2370		1578+806 or 1564+817 or 1564+806
	2428 A vw			1564+843
	2460 vvw			1578+880 or 1281+1163
	2566 A w	~2550 w		1389+1163 or $2 \times 1281$ (or 1311+1281)
	2584 A vw	~2570 w		
	2680 B vvw	~2680 w		2295+388 or 1389+1281
2750 w	2746 vvw	2750 w		1578+1163 or 3120-438
	2890 w	2890 w		1578+1311 or 2295+590 or 1564+1311
	2922 B vvw			2295+627
	2970 vvw	2950 vw		1389+1564 or 1389+1578 or 2276+682 or 2266+682

TABLE I.—Continued.

Raman	Vapor	Infrared	Liquid	Assignment
3049 w	3080 w	3060 s 3110 w		2276+789 or 2266+806 or 2270+806 2270+843 or 2275+843 or 2295+806 or 2295+817 or 2276+843
	3162 B vw 3256 w 3500 w 3750 vw 3930 vw 4090 vw 4590 m	3270 w 3480 w 3748 vw 3830 vw 4090 vw 4595 m		1578+1564 or 2266+880 2295+959 2295+1163
				2266+1564 or 2276+1564 or 2270+1564 2×2295

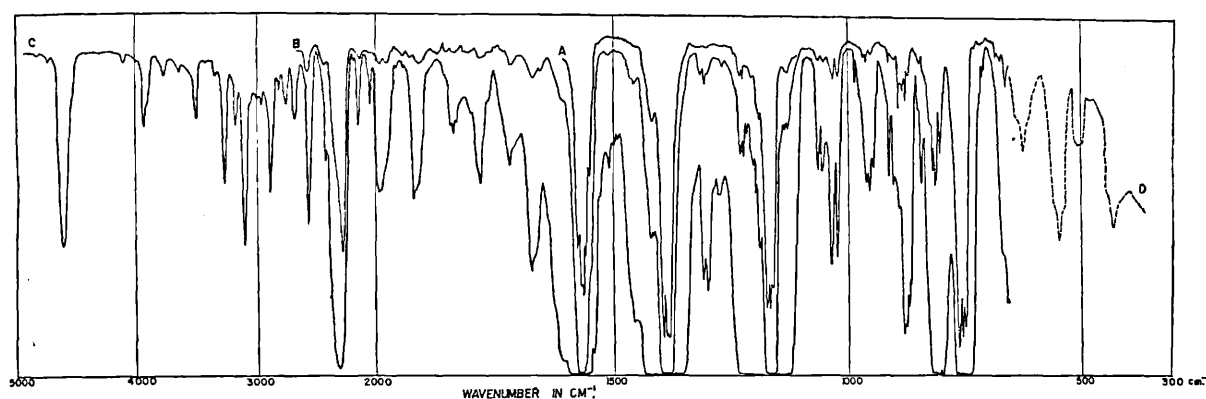


FIG. 1. Vapor phase spectrum of  $C_6D_5F$ . A. 10 cm cell, 2 mm pressure; B. 10 cm cell, 60 mm pressure; C. 1 meter cell, 60 mm pressure; D. 10 cm cell, 60 mm pressure—using CsBr prism.

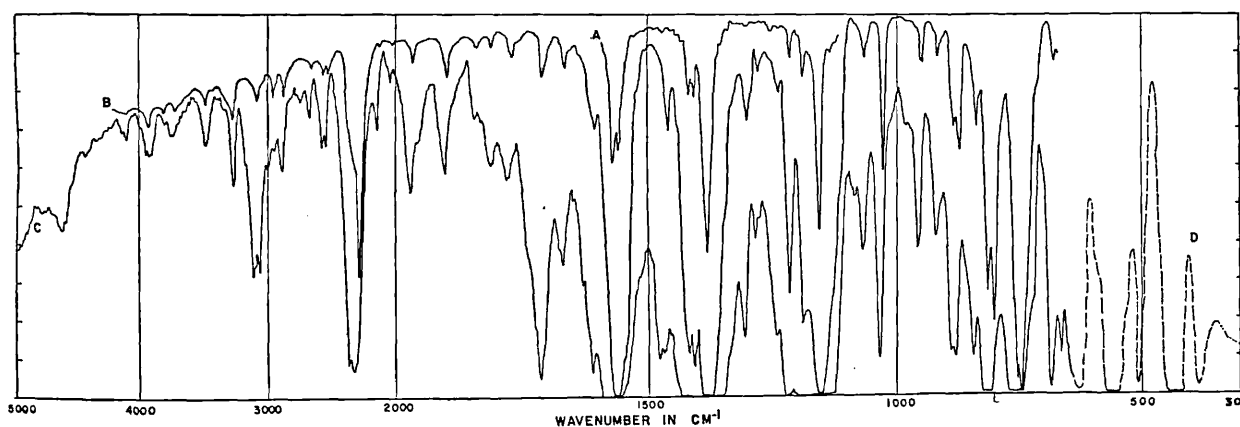


FIG. 2. Liquid phase spectrum of  $C_6D_5F$ . A. Very thin film between salt plates; B. Thin film between salt plates; C. 0.004 cm AgCl cell; D. 0.004 cm AgCl cell—using CsBr prism.

TABLE II.  $C_{2v}$  selection rules.

Symmetry class	Number of fundamentals	Raman activity	Infrared band shapes
$a_1$	11	pol.	Type A PR sep. 13 $cm^{-1}$ medium Q branch
$a_2$	3	dp.	Forbidden
$b_1$	6	dp.	Type C PR sep. 9–10 $cm^{-1}$ prominent Q branch
$b_2$	10	dp.	Type B PR sep. 9 $cm^{-1}$

## IN-PLANE VIBRATIONS

 $a_1$  Class

The vibrations of this class are infrared active vibrations of type  $A$  and give polarized Raman bands. Strong polarized Raman bands at 2295, 1155, 956, 885, 820, and 750  $\text{cm}^{-1}$  and strong type  $A$  infrared bands at 2292, 1577, 1391, 1163, and 756  $\text{cm}^{-1}$  must therefore be identified as  $a_1$  fundamental bands. The weakness of the infrared bands at 959 and 880  $\text{cm}^{-1}$  corresponding to the Raman shifts at 956 and 885  $\text{cm}^{-1}$  is understandable since both are essentially ring modes and are derived from infrared inactive bands of  $\text{C}_6\text{D}_6$  at 970  $\text{cm}^{-1}$  ( $b_{1u}$ ) and 945  $\text{cm}^{-1}$  ( $a_{1g}$ ). (All  $\text{C}_6\text{H}_6$  and  $\text{C}_6\text{D}_6$  frequencies quoted are from the paper by Broderson and Langseth.<sup>8</sup>)

Two of the three C-D stretching bands belonging to this class could not be observed because of band overlapping, but application of the inequality rule to  $\text{C}_6\text{D}_6$  and  $\text{C}_6\text{D}_5\text{F}$  indicates their frequencies to be about 2275 and 2270  $\text{cm}^{-1}$ . The remaining  $a_1$  fundamental is that derived from the  $e_{2g}$  ring deformation mode of  $\text{C}_6\text{D}_6$  at 579  $\text{cm}^{-1}$ . Although the frequency of this mode drops only from 606  $\text{cm}^{-1}$  in  $\text{C}_6\text{H}_6$  to 579  $\text{cm}^{-1}$  in  $\text{C}_6\text{D}_6$  and although there is no CX deformation in the  $a_1$  class, the frequency appears to be very sensitive to the mass of X since in  $\text{C}_6\text{H}_5\text{F}$  it drops to 520  $\text{cm}^{-1}$ .<sup>9,10</sup> The  $\text{C}_6\text{D}_5\text{F}$  fundamental must lie below its  $\text{C}_6\text{H}_5\text{F}$  counterpart and is quite clearly associated with the moderately strong Raman band at 505  $\text{cm}^{-1}$  and the infrared band at the same frequency.

The Redlich-Teller product rule ratio for  $\text{C}_6\text{H}_5\text{F}$  and  $\text{C}_6\text{D}_5\text{F}$  have been evaluated using both the assignments for  $\text{C}_6\text{H}_5\text{F}$  given in footnote 9 and those in footnote 10. The assignments differ only in minor details and both lead to acceptable  $\tau$  values (Table III). Application of the inequality rule to  $\text{C}_6\text{D}_6$ ,  $\text{C}_6\text{D}_5\text{H}_{11}$  and  $\text{C}_6\text{D}_5\text{F}$  (Table IV) indicates consistency between the assignments.

 $b_2$  Class

The only strong infrared band with a type  $B$  contour in the vapor phase is that at 1564  $\text{cm}^{-1}$  which overlaps the  $a_1$  fundamental. All other  $b_2$  bands are surprisingly

TABLE III. Redlich-Teller product ratios.

Symmetry class	Theoretical	Observed $\text{C}_6\text{H}_5\text{F}$ as footnote 9	Observed $\text{C}_6\text{H}_5\text{F}$ as footnote 10
$a_1$	5.52	5.26	5.38
$b_2$	4.97	5.34	5.08
$b_1$	2.49	2.62	2.66
$a_2$	1.82	1.7	1.7

<sup>8</sup> S. Broderson and A. Langseth, Kgl. Danske Videnskab Selskab Mat.-fys. Skr. 1, No. 1 (1956).

<sup>9</sup> D. H. Whiffen, J. Chem. Soc. 1956, 1350.

<sup>10</sup> D. W. Scott *et al.*, J. Am. Chem. Soc. 78, 5457 (1956).

<sup>11</sup> S. Broderson and A. Langseth, Kgl. Danske. Videnskab Selskab Mat.-fys. Skr. 1, No. 7 (1959).

TABLE IV.<sup>a</sup> Comparison of vibrational assignments.

$\text{C}_6\text{D}_5\text{H}$	$\text{C}_6\text{D}_6$	$\text{C}_6\text{D}_5\text{F}$	$\text{C}_6\text{H}_5\text{F}^{10}$	Description of $\text{C}_6\text{D}_5\text{F}$ mode
$a_1$				
3050	2293	2295	3101	CD stretch
2291	2276	(2275)	3067	CD stretch
2275	2275	(2270)	3044	CD stretch
2275	2266	1578	1596	CC stretch
1564	1553	1389	1499	CC stretch
1341	1330	1163	1220	CF stretch
980	970	959	1157	Ring breathing
950	945	880	1022	CC stretch
859	869	817	1008	$\beta$ CD deformation
814	812	753	808	$\beta$ CD deformation
(579)	579	505	519	Ring deformation
$b_2$				
(2288)	2276	(2276)	3091	CD stretch
(2275)	2266	(2266)	3058	CD stretch
1564	1553	1564	1603	CC stretch
1388	1330	1311	1460	CC stretch
1289	1282	1281	1323	CC stretch
1175	1055	1035	1236	$\beta$ CD deformation
984	869	843	1157	$\beta$ CD deformation
840	823	806	1066	$\beta$ CD deformation
815	812	590	614	Ring deformation
584	579	388	405	CF deformation
$b_1$				
928	830	(825)	997	$\gamma$ CD deformation
818	789	717	894	$\gamma$ CD deformation
711	664	627	754	$\gamma$ CD deformation
613	599	563	685	Ring deformation
514	497	438	500	Ring deformation
367	351	229	242	$\gamma$ CF deformation
$a_2$				
(789)	789	(789)	(970)	$\gamma$ CD deformation
664	664	682	826	$\gamma$ CD deformation
(351)	351	350	405	Ring deformation

<sup>a</sup> ( ) estimated;  $\beta$ =in-plane;  $\gamma$ =out-of-plane.

weak. This weakness of the  $b_2$  absorptions compared with the  $a_1$  is due mainly to the symmetry restrictions on the C-F motions. Since the C-F bond lies on the  $C_2$  axis the C-F stretching motion contributes to the intensities of  $a_1$  bands only, and likewise the CF in-plane deformation contributes to the  $b_2$  intensities only. The dipole gradient associated with a C-F stretching motion is about 6.5  $D/A$  whereas the gradient for a C-F bending motion is only about 1.0  $D/A$ .<sup>12</sup> Both of these are in turn much larger than the corresponding carbon carbon and carbon hydrogen terms.<sup>13</sup> Consequently those modes in which there is an appreciable admixture of C-F stretching motion will absorb several times more strongly than the others. Such modes are those which are principally  $a_1$  C-D deformations and C-C and C-F stretching modes. The same arguments apply to the in-plane vibrations of

<sup>12</sup> D. Steele and D. H. Whiffen, Trans. Faraday Soc. 8, 177 (1960).

<sup>13</sup> H. Spedding and D. H. Whiffen, Proc. Roy. Soc. (London) A238, 245 (1956).

$C_6H_5F$  and  $p\cdot C_6H_4F_2$ . A detailed analysis of the vibrations and intensities of the absorption bands of the latter molecule has previously been carried out and confirms the above reasoning.<sup>12,14</sup>

The  $b_2$  band at  $806\text{ cm}^{-1}$  is clearly one of the C–D deformation fundamentals. There is one other C–D deformation in this class and this has been taken to be associated with the very weak  $b_2$  band at  $843\text{ cm}^{-1}$  and the moderately strong Raman line at  $849\text{ cm}^{-1}$ . This assignment is supported by application of the inequality rule which requires, by comparison with  $C_6D_6$  and  $C_6D_5H$ , that the fundamental should lie in the interval  $869 > b_2 > 823\text{ cm}^{-1}$ .

The strongest, as yet unassigned, type  $B$  bands are the weak pair at  $1071$  and  $1035\text{ cm}^{-1}$ , and the very weak band at  $1311\text{ cm}^{-1}$ . The only Raman shifts observed at any of these frequencies was a very weak one at  $1031\text{ cm}^{-1}$ , but the identification of two of the infrared bands with a  $b_2$  ring breathing and the highest of the  $b_2$  C–D deformation modes is supported by a comparison with  $C_6D_6$  and  $C_6D_5H$  which indicates that the frequencies of these ought to be in the intervals  $1330$ – $1289\text{ cm}^{-1}$  and  $1055$ – $984\text{ cm}^{-1}$ . The other component of the low-frequency pair is believed to be a combination band in resonance with the fundamental.

By comparison with other fluoro-benzenes the CF deformation frequency is to be expected between  $300$  and  $450\text{ cm}^{-1}$ . The moderately strong absorption band observed in the liquid at  $388\text{ cm}^{-1}$  must be due to this mode, the only other active mode expected in this region being a  $b_1$  mode which has a definite assignment of  $438\text{ cm}^{-1}$ .

The lowest " $e_{2g}$  like" ring deformation will have a higher frequency than in  $C_6D_6$ , where it is  $579\text{ cm}^{-1}$ , due to the presence of the C–F deformation mode. No  $b_2$  infrared bands are observable in the expected region, but it seems very probable that one of the two Raman lines at  $587$  and  $639\text{ cm}^{-1}$  is due to this mode. The corresponding vibration in  $C_6H_5F$  is at  $615\text{ cm}^{-1}$ , thus indicating that  $587\text{ cm}^{-1}$  is to be preferred as the fundamental frequency.

In the C–D stretching region the only observable type  $B$  band was a very weak one at  $2238\text{ cm}^{-1}$ . This has an alternative explanation and seems too low for one of the fundamentals. It seems very unlikely that the C–D stretching frequencies will differ much from the  $b_2$  type frequencies in  $C_6D_6$ .

The remaining  $b_2$  fundamental to be assigned is a ring stretching mode. Use of the inequality rule indicates that it is derived essentially from the  $b_{2u}$  mode of  $C_6D_6$  at  $1282\text{ cm}^{-1}$ , and its frequency should lie between  $1282\text{ cm}^{-1}$  and  $1175\text{ cm}^{-1}$ . The only absorption above the strong  $a_1$  complex, extending to  $1240\text{ cm}^{-1}$ , is an extremely weak band at  $1281\text{ cm}^{-1}$  which is proposed as the fundamental.

This set of assignments leads to the Redlich-Teller

<sup>14</sup> D. Steele and D. H. Whiffen, *Trans. Faraday Soc.* **8**, 56 (1960).

product ratios given in Table III. The assignments of  $C_6H_5F$  by Scott and others and by Whiffen differ appreciably only in their choice of one C–H in-plane deformation frequency; Scott and his co-workers assigning it a value of  $1236\text{ cm}^{-1}$ , and Whiffen a value of  $1290\text{ cm}^{-1}$ . The former assignment is favored by use of the product rule ratio and the above  $C_6D_5F$  assignments. Though one or two of the proposed assignments are open to some doubt, it is thought that none can be altered by more than a few wave numbers. The weakest assignments are those given as  $843\text{ cm}^{-1}$  and  $1281\text{ cm}^{-1}$ . The former can be no more than  $20\text{ cm}^{-1}$  low and it is difficult to understand how the assignment of the ring frequency could be placed much higher than  $1281\text{ cm}^{-1}$  when the corresponding frequency of  $C_6D_5H$  is only  $1289\text{ cm}^{-1}$ . These considerations lead to the conclusion that the  $a_1$  fundamental of  $C_6H_5F$  is near  $1230\text{ cm}^{-1}$  in agreement with the assignments of Smith<sup>15</sup> and of Scott and their co-workers.

#### OUT-OF-PLANE VIBRATIONS

##### $b_1$ Class

Bands at  $627$ ,  $563$ , and  $438\text{ cm}^{-1}$  can be assigned as fundamentals of this class on the basis of strength and vapor phase contours. The out-of-plane C–F deformation mode must be identified with the moderately strong Raman shift of  $229\text{ cm}^{-1}$ , thus leaving two of the three C–D deformations in this class to be assigned frequencies. According to the inequality rule, the frequencies of these are given by,

$$830 > b_2 > 818\text{ cm}^{-1}$$

and

$$789 > b_2 > 711\text{ cm}^{-1}.$$

No type  $C$  band could be observed within the upper limits, the band almost certainly being under the  $b_2$  and  $a_1$  fundamentals in that region. A frequency of about  $825\text{ cm}^{-1}$  has been assumed for this band. Within the lower limits, only a very weak type  $C$  band at  $717\text{ cm}^{-1}$  is observable. Taking this value for the  $b_1$  fundamental, a  $\tau$  value of  $2.62$  is obtained which is in reasonable agreement with the calculated value.

##### $a_2$ Class

Since the  $G$  matrix for this class is the same for all  $C_6D_5X$  molecules, the vibrational frequencies ought to be the same for  $C_6D_5H$ ,  $C_6D_6$ , and  $C_6D_5F$  assuming that the force constants, excluding the C–X constant, remain the same. A very weak Raman shift of  $350\text{ cm}^{-1}$  can be assigned to the lowest skeletal out-of-plane deformation mode. No Raman shift close to the other  $C_6D_6$   $a_2$  values can unambiguously be assigned to this class. However, in changing from the vapor to the liquid phase an infrared band appears at  $682\text{ cm}^{-1}$ . It

<sup>15</sup> D. C. Smith, E. E. Ferguson, R. L. Hudson, and J. Rud Nielsen, *J. Chem. Phys.* **21**, 1475 (1953).

is almost, if not completely, absent in the vapor spectrum. Since intermolecular interactions can reasonably be expected to have a greater effect on dipole derivative terms such as  $\delta^2 U / \delta^2 Q_i^2$  than on cross terms such as  $\delta^2 U / \delta Q_i \delta Q_j$ ; this is felt to be strong evidence for the assignment of  $682 \text{ cm}^{-1}$  as an  $a_2$  frequency despite the fact that this frequency is appreciably higher than those assigned for  $\text{C}_6\text{D}_6$  and  $\text{C}_6\text{D}_5\text{H}$ . This assignment

is given further support by the observation that the corresponding modes of  $\text{C}_6\text{D}_6$ ,  $\text{C}_6\text{H}_6$ , and  $\text{C}_6\text{H}_5\text{F}$  absorb in the condensed phase although in all cases the vapor selection rules forbid it.

The only Raman band in the region of the highest fundamental is one at  $767 \text{ cm}^{-1}$  which has alternative acceptable explanations. The exact value of the frequency of this mode cannot be given.

## The Crystal and Solution Vibrational Spectra of Biphenyl

D. STEELE\* AND E. R. LIPPINCOTT

*Department of Chemistry, University of Maryland, College Park, Maryland*

The infrared absorption spectra of single crystals of biphenyl, measured with polarized radiation, are here reported. These and the close similarity of the spectra to those of monosubstituted benzenes are used in assigning the vibrational frequencies of biphenyl and deca-deutero-biphenyl on a pseudo  $C_{2v}$  model. The Raman spectrum of crystalline biphenyl has been remeasured and confirms that recorded by Aziz. The crystal spectra are interpreted in terms of the crystal structure and the differences in the interactions between the bonded rings in the solution and crystal phases.

### INTRODUCTION

The vibrational spectra of biphenyl have been the subject of a considerable amount of research,<sup>1</sup> the primary aim being to investigate the structure of the molecule in the liquid and solid phases (1-4). X-ray diffraction studies (5-7) have shown that crystalline biphenyl is planar and has a molecular symmetry of  $D_{2h}$ . On the other hand electron diffraction studies of the vapor (8, 9) indicate that the interplanar angle is  $\sim 45^\circ$  and that the symmetry is consequently  $D_2$ . Aziz measured the Raman spectra of solid and liquid biphenyl (10) and found these to be very similar with respect to both frequencies and intensities.

\* National Science Foundation Post-Doctoral Fellow.

<sup>1</sup> A new set of assignments based on calculations for a  $D_{2h}$  model have appeared while this paper was in press (37). The major discrepancy between the calculated frequencies and those assigned in this work is for the lowest  $a_{1g}$  mode, which is calculated to be at  $286\text{ cm}^{-1}$ . This is very low considering that it is derived from the benzene mode at  $606\text{ cm}^{-1}$ . The remainder of the calculated  $a_{1g}$  frequencies agree well with those assigned here and with those given by Peregudov. In the  $b_{1u}$  class (Mulliken's nomenclature) the major discrepancies between the two sets of assignments are for the lowest two ring modes, which in this case are calculated to be high compared with the expected for mono-substituted benzenes. It seems likely that these discrepancies are due to difficulties in estimating the coupling force constants between the inter-ring stretching coordinate and the ring coordinates. This is probably also the explanation of the remaining major discrepancies which are for the lowest ring modes of the  $b_{2g}$  and  $b_{2u}$  classes.

We observed no features in our work which lead us to believe that the  $C_{12}D_{10}$  used contains appreciable amounts of isotopic impurities, 2 to 3% will naturally be present due to the  $D_2O$  used in the preparation being only 99.8% pure, but it is believed that the resulting weak bands do not affect the assignment presented in any way. At the worst they will have been assigned as inconsequential combination bands.

This has been interpreted as suggesting that the structures of solid and liquid biphenyl were the same. The vibrational spectra have previously been interpreted in terms of a  $D_{2h}$  model in support of this (1, 4). On the other hand Dale has interpreted the spectra of the solution in terms of a  $D_2$  model and observed small changes between the solution and solid spectra which were interpreted in terms of a change from a  $D_2$  to a  $D_{2h}$  structure (3).

Cannon and Sutherland, (11) first pointed out that the infrared spectra of diphenyl and its derivatives were similar to that which would be expected if the rings were vibrating independently. The Raman spectrum of biphenyl has been reported several times (12-16, 2, 4) and that of deca-deutero biphenyl by Landsberg *et al.* (2) and by Katon and Lippincott (4), and both of these groups also reported the infrared spectra.

In view of the confusion on the subject, a reinterpretation of the spectra of biphenyl was undertaken based in part on additional experimental evidence obtained from infrared studies of oriented crystals using polarized radiation.

It was thought to be desirable to remeasure the Raman spectrum of crystalline biphenyl in view of the possibility that Aziz had obtained predominantly a glass by rapid distillation of biphenyl into his sample tube. This has been done by a technique described briefly below.

#### EXPERIMENTAL

Biphenyl (M.P.  $\sim 70^\circ\text{C}$ ), obtained from Eastman Kodak Company, was crystallized slowly from an ethoxyethanol-water solution. This gave large monoclinic plate-like crystals. The spectrum of the crystal, mounted with its ac plane perpendicular to the radiation, was measured with a beam polarized by a Perkin-Elmer unit containing six AgCl sheets. Appreciable displacement of the beam occurred as the polarizer was rotated, but since the relative shifts of the background were quite clear, this presented no problem. Since the energy passing through the crystal and polarizer was small, it was necessary to run the spectra very slowly. Evaporation of the crystal was consequently serious, and was overcome by mounting the crystal between KBr discs. The spectra were measured using polarized radiation over the NaCl region on a Beckmann I.R.4 instrument and using unpolarized radiation over the KBr and LiF regions on a Perkin-Elmer 12C.

The spectra of biphenyl in a KBr disc and in the diamond pressure cell of Weir *et al.* (17) were also measured. The differences between the two spectra were slight and explicable in terms of small molecular orientation effects. That in KBr is similar to that given by Dale (3), but some bands he reports to be missing in the disc spectra were observed weakly. The solution and solidified melt spectra obtained in this work agree well with those given by Katon and Lippincott (4) and by Stewart and Hellmann (18), respectively.

Polarization data on the Raman spectra of  $\text{C}_{12}\text{D}_{10}$  in  $\text{CCl}_4$  were obtained with

polarized incident radiation using Huet's two-prism spectrograph (aperture F/8) with a dispersion of 18 Å/mm at 4358 Å. Excitation was accomplished with a low-pressure water-cooled Toronto arc using the 4358 Å Hg line with a  $\text{KNO}_3$  filter for radiation above this wavelength.

The Raman spectrum of crystalline biphenyl was taken by the following technique. A Raman tube was filled with small crystals of biphenyl, evacuated of all air, and sealed off. By lowering the tube very slowly (about  $1\frac{1}{2}$  inches per 12 hours) through a vertical furnace with a small temperature gradient near the M.P. of biphenyl in its lower region, a crystalline semiluculent sample was obtained. The quality of the Raman spectrum obtainable with this was extremely

TABLE I.  
ABSORPTION FREQUENCIES OF BIPHENYL

Solution Infra-red	Raman	Crystal Infra-red	pol. <sup>a</sup>	Raman	Assignment <sup>b</sup>	( $C_{2v}$ nomenclature)
4628 m		4644 m			1600+3038 ( $a_1b_2$ )	
4588 m		4596 w			3086+1484 ( $a_1b_2$ )	
4552 w		4548 w				
		4517 vw			3038+1484 ( $a_1b_2$ )	3086+1434 ( $a_1b_2$ )
		4482 vw			3052+1434 ( $b_2$ )	
4328 w		4350 w			3052+1275 ( $a_1$ )	3086+1250 ( $a_1b_2$ )
		4083 vw			3086+993 ( $a_1b_2$ )	3086+985 ( $a_2b_1$ )
4045 ms		4051 ms			3052+993 ( $b_1$ )	3052+985 ( $a_2$ )
3993 vw		4013 sh			3086+904 ( $b_1a_2$ )	
		3910 vw			3086+841 ( $a_2b_1$ )	
		3660 w			3052+606 ( $b_2$ )	
		3625 w			3086+543 ( $a_1b_2$ )	
		3470 vw			3086+399 ( $a_2b_1$ )	
	3198 m				2x1600 ( $a_1$ )	
3086 s	3083 w	3088 s			} $a_1$ and $b_2$ fundamentals	
		3076 w				
3067 vw	3052ms	3054 s			} $a_1$ fundamentals	
		3047 s		3055		



TABLE I. (continued)

Solution Infra-red	Raman	Crystal Infra-red	pol. <sup>a</sup>	Raman	Assignment <sup>b</sup> (C <sub>2v</sub> nomenclature)
8 vs	3031 w	3038 s		}	a <sub>1</sub> b <sub>2</sub> fundamentals
	3009 w	3014 s			
		3001 m			1434+1577 (a <sub>1</sub> )
2 s		2984 m			
2 s		2934 s			1434+1484 (b <sub>2</sub> );
2 vw		2874 w			1275+1600 (a <sub>1</sub> );
		2852 w			1577+1275 (b <sub>2</sub> );
3 w					1313+1484 (b <sub>2</sub> );
4 w					1577+1182 (b <sub>2</sub> ); 1275+1484 (b <sub>2</sub> ); 1162+1600 (b <sub>2</sub> )
	2737 w				1434+1313 (a <sub>1</sub> )
		2684 vw			1250+1434 (a <sub>1</sub> )
	2646vw	2638 w			2x1313 a <sub>1</sub>
w		2618 w			1434+1182 (b <sub>2</sub> )
w		2588 w			1600+985(b <sub>1</sub> ); 993+1600(a <sub>1</sub> ); 1577+1012(b <sub>2</sub> ); 1313+1275 (b <sub>2</sub> )
		2571 w			1577+993(b <sub>2</sub> ); 1082+1484(b <sub>2</sub> ); 1600+969(b <sub>1</sub> )
w		2546 w			2x1275(a <sub>1</sub> ); 1577+969 (a <sub>2</sub> )
		2370 w			2x1182 (a <sub>1</sub> )
s		2330 w	⊥		733+1600(a <sub>1</sub> ); 1082+1250 (a <sub>1</sub> )

good, very little scattering being apparent. This technique would seem to be applicable to any material which does not have very anisotropic crystals. The observed frequencies for biphenyl agree very well with those given by Aziz (10) and are given in Table I along with the other observed vibrational frequencies for this compound. The frequencies of C<sub>12</sub>D<sub>10</sub> are given in Table II.

#### INTERPRETATION

The following structures for biphenyl are possible using  $\theta$  as the interplanar angle of the rings (a)  $D_{2d}(\theta = 90^\circ)$  (b)  $D_{2h}(\theta = 0^\circ)$  (c)  $D_2(0 < \theta < 90^\circ)$  (d) Free or nearly free internal rotation-resulting in  $D_{2h}$  selection rules (19). It has

Table I. (continued)					
Solution Infra-Red	Raman	Crystal Infra-red	pol. <sup>a</sup>	Raman	Assignment <sup>b</sup> (C <sub>2v</sub> nomenclature)
2257 m		2270 w	<b>L</b>		993+1275 (a <sub>1</sub> );
2230 w		2240 w			1250+993(b <sub>2</sub> );1275+969(b <sub>1</sub> );985+1250(a <sub>2</sub> )
2201 w					1012+1182(a <sub>1</sub> );1600+606(b <sub>2</sub> )
2148 vw					1313+841(a <sub>2</sub> );1162+985(a <sub>2</sub> )·1182+969(b <sub>1</sub> )
	2086vw				1162+993(b <sub>2</sub> );1250+904(a <sub>2</sub> );543+1600(a <sub>1</sub> )
					1250+841(a <sub>2</sub> );1484+606(b <sub>2</sub> );1600+487(b <sub>1</sub> );
					1182+904(b <sub>1</sub> )
	2018 w				2x1012 (a <sub>1</sub> )
1985-90ms		1987 w			993+985(a <sub>2</sub> );1012+969(b <sub>1</sub> );1250+738(a <sub>2</sub> );
					2x993(a <sub>1</sub> );1250+733(b <sub>2</sub> );1082+904(a <sub>2</sub> )
1961 s		1952 s		}	985+969 (a <sub>1</sub> )
1945 s					
	1937 vw				2x969 (a <sub>1</sub> )
1919 wtn	1923 vw				606+1313(a <sub>1</sub> );1082+841(a <sub>2</sub> );1182+733(a <sub>1</sub> );
					1182+738(b <sub>1</sub> );1012+904(b <sub>2</sub> )
1900 ms					993+904(b <sub>1</sub> );1162+733(b <sub>2</sub> )
1886 s		1877 ms	<b>L</b>	}	969+904(a <sub>1</sub> )
1869 s					

been observed by several investigators that the spectra of biphenyl and substituted biphenyls are consistent with the individual rings absorbing almost independently (3, 4, 11, 18, 20). This suggests that the interaction between the rings is almost negligible. If this were really so, the spectra arising from the above four models would be indistinguishable apart from the spectral activities of the inter-ring deformation. Model (b) might be expected to result in strong coupling between the rings through  $\pi$ -electron overlap and through steric interaction between C—H bonds in the 2,6 and 2',6' positions. Guy (21) has calculated the stabilization energy due to  $\pi$ -electron overlap and has shown that this remains fairly constant over the interval  $-\pi/8 < \theta < \pi/8$  and that the increased stabilization energy for the configuration at  $\theta = 0$  over that at  $\theta = 90^\circ$  is 6.96

## CRYSTAL AND SOLUTION VIBRATIONAL SPECTRA OF BIPHENYL 243

Table I. (continued)

Vibration Intra-Red	Crystal		pol. <sup>a</sup>	Raman	Assignment <sup>b</sup> (C <sub>2v</sub> nomenclature)
	Raman	Infra-red			
2 m		1820 m		}	969+841 (b <sub>2</sub> )
5 ms		1811 w			
10 m				}	841+904 (b <sub>2</sub> )
10 m		1752 ms			
15 wm					969+738 (a <sub>1</sub> )
17 wm		1667 w	⊥		969+695 (a <sub>1</sub> )
18 w	1648 w	1644 vw	⊥		738+904 (a <sub>1</sub> )
19 w		1618 m			606+1012(b <sub>2</sub> ); 1082+543(b <sub>2</sub> ); 140+1484(b <sub>2</sub> )
20 vs	1603vs	1597 w	⊥	1605vs	a <sub>1</sub> fundamental
21 m	1583 w	1570 s		1589vs	b <sub>2</sub> fundamental
22 w		1548 vw			1434+120(a <sub>2</sub> ); 543+993(a <sub>1</sub> )
23 vw			⊥		
	1513 vw				543+969(b <sub>1</sub> ); 606+904(a <sub>2</sub> )
24 vs	1497m p	1481 m	⊥		a <sub>1</sub> fundamental
25 w					2x733(a <sub>1</sub> ); 2x738(a <sub>1</sub> ); 733+738(b <sub>1</sub> )
26 vs	1448 w	1435 vw	S	1459vw <sup>†</sup>	b <sub>2</sub> fundamental
27 m		1386 s	⊥	1391 w	487+904(a <sub>1</sub> ); 985+399(a <sub>1</sub> )
28 w		1357 vw			606+733(b <sub>2</sub> ); 606+738(a <sub>2</sub> )

keal mole<sup>-1</sup>. Howlett (22) has evaluated the difference in the steric interaction energies, allowing for molecular deformations, between the  $\theta = 0$  and  $\theta = 90^\circ$  conformations and obtained a value of 11.27 keal mole<sup>-1</sup>. These results are in accord with the isolated molecule having a  $D_2$  structure (minimum in the energy between  $\theta = 0$  and  $\theta = 90^\circ$ ) or a  $D_{2h}$  structure (no minimum for  $-\pi/4 < \theta < \pi/4$ ). The interaction energies are clearly small and only small frequency shifts may consequently be expected in going from a  $D_{2h}$  to a  $D_2$  structure. Such structural change effects as might occur, would be expected to show mainly in the ring deformations ( $\pi$ -electron effects), the in-plane C—H deformations due to steric interactions, and the inter-ring stretching frequency.

The solution spectra will be discussed first and interpreted in terms of a

Table I. (continued)

Solution Infra-red	Raman	Crystal Infra-red	pol. <sup>a</sup>	Raman	Assignment <sup>b</sup> (C <sub>2v</sub> nomenclature)
1313 w	1316vw	1343 s	S	1326 <sup>†</sup> vw	b <sub>2</sub> fundamental
1290 w		1307 ms	S		985+302 (b <sub>2</sub> )
		1265 m			543+733 (a <sub>1</sub> )
1274 m	1275vsP			1273vs	a <sub>1</sub> fundamental
1250 w	1235vw	1242vw	⊥		841+399 (a <sub>1</sub> )
1182 m	1185mP	1179 w	⊥	1206w	a <sub>1</sub> fundamental
		1168 m	(⊥)90°		b <sub>2</sub> fundamental; 695+487 (a <sub>1</sub> )
1162 m	1151 m	1152 m	0°	1160 m	
	1145 w			1146 <sup>†</sup> vw	606+543(b <sub>2</sub> ); 140+1012(b <sub>2</sub> ); 302+841(a <sub>2</sub> )
1110 w		1108 s			993+120(b <sub>1</sub> ); 140+969(a <sub>2</sub> )
1077 vs	1082vw	1089 vs		1097 <sup>†</sup> vw	b <sub>2</sub> fundamental
1046 s		1078 m			
1034 vw	1032wm	1030 vs			543+487 (b <sub>1</sub> )
1012 vs	1025msP	1038 w	⊥	1032 m	a <sub>1</sub> fundamental
		1019 w			
993 m	996vsP	1005 m	⊥	998vs	a <sub>1</sub> fundamental
985 vw					a <sub>2</sub> fundamental
969 w	970 w	982 w	90°		b <sub>1</sub> fundamental
		966 w	0°		

C<sub>6</sub>H<sub>5</sub>X model, maintaining, however, a distinction between the Raman and infrared frequencies. The Raman and infrared solution frequencies for biphenyl (C<sub>12</sub>H<sub>10</sub>) and deca-deutero-biphenyl (C<sub>12</sub>D<sub>10</sub>) which will be used will be those given by Katon and Lippincott. Small calibration corrections have been applied to infrared bands between 1300 and 1700 cm<sup>-1</sup>.

The crystal spectra will be interpreted in Part 2 in terms of a D<sub>2h</sub> model developed from the C<sub>6</sub>H<sub>5</sub>X model and the effects of increased planarity in the solid state discussed.

The recommendations of Mulliken (23) will be followed in naming the sym-

Table I. (continued)

Solution Infra-red	Raman	Crystal Infra-red	pol. <sup>a</sup>	Raman	Assignment <sup>b</sup> (C <sub>2v</sub> nomenclature)
		942 w			543+399 (a <sub>2</sub> )
919 m					302+606 (a <sub>1</sub> )
904 vs		902 s	0°		b <sub>1</sub> fundamental
881 vw					487+399 (b <sub>2</sub> )
876 vw	879 vw	870 vw			140+733(b <sub>2</sub> );140+738(a <sub>2</sub> )
841 m	834 w	841 w		846 † vw	a <sub>2</sub> fundamental
813 w					120+695 (a <sub>1</sub> )
	802 w				2×399 (a <sub>1</sub> )
778 s	775 w	782 w	⊥	784 w	
738 vw		731 vs	0°		b <sub>1</sub> fundamental
	733 mp			738 w	a <sub>1</sub> fundamental
	719 w				606+120 (a <sub>2</sub> )
	712 w				302+399 (b <sub>1</sub> )
695 vs	696 w	698 vs	0°		b <sub>1</sub> fundamental
670 s					120 543 (b <sub>1</sub> )
	636 vw	630 w			246+399 (b <sub>2</sub> )
	618 w				140+487 (a <sub>2</sub> )
606 s	606 m	610 w		607 w	b <sub>2</sub> fundamental
575 w					

metry classes. That is, for  $D_2$  and  $D_{2h}$  structures the  $X$  axis is chosen as perpendicular to the plane of the ring, and the  $z$  axis as passing through (carbon atoms)  $C_1, C_4 (C_1', C_4')$ .

#### PART I. SOLUTION SPECTRA

##### *a<sub>1</sub>-type motions*

On the basis of strength and polarizations, the Raman bands of C<sub>12</sub>H<sub>10</sub> at 1497, 1275, 1025, and 996 cm<sup>-1</sup>, and of C<sub>12</sub>D<sub>10</sub> at 2290, 1571, 1179, and 955 cm<sup>-1</sup>, are without doubt *a<sub>1</sub>*-type fundamentals. Those at 1275 and 1179 cm<sup>-1</sup> have

Table I. (continued)

Solution Infra-red	Raman	Crystal Infra-red	pol. <sup>a</sup>	Raman	Assignment <sup>b</sup> (C <sub>2v</sub> nomenclature)
543 vs	531 m	550 w			a <sub>1</sub> fundamental
512 m					120+399 (b <sub>2</sub> )
487 vs	470 m	460 m			b <sub>1</sub> fundamental
	430 w				733-302 (b <sub>2</sub> )
	407 w				543-140 (b <sub>2</sub> )
399 m	397 m	398 w			a <sub>2</sub> fundamental
	390 w				696-302 (a <sub>2</sub> )
	349 w				841-487 (b <sub>2</sub> )
	302 m			329 w	b <sub>2</sub> fundamental
	244-252 wb			243 w <sup>†</sup>	b <sub>1</sub> (b <sub>3u</sub> ) fundamental

- a † Observed by Aziz.
- ⊥ Dipole gradient ⊥<sup>r</sup> to ac plane
- S Adsorption for electric vector along  $\theta = 0^\circ$  that  
for electric vector along  $\theta = 90^\circ$
- 0° Adsorption maximum for electric vector along  $\theta = 0^\circ$
- b Infra-red frequencies are quoted where available.

previously been assigned to the inter-ring stretching vibrations (1, 3, 4). Polarized bands of moderate strength at 733 cm<sup>-1</sup> in C<sub>12</sub>H<sub>10</sub> and at 1129, 865, and 690 cm<sup>-1</sup> in C<sub>12</sub>D<sub>10</sub> are suggested as fundamentals. Of these, those at 690 and 865 cm<sup>-1</sup> are readily assigned to in-plane C—D deformations.

The Raman band at 1151 cm<sup>-1</sup> of C<sub>12</sub>H<sub>10</sub> is reported to be polarized, but the crystal studies indicate that a b<sub>2</sub>-type fundamental exists at this frequency and that the a<sub>1</sub>-like C—H deformation is at 1185 cm<sup>-1</sup>. The assignment of the higher frequency to the a<sub>1</sub> mode is in accord with the assignments for C<sub>6</sub>H<sub>5</sub>X molecules given by Randles and Whiffen (24).

In view of the conflict of the reported polarization data with other criteria for making the choice, the polarization spectra of biphenyl in CCl<sub>4</sub> were re-measured. The 1185-cm<sup>-1</sup> band was observed to be slightly polarized and no polarization of the lower frequency band was apparent, thus confirming the assignments suggested by the crystal spectra.

TABLE II.  
 ABSORPTION FREQUENCIES OF  $C_{12}D_{10}$

Infra-red	Raman	Assignment
4454 m		
	3273 w	2287+986 ( $b_2$ )
3245		2287+956 ( $a_1$ ); 2255+986 ( $b_2$ )
3228 m		2276+956 ( $a_1$ )
	3083 w	2255+818 ( $a_1$ )
3052 m		2276+783 ( $b_2$ )
⋮	2974 bw	2276+690 ( $a_1$ )
⋮	⋮	
2307 s	2260-90	C-D Stretching fundamentals
2287 vs		
2276 vs		
2255 s		
2242 m	2244 m sh	
2216 w		1353+863( $a_1$ ); 1269+956( $b_2$ ); 1551+626( $a_2$ )
	2176 w	1353+818( $a_1$ ); 1179+986( $b_2$ )
1818-27 wb		863+956( $a_1$ ); 986+818( $b_2$ ); 1269+553( $a_2$ )
1690 w		863+825( $a_1$ ); ~1555+130( $a_1$ )
1657 vw	1664 vw	2x825( $a_1$ ); 986+818( $a_2$ )

There are three C—H, C—D stretching vibrations of this type. The choices of C—H stretching frequencies are the same as those of Katon and Lippincott. The C—D stretching frequencies have been assumed to be the same in the infrared as in the Raman and have been selected as 2287, 2276, and 2255  $cm^{-1}$  using the criterion that they must be lower than their  $C_6D_6$  counterparts. This latter is based on the sound assumption that the effects of force constant changes are small. All  $C_6D_6$ ,  $C_6D_5H$ , and  $C_6H_6$  frequencies which will be quoted are from Refs. 25 and 26.

The highest C—C stretching frequency is expected in the range 1560 to 1610  $cm^{-1}$  for both molecules. It is necessary to choose between the Raman bands at 1603  $cm^{-1}$  (vs) and 1583  $cm^{-1}$  (vs) for  $C_{12}H_{10}$  and between 1571  $cm^{-1}$  (vs) and

TABLE II. (continued)

Infra-red	Raman	Assignment
1641 vw	1631 w	863+783( $b_2$ ); 783+843( $a_1$ )
1609 w-m		1313+297( $b_2$ )
1578 vs	1571 vs p	$a_1$ fundamental
1555 w-m	1551 m	$b_2$ fundamental
1542 w-m		956+592( $b_2$ )
1528 w	1531 w	843+690( $b_2$ ); 783+746( $a_2$ )
1490 w		1353+137( $b_2$ ); 2x746( $a_1$ )
1448 ms		818+626( $a_1$ )
1420 w	1429 m p	2x705 ( $a_1$ )
1409 m-s		553+863( $b_2$ )
1392 w sh		
1382 s	1370 w } }	626+746( $a_1$ ); 553+825( $a_1$ )
1353 vs		$a_1$ fundamental
1330 m-s	1335 m	863+485 ( $a_1$ )
1326 w sh	1320 m	843+485 ( $b_2$ )
1307 w		553+746 ( $a_1$ )
1290 vw	1296 w	592+705( $b_2$ ); 297+986( $a_1$ )
1269 w-m	1272 m	$b_2$ fundamental

1551  $\text{cm}^{-1}$  (m) for  $\text{C}_{12}\text{D}_{10}$ , the other two bands corresponding to  $b_2$ -type modes. An unambiguous choice can be made by application of the inequality rule to  $\text{C}_6\text{H}_6$  and  $\text{C}_{12}\text{H}_{10}$  and to  $\text{C}_6\text{D}_6$  and  $\text{C}_{12}\text{D}_{10}$ . This rule (27, 28) may be briefly stated as follows: "Consider two molecules  $R-X$ , and  $R-Y$ , the mass of the substituent  $X$  being greater than that of the substituent  $Y$ . Then in any given symmetry class of the molecule  $R-X$  containing ' $a$ ' modes associated with the  $RX$  group, the  $j$ th highest frequency lies between the  $j$ th and  $j+a$ th highest frequencies of the equivalent symmetry class of  $R-Y$ . Where  $R-X$  and  $R-Y$  are of different symmetries the vibrations must be classified according to the highest common symmetry groups." Comparison with  $\text{C}_6\text{H}_6$  and  $\text{C}_6\text{D}_6$  indicates that the  $a_1$  frequencies of  $\text{C}_{12}\text{H}_{10}$  and  $\text{C}_{12}\text{D}_{10}$  must lie above 1595 and above 1553



TABLE II. (continued)

Infra-red	Raman	Assignment
1226 vw	1218 m	746+485 ( $b_1$ )
1204 w-m		346+863 ( $b_1$ )
1182 vw	1179 s p	$a_1$ fundamental
	1151 m	297+863 ( $b_2$ )
1121 w		297+818 ( $b_2$ ); 130+986 ( $a_1$ )
1093 w		$\sim$ 130+956 ( $b_2$ )
	1074 vw	592+485 ( $b_2$ )
1010 w	1013 vw	
998 vw		$\sim$ 130+863 ( $b_2$ )
990 w sh		435+553 ( $a_1$ )
986 s		$b_2$ fundamental
973 vw		746+232 ( $a_1$ )
966 vw	967 m sh	$\sim$ 130+818 ( $b_2$ )
956 w-m	955 s p	} $a_1$ fundamental
952 w-m		
938 vw		825+113 ( $a_1$ ); 592+346 ( $a_2$ )
922 s		} 435+485 ( $b_1$ ); 297+626 ( $a_2$ ); $\sim$ 130+783 ( $a_1$ )
913 s	913 w	

$\text{cm}^{-1}$ , respectively, and that the  $b_2$  frequencies must lie below 1595 and 1553  $\text{cm}^{-1}$ . This clearly suggests 1603 and 1571  $\text{cm}^{-1}$  as the  $a_1$  fundamentals and 1583 and 1551  $\text{cm}^{-1}$  as the  $b_2$ .

The lowest C—C stretching vibration derived from the benzene C—C modes at 1037 ( $a_{1g}$ ), 1010 ( $b_{1g}$ ), and 993  $\text{cm}^{-1}$  ( $a_{1g}$ ) is strongly mass sensitive, dropping for example to 808  $\text{cm}^{-1}$  in  $\text{C}_6\text{H}_5\text{F}$  (29, 30). The presence of a strong mass insensitive, polarized band near 1000  $\text{cm}^{-1}$  as well as a mass sensitive C—C stretching band well below this frequency in mono-, meta-di- and symmetrical tri-substituted benzenes has been explained in terms of a mixing of the modes derived from the symmetrical ( $a_{1g}$ ) and trigonal ( $b_{1g}$ ) ring breathing modes of benzene (24). It is clear from this explanation that the new modes are roughly

TABLE II. (continued)

Infra-red	Raman	Assignment
908 w		
863 m	865 m p	$a_1$ fundamental
843 s	836 m	$b_2$ fundamental
830 m		$\sim 130+705$ ( $b_2$ )
825 s		$b_1$ fundamental
818 vs		$a_1$ fundamental
	790 w	$a_2$ fundamental
783 m	784 m	$b_2$ fundamental
769 vw	775 w	$297+485$ ( $b_2$ )
762 w		$626+130$ ( $a_2$ )
752 m		} $b_1$ fundamental
746 s		
739 w		$626+113$ ( $a_1$ )
717 w		$592+137$ ( $a_1$ )
705 ms	690 m	$a_1$ fundamental
660 m	660 w	$113+553$ ( $a_1$ )
	652 m	$346+297$ ( $b_2$ )

equal admixtures of the symmetrical and trigonal modes, and that consequently these suffixes are no longer applicable to the new modes ( $p$  and  $q$  of Fig. 1, Ref. 2). An estimate of the frequency of the mass sensitive vibration can be made by noting how closely the frequencies assigned agree with the corresponding  $C_6H_5F$  frequencies.<sup>2</sup> The inter-ring stretching frequency of  $C_6H_6 \cdot C_6H_5$  at  $1275 \text{ cm}^{-1}$  is reasonably close to the  $C-F$  stretching frequency of  $1220 \text{ cm}^{-1}$ , and the remaining frequencies are typical of the  $C_6H_5$  group. This then would indicate that the  $a_g$ -type biphenyl frequency is near  $800 \text{ cm}^{-1}$ . On the assumption, which now seems very plausible, that the Raman shifts and absorption bands are explicable in terms of a  $C_{2v}$  like independent ring vibrational model, three reasonable alternatives exist. There is a strong infrared band at  $778 \text{ cm}^{-1}$ , a

<sup>2</sup> See Table III.

TABLE II. (continued)

Infra-red	Raman	Assignment
626 s	646 s	b <sub>1</sub> fundamental
592 vs	593 w	b <sub>2</sub> fundamental
485 ms	500 w	a <sub>1</sub> fundamental
462 vs	474 vw	} 2x232 (a <sub>1</sub> ) or/and b <sub>1</sub> fundamental
435 vs	428 vw	
	393 vw	
	346 w	a <sub>2</sub> fundamental
	297 vw	b <sub>2</sub> fundamental
232-42 m		b <sub>1</sub> fundamental

moderately strong polarized Raman band at  $733\text{ cm}^{-1}$  and a very strong infrared band at  $738\text{ cm}^{-1}$ . The former is the more acceptable by comparison with  $\text{C}_6\text{H}_5\text{F}$  and has been assigned as due to this mode by Dale on the basis of differences between the spectra of a single crystal and a KBr disc of biphenyl. However, it remains to explain the Raman band. The very strong infrared band at  $738\text{ cm}^{-1}$  is certainly a  $b_1 \gamma$  C—H mode corresponding to what is almost invariably the strongest infrared band of monosubstituted benzenes (27). It, therefore, obliterates the  $a_1$  infrared counterpart of the Raman band. If the latter is not a fundamental it must be a first overtone since it is so strong, but no fundamental is expected near  $370\text{ cm}^{-1}$  on the basis of the model adopted.  $738\text{ cm}^{-1}$  is consequently taken as the  $a_1$  fundamental frequency. This agrees with the choice of Katon and Lippincott and with Kovner. It remains for an interpretation of the band at  $778\text{ cm}^{-1}$  to be made. Dale failed to observe it in the crystal spectra. It has been observed in the present work but it is considerably weaker in the un-oriented disc spectrum than in solution. Polarization studies confirm that it is an  $a_1$  band. Its weakness in the spectra of the solid may be due to it being in resonance with the  $a_1$  fundamental. In the solid phase, narrowing of the bands due to suppression of rotational transitions would be expected to weaken the resonance.

The remaining  $a_1$ -type fundamental of the lighter isotopic molecule corresponds to the  $e_{2g}$ -like C—C deformation mode. This mode gives rise to Raman bands of moderate strength in  $\text{C}_6\text{H}_6$  at  $606\text{ cm}^{-1}$ ,  $\text{C}_6\text{D}_6$  at  $579\text{ cm}^{-1}$ ,  $\text{C}_6\text{H}_5\text{F}$  at  $520\text{ cm}^{-1}$ , and in  $\text{C}_{12}\text{D}_{10}$  at  $505\text{ cm}^{-1}$ . This suggests it is to be identified either with the Raman band at  $531$  or that at  $470\text{ cm}^{-1}$  in  $\text{C}_{12}\text{H}_{10}$  and with one of the Raman bands  $539$ ,  $500$ , and  $474\text{ cm}^{-1}$  in  $\text{C}_6\text{D}_5\text{F}$ . Both those of  $\text{C}_{12}\text{H}_{10}$  have very strong

TABLE III.  
 FUNDAMENTAL FREQUENCY ASSIGNMENT FOR  $C_{12}H_{10}$  AND  $C_6H_5F$ 

	Solution		$C_{12}H_{10}$ Crystal		Mode	$C_6H_5F$
	Raman	Infra-red	Raman	Infra-red		
$a_1$ like	3083	3086		3088	CH stretch	3101
	3067	3052		3054	CH stretch	3067
	3031	3038		3038	CH stretch	3044
	1603	1600	1605	1598	CC stretch	1596
	1497	1484	1506 <sup>†</sup>	1481	CC stretch	1499
	1275	-	1273	-	inter-ring stretch	1220
	1185	1182	1206?	1179	$\beta$ C-H def.	1157
	1025	1012	1032	1038	$\beta$ C-H def.	1022
	996	993	998	1005	ring breathing	1008
	733	~ (733)	738		ring breathing	808
	531	543		550	ring def.	519
$b_2$ like	3083	3086		3088or3076	CH stretch	3091
	3031	3038		3038	CH stretch	3035
	1583	1577	1589	1570	CC stretch	1603
	1448	1434	1459 <sup>†</sup>	1435	CC stretch	1460
	1316	1313		1343	CC stretch	1323
	1235	1250		1265	$\beta$ CH def.	1236

infrared counterparts, at 543 and 487  $cm^{-1}$ . In the oriented crystal spectrum the higher frequency band almost disappears whereas the other retains its strength. Consequently the 543- $cm^{-1}$  band is taken as the  $a_1$ -type and the other is assigned as the lowest  $b_1$  out-of-plane ring deformation. Dale has assigned the band at 606  $cm^{-1}$  to the  $a_1$  fundamental and the 543- $cm^{-1}$  band to the lowest  $b_2$  ring deformation. This does not seem plausible in view of the mass sensitivity of the  $a_1$  mode. Furthermore, in view of the fact that the modes changed in going from the parent mononuclear compound to the binuclear compound are as follows:

- ( $a_1$  class) C—H stretch  $\sim$  3100  $cm^{-1}$  to C—C stretch  $\sim$  1275  $cm^{-1}$ ,  
 ( $b_2$  class) C—H deformation  $\sim$  1150  $cm^{-1}$  to C—C def.  $\sim$  300  $cm^{-1}$ ,

it is clear from the inequality rule that the  $a_1$  frequency ought to drop somewhat from its benzene counterpart, whereas the  $b_2$  frequency ought to rise.

TABLE III. (continued)

	Solution		Crystal		Mode	C <sub>6</sub> H <sub>5</sub> F
	b <sub>2</sub> like Raman	Infra-red	C <sub>12</sub> H <sub>10</sub> Raman	Infra-red		
	1151	1162	1160	1168, 1152	β CH def.	1157
			(1164, 1146†)			
	1077	1082	1097 †	1089	β CH def.	1066
	606	606	607	610	ring def.	614
	~ 302	-	~ 329	-	ring ring shearing	} 405
	-	140	-	-	ring ring scissoring	
b <sub>1</sub> like	970	969		982, 966	γ CH def.	997
		904		902	γ CH def.	894
		738		731	γ CH def.	754
	696	695		698	ring def.	685
	470	487		460	ring def.	500
	246	-	250		ring ring shearing	} 242
	-	(120)			ring ring scissoring	
a <sub>2</sub> like	985				γ CH def.	970
	834	841	846 †	841	γ CH def.	826
	397	399			ring def.	405
	-	?	-	?	Int. rotation	-

( ) estimated ; † observed by Aziz [10]

Since the a<sub>1</sub> ring mode frequency of C<sub>12</sub>D<sub>10</sub> must lie below that of C<sub>12</sub>H<sub>10</sub> the choice is between 500 cm<sup>-1</sup> and 474 cm<sup>-1</sup>. The differences between the frequencies of this mode in C<sub>6</sub>H<sub>6</sub> and C<sub>6</sub>D<sub>6</sub> and in C<sub>6</sub>H<sub>5</sub>F and C<sub>6</sub>D<sub>5</sub>F are 27 cm<sup>-1</sup> and 15 cm<sup>-1</sup>, respectively. This indicates 500 cm<sup>-1</sup> is the correct choice in accord with the greater strength of the Raman band of this frequency.

A value has yet to be assigned to one C—D deformation frequency. Comparison with C<sub>6</sub>D<sub>6</sub> and C<sub>6</sub>D<sub>5</sub>F<sup>3</sup> indicates its value to be close to 820 cm<sup>-1</sup>. Also expected in this region are two b<sub>2</sub>-like C—D deformation modes (near 840 cm<sup>-1</sup> and 800 cm<sup>-1</sup>) and a b<sub>1</sub>-like mode (near 825 cm<sup>-1</sup>) each with its infrared and Raman active components, and an a<sub>2</sub>-like Raman band (near 789 cm<sup>-1</sup>). Since neither the

<sup>3</sup>See Table IV.

TABLE IV.  
 FUNDAMENTAL FREQUENCY ASSIGNMENT FOR C<sub>12</sub>D<sub>10</sub> AND C<sub>6</sub>D<sub>5</sub>F

	Solution	C <sub>12</sub> D <sub>10</sub>	Mode	C <sub>6</sub> D <sub>5</sub> F
	Raman	Infra-red		
a <sub>1</sub> like	(2287)	2287	CD stretch	2295
	(2276)	2276	CD stretch	(2275)
	(2255)	2255	CD stretch	(2270)
	1578	1571	CC stretch	1578
	1375	1353	CC stretch	1389
	1179	-	inter ring stretch	1163
	955	956	ring breathing	959
	865	863	β CD def.	880
	(818)	818	β CD def.	817
	690	(705)	ring def.	753
500	485	ring def.	505	
b <sub>2</sub> like	(2276)	2276	CD stretch	(2276)
	(2255)	2255	CD stretch	(2266)
	1551	1551	CC stretch	1564
	1335	1330	CC stretch	1311
	1272	1269	CC stretch	1281

polarization data nor the band shapes guide the choice, a comparison with C<sub>6</sub>D<sub>5</sub>F frequencies (which were used as guide in quoting the above estimated values) and intensities seems to offer the best criterion.

This leads to the following choice:

Assignment	Infrared	Raman
b <sub>2</sub> -like	813 s	838 m
b <sub>1</sub> -like	825 s	?
a <sub>1</sub> -like	818 vs	?
a <sub>2</sub> -like	—	790 w
b <sub>2</sub> -like	783 m	784 m

TABLE IV. (continued)

	Raman	Solution Infra-red	Mode	C <sub>6</sub> D <sub>5</sub> F
like	967	986	$\beta$ CD def.	1035
	838	843	$\beta$ CD def.	843
	784	783	$\beta$ CD def.	806
	593	592	ring def.	590
	297		ring ring shearing	} 388
		~ 130	ring ring scissoring	
like	?	825	$\gamma$ CD def.	(825)
	?	746	$\gamma$ CD def.	717
	646	626	$\gamma$ CD def.	627
	539?	553	ring def.	563
	428	435,462	ring def.	438
	232		ring ring shearing	} 229
		(113)	ring ring scissoring	
like	790	?	$\gamma$ CD def.	(789)
	660	?	$\gamma$ CD def.	682
	346	-	ring def.	} 350
	-	?	Int. rotation	

The C—C mode derived from the  $e_{1g}$  benzene mode at  $1480\text{ cm}^{-1}$  contains appreciable C—H deformation (31) as is evident from its sensitivity to substitution ( $1341\text{ cm}^{-1}$  in C<sub>6</sub>D<sub>5</sub>H,  $1330\text{ cm}^{-1}$  in C<sub>6</sub>D<sub>6</sub>). Due to the inter-ring stretching frequency, however, it ought to lie above the C<sub>6</sub>D<sub>5</sub>H frequency. Katon and Lippincott chose the Raman band at  $1335\text{ cm}^{-1}$  (m) and the infrared band at  $1353\text{ cm}^{-1}$  (vs) as due to this mode. The latter seems unquestionable, but the Raman frequency is somewhat low. The corresponding mode of C<sub>6</sub>D<sub>5</sub>F gives a very strong infrared band and only a weak Raman band. This suggests that the Raman band at  $1370\text{ cm}^{-1}$  is preferable.

Those  $a_1$ -type infrared frequencies which have not been quoted are obvious apart from counterparts of the  $733\text{-cm}^{-1}$  and  $690\text{-cm}^{-1}$  bands which are obscured by out-of-plane fundamentals.

These assignments lead to a satisfactory product ratio for the  $D_{2h}$  model (see Table V). The product ratios for the  $D_2$  models are obtainable from the  $D_{2h}$  by multiplication of the ratios of the  $D_{2h}$  classes that coalesce on reducing the symmetry. Consequently, the assigned frequencies fit equally well the calculated ratios for a  $D_2$  model. Assuming a  $C_6H_6X$  model and applying the inequality rule, the present assignments are seen to be consistent with those of  $C_6H_6$  and  $C_6D_6$ . Even better evidence for the independent ring model comes from a comparison of frequencies and intensities of the assigned bands with the table of characteristic bands of monosubstituted benzenes compiled by Randle and Whiffen (27). This encourages its use in making further assignments.

*b<sub>2</sub>-type assignments*

The  $b_2$ -type C—H and C—D stretching fundamentals have been selected by a comparison with the  $C_6H_6$  and  $C_6D_6$  frequencies.

Of the  $C_6H_6$  group frequencies, two have already been assigned and the remainder are clearly chosen by correlation with the table of Randle and Whiffen.

This leaves only the in-plane ring shearing and the in-plane scissoring vibrations, both of which belong to the  $b_2$ -like group. Katon and Lippincott have assigned these frequencies of 302  $cm^{-1}$  and 140  $cm^{-1}$ , respectively, for  $C_{12}H_{10}$  and 297  $cm^{-1}$  and 137  $cm^{-1}$  for  $C_{12}D_{10}$ .

Four  $b_2$  assignments remain for  $C_{12}D_{10}$ . The strong infrared band at 986  $cm^{-1}$  and the Raman shift of 967  $cm^{-1}$  are readily assigned to the highest in-plane C—D deformation mode derived from the  $a_{2g}$  mode of  $C_6D_6$  1037  $cm^{-1}$ . The other three assignments are chosen by comparison with the spectra of  $C_6D_6F$  (32) as 1335, 1272, and 593  $cm^{-1}$ .

TABLE V.  
REDLICH TELLER PRODUCT RATIOS

	$D_{2h}$ Model	
	obs.	theor.
$a_g$	.173	0.177
$b_{1u}$	.1766	0.182
$b_{2u}$	~ .191	0.182
$b_{3g}$	.191	0.187
$a_u$	< .531	.500
$b_{1g}$	.543	0.549
$b_{3u}$	.398	0.365
$b_{2g}$		0.372



Applying the product rule to the above assignments, assuming a  $D_{2h}$  model, leads to a satisfactory ratio for the  $b_{3u}$  class, but to a slightly high ratio for the  $b_{2u}$  class. This suggests that the  $C_{12}D_{10}$  scissoring frequency is nearer  $130\text{ cm}^{-1}$ .

*b<sub>1</sub>-like assignments*

Very strong infrared bands in the spectra of  $C_{12}H_{10}$  at  $904\text{ cm}^{-1}$  and  $738\text{ cm}^{-1}$  are readily assigned as out-of-plane C—H deformations and those at  $695\text{ cm}^{-1}$  and  $487\text{ cm}^{-1}$  are clearly the two ring deformations. The highest C—D deformation has already been assigned as  $825\text{ cm}^{-1}$ , and on the basis of intensities, the remaining two are identified with the infrared bands at  $746\text{ cm}^{-1}$  and  $626\text{ cm}^{-1}$ . These correlate well with the fundamentals of  $C_6D_5F$ . The highest ring deformation is identified with the very strong infrared band at  $553\text{ cm}^{-1}$ , and the lower with one of the strong pair of bands at  $435$  and  $462\text{ cm}^{-1}$ . Since only one fundamental is expected in the region of the latter two bands, it is necessary to assume Fermi resonance of the fundamental with a  $b_1$ -like combination band. Such a low-lying combination band must arise from inter-ring deformation modes.

The highest  $\gamma$  C—H vibration frequency is expected to be about  $980\text{ cm}^{-1}$  by comparison with  $C_6H_5F$ . This mode usually gives rise to quite weak absorption in contrast to the lower frequency  $\gamma$  CH modes of this class. Only weak absorption is observed in the expected region. As pointed out by Whiffen (33), the intense combination bands of substituted benzenes, between  $2000$  and  $1500\text{ cm}^{-1}$ , arise from transitions involving the out-of-plane C—H deformation modes, and these can be used in determining the frequencies of the inactive and weakly absorbing fundamental vibrations. The crystal studies indicate that the three lowest of the strong combination bands, that is those at about  $1590$ ,  $1656$ ,  $1703$ , and  $1880\text{ cm}^{-1}$  are  $a_1$ -type modes, whereas those at  $1952$ ,  $1812$ , and  $1751\text{ cm}^{-1}$  are  $b_2$ . The corresponding frequencies in the solution spectra are very close to these, though it is clear with the better resolution available that most of the bands are double. This doubling clearly arises from weak coupling between the vibrations of the two rings leading to a splitting of the  $C_{2v}$  model frequencies. It can be readily seen from symmetry considerations that such coupling for any model with a centre of symmetry leads to an inherent doubling of all combination bands. Due to Fermi resonance between the components, it is to be expected that where the coupling is appreciable, splitting of combination bands will be observed. All the observed strong combination bands in the range  $2000$ – $1500\text{ cm}^{-1}$  are readily explained using the frequencies  $b_1$ -like ca.  $975$ ,  $904$ ,  $738$ ,  $695\text{ cm}^{-1}$ ;  $a_2$ -like *c.*  $975$ , *c.*  $840\text{ cm}^{-1}$ .

The lowest fundamentals of this class are the ring-ring shearing and the out-of-plane scissoring modes. These have been assigned as by Katon and Lippincott.

*a<sub>2</sub>-type vibrations*

The frequencies of these modes ought to be very close to those of the corresponding benzene modes. For a  $C_{2v}$  model, these bands are Raman active only, though in the liquid phase they usually absorb infrared radiation with appreciable

strength due to relaxation of the selection rules. As indicated above, the study of combination bands leads to frequencies of about 975 and 840  $\text{cm}^{-1}$  for the  $\gamma$  C—H modes. These assignments are in agreement with the assignments of Katon and Lippincott Bands at 397  $\text{cm}^{-1}$  (Raman) and 399  $\text{cm}^{-1}$  (infrared) are satisfactorily assigned as arising from the  $a_2$  like ring deformation. The corresponding  $\text{C}_{12}\text{D}_{10}$  frequencies have been chosen by comparison with  $\text{C}_6\text{D}_6$  and  $\text{C}_6\text{D}_5\text{F}$ .

#### PAIR 2. CRYSTAL SPECTRA

The crystal symmetry is  $P_{21}/b$ , thus the molecular site symmetry is  $C_1$  ( $\bar{5}$ ). This lowering of the symmetry from that of the isolated molecule leads to the formal coalescing of all the  $g$  and of all the  $u$  classes of the isolated  $D_{2h}$  molecule. As has been shown by many previous crystal studies, however, (for example, Ref. 34), the selection rules and frequencies may be taken, as a first approximation, to be those of the isolated molecule, and the relaxation of the selection rules and the frequency shifts considered subsequently as the consequence of small perturbation forces. The intensities, in the same approximation, can be taken as those of the isolated gas molecule corrected for orientation of the molecules and the change of dielectric constant in passing from the gas to crystal phases. The latter correction is given by (35)

$$\frac{I_i}{I_0} = \frac{1}{n} \left( \frac{n^2 + 2}{3} \right)^2.$$

On the basis of the above model, any large differences between the spectra of the crystal and the vapor after allowing for molecular orientation must be explained by strong crystal interactions or structural changes. Hornig (36) has shown that the potential function for a crystal may be written as  $V = V_L + \sum_i (V_j^0 + V_j') + \sum_i \sum_k V_{jk}'' + V_{ii}''$ , where  $V_L$  is the lattice potential,  $V_j^0$  is the potential of the free molecule,  $V_j'$  is the perturbation due to the crystal field,  $V_{jk}''$  is the interaction potential between different molecules and  $V_{ii}''$  is the interaction of the internal modes with the lattice vibrations.  $V_j'$  leads to frequency shifts and  $V_{jk}''$  to coupling of the vibrations and to changes in the direction of the transition moment. Assuming that the coupling term is small, no splitting of the bands should result from the presence of two molecules per unit cell, and the dichroic ratios can be evaluated easily from a knowledge of the crystal structure.

According to Dahr (5), the molecules are aligned with their  $Z$  axes parallel to the  $b$  axis of the crystal. The unit cell contains two molecules, the planes of the rings of the two being inclined at about  $64^\circ$ . For noninterference of radiation from the various parts of the crystal, the vibrations of the unit cells must be in phase. That is, the phase difference between adjacent cells must be  $2\pi n$  where  $n$  is an integer. The two molecules in the unit cell may vibrate in-phase or out-of-phase. For the  $a_1$  vibrations the out-of-phase results in no resultant dipole

change, but the out-of-phase  $b_1$ - and  $b_2$ -type vibrations result in a net dipole change at  $90^\circ$  to the in-phase change. If the coupling potential  $V''$  is sufficiently strong, this will result in two bands with electric vectors exactly at  $90^\circ$  to one another. If the peak separation is insufficient to resolve the bands, the overall dichroism will depend on the relative strengths of the two components. For very weak coupling, the strengths will be equal and the electric vector ellipsoid will degenerate to a circle.<sup>4</sup>

#### Band Assignments

The  $C_{2v}$  fundamental modes of the  $C_6H_5$  radical each give rise in crystalline  $C_{12}H_{10}$  ( $D_{2h}$  symmetry) ( $\bar{5}$ ) to two modes; a "g" and a "u" mode. Since all g modes are infrared inactive and all u modes are Raman inactive, no ambiguity is likely to arise in referring to the vibrations in terms of the  $C_{2v}$  classes from which they are derived. To facilitate comparison with the solution and  $C_6H_5X$  frequencies, the  $C_{2v}$ -type nomenclature will be retained. The  $D_{2h}$  and  $C_{2v}$  fundamentals are related as follows:

$$\begin{array}{l} C_{2v} \quad a_1 \rightarrow a_g + b_{1u} \quad D_{2h} \\ \quad \quad b_2 \rightarrow b_{2u} + b_{3g} \\ \quad \quad a_2 \rightarrow a_u + b_{1g} \\ \quad \quad b_1 \rightarrow b_{2g} + b_{3u} \end{array}$$

Taking into account the inter-ring deformations, the  $D_{2h}$  fundamentals separate as  $11a_g + 10b_{1u} + 10b_{2u} + 10b_{3g} + 4a_u + 3b_{2g} + 6b_{2g} + 6b_{3u}$ .

Since the molecules are aligned with their  $Z$  axes perpendicular to the  $ac$  plane of the crystal, the much smaller absorption intensity of infrared bands at 1700, 1644, 1567, 1520, 1481, 1386, 1238, 1179, 1038, and  $1003 \text{ cm}^{-1}$  in the crystal as compared with their counterparts in the pellet spectra, indicate that they arise from  $a_1$ -type vibrations. Also a band at  $1168 \text{ cm}^{-1}$  would appear to have considerable  $a_1$  character. A polarization study indicates that the electric vectors of the weak residual bands at 1386, 1179, and  $1003 \text{ cm}^{-1}$  were in the same direction, being a maximum when the vector was parallel to an arbitrarily chosen edge of the crystal and a minimum at  $90^\circ$  to this direction. (The angle of the electric vector in the  $ac$  plane of the crystal,  $\theta$ , will be defined with respect to this edge.) The band at  $1481 \text{ cm}^{-1}$  gained intensity in moving the electric vector from  $0$  to  $90^\circ$  indicating the presence of another band type. The other residual bands were too weak to observe in the crystal.

<sup>4</sup> Since communication of this paper, it has come to the notice of the authors that the spectrum of crystalline polyethylene, which also contains two molecules (infinite chains) per unit cell, has been interpreted in a similar manner.<sup>38</sup> Thus, two perpendicular bands namely a deformation mode at  $1460 \text{ cm}^{-1}$  and a wagging mode at  $725 \text{ cm}^{-1}$ , split into two components  $90^\circ$  out of phase with one another. Polarization and deuteration studies and the replacement of the doublets by single bands on melting have confirmed that the two components arise from interactions between the chains in the two crystallographically different sites.

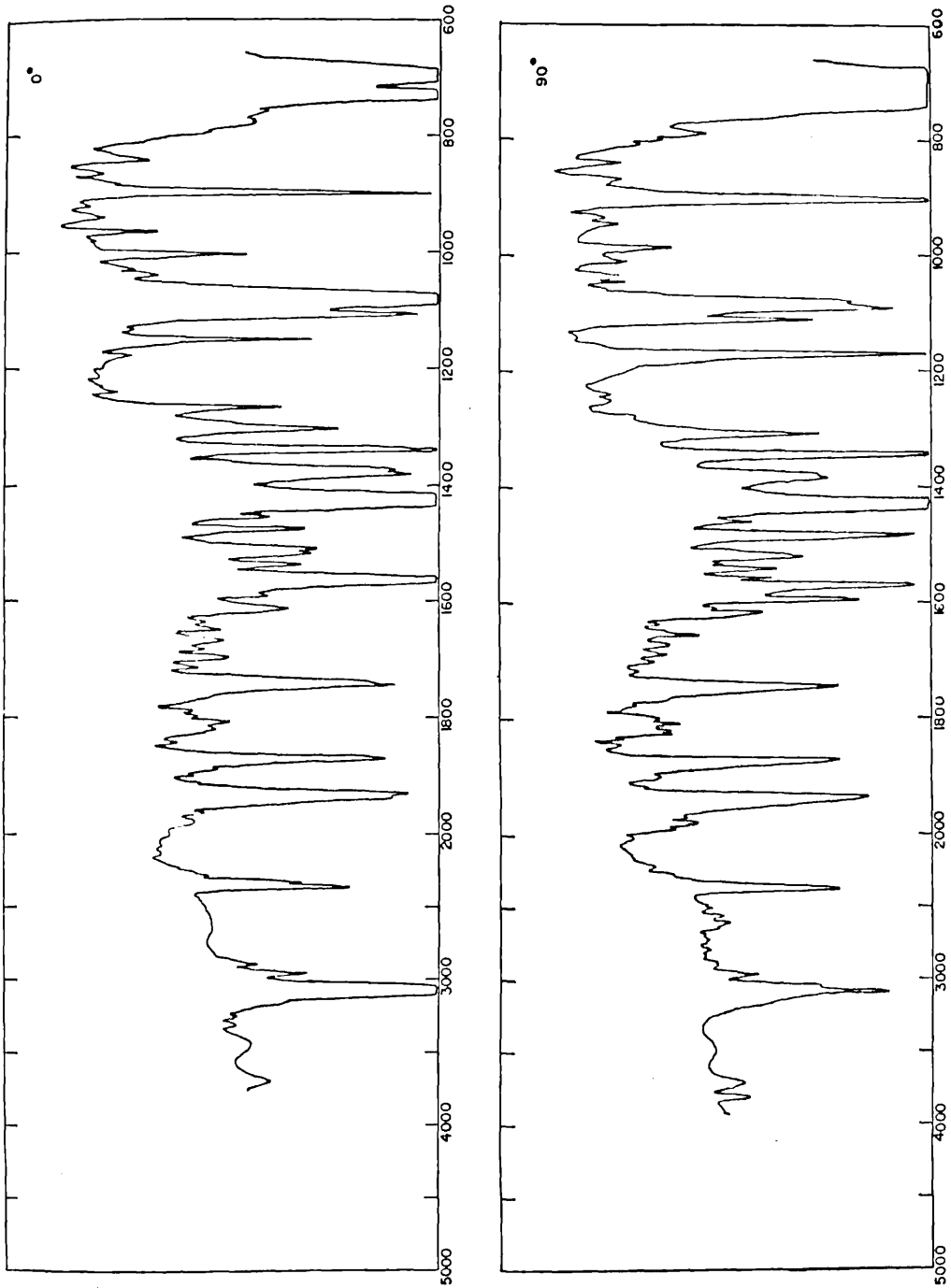


Fig. 1. Polarized infrared spectra of crystalline biphenyl. Top, curve  $\theta = 0^\circ$ . Bottom, curve  $\theta = 90^\circ$ .

The out-of-plane bands at 698, 731 and 902  $\text{cm}^{-1}$  retain the same strengths relative to the  $b_1$  bands in passing from the disc to crystal spectra, as is to be expected from the molecular alignment. The intensities of these bands show a strong dependence on the direction of the electric vectors indicating a preferred phase relationship. Since these bands are so strong, it was not possible to measure their intensities, but the half height widths, for various incident vectors given in Table VI, show clearly the marked nature of this preferred coupling.

One of the  $b_2$  C—C stretches is clearly associated with the very strong band at 1435  $\text{cm}^{-1}$ , and the lowest C—C stretch with one of the two bands at 1307 and 1343  $\text{cm}^{-1}$ . That at 1343  $\text{cm}^{-1}$  is considerably stronger than that at 1307 and is therefore taken as the fundamental. All of these bands are characterized by an independence of the direction of the incident electric vector showing that the degree of coupling is weak for the associated vibrations.

The above pattern of behavior for the different symmetry classes allows most of the observed crystal bands to be assigned. There are, however, two pairs of bands at 982 and 966  $\text{cm}^{-1}$  and at 1168 and 1152  $\text{cm}^{-1}$  which are not classified by the above behavior. None of these are  $a_1$ -type, but they all show very high dichroic ratios, the bands at 1152 and 966  $\text{cm}^{-1}$  having maximum intensity for  $\theta = 0$  and practically zero intensity at  $\theta = 90^\circ$ . The other two bands have electric displacement vectors  $90^\circ$  out-of-phase with these. The maximum intensities of the 982 and 966  $\text{cm}^{-1}$  bands were in the ratio 1.48:1. The intensities of the other pair were too strong to measure, but the 1168- $\text{cm}^{-1}$  band at  $\theta = 90^\circ$  appeared at least three times as strong as the 1152- $\text{cm}^{-1}$  band at  $\theta = 0$ . However, as previously indicated, the 1168- $\text{cm}^{-1}$  band is apparently complex and contains  $a_1$  absorption. These ratios suggest that the bands arise from a strong splitting of the in-phase and out-of-phase components of a  $b_{3u}$  or  $b_{2u}$  vibration. The higher

TABLE VI.

VARIATION OF THE HALF HEIGHT WIDTH OF 902  $\text{cm}^{-1}$  BAND  
WITH THE ANGLE OF THE INCIDENT ELECTRIC VECTOR.

$\theta$	$\Delta\nu \frac{1}{2}$
+90°	20 $\text{cm}^{-1}$
+60°	24 $\text{cm}^{-1}$
+30°	29 $\text{cm}^{-1}$
0°	29 $\text{cm}^{-1}$
-30°	26 $\text{cm}^{-1}$
-60°	21 $\text{cm}^{-1}$

pair are readily assigned to the  $b_{2u}$   $\beta$  C—H deformation. The lower pair cannot be assigned with as much certainty. Two fundamentals—a  $b_2$  and an  $a_u$  (forbidden for  $D_{2h}$  symmetry)—are expected in this region. The closeness of the ratio of the maximum intensities to that expected for an equal mixture of in-phase and out-of-phase motions distinguishes the band in question from the previously assigned  $b_{3u}$  ( $b_1$ -like) bands. However, it is tentatively assigned to the highest of the  $b_1$ -like  $\gamma$  C—H vibrations. The position of the fundamental is very unlikely to be far from this frequency.

The relative intensities of the bands at about 1600 and at about 1580  $\text{cm}^{-1}$  differ considerably in the solution and disc spectra. This in part arises from a partial alignment of the molecules in the disc, as is evidenced by the general increase of the  $b_2$ -type intensities relative to the  $a_1$ . Nevertheless, it would seem that the lower frequency band has gained considerable intensity at the expense of the higher frequency band. There is some indication of a band of  $a_1$  character superimposed on the lower frequency band which has probably taken some of the intensity from the  $a_1$  fundamental.

The corresponding Raman bands are observed at 1605 and 1589  $\text{cm}^{-1}$ . The difference between the Raman and infrared frequencies of these two fundamentals is slightly greater for the crystal than for the solution, indicating a slightly increased interaction between the rings. However, the mean frequencies remain the same indicating that there is very little increase in the  $\pi$ -electron contribution to the bonding. This is in accord with Guy's calculations (21) which indicated that the stabilization energy due to  $\pi$ -electron overlap remains fairly constant for angles between the ring planes of  $+\pi/8$  to  $-\pi/8$ . The ring breathing mode must contain appreciable C—H deformation due to the proximity of its frequency to that of the highest  $a_1$ -like  $\beta$  C—H mode. The small rise in frequency of this mode in the crystal is understandable in terms of increased C—H interaction. The other vibrations which might be expected to be sensitive to the  $\pi$ -electron density are the inter-ring stretching frequency and the out-of-plane ring deformation ( $b_1$ -type). The inter-ring stretching frequency observed in the Raman spectrum is the same within experimental error in solution and the crystal. This is surprising in view of the shortening of the ring-ring bond in the crystal (1.48 Å (10)) as compared with the vapor (1.54 Å (8, 9)). This implies either that the bond length in the liquid phase is near to that of the crystal, or that the inter-ring C—H interactions reduce the restoring force for this vibration sufficiently to counteract the shortening of bond length. The out-of-plane deformation mode clearly gives rise to the strong crystal absorption at 460  $\text{cm}^{-1}$ . This is a drop of 27  $\text{cm}^{-1}$  from the solution frequency. In view of the very small frequency shifts of other fundamentals, this is felt to be a strong indication of a thinning of the  $\pi$ -electron density above the individual rings as would be expected for increased conjugation.

Two strong  $b_2$ -type bands exist at 1265  $\text{cm}^{-1}$  and 1307  $\text{cm}^{-1}$ , one of which must

be the highest  $b_2$ -like  $\beta$  C—H deformation. The latter is the stronger, but this frequency seems far too high since the corresponding  $C_6H_6$  frequency is only  $1309\text{ cm}^{-1}$ . The former frequency is also in much better agreement with the assigned liquid value.

The in-plane C—H deformation frequencies are somewhat higher in the crystal than in solution. This is again in accord with a decrease in the inter-ring plane angle in going from solution to the crystal. These frequencies ought to be very sensitive to planarity in view of the closeness of the hydrogen atoms on 2 and 2' and 4 and 4' positions in the planar molecule (calculated  $1.78\text{ \AA}$  for non-deformed molecule). The inter-ring deformations ought to be sensitive to planarity for this same reason. In agreement with expectation the in-plane ring-ring shearing frequency rises from  $302$  to  $329\text{ cm}^{-1}$  and out-of-plane shearing from  $246$  to  $250\text{ cm}^{-1}$  in the crystal.

#### CONCLUSION

The main spectral features of biphenyl crystals and solutions can be interpreted in terms of a model consisting of two monosubstituted benzene rings which interact weakly. It appears from the C—C stretching vibrations that the  $\pi$ -electron contribution to the bonding is essentially the same in solution as in the solid. According to the calculations of Guy, this is consistent with the angle between the plane of the rings for the solution being less than  $\pi/8$ . The lowest  $b_1$ -type ring deformation frequency appears to be very sensitive to the  $\pi$ -electron density, presumably because the deformation involves considerable rehybridization and consequent distortion of the  $\pi$ -electron system. As is to be expected from the short distance between the hydrogen atoms on the 2 and 2' and 6 and 6' positions, the C—H interactions cause small increases in the vibrational frequencies of the crystal from those in solution. This interaction may also explain the lack of increase in the inter-ring stretching frequency which is expected to accompany the shortening of the inter-ring bond in going from the solution to crystal phases. It is not possible, however, on the evidence presented to eliminate the possibility that the inter-ring bond length in solution is closer to that of the crystal than that measured for the vapor.

RECEIVED: July 21, 1960

#### REFERENCES

1. M. A. KOVNER, *Optika i Spectroskopiya* **1**, 742 (1956).
2. G. S. LANDSBERG, A. I. SHATENSUTEIN, G. V. PEREGUDOV, E. A. IZRAILEVICH, AND I. A. NOVIKOVA, *Izvest. Akad. Nauk S.S.S.R., Ser. Fiz* **13**, 669 (1954).
3. J. DALE, *Acta. Chem. Scand.* **11**, 640 (1957).
4. J. E. KATON AND E. R. LIPPINCOTT, *Spectrochim. Acta.* **15**, 627 (1959).
5. J. DAHR, *Indian J. Phys.* **7**, 43 (1932).
6. J. TOUSSAINT, *Acta Cryst.* **1**, 43 (1948).
7. D. H. SAUNDER, *Proc. Roy. Soc.* **A188**, 31 (1946).
8. O. BASTIANSSEN, *Acta Chem. Scand.* **3**, 408 (1949).

9. L. O. BROCKWAY AND J. L. KARLE, *J. Am. Chem. Soc.* **65**, 1974 (1944).
10. S. A. AZIZ, *Indian J. Phys.* **13**, 247 (1939).
11. C. G. CANNON AND G. B. B. M. SUTHERLAND, *Spectrochim. Acta* **4**, 373 (1951).
12. A. DADIEU AND K. W. F. KOHLRAUSCH, *Monatsh. Chem.* **55**, 201 (1930).
13. P. DONZELOT AND M. CHAIX, *Comp. Rend.* **201**, 501 (1935).
14. S. K. MUKERJI AND S. A. AZIZ, *Indian J. Phys.* **12**, 271 (1938).
15. S. K. MUKERJI AND L. SINGH, *Phil. Mag.* [7], **37**, 877 (1937).
16. A. FRUHLING, *Ann. Physik* **6**, 401 (1951).
17. C. E. WEIR, E. R. LIPPINCOTT, A. VAN WALKENBURG, AND E. N. BUNTING, *J. Research. Natl. Bur. Standards* **63A**, 55 (1959).
18. J. E. STEWART AND M. HELLMANS, *J. Research. Natl. Bur. Standards* **60**, 125 (1958).
19. R. A. BAUMAN, *J. Chem. Phys.* **24**, 13 (1956).
20. G. H. BEAVER AND E. A. JOHNSON, *Spectrochim. Acta* **14**, 67 (1959).
21. J. GUY, *J. chim. phys.* **46**, 469 (1949).
22. K. E. HOWLETT, *J. Chem. Soc.* p. 1055 (1960).
23. R. MULLIKEN, *J. Chem. Phys.* **23**, 1997 (1955).
24. R. R. RANDLE AND D. H. WHIFFEN, in Report of the Molecular Spectroscopy Conference, London, 1954, p. 111. Institute of Petroleum, 1955.
25. S. BRODERSON AND A. LANGSETH, *Kgl. Danske Videnskab. Selskab, Mat.-fys. Skr.* **1**, No. 1 (1956).
26. S. BRODERSON AND A. LANGSETH, *Kgl. Danske Videnskab. Selskab., Mat.-fys. Skr.* **1**, No. 7 (1959).
27. D. STEELE AND D. H. WHIFFEN, *Trans. Faraday Soc.* **55**, 369 (1959).
28. M. STACEY, R. H. MOORE, S. A. BARKER, H. WEIGEL, E. J. BOURNE, AND D. H. WHIFFEN, *Proc. Second Intern. Conf. Peaceful Uses of Atomic Energy, Geneva P/1466* (1958).
29. D. H. WHIFFEN, *J. Chem. Soc.* p. 1350 (1956).
30. D. W. SCOTT, J. P. McCULLOUGH, W. D. GOOD, J. F. MESSERLY, R. E. PENNINGTON, T. C. KINCHELOE, I. A. HOSSENLOPP, D. R. DOUSLIN, AND G. WADDINGTON, *J. Am. Chem. Soc.* **78**, 5457 (1956).
31. D. H. WHIFFEN, *Phil. Trans. Roy. Soc.* **A268**, 131 (1955).
32. D. STEELE AND E. R. LIPPINCOTT, *J. Chem. Phys.* **33**, 1242 (1960).
33. D. H. WHIFFEN, *Spectrochim. Acta* **7**, 253 (1955).
34. R. D. MAIR AND D. F. HORNIG, *J. Chem. Phys.* **17**, 1236 (1949).
35. S. R. POLO AND M. K. WILSON, *J. Chem. Phys.* **23**, 2376 (1955).
36. D. F. HORNIG, *Disc. Faraday Soc.* **54**, 327 (1950).
37. G. V. PEREGUDOV, *Optics and Spect.* **9**, 155 (1960).
38. R. S. STEIN, *J. Chem. Phys.* **23**, 734 (1955).



## The vibrational spectra of tetra-fluoro-benzenes

D. STEELE,

Department of Chemistry, University College of Swansea, Singleton Park, Swansea

(Received 16 January 1962)

**Abstract**—The vibrational spectra of 1:2:3:4 and 1:2:3:5-tetra-fluoro-benzenes are interpreted in terms of  $C_{2v}$  structures and the resulting assignments shown to be consistent with assignments of other fluoro-aromatics.

The Decius and Wilson sum rule is shown to be applicable within certain limits to non-isotopic systems. The deviations in  $(\Sigma \nu^2)$  are of the order of 0.5 per cent for in-plane vibrations and about 3–5 per cent for out-of-plane vibrations.

### 1. INTRODUCTION

THE vibrational spectra of fluoro-aromatics have attracted considerable interest. There are three major reasons for this: Firstly, the fluoro-benzene series form a volatile set of planar aromatic molecules; secondly, the highly electronegative fluorine atom imparts interesting characteristics to the molecules, for instance, intense infra-red absorption and changes in force constants, without destroying the planarity of the systems; and, finally, all fluorine-substituted benzenes are now known and thus yield a complete and interesting series in which to study the effect of progressive substitution on the aromatic nucleus.

Vibrational assignments have been presented previously for  $C_6H_5F$  [1–3],  $m$ - $C_6H_4F_2$  [4] and  $C_6F_5H$  [5] in addition to all the fluoro-derivatives with symmetries greater than  $C_{2v}$  [5–12]. In the present work the spectra of 1:2:3:4 and 1:2:3:5-tetra-fluoro-benzenes have been investigated and assignments presented which are shown to be consistent with assignments of other fluoro-aromatics.

It would seem reasonable to expect both the molecules in question to be planar

- 
- [1] D. H. WHIFFEN, *J. Chem. Soc.* 1350 (1956).  
 [2] D. W. SCOTT, J. P. McCULLOUGH, W. D. GOOD, J. F. MESSERLY, R. E. PENNINGTON, T. C. KINCHELOE, I. A. HOSSENLOPP, D. R. DOUSLIN and G. WADDINGTON, *J. Am. Chem. Soc.* **78**, 5457 (1956).  
 [3] D. STEELE, E. R. LIPPINCOTT and J. XAVIER, *J. Chem. Phys.* **33**, 1242 (1960).  
 [4] E. E. FERGUSON, R. L. COLLINS, J. R. NEILSON and D. C. SMITH, *J. Chem. Phys.* **21**, 1470 (1953).  
 [5] D. STEELE and D. H. WHIFFEN, *Spectrochim. Acta* **16**, 368 (1960).  
 [6] A. STOJILKOVIC and D. H. WHIFFEN, *Spectrochimica Acta* **12**, 47 (1958).  
 [7] E. E. FERGUSON, R. L. HUDSON, J. R. NIELSON and D. C. SMITH, *J. Chem. Phys.* **21**, 1464 (1953).  
 [8] D. STEELE and D. H. WHIFFEN, *Trans. Faraday Soc.* **56**, 8 (1960).  
 [9] J. R. NIELSON, C. Y. LIANG and D. C. SMITH, *Disc. Faraday Soc.* **9**, 177 (1950).  
 [10] E. E. FERGUSON, *J. Chem. Phys.* **21**, 886 (1953).  
 [11] D. STEELE and D. H. WHIFFEN, *Trans. Faraday Soc.* **55**, 369 (1959).  
 [12] L. DELBOUILLE, *J. Chem. Phys.* **25**, 182 (1956).

in view of the planarity of  $C_6F_6$  [11, 13] and consequently their molecular symmetries can be taken as  $C_{2v}$  with reasonable confidence. The vibrations separate according to their symmetries as in Tables 1 and 2, the relevant characteristics of the interaction of the classes with electro-magnetic radiation also being presented in these tables. The recommendations of MULLIKEN [14] have been followed in labelling the symmetry classes.

Table 1. Selection rules for 1:2:3:5-tetra-fluoro-benzene

$C_{2v}$	No. of vibrations	Raman activity	I. R. activity
$a_1$	11	pol.	type <i>A</i>
$a_2$	3	dp.	inactive
$b_1$	6	dp.	type <i>C</i>
$b_2$	10	dp.	type <i>B</i>

Table 2. Selection rules for 1:2:3:4-tetra-fluoro-benzene

$C_{2v}$	No. of vibrations	Raman activity	I. R. activity
$a_1$	11	pol.	type <i>B</i>
$a_2$	5	dp.	inactive
$b_1$	4	dp.	type <i>C</i>
$b_2$	10	dp.	type <i>A</i>

## 2. EXPERIMENTAL

The materials were gifts from Professor J. C. TATLOW and his group and from Dr. L. WALL and were chromatographically pure. All infra-red spectra at frequencies greater than  $650\text{ cm}^{-1}$  were measured on a Perkin-Elmer 21 equipped with a NaCl prism, and at frequencies below this on a Beckmann I.R.4 with CsBr optics. A Hilger E612 spectrograph was used for observation of the Raman spectra of the liquids excited by the Hg 4358-Å line, other wavelengths being removed by a filter solution of Rhodamine GBN 500 and nitrobenzene in alcohol [15].

The observed frequencies are tabulated in Tables 3 and 4. For the sake of consistency, wherever possible throughout the text the vibration frequencies quoted will be the liquid-state frequencies.

### 3. 1:2:3:5-TETRA-FLUORO-BENZENE

#### $a_1$ Class

On the basis of strength of infra-red absorption and vapour-phase band contours, and of intensity of Raman shifts and the polarization of the bands,  $a_1$  fundamentals can be clearly assigned at 1124, 997, 786 and  $580\text{ cm}^{-1}$ .

No high resolution data are available for deciding the exact C—H stretching frequencies, but both the  $a_1$  and  $b_2$  are undoubtedly near  $3080\text{ cm}^{-1}$ . Apart from

[13] C. A. COULSON and D. STOCKER, *Mol. Phys.* **2**, 397 (1959).

[14] R. S. MULLIKEN, *J. Chem. Phys.* **23**, 1997 (1955).

[15] J. T. EDSALL and E. B. WILSON, *J. Chem. Phys.* **124** (1938).

Table 3. Observed vibrational spectra of 1:2:3:5-tetra-fluoro-benzene

Raman	I.R. vapour	I.R. liquid	
258 w			$b_2$ fundamental
		302 vw	} $a_1$ fundamental
		310 s	
324 w		334 vs	$b_2$ fundamental
368 mw		368 w	$b_1$ fundamental
390 w			$205 + 185(a_2 + b_1)$
		437 w	
442 w	440	445 ms	$368 + 185(b_1 + b_2)$
466 w	465	471 ms	$a_1$ fundamental
506 w	508 s B	510 s	$b_2$ fundamental
523 vvw			$2 \times 258(2 \times b_2)$
	557 w A?	558 ms	$368 + 185(b_1 + b_2)$
578 s p		580 w	$a_1$ fundamental
609 vw	610 s C	606 s	$b_1$ fundamental
641 w-vw	640 w B	641 m	$b_2$ fundamental
	707 ms	702 ms	$b_1$ fundamental
714 m p	732 vvw	736 w	$2 \times 368(2 \times b_1)$
786 ms p	787 s A	786 s	$a_1$ fundamental
	843 vs	840 s	$b_1$ fundamental
994 ms p	1002 s A	997 s	$a_1$ fundamental
	1056 vs B	1050 vs	$b_2$ fundamental
		1083 w	
1130 w	1130 vs A	1124 vs	$a_1$ fundamental
1173 vw br	1179 ms B	1176 ms	$b_2$ fundamental
1238 vw	1249 s	1240 s	$b_2$ fundamental
		1267 m	$997 + 258(a_1 + b_2)$
	1282 m	1287 w	$2 \times 641(2 \times b_2)$
		1310 w	$997 + 310(a_1 + a_1)$
		1330 w	$997 + 334(a_1 + b_2)$
1384 m p		1381 w	} $a_1$ fundamental and $334 + 1050(b_2 + b_2)$
1404 w p	1405 m	1405 m	
	1466 s	1455 s	$b_2$ fundamental
1530 w	1531 vs	1523 vs	$a_1$ fundamental
	1571 mw	1556 mw	$510 + 1050(a_1 + a_1)$
	1585 w	1587 mw	$471 + 1124(a_1 + a_1)$
1640 w br	1642 vs	1631 vs	$a_1$ and $b_2$ fundamental
		1660 w	
		1681 mw	$(b + a_2) 843 + c. 845$
		1695 mw	$1050 + 641(b_2 + b_2)$
		2510 mw	$1405 + 1124(a_1 + a_1)$
3090 m p		3100 mw	$a_1$ fundamental

the C—H stretching frequency the highest  $a_1$  fundamental is predominantly a C—C stretching vibration expected near  $1612 \text{ cm}^{-1}$  [16]. The corresponding  $b_2$  mode will also have a frequency near this value and it is necessary to assign the very strong absorption at  $1631 \text{ cm}^{-1}$  jointly to these two modes. The third highest  $a_1$  and  $b_2$  frequencies are derived from the  $e_{1u}$  fundamental at  $1530 \text{ cm}^{-1}$  in  $\text{C}_6\text{F}_6$ .

[16] R. R. RANDES and D. H. WHIFFEN, *Molecular Spectroscopy*, p. 111. Report on the conference held in London in Oct. 1954 by the Institute of Petroleum.

Table 4. Observed vibrational frequencies of *o*-C<sub>6</sub>H<sub>2</sub>F<sub>4</sub>

Raman	I. R. vapour	I. R. liquid	
170 w			$b_1$ fundamental
291 m			$b_2$ fundamental
		310 vw	$b_2$ fundamental
324 vw		325 vs	$a_1$ fundamental
374 ms		376 w	$b_1$ fundamental
		432 vw	$a_2$ fundamental
457 m. br		460 m. br	$a_1$ fundamental
489 m		487 w	$b_2$ fundamental
		500 w	
537 w		540 vw	$2 \times c. 268(2 \times a_1)$
581 vw p			$2 \times 291(2 \times b_2)$
598 vw	597 ms <i>C</i>	597 ms	$b_1$ fundamental
605 vw			
625 w p			$2 \times 310(2 \times b_2)$
	669 vvw		
684 vs p	682 s <i>B</i>	682 s	$a_1$ fundamental
746 w	748 s <i>A</i>	747 s	$b_2$ fundamental
	802 vs <i>C</i>	803 s	$b_1$ fundamental
		929 w	$a_2$ fundamental
	962 m <i>A</i>	963 s	$b_2$ fundamental
	993 w <i>A</i>	988 w	
		1003 w	
1046 m	1050 vs <i>B</i>	1048 s	$a_1$ fundamental
1070 vvw			$325 + 747(a_1 + b_2)$
	1089 w	1093 w	$922 + 170(a_2 + b_1)$
1164 vw	1165 s <i>B</i>	1162 s	$a_1$ fundamental
	1192 vvw	1211 vw	$a_1$ fundamental
1233 vvw	1243 vs <i>A</i>	1239 s	$b_2$ fundamental
1270 w	1278 s <i>A</i>	1267 s	$b_2$ fundamental
1304 vw		1314 vw	$1048 + 268(a_1 + a_1)$
1328 s p	1331 s <i>B</i>	1328 s	$a_1$ fundamental
		1402 mw	$b_2$ fundamental
	1446 vw	1438 w	
	1475 vw	1476 mw	$1162 + 310(a_1 + b_2)$
	1517 vvs	1515 vvs	$b_2$ fundamental
1523 w. p.	1525 vvs	1522 vs	$a_1$ fundamental
	1531 s	1541 s	} $1048 + 489(a_1 + b_2)$
	1565 m	1560 w	
	1606 w	1607 m	$b_2$ fundamental
1634 m	1634 m	1632 s	$a_1$ fundamental
		1638 m	$1162 + 460(a_1 + a_1)$
		1648 w	$682 + 963(a_1 + b_2)$
		1725 m	$988 + 747(b_2 + b_2)$
		1787 m	$747 + 1048(b_2 + a_1)$
		1840 s	$1162 + 682(a_1 + a_1)$
		1904 m	$1162 + 747(a_1 + b_2)$
		1919 mw	$682 + 1239(a_1 + b_2)$
		1931 mw	$1328 + 597(a_1 + b_1)$
		2011 mw	$1211 + 803(a_1 + b_1)$
		2074 mw	$1402 + 682(b_2 + a_1)$

Table 4 (cont.)

Raman	I.R. vapour	I.R. liquid
		2200 mw
		2309 mw
		2426 mw
		2474 mw
		2059 mw
		2568 m
		3038 w
		3104 m
		682 + 1522( $a_1 + a_1$ )
		1048 + 1278( $a_1 + b_2$ )
		1632 + 803( $a_1 + b_1$ )
		1328 + 1162( $a_1 + a_1$ )
		1515 + 988( $b_2 + b_2$ )
		1328 + 1211( $a_1 + a_1$ )
		$b_2$ fundamental
		$a_1$ fundamental

Two candidates exist for these, the very strong absorption at  $1523\text{ cm}^{-1}$  and the strong absorption at  $1455\text{ cm}^{-1}$ . An unambiguous choice between these can be made by noting that the frequency of this  $a_1$ -type mode drops only from  $1530\text{ cm}^{-1}$  in  $\text{C}_6\text{F}_6$  to  $1511\text{ cm}^{-1}$  in  $p\text{-C}_6\text{H}_4\text{F}_2$  due to the removal of two CF stretching modes and replacement by two CH stretching modes, while the analogous  $b_2$ -type frequency drops from  $1530$  to  $1437\text{ cm}^{-1}$ . In  $m\text{-C}_6\text{F}_4\text{H}_2$  we may consider one CF stretch and one CF deformation to have been replaced by their CH counterparts and thus the ring assignments ought to be intermediate between those of  $\text{C}_6\text{F}_6$  and  $p\text{-C}_6\text{H}_4\text{F}_2$ . This clearly places the intermediate  $a_1$   $o\text{-C}_6\text{H}_2\text{F}_4$  frequency at  $1523\text{ cm}^{-1}$  and the  $b_2$  at  $1455\text{ cm}^{-1}$ . Polarized Raman shifts at  $1404$  and  $1384\text{ cm}^{-1}$  and the corresponding infra-red absorption at  $1405\text{ cm}^{-1}$  (m) and  $1381\text{ cm}^{-1}$  (w) are proposed as due to the fourth highest  $a_1$  fundamental frequency interacting with an  $a_1$  combination band. This leaves one  $a_1$  vibration with a frequency in the NaCl region to be assigned. A comparison of the corresponding modes of  $\text{C}_6\text{F}_6$  and  $p\text{-C}_6\text{H}_4\text{F}_2$  (Table 5) places this between  $1245$  and  $1157\text{ cm}^{-1}$ . The only band in this region which is clearly a fundamental is that at  $1240\text{ cm}^{-1}$ . However, it seems preferable to assign this as a  $b_2$  CF-stretching mode.

No vapour-phase band contours or clear Raman polarization data are available to assist with the choice of the lowest two modes. These are a CF-deformation mode and a ring-deformation mode. Since the ring-deformation frequency is at  $451\text{ cm}^{-1}$  in  $p\text{-C}_6\text{H}_4\text{F}_2$ , the tetra-fluoro frequency must lie above this value due to interaction with the low-lying  $\beta$ -CF mode. The absorption at  $471\text{ cm}^{-1}$  almost certainly arises from this mode. The CF-deformation frequency is likely to be associated with strong absorption near  $300\text{ cm}^{-1}$  and the choice is between bands at  $334\text{ cm}^{-1}$  and  $310\text{ cm}^{-1}$ . The latter is preferred though no clear criterion exists for making the choice. The absorption at  $334\text{ cm}^{-1}$  is assigned to the  $b_2$ -CF absorption.

#### $b_2$ Class

Fundamentals of the  $b_2$  class have already been assigned at  $3080$ ,  $1631$ ,  $1455$ ,  $1240$  and  $334\text{ cm}^{-1}$ . Strong infra-red bands with type-B contours in vapour-phase absorption locate other fundamentals at  $1176$ ,  $1050$ ,  $641$  and  $510\text{ cm}^{-1}$ . This leaves just the lowest  $\beta$ -CF deformation to be located. The weak Raman shift at  $258\text{ cm}^{-1}$  is satisfactorily accounted for by this mode and has a frequency close to that expected from a comparison with  $\text{C}_6\text{F}_6$ .

Table 5. Comparison of vibrational assignments of  $C_6F_6$ , 1:2:3:5- $C_6F_4H_2$  and  $p$ - $C_6H_4F_2$ .

	$C_6F_6$	$m$ - $C_6H_2F_4$	$p$ - $C_6H_4F_2$	1:3:5- $C_6F_3H_3$
$a_1$	1655	3090	3084	3111
	1530	1631	3050	3081
	1490	1523	1617	1620
	1323	1405	1511	1471
	1157	?	1245	1350
	1006	1124	1225	1122
	640	997	1142	1010
	559	786	1012	993
	443	580	858	578
	315	471/445	737	502
	264	310	451	326
$a_2$	595	845	943	845
	370	(645)	800	665
	175	c. 205	410	214
$b_2$	1655	(3080)	3084	3111
	1530	1631	3080	1620
	1253	1455	1617	1471
	1157	1240	1437	$a_2'$
	1006	1176	1304	$a_2'$
	691	1050	1285	1122
	443	641	1085	993
	315	510	635	$a_2'$
	264	334	427	502
	208	258	350	326
$b_1$	714	840	928	1191
	595	702	833	845
	370	606	692	665
	249	368	509	595
	215	?	375	253
	175	c. 185	186	214

 $b_1$  Class

The three highest  $b_1$  fundamentals are at 840, 702 and 606  $cm^{-1}$ . The lowest  $\gamma$ -CF deformation is unlikely to be far from the  $C_6F_6$  and  $p$ - $C_6H_4F_2$  frequencies at 175 and 186  $cm^{-1}$  respectively. No Raman band is observed in this region. The lowest ring mode is likely to be depressed slightly from its frequency in  $C_6F_6$  (370  $cm^{-1}$ ) due to the  $\gamma$ -CH mode. The Raman and infra-red bands at 368  $cm^{-1}$  may be safely assigned to this mode though the frequency has changed but little from 370  $cm^{-1}$ . No observed low-frequency band remains to be assigned as the last  $\gamma$ -CF mode. Application of the inequality rule [11, 17] indicates its frequency to be between 249 and 215  $cm^{-1}$ .

[17] M. STACEY, R. H. MOORE, S. A. BARKER, H. WEIGEL, E. J. BOURNE and D. H. WHIFFEN, *Proc. 2nd Int. Conf. Peaceful Uses of Atomic Energy, Geneva 1958* P. 1466. Pergamon Press, London (1959).

*a*<sub>2</sub> Class

The *G*-matrix for this class is identical with that of the *a*<sub>2</sub>" class of sym-tri-fluoro-benzene. This indicates that the fundamental frequencies are near 845, 665 and 214 cm<sup>-1</sup> [9]. None is observed. However, the strongest combination bands of aromatics above the finger-print region usually arise from combinations of  $\gamma$ -CH frequencies [18]. In this case the strongest band is a doublet at 1695/1681 cm<sup>-1</sup>. The major component is most probably  $\gamma$ -CH (*b*<sub>1</sub>) +  $\gamma$ -CH *a*<sub>2</sub>, thus confirming a value of about 845 cm<sup>-1</sup> for the highest *a*<sub>2</sub> fundamental.

Due to the low symmetry of the molecule little is to be gained by trying to interpret the weak combination bands throughout the spectrum, except where they are at low frequencies, since so many possible assignments invariably exist. For this reason the infra-red spectral absorptions listed do not include weak absorptions above 1700 cm<sup>-1</sup>, nor do they include very weak absorptions between 1700 and 800 cm<sup>-1</sup>. Where several alternative explanations are possible for the combination bands—as is usually the case—only one is listed.

Only one combination band is unexplained using the previous assignments. It is the weak Raman line at 390 cm<sup>-1</sup>. The number of possible non-fundamental assignments for such a low-frequency band is very limited and the most probable explanation is that it is due to combination of the lowest *a*<sub>2</sub> and *b*<sub>1</sub>  $\gamma$ -CF fundamentals. Assuming a value of about 185 cm<sup>-1</sup> for the lowest *b*<sub>1</sub> yields an *a*<sub>2</sub> frequency of 205 cm<sup>-1</sup>.

The vibrational assignments for 1:3:5-tri-fluoro-benzene are also included in Table 5. Agreement with those proposed above for *m*-C<sub>6</sub>H<sub>2</sub>F<sub>4</sub> is satisfactory. The question mark against the highest *e*" (*b*<sub>1</sub> in *C*<sub>2v</sub>) is the author's.

## 4. 1:2:3:4-TETRAFLUOROBENZENE

The following assignments for the fundamental vibrational frequencies of 1:2:3:4-tetra-fluoro-benzene are readily made on the basis of intensities, band contours and polarization data:

*a*<sub>1</sub>: 3090, 1522, 1328, 1162, 1048 and 682 cm<sup>-1</sup>

*b*<sub>2</sub>: 1239, 988 and 747 cm<sup>-1</sup>

*b*<sub>1</sub>: 803, 597 cm<sup>-1</sup>

As with *m*-C<sub>6</sub>F<sub>4</sub>H<sub>2</sub> the two highest ring modes (*a*<sub>1</sub> and *b*<sub>2</sub>) are to be expected at approximately 1600 cm<sup>-1</sup>. One Raman band exists at 1634 cm<sup>-1</sup> and two infra-red bands at 1632, (s) and 1607 cm<sup>-1</sup> (m). It is tentatively suggested that the higher-frequency bands are associated with the *a*<sub>1</sub> class on the basis of the intensity of the Raman band. The higher component of the very strong complex at about 1520 cm<sup>-1</sup> has an associated weak polarized Raman line indicating its assignment as an *a*<sub>1</sub>. This indicates that the second major component at 1515 cm<sup>-1</sup> is to be identified with the *b*<sub>2</sub> fundamental.

Two  $\beta$ -CF deformation modes exist in each of the in-plane classes. Two of these are clearly associated with the transition frequencies of 291 and 325 cm<sup>-1</sup>. Also the very weak absorption at 310 cm<sup>-1</sup> may be a third  $\beta$ -CF fundamental.

[18] D. H. WHIFFEN, *Spectrochim. Acta* **7**, 253 (1955).

[19] S. BRODERSON and A. LANGSETH, *Kgl. Danske Videnskab. Selskabs Mat. fys. Skrifter* **1**, (1959).

These frequencies are readily accommodated by comparison with  $o\text{-C}_6\text{H}_4\text{F}_2$  and  $\text{C}_6\text{F}_6$  as the higher  $a_1$  frequency ( $325\text{ cm}^{-1}$ ) and the two  $b_2$  fundamentals ( $310\text{ cm}^{-1}$  and  $291\text{ cm}^{-1}$ ). The assignment of two low  $\beta\text{-CF}$  frequencies in the  $b_2$  class is supported by noting that the ring-deformation frequencies are considerably higher in  $o\text{-C}_6\text{F}_4\text{H}_2$  ( $747, 489\text{ cm}^{-1}$ ) than in  $\text{C}_6\text{F}_6$  ( $640, 443\text{ cm}^{-1}$ ).

The Raman bands at  $489$  and  $457\text{ cm}^{-1}$  clearly arise from  $a_1$  and  $b_2$  (or  $b_2$  and  $a_1$ ) ring-deformation modes. The former pair of assignments is preferred.

The strength of the  $a_1$  absorption bands at  $1328$  and  $1048\text{ cm}^{-1}$  indicates that they are predominantly C—F stretching modes. By following the frequency changes of the  $b_{2u}$  like C—C stretching mode from benzene ( $1309\text{ cm}^{-1}$ ) to  $\text{C}_6\text{F}_6$  ( $1253\text{ cm}^{-1}$ ) it would appear that the  $1162\text{ cm}^{-1}$  band in  $o\text{-C}_6\text{F}_4\text{H}_2$  is predominantly  $\beta\text{-CH}$  and that the  $b_{2u}$ -like ring mode is at a slightly higher frequency and masked by the pair of strong  $b_2$  absorption bands at  $1239, 1267\text{ cm}^{-1}$ . The strongest unassigned absorption is at  $1402\text{ cm}^{-1}$  but appears to be too high for this ring mode, both according to mode tracing and by application of the sum rule described in the final section.

In the  $b_2$  class the remaining assignments are for the CH stretching frequency, which is assigned as  $3070\text{ cm}^{-1}$  and for the  $\beta\text{-CH}$  mode. The pair of  $b_2$  modes at  $1267/1239\text{ cm}^{-1}$  is due to Fermi resonance of a combination band with the higher CF-stretching mode. This is indicated by the considerable difference in relative intensities in the liquid and vapour phases coupled with the result that using both frequencies as fundamentals leads to a  $\delta$  value (see Section 5) of 2.0 per cent. The latter suggests a considerably higher frequency and the strongest unassigned band at  $1402\text{ cm}^{-1}$  is readily accommodated as the sought-for fundamental.

The out-of-plane  $b_1$ -CF deformations are assigned as  $374\text{ cm}^{-1}$  and  $170\text{ cm}^{-1}$ . In the  $a_2$  class the only assignment that can be advanced on the present experimental findings is the  $\gamma\text{-CH}$ . The moderately strong infra-red band at  $1725\text{ cm}^{-1}$  is very likely the combination band resulting from the two  $\gamma\text{-CH}$  deformations. As the  $b_1$  is located at  $802\text{ cm}^{-1}$  this suggests a frequency of  $922\text{ cm}^{-1}$  for the  $a_2$ .

The assignments are summarized in Table 6 where the vibrational frequencies are compared with those of the analogous transitions of the series  $\text{C}_6\text{D}_6$ ,  $o\text{-C}_6\text{H}_4\text{D}_2$ ,  $o\text{-C}_6\text{H}_4\text{F}_2$  and  $\text{C}_6\text{F}_6$ . While it is often difficult as a result of mode mixing, to assign with certainty the nature of the mode to an observed vibrational transition for the partially fluorinated series, the modes of the  $D_{6h}$  molecules are well known from force-constant treatments. The  $D_{6h}$  frequencies are labelled according to the mode involved so as to assist in the identification of the vibrations of the intermediate molecules.

##### 5. THE APPLICATION OF THE SUM RULE TO NON-ISOTOPIC MOLECULES

The sum rules for isotopically related molecules [20, 21] hold to a greater degree of precision than does the product rule of REDLICH and TELLER [22]. This is due

[20] S. BRODERSON and A. LANGSETH, *Kgl. Danske Videnskab. Selskabs Mat. fys. Skrifter* **1** (1956).

[21] J. C. DECIUS and E. B. WILSON, *J. Chem. Phys.* **19**, 1409 (1951).

[22] O. REDLICH, *Z. physik. Chem. (Leipzig)* **B 28**, 371 (1935); E. TELLER quoted by W. R. ANGUS, C. R. BAILEY, J. B. HALE, C. K. INGOLD, A. H. LECKIE, C. G. RAISIN, J. W. THOMPSON, and C. L. WILSON, *J. Chem. Soc.* 971 (1936).



Table 6. Comparison of vibrational assignments of  $C_6H_6$ ,  $o-C_6H_4D_2$ ,  $o-C_6H_4F_2$ ,  $o-C_6F_4H_2$  and  $C_6F_6$ 

	$C_6H_6$	$o-C_6H_4D_2$ [18]	$o-C_6H_4F_2$	$o-C_6F_4H_2$	$C_6F_6$
$a_1$	3073 r	c. 3074	3092	3090	1655 R
	3068 r	c. 3074	3053	1632	1530 R
	3055 r	2291	1616	1522	1490 r
	1600 R	1582	1506	1328	1253 R
	1482 R	1461	1399	1211?	1157 r
	1309 R	1299	1269	1162	1006 r
	1177 $\beta$	1159	1152	1048	559 R
	1146 $\beta$	1055	1023	682	443 $\alpha$
	1037 $\beta$	977	763	460	315 $\beta$
	993 R	843	565	325	264 $\beta$
	607 $\alpha$	592	295	(268)	208 $\beta$
$b_2$	3068 r	c. 3074	c. 3070	3070	1655 R
	3057 r	c. 3055	3039	1607	1530 R
	3055 r	2281	1610	1515	1323 r
	1600 R	1595	1464	1402	1157 r
	1482 R	1437	1348	1278/1239	1006 r
	1350 $\beta$	1271	1212	988	691 $\beta$
	1177 $\beta$	1130	1101	747	640 $\alpha$
	1037 $\beta$	997	857	489	443 $\alpha$
	1010 $\alpha$	872	597	310	315 $\beta$
	607 $\alpha$	603	450	291	264 $\beta$
	$b_1$	967 $\gamma$	954	917	803
845 $\gamma$		780	750	597	370 $\gamma$
673 $\gamma$		579	549	374	215 $\gamma$
398 $\phi$		c. 385	195	170	175 $\gamma$
$a_2$	990 $\gamma$	982	982	922	714 $\phi$
	967 $\gamma$	887			595 $\phi$
	845 $\gamma$	779			370 $\gamma$
	707 $\phi$	661	437		249 $\gamma$
	398 $\phi$	c. 385			175 $\gamma$

r = extra nuclear bond stretching;  $\beta$  = in-plane CH or CF bond deformation;  $\gamma$  = out-of-plane bond deformation; R = Ring stretching;  $\alpha$  = ring deformation;  $\phi$  = CC twisting

to the partial balancing out of deviations from the harmonic frequencies which is inherent in the superimposition nature of the rule.

Extending the application of cancellation of non-harmonic terms it might be expected that changes in force constants would also be partially compensated for as long as the rates of change of force constants with perturbing influence are uniform throughout the series under consideration. In other words, the sum rule might be expected to hold reasonably well for non-isotopic molecules. The reasoning has been confirmed by application of the rule to the fluoro-aromatic series [23]. It is also implicit in the application by BRODERSON and LANGSETH of their sum rules to series of non-isotopic molecules [24].

[23] D. STEELE. M.Sc. thesis (qual.) Birmingham University (1957).

[24] S. BRODERSON and A. LANGSETH, *Acta Chem. Scand.* **12**, 1111 (1958).

In Tables 7 and 8 are given the results of application of the sum rule to various fluoro-aromatic series. For in-plane vibrations the percentage deviation, expressed by

$$\delta = \frac{a\Sigma\nu_A^2 + b\Sigma\nu_B^2 - (a + b)\Sigma\nu_C^2}{(a + b)\Sigma\nu_C^2} \times 100$$

Table 7

Common symmetry in superimposition		$\Sigma\nu^2$ $C_6H_6$	$\Sigma\nu^2$ $C_6F_6$	$\Sigma\nu^2$ $p-C_6H_4F_2$	$\delta$ (%)
$C_{2h}$	$[A_g]$	39,345,700 (11,389,300)	11,697,300 11,697,300	30,278,200 (11,256,300)	-0.5 (+2.2)
	$[b_u]$	38,496,200 (10,564,200)	10,681,500 10,681,500	29,240,500 (10,335,300)	-0.05 (+2.6)
	$[b_g]$	2,926,900	845,600	2,120,700	+5.3
		$C_6D_6$	$C_6F_6$	$p-C_6D_4F_2$	
$C_{2h}$	$[b_u]$	23,654,200 (8,118,241)	10,681,500 10,681,500	19,334,100 (8,813,298)	-0.02 (+1.8)
		$C_6H_6$	$C_6F_6$	$p-C_6H_2F_4$	
$C_{2h}$	$[A_g]$	39,345,700 (11,389,300)	11,697,300 11,697,300	20,968,100 (11,376,700)	-0.26 (+1.9)
	$[b_u]$	38,496,200 (10,564,200)	10,681,500 10,681,500	19,856,000 (10,314,000)	+0.5 (+3.2)
	$[b_g]$	2,926,900	845,600	1,467,100	+4.9
	$[A_u]$	2,660,000	815,500	1,387,000	+3.2
		$C_6H_6$	$C_6F_6$	sym. $C_6F_3H_3$	
$D_{3h}$	$[E']$	26,165,500 (7,554,400)	7,803,800 7,803,800	17,045,200 (7,398,000)	-0.35 (+5.1)
	$[A_1']$	20,672,300 (2,006,100)	4,689,500 4,689,500	12,662,500 (3,176,100)	+0.15 (+3.6)
	$[A_2'']$	1,937,500	618,000	1,202,000	6.3
	$[E'']$	1,824,700	523,300	1,135,400	3.4
		$C_6F_6$	$p-C_6H_4F_2$	$C_6H_2F_4$	
$C_{2v}$	$[a_1]$	12,493,400 12,493,400	30,657,600 (11,727,800)	21,471,300 (11,923,200)	+0.48 (+1.57)
	$[b_2]$	9,904,600 9,904,600	28,861,000 (9,863,500)	19,135,800 (9,649,400)	+1.29 (+2.4)
	$[b_1]$	1,139,600	2,468,200	1,792,900	+0.61

Table 8

Common symmetry	$\Sigma\nu^2$	$\Sigma\nu^2$	$\Sigma\nu^2$	$\Sigma\nu^2$	$\delta^*$
$C_{2v}$	$C_6F_6$	$C_6H_6$	$p-C_6F_4H_2$	$o-C_6F_4H_2$	(%)
$[a_1]$	11,943,600	39,554,200	21,187,800	21,041,900	-0.27
	11,943,600	(11,567,300)	(11,596,400)	(11,493,800)	(-2.52)
$[b_2]$	10,435,200	38,287,700	19,636,300	19,425,000	-1.13
	10,435,200	(10,386,200)	(10,094,400)	(10,000,100)	(-3.86)
$[b_1]$	567,800	2,280,300	1,176,300	1,170,000	+2.85

( ) CH stretching frequencies removed

$$\delta^* = \frac{2\Sigma\nu^2 o-C_6F_4H_2 + \Sigma\nu^2 p-C_6F_4H_2 - 2\Sigma\nu^2 C_6F_6 - \Sigma\nu^2 C_6H_6}{2\Sigma\nu^2 o-C_6F_4H_2 + \Sigma\nu^2 p-C_6F_4H_2}$$

is usually less than 0.5 per cent. Separation and discarding of the C—H stretching frequencies increases  $\delta$  to about 2 per cent, mainly as a result of the decreased value of the denominator. It is interesting, however, that in all cases  $\delta$  changes in a positive sense, even though in some cases  $\delta$  with CH stretch included is negative. This change is in the sense required for mixing of the CH stretch with CF modes. For the out-of-plane classes  $\delta$  is slightly greater being usually in the range +3 to +6 per cent.

In many frequency assignments it is very difficult to decide without a detailed force-constant calculation whether or not a frequency has been misassigned by a considerable amount due to serious admixing of the modes. In such cases the rule could be of very considerable use.

*Acknowledgements*—I gratefully acknowledge the gifts of samples by Dr. L. WALL and Dr. J. C. TATLOW; the use of instruments at the University of Birmingham and at the National Bureau of Standards, Washington D.C., and of the interest and advice of Dr. D. H. WHIFFEN. Finally, I acknowledge the tenure of an I.C.I. fellowship during which the final phase of this work was completed.

## The far infra-red spectra of *p*-difluorobenzene and *p*-difluorodeuterobenzene

(Received 18 September 1962)

AS PART of a programme of study of substituted aromatic systems it was important to know the absorption frequencies of  $p\text{-C}_6\text{H}_4\text{F}_2$  and  $p\text{-C}_6\text{D}_4\text{F}_2$  in the far infra-red. These have been measured in the liquid phase using a Michelson interferometer, the spectra being obtained by Fourier transformation of the interferograms using the N.P.L. Ace computer [1]. The  $p\text{-C}_6\text{D}_4\text{F}_2$  was prepared by Friedel-Crafts exchange with DCl and was of 94 per cent isotopic purity (98.5 per cent deuteration). The spectrum of the lighter isotopic system is reproduced in Fig. 1., and the observed frequencies and band assignments given in Table 1. The observed  $p\text{-C}_6\text{D}_4\text{F}_2$  spectrum differs from that of  $p\text{-C}_6\text{H}_4\text{F}_2$  only in respect to small frequency shifts of the bands.

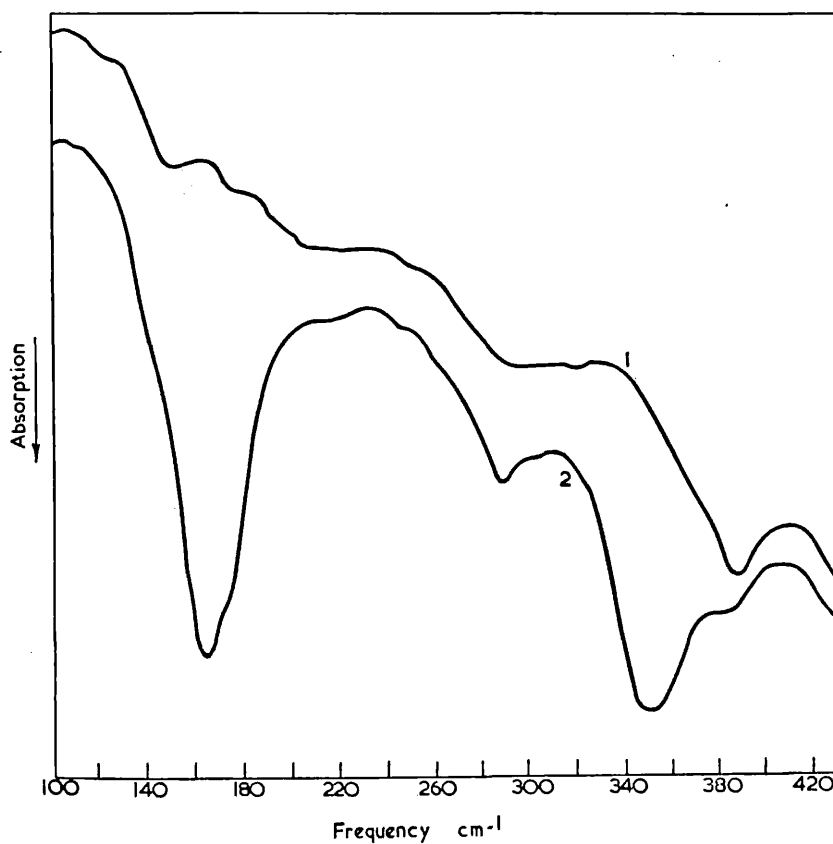


Fig. 1. Curve 1—Blank cell. Curve 2—*p*-Difluorobenzene.

[1] J. H. S. GREEN, W. KYNASTON and H. A. GEBBIE, *Nature*, **195**, 595 (1962).

The frequency range covered in the present study overlaps that investigated by FERGUSON, HUDSON, NIELSON and SMITH [2] using conventional prism spectrometry (250–5000  $\text{cm}^{-1}$ ). These authors reported a strong absorption band at 265  $\text{cm}^{-1}$  as well as a questionable, weak band at 288  $\text{cm}^{-1}$ . The former was assigned as a difference band involving the lowest  $b_{3u}$  mode and led them to a value of 186  $\text{cm}^{-1}$  for the unobserved frequency. This strong band is certainly absent in our spectra.

The  $b_{3u}$  frequency of 164  $\text{cm}^{-1}$  now observed is in good agreement with that calculated by STEELE and WHIFFEN [3] (168  $\text{cm}^{-1}$ ) and is also in accord with the assignment of the analogous mode of *p*-fluorotoluene [4] at 152  $\text{cm}^{-1}$  and of *p*-xylene [1] at 166  $\text{cm}^{-1}$ . A Raman band at 165  $\text{cm}^{-1}$  is clearly due to the  $b_{3u}$  fundamental appearing in violation of the ground state selection rules.

It is the general experience of the authors that the lowest frequency, out of plane, infrared active fundamental of aromatic molecules frequently appears in the Raman effect in violation of the selection rules. A possible explanation arises from the fact that the excited state population of the level near 160  $\text{cm}^{-1}$  is approximately half of that of the ground state. The molecular geometry may be reduced sufficiently in this state to allow forbidden transitions to be observed. However, it is not clear why the observed forbidden transitions should be restricted usually to the lowest lying fundamental.

Table 1

Frequency		Assignment
<i>p</i> -C <sub>6</sub> H <sub>4</sub> F <sub>2</sub>	<i>p</i> -C <sub>6</sub> D <sub>4</sub> F <sub>2</sub>	
164 $\text{cm}^{-1}$	163 $\text{cm}^{-1}$	$\gamma_F b_{3u}$
284 $\text{cm}^{-1}$	284 $\text{cm}^{-1}$	451–164( $\alpha_g - b_{3u}$ )
352 $\text{cm}^{-1}$	348 $\text{cm}^{-1}$	$\gamma_F b_{2u}$

The 164  $\text{cm}^{-1}$  band must be designated as an out-of-plane CF deformation mode, though the calculated  $\mathcal{L}$  matrix of STEELE and WHIFFEN [5] largely obscures this due to the nature of the symmetry co-ordinates chosen. Thus  $S_{30} = 2^{-1/2}(\gamma_1 + \gamma_4)$  implies movements of carbon atoms at  $C_1$  and  $C_4$ . For a pure CF deformation it is necessary to mix in some  $\phi$  and  $\gamma_H$  deformations. The internal co-ordinates  $\gamma$  and  $\phi$  are as defined by WHIFFEN [6]. Use of these co-ordinates then results in an apparent considerable mixing of the ring and  $\gamma_F$  modes. This is readily seen if one transforms the normal co-ordinates into cartesian co-ordinates. Then

$$Q_{164} = 0.56(\eta_1 + \eta_4) - 0.20(\eta_2 + \eta_3 + \eta_5 + \eta_6) - 0.20(z_1 + z_4) + 0.02(z_2 + z_3 + z_5 + z_6)$$

The  $\eta$ 's refer to displacements of the hydrogen and fluorine atoms and the  $z$ 's to carbon displacements.

The observed frequency for the lowest  $b_{2u}$  mode is in good agreement with that observed by FERGUSON, HUDSON, NIELSON and SMITH [2] using conventional prism spectrometry.

*Department of Chemistry, University College, Swansea*  
*National Chemical Laboratory, Teddington, Middx*  
*National Physical Laboratory, Teddington, Middx*

D. STEELE\*  
 W. KYNASTON  
 H. A. GEBBIE

\* Present address: Department of Chemistry, Royal Holloway College, Englefield Green, Surrey.

- [2] E. E. FERGUSON, R. L. HUDSON, J. R. NIELSON and D. C. SMITH, *J. Chem. Phys.*, **21**, 1457 (1953).  
 [3] D. STEELE and D. H. WHIFFEN, *Trans. Faraday Soc.*, **56**, 8 (1960).  
 [4] E. E. FERGUSON, R. L. HUDSON, J. R. NIELSON and D. C. SMITH, *J. Chem. Phys.*, **21**, 1736 (1953).  
 [5] D. STEELE and D. H. WHIFFEN, *Trans. Faraday Soc.*, **56**, 177 (1960).  
 [6] D. H. WHIFFEN, *Phil. Trans. Roy. Soc. London. Ser. A*, **248**, 131 (1955).

The in-plane frequencies and atomic displacements for  
 $C_6F_5H$ ,  $C_6F_5D$  and the model compounds  $C_6F_5X$   
( $X = \text{mass } 35.5, 80 \text{ and } 127$ )

D. A. LONG and D. STEELE  
Department of Chemistry, University College of Swansea

(Received 11 April 1963)

**Abstract**—The vibrational frequencies and atomic displacements for  $C_6F_5H$  and  $C_6F_5D$  have been calculated using a force field based on force constants transferred from  $C_6F_6$  and  $C_6H_6$ . This field which proved very successful has also been slightly modified and used to calculate the frequencies and atomic displacements in the model compounds  $C_6F_5X$  where  $X$  has successively mass 35.5, 80 and 127.

RECENT papers from this laboratory have shown that a reasonably successful force field for pyridine, pyridine- $d_5$  [1], pyridine-3,5- $d_2$ , pyridine-2,4- $d_2$  and pyridine-4- $d$  [2] may be obtained by transferring force constants from benzene, making due allowance for the reduced symmetry. This field was also used to predict the skeletal frequencies in  $\gamma$ -picoline and  $\gamma$ -picoline- $d_7$  [3] by calculating the frequencies for various values of the mass of the 4-substituent in pyridine and pyridine- $d_5$ . In the present paper we give an account of somewhat similar force field studies in compounds of the general formula  $C_6F_5X$  using as a starting point the force field derived by STEELE and WHIFFEN [4] for  $C_6F_6$ . Two types of calculation have been carried out.

(i) The in-plane frequencies of  $C_6F_5H$  and  $C_6F_5D$  have been calculated using a force field based on force constants transferred from  $C_6F_6$  and  $C_6H_6$ . Since independent assignments [5] of the in-plane fundamentals of  $C_6F_5H$  and  $C_6F_5D$  have been made the extent of the agreement between calculated and assigned frequencies serves as a further test of the field proposed for  $C_6F_6$  and the assignments on which it is based [6].

(ii) The frequencies of model compounds of the general formula  $C_6F_5X$  have been calculated using force constants from  $C_6F_6$  throughout but with the mass of  $X$  taken successively as 35.5, 80 and 127. The two types of calculation have many features in common and as far as the mechanics of the calculations are concerned they are best considered together.

#### DETAILS OF FORCE FIELD CALCULATIONS

All the molecules were assumed to be planar. They thus have  $C_{2v}$  symmetry

- [1] D. A. LONG, F. S. MURFIN and E. L. THOMAS, *Trans. Faraday Soc.* **59**, 12 (1963).
- [2] D. A. LONG and E. L. THOMAS, *Trans. Faraday Soc.* **59**, 783 (1963).
- [3] D. A. LONG and W. O. GEORGE, *Spectrochim. Acta* (In press).
- [4] D. STEELE and D. H. WHIFFEN, *Trans. Faraday Soc.* **56**, 5 (1960).
- [5] D. STEELE and D. H. WHIFFEN, *Spectrochim. Acta* **16**, 368 (1960).
- [6] D. STEELE and D. H. WHIFFEN, *Trans. Faraday Soc.* **55**, 369 (1959).

and the vibrations are classified as follows:  $11a_1 + 10b_1$  (in-plane) and  $3a_2 + 6b_2$  (out-of-plane.) The molecular parameters used were as follows:

$$\begin{aligned} \text{C—F bond length } 1.30 \text{ \AA}; & \quad \text{C—H bond length } 1.084 \text{ \AA}; \\ \text{C—C bond length } 1.394 \text{ \AA}; & \quad \text{all interbond angles } 120^\circ. \end{aligned}$$

The valence force field used for both types of calculation had the following general form.

$$\begin{aligned} 2V = & f_l \Delta l^2 + f_r \sum \Delta r_i^2 + 2f_{(rr)_o} \sum \Delta r_i \Delta r_{i+1} + 2f_{(rr)_m} \sum \Delta r_i \Delta r_{i+2} \\ & + 2f_{(rr)_p} \sum \Delta r_i \Delta r_{i+3} + 2f_{(lr)_o} \Delta l (\Delta r_2 + \Delta r_6) + 2f_{(lr)_m} \Delta l (\Delta r_3 + \Delta r_5) \\ & + 2f_{(lr)_p} \Delta l \Delta r_4 + f_R \sum \Delta R_i^2 + 2f_{(RR)_o} \sum \Delta R_i \Delta R_{i+1} \\ & + 2f_{(RR)_m} \sum \Delta R_i \Delta R_{i+2} + 2f_{(RR)_p} \sum \Delta R_i \Delta R_{i+3} + f_\alpha \sum (R \Delta \alpha_i)^2 \\ & + 2f_{(\alpha\alpha)_o} \sum R \Delta \alpha_i R \Delta \alpha_{i+1} + f_w (lw)^2 + f_\beta \sum (r\beta_i)^2 + 2f_{(\beta\beta)_o} \sum r\beta_i r\beta_{i+1} \\ & + 2f_{(\beta\beta)_m} \sum r\beta_i r\beta_{i+2} + 2f_{(\beta\beta)_p} \sum r\beta_i r\beta_{i+3} + 2f_{(w\beta)_o} lwr(\beta_2 + \beta_6) \\ & + 2f_{(w\beta)_m} lwr(\beta_3 + \beta_5) + 2f_{(w\beta)_p} lwr\beta_4 + 2f_{(lR)_o} \Delta l (\Delta R_2 + \Delta R_6) \\ & + 2f_{(lR)_m} \Delta l (\Delta R_3 + \Delta R_5) + 2f_{(lR)_p} \Delta l \Delta R_4 + 2f_{(rR)_o} \sum \Delta r_i (\Delta R_i + \Delta R_{i-1}) \\ & + 2f_{(rR)_m} \sum \Delta r_i (\Delta R_{i+1} + \Delta R_{i-2}) + 2f_{(rR)_p} \sum \Delta r_i (\Delta R_{i+2} + \Delta R_{i-3}) \\ & + 2f_{(r\alpha)_o} \sum r_i R \Delta \alpha_i + 2f_{(r\alpha)_m} \sum R \alpha_i (\Delta r_{i+1} + \Delta r_{i-1}) + 2f_{(l\alpha)} \Delta l R \alpha_1 \\ & + 2f_{(l\alpha)_o} \Delta l (R \alpha_2 + R \alpha_6) + 2f_{(l\beta)_o} \Delta l r (\Delta \beta_6 - \Delta \beta_2) \\ & + 2f_{(l\beta)_m} \Delta l r (\Delta \beta_5 - \Delta \beta_3) + 2f_{(r\beta)_o} \sum r \Delta \beta_i (\Delta r_{i+1} - \Delta r_{i-1}) \\ & + 2f_{(r\beta)_m} \sum r \Delta \beta_i (\Delta r_{i+2} - \Delta r_{i-2}) + 2f_{(rw)_o} lw (\Delta r_2 - \Delta r_6) + 2f_{(rw)_m} lw (\Delta r_3 - \Delta r_5) \\ & + 2f_{(R\alpha)} \sum R \alpha_i (\Delta R_i + \Delta R_{i-1}) + 2f_{(R\beta)_o} \sum r \beta_i (\Delta R_i - \Delta R_{i-1}) \\ & + 2f_{(R\beta)_m} \sum r \beta_i (\Delta R_{i+1} - \Delta R_{i-2}) + 2f_{(R\beta)_p} \sum r \beta_i (\Delta R_{i+2} - \Delta R_{i-3}) \\ & + 2f_{(Rw)_o} lw (\Delta R_1 - \Delta R_6) + 2f_{(Rw)_m} lw (\Delta R_2 - \Delta R_5) \\ & + 2f_{(Rw)_p} lw (\Delta R_3 - \Delta R_4) + 2f_{\alpha\beta} \sum r \beta_i (R \alpha_{i+1} - R \alpha_{i-1}) \\ & + 2f_{\alpha w} \sum lw (R \alpha_2 - R \alpha_6) \end{aligned}$$

The internal co-ordinates are defined in Fig 1. The values of the force constants used for (i)  $C_6F_5H$  and  $C_6F_5D$  and (ii)  $C_6F_5X$  with the mass of X taken successively as 35.5, 80 and 127 are given in Table 1. The values used for  $C_6F_5X$  have been transferred from  $C_6F_6$  without any changes. The values used for  $C_6F_5H$  and  $C_6F_5D$  although largely based on  $C_6F_6$  have been modified to take account of the replacement of one fluorine atom by a hydrogen atom. The C—H stretching constant and the C—H deformation constant have been taken from benzene [7]. All interactions of the C—H stretch have been assumed zero. The interactions of the C—H deformation with the C—F deformations and C—F stretches have also been taken as zero. The constants for the interaction of the C—H deformation with the ring stretching and ring angle terms have been given slightly modified values compared with  $C_6F_6$ .

[7] D. H. WHIFFEN, *Phil. Trans.* A248, 131 (1955).

The vibrational frequencies and the Cartesian displacements of the atoms for each normal mode were calculated on a computer using the methods described by LONG *et al.* [8]. The calculated frequencies for  $C_6F_5H$  and  $C_6F_5D$  are compared with the assigned values in Table 2. This table also gives the calculated frequencies for the model compounds  $C_6F_5X$  ( $X = \text{mass } 35.5, 80 \text{ and } 127$ ) and the calculated and observed frequencies for  $C_6F_6$ . The calculated atomic displacements for all the in-plane modes of  $C_6F_5H$ ,  $C_6F_5D$ ,  $C_6F_6$ ,  $C_6F_5X$  ( $= 35.5$ ),  $C_6F_5X$  ( $= 127$ ) are presented in Fig. 2. The arrangement is such that corresponding modes in each molecule appear in a given row.

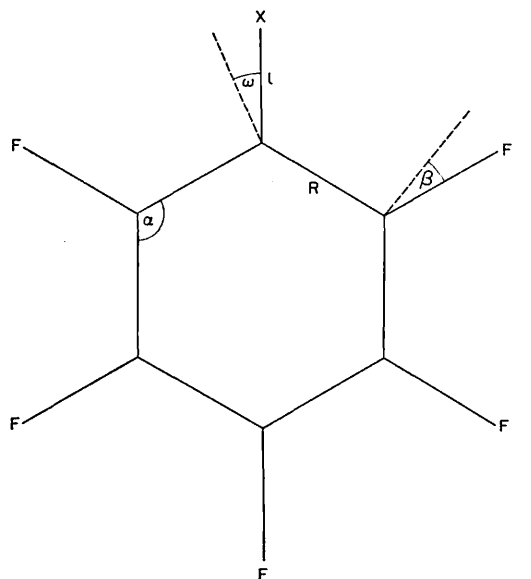


Fig. 1

## DISCUSSION

The agreement between the observed and calculated frequencies for  $C_6F_5H$  and  $C_6F_5D$  is very satisfactory. As the assignments for  $C_6F_5H$  and  $C_6F_5D$  are based very largely on intensities of infra-red bands, contours of bands in the infra-red spectra of the vapours and polarization measurements on Raman shifts this good agreement affords additional support for the force field proposed for  $C_6F_6$  and the assignments upon which it is based.

The correlation of the modes in successive molecules is relatively straightforward. In the  $a_1$  class three modes have essentially constant frequencies throughout and are clearly characteristic of the  $C_6F_5X$  ring system. Two of these are ring deformation modes and the other is a C—F deformation. One ring deformation mode varies only over the range  $1625\text{--}1648\text{ cm}^{-1}$  in the whole six molecules. The other ring deformation mode varies only over the range  $1509\text{--}1531\text{ cm}^{-1}$ . The constancy of the frequency of the C—F deformation mode is even more

[8] D. A. LONG, R. B. GRAVENOR and M. WOODGER, *Spectrochim. Acta* **19**, 937 (1963).



Table 1. Valence force constants (mD/Å) for  $C_6F_5X$ 

$f$	X = H,D	X $\neq$ H	$f$	X = H,D	X $\neq$ H
$f_R$	5.478	5.478	$f_{(\beta l)_m}$	0.000	-0.054
$f_{(RR)_o}$	0.660	0.660	$f_{\alpha R}$	-0.180	-0.180
$f_{(RR)_m}$	0.071	0.071	$f_l$	5.093	7.405
$f_{(RR)_p}$	0.459	0.459	$f_{(lr)_o}$	0.000	0.087
$f_{(LR)_o}$	0.000	0.708	$f_{(lr)_m}$	0.000	-0.050
$f_{(LR)_m}$	0.000	0.001	$f_{(lr)_p}$	0.000	0.032
$f_{(LR)_p}$	0.000	-0.263	$f_r$	7.405	7.405
$f_{(rR)_o}$	0.708	0.708	$f_{(rr)_o}$	0.087	0.087
$f_{(rR)_m}$	0.001	0.001	$f_{(rr)_m}$	0.050	-0.050
$f_{(rR)_p}$	-0.263	-0.263	$f_{(rr)_p}$	0.032	0.032
$f_{(wR)_o}$	+0.050	+0.112	$f_{(wr)_o}$	0.000	0.170
$f_{(wR)_m}$	-0.041	-0.041	$f_{(wr)_m}$	0.000	-0.054
$f_{(wR)_p}$	+0.050	0.033	$f_{(\beta r)_o}$	0.170	+0.170
$f_{(\beta R)_o}$	+0.112	+0.112	$f_{(\beta r)_m}$	-0.054	-0.054
$f_{(\beta R)_m}$	-0.041	-0.041	$f_{\alpha r}$	-0.076	-0.076
$f_{(\beta R)_p}$	-0.033	-0.033	$f_{(\alpha r)_o}$	0.344	0.344
$f_w$	0.866	0.826	$f_\alpha$	1.030	1.030
$f_\beta$	0.826	0.826	$f_{(\alpha\alpha)_o}$	0.141	0.141
$f_{(w\beta)_o}$	0.000	0.072	$f_{\alpha l}$	0.000	-0.076
$f_{(w\beta)_m}$	0.000	-0.093	$f_{(\alpha l)_o}$	0.000	0.344
$f_{(w\beta)_p}$	0.000	0.002	$f_{(\beta\beta)_o}$	0.072	0.072
$f_{w\alpha}$	-0.127	-0.103	$f_{(\beta\beta)_m}$	-0.093	-0.093
$f_{\beta\alpha}$	-0.103	-0.103	$f_{(\beta\beta)_p}$	0.002	0.002
$f_{(\beta l)_o}$	0.000	+0.170			

Table 2. Calculated and observed frequencies ( $cm^{-1}$ ) for  $C_6F_5H$ ,  $C_6F_5D$ ,  $C_6F_6$  predicted frequencies for  $C_6F_5X$ 

class.	$C_6F_5H$		$C_6F_5D$		$C_6F_6$		$C_6F_5X$			
	calc.	obs.	calc.	obs.	calc.	obs.	X = 35.5	X = 80	X = 127	
$a_1$	3064	3105	2284	2315	1006	1011	969	942	934	
	1629	1648	1625	1638	1654	1655	1648	1646	1645	
	1510	1514	1509	1511	1531	1530	1523	1520	1519	
	1407	1410	1399	1400	1488	1490	1476	1469	1467	
	1284	1286	1270	1277	1323	1323	1316	1312	1311	
	1083	1075	1077	1067	1160	1157	1138	1128	1125	
	750	718	738	701	640	640	622	614	612	
	590	578	589	578	559	559	537	522	518	
	479	470	477	467	443	443	407	365	354	
	320	325	319	325	311	315	302	279	239	
	265	272	265	?	264	264	263	255	271	
	$b_1$	1652	1648	1649	1638	1654	1655	1653	1653	1653
		1528	1540	1510	1525	1531	1530	1531	1530	1530
1305		1268	867	870	264	264	242	233	231	
1246		1182	1268	1268	1259	1253	1259	1259	1259	
1132		1138	1186	1175	1160	1157	1160	1160	1160	
960		953	1030	1018	1006	1011	1005	1005	1004	
622		688	594	625	696	691	692	690	689	
435		436	433	435	443	443	442	441	441	
291		304	291	?	311	315	301	297	297	
225		247	225	?	210	208	193	164	152	

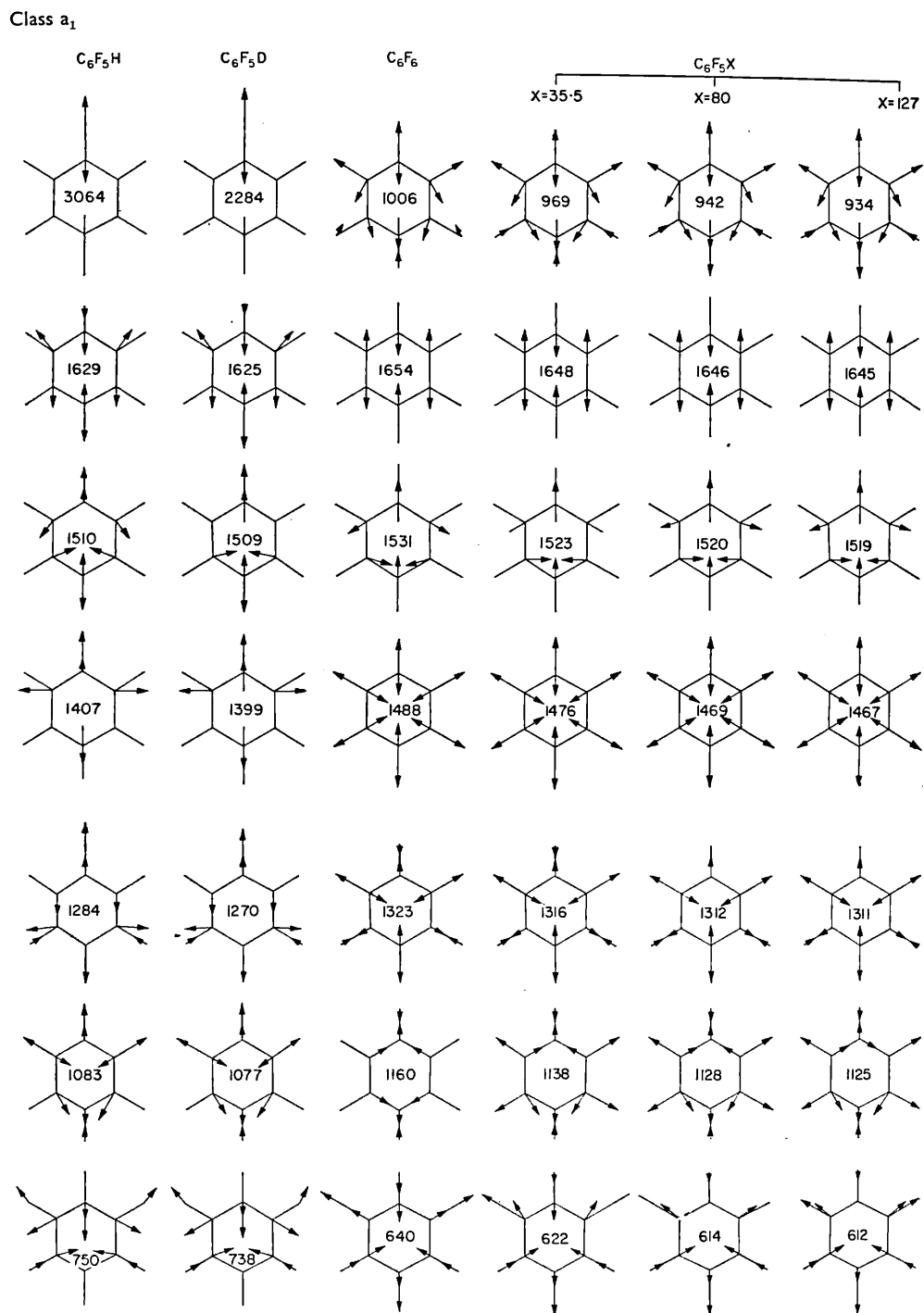
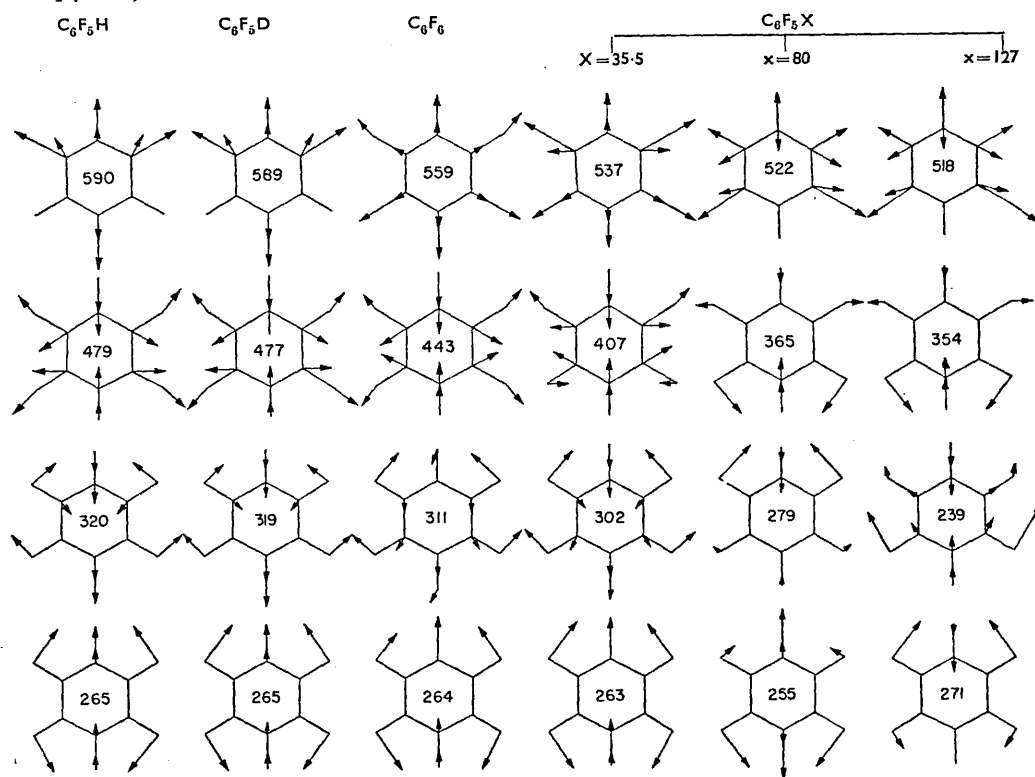


Fig. 2. Atomic displacements.

Class  $a_1$  (contd)



Class  $b_1$

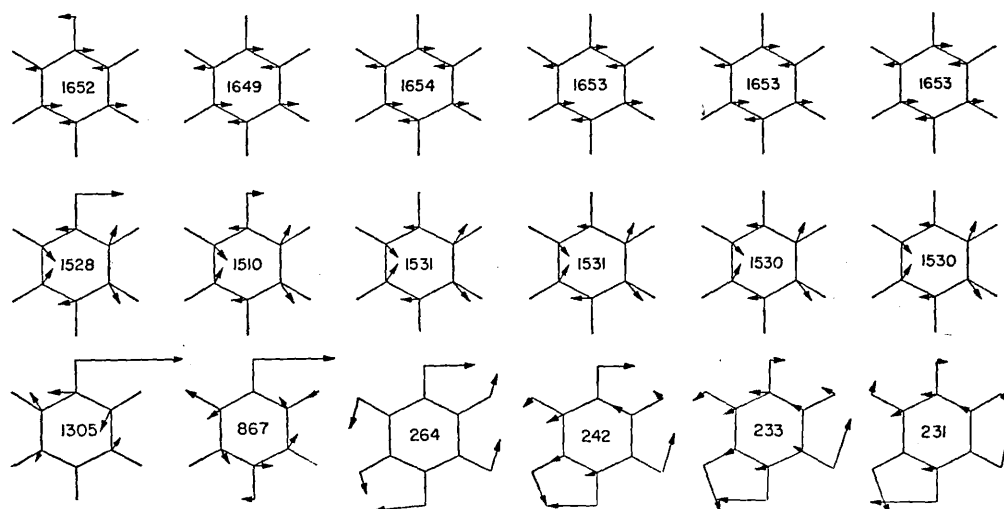


Fig. 2 (contd)

Class  $b_1$  (contd)  
 $C_6F_5H$

$C_6F_5D$

$C_6F_6$

$C_6F_5X$

X=35.5

X=80

X=127

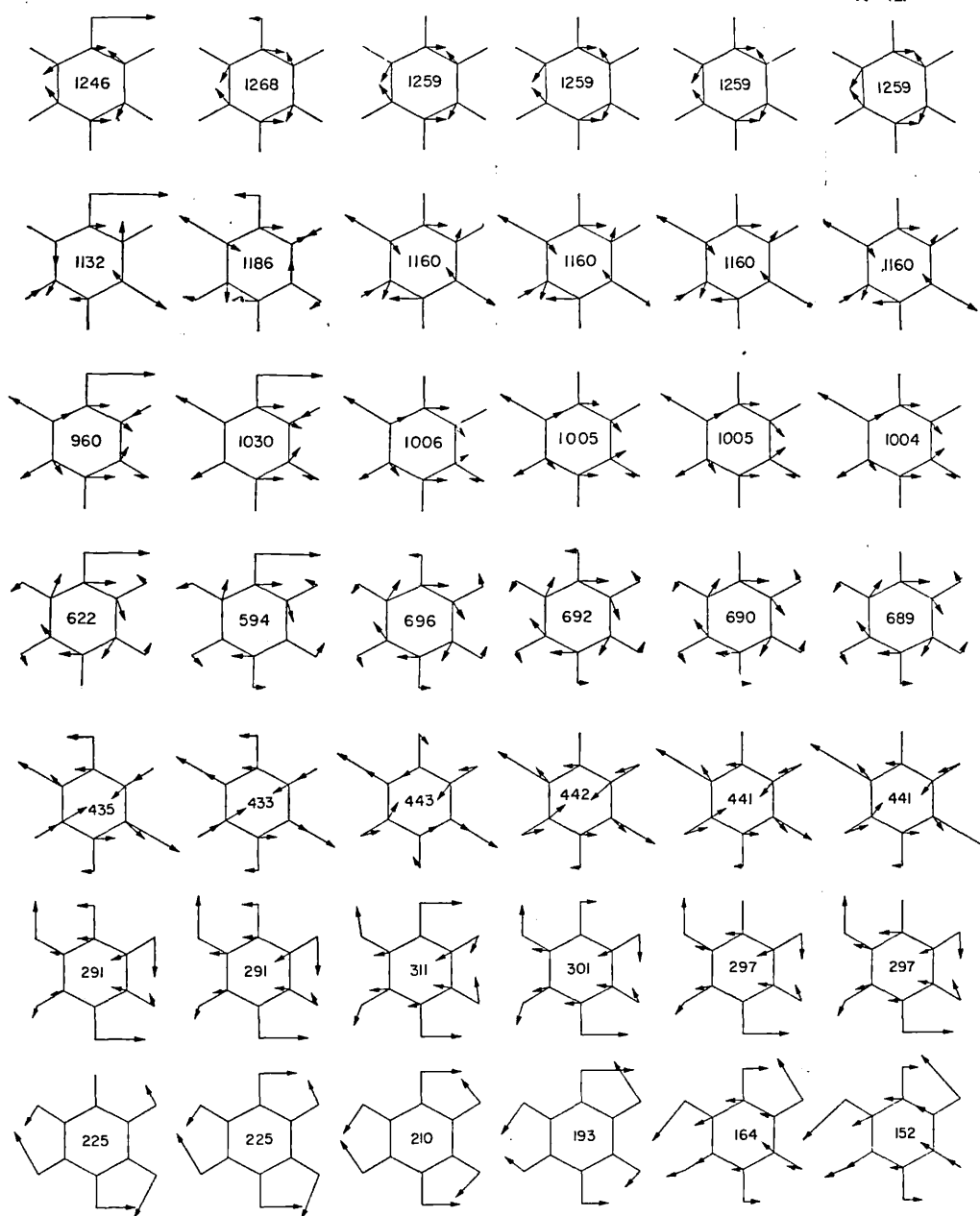


Fig. 2 (contd)

striking, the values ranging only from 263 to 271  $\text{cm}^{-1}$ . In five more modes in this class the biggest change comes when passing from  $\text{C}_6\text{F}_5\text{H}$  and  $\text{C}_6\text{F}_5\text{D}$  to  $\text{C}_6\text{F}_6$ . Thereafter, the frequencies show only a slight decrease with increasing mass of the X substituent and tend to limiting values for large X masses. There are three modes in which marked changes of frequency occur right throughout the series and we shall consider these in a little more detail. One of these may be described approximately as the C—X stretching mode. In  $\text{C}_6\text{F}_5\text{H}$  and  $\text{C}_6\text{F}_5\text{D}$  this is an excellent description of the modes with frequencies 3064 and 2284  $\text{cm}^{-1}$ . In the other compounds other motions are involved too, but the modes at 1006  $\text{cm}^{-1}$  in  $\text{C}_6\text{F}_6$ , 969  $\text{cm}^{-1}$  in  $\text{C}_6\text{F}_5\text{Cl}$ , 942  $\text{cm}^{-1}$  in  $\text{C}_6\text{F}_5\text{Br}$  and 934  $\text{cm}^{-1}$  in  $\text{C}_6\text{F}_5\text{I}$  are predominantly C—X stretching modes. The second mass sensitive mode is essentially a ring angle deformation mode which ranges from 479  $\text{cm}^{-1}$  in  $\text{C}_6\text{F}_5\text{H}$  to 354  $\text{cm}^{-1}$  in  $\text{C}_6\text{F}_5\text{I}$ . As the mass of the X substituent increases there are larger contributions from CF angle deformation *meta* to the X substituent. The third mass sensitive mode is a CF angle deformation mode which varies from 320 to 239  $\text{cm}^{-1}$ .

In the  $b_1$  class there are four modes, all ring modes, whose frequencies are essentially constant throughout the series. The ranges of frequency are 1649–1654  $\text{cm}^{-1}$ , 1510–1531  $\text{cm}^{-1}$ , 1246–1268  $\text{cm}^{-1}$  and 433–443  $\text{cm}^{-1}$ . In four more modes the only changes occur between  $\text{C}_6\text{F}_5\text{H}$  and  $\text{C}_6\text{F}_6$  and thereafter the frequency is essentially constant. From  $\text{C}_6\text{F}_6$  to  $\text{C}_6\text{F}_5\text{I}$  the frequency ranges of these modes are 1160, 1006–1004  $\text{cm}^{-1}$ , 696–689  $\text{cm}^{-1}$  and 311–297  $\text{cm}^{-1}$ . This leaves only two modes in this class showing mass sensitivity over the whole range of compounds. One of these is the C—X angle deformation mode the frequency of which varies from 1305  $\text{cm}^{-1}$  in  $\text{C}_6\text{F}_5\text{H}$  to 231  $\text{cm}^{-1}$  in  $\text{C}_6\text{F}_5\text{I}$ . The other is a C—F angle deformation mode linked with a C—X angle deformation the frequency of which ranges from 225  $\text{cm}^{-1}$  in  $\text{C}_6\text{F}_5\text{H}$  to 152  $\text{cm}^{-1}$  in  $\text{C}_6\text{F}_5\text{I}$ .

These calculations therefore establish the general pattern of frequencies in compounds of the type  $\text{C}_6\text{F}_5\text{X}$ . The predictions made by these calculations will be most reliable for the  $\text{C}_6\text{F}_5$ — frequencies and less reliable for the  $(\text{C}_6\text{F}_5)$ —X frequencies since one value of the C—X stretching constant and one value of the C—X deformation constant has been assumed throughout.

*Acknowledgements*—We are greatly indebted to the English Electric Company for the computing facilities so generously placed at our disposal and to Albright and Wilson (Mfg.) Company for financial support. One of us (D. S.) acknowledges the award of an I.C.I. Fellowship during the tenure of which this work was carried out.

## The vibrational spectra and assignments for $C_6F_5Cl$ , $C_6F_5Br$ and $C_6F_5I$

D. A. LONG and D. STEELE

Department of Chemistry, University College of Swansea

(Received 11 April 1963)

**Abstract**—The infra-red spectra of  $C_6F_5Cl$ ,  $C_6F_5Br$  and  $C_6F_5I$  and the Raman spectrum of  $C_6F_5Br$  are reported. Assignments are proposed for the in-plane fundamentals of these molecules.

IN A previous paper [1] we have reported calculations of the in-plane vibrational frequencies of some model pentafluorobenzenes of the type  $C_6F_5X$  in which the mass of X was taken successively as 35.5, 80 and 127. In these calculations the force constants have been transferred from hexafluorobenzene [2],  $C_6F_6$ , without modification so that the force constants associated with the C—X bond are taken to be the same as those for a C—F bond. The calculations therefore give the frequencies of hypothetical derivatives of hexafluorobenzene in which one fluorine is replaced by hypothetical isotopes of mass 35.5, 80 or 127. The frequencies calculated for these hypothetical derivatives will serve as a good guide to the frequencies of the real molecules of the type  $C_6F_5X$ . The twenty-one in-plane frequencies of such a system ( $11a_1 + 10b_1$ ) may be regarded as made up of ( $10a_1 + 9b_1$ ) for the  $(C_6F_5)$ —system and ( $1a_1 + 1b_1$ ) for the  $(C_6F_5)$ —X system. The frequencies for  $(C_6F_5)$ —in  $(C_6F_5)$ —(X) will differ from those for  $(C_6F_5)$ —in  $C_6F_6$  partly because of the mass of X and partly because of the different interactions between  $(C_6F_5)$ —and—(F) and  $(C_6F_5)$ —and—(X). The effect of mass will predominate and hence the calculations which take no account of changes in force constants should give good predictions of the actual frequencies in the  $(C_6F_5)$ —system in  $C_6F_5X$  molecules. In particular the calculations indicate the extent to which frequencies of individual modes are sensitive to change of mass. The frequencies of  $(C_6F_5)$ —(X) modes will differ from the frequencies of the  $(C_6F_5)$ —(F) modes because of changes in mass and changes in force constants. The force constant will be more important here and so the calculations, which only take account of mass change, will give zero order approximations to the observed frequencies of the  $(C_6F_5)$ —(F) modes.

The existence of these calculations makes it feasible to attempt assignments for some pentafluorobenzene derivatives. In this paper we consider in some detail the assignments of the in-plane vibrations of the following compounds;  $C_6F_5Cl$ ,  $C_6F_5Br$ ,  $C_6F_5I$ .

[1] D. A. LONG and D. STEELE, *Spectrochim. Acta* **19**, 1947 (1963)

[2] D. STEELE and D. H. WHIFFEN, *Trans Faraday Soc.* **56**, 5 (1960).

*Observed spectra*

The vibrational spectra of these compounds have not been recorded previously. The compounds were prepared at the University of Birmingham by NIELD *et al* [3]. The following vibrational spectra were obtained:  $C_6F_5Cl$ , infra-red spectra of the vapour and the liquid (4000–650  $cm^{-1}$ );  $C_6F_5Br$ , infra-red spectra of the vapour and the liquid (4000–400  $cm^{-1}$ ) and Raman spectrum of the liquid;  $C_6F_5I$ , infra-red spectrum of the liquid (5000–400  $cm^{-1}$ ). The infra-red spectra were recorded with a Perkin-Elmer 21 with NaCl prism and with a Grubb-Parsons single beam instrument employing a KBr prism. The precision of the infra-red frequencies is  $\pm 2 cm^{-1}$ . The Raman spectrum was obtained photographically using the Hilger E 612 spectrograph and E 614 camera. Qualitative polarization measurements were made using the method of polarized incident light. The precision of the Raman frequencies is  $\pm 2 cm^{-1}$  for strong sharp lines and somewhat less for weaker, more diffuse lines.

Figures 1, 2 and 3 give the infra-red spectra below 2000  $cm^{-1}$  of the liquids  $C_6F_5Cl$ ,  $C_6F_5Br$  and  $C_6F_5I$ . Table 1 gives the frequencies and approximate intensities of the infra-red bands of these liquids below 2000  $cm^{-1}$  together with the frequencies and qualitative intensities and polarizations of the lines observed in the Raman spectrum of liquid  $C_6F_5Br$ . We have limited the published details of the spectra and have listed the frequencies below 2000  $cm^{-1}$  since we are concerned only with the assignment of fundamentals. We have given details of the spectra of the liquids since it is only for this state that the frequencies are available for all three compounds.

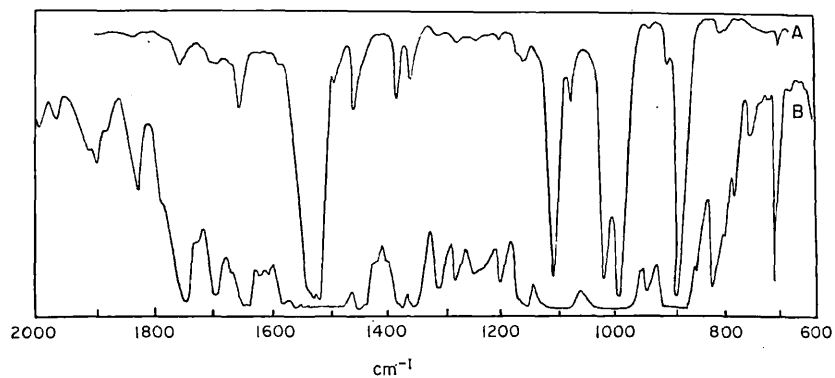
*Assignments*

The following discussion only deals in detail with  $C_6F_5Br$  for which the spectroscopic information is by far the most complete. The calculations predict that the majority of the vibrations will have very similar frequencies in  $C_6F_5Cl$ ,  $C_6F_5Br$  and  $C_6F_5I$  and hence most of the assignments in  $C_6F_5Cl$  and  $C_6F_5I$  follow automatically once they have been established in  $C_6F_5Br$ . Any discussion of the assignments in  $C_6F_5Cl$  and  $C_6F_5I$  will be confined to those which differ appreciably from those in  $C_6F_5Br$ .

*Class  $a_1$* 

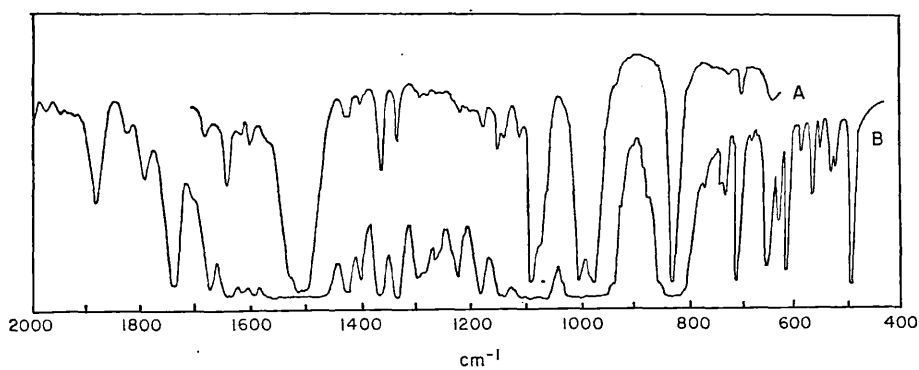
The polarization of the Raman lines leads to a ready identification of some of the  $a_1$  frequencies. The Raman spectrum of  $C_6F_5Br$  contains seven polarized lines at 1429, 835, 585, 524, 497, 361 and 241  $cm^{-1}$ . Six of these are reasonably strong and are certainly  $a_1$  fundamentals. The polarized line at 524  $cm^{-1}$  is weak and its designation is less certain. With the aid of the calculations we can associate these frequencies with particular modes. The calculations predict three  $a_1$  frequencies below 400  $cm^{-1}$  and since this is the lower limit of the infra-red measurements these frequencies can be identified only from the Raman spectrum. The predicted values of these low frequencies are 365, 279 and 255  $cm^{-1}$ . The highest of these frequencies is predominantly a ring deformation mode derived from an  $e_{2g}$  mode in  $C_6F_6$ . The two lower frequencies are predominantly C—F deformation modes derived from

[3] E. NIELD, R. STEPHENS and J. C. TATLOW, *J. Chem. Soc.* 166 (1959).



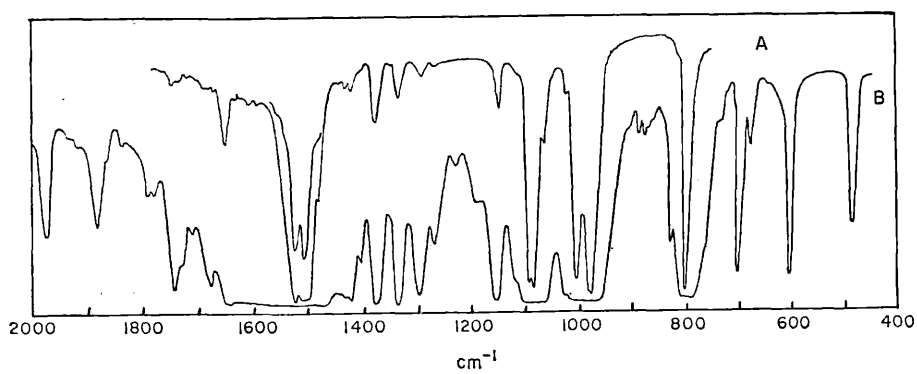
A = thin film, B = 0.2 mm.

Fig. 1. Infra-red spectra of  $C_6F_5Cl$  (liquid).



A = thin film, B = 0.2 mm.

Fig. 2. Infra-red spectra of  $C_6F_5Br$  (liquid).



A = thin film, B = 0.2 mm.

Fig. 3. Infra-red spectra of  $C_6F_5I$  (liquid).



Table 1. Frequencies ( $\text{cm}^{-1}$ ) below  $2000 \text{ cm}^{-1}$  in the infra-red spectra of  $\text{C}_6\text{F}_5\text{Cl}$ ,  $\text{C}_6\text{F}_5\text{Br}$  and  $\text{C}_6\text{F}_5\text{I}$  and the raman spectrum of  $\text{C}_6\text{F}_5\text{Br}$ 

$\text{C}_6\text{F}_5\text{Cl}$			$\text{C}_6\text{F}_5\text{Br}$				$\text{C}_6\text{F}_5\text{I}$			
I.R.	I	ass.	I.R.	I	Raman	Ass.	I.R.	I	Ass.	
1985	w		1987	m						
1961	w		1950	vw			1954	m		
			1925	vvw						
1904	w		1905	vvw			1908	vw		
1891	w						1891	vw		
1872	w		1877	m			1862	m		
							1844	vw		
1821	m		1815	vw			1815	vw		
							1773	w		
			1789	m			1760	w		
1743	vs		1739	s			1729	s		
1719	w									
1693	s		1703	w			1695	w		
1665	m		1675	vs	1671	w	1666	s		
1644	vvs	$a_1, b_1$	1639	vvs	1635	s. dp	$a_1, b_1$	1634	vvs	$a_1$
1615	m		1614	vs			1605	s		
1597	m		1595	vs			1590	s		
1576	m		1567	m	1579	w	1573	s		
1530	m								$b_1$	
1519	vs	$a_1, b_1$	1510	vvs	1511	w	$a_1, b_2$	1512	vvs	$a_1$
1509	m									
							1494	vvs		
							1476	vw		
1445	vs	$a_1$	1428	s	1429	s.p.	$a_1$	1432	s	$a_1$
					1421	m		1421	s	
			1400	s				1409	s	
								1391	s	
1370	vs		1366	vs				1365	vs	
1347	vs		1335	vs				1326	vs	
1311	s	$a_1$								
			1295	vs	1292	w	$a_1$	1286	vs	$a_1$
			1285	s						
1274	s		1268	s				1263	s	
1244	s		1238	s						
1219	m		1228	vs				1224	m	
1196	s		1186	vs				1189	m	
1162	s	$b_1$	1154	vs	1151	w	$b_1$	1149	vs	$b_1$
1153	s		1145	s						
			1119	vs				1113	vw	
1101	vvs	$a_1$	1093	vvs			$a_1$	1092	vvs	$a_1$
			1083	m				1083	vvs	
1075	m		1069	m				1064	m	
			1038	m						
			1025	vw				1026	w	
1013	vvs	$b_1$	1007	vvs			$b_1$	1005	vvs	$b_1$
986	vvs		979	vvs				977	vvs	
938	s		943	vs						
912	m		930	m						
			892	w				893	w	

Table 1 (contd.)

$C_6F_5Cl$			$C_6F_5Br$				$C_6F_5I$			
I.R.	I	ass.	I.R.	I	Raman	Ass.	I.R.	I	Ass.	
885	vvs	$a_1$	883	w			884	w		
			874	m			870	w		
			836	vvs	835	m.p.	$a_1$	836	m	
824	m									
806	w		811	vw			808	vvs	$a_1$	
790	w		781	m			792	v		
765	vw		765	w			772	vw		
750	vw		753	w			750	vw		
			746	m						
739	vw		740	m						
722	vw		717	s						
716	s	$b_1$	714	s			$b_1?$	714	s	$b_1$
700	vw		692	vw				694	w	
			668	vw				667	vw	
			657	m						
			637	w				600	s	
			618	m	616	w				
			595	w	585	s.p.	$a_1$			
			568	w						
			555	w						
			524	w	524	w.p.				
			518	w						
			498	s	497	s.p.	$a_1$	480	s	$a_1$
					443	m.dp.	$b_1$			
					379	m.dp.				
					361	m.p.	$a_1$			
					350	m.dp.				
					281	w?	$a_1$ and/or $b_1$			
					241	m.p.	$a_1$			
					157	m.dp.	$b_1$			

$e_{1u}$  and  $e_{2g}$  modes in  $C_6F_6$ . The Raman spectrum of  $C_6F_5Br$  contains only two polarized Raman lines below  $400\text{ cm}^{-1}$ . One at  $361\text{ cm}^{-1}$  is the ring deformation mode and that at  $241\text{ cm}^{-1}$  is one of the C—F deformation modes. The other C—F deformation mode expected around  $279\text{ cm}^{-1}$  cannot be identified with certainty but the weak Raman line of unknown polarization at  $281\text{ cm}^{-1}$  might arise from this mode although it is also a possible candidate for the  $b_1$  class.

The calculations suggest two ring modes in the region  $500\text{--}600\text{ cm}^{-1}$ . A ring stretch derived from an  $a_{1g}$  mode in  $C_6F_6$  has a predicted frequency of  $522\text{ cm}^{-1}$  and a ring deformation mode derived from a  $b_{1u}$  mode in  $C_6F_6$  has a calculated frequency of  $614\text{ cm}^{-1}$ . We associate the two polarized Raman lines at  $497$  and  $585\text{ cm}^{-1}$  with these two modes. The infra-red spectrum of  $C_6F_5Br$  has corresponding bands at  $498\text{ cm}^{-1}$  (strong) and at  $595\text{ cm}^{-1}$  (weak).

The polarized Raman line next highest in frequency is at  $835\text{ cm}^{-1}$  and there is a corresponding very intense infra-red band at  $836\text{ cm}^{-1}$ . We assign this to the  $(C_6F_5)\text{—Br}$  stretching mode. The calculations predicted  $942\text{ cm}^{-1}$  for this mode but the calculations assumed that the stretching force constant for the C—F bond was the same as that for the C—Br bond. The stretching force constant for the C—

halogen bond decreases from fluorine to iodine the biggest change coming between fluorine and chlorine. It is therefore to be expected that the observed frequencies for the  $(C_6F_5)$ -halogen stretching modes in  $C_6F_5Cl$ ,  $C_6F_5Br$  and  $C_6F_5I$  will all be less than the calculated values. The identification of the  $(C_6F_5)$ -Br stretching frequency is made possible by the existence of only one polarized Raman frequency in this region. Although no Raman frequencies are available for  $C_6F_5Cl$  and  $C_6F_5I$  the identification of the frequency in  $C_6F_5Br$  defines the regions of the infra-red spectra of  $C_6F_5Cl$  and  $C_6F_5I$  in which to look for the intense absorption associated with the  $(C_6F_5)$ -X stretching mode. In  $C_6F_5Cl$  we assign  $885\text{ cm}^{-1}$  to this mode and in  $C_6F_5I$  the assignment is  $808\text{ cm}^{-1}$ .

The remaining polarized Raman line has a frequency of  $1429\text{ cm}^{-1}$ . There is a corresponding strong infra-red band at  $1428\text{ cm}^{-1}$ . This is assigned to the symmetric C—F stretching mode derived from the  $a_{1g}$  mode of  $C_6F_6$  at  $1490\text{ cm}^{-1}$  and predicted by the calculations to lie at a lower frequency (calculated  $1469\text{ cm}^{-1}$ ) in  $C_6F_5Br$ .

In  $C_6F_6$  there are two doubly degenerate ring stretching modes one at  $1655\text{ cm}^{-1}$  ( $e_{2g}$ ) and one at  $1550\text{ cm}^{-1}$  ( $e_{1u}$ ). In  $C_6F_5Br$  these degeneracies will be removed but the calculations show that the splitting of the degeneracies will be very small. Thus  $1655\text{ cm}^{-1}$  in  $C_6F_6$  becomes  $1646\text{ cm}^{-1}$  ( $a_1$ ) and  $1653\text{ cm}^{-1}$  ( $b_1$ ) in  $C_6F_5Br$  and  $1530\text{ cm}^{-1}$  in  $C_6F_6$  becomes  $1520\text{ cm}^{-1}$  ( $a_1$ ) and  $1530\text{ cm}^{-1}$  ( $b_1$ ) in  $C_6F_5Br$ . In practice this splitting may be so small that only one frequency, assignable to both the  $a_1$  and  $b_1$  ring modes, is observed in one or both cases. An example of this occurs in  $C_6F_5H$  where  $1648\text{ cm}^{-1}$  is assigned to both the  $a_1$  and  $b_1$  modes derived from the  $e_{2g}$  modes of  $C_6F_6$ . The calculations show that the frequencies of these modes are essentially mass independent in the  $C_6F_5X$  molecules. The infra-red spectrum of each of these compounds shows two intense absorption bands of nearly constant frequency in this region:— $C_6F_5Cl$ ,  $1644$  and  $1519\text{ cm}^{-1}$ ;  $C_6F_5Br$ ,  $1639$  and  $1510\text{ cm}^{-1}$ ;  $C_6F_5I$ ,  $1634$  and  $1512\text{ cm}^{-1}$ . In each case we assign each frequency to one  $a_1$  and one  $b_1$  ring stretching mode. Support for this assignment is found by comparing the infra-red and Raman spectra of  $C_6F_5Br$ . The intense infra-red band at  $1639\text{ cm}^{-1}$  has an essentially coincident Raman line at  $1635\text{ cm}^{-1}$  which is strong but depolarized. There is no polarized Raman line in this region and since the  $a_1$  ring stretching mode would give a strong Raman line we must conclude that the line at  $1635\text{ cm}^{-1}$  arises from the coincidence of an  $a_1$  and a  $b_1$  mode of identical frequency. As the  $a_1$  line would be polarized and the  $b_1$  line depolarized the observed line would appear to be depolarized. The Raman spectrum of  $C_6F_5Br$  also contains a line at  $1511\text{ cm}^{-1}$  which is essentially coincident with the infra-red band at  $1510\text{ cm}^{-1}$ . The Raman line is weak and its polarization was not measured but it can be assigned to the other  $a_1$  and  $b_1$  ring stretching modes.

The two remaining  $a_1$  modes are both derived from C—F stretching modes in  $C_6F_6$ ,  $1157\text{ cm}^{-1}$  ( $e_{2g}$ ) and  $1323\text{ cm}^{-1}$  ( $b_{1u}$ ). In going from the  $D_{6h}$  symmetry of  $C_6F_6$  to the  $C_{2v}$  symmetry of  $C_6F_5Br$  the two-fold degenerate  $e_{2g}$  mode splits into one  $a_1$  and one  $b_1$  mode. The calculations show that the  $b_1$  mode in  $C_6F_5Br$  will have essentially the same frequency as the  $e_{2g}$  mode in  $C_6F_6$  but that the frequency of the  $a_1$  mode will be somewhat lower. On this basis we assign the infra-red band at  $1093\text{ cm}^{-1}$  to the  $a_1$  mode and the strong infra-red band at  $1154\text{ cm}^{-1}$  to the  $b_1$  mode. The

$b_1$  mode has a weak Raman counterpart at  $1151\text{ cm}^{-1}$  (depolarized) but no Raman counterpart of the  $a_1$  mode was observed. The last mode in this class should have a frequency only slightly lower than the value of  $1323\text{ cm}^{-1}$  assigned to it in  $C_6F_6$ . On this evidence we select the strong infra-red band at  $1295\text{ cm}^{-1}$  as the assignment for this mode. This is supported by the existence of a weak Raman line at  $1292\text{ cm}^{-1}$ .

#### Class $b_1$

Three assignments in this class have already been made in the course of the discussion of the  $a_1$  assignments. These are  $1639$ ,  $1510$  and  $1154\text{ cm}^{-1}$ . The calculations show that three modes should have frequencies below  $400\text{ cm}^{-1}$ , the lower limit of the infra-red measurements. The predicted values are  $297$ ,  $233$  and  $164\text{ cm}^{-1}$ . The Raman spectrum has two unassigned frequencies in this region. The medium strength depolarized line at  $157\text{ cm}^{-1}$  is certainly to be associated with the mode of lowest frequency in this class. It is derived from the  $b_{2u}$  mode of  $C_6F_6$  which occurs at  $208\text{ cm}^{-1}$ . In  $C_6F_6$  it is a pure C—F angle deformation mode but in  $C_6F_6Br$  it is to be described as partly C—F deformation and partly C—Br deformation. The weak Raman line at  $281\text{ cm}^{-1}$  could be assigned to this class also. In  $C_6F_6$  there is a degenerate ( $e_{1u}$ ) C—F angle deformation mode at  $315\text{ cm}^{-1}$ . On removal of the degeneracy in  $C_6F_5Br$  the calculations indicate that the  $a_1$  component will have a frequency around  $279\text{ cm}^{-1}$  and the  $b_1$  component a frequency at  $297\text{ cm}^{-1}$ . The Raman line at  $281\text{ cm}^{-1}$  could therefore be assigned either to the  $a_1$  component (as previously discussed) or to the  $b_1$  component. There is a slight preference for the latter as the line is so weak. No assignment can be put forward for the mode for which the calculated frequency is  $233\text{ cm}^{-1}$ . This mode is a mixture of C—Br and C—F angle deformations.

The ring angle deformation mode with the lowest frequency is well established at  $443\text{ cm}^{-1}$  in  $C_6F_6$  ( $e_{2g}$ ). The  $b_1$  component of this in  $C_6F_5Br$  according to the calculations should have almost the same frequency. This mode can therefore confidently be associated with the medium strength, depolarized Raman line at  $443\text{ cm}^{-1}$ .

The C—F deformation mode of  $a_{2g}$  symmetry occurs at  $691\text{ cm}^{-1}$  in  $C_6F_6$ . The calculations show that the corresponding mode which has  $b_1$  symmetry in the  $C_6F_5X$  molecules is not mass sensitive. The choice therefore lies between a strong infra-red band at  $714\text{ cm}^{-1}$  or the very weak infra-red band at  $692\text{ cm}^{-1}$ .

A feature of the infra-red spectrum of each of these compounds is the appearance of two very strong bands around  $1000\text{ cm}^{-1}$ . In  $C_6F_5Br$  the two bands are at  $1007$  and  $979\text{ cm}^{-1}$ . The two bands arise from Fermi resonance. One component is a C—F stretching mode with  $b_1$  symmetry for which the calculated frequency is  $1005\text{ cm}^{-1}$ . The other component could be the combination band  $714 (b_1) + 281 (a_1) = 995 (b_1)$ .

The remaining  $b_1$  mode, is a ring stretching mode for which the predicted frequency is  $1259\text{ cm}^{-1}$ . The infra-red band at  $1268\text{ cm}^{-1}$  is assigned to this mode.

The assignments for  $C_6F_5Cl$ ,  $C_6F_5Br$  and  $C_6F_5I$  are included in Table 1.

*Acknowledgements*—One of us (D. S.) acknowledges the award of an I.C.I. Fellowship during the tenure of which this work was carried out. The spectroscopic measurements were made at Birmingham by one of us (D. S.).

## Spectroscopic and thermodynamic studies of pyridine compounds—VI

### Force constants and atomic displacements for pentafluoropyridine

D. A. LONG and D. STEELE

Department of Chemistry, University College of Swansea

(Received 11 April 1963)

**Abstract**—Details of a force field for pentafluoropyridine based on force constants transferred from  $C_6F_6$  are presented. The calculated frequencies and atomic displacements for both the in-plane and out-of-plane vibrations are listed.

THE infra-red and Raman spectra of pentafluoropyridine  $C_5F_5N$  have recently been reported and assignments of the fundamental vibrational frequencies made [1]. The assignments were made by using infra-red band shapes and polarization of Raman lines, and by comparison with  $C_6F_5H$  and with  $C_6F_6$ . The assignments were supported by calculations of the frequencies using a force field transferred from  $C_6F_6$ . Details of these calculations are presented here.

Pentafluoropyridine was assumed to be planar and to have  $C_{2v}$  symmetry. It thus has nineteen in-plane vibrations ( $10a_1 + 9b_1$ ) and eight out-of-plane vibrations ( $3a_2 + 5b_2$ ). The following parameters were assumed: C—C and C—N bond lengths 1.40 Å; C—F bond length 1.30 Å; all interbond angles 120°.

The in-plane force field had the form

$$\begin{aligned}
 2V_{\text{in-plane}} = & f_r \sum \Delta r_i^2 + 2f_{(rr)_0} \sum \Delta r_i \Delta r_{i+1} + 2f_{(rr)_m} \sum \Delta r_i \Delta r_{i+2} & (1) \\
 & + 2f_{(rr)_p} \sum \Delta r_i \Delta r_{i+3} + f_R \sum \Delta R_i^2 + 2f_{(RR)_0} \sum \Delta R_i \Delta R_{i+1} \\
 & + 2f_{(RR)_m} \sum \Delta R_i \Delta R_{i+2} + 2f_{(RR)_p} \sum \Delta R_i \Delta R_{i+3} \\
 & + f_\alpha \sum (R \Delta \alpha_i)^2 + 2f_{(\alpha\alpha)_0} \sum (R \Delta \alpha_i R \Delta \alpha_{i+1}) \\
 & + f_\beta \sum (r \beta_i)^2 + 2f_{(\beta\beta)_0} \sum r \beta_i r \beta_{i+1} + 2f_{(\beta\beta)_m} \sum r \beta_i r \beta_{i+2} \\
 & + 2f_{(\beta\beta)_p} \sum r \beta_i r \beta_{i+3} + 2f_{(rR)_0} \sum \Delta r_i (\Delta R_i + \Delta R_{i-1}) \\
 & + 2f_{(rR)_m} \sum \Delta r_i (\Delta R_{i+1} + \Delta R_{i-2}) + 2f_{(rR)_p} \sum \Delta r_i (\Delta R_{i+2} + \Delta R_{i-3}) \\
 & + 2f_{(r\alpha)} \sum r_i R \Delta \alpha_i + 2f_{(r\alpha)_0} \sum R \alpha_i (\Delta r_{i+1} + \Delta r_{i-1}) \\
 & + 2f_{(r\beta)_0} \sum r \Delta \beta_i (\Delta r_{i+1} - \Delta r_{i-1}) + 2f_{(r\beta)_m} \sum r \Delta \beta_i (\Delta r_{i+2} - \Delta r_{i-2}) \\
 & + 2f_{(R\alpha)} \sum R \alpha_i (\Delta R_i + \Delta R_{i-1}) \\
 & + 2f_{(R\beta)_0} \sum r \beta_i (\Delta R_i - \Delta R_{i-1}) + 2f_{(R\beta)_m} \sum r \beta_i (\Delta R_{i+1} - \Delta R_{i-2}) \\
 & + 2f_{(R\beta)_p} \sum r \beta_i (\Delta R_{i+2} - \Delta R_{i-3}) + 2f_{\alpha\beta} \sum r \beta_i (R \alpha_{i+1} - R \alpha_{i-1})
 \end{aligned}$$

The internal co-ordinates are defined in Fig 1. The values of the valence force constants used were transferred directly without modification from  $C_6F_6$  [2] and are given in Table 1.

[1] D. A. LONG and R. T. BAILEY, *Trans. Faraday Soc.* **59**, 599 (1963).

[2] D. STEELE and D. H. WHIFFEN, *Trans. Faraday Soc.* **56**, 5 (1960).

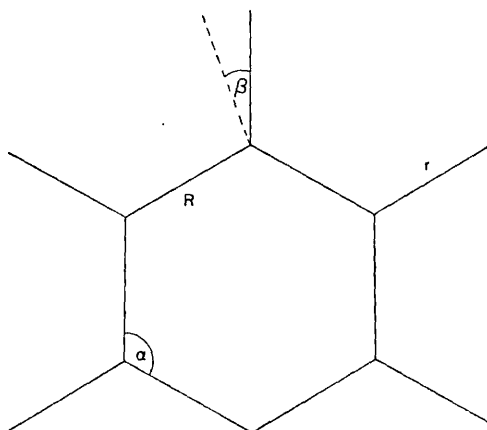


Fig 1. Internal co-ordinates.

Table 1. In-plane force constants (md/Å)

$f_R$	5.478	$f_{(\alpha\alpha)_o}$	0.141
$f_{(RR)_o}$	0.660	$f_{\alpha R}$	-0.180
$f_{(RR)_m}$	0.071	$f_{(rR)_o}$	0.708
$f_{(RR)_p}$	0.459	$f_{(rR)_m}$	0.001
$f_r$	7.405	$f_{(rR)_p}$	-0.263
$f_{(rr)_o}$	0.087	$f_{(\beta R)_o}$	0.112
$f_{(rr)_m}$	-0.050	$f_{(\beta R)_m}$	-0.041
$f_{(rr)_p}$	0.032	$f_{(\beta R)_p}$	-0.033
$f_\beta$	0.826	$f_{\alpha r}$	-0.076
$f_{(\beta\beta)_o}$	0.072	$f_{(\alpha r)_o}$	0.344
$f_{(\beta\beta)_m}$	-0.093	$f_{(\beta\alpha)_o}$	-0.103
$f_{(\beta\beta)_p}$	0.002	$f_{(\beta r)_o}$	0.170
$f_\alpha$	1.030	$f_{(\beta r)_m}$	-0.054

The out-of-plane force field had the form

$$\begin{aligned}
 2V_{\text{Out-of-plane}} = & f_\gamma r^2 \sum \gamma_i^2 + 2f_{(\gamma\gamma)_o} r^2 \sum \gamma_i \gamma_{i+1} + 2f_{(\gamma\gamma)_m} r^2 \sum \gamma_i \gamma_{i+2} \\
 & + 2f_{(\gamma\gamma)_p} r^2 \sum \gamma_i \gamma_{i+3} + f_\delta R^2 \sum \delta_i^2 + 2f_{\delta\delta} R^2 \sum \delta_i \delta_{i+1} \\
 & + 2f_{(\gamma\delta)_o} r R \sum \gamma_i (\delta_{i-1} - \delta_i) + 2f_{(\gamma\delta)_m} r R \sum \gamma_i (\delta_{i-2} - \delta_{i+1})
 \end{aligned} \quad (2)$$

The co-ordinates  $r\gamma$  and  $R\delta$  are associated with out-of-plane C—F wagging motions and torsions about C—C or C—N bonds respectively [3]. The out-of-plane valence constants are given in Table 2 and were calculated from the out-of plane constants used in  $C_6F_6$ . In  $C_6F_6$  the torsional motions were defined in terms of the  $\phi$  co-ordinate by BELL [4] and used by WHIFFEN [5] in benzene. It is not possible to use this co-ordinate with the ring system of  $C_5F_5N$  where there is no substituent at one ring atom. For this reason the alternative co-ordinate  $\delta$  was used. The

[3] D. A. LONG, F. S. MURFIN and E. L. THOMAS, *Trans. Faraday Soc.* **59**, 12 (1963).

[4] R. P. BELL, *Trans. Faraday Soc.* **41**, 293 (1945).

[5] D. H. WHIFFEN, *Phil. Trans.* **A248**, 131 (1955).

Table 2. Out-of-plane force constants (md/Å)

$f_\gamma$	0.423
$f_{(\gamma\gamma)_o}$	-0.167
$f_{(\gamma\gamma)_m}$	0.080
$f_{(\gamma\gamma)_p}$	-0.048
$f_\delta$	0.320
$f_{\delta\delta}$	-0.004
$f_{(\gamma\delta)_o}$	-0.179
$f_{(\gamma\delta)_m}$	0.078

relationships between the force constants in the two systems are as follows:

$$\begin{aligned}
 f_\delta &= 4F_\phi \\
 f_{\delta\delta} &= 4F_{\phi\phi} \\
 f_\gamma &= F_\gamma + 8 \cdot 3^{-1} \rho^{-2} (F_\phi - F_{\phi\phi}) - 8 \cdot 3^{-1/2} \rho^{-1} F_{(\gamma\phi)_o} \\
 f_{(\gamma\gamma)_o} &= F_{(\gamma\gamma)_o} + 4 \cdot 3^{-1/2} \rho^{-1} (F_{(\gamma\phi)_o} - F_{(\gamma\phi)_m}) - 4 \cdot 3^{-1} \rho^{-2} (F_\phi - 2F_{\phi\phi}) \\
 f_{(\gamma\gamma)_m} &= F_{(\gamma\gamma)_m} + 4 \cdot 3^{-1/2} \rho^{-1} F_{(\gamma\phi)_m} - 4 \cdot 3^{-1} \rho^{-2} F_{\phi\phi} \\
 f_{(\gamma\gamma)_p} &= F_{(\gamma\gamma)_p} \\
 f_{(\gamma\delta)_o} &= 2F_{(\gamma\phi)_o} + 4 \cdot 3^{-1/2} \rho^{-1} (F_{\phi\phi} - F_\phi) \\
 f_{(\gamma\delta)_m} &= 2F_{(\gamma\phi)_m} - 4 \cdot 3^{-1/2} \rho^{-1} F_{\phi\phi}
 \end{aligned} \tag{3}$$

The vibrational frequencies (Table 3) and atomic displacements (in-plane Fig. 2, out-of-plane, Fig. 3) were calculated on a computer using the procedure

Table 3. Calculated and assigned frequencies (cm<sup>-1</sup>)

Class.	Calc.	Ass.	Class.	Calc.	Ass.
$a_1$	1629	1650	$b_2$	718	736
	1510	1529		659	620
	1404	1420		376	353
	1278	1285		236	224
	1080	1077		202	174
	741	694	$a_2$	594	570
	589	593		371	428
	478	476		175	174
	319	310			
	265	273			
$b_1$	1639	1650			
	1487	1492			
	1251	1285			
	1150	1172			
	970	983			
	632	706 or 620			
	438	457			
	291	273 or 310			
	225	224			

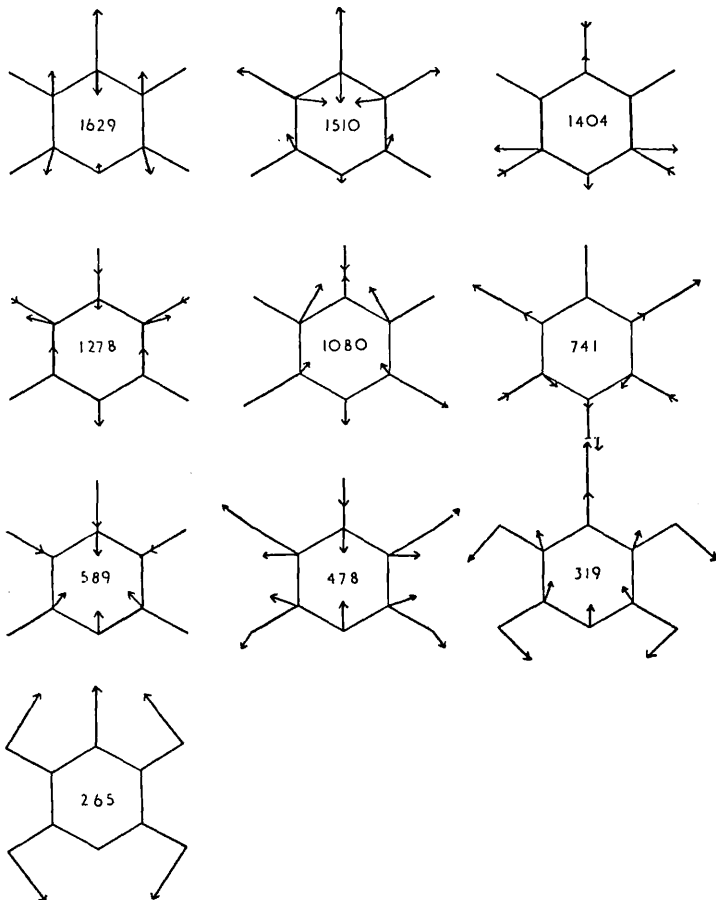
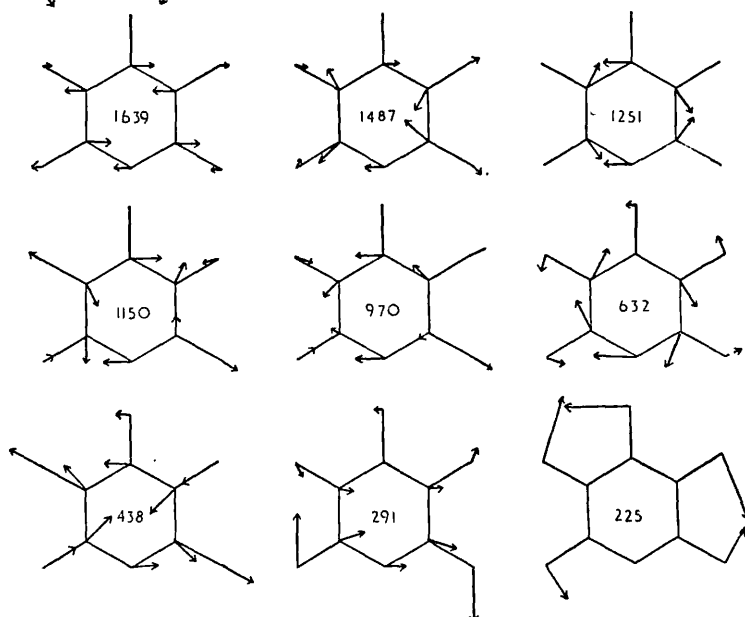
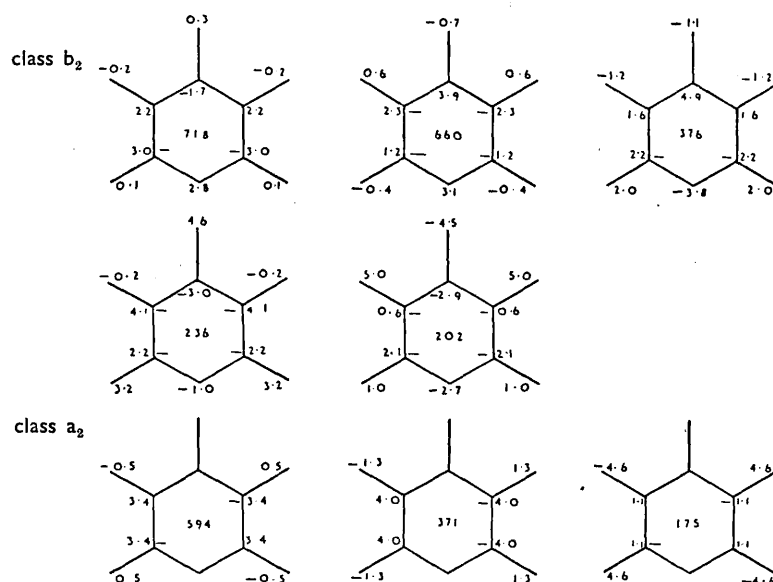
class  $a_1$ class  $b_1$ 

Fig. 2. In-plane atomic displacements (X40)



Fig 3. Out-of-plane atomic displacements ( $10^{-2}$  Å)

described by LONG [6]. The assigned vibrational frequencies are also included in Table 3 for comparison. The agreement between calculated and observed frequencies is very satisfactory for the in-plane modes. The average percentage error is 1.8 per cent in the  $a_1$  class and 2.4 per cent in the  $b_1$  class. The error only exceeds 3 per cent for three vibrations. The  $b_1$  mode with a calculated frequency of  $291\text{ cm}^{-1}$  shows a large percentage error of +8.6 or -8.6 per cent depending on whether the assigned frequency is  $310$  or  $273\text{ cm}^{-1}$ , but the absolute error is only  $\pm 18\text{ cm}^{-1}$ . If this mode is excluded from the averaging of the class  $b_1$  percentage errors the mean error drops to 1.6 per cent. The other mode with a relatively large discrepancy between the calculated and observed frequencies is in the  $a_1$  class. The ring mode assigned at  $694\text{ cm}^{-1}$  has a calculated frequency of  $741\text{ cm}^{-1}$ . The agreement between calculated and observed frequencies is somewhat less satisfactory for the out-of-plane modes but the calculations are nevertheless helpful in making assignments.

The calculated forms of the modes bear a marked resemblance to those for  $\text{C}_6\text{F}_5\text{H}$ . This is to be expected for the  $a_1$  class since the C—H stretching mode will have no appreciable interaction with the other  $a_1$  modes. It is more surprising in the  $b_1$  class where an appreciable mixing of the CH deformation with modes of similar frequency might have been expected.

*Acknowledgements*—We are greatly indebted to the English Electric Company for the extensive computing facilities so generously made available to us and to Albright and Wilson (Mfg.) Company Limited for financial support. D. S. acknowledges the award of an I.C.I. Fellowship during the tenure of which this work was carried out.

[6] D. A. LONG, R. B. GRAVENOR and M. WOODGER, *Spectrochim. Acta* **19**, 937 (1963).

A 14

**THE ABSOLUTE INTENSITIES OF  
INFRARED ABSORPTION BANDS**

BY  
**D. STEELE**

---

Reprinted from Quarterly Reviews  
1964, Vol. XVIII, No. 1

London  
The Chemical Society

## THE ABSOLUTE INTENSITIES OF INFRARED ABSORPTION BANDS

By D. STEELE

(DEPARTMENT OF CHEMISTRY, ROYAL HOLLOWAY COLLEGE, ENGLEFIELD GREEN, SURREY)

THE intensity of absorption of infrared radiation by a given system is intimately related to the electronic charge movements during the associated vibrational quantum transition. Molecular deformations must involve bond deformations and are very unlikely to affect any but the valence-shell electrons. Consequently, in principle, absorption intensities could yield not only information on charge distributions in molecules but also information on the manner in which the valence electrons redistribute themselves during molecular deformations. Since chemical reactions, of necessity, involve specific bond deformations, such information could lead to a deeper understanding of reaction mechanisms. The equilibrium charge distributions can lead to a better understanding of the bonding.

During recent years a large number of publications on the theory, measurement, and interpretation of the absolute intensities of infrared absorption bands has appeared in the literature. Many serious difficulties still beset the spectroscopist in the interpretation of the results, but the information gleaned has reached the state where a survey of the gains, the difficulties, and the prospects can be usefully made.

**Experimental Techniques.**—It has proved to be extremely difficult to make accurate absolute measurements of absorption intensities. The intensities are usually defined as

$$I_k = 1/cl \int \ln[(I_0)_\nu / (I)_\nu] d \ln \nu \quad (1)$$

where  $c$  is the absorbent concentration,  $l$  is the path length of the beam through the absorbing material,  $(I_0)_\nu$  and  $(I)_\nu$  are the initial and final intensities of the beam of frequency  $\nu$  (expressed in  $\text{cm.}^{-1}$  in all subsequent equations), and the integration is over the complete band. Such a definition follows readily from the usual exponential law of absorption. The experimental difficulties were first made apparent by the early measurements of Bourgin<sup>1</sup> and Bartholomé.<sup>2</sup> Independently they measured the intensity of the vibration-rotation band of hydrogen chloride in the gas phase and obtained results which differed by a factor of four. The major reason for this was that, for finite slit-widths, the beam is not monochromatic and consequently the measured fractional absorption of the sample,  $[(T_0 - T)/T_0]_\nu$ , at a given frequency setting,  $\nu$ , generally differs from the true transmission in such a way that the measured absorption value is too low. Bourgin,<sup>3</sup> Bartholomé,<sup>2</sup> Penner and Weber,<sup>4</sup> Wilson and Wells,<sup>5</sup> and others

<sup>1</sup> D. G. Bourgin, *Phys. Rev.*, 1927, 29, 794; *ibid.*, 1928, 32, 237.

<sup>2</sup> E. Bartholomé, *Z. phys. Chem.*, 1933, b23, 131.

<sup>3</sup> D. G. Bourgin, *Phys. Rev.*, 1928, 31, 503.

<sup>4</sup> S. S. Penner and D. Weber, *J. Chem. Phys.*, 1951, 19, 801, 817, 974, *ibid.*, 1953, 21, 649.

<sup>5</sup> E. B. Wilson and A. J. Wells, *J. Chem. Phys.*, 1946, 14, 578.

have investigated the conditions under which these two values approach one another and how the true absorption can be evaluated with an instrument of limited resolving power. In the procedure of Wilson and Wells the measured integrated optical density  $\int \log_{10} (T_0/T)_\nu d \ln \nu$ , divided by the concentration, is graphed against the concentration and the plot extrapolated to zero concentration. It was shown that the limiting value of the integral for zero concentration is equal to  $\int \log_{10} (I_0/I)_\nu d \ln \nu$  if (a) the incident intensity,  $I_0$ , does not vary over the slit-width, and (b) the resolving power is high compared with the variations in the absorption coefficient.

In Bourgin's method  $[\int (T_0/T)_\nu d \nu]/c$  is graphed against  $c$  and the ratio extrapolated, as in the Wilson-Wells technique, to zero concentration. However the curvature of the plot is far greater and the extrapolation consequently less accurate.

Since the aim of absorption intensity measurements is usually to study intramolecular properties, it is necessary to carry out studies on the gaseous phase where intermolecular interactions are reduced to a minimum. Unfortunately, the removal of intramolecular interactions results in sharp vibrational-rotational absorption lines. As a consequence condition (b) is difficult to attain. In order that this condition should be satisfied the rotational bands must be collision-broadened by adding a high pressure of a chemically inert, non-absorbing gas, or, for the study of weak absorption bands, by self-broadening at high pressures. The pressure-broadening is considered to be sufficient when an increase of total pressure produces no further change in the molecular extinction coefficient,  $\epsilon = 1/cl \log_{10} (I_0/I)_{\max}$ . However, even when the individual rotational lines are sufficiently broadened to yield an overall smooth absorption curve, the band contour may still have sufficiently steep gradients to result in low measured values of the absorbance. This is particularly the case with bands having strong sharp  $Q$  branches (corresponding to no change in the rotational quantum number,  $J$ ) such as the out-of-plane deformation bands in aromatic systems. The pressure required to produce broad  $Q$  branches may be excessively high, and it is to be noted that in such cases the extrapolation procedure still may not be strictly valid if condition (b) has not been fully met. Consequently the use of instruments of high resolving power is really required in such cases.

At very high pressures the molecule is being subjected to excessive collisional perturbations which are often undesirable. Thus it has been shown that absorption by the infrared-inactive  $a_{1g}$  mode of methane can be induced in this manner,<sup>6</sup> and many examples are now known of simultaneous transitions in mixed gases at high pressures.<sup>7</sup> In a simultaneous transition, absorption occurs at a frequency  $\nu_a \pm \nu_b$ , where  $\nu_a$  and  $\nu_b$  are transition frequencies for two different molecules and can be for two different

<sup>6</sup> R. Coulon, B. Oksengorn, J. Robin, and B. Vodar, *J. Phys. Radium*, 1953, 14, 63.

<sup>7</sup> H. L. Welsh, M. F. Crawford, J. C. F. McDonald, and D. A. Chisholm, *Phys. Rev.*, 1951, 83, 1264; J. Fahrenfort and J. A. A. Ketelaar, *J. Chem. Phys.*, 1954, 22, 1631.

chemical species. Such evidence indicates that pressure-broadening must be treated cautiously, especially when dealing with weak bands and easily polarisable molecules.

The sources of error in the Wilson–Wells and Bourgin procedures are so serious that efforts have been made to find alternative techniques. The dispersion of infrared rays has proved to be a very valuable tool in this connection since a vibrating electric moment in a molecule gives a contribution to the refractive index. Molecular vibrations are separable into normal modes each of which makes a contribution to the refractive index,  $n$ , of

$$\Delta_i (n - 1) = \frac{N}{6\pi^2 c} \left( \frac{\partial \mu}{\partial Q_i} \right)^2 \left/ \nu_i^2 - \nu^2 \right., \quad (2)$$

where  $N$  is the number of molecules per ml.,  $\mu$  is the molecular dipole moment,  $Q_i$  is the  $i$ th normal co-ordinate,  $\nu_i$  is the frequency of the corresponding vibration and  $\nu$  is that of the incident light (in  $\text{cm.}^{-1}$ ). (This formula, known as the Kramers–Heisenberg formula, assumes that the absorption line is infinitely narrow, and has to be modified slightly for finite line widths).

The infrared absorption intensity of a given fundamental band has been shown to be equal to

$$\Gamma_i = \frac{1}{\nu_i} \frac{N\pi}{3c} \left( \frac{\partial \mu}{\partial Q_i} \right)^2. \quad (3)$$

(This formula is derived neglecting rotational quantisation. An exact summation of intensity over the rotational components of a parallel band of a symmetric rotor molecule<sup>8</sup> leads to a correction factor equivalent to multiplying the right-hand side of (3) by

$$1 + \frac{2 B c [1 + \exp(-h\nu_0/kT)]}{\nu [1 - \exp(-h\nu_0/kT)]}$$

$B$ , the rotational constant, is equal to  $h/8\pi^2 c I_B$ , where  $I_B$  is the moment of inertia perpendicular to the axis of the top, and  $c$  is the velocity of light. This factor is unlikely to lead to an error exceeding 5% in  $(\partial\mu/\partial Q)^2$ , and is usually neglected on the excuse that the experimental uncertainty is generally of the same order of magnitude.)

Thus the vibrational contribution to the refractive index is intimately related to the infrared absorption intensity, and, in fact, these two phenomena are manifestations of the same property. Consequently, absolute infrared absorption intensities can be deduced from dispersion studies. The particular advantage of the dispersion method, as can be seen from equation (2), is that even for infinitely narrow absorption lines the change of the refraction with frequency is quite gradual. A typical refraction spectrum due to the  $R_2-0$  bands of  $\text{H}^{35}\text{Cl}$  and  $\text{H}^{37}\text{Cl}$  is shown in Fig. 1,<sup>9</sup>

<sup>8</sup> B. L. Crawford and H. L. Dinsmore, *J. Chem. Phys.*, 1950, 18, 1682.

<sup>9</sup> F. Legay, *Rev. Opt. (theor. instrum.)*, 1958, 37, 11.

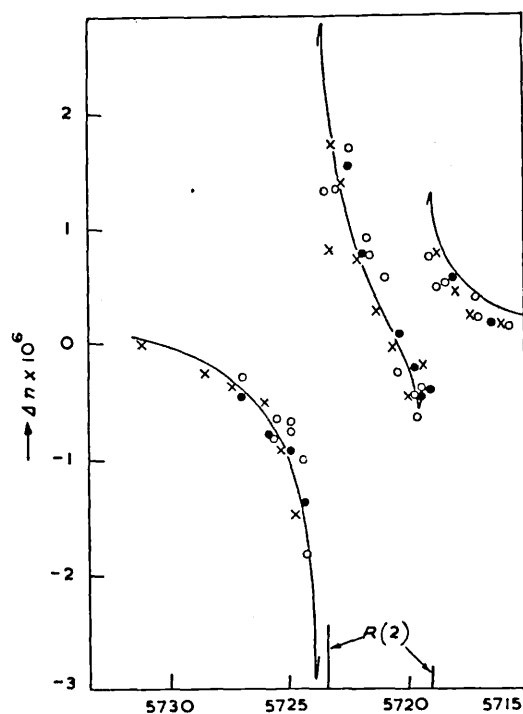


FIG. 1. The vibration-rotation contribution to the refractive index by the  $R(2)$  bands of the 2-0 vibrational transitions of  $\text{H}^{35}\text{Cl}$  and  $\text{H}^{37}\text{Cl}$ . The vertical lines indicated as  $R(2)$  represent the relative intensities of the corresponding absorption lines.

and is compared with the corresponding absorption curve. It can be seen that the distance between opposite branches of the refraction curve is a function of the absorption intensity. The technique is only suitable, at present, for simple molecules with well-separated strong absorption bands. This is a very severe restriction, but fortunately it is for such molecules that the Wilson-Wells procedure is most unsuitable. The results of the dispersion measurements generally compare quite favourably with those of the best absorption measurements and are usually, though by no means always, higher than their Wilson-Wells counterparts. An excellent summary of measurements up to 1960 is given in ref. 10.

Another recent technique capable of giving relatively accurate results is the curve-of-growth method.<sup>11</sup> This involves making measurements at different path-lengths and allows the error due to finite slits to be eliminated if the band shape is known. It can be applied only if the individual rotational lines can be resolved, which seriously restricts its applicability. Where it can be applied, it is usual to assume that the lines can be des-

<sup>10</sup> J. H. Jaffé, "Advances in Spectroscopy," Interscience, New York, 1961, Vol. 2, p. 263.

<sup>11</sup> S. S. Penner and H. Aroeste, *J. Chem. Phys.*, 1955, **23**, 2244.

cribed by the Lorentzian function. In such cases the technique would be expected to be of superior accuracy to the Wilson-Wells procedure. Consequently there was a great deal of consternation when the intensity of the  $670\text{ cm.}^{-1}$  band of carbon dioxide was measured in this way and a result obtained which was 50% higher than previous results.<sup>12</sup> As pointed out by Kaplan and Eggers,<sup>12</sup> this  $670\text{ cm.}^{-1}$  band is an extremely difficult band to study as far as the Wilson-Wells procedure is concerned, since: (a) it has a great deal of its intensity concentrated in a sharp  $Q$  branch (half-width, *ca.*  $0.35\text{ cm.}^{-1}$ ); (b) to measure it, it is necessary to remove absorption due to atmospheric carbon dioxide; and (c) it lies in a range of the spectrum where sodium chloride prisms begin to absorb appreciably and where the dispersion of potassium bromide prisms is low. This means that all the serious problems characteristic of this technique are in force for this case. Crawford and his co-workers<sup>13</sup> have remeasured the intensity by the Wilson-Wells procedure, exercising great care to overcome these problems, and have obtained a result very close to that of the curve-of-growth method (see Table 1). Also they pointed out that calcula-

TABLE 1. *Measured intensities of  $15\mu$  band of carbon dioxide.*

Ref.	15	16	17	18	12	13
Method	C-o-G	W-W	W-W	D	C-o-G	W-W
Intensity ( $10^3\text{cm.}^2/\text{mole}$ )	7.40	6.28	5.41	6.02	8.07	8.09

C-o-G, curve-of-growth. W-W, Wilson-Wells. D, dispersion.

tions made by Kostkowski and Bass<sup>14</sup> on the functional dependence of the errors in measuring intensities of individual rotational lines should be applicable to measurements on sharp  $Q$  branches. Using Kostkowski and Bass's results and estimating the pressure-broadened line-widths from collision theory, they showed that the pressure-broadening in previous determinations of the intensity (at total pressures of up to 5 atm.) had been inadequate. At the pressures of about 68 atm. that they had employed, the error resulting from slit-widths should be negligible. Also they had failed to observe any induced absorption. These careful measurements indicate that the Wilson-Wells procedure is capable of reasonable accuracy (within 2–3%) if sufficient care is exercised.

**Interpretation of Results.**—The interpretation of the measured intensities in terms of bond properties is best appreciated by considering what can be deduced, with and without assumptions, from the intensity measurements. Equation (3) is derived on the assumption that the dipole moment,  $\mu$ , can

<sup>12</sup> L. D. Kaplan and D. F. Eggers, *J. Chem. Phys.*, 1956, **25**, 876.

<sup>13</sup> J. Overend, M. J. Youngquist, E. C. Curtis, and B. Crawford, *J. Chem. Phys.*, 1959, **30**, 532.

<sup>14</sup> H. J. Kostkowski and A. M. Bass, *J. Opt. Soc. Amer.*, 1956, **46**, 1060.

<sup>15</sup> L. D. Kaplan, *J. Chem. Phys.*, 1947, **15**, 809.

<sup>16</sup> A. M. Thorndike, *J. Chem. Phys.*, 1947, **15**, 868.

<sup>17</sup> D. F. Eggers and B. L. Crawford, *J. Chem. Phys.*, 1951, **19**, 1554.

<sup>18</sup> Values reviewed by O. Fuchs, *Z. Physik*, 1927, **46**, 519.

be expanded as a Taylor series in terms of displacements from the equilibrium positions, and all but the first derivatives can be neglected. That is

$$\mu = \mu_0 + \sum_k (\partial\mu/\partial Q_k)_0 Q_k + \text{higher terms (negligible)}.$$

$Q_k$  represents the molecular distortion in the vibration  $k$  (*i.e.*, normal co-ordinate for  $k$ ). This is the assumption of electrical harmonicity which is true only to a first approximation. The intensity of infrared combination bands ought to be zero in this approximation. This is certainly not so, but the intensities are usually far less than those of fundamentals, unless a combination band gains intensity from a fundamental of the same symmetry, by resonance. This confirms the validity of the assumption. The error involved is certainly much less than the present experimental errors and those, which are to be discussed later, arising from the uncertainty in the normal co-ordinate  $Q$ .

If the molecule has any symmetry, the vibrations can be separated into independent groups, each group being characterised by the behaviour of its constituents towards the symmetry elements. This means that the normal co-ordinates,  $Q_k$ , separate according to this behaviour. For example, in carbon dioxide there are two non-degenerate vibrations and one doubly degenerate vibration. The linear molecule has three planes of symmetry, mutually perpendicular, and passing through the carbon nucleus. This also implies a centre of symmetry and rotation axes, but a consideration of the symmetry of the vibrations, with respect to the planes, suffices for our present purpose. Each vibration must be symmetric or antisymmetric with respect to a particular plane. If a vibration is symmetric with respect to the  $XZ$  and  $YZ$  planes (axes defined in Fig. 2), then

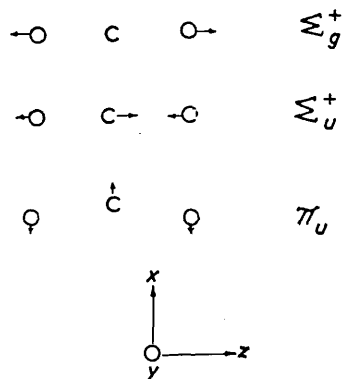


FIG. 2. The vibrational modes of carbon dioxide, and the definition of the cartesian axes.

clearly this cannot involve movements of the nuclei in the  $Z$  direction. Consequently, only CO stretching motions belong to the symmetry classes involving these symmetry characteristics. In addition, the CO stretching



vibrations must be symmetric or antisymmetric with respect to the  $XY$  plane. This means that the CO bonds must vibrate either in phase (symmetric stretch) or out of phase (antisymmetric stretch). Similar reasoning shows that the only deformation which can be antisymmetric with respect to either the  $XZ$  or the  $YZ$  plane is that of the O-C-O angle. Thus in this simple case, the normal co-ordinates are, apart from normalisation factors,  $\Delta r_1 + \Delta r_2$ ,  $\Delta r_1 - \Delta r_2$ , and  $\Delta\alpha$ . In general the symmetry of  $Q_k$ , and hence of  $\partial\mu/\partial Q_k$ , is known, but in solving for the dipole gradients from the measured intensities, using equation (3), there are sign ambiguities arising from taking the square root of the intensities. Furthermore, the exact form of the vibrations,  $Q_k$ , must be determined before any further interpretation of the gradients is possible. That is, it is necessary to obtain a relationship between the normal co-ordinates,  $Q$ , and a set of co-ordinates, such as cartesian, which are defined with respect to the molecular axes. Provided that the potential energy can be expressed as a function of all possible distortions of the molecule, molecular-vibration theory will yield the required relationship as well as the vibration frequencies. In order to know the potential energy it is sufficient to know the force field, *i.e.*, the force constants connecting all atoms in the molecule. Unfortunately, these are known with precision for very few molecules. A simple example is that for the harmonic oscillator, for which the vibrational frequency,  $\nu$ , is given by

$$\nu = \frac{1}{2\pi} \sqrt{k/\mu} \text{ and } V = \frac{1}{2}kq^2, \quad (4)$$

where  $k$  is the force constant for the distortion,  $q$ , and  $\mu$  is the reduced mass of the system. Such equations describe, to a first approximation, the vibrational motions of a diatomic molecule. Purely theoretical approaches to evaluating the force constants of the system are impossible at present, except for the simplest of molecules. Force constants have been calculated for a number of simple systems such as  $\text{LiH}^{19}$ , C-H,<sup>20</sup>  $\text{CH}_4$  (C-H stretch),<sup>21</sup> and  $\text{O}_2$ .<sup>22</sup> Except for diatomic molecules, there are more quadratic force constants than fundamental vibrational frequencies. Thus for the non-linear triatomic system  $\text{XYX}$  a complete description of the potential energy arising from molecular deformations requires a knowledge of four force constants—those for the X-Y stretch, the  $\text{XYX}$  deformation, the interaction between the X-Y stretches, and between the stretch and angle motions—whereas there are only three fundamental vibrational frequencies. (The number of vibrational frequencies is  $3N - 6$  for a non-linear molecule, or  $3N - 5$  for a linear molecule). For molecules with a high degree of symmetry, certain of the fundamental vibrations have the

<sup>19</sup> A. M. Karo and A. R. Olsen, *J. Chem. Phys.*, 1959, **30**, 1232.

<sup>20</sup> J. Higuchi, *J. Chem. Phys.*, 1954, **22**, 1339.

<sup>21</sup> R. G. Parr and A. F. Saturno, unpublished data; I. M. Mills, *Mol. Phys.*, 1958, **1**, 99, 107.

<sup>22</sup> A. Meckler, *J. Chem. Phys.*, 1953, **21**, 1750.

same frequencies, *i.e.*, they are degenerate. As the number of atoms increases and the molecular symmetry decreases, the situation becomes rapidly more unfavourable. Clearly, additional sources of experimental data are needed in order to deduce the force field.

By means of isotopic substitution, the harmonic vibrational frequencies are altered without affecting the electronic binding. By this expediency, it is possible to obtain further sets of experimental data from which to determine the force constants. At first it would appear that  $M$  isotopic substitutions would yield  $Mx$  sets of data, where  $x$  is the number of fundamental frequencies. In practice, this is not so. There are several reasons for this. First, whilst the molecular vibrational frequencies are properties of the molecule as a whole, it is well known that many bonds vibrate almost independently of the remainder of the molecule. Thus,  $>X-H$  stretching modes interact only very weakly with other modes. This clearly means that isotopic substitution of such atoms will not give significant data on the interaction terms which do not involve the  $X-H$  stretching motion. Secondly, whilst all the vibrational frequencies may change on isotopic substitution, it may be found that all changes are not independent. Vibrational theory shows that the product of the vibrational frequencies of any symmetry class are related, by the geometry of the molecule and the masses of the atoms, to the product of the equivalent vibrations of an isotopically substituted molecule.<sup>23</sup> Such internal relationships reduce the number of independent equations relating frequencies to force constants. A third limitation arises from the extremely small changes in the majority of the vibrational frequencies which result from isotopic mass changes of atoms other than hydrogen. This insensitivity of the vibrational frequencies to the isotopic masses drastically restricts the usefulness of the observed data. Frequently, all the vibrational frequencies may prove quite insensitive to a particular interaction force constant, thus making the uncertainty in the value of that constant large compared with its actual magnitude. An interesting case of this type has been discussed by Linnett.<sup>24</sup> The two stretching vibrations of HCN belong to the  $\Sigma$  symmetry class and may be considered independently of the angular deformation frequency of the  $\pi$  class. Writing the stretching part of the potential energy as

$$2v = k_1 (\Delta r_{CH})^2 + k_2 (\Delta r_{CN})^2 + 2k_{12} (\Delta r_{CH}) (\Delta r_{CN}),$$

and using the values of  $k_1$  and  $k_2$  as determined from HCN and DCN, it may be shown that a change in the interaction constant,  $k_{12}$ , from 0 to  $1 \times 10^5$  dynes/cm. results in a change in the calculated stretching frequencies of  $HC^{14}N$  and  $HC^{15}N$  of only 1.7 and 1.1  $cm^{-1}$ , whilst for DCN the corresponding changes are 100 and 74  $cm^{-1}$ . The actual value of  $k_{12}$  is near  $-0.4 \times 10^5$  dynes/cm. Clearly the constant  $k_{12}$  contributes little to

<sup>23</sup> O. Redlich *Z. phys. Chem.*, 1935, b28, 371; see also W. R. Angus, C. R. Bailey, J. B. Hale, C. K. Ingold, A. H. Leckie, C. G. Raisin, J. W. Thompson, and C. L. Wilson, *J.*, 1936, 971.

<sup>24</sup> J. W. Linnett, *Ann. Reports*, 1952, 49, 8.

the potential energy of  $\text{HC}^{14}\text{N}$  and  $\text{HC}^{15}\text{N}$ , and would be difficult to estimate from the vibrational frequencies of those systems. The reason why the frequencies of DCN are so much more sensitive to  $k_{12}$  is that the CD stretching frequency near  $2320\text{ cm}^{-1}$  is much closer to the stretching frequency of the CN group (at  $2089\text{ cm}^{-1}$  in HCN) than is the CH frequency of  $3310\text{ cm}^{-1}$ .

If we are to arrive generally at a realistic force field and hence at a good description of the vibrational distortions, we must seek additional sources of information about the force constants. Such information can be obtained, in principle, from the magnitudes of vibration-rotation interactions and centrifugal distortions, from mean-square vibrational amplitudes as determined by electron diffraction, and, in certain circumstances, from absorption intensity studies. According to the Born-Oppenheimer approximation, electronic, vibrational, and rotational motions are independent of one another for non-degenerate vibrational states. For example, the rotational energy levels of a spherical rotor (*e.g.*,  $\text{CH}_4$ ,  $\text{SF}_4$ ) can be written as

$$E_{\text{rot.}}/\hbar = BJ(J + 1), \quad (5)$$

where  $E_{\text{rot.}}$  is the rotational energy,  $\hbar$  is Planck's constant, and  $B$  is the moment of inertia about any axis. Hence, since  $\Delta J = \pm 1$  for the  $P$  and  $R$  branches of a vibrational band, we have

$$\Delta E_{\text{rot.}}/\hbar = 2BJ, \quad (6)$$

which is independent of the vibrational and electronic states. In the case of a degenerate vibrational band, the rotational spacings in the  $R$  ( $\Delta J = +1$ ) and the  $P$  ( $\Delta J = -1$ ) branches are different as a result of vibration-rotation interaction. The rotational spacings are now  $2B_v(J + \zeta_i)$  and  $2B_v(J - \zeta_i)$ , respectively.  $\zeta_i$  is the magnitude of the angular momentum arising from the interaction, and may be expressed in terms of the potential constants and the masses. This has been done in algebraic form for many of the more important types of vibration of simple molecules.<sup>25</sup> Clearly, each  $\zeta_i$  value gives an extra relationship between the force constants and the result of an observation. Unfortunately, Coriolis constants, which is the name given to the vibration-rotation coupling parameters, can only be determined with reasonable precision for small molecules. In a similar manner, the change in rotational spacing with changes in the rotational parameter,  $J$ , can be related to the force constants and molecular parameters. This effect of centrifugal distortion has proved of little value, owing to the rather large uncertainties in the observed values.

In principle, it is possible to determine, from the electron-diffraction patterns of gases, the mean-square amplitudes of bond and angle vibrations as well as the bond and angle values themselves.<sup>26</sup> These amplitudes are

<sup>25</sup> G. Herzberg "Infrared and Raman Spectra of Polyatomic Molecules," Van Nostrand, New York, 1945.

<sup>26</sup> J. L. Karle and J. Karle, *J. Chem. Phys.*, 1949, **17**, 1052.

readily evaluated from the force field, and have been used to test assumed fields.<sup>27,28</sup> The precision of the experimental data is again low. Even so, such calculations have served to show inadequacies of assumed fields.

The mathematical difficulties involved in determining the set of force constants which give the most satisfactory fit between observed and calculated frequencies, distortion constants, etc., are very formidable for all but the very simplest of molecules. Electronic computers have been programmed by several groups of research workers to derive optimum sets of force constants.<sup>28-30</sup> Early optimism in obtaining good fields in this way was rapidly dispelled when it was discovered that further mathematical problems were of prime importance. The major problem arises from the fact that the solution of a vibrational problem involving  $n$  vibrational frequencies involves the solution of an equation of order  $n$ , to which there are generally  $n$  solutions. In the computing procedure, a guessed set of constants is used to derive a calculated set of frequencies, distortion constants etc. The difference between the calculated and observed sets are then used to derive an improved set of force constants by a perturbation technique. It was expected that, if a reasonable set of force constants was chosen initially, from previous experience with simpler molecules, then the perturbation would lead to convergence on a unique set of improved constants, which would yield a description of the vibrational distortions close to the truth. In practice it was found that the perturbation problem was often unstable and the perturbed constants diverged to impossible values. This usually arises from the differences between the calculated and observed frequencies being too large for a perturbation treatment, and can sometimes be overcome by taking small fractional improvements, *i.e.*, if  $f_i$  is a typical input constant and  $f_j$  is its "improved" value, then using  $f_i + (f_j - f_i)x$ , where  $x \ll 1$ , in the next cycle may remove the divergence of the constants. Occasionally the cause of the divergence is more deep-seated and arises from an unstable situation in the perturbation solution due to a special case of ill-conditioned behaviour.<sup>31</sup> Another frequent occurrence is that the convergence of the force constants terminates at a stage of oscillation. This behaviour has been shown to correspond to a set of complex solutions. Such complex solutions may arise as a result of simplifying assumptions made in the force field to make the problem tractable. It has been shown, however, that the oscillations occur about the real components of the converged set. Finally, and perhaps most disturbing of all, it has been found that in certain cases slightly different initial guesses lead to a different set of converged solutions.<sup>32</sup> Various criteria have been described to test the validity of the final answers, but the uncertainty in the

<sup>27</sup> D. A. Long and E. A. Seibold, *Trans. Faraday. Soc.*, 1960, **56**, 1105.

<sup>28</sup> D. E. Mann, T. Shimanouchi, J. H. Meal, and L. Fano, *J. Chem. Phys.*, 1957, **27**, 43.

<sup>29</sup> J. Overend and J. R. Scherer, *J. Chem. Phys.*, 1960, **32**, 1289.

<sup>30</sup> D. A. Long, R. B. Gravenor, and M. Woodger, *Spectrochim. Acta*, 1963, **19**, 937.

<sup>31</sup> D. A. Long and R. B. Gravenor, *Spectrochim. Acta*, 1963, **19**, 961.

<sup>32</sup> Joan Aldous and I. M. Mills, *Spectrochim. Acta*, 1962, **18**, 1073.

reliability of the distortional co-ordinates remains a major obstacle to progress in the interpretation of absorption intensities.

Once the force field has been deduced and hence the form of the normal co-ordinates determined, or approximated, the next step is to visualise what the resulting  $\partial\mu/\partial Q_j$  mean. The molecular dipole gradient will generally be difficult to visualise and to utilise. Since physical chemists almost invariably find life a great deal easier if they can translate molecular properties into comparatively simple, directed, and more-localised properties, the next step is to find a suitable set of assumptions that will yield the desired simplifications. The obvious assumptions are those that will decompose the molecular properties into the sum of a set of bond properties, and are generally chosen as:

(a) the stretching of a bond by  $dr$  produces a change of dipole moment along the bond of  $(\partial\mu/\partial r) dr$ ;

(b) the deformation of a bond through an angle  $d\theta$  produces a dipole change  $(\partial\mu/\partial\theta)d\theta$  perpendicular to the bond and in the plane of movement;

(c) changes in one bond do not result in changes in another bond, except when this is geometrically necessary.

The test of the validity and usefulness of these assumptions is whether any or all of the following criteria are found to hold, and, if not, whether anything positive can be deduced from the discrepancies.

(i) Values of the deduced bond moments and gradients in different molecules are comparable.

(ii) Values of given gradients and moments derived from different symmetry classes of the same molecule are equal.

(iii) The perpendicular gradients to any bond are negligible.

(iv) Values of the bond dipoles derived are comparable with the static dipoles as measured by other methods.

TABLE 2. *Effective bond dipole moments and derivatives for C-H bonds.*

Compound	Symmetry Class	Dipole-moment derivative (D/Å)	Effective bond dipole moment (D)	Measurement	Ref.
CH <sub>4</sub>	$f_2$	$\pm 0.83$	$\mp 0.37$	W-W	33
CH <sub>3</sub> D, CH <sub>2</sub> D <sub>2</sub>	$a_{1,e}$	-0.61	0.33	W-W	34
CD <sub>3</sub> H					
C <sub>2</sub> H <sub>4</sub> , C <sub>2</sub> H <sub>2</sub> D <sub>2</sub>	$b_{2u}$	$\pm 0.26$	$\mp 0.42$	W-W	35
C <sub>2</sub> D <sub>4</sub>	$b_{3u}$	$\mp 0.23$	$\mp 0.60$		
	$b_{1u}$	0.67			

<sup>33</sup> I. M. Mills, *Mol. Phys.*, 1958, 1, 107.

<sup>34</sup> R. E. Hiller and J. W. Straley, *J. Mol. Spectroscopy*, 1960, 5, 24.

<sup>35</sup> R. C. Golike, I. M. Mills, W. B. Person, and B. L. Crawford, *J. Chem. Phys.*, 1956, 25, 1266.

TABLE 2.—*continued.*

Compound	Symmetry Class	Dipole-moment derivative	Effective bond dipole moment	Measurement	Ref.
C <sub>2</sub> H <sub>2</sub>	$\Sigma_u^+$	0.8		D	36
	$\Pi_u$		1.05		
C <sub>2</sub> D <sub>2</sub>	$\Sigma_u^+$	0.78		W-W	37
	$\Pi_u$		0.89		
C <sub>2</sub> H <sub>2</sub>	$\Sigma_u^+$	0.87		W-W	37
	$\Pi_u$		1.05		
C <sub>2</sub> HD	$\Sigma_u^+$	0.79(H)	0.90(H)	W-W	37
	$\Pi$	0.78(D)	0.92(D)		
C <sub>2</sub> H <sub>6</sub>	$a_{2u}$	$\pm 1.24$	$\mp 0.23$	W-W	40
	$e_u$	$\pm 0.75$	$\mp 0.26$		
C <sub>6</sub> H <sub>6</sub>	$e_{1u}$	+0.45	-0.31	W-W	38
	$a_{2u}$		-0.61		
CH <sub>3</sub> Cl	$a_1$	+1.00	+0.17	W-W	39
	$e$	+0.24	-0.45		
CH <sub>3</sub> Br	$a_1$	+0.98	+0.27	W-W	39
	$e$	+0.19	-0.48		
CH <sub>3</sub> I	$a_1$	+0.73	+0.42	W-W	39
	$e$	+0.13	-0.46		
NH <sub>3</sub> *	$a_1$	0.61	1.04	W-W	41
	$e$	0.16	0.52		
PH <sub>3</sub>	$a_1$	1.2		W-W	41
	$e$	0.8			
SiH <sub>4</sub> , SiD <sub>4</sub>	$f_2$	$\pm 1.23$	$\mp 1.58$	W-W	42
	$f_2$	$\pm 1.44$		W-W	43

W-W, Wilson-Wells method. D, dispersion method.

\* Introduction of  $\partial\mu_{u,p}/\partial x$  and assumption of complete bond following leads to:  $a_1, \mu_{u,p} = 0.74D$  and  $\mu_{NH} = -0.65D$ ;  $e, \mu_{u,p} = 0.70D$  and  $\mu_{NH} = -0.68D$ .

It can be seen from Tables 2 and 3 that criteria (i), (ii), and, hence, (iv) certainly do not hold, though there is a certain amount of consistency between the gradients and dipoles for similar molecules, and some trends are apparent. The situation is particularly bad for carbon-hydrogen bonds. It is from an analysis of these inconsistencies that a great deal of useful information and knowledge of molecular structure has been gleaned. The first step in such an analysis must be a consideration of the four major reasons for the failure of the model.

<sup>36</sup> R. L. Kelly, R. Rollefson, and B. S. Schurin, *J. Chem. Phys.*, 1951, **19**, 1595.

<sup>37</sup> D. F. Eggers, I. C. Hisatsune, and I. Van Alten, *J. Phys. Chem.*, 1955, **59**, 1124.

<sup>38</sup> H. Spedding and D. H. Whiffen, *Proc. Roy. Soc.*, 1956, *A*, **238**, 245.

<sup>39</sup> A. D. Dickson, I. M. Mills, and B. L. Crawford, *J. Chem. Phys.*, 1957, **27**, 445.

<sup>40</sup> I. M. Nyquist, I. M. Mills, W. B. Person, and B. L. Crawford, *J. Chem. Phys.*, 1957, **26**, 552.

<sup>41</sup> D. C. McKean and P. N. Schatz, *J. Chem. Phys.*, 1956k **24**, 316.

<sup>42</sup> D. F. Ball and D. C. McKean, *Spectrochim. Acta*, 1962, **18**, 1019.

<sup>43</sup> I. W. Levin and W. T. King, *J. Chem. Phys.*, 1962, **37**, 1375.

TABLE 3. *Effective bond dipole moments and derivatives for X-F bonds.*

Compound	Symmetry class	Dipole moment derivative (D/Å)	Effective bond dipole moment (D)	Measurement	Ref.
CF <sub>4</sub>	f <sub>2</sub>	5.99	1.11	D	44
		or 3.71	or 2.98		
		4.9	1.1	W-W	45
		or 3.4	or 2.4		
CH <sub>3</sub> F	a <sub>1</sub>	4.0		W-W	46
CF <sub>3</sub> Br	a <sub>1</sub>	+8.1	+2.8	W-W	47
		e	+4.1	+0.5 (ν <sub>5</sub> )	
			+1.1 (ν <sub>6</sub> )		
C <sub>2</sub> F <sub>6</sub>	a <sub>2u</sub>	+3.4	+2.2	W-W	48
		e <sub>u</sub>	+3.8	+1.6	
			+0.7		
C <sub>6</sub> F <sub>6</sub>	e <sub>1u</sub>	+5.0	1.6	W-W	49
p-C <sub>6</sub> H <sub>4</sub> F <sub>2</sub>	b <sub>1u</sub>	+6.5	1.3	W-W	50
p-C <sub>6</sub> D <sub>4</sub> F <sub>2</sub>		+5.2		W-W	50
p-C <sub>6</sub> H <sub>2</sub> F <sub>4</sub>		e'	±4.0	±2.6	W-W
BF <sub>3</sub>		or ∓6.1	or ∓0.9		
	a <sub>2</sub> ''		1.7		
NF <sub>3</sub> *	a <sub>1</sub>	+1.5	+0.9	W-W	52
		to +2.0	to +1.2		
		or 3.3	0 to 0.3		
	e	ca. +4.7			
SF <sub>6</sub>	f <sub>1u</sub>	3.85	2.65	W-W	53
SiF <sub>4</sub>	f <sub>2</sub>	3.3	3.3	W-W	53
		or 7.5	2.3		

D, dispersion method. W-W, Wilson-Wells method.

\* Introduction of  $\partial\mu_{u,p}/\partial\alpha$  and assumption of complete bond following for the a<sub>1</sub> class leads to:  $\mu_{u,p} \sim 1.7$  or  $1.2D$ ;  $\mu_F \sim 1.1D$ .

(a) In criterion (i) it is implicitly assumed that the charge distribution in the bond XY is always the same and always alters in the same manner. It is common experience that all XY bonds do not have the same chemical reactivity, apart from steric effects, and since chemical reactivity is intimately related to the valence-shell electronic structure of the bonds, this contradicts the above assumption. Furthermore, all XY bonds do not have

<sup>44</sup> B. Schurin, *J. Chem. Phys.*, 1959, 30, 1.

<sup>45</sup> P. N. Schatz and D. F. Hornig, *J. Chem. Phys.*, 1953, 21, 1516.

<sup>46</sup> G. M. Barrow and D. C. McKean, *Proc. Roy. Soc.*, 1952, A, 213, 27.

<sup>47</sup> W. B. Person and S. R. Polo, *Spectrochim. Acta*, 1961, 17, 101.

<sup>48</sup> I. M. Mills, W. B. Person, J. R. Scherer and B. Crawford, *J. Chem. Phys.*, 1958, 28, 851.

<sup>49</sup> D. Steele and D. H. Whiffen, *J. Chem. Phys.*, 1958; 29, 1194.

<sup>50</sup> D. Steele and D. H. Whiffen, *Trans. Faraday Soc.*, 1960, 56, 177.

<sup>51</sup> D. C. McKean, *J. Chem. Phys.*, 1956, 24, 1002.

<sup>52</sup> P. N. Schatz and I. W. Levin, *J. Chem. Phys.*, 1958, 29, 475.

<sup>53</sup> P. N. Schatz and D. F. Hornig, *J. Chem. Phys.*, 1953, 21, 1516.

the same bond length, but this in turn depends on the environment of X and Y. Thus the CH bond decreases in length as the local hybridisation at the carbon atoms takes on less *p* and more *s* character. Thus, this is a further manifestation of the variation of the electronic structure of the bond between two given atoms.

(b) The effect of lone-pair electrons on the dipole change during a vibration is ignored. As the molecule vibrates, the hybridisation of the orbitals will generally change and consequently affect the infrared absorption. Burnelle and Coulson<sup>62</sup> have shown, using wave-mechanical

TABLE 4. *Effective bond dipole moments and derivatives for various bonds.*

Compound	Symmetry class	Bond	Dipole-moment derivative (D/Å)	Effective bond dipole moment (D)	Measurement	Ref.
C <sub>6</sub> H <sub>6</sub>	<i>e</i> <sub>1u</sub>	C-C	0.0		W-W	38
C <sup>16</sup> O <sup>18</sup> O	$\Sigma^+$	C=O	5.79		W-W	54
CO <sub>2</sub>	$\Sigma_u^+$	C=O	6.0		W-W	16
	$\Sigma_u^+$	C=O	5.85		W-W	17
	$\Pi_u$	C=O		1.33	W-W	13
	$\Pi_u$	C=O		1.33	C-o-G	12
(CN) <sub>2</sub>	$\Sigma_u$	C≡N	0.585		W-W	55
	$\Pi_u$	C≡N		1.2		
<sup>12</sup> CN <sup>13</sup> CN	$\Sigma$	<sup>12</sup> C≡N	0.595		W-W	56
		<sup>13</sup> C≡N	0.605			
ClCN	$\Sigma$	C≡N	0.3		W-W	57
			to 0.7			
BrCN	$\Pi$	C≡N		1.4		
	$\Sigma$	C≡N	0.5	1.3	W-W	58
			to 0.8			
CH <sub>3</sub> CN	$\Pi$	C≡N				
	<i>a</i> <sub>1</sub>	C≡N			W-W	59
HCl	$\Sigma$	H-Cl	1.21	1.3		
HCN } DCN }	$\Sigma$	C≡N	0.66		W-W	60
SO <sub>2</sub>	$\Pi$	C≡N		1.8		
	<i>b</i> <sub>1</sub>	S=O	4.17		W-W	33
	<i>a</i> <sub>1</sub>	S=O	±2.0 or ±4.3	∓1.3 ±1.2		

W-W, Wilson-Wells method. C-o-G, curve-of-growth method.

<sup>54</sup> D. F. Eggers and C. B. Arends, *J. Chem. Phys.*, 1957, **27**, 1405.

<sup>55</sup> T. Miyazawa, *J. Chem. Phys.*, 1958, **29**, 421.

<sup>56</sup> J. W. Schultz and D. F. Eggers, *J. Mol. Spectroscopy*, 1958, **2**, 113.

<sup>57</sup> R. W. Hendricks and D. F. Hornig, see ref. 58.

<sup>58</sup> D. F. Hornig and D. C. McKean, *J. Phys. Chem.*, 1955, **59**, 1133.

<sup>59</sup> A. V. Golton, D.Phil. Thesis, Oxford, 1953.

<sup>60</sup> S. S. Penner and D. Weber, *J. Chem. Phys.*, 1953, **21**, 649.

<sup>61</sup> G. E. Hyde and D. F. Hornig, *J. Chem. Phys.*, 1952, **20**, 647.

<sup>62</sup> L. Burnelle and C. A. Coulson, *Trans. Faraday Soc.*, 1957, **53**, 403.



calculations of Ellison and Shull<sup>63</sup> and Higuchi,<sup>64</sup> that the lone-pair contribution to the molecular-dipole change associated with the bending vibrations of  $\text{H}_2\text{O}$  and  $\text{NH}_3$  is nearly as large as the contribution resulting from the bond deformations. Thus, for  $\text{H}_2\text{O}$ ,  $\partial\mu_L/\partial\alpha \sim 1.41\text{D}$  and  $\partial\mu_B/\partial\alpha \sim -2.13\text{D}$ , where  $\mu_L$  and  $\mu_B$  are the lone-pair and bonding contributions, respectively, to the molecular dipole. That this must be the case can be seen from the fact that the lone-pair contribution to the molecular dipole is calculated to be  $1.69\text{D}$  for  $\text{H}_2\text{O}$ . In the deformed state where the oxygen and hydrogen atoms are collinear, the lone-pair contribution must be zero, by symmetry.

Several of the discrepancies between the effective bond moments given in Tables 2, 3, and 4 can be explained by similar reasoning to the above. Thus in boron trifluoride, which in its equilibrium position is planar, there is a vacant  $p$  orbital associated with the boron atom and perpendicular to the plane of the molecule. During the symmetrical, out-of-plane, bending vibration, rehybridisation of the B-F bonding electrons at the boron atom

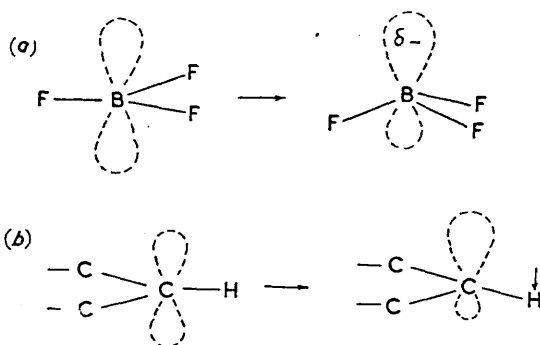


FIG. 3. Electron rehybridisations in the  $p_z$  orbitals during the transitions of symmetry: (a)  $a_2''$  of boron trifluoride; (b)  $a_{2u}$  of benzene.

results in electron-flow into an orbital on the opposite side of the original atomic plane to the fluorine atoms [see Fig. 3(a)]. This makes the fluorine atoms appear to carry less negative charge than they actually do. In the  $e'$  class, the F-B-F angular deformation cannot result in electron flow into the vacant  $p_z$  orbital. In agreement with this reasoning, the effective BF dipole, as deduced from the  $a_2''$  class, is only  $1.7\text{D}$  compared with  $2.6\text{D}$ , as deduced from the  $e'$  class. In the out-of-plane CH deformation of benzene, a similar effect occurs in the  $a_{2u}$  out-of-plane deformation. The  $p_z$  orbital is fully occupied in this case, but rehybridisation at the carbon atom takes place in the form of  $s$  character being introduced in the  $p_z$  orbital (Fig. 3(b)). That this must be so, is readily apparent from the fact that when the HCH angles are deformed to  $108^\circ$ , the carbon hybridisation must be  $sp^3$  compared with  $sp^2$  for the planar configuration. The effect

<sup>63</sup> F. O. Ellison and H. Shull, *J. Chem. Phys.*, 1953, 23, 2348.

<sup>64</sup> J. Higuchi, *J. Chem.*, 1956, 24, 535.

once again is to make the substituent appear less negative. Since the hydrogen atoms in benzene are known to be at the positive end of the CH dipole,<sup>65</sup> the numerical value of the effective dipole should be greater for the  $a_{2u}$  class than for the in-plane  $e_{1u}$  class. The observed values are 0.61D and 0.31D, respectively. Clearly an adequate theory of infrared intensities must incorporate terms of the nature of  $\partial\mu_{p_z}/\partial\alpha$ .

Coulson and Stephen<sup>66</sup> have shown that the variations in the deduced effective dipoles in benzene, acetylene, and ethylene are compatible with reasonable degrees of rehybridisation and bond following (see below). However, they were unable to deduce the relative contributions of the two effects.

(c) Hybridisation changes can also occur as a bond stretch. If we consider the CH stretching in methane, and assume that in the extreme case we have a  $\text{CH}_3$  radical and an H atom, then it can be seen that rehybridisation of the orbitals around the carbon atom must have occurred. The configuration of the  $\text{CH}_3$  radical is still uncertain, but it seems probable that it is planar. In this case, the hybridisation at the carbon atom will be  $sp^2$  as compared with  $sp^3$  in  $\text{CH}_4$ . Though in both the extreme cases *i.e.*, those of the unperturbed  $\text{CH}_4$  molecule and of a  $\text{CH}_3$  radical and an H atom, there is no total dipole moment, it seems necessary to assume that there is a dipole gradient during the vibrational motion. This gradient can be expected, on the above grounds, to be different from that in, say, the vibrational motion in which the stretching of one CH bond is out of phase with the remaining two ( $\nu_3$  of symmetry class  $f_2$ ).

(d) A bond is usually thought of as being directed along the line connecting the bonded atoms. This is frequently a false picture, particularly for vibrationally distorted configurations. Wave-functions are not usually localised in one bond. Indeed, the orthogonality of the wave-functions generally forbids this. By their delocalisation, these wave-functions are not directly related to the usual conception of chemical bonds. Burnelle and Coulson<sup>62</sup> transformed the accurate SCF-LCAO wave-functions for  $\text{H}_2\text{O}$  and  $\text{NH}_3$  so that the resulting wave-functions satisfied the following conditions: (a) that they were orthogonal; (b) that the orbitals associated with identical bonds should be equivalent; and (c) that the lone-pair orbitals should contain only orbitals of the central atom. The resulting picture of the molecular orbitals showed that the hybrid orbitals at the central atom are not in general directed along the bond direction. This means that the bonds may be considered to be bent and to have dipole gradients perpendicular to the internuclear axis. The individual contributions to the dipole moment of  $\text{H}_2\text{O}$  are, for an inter-bond angle of  $105^\circ$ ,  $\mu_L = 1.69\text{D}$ ,  $\mu_B = 0.20\text{D}$ , and  $\mu_B^Y = -0.37\text{D}$ , where  $\mu_L$ ,  $\mu_B$ , and  $\mu_B^Y$  are the contributions due to the lone-pair electrons, the

<sup>65</sup> (a) R. P. Bell, H. W. Thompson, and E. E. Vago, *Proc. Roy. Soc., A*, **192**, 498;

(b) A. R. H. Cole and H. W. Thompson, *Proc. Roy. Soc.*, 1951, *A*, **208**, 341.

<sup>66</sup> C. A. Coulson and M. J. Stephen, *Trans. Faraday Soc.*, 1957, **53**, 272.

bond electrons in the direction of the internuclear axis, and the bond electrons in a direction perpendicular to the internuclear axis, respectively. If the HOH angle is deformed, the resulting molecular dipole gradient of  $-0.72\text{D/radian}$  is derived from the following contributions:  $\partial\mu_x/\partial\alpha = 1.41\text{ D/Radian}$ ;  $\partial\mu_y^Z/\partial\alpha = -0.20\text{ D/Radian}$ ; and  $\partial\mu_y^Y/\partial\alpha = 1.93\text{ D/Radian}$ . The transverse moment is very sensitive to the inter-bond angle, and its derivative is the major contributing term to the absorption intensity.

An analysis of the absolute absorption intensities of the infrared bands of 1,2,4,5-tetrafluorobenzene<sup>50</sup> showed that the dipole gradient,  $\partial\mu/\partial r_{\text{CF}}$ , lies along the internuclear axis, within the experimental error. However, the asymmetry of the CF bond in this compound is not very pronounced, and it is not unreasonable to expect the above result.

**The Polarity of the Dipole Gradients.**—According to equation (3), the absorption intensity is proportional to the square of the dipole gradient. In the preceding section it has been assumed that in solving for the gradient, the sign of the square root of the intensity is known. In fact, the question of these signs introduces what is frequently a serious uncertainty into the interpretations. The seriousness of this problem can be appreciated from the fact that, if there are  $n$  fundamental vibrations in a given symmetry class, then there are  $2^n$  possible ways of choosing the sign combinations, leading to  $2^n$  distinct solutions for the bond parameters. Isotopic substitution should leave the dipole gradients unchanged, whilst changing the form of the vibrational modes. The sets of dipole gradients with respect to bond co-ordinates—or with respect to combinations of the co-ordinates in the form of symmetry co-ordinates—will not all be consistent with the observed intensities of the other isotopic system. Generally, there are rarely more than three sets which yield acceptable values for the intensities of the other isotopic system. A choice between sets acceptable by the above criterion is usually made on the basis of lack of credulity of the authors to certain of the derived gradients. When no isotopic data existed, sign choices have often been made on the basis of one set giving bond gradients and dipoles which were in line with values for similar molecules. Clearly this is not an acceptable criterion, especially as the aim has usually been to discover if the gradients and dipoles were indeed comparable for bonds of a given type in similar molecules. Blatant cases of this practice have been excluded from the Tables.

As an example of the above technique, the CN dipole gradient for cyanogen, derived from the infrared-active  $\text{C}\equiv\text{N}$  stretching vibration of  $^{13}\text{CN}^{12}\text{CN}$ , is compared in Table 5 with those derived from the “almost symmetric” CN and CC stretching vibrations of  $^{13}\text{CN}^{12}\text{CN}$ .<sup>56</sup> Owing to the presence of normal cyanogen in the heavy-isotopic system, the intensity of the antisymmetric mode was not measured. In this case it is very clear that the  $\partial\mu/\partial Q$  values must have the same sign.

Occasionally the sign of the square root in equation (3) can be deter-

TABLE 5. Dipole-moment derivatives for cyanogen D/Å

Dipole-moment derivative	$(^{12}\text{CN})_2$	Relative signs for $\partial\mu/\partial Q$ values	$^{12}\text{CN}^{13}\text{CN}$
$\partial\mu/\partial r_{(\text{CN})_1}$	$\pm 0.585$	same	$\pm 0.595$
		different	$\mp 0.416$
$\partial\mu/\partial r_{(\text{CN})_2}$	$\mp 0.585$	same	$\mp 0.607$
		different	$\pm 0.718$
$\partial\mu/\partial r_{(\text{C}-\text{C})}$	zero, by symmetry	same	$\mp 0.0003$
		different	$\mp 0.107$

mined from vibration-rotation interaction studies. Thus Hermann and Wallis<sup>67</sup> were able to show that, for a diatomic molecule, the ratio of intensities of corresponding rotational absorption lines in *P* and *R* branches is proportional to  $(1 + 4\gamma\theta J)J$ , where  $\gamma = 2B_e/\nu_e$ ,  $\theta = [\mu_0/(\partial\mu/\partial r)]1/r_e$ , and  $J$  is the rotational quantum number of the initial state.  $B_e$  is the rotational constant for the equilibrium bond length,  $r_e$ ;  $\mu_0$  is the molecular dipole; and  $\partial\mu/\partial r$  is the dynamic dipole gradient. If the sign of  $\mu_0$  is known then the sign of the dipole gradient can be deduced. In this way they were able to show that  $\partial\mu/\partial r$  for HCl has the same sign as  $\mu_0$ . Clearly, it is also possible to use the above technique to evaluate the ratio of the magnitude of the gradient to the static dipole. Thus  $\mu/(\partial\mu/\partial r)r_e$  for LiH has been determined as  $-1.8 \pm 0.3\text{D}$ .<sup>68</sup> Clearly a prerequisite of this technique is the existence of an equilibrium molecular dipole. The Hermann-Wallis theory has been extended to the case of linear polyatomic molecules<sup>69</sup> (group  $C_{\infty v}$ ), but no application to intensity interpretation has yet been made.

Bell, Thompson, and Vago, and Cole and Thompson, have shown<sup>65</sup> that the intensities of the out-of-plane deformations in various alkyl- and halogen-substituted benzenes indicate that the effective CH dipole is of opposite sign to the effective halogen dipole. As it is reasonably certain that the halogen atom is at the negative end, then this implies that the hydrogen atom is at the positive end of the CH dipole in benzenes in the out-of-plane deformations. Since out-of-plane deformations have the effect of making the dipoles appear less positive, the hydrogen atom must also be at the positive pole of the static bond.

Interaction between two vibration-rotation bands can occur if the symmetry of the vibrations and of a principal rotation axis bear a certain simple relationship to one another. Specifically, the Coriolis force on each atom is of magnitude  $2m_a v_a w \sin \phi$ , where  $m_a$  is the mass of the atom,  $w$  is the angular velocity of the co-ordinate system with respect to a fixed co-ordinate system,  $v_a$  is the velocity of atom "a", and  $\phi$  is the angle between the axis of rotation and the direction of  $v_a$ . The force is directed at right-angles to the direction of  $v_a$  and to the axis of rotation. If the forces on the

<sup>67</sup> R. Hermann and R. F. Wallis, *J. Chem. Phys.*, 1955, **23**, 637.

<sup>68</sup> T. C. James, W. G. Norris, and W. Klemperer, *J. Chem. Phys.*, 1960, **32**, 728.

<sup>69</sup> G. A. Gallup, *J. Chem. Phys.*, 1957, **27**, 1338.

atoms constituting the molecule, which arise from a vibration,  $j$ , and from rotation about a specific axis,  $m$ , have the same symmetry as a second vibration,  $k$ , which is not too far removed in frequency from  $j$ , then the two vibrations will interact. The effect of this interaction on the vibrational frequencies is to make the  $P$  and  $R$  rotational band spacings different from one another (apart from the small effect arising from centrifugal distortion). This Coriolis interaction has been mentioned previously in connection with the dependence of the  $\zeta$  constants on the potential constants. In addition to the frequency effect, the intensities are also altered. In the approximation of no vibration-rotation interaction, the lines in the  $P$  and  $R$  branches, arising from transitions from the same initial state have equal strengths. The effect of the Coriolis interaction is to increase (or decrease) the  $R$ -line intensities of the higher-frequency band, and also the  $P$ -line intensities of the lower band, whilst decreasing (or increasing) the intensities of the other  $\Delta J = \pm 1$  lines. Which, in fact, occurs, depends on the sign of  $\zeta_{jk} = (\partial\mu/\partial Q_j)^x(\partial\mu/\partial Q_k)^y$ , where the  $j$  and  $k$  subscripts specify the two vibrations. The sign of  $\zeta_{jk}$  is generally determinable, and hence from the intensity asymmetry of the bands, the relative signs of the two dipole transitions can be deduced.<sup>70</sup> This new technique has considerable promise.

**The Effect of Change of State on Intensities.**—Recently there has been a renewed interest in the intensities of absorption bands in condensed phases. Until the last two or three years, it was believed that intensity changes arising from intermolecular interactions would be small, except where structural changes took place or where definite bonds were formed between molecules. Examples of these special cases are the crystallisation of *trans*-dichloroethane from a mixture of the *trans*- and *gauche*-forms, and the formation of intermolecular hydrogen bonds in hydroxyl-containing compounds. Considerable theoretical work has been carried out to evaluate the magnitude of the intensity changes in the absence of appreciable intermolecular interactions.<sup>71-75</sup> The basic theory is encompassed in the equation<sup>71,72</sup>

$$\frac{I_{\text{liq}}}{I_{\text{gas}}} = \frac{(n^2 + 2)^2}{9n}, \quad (7)$$

which is derived for an oscillating dipole in a spherical cavity in a medium of refractive index  $n$ . This equation implies that the intensities ought always to be greater in a condensed phase than in the gaseous phase. Experimental work, until very recently, was restricted to isolated absorption bands—isolated in the sense of a single band of a certain molecule. Equation (7) and its refined forms have met with very limited success.

<sup>70</sup> I. M. Mills, unpublished work.

<sup>71</sup> N. Q. Chako, *J. Chem. Phys.*, 1934, **2**, 644.

<sup>72</sup> S. R. Polo and M. K. Wilson, *J. Chem. Phys.*, 1955, **23**, 2376.

<sup>73</sup> J. van Kranendonk, *Physica*, 1957, **23**, 825.

<sup>74</sup> A. D. Buckingham, *Proc. Roy. Soc.*, 1960, *A*, **255**, 32.

<sup>75</sup> L. Onsager, *J. Amer. Chem. Soc.*, 1936, **58**, 1486.

Intensity data now exist for all infrared active bands of benzene<sup>38,76-78</sup> in vapour, liquid, and solid phases. The results are very disturbing. The intensity changes are far greater than can be accounted for by dielectric changes or by the expected magnitudes of intermolecular perturbations. Similar results have been reported for ethylene.<sup>79</sup> The results for benzene are shown in Table 6. These results pose a fascinating theoretical problem

TABLE 6. *Absolute intensities of benzene transitions in various phases* ( $10^3\text{cm}^2/\text{mole}$ ).

Band ( $\text{cm}^{-1}$ )	$\Gamma_g$	$\Gamma_l$	$\Gamma_s$
3060	1.95	1.45	0.65
1480	0.878	1.29	2.56
1036	0.850	1.11	1.69
673	12.95	14.1	13.6

on which no headway has been made at the present time, and which is certain to attract considerable attention from theoretical chemists and physicists in the future.

**Applications of Absolute Intensity Measurements to Determination of Chemical Structure.**—The intensities of some absorption bands characteristic of certain groupings, such as those generally associated with the stretching of  $-\text{C}\equiv\text{N}$ ,  $-\text{C}=\text{O}$ ,  $-\text{C}-\text{H}$  (in hydrocarbons), and  $-\text{OH}$  bonds, have been correlated in an empirical manner with the structure of the attached group. In many cases it is possible to deduce the number of absorbing centres in an unknown molecule. This aspect of intensity measurement has been thoroughly reviewed by T. L. Brown.<sup>80</sup> It is interesting that such empirical correlations actually do exist. The so-called characteristic group vibrations are rarely confined to one bond, and the mode may change quite drastically for small structure changes without the frequency being much affected. It is likely that the main reason for the success of these empirical correlations is that the groups studied usually have very large dipole gradients associated with their stretching motions so that participation in the vibration by other parts of the molecule is relatively unimportant. Even so, these correlations imply that the stretching gradients of these groups are reasonably constant. Very few detailed studies of molecules involving these groupings have been carried out at present.

As a consequence of the interpretational difficulties of intensity measurements, absorption intensities have been little used in elucidating molecular structure, apart from the empirical approach mentioned above. The following examples show that, in special circumstances, absolute intensity measurements can be used in structure determinations.

<sup>76</sup> D. A. Dows and A. L. Pratt, *Spectrochim. Acta*, 1962, **18**, 433.

<sup>77</sup> I. S. Hisatsune and E. S. Jayadevappa, *J. Chem. Phys.*, 1960, **32**, 565.

<sup>78</sup> J. L. Hollenberg and D. A. Dows, *J. Chem. Phys.*, 1962, **37**, 1300.

<sup>79</sup> G. M. Wieder and D. A. Dows, *J. Chem. Phys.*, 1962, **37**, 2990.

<sup>80</sup> T. L. Brown, *Chem. Rev.*, 1958, **58**, 581.

Until recently, magnesium dicyclopentadienyl was believed to be an ionic salt. However, its solubility in benzene was inconsistent with this belief. An analysis of its vibrational spectrum indicated a marked similarity in its vibrational modes to ferrocene.<sup>81</sup> If it is principally ionic, then the absorption intensity of the antisymmetric ring-metal stretching vibration ought to be well represented by the ionic model Fig. 4, where the rings

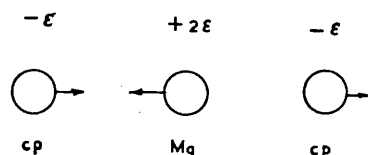


FIG. 4. An ionic model for the antisymmetric stretching vibration of magnesium dicyclopentadienyl ( $\text{MgCp}_2$ )

and the metal atom are represented by point charges. The absolute intensity calculated for this model was approximately seventy times as large as the observed value.<sup>81</sup> This can only be explained on the basis of principally covalent bonding. Magnesium dicyclopentadienyl, or magnacene, is the first established covalently bonded sandwich compound of a non-transition element.

The vibrational stretching frequencies of cyanide bonds are outstanding in their insensitivity to the presence of other groups. Furthermore, there is little coupling between the stretching vibrations of cyanide groups attached to a common atom. Thus, in maleonitrile, only one  $\text{C} \equiv \text{N}$  stretching frequency is observed in the infrared and Raman spectra,<sup>82</sup> and in sulphur dicyanide, the symmetric and antisymmetric modes are at 2184 and 2179  $\text{cm}^{-1}$ , respectively, only 5  $\text{cm}^{-1}$  apart.<sup>83</sup> This indicates that the electronic wave-functions are highly localised in the bonds themselves. The stretching gradients for cyanides are all of the same order of magnitude. The only reported absolute intensity measurements on a dicyanide are those on cyanogen.<sup>56</sup> Rather surprisingly, the stretching gradients derived from the symmetric stretching modes of  $^{12}\text{CN}^{13}\text{CN}$  and from the antisymmetric mode of  $^{12}\text{CN}^{12}\text{CN}$  are in excellent agreement. These facts have been used as the basis for a determination of the angle between the cyanide groups in the dicyanamide ion,  $\text{N}(\text{CN})_2^-$ .<sup>84</sup> Assuming that the bond-moment hypothesis holds for this ion, then it is easy to show that the ratio of the intensities of the antisymmetric to the symmetric stretching modes is given by

$$\frac{I_{\text{as}}}{I_{\text{s}}} = \frac{\sin^2\theta/2}{\cos^2\theta/2},$$

where  $\theta$  is the inter-bond angle. A fortuitous splitting of the antisymmetric

<sup>81</sup> E. R. Lippincott, J. Xavier, and D. Steele, *J. Amer. Chem. Soc.*, 1961, **83**, 2262.

<sup>82</sup> F. Halverson and R. J. Francel, *J. Chem. Phys.*, 1948, **17**, 694; K. W. F. Kohlrusch and G. P. Ypsilanti, *Z. phys. Chem.*, 1934, **b29**, 274.

<sup>83</sup> D. A. Long and D. Steele, *Spectrochim. Acta*, 1963, **19**, 1731.

<sup>84</sup> D. A. Long, J. Y. H. Chau, and D. Steele, unpublished results.

mode occurs as a result of Fermi resonance. This allowed the relative intensities of the two cyanide bands to be measured with reasonable precision. The value derived for the inter-bond angle was  $145^\circ$ . The original measurements were made in potassium bromide media. According to the dielectric theories of the effects of phase on intensities, the relative intensities should be unaffected by phase changes. However, in view of the previously noted influences on the bands of benzene and ethylene, the measurements have been repeated in aqueous solution.<sup>85</sup> The two results agree well.

**Other Aspects and Present Trends.**—A certain amount of research has been devoted towards the evaluation of higher-order derivatives of the dipole moment in suitable systems—generally diatomic systems.<sup>86–90</sup> An interesting special case was the interpretation of the intensities of certain combination bands of benzene arising from the out-of-plane motions of the C–H bonds.<sup>91</sup> These bands, which are characteristic of benzene and substituted benzenes, occur in the region  $2000–1500\text{ cm}^{-1}$ . It was shown that the intensities of these bands of  $\text{C}_6\text{H}_6$ ,  $\text{C}_6\text{D}_6$ , and  $p\text{-C}_6\text{H}_4\text{D}_2$  could be interpreted satisfactorily using only one parameter. This parameter, which is the second derivative of the dipole moment with respect to the out-of-plane deformation of the  $j$ th bond,  $\partial^2\mu/\partial\gamma_j^2$ , has the value  $1.10\text{D}$ .

Several important theorems concerning the vibrational frequencies and intensities of isotopically related systems have been advanced by B. Crawford.<sup>92,93</sup> The most important of these shows that the function  $\Sigma I/\nu_a$  is invariant to isotopic substitution when the summation is over all vibrational bands in a given symmetry class.  $I_a$  is the absorption intensity of the band centred at a frequency  $\nu_a$ . This theorem, when applicable, provides a very useful test on measured intensities. A typical set of results is shown below for  $\text{C}_2\text{H}_6$  and  $\text{C}_2\text{D}_6$ <sup>40</sup>

$\text{C}_2\text{H}_6$	$\text{C}_2\text{D}_6$
class $2.810 \pm 0.024$	$2.942 \pm 0.140\text{ cm}^3/\text{mole}$ .
class $0.737 \pm 0.008$	$0.775 \pm 0.037\text{ cm}^3/\text{mole}$ .

Le Fèvre and Rao,<sup>94,95</sup> Whiffen,<sup>96</sup> and Illinger and Smyth<sup>97</sup> have shown

- <sup>85</sup> D. Steele, unpublished results.  
<sup>86</sup> W. S. Benedict, R. Hermann, G. E. Moore, and S. Silvermann, *J. Chem. Phys.*, 1957, **26**, 1671.  
<sup>87</sup> G. A. Kuipers, *J. Mol. Spectroscopy*, 1958, **2**, 75.  
<sup>88</sup> S. S. Penner and D. Weber, *J. Chem. Phys.*, 1953, **21**, 649.  
<sup>89</sup> B. Schurin and R. Rollefson, *J. Chem. Phys.*, 1957, **26**, 1089.  
<sup>90</sup> E. K. Plyler, W. S. Benedict and S. Silvermann, *J. Chem. Phys.*, 1952, **20**, 175.  
<sup>91</sup> F. E. Dunstan and D. H. Whiffen, *J.*, 1960, 5221.  
<sup>92</sup> B. Crawford, *J. Chem. Phys.*, 1952, **20**, 977.  
<sup>93</sup> I. M. Mills and D. H. Whiffen, *J. Chem. Phys.*, 1959, **30**, 1619.  
<sup>94</sup> D. A. A. S. N. Rao, *Trans. Faraday Soc.*, 1963, **59**, 43.  
<sup>95</sup> R. J. W. Le Fèvre and D. A. A. S. N. Rao, *Austral. J. Chem.*, 1955, **8**, 39.  
<sup>96</sup> D. H. Whiffen, *Trans. Faraday Soc.*, 1958, **54**, 327.  
<sup>97</sup> K. H. Illinger and C. P. Smyth, *J. Chem. Phys.*, 1960, **32**, 787.



that the atomic polarisation of a molecule is related to its infrared absorption by the relationship

$$P_A = \frac{Nc}{3\pi^2} \sum_j \frac{f_j}{\nu_j}$$

The significance of the atomic polarisation can be understood by considering the effect of an applied oscillating electric field on a molecular gas. The induced and the permanent dipole moments align, as far as permitted by the thermal motions, against the applied field, thus reducing the effective field. The molecular polarisation is defined as the total dipole moment per unit volume, parallel to the field arising from the above contributions. As the field frequency is decreased, the total molecular polarisation decreases in certain frequency ranges. At very high oscillating frequencies, only the electrons are mobile enough to follow the field changes. In the infrared frequency range, the nuclei become able to follow the field, and, finally, at still lower frequencies, the molecular dipoles are able to align with the field (see Fig. 5). Clearly it is reasonable to consider the molecular

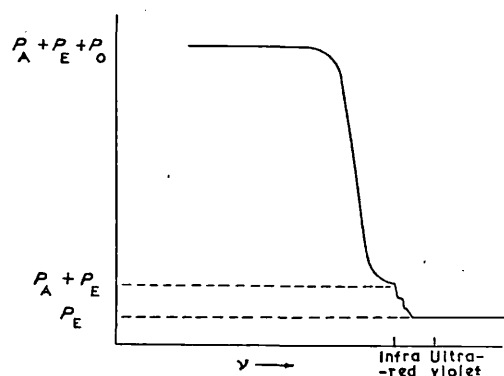


FIG. 5. The variation of molecular polarisability with frequency.

polarisation as consisting of three parts, the electron and the atomic induced polarisations, and that arising from the permanent dipoles. ( $P_E$ ,  $P_A$  and  $P_0$ ).

Values for the atomic polarisation of non-polar molecules, as determined from refractive-index and dielectric-constant studies (see *e.g.*, ref. 94), agree very well with those deduced from intensity measurements. Some typical results are shown in Table 7.

In the case of polar molecules, the discrepancies are generally much greater, but it is very likely that these discrepancies arise from difficulties in determining the total polarisability at frequencies such that only  $P_0$  is measured.

It is clear from preceding sections that any successful theory of absorption intensities must incorporate terms involving derivatives of the dipole

TABLE 7.

Compound	$P_A$		Compound	$P_A$	
	Infrared studies (cm. <sup>3</sup> )	Dielectric studies (cm. <sup>3</sup> )		Infrared studies (cm. <sup>3</sup> )	Dielectric studies (cm. <sup>3</sup> )
BF <sub>3</sub>	2.19	2.81	C <sub>2</sub> H <sub>6</sub>	0.12	0.09
CF <sub>4</sub>	2.89	2.86	C <sub>6</sub> H <sub>6</sub>	0.73	0.80
CH <sub>4</sub>	0.11	0.08	SiF <sub>4</sub>	4.82	5.46
C <sub>2</sub> H <sub>2</sub>	1.28	1.27	SF <sub>6</sub>	5.07	5.20

contribution of lone-pair electrons, rehybridisable orbitals, conjugated systems, etc., with respect to bond deformations. McKean and Schatz<sup>41</sup> and Hornig and McKean<sup>58</sup> have utilised terms involving the lone-pair electrons. Sverdlov<sup>98</sup> has developed a complete second-order bond-moment theory which incorporates terms such as  $\partial\mu_i/\partial R_j$ , where the  $i$  and  $j$  subscripts refer to different bonds. In this way, instead of single terms being determinable, only combinations of terms such as  $(\partial\mu/\partial\theta_1)_{(1)} - (\partial\mu/\partial\theta_1)_{(4)}$  can be evaluated. An appreciation of these results necessitates a judicious assessment of the relative importance of the additional terms.

Much of the present experimental data cannot be satisfactorily treated, owing to the sensitivity of the modes to uncertainties in the force fields. Further developments in gas-phase intensities must come through the deduction of satisfactory force fields and the use of treatments such as those of Hornig and McKean and of Sverdlov.

It is usually the unexpected results which prove to be the most fascinating and the most rewarding. The changes of intensities with phase changes are certainly the most surprising results during recent years of the field reviewed. It is too early to even surmise the importance of an interpretation, but it must modify the present concepts of condensed phases.

In conclusion, much has been achieved in the interpretation of infrared intensities, but many important problems remain to be solved.

I sincerely thank Dr. I. M. Mills for describing his work on the determination of the sign of dipole gradients from Coriolis interaction studies, prior to its publication.

<sup>98</sup> L. M. Sverdlov, *Optics and Spectroscopy*, 1959, 6, 477; 1959, 7, 11; 1960, 8, 316; 1960, 8, 96.

Reprinted from JOURNAL OF MOLECULAR SPECTROSCOPY, Volume 15, No. 3, March, 1965  
Copyright © by Academic Press Inc. Printed in U.S.A.

JOURNAL OF MOLECULAR SPECTROSCOPY 15, 333-343 (1965)

## The Out-of-Plane Vibrations of Azulene

D. STEELE

*Department of Chemistry, Royal Holloway College, Englefield Green, Surrey, England*

The out-of-plane vibrational frequencies and modes have been calculated for azulene,  $d_1$  (1) azulene,  $d_6$  (2 3 4 6 7 8) azulene and  $d_8$  azulene using a modified valence force field derived from that of benzene. The agreement between the calculated frequencies and unequivocal assignments is good. A revised set of assignments is presented based on an analysis of the spectra between 2000 and 1500  $\text{cm}^{-1}$ , on the calculations and on previous crystal studies of other authors.

### I. INTRODUCTION

The spectra of azulene have attracted considerable attention in the past as a result of the unique structural characteristics of the bicyclic aromatic system (1, 2).<sup>1</sup> However a complete vibrational assignment is rendered much more difficult by the failure to obtain Raman spectra of azulene and its derivatives as a result of the long wavelength electronic absorption bands extending well beyond the visible region. Crystal studies in the infrared, coupled with vapor phase band contours, have permitted a classification of the absorption bands according to symmetry, but a unique selection of the vibrational fundamentals has not yet been achieved.

The vibrational spectra of the isomeric naphthalene are now understood and little doubt remains about the assignment of the fundamental vibrational frequencies (3-6).<sup>2</sup> Computations of the vibrational frequencies using a valence force field transferred from benzene have contributed in no small measure to this achievement (4, 5). It seemed well worthwhile to carry out a similar approach to an understanding of the azulene spectra. In this paper are summarized the results of the first part of such a study on the out-of-plane motions.

### II. THEORY AND COMPUTATIONAL PROCEDURE

Azulene is a planar molecule of  $C_{2v}$  symmetry for which the out-of-plane normal vibrations may be classified as  $9b_1 + 6a_2$ . The class designations are as determined by the recommendations of Mulliken with the axes as shown in

<sup>1</sup> For earlier work, see References 1 and 2 of van Tets and Günthard (2).

<sup>2</sup> For earlier work, see references cited in Lippincott and O'Reilly (3) and Mitra and Bernstein (3).

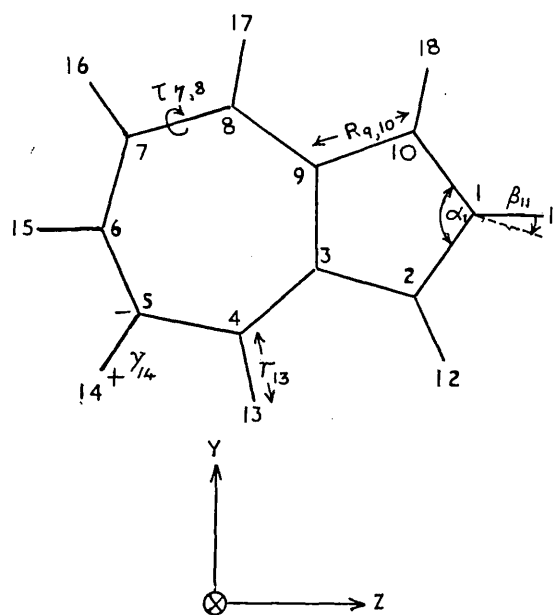


FIG. 1. Definition of axes and internal coordinates

Fig. 1. Solution of such a vibrational problem would be extremely tedious using desk calculators. An autocode program has been written for the solution of vibrational problems. The secular equation is set up in the form

$$A - I\Lambda = D^\dagger F D - I\Lambda, \quad (1)$$

where  $DD^\dagger = G$  and where, as usual,  $G$  and  $F$  represent the kinetic energy and potential energy matrices.  $I$  is the unit matrix. Premultiplication of (1) by  $D$  shows that the roots of  $A$  are equivalent to those of  $GF$  and that the eigenvectors,  $Y$ , are related to the usual  $L$  vectors by  $L = DY$ . The  $Y$  vectors themselves are related to the absolute mean amplitudes of vibration  $x$  by

$$x = M^{-1/2} Y Q,$$

where

$$Q = h^{1/2} (4\pi^2 \nu_p)^{-1/2}.$$

The  $D$  matrix is related to the  $B$  matrix by  $D = BM^{-1/2}$  where  $B$  is the transformation matrix from internal to Cartesian coordinates—that is,  $R = BX$ —and  $M^{-1/2}$  is a diagonal matrix with entries equal to the inverse square roots of the atomic masses appropriate to the corresponding atomic Cartesian axes. The advantages of setting up the problem in this manner are worthy of comment. A transformation of the type  $D^\dagger F D$ , where  $F$  is symmetric, yields a symmetric matrix. Fast computer programs, such as Householder's program (7), exist for

diagonalizing symmetric matrices. This advantage is in part offset by the increase in the order of the secular matrix, the matrix  $A$  being of dimension  $3N \times 3N$ . However the real gain is in the elimination of the well-known and vexing problem of redundancies. Each and every coordinate should be introduced into  $B$  and its corresponding force constants included in  $F$ . The redundancies become irrelevant in the transformation to cartesians implicit in forming  $A$ .

The  $B$  matrix for azulene is readily written down from the general definition of the internal coordinates in terms of the Cartesian coordinates:

$$r\Delta y_i = x_i + X_{i-1} \frac{r}{R_{i-1,i}} \frac{\sin(\pi - \frac{1}{2}\alpha_i)}{\sin \alpha_i} + X_{i+1} \frac{r}{R_{i,i+1}} \frac{\sin(\pi - \frac{1}{2}\alpha_i)}{\sin \alpha_i} - X_i \left[ \frac{r}{R_{i-1,i}} \frac{\sin(\pi - \frac{1}{2}\alpha_i)}{\sin \alpha_i} + \frac{r}{R_{i,i+1}} \frac{\sin(\pi - \frac{1}{2}\alpha_i)}{\sin \alpha_i} + 1 \right],$$

$$R_{i,i+1} \Delta \phi_i = \frac{R_{i,i+1}}{R_{i,i-1}} \frac{(X_i - X_{i-1})}{\sin \alpha_i} - \frac{R_{i,i+1}}{R_{i+1,i+2}} \frac{(X_{i+1} - X_{i+2})}{\sin \alpha_{i+1}} - \frac{R_{i,i+1}}{r_i} \frac{(X_i - x_i)}{\sin(\pi - \frac{1}{2}\alpha_i)} + \frac{R_{i,i+1}}{r_{i+1}} \frac{(x_{i+1} - X_{i+1})}{\sin(\pi - \frac{1}{2}\alpha_{i+1})}.$$

$x_i$  and  $X_i$  refer to the displacements of the  $i$ th substituent atom and the  $i$ th carbon atom, respectively.  $\alpha_i$  is the ring angle at the carbon atom  $i$ , and it has been assumed that the bond to the substituent bisects the external angle. When this latter condition is relaxed, as it was for twisting about bonds adjacent to the bond common to both rings, the angles  $(\pi - \frac{1}{2}\alpha)$  are replaced by angles which are readily ascertained from an inspection of the appropriate equations in Reference 8. [Eqs. (17) on page 51 and Eqs. (21) to (24) on page 61].<sup>3</sup>

In converting the  $B$  matrix to numerical form the structural data of Robertson, Shearer, Sim, and Watson (9) was used. Since there is a slight asymmetry in the values of the bond angles derived for the molecule in the crystal lattice the average of the values for equivalent angles in the isolated molecule sense was used.

The potential function can be expressed as

$$2V = \sum_i Pr^2 \Gamma_i^2 + 2 \sum_i p_0 r^2 \gamma \gamma_{i+1} + 2 \sum_i p_n r^2 \gamma_i \gamma_{i+2} + 2 \sum_i p_p r^2 \gamma_i \gamma_{i+3} + \sum_i QR_{i,i+1}^2 \phi_{i,i+1}^2 + 2 \sum_i q_0 R_{i,i+1} R_{i+1,i+2} \phi_{i,i+1} \phi_{i+1,i+2} - 2 \sum_i t_0 r R_{i,i+1} \gamma_i \phi_{i,i+1} + \sum_i P_{cc} (R \cdot \gamma_{cc})^2,$$

<sup>3</sup> Equation (22) on page 61 of Reference 8 is incorrect in that there is a sign error. It ought to read

$$S_{12} = \frac{r_{23} - r_{12} \cos \phi_2}{r_{23} r_{12} \sin \phi_2} \frac{e_{12} \times e_{23}}{\sin \phi_2} + \frac{\cos \phi_3}{r_{23} \sin \phi_3} \frac{e_{43} \times e_{32}}{\sin \phi_3}.$$

This error was noted and the correct formula deduced by Dr. R. B. Gravenor and by the present author independently.

TABLE I  
ADOPTED FORCE CONSTANTS IN UNITS OF  $10^{-12}$  DYNE  
cm/RADIAN<sup>2</sup>

$P_r^2 = +3.15$	$QR^2 = +0.57$
$p_{\theta}^2 = +0.13$	$q_{\theta}R^2 = -0.20$
$p_m^2 = -0.24$	$t_{\theta}R = +0.21$
$p_p^2 = -0.19$	$P_{cc}R^2 = +3.15$

where the summations are taken over all possible interactions whether in the same ring or not, except in that, following Scully and Whiffen's procedure for naphthalene,  $p_p$  is defined only for both substituents in the one ring. The values of the force constants in dyne cm/radian<sup>2</sup> were transferred directly from benzene except for  $P_{cc}$ . In the latter case it was assumed that  $P_{cc}R^2 = P_r^2$ . The values are given in Table I.

The frequencies computed for azulene,  $d_i(1)$ azulene,  $d_6(2, 4, 5, 6, 7, 8)$  azulene and  $d_8$  azulene are given in Table II, and the vibrational distortions are depicted in Fig. 2 for the  $d_0$  and  $d_8$  systems. The distortions are given as  $[10^{5/2}/(\nu_i M_j)^{1/2}]Y_{ij}$ , where the  $Y$  matrix is normalized to unity,  $\nu_i$  is the  $i$ th vibrational frequency in  $\text{cm}^{-1}$  and  $M_j$  is the mass in atomic units corresponding to the  $j$ th coordinate.

### III. FAR INFRARED SPECTRUM

An investigation of the far infrared spectrum of azulene carried out by the author prior to the publication of van Tets and Gunthard affords excellent confirmation of the low-frequency spectra reported in the latter work. The measurements were made on an evacuable grating spectrograph built in the department—the design of which has been reported elsewhere (10). The spectral slit widths used were of the order of  $1.5 \text{ cm}^{-1}$ . Bands were observed in benzene solution at  $402 \text{ cm}^{-1}$  (m),  $331.5 \text{ cm}^{-1}$  (m),  $311.2 \text{ cm}^{-1}$  (vs.), and  $162 \text{ cm}^{-1}$  (s).

### IV. VIBRATIONAL ASSIGNMENTS

The excellent infrared data of Hunt and Ross (1) and of van Tets and Gunthard (2) (hereafter referred to as H & R, and T & G, respectively) of crystals and solutions of azulene and the deuterium isotopic systems has allowed virtually all the absorption bands to be assigned to their appropriate symmetry classes. However intensity data alone do not suffice to choose the fundamentals since, as is well known, the local symmetry of a normal mode, even when infrared absorption is allowed, may give rise to a small dipole gradient and, hence, low intensity. H & R and T & G are unanimous in their choice of the following fundamentals as  $b_2$  fundamentals: 960, 946, 764, 721, and  $165 \text{ cm}^{-1}$ . The present experimental data and that of T & G leave no doubt that the frequency  $311 \text{ cm}^{-1}$  has to be added to this list.

The absence of several bands in the solution spectrum while they appear with

TABLE II  
 COMPARISON OF CALCULATED AND ASSIGNED FREQUENCIES

$d_0$		$d_1$	$d_6$		$d_8$	
Calc.	Assigned	Calc.	Calc.	Assigned	Calc.	Assigned
$b_1$ Class						
1028	<i>c.</i> 1000	1026	957	<i>c.</i> 957	919	<i>c.</i> 920
982	960	960	927	890	798	833
958	946	914	868	840	770	798
791	764	741	663	681	611	612
735	721	690	627	610	556	
681	664	670	539		537	538
515	<i>c.</i> 492	481	490	<i>c.</i> 477	463	<i>c.</i> 470
272	311	269	245	<i>c.</i> 275	239	272
161	165	156	155	<i>c.</i> 155	147	<i>c.</i> 145
$a_2$ Class						
994	<i>c.</i> 1000	994	853	(844)	853	844
931	908	931	734	733	734	(733)
863	795	863	689	706	689	707
547	531	547	474		474	
323		323	295		295	
163		163	146		146	

moderate strength in the crystal spectrum is indicative of  $a_2$  symmetry. The value of such data has been demonstrated recently for naphthalene by Chantry, Anderson, and Gebbie (6). Bands at 908, 795, and 531  $\text{cm}^{-1}$  assigned on this basis to the  $a_2$  class are confirmed as such by the present calculations, but there is no place for the 744- $\text{cm}^{-1}$  band which in any case is quite weak.

The agreement between the calculated and the above assigned frequencies is very satisfactory. This encourages a reliance on the calculations for locating the other fundamentals. The calculations show that one  $b_1\gamma_{\text{CH}}$  band has yet to be located in the range 1000–900  $\text{cm}^{-1}$ . T & G and H & R place this fundamental near 700  $\text{cm}^{-1}$  which is clearly far too low. Polarization data give little help in locating a third  $b_1$  fundamental in the range 1000–900  $\text{cm}^{-1}$ . An analysis of the combination bands between 2000 and 1900  $\text{cm}^{-1}$  will be shown to suggest that this fundamental is near 1000  $\text{cm}^{-1}$ . The two highest  $b_1$  ring deformations have yet to be located. H & R place these at 707 and 664  $\text{cm}^{-1}$ —both corresponding to weak bands. T & G prefer very low frequencies, namely, 333, 319, 180, and 170  $\text{cm}^{-1}$  to the four twisting modes. There seems little doubt that the bands at 180 and 170  $\text{cm}^{-1}$  arise from a crystal splitting of the low pure skeletal mode and must be considered as due to one fundamental. On the basis of the calculations the modes should have frequencies close to 680 and 520  $\text{cm}^{-1}$ . These frequencies are also in better accord with the corresponding benzene frequencies, 705 ( $b_{2g}$ ) and 405 ( $e_u$ )  $\text{cm}^{-1}$ —and in naphthalene the range of the analogous twisting

modes is  $770\text{--}385\text{ cm}^{-1}$ . This leads the author to the belief that the weak bands at  $664$  and  $473\text{ cm}^{-1}$  chosen by H & R as arising from the skeletal deformations are at least close in frequency to the correct assignments. The latter frequency has been slightly modified using the data of T & G to raise this frequency above its  $d_1$  counterpart.

In the  $a_2$  class the highest  $\gamma_{CB}$  frequency is required. The summation bands unambiguously locate this at about  $1000\text{ cm}^{-1}$ . No observed crystal band can be identified with this mode. The present evidence does not permit the lowest two  $a_2$  fundamentals to be assigned frequencies.

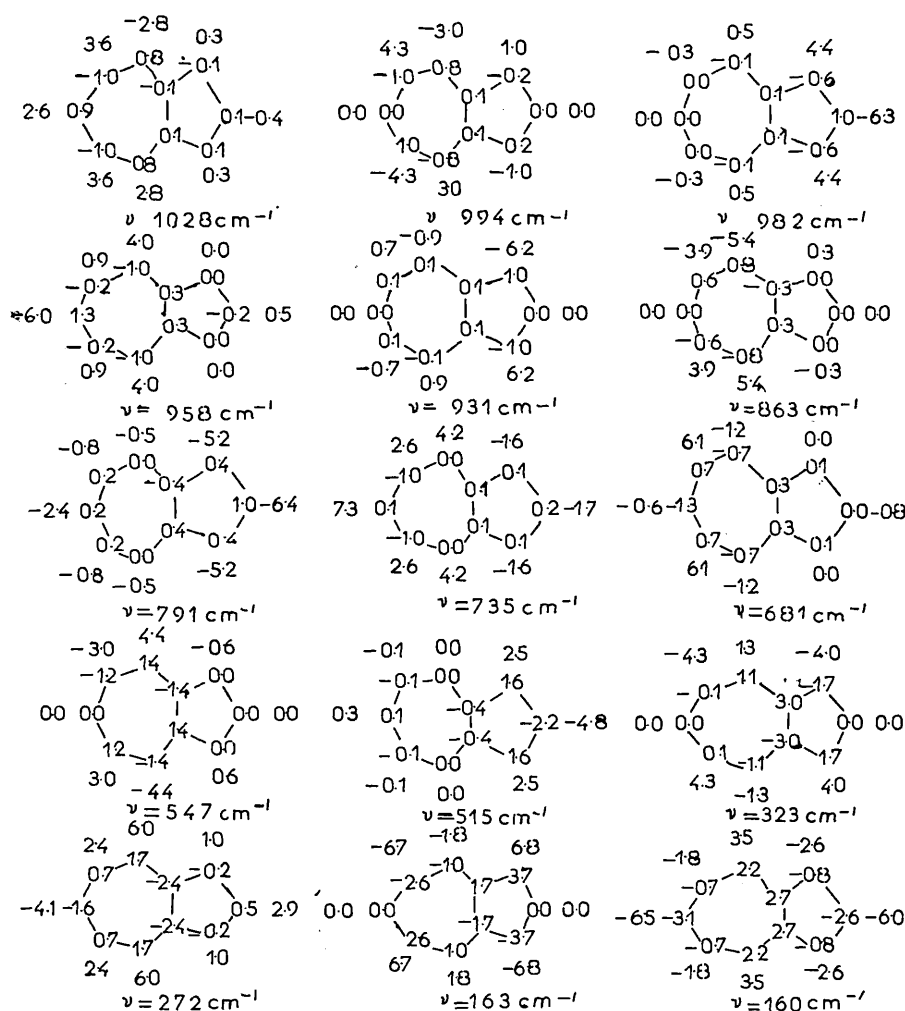
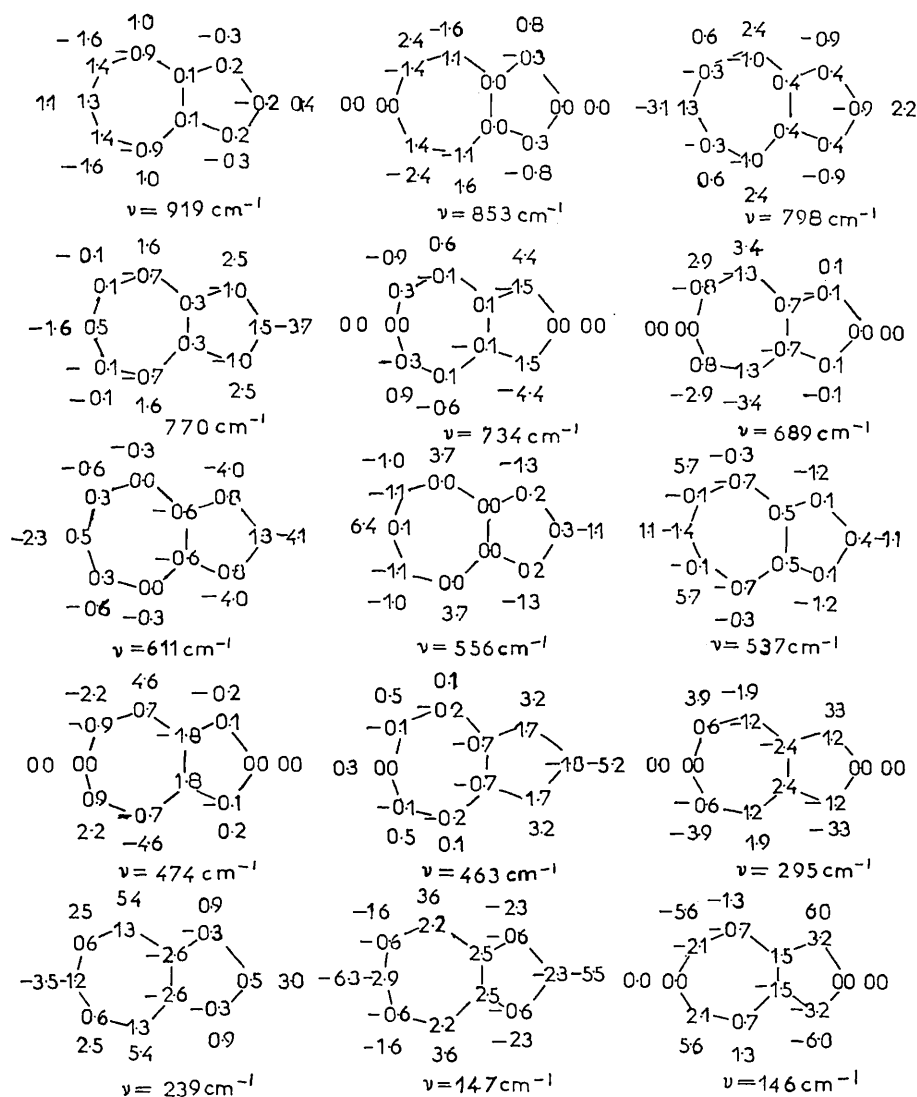


FIG. 2. (a) Normal coordinates of azulene. (b) Normal coordinates of  $d_8$  azulene





## V. SUMMATION BANDS

It is well known that aromatic systems show a series of strong combination bands in the range  $2000$  to  $1600 \text{ cm}^{-1}$  which arise from combination transitions involving the out-of-plane CH deformations (11, 12). These have been shown to be very useful in identifying uncertain  $\gamma_{\text{CH}}$  frequencies (e.g., see Reference 5). The observed bands of azulene in this region are no exception to the general rule. The situation is further improved by the identification of the overall sym-

TABLE III  
 OBSERVED ABSORPTION BANDS BETWEEN 2000 AND 1600  $\text{cm}^{-1}$  AND ASSIGNMENTS

Vapor	H & R Crystal	T & G Crystal	Soln.	Symmetry	Assignment
<i>d</i> <sub>3</sub> Azulene					
1970 (1)	1970 (2)	1959 m	1968 m	<i>b</i> <sub>2</sub>	(1000) + 963 ( <i>b</i> <sub>2</sub> )
			1948 m	<i>a</i> <sub>1</sub>	(1000) + 952 ( <i>a</i> <sub>1</sub> )
1935 (1)	1935 (2)	1926 m	1930 m	<i>a</i> <sub>1</sub> or <i>b</i> <sub>1</sub>	2 × 963 ( <i>a</i> <sub>1</sub> )
		1907 vw	1908 m	<i>a</i> <sub>1</sub>	(1000) + 908, 952 + 963; 2 × 952 ( <i>a</i> <sub>1</sub> )
		1884 vw	1889 w		908 + 963 ( <i>a</i> <sub>1</sub> )
	1865 (1)	1864 vw	1858 w	<i>b</i> <sub>2</sub>	908 + 952 ( <i>b</i> <sub>2</sub> )
1825 (2)	1815 (1)	1815 w	1820 s	<i>a</i> <sub>1</sub>	2 × 908 ( <i>a</i> <sub>1</sub> )
		n.o.	1799 w	<i>a</i> <sub>1</sub> or <i>b</i> <sub>1</sub>	(1000) + 795, 2 × 900 ( <i>a</i> <sub>1</sub> ) etc.
		1697 w	1694 m	<i>a</i> <sub>1</sub> or <i>b</i> <sub>2</sub>	765 + 952 ( <i>a</i> <sub>1</sub> )
		n.o.	1670 w	<i>a</i> <sub>1</sub> or <i>b</i> <sub>2</sub>	908 + 765 ( <i>b</i> <sub>2</sub> ) 765 + 900 ( <i>a</i> <sub>1</sub> )
<hr/>					
	Crystal	Soln.		Symmetry	Assignment
<i>d</i> <sub>6</sub> Azulene					
	n.o.	1795 m		<i>a</i> <sub>1</sub>	(957) + 840 ( <i>a</i> <sub>1</sub> )
	1745 vw	1735 m		<i>a</i> <sub>1</sub>	890 + 840 ( <i>a</i> <sub>1</sub> )
	1671 m	1662 m		<i>b</i> <sub>2</sub>	957 + 706 ( <i>b</i> <sub>2</sub> )
	1640 w	1635 vw			
	1619 m	1619 w		<i>b</i> <sub>2</sub>	890 + 733 ( <i>b</i> <sub>2</sub> )
		1606 m		<i>a</i> <sub>1</sub>	
	1590 m	1580 s		<i>a</i> <sub>1</sub>	844 + 733 ( <i>a</i> <sub>1</sub> )
<hr/>					
<i>d</i> <sub>8</sub> Azulene					
		1799 w		<i>a</i> <sub>1</sub>	
	1718 vw	1719 m		<i>a</i> <sub>1</sub>	(920) + 798 ( <i>a</i> <sub>1</sub> )
	1667 w	1658 vw		<i>b</i> <sub>2</sub>	(920) + 733 ( <i>b</i> <sub>2</sub> )
	1626 w	1622 w			(920) + 707 ( <i>b</i> <sub>2</sub> )

metry of the transitions involved in many cases by crystal studies. Using the assignments which are unambiguous only two moderately strong bands, those at 1968 and 1948  $\text{cm}^{-1}$ , remain unexplained in the spectrum (see Table III). These strongly suggest that the highest  $\gamma_{\text{CH}}$  frequency of the *a*<sub>2</sub> class is approximately 1000  $\text{cm}^{-1}$ . This forms the basis of the previous assignments of 1000  $\text{cm}^{-1}$  to the highest *a*<sub>2</sub> mode. It appears from the calculations that the highest *b*<sub>1</sub> mode ought to appear at about either 1000  $\text{cm}^{-1}$  or 920  $\text{cm}^{-1}$  depending on the correlation of the two assigned bands with the calculated frequencies. The former would explain the solution band at 1948  $\text{cm}^{-1}$ . This value is made virtually certain by an analysis of the combination bands of the deuterated species. In

$d_8$  azulene and in  $d_6$  azulene the strongest bands in the region 2000–1600  $\text{cm}^{-1}$  are  $a_1$  type at 1719 and 1795  $\text{cm}^{-1}$ , respectively. These frequencies are too high to arise from  $a_2$  modes and necessitate the assignment of the highest  $b_2$  fundamentals at frequencies almost exactly equal to the calculated. Furthermore the modes involved should have considerable intensity on the criterion that the principal displacements arise from the same atoms in each case (13). The resulting pattern of agreement between calculated and observed frequencies for  $d_6$  and  $d_8$  shows that the  $d_0$  frequency must lie near 1000  $\text{cm}^{-1}$ . In none of the spectra can this fundamental transition be observed. An examination of the mode depicted in Fig. 2 shows an alternating sequence in the phases of the CH deformations which gives rise to a pseudo centro-symmetric mode. This is likely to be of low intensity by comparison with its inactive benzene counterpart.

#### VI. THE SPECTRA OF $d_6$ AND $d_8$ AZULENES

The bulk of the assignments in Table II for the  $b_1$  species require no further comment. In several cases van Tets and Gunthard note splitting of bands into two components, one component being polarized parallel to the  $a$  axis, and the second to the  $b$  axis. They generally assign these to two bands. However such splittings—especially where high dichroic ratios are concerned—most likely arise from coupling between vibrations within the unit cell. Such coupling has been well established in biphenyl (14). T & G note that crystal splitting will give rise to such doublets.

In the  $a_2$  class, as might be expected, the available experimental evidence as to the frequencies for any one molecular species is meager. However it is a symmetry requirement that the G matrix for the  $a_2$  species should be invariant to the substituent at ring positions 1 and 5. This means that for isotopic substitution at these positions the  $a_2$  frequencies must be identical. This stringent requirement permits the elimination of many spectral bands as possible  $a_2$  fundamentals in the  $d_6$  and  $d_8$  spectra. Weak bands at 706 and 707  $\text{cm}^{-1}$  probably arise from one fundamental, and bands at 844  $\text{cm}^{-1}$  in the  $d_8$  spectra and 733  $\text{cm}^{-1}$  in the  $d_6$  spectra are further likely candidates. In the latter cases the corresponding bands in the other species are probably overlaid by stronger bands of other symmetries.

The Redlich–Teller product ratios are of little interest since the calculated and assigned frequencies agree so well. Discrepancies between the theoretical and observed ratios can be explained easily in terms of phase shifts and anharmonicity corrections. The observed ratio for  $d_8$  to  $d_0$  species is 0.255 for the  $b_1$  class compared with the theoretical of 0.1986 if we take the missing frequency as equal to the calculated. The difference amounts to 3% for each frequency. For the  $d_6$  to  $d_0$  the calculated ratio is 0.3718 and the observed ratio 0.399. It is to be noted that T & G are in error in giving the theoretical ratio 0.265 for these latter species.

TABLE IV  
 POTENTIAL ENERGY DISTRIBUTION FOR  $d_0$  AZULENE

Freq.	$\gamma_{11}$	$2\gamma_{12}$	$2\gamma_{13}$	$2\gamma_{14}$	$\gamma_{15}$	$2\phi_{12}$	$2\phi_{23}$	$2\phi_{34}$	$2\phi_{45}$	$2\phi_{56}$	$\phi_{39}$	$2\gamma_{cc}$
1028	0	0	26	49	16	0	0	0	5	4	0	0
994	0	1	32	54	0	0	0	0	9	3	0	0
982	37	35	1	0	0	23	4	0	0	0	0	0
958	0	0	38	3	40	0	0	4	3	12	0	0
931	0	71	2	1	0	13	12	0	0	0	0	0
863	0	0	59	27	0	0	0	7	0	6	0	0
791	41	39	0	2	3	0	13	0	0	1	0	0
735	3	3	16	41	20	0	1	7	1	9	0	0
681	0	0	8	2	40	0	0	1	27	20	0	1
547	0	5	7	7	0	0	0	18	31	5	2	25
515	16	31	0	0	0	38	6	2	0	0	0	5
323	0	6	0	1	0	7	15	0	3	4	2	62
272	3	0	6	1	1	0	6	8	13	21	0	40
163	0	0	0	0	0	3	29	12	9	9	22	16
160	1	3	6	1	1	0	0	62	0	3	0	22

## VII. POTENTIAL ENERGY DISTRIBUTION

The potential energy distribution (P.E.D.) in a vibration  $i$  is given by  $\sum_{j,k} l_{ij} l_{ik} f_{jk}$ . In an effort to classify the modes according to type the contribution of the diagonal force constants to the P.E.D. has been evaluated and tabulated in Table IV for  $d_0$  azulene. The results are given in the form  $l_{ij}^2 f_{jj} \times 100 / \sum_k l_{ik}^2 f_{kk}$ . It is apparent from the results that the eight highest frequency vibrations are almost pure CH deformations. Even so the two highest frequency  $b_1$  skeletal modes contain a very appreciable amount of C—H deformation. The  $a_2$  skeletal modes on the other hand are virtually pure. The results also show very clearly that the deformations for any particular vibration are localized in one of the rings.

## VIII. CONCLUSIONS

The good agreement between calculated and observed frequencies shows that the azulene force field is not very different from that in benzene. This in itself is interesting in view of the pseudo-aromatic character of the molecule. The localization of vibrations in one or the other ring suggests that it might well be possible to treat polynuclear systems as conglomerates of mononuclear systems with substituents of particular masses. Thus in this case the out-of-plane vibrations of azulene might be considered as arising from 1,2 di  $X$  cycloheptatrienyl and 1,2 di  $X$  cyclopentadienyl radicals. The vibrations common to the two groups would then have to be averaged. This might prove to be a suitable approximation for the higher polynuclear systems.

The majority of the out-of-plane assignments now seem to be satisfactory.

One or two doubts as to exact frequencies remain in the  $b_2$  classes—particularly for the two highest frequency ring modes. The inactive  $a_2$  ring modes can not yet be identified.

## ACKNOWLEDGMENTS

I wish to thank Dr. D. H. Whiffen for helpful discussions, Dr. K. Singer for assistance in programming, and the U. S. Navy for a grant for research in far infrared spectroscopy.

RECEIVED May 18, 1964

## REFERENCES

1. G. R. HUNT AND I. G. ROSS, *J. Mol. Spectry.* **3**, 604 (1959).
2. A. VAN TETS AND HS. H. GÜNTARD, *Spectrochim. Acta* **19**, 1495 (1963).
3. E. R. LIPPINCOTT AND E. J. O'REILLY, *J. Chem. Phys.* **23**, 238 (1955);  
S. S. MITRA AND H. J. BERNSTEIN, *Can. J. Chem.* **37**, 553 (1959).
4. D. B. SCULLY AND D. H. WHIFFEN, *Spectrochim. Acta* **16**, 1409 (1960).
5. D. B. SCULLY AND D. H. WHIFFEN, *J. Mol. Spectry.* **1**, 257 (1957).
6. W. CHANTRY, A. ANDERSON, AND H. A. GEBBIE, *Spectrochim. Acta* **20**, 1465 (1964).
7. A. S. HOUSEHOLDER AND F. L. BAUER, *Numerische Math.* **1**, 29 (1959).
8. E. B. WILSON JR., J. C. DECIUS, AND P. C. CROSS, "Molecular Vibrations." McGraw-Hill, New York, 1955.
9. J. M. ROBERTSON, H. M. M. SHEARER, G. A. SIM, AND D. G. WATSON. *Acta Cryst.* **15**, 1 (1962).
10. P. J. HENDRA, R. D. G. LANE, AND B. SMETHURST. *J. Sci. Instr.* **40**, 457 (1963).
11. D. H. WHIFFEN, *Spectrochim. Acta* **7**, 253 (1955).
12. Y. KAKIUTI, *J. Chem. Phys.* **25**, 777 (1956)
13. F. E. DUNSTAN AND D. H. WHIFFEN, *J. Chem. Soc.* p. 5221 (1960).
14. D. STEELE AND E. R. LIPPINCOTT, *J. Mol. Spectry.* **6**, 238 (1961).

## The vibrational spectrum and geometrical configuration of decafluorobiphenyl\*

D. STEELE

Royal Holloway College, Englefield Green, Egham, Surrey

T. R. NANNEY and E. R. LIPPINCOTT

Department of Chemistry, University of Maryland, College Park, Maryland

(Received 5 July 1965)

**Abstract**—The Raman and infrared spectra of decafluorobiphenyl in solution and solidified melt are reported. A partial vibrational assignment is presented for the solution data assuming  $D_2$  symmetry.

It appears that the molecule is not planar in solution, however a comparison of solution and solidified melt spectra indicates that the molecules are aligned in the crystal and favours a planar or near-planar structure in this phase. The vibrational frequencies show little interaction between the vibrations in the two rings.

### 1. INTRODUCTION

THE PRIMARY purpose of this investigation of decafluorobiphenyl was to obtain information as to the relative conformations of the two rings. Also, it is of interest to know to what extent the vibrations of the pentafluorophenyl units couple.

In biphenyl and in polyphenyls the individual aromatic units are coupled very weakly with the result that the spectra of the units are nearly additive [1, 2]. This situation considerably facilitates the analysis of the spectra, but it prevents unequivocal deductions being made as to the relative conformations of the rings. It is conceivable that introduction of fluorine into the rings will alter this situation on two grounds. The increased mass of the substituents will considerably increase the kinetic mixing of the vibrational modes, and the increased dimensions of the substituents will introduce steric interaction between the rings. A consequence of the former in hexafluorobenzene was the increased importance of CX interactions with the ring modes. In benzene these interactions are assumed to be of small magnitude, but this assumption is not permissible for  $C_6F_6$  if agreement between calculated and observed frequencies is desired [3].

The conformation of the phenyl rings of fluorobiphenyls has been the subject of considerable research. Electron diffraction [4], ultraviolet spectra [5] and dipole

\* This work was supported in part by a Materials Science Program from the Advanced Research Projects Agency, Department of Defense and a grant from the U.S. Atomic Energy Commission.

[1] D. STEELE and E. R. LIPPINCOTT, *J. Mol. Spectroscopy* **6**, 238 (1961).

[2] J. DALE, *Acta Chem. Scand.* **11**, 640 (1957).

[3] D. STEELE and D. H. WHIFFEN, *Trans. Faraday Soc.* **56**, 5 (1960)

[4] O. BASTIASEN and L. SMEDVIK, *Acta Chem. Scand.* **8**, 1953 (1954).

[5] G. H. BEAVEN and D. M. HALL, *J. Chem. Soc.* 4637 (1956).

Table I. Observed vibrational spectrum of  $C_{10}F_{12}$ 

Solidified Melt	Infrared		Raman			Solidified Melt	Assignment*	Equiv. $D_{2h}$ class
	Melt	$CS_2$ Solution	$CCl_4$ Solution	$CS_2$ Solution	$CCl_4$ Solution			
		183 <sup>b</sup> m		15 <sup>g</sup> w			$b_{1g}, b_{2g}, b_{3g}$	
		240 <sup>b</sup> s					fundamentals	
		~270 vw		235 vw (dp)	187 vvw	238 vw	$b_2, b_3$	$b_{2u}, b_{3u}$
		280 w	280 w				$b_2$	$b_{2g}, b_{3g}$
		295 vvw		273 vvw (dp)			$a_1, b_2, b_3$	$a_g, b_{2g}, b_{3g}$
		305 vw sh					$b_1, b_2$	$b_{1u}, b_{2u}$
305 vw sh		313 w	313 w				$b_3$	$b_{3g}$
312 w-m		344 w	344 w				$b_2$	$b_{2u}$
336 w-m (I)								
		339 w						
		387 vvw	387 vvw	363 vw sh	362 vvw	390 s	$b_2$	$b_{2g}$
389 vvw		411 vvw	410 vvw	386 m	386 m (dp)		$b_1, b_3$	$b_{1u}, b_{3u}$
411 vvw				408 w-m (dp)	411 w-m (dp)	411 w-m	$b_2, b_3$	$b_{2u}, b_{3u}$
452 vw			456 <sup>c</sup> w	440 w (dp)		446 w	$a$ or $b_3$	$a_g$ or $b_{3g}$
469 w (I)				469 vw (dp)			$b_2$	$b_{2u}$
475 vw sh		478 w	478 <sup>c</sup> w			480 vw	$b_1$	$b_{1u}$
510 vvvw				509 m (P)	511 m (P)	513 m	$a$	$a_g$
		542 vvvw					$b_1$	$b_{1g}$
		556 vvvw		553 <sup>c</sup> vvw		548 vvw?		
~559 vvvw sh		580 w	588 w				$b_1$	$b_{1u}$
578 vw							$b_1$	$a_g$
619 vvw		620 vvw	618 vvw	585 m (P)	588 m (P)	593 m	$a$	$a_g$
652 vw		652 vvw	653 vw		~621 vvw?		$b_2$	$b_{2u}$
		681 vvw	678 vw		652 w	654 w	$b_2$	$b_{2u}, b_{2g}$
699 vvw		~702 vvw sh					$b_3$	$b_{3u}$
726 m (I)		728 s	727 <sup>c</sup> s				$b_2$	$b_{2u}$
752 vvw		750 w						
778 vw		771 vw						
794 vvw		~792 w						
806 vvw		~805 vvw						
		832 vvvw						
		850 vvvw						
880 vw		855 vvvw						
934 vw sh		889 vvw	889 <sup>c</sup> vw					
		~937 vw sh	937 <sup>c</sup> w					
				957 w (P)	960 w (P)	959 w	$a$	$a_{1g}$
~967 ms sh		~964 m sh						
~975 ms sh (I)		981 s	982 <sup>c</sup> s				$b_2$	$b_{2u}$
		1000 s	1000 s					
		1009 s	1010 s					
1008 s				1003 vvw?	1004 vvw		$b_3$	$b_{3g}$

1038 s	1038 m	1037 m	1038 w	$b_{1u}$
1064 ms	~1065 m sh	1060 w-m sh	1064 w	
1073 m	1078 s	1078 s	1079 s	$b_{2u}$
1086 m } (l)				$b_{2g}$
1092 w-m sh	~1091 w sh?	1089 w sh	1091 w sh	$a_{1g}$
1106 w-m	~1104 w sh	~1102 vw	1103 vvw	$b_{1u}$
1132 w	1131 w	1128 vw	1128 vw	$a$
1147 m			~1147 vvw	$b_1$
1156 w	1155 w-m	1154 w	1155 w	$b_3 ?$
1169 vvw	1171 vw sh	1169 vvw sh	1170 vvw	$b_2$
1259 vw sh	~1255 vw	~1254 vvw sh	~1262 <sup>c</sup> vvw	$a_{1g}$
1272 w	1274 w	1269 vvw	1274 vw	$b_{2u}$
1289 w-m (l)	1293 m	1292 m	~1271 vvw	$a_{1g}$
1304 vvw			~1300 vvw (P)	$b_{1u}$
1345 w	1346 w	1342 vw	1305 vvw?	
1374 ms	1377 m	1370 w-m	~1338 vvw	$b_1 ?$
1409 w	1408 w	1407 vw	~1342 vw	$b_2$
1434 m	1436 w	1433 vw	~1339 vvw	$a$
~1470 ms sh	1473 ms sh?	~1460 w sh		$b_1 ?$
1501 s	~1494 vs	~1474 ms sh?	1472 s (l)	$b_{1u} ?$
1509 s (l)	~1514 vs		1476 s (P)	$a_{1g}$
1524 s				$b_{2u}$
~1532 ms sh	~1532 ms sh	1530 ms sh		
1593 m	~1564 vvw		1533 w (P)	$b_1, b_3$
~1616 w-m	1591 w	1591 w	1555 w (P)	$a, b_3$
1632 m	1616 vvw	1617 vw		$b_{1u}, b_{2g}$
1651 m (l)	1627 m sh	1629 w		
1655 m	1634 m sh	1634 w sh		
1666 w-m	1651 ms	1650 ms		$b_{2u}$
1682 vw sh	1656 ms sh	1655 m	1657 s (P)	$b_1$
1700 vvw	1666 ms	1665 w-m	1662 vs	$a, b_3$
1717 vw sh	~1712 vw sh	1666 w-m sh		
1728 w	overlap	1687 vvw	1716 vvw?	
1733 w		1714 vw		
1739 w				
1785 vw	1739 w	1736 vw		
1797 vvw	~1782 vvw	1785 vvw		
1872 w	~1804 vvw	1803 vvw		
	1877 w	1877 w		

\* Only assignments for fundamentals are given.

a Obtained with Cary White spectrometer.

b Obtained with far infrared spectrophotometer of special design.

c Partially contributed by solvent.



moment [6] studies for 2,2'-difluorobiphenyl have been interpreted by assuming that the interplanar angle is near  $60^\circ$  with the fluorine atoms in a "cis" configuration. More recently, the observed chemical shifts of  $^{19}\text{F}$  in the n.m.r. spectrum of decafluorobiphenyl have been used to estimate its interplanar angle [7].

## 2. EXPERIMENTAL

A sample of decafluorobiphenyl was obtained from Imperial Smelting Corporation and was recrystallized twice from benzene before use. A gas chromatogram of the compound after recrystallization gave no indication of impurities. The reported infrared spectra were obtained with a Perkin-Elmer 421 equipped with an accessory 2000-200  $\text{cm}^{-1}$  interchange. Infrared spectra were obtained for  $\text{CS}_2$  and  $\text{CCl}_4$  solutions, melt and a solidified melt between NaCl and CsBr windows. The reported Raman spectra were obtained with a Cary 81 spectrophotometer. Raman spectra were obtained for  $\text{CS}_2$  and  $\text{CCl}_4$  solutions and for a solidified melt prepared by allowing 1 ml of melt approximately two degrees above its melting point to cool in a 7 mm Raman tube over a two hour period. All data are listed in Table 1, and representative spectra are given in Fig. 1 and 2.

An independent study by one of us\* using a different sample of  $\text{C}_{12}\text{F}_{10}$ , a Unicam SP 100 with 130 grating accessories and a far infrared grating spectrophotometer of special design [8] confirmed all the main features of the infrared spectra reported in this work. In both infrared studies large decreases in intensity were observed for some lines upon going from solution to solidified melt. Using a set of data obtained with the Unicam the ratios of intensities (intensity solution/intensity crystal) were measured above  $500 \text{ cm}^{-1}$  taking the ratio of intensities for the  $1372 \text{ cm}^{-1}$  line as unity. Most of the absorption bands have the same relative intensities in solution and solidified melt, but a number of bands have ratios in the range from 3 to 21. All bands showing these large intensity changes are marked with "I" in Table 1. The Raman spectrum of  $\text{C}_{12}\text{F}_{10}$  in  $\text{CCl}_4$  was also obtained in the independent study using a Cary White spectrometer.

## 3. THEORY AND RESULTS

Spectral evidence indicates that hexafluorobenzene is planar [9], and therefore, it appears safe to assume that the pentafluorophenyl units are planar. A further assumption which will be made is that the phenyl units are colinear. Based on these assumptions three structures are possible.

3.1 A planar system of  $D_{2h}$  symmetry. The representation of the modes is then

$$11 a_g (\text{R}) + 3b_{1g} (\text{R}) + 6b_{2g} (\text{R}) + 10b_{3g} (\text{R}) + 4a_u (\text{i.a.}) \\ + 10b_{1u} (\text{i.r.}) + 10b_{2u} (\text{i.r.}) + 6b_{3u} (\text{i.r.})$$

The activities of the transitions are shown in parentheses. For this representation as well as those that follow, the recommendations of MULLIKEN [10] have

\* D. STEELE.

- [6] A. C. LITTLEJOHN and J. W. SMITH, *J. Chem. Soc.* 2552 (1954).  
 [7] N. BODEN, J. W. EMSLEY, J. FEENEY and L. H. SUTCLIFFE, *Mol. Phys.* **8**, 467 (1964).  
 [8] P. J. HENDRA, R. D. G. LANE and B. SMETHURST, *J. Sci. Instr.* **40**, 457 (1963).  
 [9] D. STEELE and D. H. WHIFFEN, *Trans. Faraday Soc.* **55**, 369 (1959).  
 [10] R. MULLIKEN, *J. Chem. Phys.* **23**, 1997 (1955).

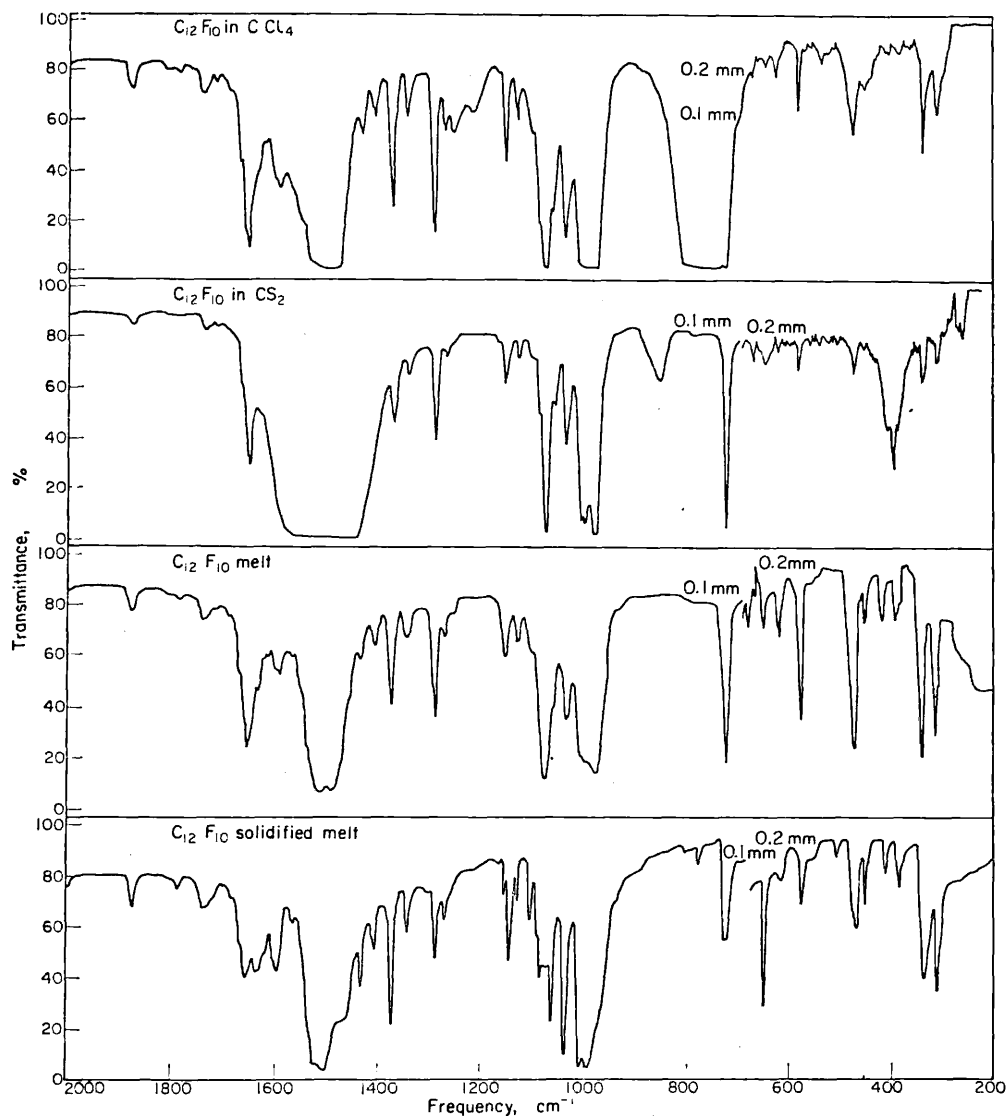


Fig. 1. Representative infrared spectra of  $C_{12}F_{10}$ . From top to bottom:  $CCl_4$  solution,  $CS_2$  solution, melt, solidified melt. Typical conditions: Slit program, 1000; gain 4.5; attenuator, 1100; scan time, 50 min; suppression, 6; source current, 0.32 A.

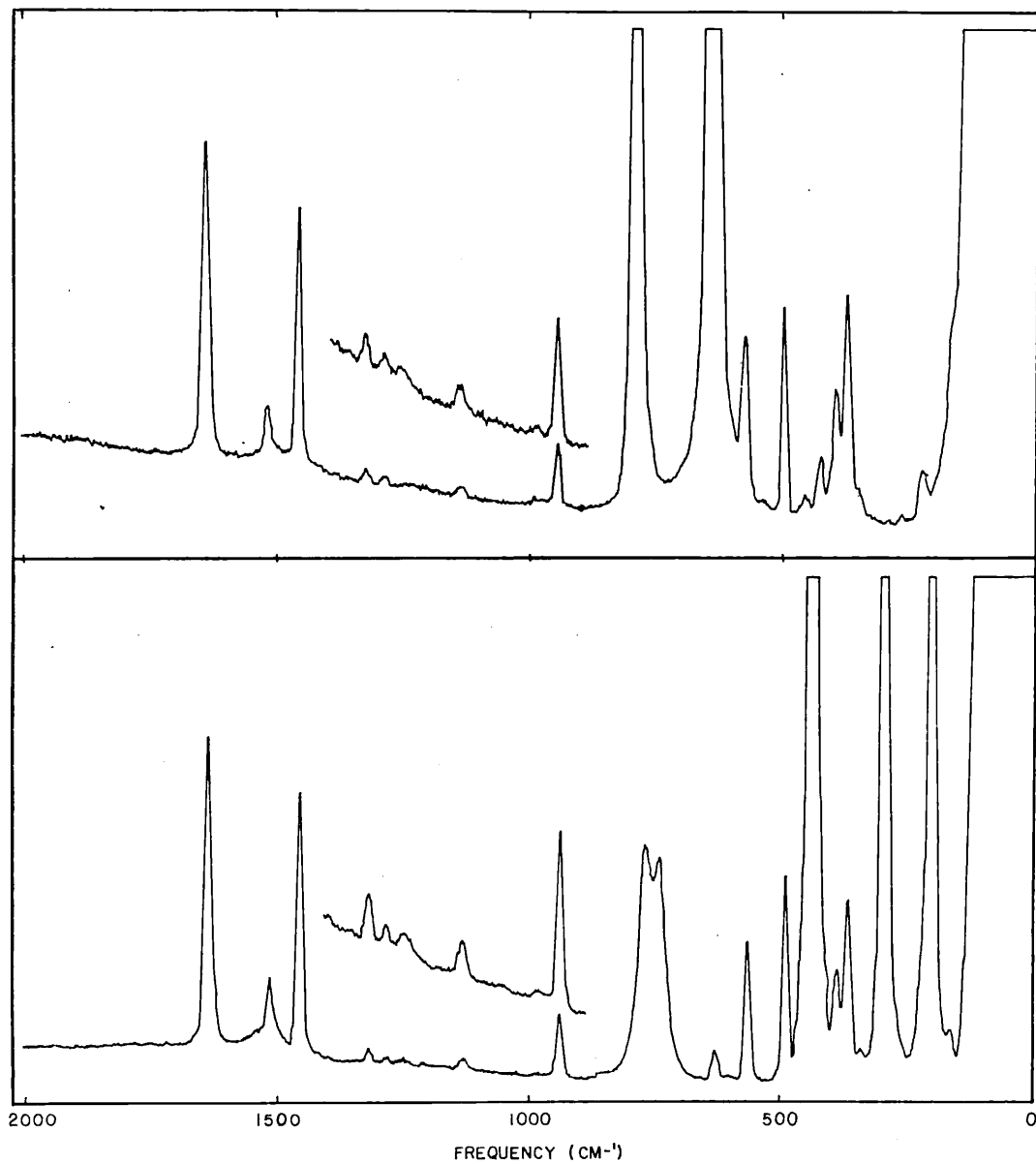


Fig. 2. Representative solution Raman spectra of  $C_{12}F_{10}$ . Top,  $CS_2$  solution; bottom,  $CCl_4$  solution. Typical conditions: Scan speed,  $1\text{ cm}^{-1}/\text{sec}$ ; slit width,  $10\text{ cm}^{-1}$ ; slit height,  $10\text{ cm}$ ; zero suppression, 100; period, 10; sensitivity.

been adopted in selecting molecular axes. The  $z$ -axis is colinear with the phenyl-phenyl bond. For the planar case the  $x$ -axis bisects the phenyl-phenyl bond and is perpendicular to the plane of the molecule.

3.2 A symmetric rotor structure of  $D_{2d}$  symmetry. The associated vibrational representation is

$$11a_1 (\text{R}) + 3a_2 (\text{i.a.}) + 4b_1 (\text{R}) + 10b_2 (\text{R,i.r.}) + 16e (\text{R,i.r.})$$

3.3 A  $D_2$  structure in which the angle between the planes of the rings is between 0 and  $\pi/2$ . The corresponding representation is

$$15a (\text{R}) + 13b_1 (\text{R,i.r.}) + 16b_2 (\text{R,i.r.}) + 16b_3 (\text{R,i.r.})$$

For the  $D_{2h}$  structure the fundamental vibrations are forbidden to give rise simultaneously to infrared and Raman lines. For  $\text{C}_{12}\text{F}_{10}$  twelve of twenty-three observed Raman lines in solution appear to be coincident with infrared lines. For many molecules these coincidences would be sufficient grounds for rejecting the  $D_{2h}$  model, but in the case of symmetrically substituted biphenyls many accidental coincidences are expected. In this regard it may be noted that in the cases of biphenyl and decadeuterobiphenyl [11] nineteen of a total of fifty and twenty-five of a total of forty-seven, respectively, of the observed Raman lines appear to be coincident with infrared lines. Yet for both of these compounds the observed frequencies were successfully assigned assuming a  $D_{2h}$  model, although the final assignment was one based essentially on  $D_2$  symmetry. Additional spectral evidence for the  $D_{2h}$  model for  $\text{C}_{12}\text{H}_{10}$  and  $\text{C}_{12}\text{D}_{10}$  was furnished subsequently by a study of the crystal spectrum [1]. In view of these points it appears that the main evidence for the conformation in solution of the pentafluorophenyl units of  $\text{C}_{12}\text{F}_{10}$  must arise from the ability of the various models to provide an adequate explanation for the observed frequencies.

For the three proposed models a reasonable assignment of the observed lines is most easily made on the basis of a  $D_2$  model. While the  $D_{2d}$  model is not completely eliminated by the available data, the complexity of the infrared spectrum makes the assignment difficult and is strong evidence against the  $D_{2d}$  model. Assignment of the coincident lines below  $1000 \text{ cm}^{-1}$  is considerably easier using the  $D_2$  model than with the  $D_{2h}$  model. However the pattern of coincidences is such that modes expected to be infrared (or Raman active) on the basis of  $D_{2h}$  symmetry appear but weakly in the Raman effect (or infrared absorption). This would suggest that the structural deviation from planarity was not as great as suggested by the n.m.r. results. Even so it is surprising that the Raman intensity of the CF modes is so low. We interpret these points as strong support for the conclusion of BODEN [7] that  $\text{C}_{12}\text{F}_{10}$  is non-planar in solution but probably with an azimuthal angle between pentafluorophenyl rings of less than that suggested (approximately  $50^\circ$ ). Consequently, for the vibrational assignment of  $\text{C}_{12}\text{F}_{10}$  in solution, the molecule will be treated as having  $D_2$  symmetry.

#### 4. VIBRATIONAL ASSIGNMENT

An important and as yet unexplained feature of the observed infrared spectra of  $\text{C}_{12}\text{F}_{10}$  is the large decrease in intensity observed for some lines in going from solution to solidified melt. The following points regarding these changes are pertinent.

[11] J. E. KATON and E. R. LIPPINCOTT, *Spectrochim. Acta* **15**, 627 (1959).

- (a) Not all the infrared lines change intensity in going from solution to solid. Ordinarily, this behavior implies the existence of two sets of transition moments in the solid state, one set perpendicular to the surface of the solid and the other set parallel to the surface.
- (b) The magnitudes of the intensity changes appear to be too great to be explained by changes in band shape and crystal field effects.
- (c) The magnitudes of the intensity changes are of the order expected if neighboring molecules in the solid state are aligned with the affected transition moments parallel.
- (d) Comparison of the observed frequencies with those calculated for  $C_6F_5X^{12}$  systems shows that all lines of weakened intensities have frequencies within ranges expected for  $b_2$  modes.

All these points can be explained by assuming that in the solid state  $C_{12}F_{10}$  is planar with symmetry  $D_{2h}$  or nearly planar with symmetry  $D_2$ . The available data do not allow an unequivocal decision between these models, but in either case the intensity changes observed for some infrared lines facilitates the assignment of fundamentals. For the  $D_{2h}$  model of the solid all lines exhibiting large intensity changes will be  $b_{2u}$  modes. For the  $D_2$  model these lines will be  $b_2$  modes, but complete exclusion of coincident Raman lines is not required as is the case for the  $D_{2h}$  model.

Another technique frequently used for the assignment of fundamentals assumes the  $D_2$  structure of  $C_{12}F_{10}$  to be derived from a  $D_{2h}$  structure. If this approximation is satisfactory as the data appear to indicate, the relative intensities of the Raman and infrared lines of a given  $D_2$  mode can be predicted. For example, many of the  $b_3$  modes may be considered to be derived from  $b_{3g}$  modes. All such modes should have Raman lines which are more intense than the corresponding infrared lines. All assignments are given in Table 2.

#### 4.1 "a" class

On the basis of polarization data the Raman lines at 1659, 1534, 1474, 1302, 959, 587 and 510  $cm^{-1}$  are immediately assigned to the "a" class. Coincidences occur in the cases of the lines at 1534 and 587  $cm^{-1}$ . It will be assumed that these coincidences are accidental, and we anticipate assigning the coincident infrared lines as fundamentals in another symmetry class.

A polarized Raman line is expected between 959 and 1302  $cm^{-1}$  at approximately 1150  $cm^{-1}$ . The only Raman line in this region is the very, very weak line at 1150  $cm^{-1}$  which is tentatively assigned to this mode. Due to the weakness of the line, polarization data could not be obtained for it. It will also be necessary to assign the coincident infrared line at 1154  $cm^{-1}$  as a fundamental of another class.

The Raman line at 363  $cm^{-1}$  has been assigned to the mode which occurs at 370  $cm^{-1}$  in  $C_6F_6$ . Not only is it the only line in the anticipated region, but it is the only Raman line between 200  $cm^{-1}$  and 500  $cm^{-1}$  which is not known to be depolarized. Furthermore, no coincident infrared line is observed.

[12] D. A. LONG and D. STEELE, *Spectrochim. Acta* **19**, 1947 (1963).

Table 2. Comparison of fundamental frequencies for  $C_6F_6$ ,  $C_6F_5Cl$ ,  $C_6F_5Br$  and  $C_{12}F_{10}$  (classified as for  $D_{2h}$  structure)

$C_{2v}$ class	$C_6F_6^{9,14}$	$C_6F_5Cl^{13,14}$	$C_6F_5Br^{13,14}$	$g$ class	$C_{12}F_{10}$ $u$ class	$D_{2h}$ classes		
$a_1$	1655	1643	1639	1661	1656	$a_g b_{1u}$		
	1530	1518	1515	1534	1530			
	1490	1448	1426	1474	1374			
	1323	1300	1291	1302	1154			
	1157	1102	1093	1152	1038			
	1011	882	834	960	—			
	640	589	583	587	?			
	559	516	496	510	588			
	443	394	378	362	478			
	315	310	280	273	312			
	264	277	239	235	240			
	$b_1$	1655	1643	1639	1661		1650	$b_{3g} b_{2u}$
		1530	1518	1515	1533		1515/1494	
1253		1274	1268	1272	1294			
1157		1153	1154	1092	1078			
1011		1013/986	1007/979	1003	1010/981			
691		717	714	678	728			
443		441	440	440	471			
315		310	310	344	344 or 313?			
264		217	217	273	280			
208		202	151	190	183			
$b_2$		714	717	714	653	678	$b_{2g} b_{3u}$	
		595	?	?	?	618		
		370	357	350	386	379		
	249	217	217	235	240			
	215	?	?	187	183			
	125	116	114	156	?			
$a_2$	595	?	?	?	?	$b_{1g} a_u$		
	370	379	360	411	?			
	125	116	114	156	?			

For the modes which occur at 315 and 264  $cm^{-1}$  in  $C_6F_6$  no Raman lines were observed which could be definitely assigned. Except for the fact that they are depolarized, the Raman lines at 273 and 235  $cm^{-1}$  appear to be excellent candidates for assignment to these modes. Examination of the assignments of related  $C_6F_5X$  compounds reveals that vibrations of other symmetry classes are also expected to occur in these regions. Such accidental degeneracies are likely to make the Raman lines appear depolarized. For this reason and because no other Raman lines are observed in this region, the lines at 273 and 235  $cm^{-1}$  have been tentatively assigned to this class.

No lines were observed which could be assigned to the remaining four modes of this symmetry class. These arise from vibrations which would be inactive if the symmetry were  $D_{2h}$ . For  $D_2$  symmetry it is expected that these modes would still be quite weak.

[13] D. A. LONG and D. STEELE, *Spectrochim. Acta* **19**, 1955 (1963).

[14] I. HYAMS, *Private communication*, 1965. (To be published by I. HYAMS.)

#### 4.2 " $b_2$ " class

Infrared lines which show an appreciable decrease in intensity upon going from solution or melt to solid are candidates for assignment as  $b_2$  fundamentals. On the basis of their intensity changes the infrared lines at 1651, 1514/1494, 1293, 1078, 1010/981, 726, 470 and 344  $\text{cm}^{-1}$  are assigned to this class. As these lines are derived from the strongly infrared active  $b_{2u}$  modes of the  $D_{2h}$  model, they should also be strong. Indeed, the lines assigned on the basis of intensity changes include the most intense infrared lines in the solution spectrum. Of the eight lines assigned so far to this class none has a coincident line in the Raman spectrum of the solid; and only one, the line at 470  $\text{cm}^{-1}$ , has a coincident line in the solution Raman spectrum. This is additional evidence for the proposed model of the solid. On the basis of their strength and position the infrared lines at 280  $\text{cm}^{-1}$  and 183  $\text{cm}^{-1}$  have been assigned to the modes derived from the 264 and 208  $\text{cm}^{-1}$  lines of  $\text{C}_6\text{F}_6$ .

The remaining modes of this symmetry class are derived from modes which are Raman active in the  $D_{2h}$  model. Consequently, whenever several lines appeared to be suitable for assignment to a given mode, the line was selected for which the Raman line was stronger than its coincident infrared line. Using this criterion and a comparison with  $\text{C}_6\text{F}_5\text{X}$  compounds, lines at 653, 386, 235, 187 and 156  $\text{cm}^{-1}$  have been assigned as  $b_2$  modes.

#### 4.3 " $b_1$ " class

The five modes of highest frequency of the  $b_1$  class are derived from infrared active  $b_{1u}$  modes of the  $D_{2h}$  model. If the origin of the corresponding modes of the  $b_3$  symmetry class is considered, they are found to be derived from Raman active  $b_{3g}$  modes. These observations indicate that the  $b_1$  modes should be stronger in the infrared than the  $b_3$  modes. The five strongest unassigned infrared lines above 1000  $\text{cm}^{-1}$  occur at 1656, 1530, 1372, 1154 and 1038  $\text{cm}^{-1}$  and have been assigned to the  $b_1$  class. The values observed for the latter three lines appear low relative to the corresponding modes of  $\text{C}_6\text{F}_5\text{Cl}$ . This may be due to the removal of the  $\text{C}_6\text{F}_5\text{—X}$  stretching mode from this class. A shoulder at 1474  $\text{cm}^{-1}$  indicative of a line of moderately strong intensity was observed in several spectra. This line is an excellent candidate for the fundamental which was tentatively assigned to the 1372  $\text{cm}^{-1}$  line. Due to the questionable reality of the shoulder and to the possibility of this being a combination mode in resonance with the fundamental near 1500  $\text{cm}^{-1}$  the former assignment is preferred.

The infrared lines at 411 and 387  $\text{cm}^{-1}$  are of almost equal intensity and both appear to be reasonable for assignment to the slightly mass sensitive 443  $\text{cm}^{-1}$  mode of  $\text{C}_6\text{F}_6$  which falls to a value of 378  $\text{cm}^{-1}$  in  $\text{C}_6\text{F}_5\text{Br}$ . The line at 387  $\text{cm}^{-1}$  has been previously assigned to the  $b_2$  symmetry class, indicating that the 411  $\text{cm}^{-1}$  line is to be assigned to this class. The intensities of the coincident Raman lines are both consistent with these assignments.

Infrared lines at 478, 313, 240 and 156  $\text{cm}^{-1}$  have been assigned to the remaining modes expected below 500  $\text{cm}^{-1}$ . These lines are all of reasonable intensity, and none has a coincident line in the solution Raman spectrum. No line was observed which could be assigned to the mode derived from the 595  $\text{cm}^{-1}$  line of  $\text{C}_6\text{F}_6$ .

#### 4.4 " $b_3$ " class

The two highest  $b_3$  modes are assumed to be hidden by the strong Raman lines of the  $a$  class at 1659 and 1534  $\text{cm}^{-1}$ . The exact frequencies are probably close to these. The Raman line at 1268  $\text{cm}^{-1}$  is a plausible choice for the mode corresponding to the 1253  $\text{cm}^{-1}$  mode of  $\text{C}_6\text{F}_6$ . A Raman line at 1340 is also a possibility for this mode.

Primarily on the basis of their positions, lines at 1092, 1003, 678 and 618  $\text{cm}^{-1}$  have been tentatively assigned to the next four modes of the  $b_3$  class. With the exception of the line at 1090  $\text{cm}^{-1}$  these assignments are consistent with the anticipated strengths of the lines in the infrared and Raman spectrum. Although it is derived from a Raman active  $b_{3g}$  mode, no Raman line is coincident with the weak 1090  $\text{cm}^{-1}$  infrared line. Consequently, this assignment must be considered speculative.

The depolarized Raman line at 440  $\text{cm}^{-1}$  has been assigned to the mass insensitive mode derived from the 443  $\text{cm}^{-1}$  line of  $\text{C}_6\text{F}_6$ . The infrared line at 344  $\text{cm}^{-1}$  has several shoulders of questionable reality in the solution spectrum. Also, the frequency of this line shifts from 344 to 336  $\text{cm}^{-1}$  when the intensity of the line decreases in going from solution to solid. These points may be interpreted by assuming the line to arise from several vibrations. For these reasons the 344  $\text{cm}^{-1}$  line has been assigned to both the  $b_3$  and  $b_2$  symmetry classes.

The candidate lines for assignment to the remaining low frequency modes of this class have all been previously assigned to other classes. In several cases the previous assignments were rather arbitrary, but the assignment of these lines to this class would be equally arbitrary. A final decision as to the proper class for assignment of these lines will have to await further data. Although this situation is not satisfactory, it appears superior to the unexplained coincidences which arise when the frequencies are assigned on a  $D_{2h}$  basis. While it is true that arbitrary assignments have been made in all  $D_2$  classes, the overall assignment is reasonable; and it seems probable that for  $\text{C}_{12}\text{F}_{10}$  in solution additional data will result only in changes of the  $D_2$  assignment.

#### 4.5 Consideration of the mode mixing

As has already been noted the band intensities follow very much the pattern which might be expected for a planar structure. This is a similar effect to that in biphenyl. It is easy to classify the bands according to their "would have been"  $D_{2h}$  classes. In this classification the effect of interaction between the rings is most easily seen (Table 2). The  $g$  and  $u$  counterparts have closely similar frequencies except in the  $a_g b_{1u}$  classes. In this case the mixing of the  $\text{C}_6\text{F}_5$  modes with the inter-ring C—C stretching vibration occurs in the gerade class but is not possible in the ungerade class. As a result the  $b_{1u}$  modes converge on the inter-ring stretching frequency of about 968  $\text{cm}^{-1}$ . Thus apart from this expected mixing with the C—C mode little interaction between the rings can be observed. This of course explains why so many near coincidences occur in the spectra.



## The in-plane vibrations of azulene

D. STEELE

Department of Chemistry, Royal Holloway College, Englefield Green, Surrey

(Received 6 December 1965)

**Abstract**—The in-plane vibrations of azulene have been computed using two different force fields based on the benzene fields of CRAWFORD *et al.* and of DUINKER and MILLS. The agreement between the two sets of results and obvious assignments is very satisfactory. An almost complete assignment of azulene is presented based on the calculations and previous experimental data. The results of calculations of the frequencies of per-deutero azulene are given but not discussed.

THE VIBRATIONAL spectrum of azulene has attracted considerable attention in recent years as a result of its interesting quasi-aromatic character and of its isomeric relationship with naphthalene. The inability to write a Kekulé type structure for azulene with a double bond between the rings suggests that the central bond should have single bond character. X-ray analysis shows that the bond length is 1.48 Å and that consequently the bond must indeed be considered as essentially a single bond. On the other hand the peripheral conjugated system is endless and would therefore be expected to have some aromatic character. The planarity of azulene and its chemical behaviour confirm this.

The infra-red spectrum has been thoroughly investigated for both solution and crystal phases [1, 2] and the out-of-plane vibrations have been computed using a benzene force field [3]. Until recently the Raman spectrum of azulene was unobtainable since azulene is virtually opaque to visible radiation. The advent of powerful sources of monochromatic long wave-length radiation [4] has recently permitted its measurement [5]. Despite this wealth of data the analysis of the spectra is still far from unequivocal due to the complexity of the system. As a further aid to this problem, and to endeavour to analyse to what extent the vibrations were aromatic in character, the in-plane vibrational frequencies and modes have been computed using two different force fields. These force fields are based on two different fields for benzene.

### 1. COMPUTATIONS

The procedure adopted was to determine the eigenvalues and eigenvectors of the matrix  $D^+FD$  where  $DD^+ = G$ , the inverse kinetic energy matrix, and  $F$  is the force constant matrix, both defined for internal co-ordinates.  $D$  is evaluated as  $B \cdot M^{-1/2}$  where  $B$  is the transformation matrix between internal and cartesian co-ordinates

- 
- [1] G. R. HUNT and I. G. ROSS, *J. Mol. Spectry* **3**, 604 (1959).  
[2] A. VAN TETS and HS. H. GÜNTARD, *Spectrochim. Acta* **19**, 1495 (1963).  
[3] D. STEELE, *J. Mol. Spectry* **15**, 333 (1965).  
[4] F. X. POWELL, E. R. LIPPINCOTT and D. STEELE, *Spectrochim. Acta* **17**, 880 (1961); F. X. POWELL, O. FLETCHER and E. R. LIPPINCOTT. *Rev. Sci. Instr.* **34**, 36 (1963).  
[5] R. T. BAILEY and E. R. LIPPINCOTT, *J. Chem. Phys.* **42**, 1121 (1965).

i.e.  $R = Bq$  and  $M^{-1/2}$  is a diagonal matrix, the entries of which are the square roots of the inverse atomic masses in atomic units. The advantages of this procedure over the familiar Wilson  $GF$ -matrix method have been discussed previously [3]. The  $B$ -matrix is readily evaluated in terms of unit vectors along the bonds using  $\mathbf{S}$  vector formulae of Wilson. With the geometry as shown in Fig. 1 the  $\mathbf{e}$  vectors are:

$$\begin{aligned} e_{1,11} &= x; e_{2,12} = x \sin 20 - y \cos 20; e_{4,13} = x \sin 12 - y \cos 12 \\ e_{5,14} &= -x \sin 37^\circ 30' - y \cos 37^\circ 30'; e_{6,15} = -x; \\ e_{1,2} &= -x \cos 58 - y \sin 58; \\ e_{2,3} &= -x \cos 18 + y \sin 18; e_{3,4} = -x \cos 38 - y \sin 38; \\ e_{4,5} &= x \cos 14 + y \sin 14; e_{5,6} = -x \sin 29 + y \cos 29. \end{aligned}$$

(Remainder by symmetry)

The final  $B$ -matrix is available on request.

The benzene force field has been assumed to transfer to azulene except in that the C—C diagonal force constants are modified to take into account non-equivalence

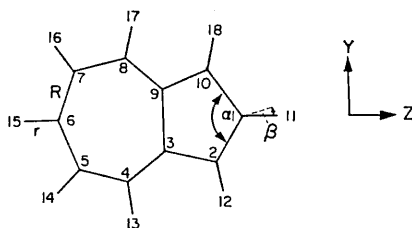


Fig. 1. Co-ordinate definitions, cartesian axes and numbering of nuclei. Geometry according to Ref. [6]

$$\begin{aligned} R_{1,2} &= 1.39 \text{ \AA}; R_{2,3} = 1.41 \text{ \AA}; R_{3,4} = 1.38 \text{ \AA}; R_{4,5} = 1.40 \text{ \AA}; R_{5,6} = 1.385 \text{ \AA}; \\ R_{3,9} &= 1.48 \text{ \AA}; \text{ All } r_{\text{CH}} = 1.08 \text{ \AA (assumed)} \alpha_1 = 116^\circ; \alpha_2 = 104^\circ; \alpha_3(239) = 108^\circ; \\ \alpha_3(439) &= 128^\circ; \alpha_4 = 128^\circ; \alpha_5 = 133^\circ; \alpha_6 = 122^\circ. \end{aligned}$$

of the different CC bonds. Two quite different quadratic force fields have been derived for benzene. The CRAWFORD-MILLER-WHIFFEN field [7, 8] is based on the supposition that with a suitable co-ordinate basis interaction force constants are minimized. In the derivation of the DUINKER-MILLS field [9] the MILLS Hybrid Orbital Force Field [10] is assumed to apply and the constants were determined by perturbation procedures. As no Coriolis data is available for benzene the experimental data on which the fields are based is restricted to isotopic substitution data. The two fields are very different and yet both have been employed with considerable success in the calculations of a wide range of aromatic systems. However, the mode

[6] J. M. ROBERTSON, H. M. M. SHEARER, G. A. SIM and D. G. WATSON, *Acta Cryst.* **15**, 1 (1962).

[7] B. L. CRAWFORD and F. A. MILLER, *J. Chem. Phys.* **17**, 249 (1949).

[8] D. H. WHIFFEN, *Phil. Trans. Roy. Soc. London* **A248**, 131 (1955).

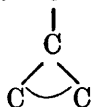
[9] J. C. DUINKER and I. M. MILLS, Private communication.

[10] I. M. MILLS, *Spectrochim. Acta* **19**, 1585 (1963).

patterns differ markedly in the two cases. By comparing the results of using the two fields for azulene it was hoped that some idea of the reliability of the calculations could be made. A direct comparison of the results for the two fields for a bicyclic system was a secondary consideration.

The force constants for C—C bonds of aliphatic systems can be related well to bond lengths by a relationship  $f = Ae^{-x/r}$  where  $A$  and  $x$  are parameters. For  $A = 1239$  and  $x = 3.65$  the force constants for single, double and triple bonds are deduced to be 4.3, 9.4 and 15.6 mdyn/Å compared with the usually quoted values of 4.5, 9.6 and 15.6 mdyn/Å. For the aromatic bond length of 1.40 Å this equation predicts an  $f_{cc}$  of 7.43 mdyn/Å, a value close to the DUINKER—MILLS value of 7.015 but far from WHIFFEN's value of 5.55. For the DM calculations the variations of  $f_{cc}$  with bond length have been represented by the various formula but with  $A = 1170$  so as to reproduce the standard value for 1.40 Å. For the WHIFFEN field it was necessary to assume that  $\log f_{cc}$  was proportional to  $R_{cc}$ , the linear plot passing through WHIFFEN's aromatic value and the accepted single bond value.

A second problem in the choice of a force field is choosing a value for the force constant for the  $\alpha$  C angles at the ring junctions. For naphthalene SCULLY and



WHIFFEN chose the constants so that an angular distortion at the ring junctions produced the same energy as an equivalent distortion at other positions [11]. In the present calculations the ring junction force constants are taken to have two thirds of the value of the other  $\alpha_{CCC}$  constants since one of the three angles enclosing a junction carbon atom is redundant. The effect of increasing this value was explored. The highest ring frequencies rose sharply and for the normal ring angle constant value exceeded observed frequencies by over 100  $\text{cm}^{-1}$ .

All interaction constants were assumed to be applicable between the rings. The final force fields are given in Table 1.

## 2. RESULTS and DISCUSSION

The frequency agreement for the two fields is good except for highest ring frequency of each class, for the lowest  $b_2$  mode and for the tenth highest  $a_1$  mode. With the exception of the latter mode these vibrations are characterized by considerable energy contributions from the inter-ring deformations. This is particularly so for the lowest  $b_2$  mode (see Table 2). Whilst generally the vibrational frequencies agree very well the potential energy distributions differ markedly as inspection of Table 2 shows. This is hardly surprising in view of the great differences in the fields used. The surprise is that the frequency agreement is so good. It would appear from this that one can rely on the frequency results as a guide to vibrational assignments, but for any purpose for which the normal co-ordinate to internal co-ordinate transformation matrix is required, little reliance can be placed on the present values without further investigations into the reality of the fields. In Fig. 2 a number of arbitrarily

[11] D. B. SCULLY and D. H. WHIFFEN, *Spectrochim. Acta* **16**, 1409 (1960).

Table 1. Force constants used in the calculations

$fA, B$ $A, B \equiv$	WHIFFEN	DUINKER-MILLS mdyn/Å
$rr$	5.093	5.125
$(rr)_0$	0.025	0
$(rr)_m$	0.008	0
$(rr)_p$	-0.040	0
$RR = 1.40 \text{ \AA}$	5.553	7.015
$RR = 1.48 \text{ \AA}$	4.65	5.9
$(RR)_0$	0.633	0.531
$(RR)_m$	0.113	0
$(RR)_p$	0.573	0
$\alpha_{\text{CCO}}^{\text{H}}$	1.031	0.564
$\alpha_{\text{CCO}}^{\text{O}}$	0.688	0.375
$(\alpha\alpha)_0$	0.185	-0.05
$\beta\beta$	0.866	0.881
$(\beta\beta)_0$	0.016	0.024
$(\beta\beta)_m$	-0.013	-0.020
$(\beta\beta)_p$	-0.015	-0.027
$(r_i\alpha_i)$	0	-0.01
$(R_i\alpha_i)$	-0.180	0.316
$(R_i\beta_i)$	0.049	0.337
$(R_{i+1}\beta_i)$	-0.050	0
$(R_{i+2}\beta_i)$	0.049	0
$(\beta_i\alpha_{i+1})$	-0.127	0.042

( ) denote interaction force constants.

chosen modes as calculated with the two fields have been displayed to give a visual indication of the mode differences.

As further investigations of the Raman spectra of deuterated azulenes are in progress elsewhere [12] a detailed analysis of the available spectra in the light of the present calculations would be premature. The subsequent discussion will be restricted to an attempt to identify the fundamental frequencies of the normal azulene.

### 2.1 $a_1$ class

The recent Raman data of BAILEY and LIPPINCOTT [5] shows four strong polarized bands at 1265, 940, 820 and 673  $\text{cm}^{-1}$ . From crystal polarization data HUNT and ROSS [1] and VAN TETS and GUNTARD [2] derived that the 1267 and 820  $\text{cm}^{-1}$  bands were  $a_1$ . Absorption at 673  $\text{cm}^{-1}$  was too weak to measure polarization values but the loss of intensity in going from solution phase to crystal phase confirmed  $a_1$  character. An infra-red band at 942  $\text{cm}^{-1}$  in the crystal spectrum appears to have  $b_2$  character but the result is rendered questionable by the proximity of the far more intense  $b_1$  or  $b_2$  band at 952  $\text{cm}^{-1}$ . The agreement of these analyses with Raman polarization data lends support to the general interpretation of HUNT and ROSS and VAN TETS and GUNTARD. These authors have demonstrated on the bases of intensity changes and crystal polarization data that further  $a_1$  fundamentals can be identified at 1392, 1054 and 403  $\text{cm}^{-1}$  and possibly at 900  $\text{cm}^{-1}$ . The evidence for the 900  $\text{cm}^{-1}$  band is conflicting and on the basis of the present calculations the author prefers to assign this as a  $b$  mode. Strong Raman bands—not apparently polarized—at 1396, 980 and 404  $\text{cm}^{-1}$  are also indicative of  $a_1$  fundamentals. It is clear from this that

[12] R. T. BAILEY, I. J. HYAMS and E. R. LIPPINCOTT, Private communication.

Table 2. Calculated and observed frequencies and potential energy distribution for the in-plane vibrations of azulene

Calc. freq. (cm <sup>-1</sup> )	WHIFFEN field				Calc. freq. (cm <sup>-1</sup> )	DUNKER-MILLS field				Obs. freq. (cm <sup>-1</sup> ) (Raman)	(i.r.)
	% Potential energy distribution					% Potential energy distribution					
	R <sub>CC</sub>	β <sub>CH</sub>	α <sub>COH</sub> <sup>H</sup>	α <sub>CCO</sub> <sup>C</sup>		R <sub>CC</sub>	β <sub>CH</sub>	α <sub>COH</sub> <sup>H</sup>	α <sub>CCO</sub> <sup>C</sup>		
<i>A<sub>1</sub> class</i>											
3080					3078						
3073					3073						
3061	99-100% ν <sub>CH</sub>				3070	99-100% ν <sub>CH</sub>					
3056					3069						
3054					3067						
1709	53	14	16	18	1617	89	5	2	3		1638 m ⊥ s >> c
1551	65	26	2	7	1502	66	29	3	2		1537 m ⊥ s >> c
1475	46	35	13	6	1469	69	19	7	6	1440 (m)	1443 vs    ? s > c
1407	41	49	10	0	1430	39	56	4	1	1396 (s)	1392 vs ⊥ s >> c
1234	54	45	2	0	1317	49	50	1	0	1265 (s) pol	1267 w ⊥ s >> c
1160	14	72	14	0	1186	13	85	2	0	1149 (m)	1140 w ⊥ ?
1111	47	38	14	1	1118	62	32	3	3		1054 vs ⊥ s >> c
969	11	4	83	2	987	35	3	59	3	980 (s)	976 m    s = c
935	77	13	6	4	940	35	7	57	1	940 (s) pol	940 w    ?
834	51	2	45	2	812	51	4	45	0	820 (s) pol	820 s ⊥ s >> c
694	27	4	62	7	686	36	1	47	16	673 (vs) pol	671 m ? s >> c
446	31	5	48	17	425	12	1	26	60	404 (vs)	403 m ⊥ s >> c
<i>B<sub>2</sub> class</i>											
3076					3073						
3064	99-100% ν <sub>CH</sub>				3070	99-100% ν <sub>CH</sub>					
3053					3067						
1692	60	19	4	16	1626	88	5	0	7	1699 (m)	1694 m    c << s
1544	57	19	16	7	1552	81	13	2	4	1586 (ms)	1580 vs    c << s
1461	44	41	5	10	1490	65	28	5	1	1478 (w)	1479 vs
1435	67	26	4	3	1437	51	44	4	1	1456 (m)	1453 s
1372	15	81	3	1	1385	33	63	3	1		
1337	24	45	12	18	1338	16	66	7	10	1301 (w)	1301 s
1265	12	79	2	7	1269	25	72	3	0		
1164	13	81	6	0	1184	1	98	1	0		1205 s ? c > s
1148	18	80	1	1	1157	14	85	1	0	1149 (w)	1151 w    c > s
1030	56	28	9	7	1027	65	21	7	7		1007 m
776	27	5	53	15	779	14	4	71	11		
479	36	6	17	41	477	16	2	45	36		593 s
441	25	3	19	53	349	17	1	14	67	480 (m)	478 m

⊥, || polarization characteristics || to *b* axis.

s > c relative intensities in solution and crystal phases.

the only doubt in the assignments up to this point is a choice between the 980 and 900 cm<sup>-1</sup> bands. A comparison with the calculations indicates that only one of these can be accepted and strongly favours the 980 cm<sup>-1</sup> assignment. It is also clear that the assignments are in good agreement with the calculations and the latter can therefore be safely used as a guide to the other fundamental frequencies. Apart from the C—H stretching modes on which it is believed that no new significant data can be presented here, only the three highest ring modes and a β mode near 1200 cm<sup>-1</sup> remain to be identified in the *a*<sub>1</sub> class. HUNT and ROSS and VAN TETS and GUNTARD agree in the choice of bands at 1638 and 1537 cm<sup>-1</sup> as *a*<sub>1</sub> fundamentals on the basis of crystal data and HUNT and ROSS also suggest 1443 cm<sup>-1</sup>. The polarization data on the latter does not support this choice but a considerable loss of intensity in passing from solution to crystal phase appears to be stronger evidence in favour. The missing CH mode is probably to be identified with the moderately strong Raman

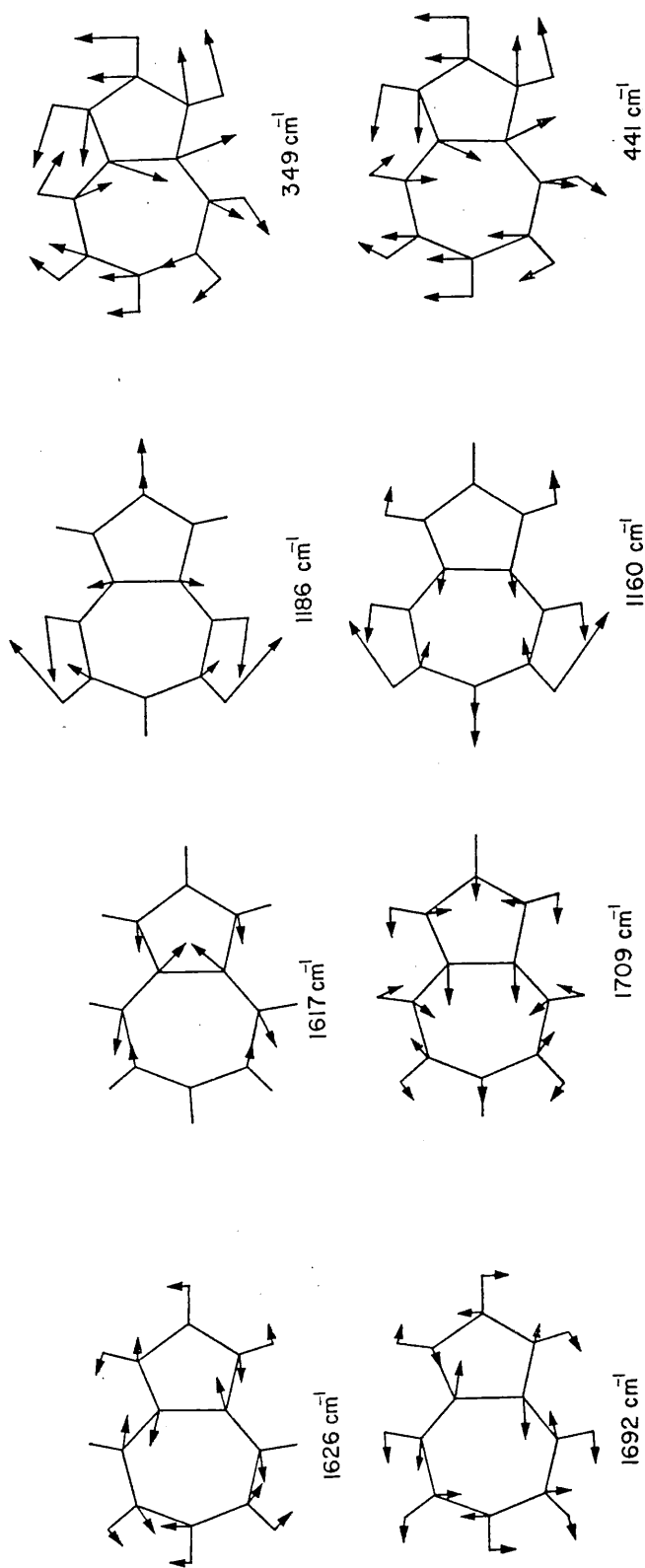


Fig. 2. Some corresponding normal modes according to the Whiffen field (lower line) and the Duinker-Mills field (upper line).

band at  $1149\text{ cm}^{-1}$  and the weak infra-red band at  $1140\text{ cm}^{-1}$ . The latter has the crystal polarization character of an  $a_1$  mode.

## 2.2 $b_2$ class

Distinguishing between  $b_1$  and  $b_2$  modes is straightforward in principle on the basis of infra-red crystal polarization data, the  $b_2$  being polarized parallel to the  $b$  axis and the  $b_1$  parallel to the  $a$  axis [1, 2]. In contrast to the  $a_1$  modes the intensities in the crystal phase should be comparable to those in the solution phase for both symmetries. Furthermore, since no  $b_1$  fundamentals will have frequencies greater than  $1000\text{ cm}^{-1}$  we can safely identify  $b_2$  fundamentals at 1478, 1453, 1301, 1205 and  $1152\text{ cm}^{-1}$ . In addition low frequency  $b_2$  fundamentals are indicated at 593 and  $478\text{ cm}^{-1}$ .

Table 3. The calculated vibrational frequencies for per-deutero azulene

WHIFFEN field		DUINKER-MILLS field	
$A_1$	$B_2$	$A_1$	$B_2$
2311	2298	2302	2291
2284	2282	2289	2279
2282	2276	2280	2270
2278	1654	2277	1622
2273	1492	2274	1534
1652	1416	1608	1441
1508	1375	1456	1368
1405	1233	1429	1216
1272	1087	1286	1073
1098	991	1151	996
948	860	944	851
863	829	891	836
833	807	845	815
820	715	807	723
756	454	738	459
650	402	648	319
428		411	

All but the  $593\text{ cm}^{-1}$  band are confirmed as  $b_2$  by the calculations. However, the out-of-plane calculations of the author and the available data show no possibility of accepting an assignment of this  $593\text{ cm}^{-1}$  band as a  $b_1$  mode. It must be assumed that the observed bands at  $593$  and  $478\text{ cm}^{-1}$  correspond to the two lowest frequency modes calculated at  $479$  and  $441\text{ cm}^{-1}$  (WHIFFEN field) and at  $477$  and  $349\text{ cm}^{-1}$  (DUINKER-MILLS field). In support of this no other strong low frequency  $b_2$  candidate exists. This point will be discussed below.

Whilst the evidence is not unquestionable there seems little doubt that the two highest frequency ring modes are at  $1694\text{ cm}^{-1}$  ( $1699\text{ cm}^{-1}$  (ms) in Raman;  $1694\text{ cm}^{-1}$  in infra-red in  $\text{CCl}_4$  solution with crystal polarization parallel to the  $b$  axis, but showing a marked decrease in intensity in going from solution to crystal phase) and  $1580\text{ cm}^{-1}$  ( $1586\text{ cm}^{-1}$  (ms) in Raman;  $1580\text{ cm}^{-1}$  (vs) in infra-red with crystal polarization parallel to the  $b$  axis but again showing a decrease in intensity in going from solution to crystal phase). Of the four remaining assignments only one can be made with any assurance on the available data. The moderately strong band at  $1007\text{ cm}^{-1}$  has  $b_2$  character and the calculations confirm its assignment as a fundamental. No other strong Raman bands or infra-red bands of appreciable strength and of  $b_2$  character remain to be correlated with the three missing fundamentals expected near

1380, 1260 and 780  $\text{cm}^{-1}$ . This sort of situation is usual in complex molecules and it seems sensible to leave these assignments till the Raman data on the deuterated azulenes becomes available.

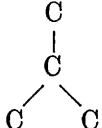
### 2.3 Further out-of-plane assignments

The present calculations in no way affect the assignment of the out-of-plane modes presented previously. However the Raman data of BAILEY and LIPPINCOTT show two low frequency bands at 330 and 184  $\text{cm}^{-1}$  which have not yet been assigned. These frequencies agree well with the o/p calculation for the  $a_2$  class (calculated 323 and 163  $\text{cm}^{-1}$ ) [3]. Failure to observe infra-red absorption at these frequencies confirms these assignments [2, 3].

### 3. DISCUSSION

The assignments presented are based largely on the Raman and infra-red polarization data. The calculations have been used primarily as a guide to the general region of absorption. Agreement between calculated and assigned frequencies is generally good thus vindicating the use of aromatic force fields based on those of benzene. There is little to choose between the results of the WHIFFEN field and the DUINKER-MILLS field except in that the latter field predicts a very low frequency for the lowest  $b_2$  mode. The source of discrepancies is difficult to see. However the following points are clear—

(a) the major discrepancies are in those frequencies largely governed by the inter-ring angle deformations. As some of these discrepancies are high whilst others are low

it appears that interaction constants involving the  angles are involved. In

this sense the major fault does not arise from transference of the benzene force field.

(b) The force constant for stretching of the common CC bond can only contribute to the  $a_1$  class. It affects primarily the calculated frequencies corresponding to the 820, 1638 and 1443  $\text{cm}^{-1}$  bands in that order of importance. The agreement between calculated and observed frequencies confirms the magnitude of the force constant used which was practically that of a single order bond.

Clearly there is little hope in assessing the relative merits of the two force fields until Coriolis coupling constants become available for aromatic systems.

A comparison of the present results with the calculations of SCULLY and WHIFFEN on naphthalene [11] shows a very similar pattern of discrepancies and of frequencies. As in the present case the major discrepancies for naphthalene were in the lowest and highest frequency ring modes. The final assigned frequencies for these vibrations are also very similar. This confirms the origin of the discrepancies as due to the force fields and lends support to the assignments. It also verifies that the vibrations of azulene are aromatic in nature.

*Acknowledgements*—I wish to thank Drs. J. C. DUINKER and I. M. MILLS for details of their benzene force field prior to publication and the staff of the University of London computer unit for running of all computer tapes.



## ERRATUM

### The in-plane vibrations of azulene\*

D. STEELE

Department of Chemistry, Royal Holloway College, Englefield Green, Surrey

(Received 10 January 1967)

As a result of a misunderstanding in correspondence two terms were inadvertently left out of the DUINKER-MILLS field [1] for benzene as reported in the above article. The D. M. field is based on the known fundamental frequencies of benzene and its deuterated isomers and on the Coriolis coupling constants for the ring angle deformations,  $\nu_6$ , in the  $E_{2g}$  class of benzene and benzene- $d_6$ . Amongst the assumptions made to render the problem tractable were (a) that the Hybrid Orbital Force Field of MILLS [2] applied and (b) that  $f(RR)_0 = -f(RR)_m = f(RR)_p$ . In the previously reported calculations  $f(RR)_m$  and  $f(RR)_p$  were assumed to be zero. The frequencies of benzene and benzene- $d_6$  have been recalculated and the new frequencies are shown in Table 1.

Table 1. The calculated vibration frequencies (in  $\text{cm}^{-1}$ ) for azulene and azulene  $d_8$  as obtained using the Duinker-Mills field for benzene

Azulene					
$A_1$	$d_0$	$d_8$	$B_2$	$d_0$	$d_8$
	3078	2303		3073	2290
	3073	2288		3070	2283
	3070	2281		3066	2269
	3069	2279		1673	1648
	3069	2275		1540	1536
	1652	1615		1482	1401
	1536	1522		1403	1378
	1449	1415		1367	1183
	1423	1281		1334	1073
	1330	1129		1276	995
	1194	943		1183	852
	1113	890		1165	838
	976	844		1003	809
	920	801		769	714
	802	729		475	457
	675	636		346	316
	424	410			

The only significant frequency changes are for the highest ring modes. Most of the changes improve the fit with observed, but as might be expected there is still little to choose between the Whiffen and D. M. fields on the basis of frequency fit. Both are generally good. The potential energy distribution is not markedly affected. Neither the discussion nor the assignments require revision as a result of these corrections.

\* *Spectrochim. Acta* **22**, 1275 (1966).

[1] J. C. DUINKER. *Normal Co-ordinate Analysis of Molecules—Benzene and Derivatives*. Thesis, Amsterdam (1964).

[2] I. M. MILLS. *Spectrochim. Acta* **19**, 1585 (1963).

## The vibrational spectra of substituted nitrogen heterocyclic systems—I 2,4,6-trifluoropyrimidine

R. T. BAILEY

Department of Pure and Applied Chemistry, University of Strathclyde, Glasgow

and

D. STEELE

Department of Chemistry, Royal Holloway College, Englefield Green, Surrey

(Received 14 April 1967)

**Abstract**—The infra-red and Raman spectra of 2,4,6-trifluoropyrimidine are reported. An assignment of the vibrational modes is proposed based on the character of the observed bands, comparison with *sym*-trifluorobenzene and calculated frequencies based on a force-field derived from  $C_6H_6$  and  $C_6F_6$ .

### 1. INTRODUCTION

In spite of the considerable biological importance of the pyrimidine nucleus very little detailed spectroscopic work has been carried out on pyrimidine compounds. Vibrational assignments have however been recently made for pyrimidine itself [1–3]. Trifluoropyrimidine has recently been synthesized [4] and in view of its physical properties forms an ideal starting point for a spectroscopic study of pyrimidine derivatives. In addition, reliable assignments for most fluorobenzenes are now available and normal co-ordinate calculations have been carried out for several of these compounds. Also, since it has been well established that force constants from benzene and hexafluorobenzene can be transferred to other aromatic systems [5, 6], the vibrational frequencies of trifluoropyrimidine can be calculated. In this paper, details of the infra-red and Raman spectra and vibrational assignments for trifluoropyrimidine are presented.

### 2. EXPERIMENTAL

A sample of trifluoropyrimidine was kindly supplied by Dr. E. H. Kober. It was a colourless volatile liquid b.p.  $98^\circ$  and was shown to be at least 99% pure by analytical gas chromatography. The compound was vacuum distilled immediately prior to the spectroscopic measurements. Raman spectra were excited by the Hg 4358 Å line and recorded photographically on a conventional prism spectrograph and also photoelectrically using a Cary 81 Raman spectrophotometer. Qualitative polarization measurements using the method of polarized incident light were also made. The vibrational frequencies are estimated to be accurate to  $\pm 3\text{ cm}^{-1}$  for strong bands but for weak features the error will be greater.

- [1] R. C. LORD, A. J. MARSTON and F. A. MILLER, *Spectrochim. Acta* **9**, 113 (1957).
- [2] J. D. SIMMONS and K. K. INNES, *J. Mol. Spectry* **13**, 435 (1964).
- [3] G. SBRANA, G. ADEMBRI and S. CALIFANO, *Spectrochim. Acta* **22**, 1831 (1966).
- [4] E. KOBER, H. AGANIGIAN, H. ULRICH, R. F. W. RATZ and C. GRUNDMANN, *J. Org. Chem.* **27**, 2580 (1962).
- [5] D. A. LONG and R. T. BAILEY, *Trans. Faraday Soc.* **59**, 599 (1963).
- [6] D. A. LONG and D. STEELE, *Spectrochim. Acta* **19**, 1791 (1963).

Table 1. Infra-red and Raman spectra and assignments for  $C_4N_2F_3H$ 

Raman	Infra-red		Assignment
	Liquid	Vapour	
210 vs			$a_2$
233 vs			$b_1$
260 vs	258 m		$b_1$
356 m, p	352 s		$a_1$
369 m	365 s		$b_2$
465 w	458 w		$b_2$
511 w			$a_2$
528 s	526 s	521 m	$b_2$
567 vs, p	566 vs	564 m B	$a_1$
	600 m		258 + 352 ( $b_1$ )
624 vs, p	621 s		$a_1$
643 m	639 s		210 + 465 ( $b_1$ )
		688	
693 s	694 vs	697 Q } C	$b_1$
		705	
	736 w		
		768	
774 w	772 vs	777 Q } C	$b_1$
		785	
		829	
842 w	841 vs	836 Q } C	$b_1$
		845	
900 w	878 m		369 + 528 ( $a_1$ )
926 w			233 + 693 ( $b_2$ )
947 m, p	945 m		356 + 624 ( $a_1$ )
1000 vs, p	999 vs	997 m B?	$a_1$
		1012	
1018 m	1017 vs	1016 Q } A	$b_2$
		1022	
		1076 } B	$a_1$
1071 m, p	1073 vs	1084 }	
1145 vw	1145 vs		528 + 624 ( $b_1$ )
		1154	
1161 s	1160 vs	1158 Q } A	$b_2$
		1164 }	
	1207 m		567 + 643 ( $b_1$ )
	1225 w		210 + 1018 ( $b_1$ )
1258 m	1258 m	1260 w	$b_2$
1356 w, p	1353 s	1347 vw	356 × 1000 ( $a_1$ )
1383 w, p	1387 sh		2 × 693 ( $a_1$ )
1405 w	1403 vs	1408 } B	$a_1$
		1417 }	
1437 vs, p	1438 sh		$a_1$
		1453	
	1455 vs	1457 Q } C	$b_2$
		1463 }	
	1521 vs	1525	526 + 999 ( $b_2$ )
1542 w, p	1546 s	1538 } B	528 + 1018 ( $a_1$ )
		1547 }	
	1562 s		566 + 999 ( $a_1$ )
1597 vs, p	1594 vs		$a_1$
	1627 vs	complex	369 + 1258 or 624 + 1000 ( $a_1$ )
1640 m	1642 vs	bandshape }	$b_2$
	1693 s		1000 + 693 ( $a_1$ )
			or 260 + 1437 ( $b_1$ )
	1714 m		465 + 1258 ( $a_1$ )
	1766 m		693 + 1071 ( $b_1$ )
	1784 m		624 + 1161 ( $b_2$ )
	1808 m		369 + 1438 ( $b_2$ )
	1822 m		369 + 1455 ( $a_1$ )
	2000–3000 $cm^{-1}$ —many weak to medium bands		
3123 vs, p	3123 vs		$a_1$
	3170 sh		
	3212 s		2 × 1597 ( $a_1$ )

All frequencies are in  $cm^{-1}$ .

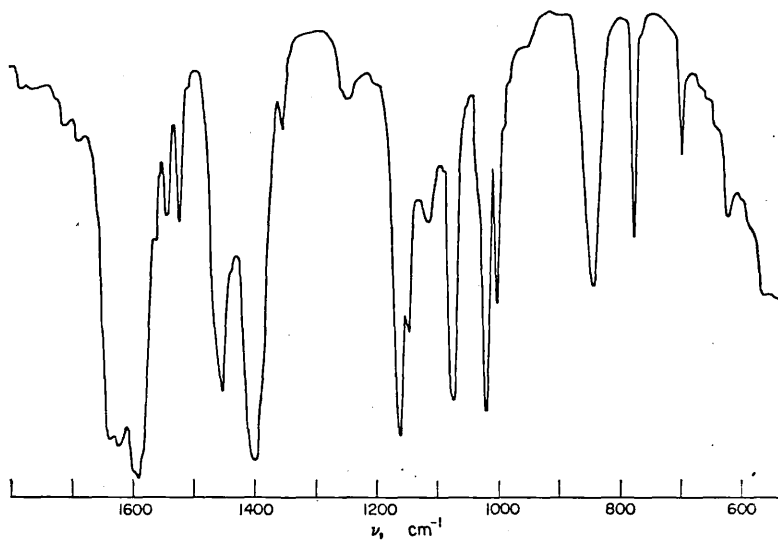


Fig. 1. Infra-red spectra of liquid trifluoropyrimidine (thin film).

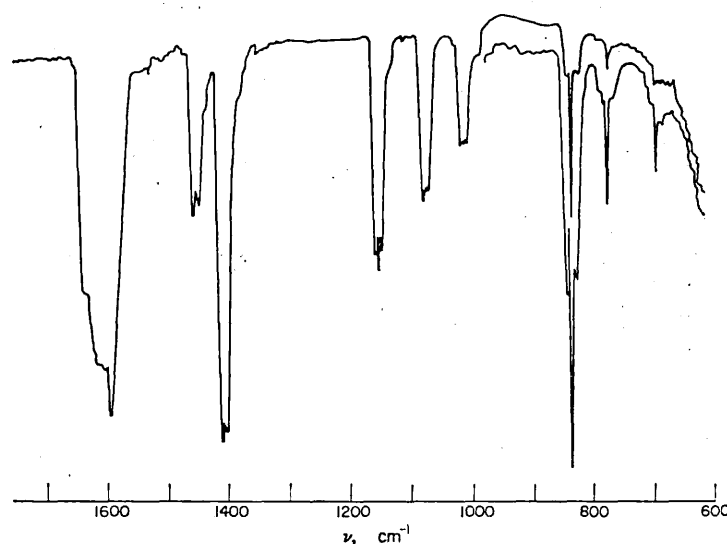


Fig. 2. Infra-red spectra of trifluoropyrimidine vapour (1 and 12 torr).

The infra-red spectra were obtained using a Unicam SP100 spectrometer with SP 130 grating attachment and a Perkin-Elmer 421 grating spectrometer equipped with low frequency interchange. Measurements on the liquid were carried out in the frequency range  $4000\text{--}250\text{ cm}^{-1}$  and for the vapour in the range  $4000\text{--}400\text{ cm}^{-1}$ . The observed infra-red and Raman frequencies together with assignments are listed in Table 1. For many of the overtone and combination bands several possibilities exist, especially for the higher frequencies. In these cases not all the possibilities are listed. The infra-red spectra are illustrated in Figs. 1 and 2.

## 3. COMPUTATIONS

The vibrational frequencies and modes were evaluated using the secular equation in the form  $D^t F D$  where  $DD^t = G$ , the inverse kinetic energy matrix,  $F$  is the force constant matrix for internal co-ordinates and  $D$  is the transformation matrix from internal to mass weighted co-ordinates. The eigenvector matrix,  $Y$ , is related to that of  $L$  by  $L = DY$ .

In *sym*-triazine and in 2-amino 4,6-dichloro pyrimidine [7] the  $\hat{N}\hat{C}\hat{N}$  angle is near  $128^\circ$  and the  $\hat{C}\hat{N}\hat{C}$  angle near  $114^\circ$ . The CN and (for the latter molecule) the CC bond lengths are 1.32 and 1.36 Å respectively. The geometry assumed for trifluoropyrimidine was based on these values. The determination of the  $B$  matrix is trivial. It will not be reproduced here but is available on request. The values of the  $F$  matrix elements were transferred from benzene [8] and hexafluorobenzene [9] and are listed in Table 2.

Table 2. Assumed force constant values based on benzene and hexafluorobenzene force fields. All values in mdyn/Å

In-plane		Out-of-plane	
$f_{CH}$	5.093	$f_{\gamma(H)}$	0.385
$f_{CF}$	7.405	$f_{\gamma(F)}$	0.423
$f_{CC}$	$f_{CN} = 5.5$	$f_\delta$	0.32
$f_{\hat{C}\hat{C}\hat{C}} = f_{\hat{C}\hat{N}\hat{C}} = f_{\hat{N}\hat{C}\hat{N}} = f_\alpha$			
1.03			
Interaction terms			
(CF/CF) <i>meta</i>	-0.05	$\gamma(H)_i \gamma(F)_{i+1}$	-0.01
(CY/CX) <i>ortho</i>	0.66	$\gamma(H)_i \gamma(F)_{i+2}$	-0.03
(CY/CX) <i>meta</i>	0.07	$\gamma(F)_i \gamma(F)_{i+2}$	0.08
(CY/CX) <i>para</i>	0.46	$\gamma(H)_i \delta_i$	-0.092
$CF_j/\alpha_j$	-0.076	$\gamma(F)_i \delta_i$	-0.179
$CF_j/\alpha_{j+1}$	0.344	$\gamma(F)_i \delta_{i+1}$	0.078
$CF_j/\beta(F)_{j+2}$	-0.054	$\delta_i \delta_{i+1}$	-0.004
$CX_i/\beta(H, F)_i$	0.112		
$CX_i/\beta(H, F)_{i-1}$	-0.041		
$CX_i/\beta(H, F)_{i-2}$	0.033		
$CX_i/\alpha_i$	-0.18		
$\alpha_i \alpha_{i+1}$	0.016		
$\beta(F)_i \beta(F)_{i+1}$	-0.09		

Since the valency co-ordinates,  $\phi$ , introduced by Bell for twisting of the carbon and substituent atoms in a torsional motion cannot be defined for pyridine systems it was necessary to use the older  $\delta$  co-ordinates for twisting of the carbon skeleton only.

The out-of-plane calculations are less reliable than the in-plane. There are two main reasons for this.

(i) The out-of-plane assignments for hexafluorobenzene are less reliable than the in-plane. The lowest  $e_{2u}$  mode has been re-assigned [10] from the value used in deriving the field. Due to (ii) and other frequency uncertainties no revision of the field seems warranted at the present time.

[7] J. E. LANCASTER and B. P. STOICHEFF, *Can J. Phys.* **34**, 1016 (1956); N. E. WHITE and C. J. B. CLEWS, *Acta Cryst* **9**, 586 (1956).

[8] D. H. WHIFFEN, *Phil. Trans. Roy. Soc.* **A248**, 131 (1955).

[9] D. STEELE and D. H. WHIFFEN, *Trans. Faraday Soc.* **56**, 5 (1960).

[10] J. H. S. GREEN, W. KYNASTON and H. M. PAISLEY, *Spectrochim. Acta* **19**, 549 (1963).

(ii) The choice of a set of force constants for a molecule such as  $C_6F_6$  necessitates a large number of force constants. The transferability of the force constants in the sense of producing an acceptable set of computed frequencies in other molecules depends on the errors cancelling

$$\text{i.e.} \quad \lambda_{\text{true}} - \lambda_{\text{calc}} \sim \sum_{j,k} l_{ij} l_{ik} \Delta f_{jk} \sim 0$$

Where  $\Delta f_{jk}$  is the deviation of the transferred force constants from the true value. When certain co-ordinates disappear in the transference—as when a CX is changed for an N—the likelihood of this being a good approximation is reduced. For the out-of-plane calculations the situation is rendered much worse by the necessity for using  $\delta$  co-ordinates instead of  $\phi$  co-ordinates as the former include  $\gamma$  type motions in benzene systems. All computations were carried out on an Atlas computer. The computed frequencies are given in Table 3 along with the approximate potential energy distribution.

Table 3. Potential energy distribution

$\nu$ ( $\text{cm}^{-1}$ )	Sym.	$\Delta d$	$r_{10}$ $r_8$	$r_9$	$R_{12}$ $R_{16}$	$R_{23}$ $R_{56}$	$R_{34}$ $R_{45}$	$\alpha_1$	$\alpha_2$ $\alpha_6$	$\alpha_3$ $\alpha_5$	$\alpha_4$	$\beta_7$	$\beta_8$ $\beta_{10}$	$\beta_9$
3067	$a_1$	99						0.5						
1618	$b_2$	0	20	0	26	0	20	0	16	10	0	4	1	2
1601	$a_1$	0	8	14	7	31	7	9	6	4	10	0	3	0
1473	$a_1$	0	37	17	3	1	1	5	14	14	7	0	0	0
1430	$b_2$	0	15	0	2	15	26	0	3	3	0	26	3	6
1381	$a_1$	0	10	28	31	7	9	2	1	0	4	0	8	0
1290	$b_2$	0	24	0	18	19	4	0	1	0	0	34	0	0
1227	$b_2$	0	2	0	20	26	34	0	0	0	0	12	3	2
1118	$a_1$	0	5	2	12	16	14	8	18	16	8	0	0	0
1013	$a_1$	0	11	20	4	17	36	5	0	2	0	0	3	0
983	$b_2$	0	24	0	26	24	1	0	1	6	0	14	0	3
602	$a_1$	0	23	12	13	14	14	3	6	7	8	0	0	0
576	$b_2$	0	8	0	10	0	7	0	35	35	0	1	0	3
575	$a_1$	0	3	6	2	12	5	23	11	12	23	0	4	0
457	$b_2$	0	0	0	0	0	0	0	0	0	0	0	70	30
295	$a_1$	0	0	0	8	2	0	0	2	0	4	0	83	0
293	$b_2$	0	0	0	0	5	10	0	6	0	0	0	24	55

$b_1$  frequencies calculated as, 876, 791, 572, 321 and 290  $\text{cm}^{-1}$ .

$a_2$  frequencies calculated as 631 and 330  $\text{cm}^{-1}$ .

#### 4. ASSIGNMENTS AND DISCUSSION

The structures of several pyrimidine compounds have been determined [e.g. 7, 11] and in all cases the molecules were found to be planar. It can reasonably be assumed therefore, that trifluoropyrimidine will be planar and belong to the  $C_{2v}$  point group. Following Mulliken's recommendations [12] and choosing the  $x$ -axis as perpendicular to the plane of the ring then the 24 normal modes will be distributed among the symmetry classes as follows

- class  $a_1$ —9 vibrations, infra-red and Raman active.
- class  $b_2$ —8 vibrations, infra-red and Raman active.
- class  $a_2$ —2 vibrations, Raman active only.
- class  $b_1$ —5 vibrations infra-red and Raman active.

[11] P. J. WHEATLEY, *Acta Cryst.* **13**, 80 (1960).

[12] R. S. MULLIKEN, *J. Chem. Phys.* **23**, 1997 (1955).

To assist in the assignment the vapour phase infra-red band contours were calculated using the data of BADGER and ZUMWALT [13]. Modes of  $b_2$  symmetry should give rise to type  $A$  bands with a medium  $Q$  branch and a  $PR$  separation of 9–10  $\text{cm}^{-1}$ ;  $a_1$  modes should have type  $B$  band structures with a separation of 9–10  $\text{cm}^{-1}$ ; and  $b_1$  modes should be associated with type  $C$  bands with strong  $Q$  branches and  $PR$  separations of 17–18  $\text{cm}^{-1}$ .

Table 4. Comparison of assignments for  $\text{C}_6\text{F}_3\text{H}_3$  and  $\text{C}_4\text{N}_2\text{F}_3\text{H}$ 

Symmetry class ( $C_{2v}$ )	$\text{C}_6\text{F}_3\text{H}_3$	$\text{C}_4\text{N}_2\text{F}_3\text{H}$		Approximate description of mode
	Assigned [14]	Calculated	Assigned	
$a_1$	3109	3067	3123	CH stretch
	3080			CH stretch
	1624	1601	1597	CC stretch
	1475	1473	1437	CF stretch
	1350	1381	1405	CF/CC stretch
	1122	1118	1071	CC stretch
	1010	1013	1000	CC stretch
	993			
	578	602	624	CC stretch
	500	575	567	ring deformation
326	295	356	CF deformation	
$b_2$	3109			CH stretch
	1624	1618	1640	CC stretch
	1475	1430	1455	CF stretch/CH defn.
	1294	1290	1258	CH deformation
	1165	1227	1161	CC stretch
	1122			
	993	983	1018	(very mixed mode)
	564	576	528	ring deformation
	500	457	465	CF deformation
326	293	369	CF deformation	
$b_1$	847	876	842	CH deformation
	843	791	774	torsion
	663	572	693	torsion
	595			
	253	321	260	CF deformation
	214	290	233	CF deformation
$a_2$	847			
	595	631	511	torsion
	253	330	210	CF deformation

In addition to symmetry properties and calculations of the normal modes the vibrational frequencies of *sym*-trifluorobenzene provided a further guide to the assignment. A recent assignment for this molecule, based on normal co-ordinate calculations, was made by SCHERER *et al.* [14]. Trifluoropyrimidine might be expected to have a similar spectrum to this molecule in many respects. Since CH and N are isoelectronic and nearly isobaric, replacement of CH by N should not markedly alter the system. There will of course be six more fundamentals for trifluorobenzene when allowance is made for reduced symmetry. They will consist of two CH stretches ( $a_1$  and  $b_2$ ), two in-plane CH deformations ( $a_1$  and  $b_2$ ) and two out-of-plane CH deformations ( $a_2$  and  $b_1$ ). These modes are fairly readily identified and although some interaction between the CH deformations and modes of similar frequency might be

[13] R. M. BADGER and L. R. ZUMWALT, *J. Chem. Phys.* **6**, 711 (1938).[14] J. R. SCHERER, J. C. EVANS and W. W. MUELDER, *Spectrochim. Acta* **18**, 1579 (1962).

expected, in general there should be a strong resemblance between the corresponding modes in the two molecules.

The assignments for trifluoropyrimidine are compared with those for trifluorobenzene and with the calculated frequencies in Table 4. For consistency liquid phase frequencies will be used throughout unless otherwise specified. The assignments will now be considered class by class.

#### *Class $a_1$*

All the nine frequencies in this class are readily identified by the character of the infra-red bands or of the Raman bands or of both. Strong polarized Raman bands at 3109, 1597, 1437, 1071, 1000, 624, 567 and 356  $\text{cm}^{-1}$  and strong type *B* infra-red bands at 1405, 1071 and 567  $\text{cm}^{-1}$  can be immediately attributed to in-plane symmetric normal modes. The assignments are also fully supported by the calculations and the correlation with trifluorobenzene.

#### *Class $b_2$*

Most substituted benzene derivatives have two C—C stretching fundamentals near 1600  $\text{cm}^{-1}$  which are prominent in the Raman spectrum. Two Raman bands were in fact found near 1600  $\text{cm}^{-1}$  but the lowest band at 1597  $\text{cm}^{-1}$  is polarized so that the 1640  $\text{cm}^{-1}$  frequency must be associated with a  $b_2$  mode. The calculations, comparison with trifluorobenzene and gas phase infra-red band contours allow the remaining  $b_2$  modes to be selected with reasonable assurance. Bands at 1455, 1258, 1161 (type *A*), 1018 (type *A*), 528, 465 and 369  $\text{cm}^{-1}$  are assigned to the  $b_2$  class on this basis.

#### *Class $b_1$*

The strong infra-red bands at 694, 772 and 841  $\text{cm}^{-1}$  exhibit characteristic type *C* contours and are thus assigned  $b_1$  symmetry. On the existing evidence it is difficult to assign the two lowest  $b_1$  modes with any degree of certainty. In identifying those modes we have been guided chiefly by the calculations and the trifluorobenzene spectra. As discussed previously the calculated frequencies are not as reliable for the out-of-plane modes as they are for the in-plane. Keeping this in mind, the Raman bands at 233 and 260  $\text{cm}^{-1}$  were assigned to the  $b_1$  class in preference to the 210  $\text{cm}^{-1}$  frequency since the strong infra-red and Raman band at 643  $\text{cm}^{-1}$  can then be explained as a binary combination (210 + 465) in Fermi resonance with the  $a_1$  mode at 693  $\text{cm}^{-1}$ . It is difficult to explain the existence of this band in any other way. More extensive vapour phase infra-red data is needed before a more definite assignment of the low frequency modes can be made.

#### *Class $a_2$*

In this class the Raman active mode at 511  $\text{cm}^{-1}$  was assigned as the highest mode of  $a_2$  symmetry since it does not appear to be infra-red active. The frequency at 210  $\text{cm}^{-1}$  has already been assigned to the other mode in this class. No infra-red data is available in this region.

*Acknowledgement*—We are indebted to Dr. E. H. KOBER for providing us with a sample of trifluoropyrimidine.



## The vibrational spectra of substituted nitrogen heterocyclic systems—II 2,6 difluoropyridine

R. T. BAILEY

Department of Pure and Applied Chemistry, University of Strathclyde  
Glasgow

and

D. STEELE

Department of Chemistry, Royal Holloway College, Englefield Green  
Surrey

(Received 20 April 1967)

**Abstract**—The infra-red (vapour and liquid phase) and Raman (liquid phase) spectra of 2,6-difluoropyridine have been measured. A complete set of assignments is proposed based on analogy with known vibrational frequencies of related compounds and calculations for 2,6-difluoropyridine itself. Some revision of previous assignments for methyl substituted pyridines is suggested.

### 1. INTRODUCTION

A CONSIDERABLE effort has been made to understand in detail the vibrational spectra of pyridine and its deuterioanalogues [e.g. 1–3] but little is known as yet about the spectra of substituted pyridines. Detailed assignments have been made for a number of monosubstituted pyridines [4, 5], for 2,6 and 2,4 lutidines [6] and for penta-fluoro-pyridine [7]. However it will be shown that even in these cases a number of assignments require revision. The availability, volatility and small moments of inertia of 2,6 di-fluoropyridine make it a most attractive substituted pyridine system for study. In addition it is well established [e.g. 5, 8–11] that the force constants of benzene [12, 13] and hexafluoro benzene [14] are transferable to other aromatic systems. This makes it feasible to calculate the vibrational frequencies of the di-fluoro pyridine. It must be emphasised that this does not

- 
- [1] J. K. WILMSHURST and H. J. BERNSTEIN, *Can. J. Chem.* **35**, 1183 (1957).  
[2] D. A. LONG, F. S. MURFIN and E. L. THOMAS, *Trans. Faraday Soc.* **59**, 12 (1963).  
[3] V. I. BEREZIN, *Opt. Spectry* **15**, 167 (1963).  
[4] J. H. S. GREEN, W. KYNASTON and H. M. PAISLEY, *Spectrochim. Acta* **19**, 549 (1963).  
[5] D. A. LONG and W. O. GEORGE, *Spectrochim. Acta* **19**, 1777 (1963).  
[6] K. C. MEDHI and D. K. MUKHERJEE, *Spectrochim. Acta* **21**, 895 (1965).  
[7] D. A. LONG and R. T. BAILEY, *Trans. Faraday Soc.* **59**, 599 (1963).  
[8] D. STEELE, *Spectrochim. Acta* **22**, 1275 (1966).  
[9] D. B. SCULLY and D. H. WHIFFEN, *Spectrochim. Acta* **16**, 1409 (1960).  
[10] D. STEELE and D. H. WHIFFEN, *Trans. Faraday Soc.* **56**, 8 (1960).  
[11] D. A. LONG and D. STEELE, *Spectrochim. Acta* **19**, 1791 (1963).  
[12] D. H. WHIFFEN, *Phil. Trans. Roy. Soc.* **A248**, 131 (1955).  
[13] J. DUINKER and I. M. MILLS, personal communication.  
[14] D. STEELE and D. H. WHIFFEN, *Trans. Faraday Soc.* **56**, 5 (1960).

mean that the force fields of these molecules are at all reliable but rather that the assignments of the molecules on which they are based are essentially correct. It has been shown that two drastically different fields for benzene reproduce the frequencies of benzene and its derivatives with equal success [8, 13]. The field of hexafluorobenzene is based on very limited data, as no isotopic information is readily obtained, and a considerable number of assumptions were necessary to fix a set of values for the force constants. These fields have been used with success in the computation of the vibrational frequencies of pyridine, its deuterio analogues [5] and of pentafluoro pyridine [11] by treating the nitrogen ring atom as  $^{14}\text{C}$ .

No information is available on the geometry of 2,6 difluoro pyridine. For the computation of vibrational frequencies small deviations in the geometry are

Table 1. Activities, model distribution and band shapes  
2,6 di-fluoropyridine

Symmetry class	No. of vibrations	Activity	Vapour phase band shapes
$a_1$	10	i.r.; R(p)	Type B. Separation 8–9 $\text{cm}^{-1}$
$b_2$	9	i.r.; R(dp)	Type A. Medium strength Q; PR separation of $\sim 10 \text{ cm}^{-1}$
$b_1$	5	i.r.; R(dp)	Type C. Very strong Q Very broad and weak P and R
$a_2$	3	R(dp)	—

unimportant. Consequently a regular, planar and hexagonal ring system has been assumed. By analogy with related systems the bond lengths were taken as  $r_{\text{CN}} = r_{\text{CC}} = 1.40 \text{ \AA}$ ;  $r_{\text{CF}} = 1.30 \text{ \AA}$  and  $r_{\text{CH}} = 1.08 \text{ \AA}$ . Band shapes and frequencies computed on the basis of this geometry agree well with observed thus vindicating the use of this model.

The nuclear point group is  $C_{2v}$ . Taking the  $C_2$  axis as the  $Z$  axis, as recommended by MULLIKEN [15], the vibrations classify as  $10a_1 + 9b_2 + 3a_2 + 5b_1$ . With this choice of axes the  $b_1$  and  $b_2$  labels are reversed from the usual convention.

On the basis of the geometry described above the principal moments of inertia are calculated to be 132, 288 and 420 a.m.u. For these values the graphs of GERHARD and DENNISON [16] predict the vapour band shapes listed in Table 1. The agreement with observed is good.

## 2. EXPERIMENTAL

A 2 ml sample of 2,6 difluoropyridine was kindly donated by Dr. G. C. Finger of the Illinois State Geological Survey. It was a clear colourless very volatile liquid, b.p.  $126^\circ\text{C}$ ;  $n_{\text{D}}^{25} 1.4345$ . No impurities were detected by vapour phase chromatography.

[15] R. S. MULLIKEN, *J. Chem. Phys.* **23**, 1997 (1955).

[16] S. L. GERHARD and D. M. DENNISON, *Phys. Rev.* **43**, 197 (1933).

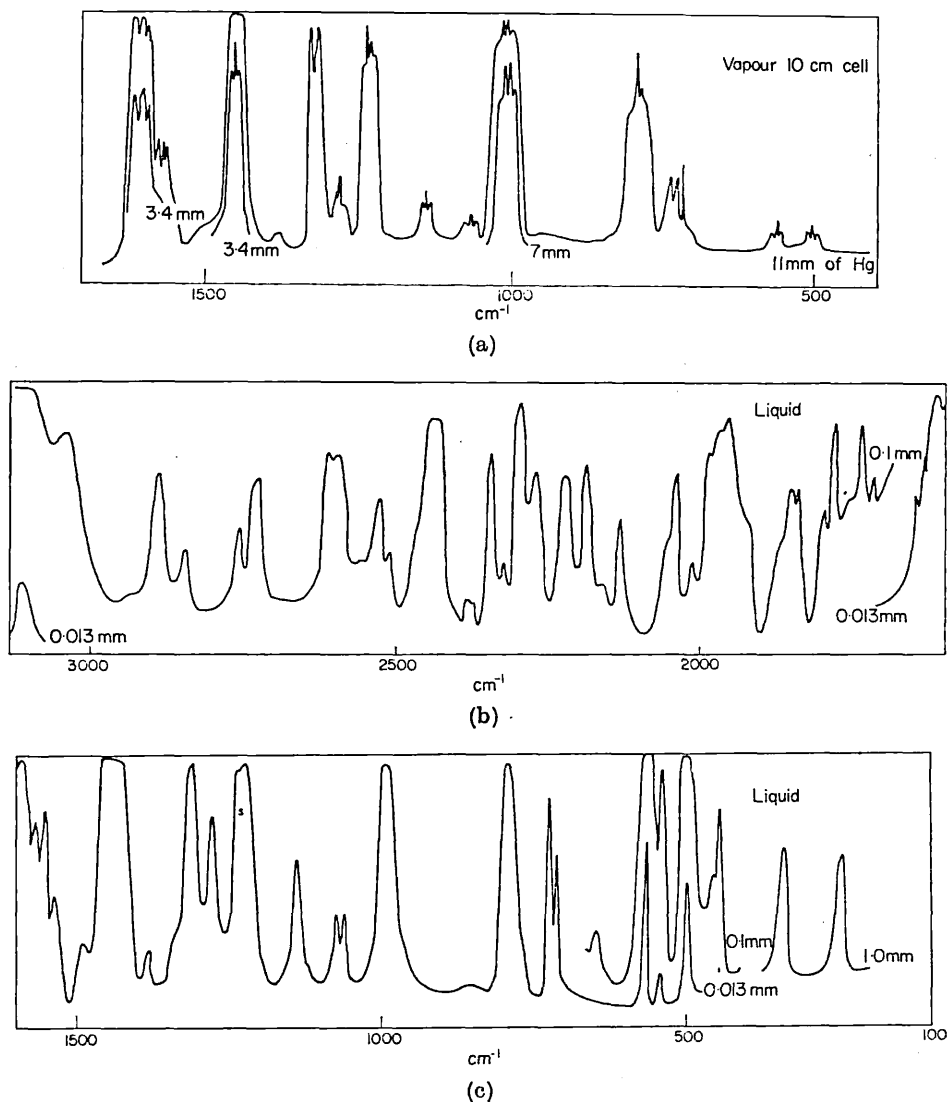


Fig. 1. (a), (b), (c). The infra-red spectra of 2,6 difluoropyridine in the vapour and pure liquid phases.

Spectra were measured as described in part I [17]. Redrawn infra-red spectra are shown in Fig. 1 and the observed frequencies are listed in Table 2.

### 3. CALCULATIONS

The procedure and force constants employed also are as described in part I. The evaluation of the  $B$  matrix elements for the regular hexagonal case is too trivial to warrant their reproduction here. They are available on request.

[17] R. T. BAILEY and D. STEELE, *Spectrochim. Acta* **23A**, 2989 (1967).

Table 2. Observed Raman shifts and infra-red absorption frequencies for 2,6 difluoropyridine

Raman	Infra-red		Assignments
	Vapour	Liquid	
219(8)			$a_2$ fundamental
247(5)		247 ms	$b_1$ fundamental
348(1)		346 ms	$a_1$ fundamental
458(1)		461 w	$b_2$ fundamental
498(2)	494 } 501 Q } 507 } A	501 ms	$b_1$ fundamental
546(5) p		548 w	$a_1$ fundamental
566(4)	563 } 568 Q } 575 } A	568 s	$b_2$ fundamental
657(3)		658 vw	
	721 Q C	720 ms	$b_1$ fundamental
736(10) p	735 } 744 } B	736 s	$a_1$ fundamental
795(1)	796 Q C	796 vs	$b_1$ fundamental
879(0)			$a_2$ fundamental
941(0)			720 + 219 ( $b_1$ ) or $b_1$ fundamental
998(10) p			$a_1$ fundamental
	1001 Q	993 vvs	} $b_2$ fundamental
	1007 Q	998 vvs	
1064 sh	1062	1066 m	348 + 720 ( $b_2$ )
1071(5) p	1070	1074 m	$a_1$ fundamental
1142(2)	1134 } 1140 Q } 1146 } A or C	1145 ms	$b_2$ fundamental
1228(0)	1237 Q	1233 vs	$b_2$ fundamental
	1244 Q	1240 s	
1255(0)			
1281(2)	1281 Q	1284 ms	$b_2$ fundamental
1307(7) p	1316 } 1325 } B	1310 vs	$a_1$ fundamental
		1385 w	
1446(1)	1451 } 1456 Q } 1460 } A	1455 vs	$b_2$ fundamental
		1486 w	
		1546 m	
1560(2)	1562 Q	1562 ms	
	1574 Q	1574 m	
1590(4)	1593 Q	1592 vs	$b_2$ fundamental
1612(3)	1609 } 1618 } B	1614 vvs	$a_1$ fundamental
1636(1)		1633 m	
		1644 mw	
		1712 vvw	796 + 924 ( $a_1$ )
		1735 w	
		1780 w	
		1797 w	879 + 924 ( $b_2$ )
		1847 w	2 × 924 ( $a_1$ )
		1860 w	
		1964 wm	
		2000-3000 many w to m bands	
3052(3)		3048 w	$a_1$ fundamental
3090 sh			$b_2$ fundamental
3108(8) p		3107 s	$a_1$ fundamental
		3199 w	
		3221 w	

Table 3. The calculated frequencies and potential energy distributions of 2,6 difluoropyridine and the assigned frequencies of 2,6 difluoropyridine and 2,6 dimethylpyridine

	2,6 difluoro		2,6 dimethyl		Approximate potential energy distribution for difluoro		
	calc.	ass.	ass. (B&S)	ass. (M&M)			
$a_1$	3077	3108	3064	3064}	99% $r_{CH}$		
	3059	3048	3040	3040}			
	1614	1614	1599	1599	48% $R_{CO}$	13% $r_{CF}$	20% $\beta_{CH}$
					18% $\alpha$		
	1423	?	1418	1470	50% $R_{CO}$	12% $r_{CF}$	10% $\beta_{CH}$
					13% $\beta_{CF}$		
	1329	1310	1264	1264/1225	15% $R_{CO}$	46% $r_{CF}$	20% $\beta_{CH}$
					19% $\alpha$		
	1088	1074	1094	1094	38% $R_{CO}$	40% $\beta_{CH}$	19% $\alpha$
	1006	998	996	996	12% $R$	86% $\alpha$	
740	736	718	718	39% $R$	14% $r_{CF}$	44% $\alpha$	
552	547	555	555	17% $R$	69% $\alpha$		
305	346	342	342	12% $R$	83% $\beta_{CF}$		
$b_2$	3066	3090		3040	99% $r_{CH}$		
	1610	1592	1580	1580	46% $R_{CO}$	21% $r_{CF}$	10% $\beta_{CH}$
					23% $\alpha$		
	1473	1456	1470?	1418	32% $R_{CO}$	12% $r_{CF}$	50% $\beta_{CH}$
	1281	1284	1340	1340	71% $R_{CO}$	21% $\beta_{CH}$	
	1235	1233	1245	1245	33% $R_{CO}$	25% $r_{CF}$	36% $\beta_{CH}$
	1152	1145	1156	1225	29% $R_{CO}$	66% $\beta_{CH}$	
	987	998	995	1156	55% $R$	24% $r_{CF}$	12% $\alpha$
	534	568	539	539	15% $R$	67% $\alpha$	
	404	461	289	218	84% $\beta_{CF}$		
$b_1$	997	924?	890	890	% $\gamma_{CF}$	% $\gamma_{CH}$	% $\tau$
	841	796	770	770	3	91	6
	768	720	725	725	36	20	44
	501	501	486	486	0	100	0
	270	247	218	200	8	17	75
$a_2$	912	879	?	940	39	6	55
	569	?	?	430	2	94	4
	242	219	200	289	73	2	25
				4	13	83	

Computed frequencies and approximate potential energy distributions are listed in Table 3.

#### 4. ASSIGNMENTS

##### $a_1$ class

Intensities and Raman polarisation data leave no doubt as to the assignment of bands at 3108, 1307, 1071, 998, 736 and 546  $\text{cm}^{-1}$  to the  $a_1$  class. The average discrepancy between observed and calculated frequencies is only 0.95%. This encourages reliance on the calculations. Infra-red absorption bands in the vapour phase at 1310 and 736  $\text{cm}^{-1}$  (liquid phase frequencies) are type *B* with peak separations in good agreement with those computed. By contrast absorption at 998  $\text{cm}^{-1}$  shows two sharp *Q* branches in the vapour phase. This shows conclusively that there are two fundamentals of different symmetry classes at 998  $\text{cm}^{-1}$ . The

second fundamental is of the  $b_2$  class. Band shapes also serve to identify the highest ring mode at  $1614\text{ cm}^{-1}$ . No evidence can be cited for the exact position of the ring mode computed to be at  $1423\text{ cm}^{-1}$ .

The remaining and lowest  $a_1$  fundamental is correlated with the  $348\text{ cm}^{-1}$  absorption and Raman shifts. Absorption is too weak below  $400\text{ cm}^{-1}$  for the vapour band contours to be observable with the available equipment. However this frequency correlates well with that of the analogous mode assigned to 2,6 lutidine. The failure to observe any polarisation of the Raman scattering at the frequency in either compound does not contradict the assignment. It frequently happens that the polarisation of very low frequency deformation modes of the fully symmetric class have too small polarisation to be detectable. The remaining  $\nu_{\text{CH}}$  fundamental is correlated with the  $3048\text{ cm}^{-1}$  band.

#### $b_2$ class

Vapour phase band shapes and absorption or scattering intensities serve to identify fundamentals of the  $b_2$  class at  $1592$ ,  $1456$ ,  $1233$ ,  $1145$ ,  $998$  and  $568\text{ cm}^{-1}$ . Band shape and calculations indicate that a further  $b_2$  fundamental is at  $1284\text{ cm}^{-1}$ . The remaining fundamental is calculated to have a frequency of  $404\text{ cm}^{-1}$ . No other mode is computed to be within  $100\text{ cm}^{-1}$  of this frequency. Weak Raman bands at  $458$  and  $348\text{ cm}^{-1}$  consequently are both reasonable candidates for assignment to this vibration. However as the lower mode has already been correlated with the lowest  $a_1$  mode and since remaining strong bands are satisfactorily correlated with all other expected low frequency modes (see below) there appears little room for doubt in the choice of the higher frequency band as the  $b_2$ . The CH stretching frequency is identified with the shoulder on the  $a_1$  Raman band at  $3090\text{ cm}^{-1}$ .

#### $b_1$ class

Strong type  $C$  bands at  $796$  and  $721\text{ cm}^{-1}$  serve to identify two  $b_1$  modes. Further  $b_1$  modes are calculated to be at  $997$ ,  $501$  and  $270\text{ cm}^{-1}$ . However the out-of-plane calculations are not as reliable as the in-plane for reasons described in part I. It is not possible to rely on these to better than 10%. Strong Raman and infra-red bands at  $247\text{ cm}^{-1}$  are unambiguously identified as due to one of these  $b_1$  modes. Strong infra-red absorption at  $568\text{ cm}^{-1}$  appears to have a type  $A$  vapour phase band contour. However as another strong type  $A$  band well removed from this frequency is more readily correlated with the only  $b_1$  mode anticipated or calculated near here it appears very likely that it is indeed a type  $C$  band with a rather broadened  $Q$  branch either due to hot bands or due to lower resolution. Absorption due to the highest  $b_1$  mode is not seen. Analysis of combination bands in the  $2000\text{--}1700\text{ cm}^{-1}$  region suggests that the frequency is about  $924\text{ cm}^{-1}$  (see below).

#### $a_2$ class

Strong Raman scattering at  $219\text{ cm}^{-1}$  is clearly due to an  $a_2$  mode. Other much weaker Raman bands without corresponding infra-red absorption bands occur at  $941$  and  $879\text{ cm}^{-1}$ . The former appears at too high a frequency by

correlation with vic-trideutero benzene in which the  $a_2$  modes occur at 920, 712 and 374  $\text{cm}^{-1}$  [18]. By symmetry, the nuclei on the  $C_2$  axis cannot contribute to an  $a_2$  vibration, and since the mass effect of substituting fluorine for hydrogen may reasonably be expected to have a greater effect on frequencies than any force constant changes, it is reasonable to expect the 2,6 difluoropyridine frequencies to lie below those of vic-trideutero-benzene. The remaining  $a_2$  mode is unidentified.

### Combination bands

As in other fluoro-aromatic systems there is a wealth of strong combination bands. However due to the low symmetry these are of little value in deducing fundamentals, many assignments generally being possible.

As in the spectra of benzene and its derivatives [19] absorption bands of substituted pyridines in the region 2000–1600  $\text{cm}^{-1}$  are characteristics of substitution pattern and arise from summation bands involving  $\gamma_{\text{CH}}$  modes. These patterns have been established for monosubstituted alkyl pyridines [20] and used to establish the  $\gamma_{\text{CH}}$  fundamentals for alkyl and halogen substituted pyridines [4]. Unfortunately no study of this region has been carried out for any disubstituted pyridines. The analysis in this case is rendered much more complicated by the presence of other strong summation bands in the appropriate range involving the  $\nu_{\text{CF}}$  modes. However the speculative  $a_2$  assignment at 879  $\text{cm}^{-1}$  and bands of appreciable strength of 1847 and 1797  $\text{cm}^{-1}$  suggest that the missing  $b_1 \gamma_{\text{CH}}$  frequency is about 924  $\text{cm}^{-1}$ —the assignments then being 879 + 924 and  $2 \times 924$  respectively.

## 5. COMPARISON OF ASSIGNMENTS WITH THOSE OF METHYL SUBSTITUTED PYRIDINES

### (a) 2,6 Lutidine

The agreement between the  $a_1$  assignments of the difluoro compound and those of 2,6 lutidine is good. This is in accord with the similarity of the spectra of alkyl substituted and halogen substituted benzene systems [e.g. 21]. In the  $b_2$  class two discrepancies are readily apparent. Medhi and Mukherjee place the lowest  $b_2$  frequency, which arises primarily from ring methyl deformation, at 218  $\text{cm}^{-1}$ . This seems far too low for such an in-plane mode. The  $\beta$  methyl mode of toluene is at 347  $\text{cm}^{-1}$  [22]. In the  $b_2$  class of 2,6 lutidine we have one out-of-phase methyl mode and one C—CH<sub>3</sub> stretch. It would appear reasonable to expect the  $\beta$  methyl mode to be below, but not much below, that of its toluene counterpart. The  $a_1$

$\beta\text{C}-\text{CH}_3$  mode is assigned at 342  $\text{cm}^{-1}$ —admittedly on slender grounds—thus

[18] A. LANGSETH and R. C. LORD, *Mat. Fys. Medd. Dan. Vid. Selsk.* **16**, No. 6 (1938); S. BRODERSEN and A. LANGSETH, *Mat. Fys. Skrifter Dan. Vid. Selsk.* **1**, No. 1 (1959).

[19] D. H. WHIFFEN, *Spectrochim. Acta* **7**, 253 (1955).

[20] G. L. COOK and F. M. CHURCH, *J. Phys. Chem.* **61**, 458 (1957).

[21] R. R. RANDLE and D. H. WHIFFEN, *Molecular Spectroscopy*. Institute of Petroleum (1955).

[22] N. FUSON, C. GARRIGOU-LAGRANGE and M. L. JOSIEN, *Spectrochim. Acta* **16**, 106 (1960).

supporting this argument. The strong Raman band at  $289\text{ cm}^{-1}$  is chosen in preference to the  $218\text{ cm}^{-1}$  band as the  $b_2$ .

The second re-assignment can be made on much firmer evidence. The Raman band at  $1225\text{ cm}^{-1}$  is noted to be polarised rendering its assignment to the  $b_2$  class unsatisfactory. Its strength presumably arises by Fermi interaction of a combination mode with the  $a_1$  fundamental giving rise to 1264, 1225 doublet. The present investigation of difluoropyridine shows that the frequency ought to be close to  $1000\text{ cm}^{-1}$ . The strong  $a_1$  absorption and scattering in this region renders its exact location unfeasible with the present evidence.

(b) *Monosubstituted pyridines*

The spectral data on 2-F pyridine is restricted to Raman data. This precludes any detailed spectral comparisons between the mono and disubstituted fluoropyridine. However a comparison of the revised assignments of the dimethyl and mono-methyl pyridines by means of two approximate, but extremely useful, theorems permits an indirect check on the fluoro assignments.

It has been demonstrated that the sum rule of DECIUS *et al.* [23] is applicable to non-isotopic systems due to compensation of force constant changes inherent in the superimposition nature of the rule [24]. For the systems  $A$ ,  $B$  and  $C$  where the nuclear configuration (and, it is hoped, electron density) of  $C$  is reproduced by super-imposing  $A$  on  $B$  with suitable weight factors, a percentage deviation from prediction can be expressed by

$$\delta = \frac{a\nu_A^2 + b\nu_B^2 - (a + b)\nu_C^2}{(a + b)\nu_C^2} \times 100$$

where  $a/a + b$  and  $b/a + b$  are appropriate weight factors for  $A$  and  $B$ .

Some typical  $\delta$  values for the in-plane vibrations of substituted fluoro-aromatics are

A	B	C	Sym. class	$\delta$
$\text{C}_6\text{H}_6$	$\text{C}_6\text{F}_6$	$p\text{ C}_6\text{H}_4\text{F}_2$	$a_g$	-0.5 (+2.2)
			$b_u$	-0.05 (+2.6)
$\text{C}_6\text{D}_6$	$\text{C}_6\text{F}_6$	$p\text{ C}_6\text{D}_4\text{F}_2$	$b_u$	-0.02 (+1.8)
$\text{C}_6\text{H}_6$	$\text{C}_6\text{F}_6$	$p\text{ C}_6\text{H}_2\text{F}_4$	$a_g$	-0.26 (+1.9)
			$b_u$	+0.5 (+3.2)
$\text{C}_6\text{H}_6$	$\text{C}_6\text{F}_6$	sym $\text{C}_6\text{F}_3\text{H}_3$	$e'$	-0.35 (+5.1)
			$a_1'$	+0.15 (+3.6)

The symmetry class designations refer to those of the common denominator symmetry group. The  $\delta$  values in parentheses are obtained by factoring out the  $\nu_{\text{CH}}$  stretching frequencies. It is to be noted that the change in  $\delta$  is in the sense required for interaction between the CH stretches and the other modes. However the magnitude of the change in  $\delta$  is amplified by the large drop in  $\nu_C^2$  in the denominator arising from elimination of the CH stretching frequencies.

[23] J. C. DECIUS and E. B. WILSON, *J. Chem. Phys.* **19**, 1409 (1951); L. M. SVERDLOV, *Dokl. Akad. Nauk S.S.S.R.* **78**, 1115 (1951).

[24] D. STEELE, *Spectrochim. Acta* **18**, 915 (1962).



Applying this rule to 2,6 dimethyl pyridine, pyridine and 2 methyl pyridine the only common symmetry element is the plane of symmetry and  $\delta$  is  $-0.5\%$  ( $-0.10\%$ ) for the sole in-plane class of common denominator group. In this case  $\delta$  computed without the CH stretching modes is very satisfactory indicating consistency of the assignments but  $\delta$  with the  $\nu_{\text{CH}}$  is high. This is due to arbitrary assignments of each of the two observed CH bands of the mono methyl compound to two fundamentals. Comparison with pyridine shows that this gives too high a value  $\nu_{\text{CH}}^2$  (Table 3).

The second rule is the interpolation rule [25]. This predicts that for the in-plane classes the  $j$ -th frequency of 2 Me pyridine will lie between the  $j$ -th and  $(j + 2)$ th frequency of pyridine. A similar relation exists between the in-plane frequencies of 2,6 dimethyl pyridine and 2 methyl pyridine. This holds in both cases. However the assignments of Medhi and Mukherjee for the dimethyl compound are not consistent with those of monomethyl compound on this basis.

[25] D. STEELE and D. H. WHIFFEN, *Trans. Faraday Soc.* **55**, 369 (1959).

## The vibrational spectra of substituted nitrogen heterocyclic systems—III. 1,3,5 trichloropyrimidine

R. T. BAILEY

Department of Pure and Applied Chemistry, University of Strathclyde, Glasgow  
and

D. STEELE

Department of Chemistry, Royal Holloway College, University of London  
Englefield Green, Surrey

(Received 27 March 1968)

**Abstract**—Raman and infra-red spectra of 1,3,5 trichloropyrimidine and its 4D derivative have been measured in the liquid phase. An almost complete set of assignments are proposed which are based on the spectral characteristics and on frequencies computed for a  $C_{2v}$  model using Scherer's force fields for chlorinated benzenes.

### 1. INTRODUCTION

IN Part I of this series [1] the vibrational spectra of 2,4,6-trifluoropyrimidine were discussed. It is interesting to compare the spectra with those of the trichloro-analogue and to establish a close analogy between the chloropyrimidine spectra and the chlorobenzene spectra as has been done for the fluoro-derivatives. Furthermore from comparison of the mass and force constant effects accompanying substitution of chlorine for fluorine it ought to be possible to interpolate or extrapolate to predict the spectrum of other pyrimidine systems. This, it is hoped, will serve as a basis on which a spectral study of cytosine may be undertaken.

The problem of spectral interpretation is greatly facilitated by the availability of force fields for the in-plane [2] and for the out-of-plane vibrations of chlorobenzenes [3]. Success in predicting the frequencies of fluorinated pyrimidines [1] and pyridines [4, 5] using force fields of benzene and hexafluorobenzene encourage the hope that similar success might be experienced for other substituents.

### 2. EXPERIMENTAL

A commercial sample of trichloropyrimidine (Koch-Light) was vacuum distilled and was found to have a purity of at least 99% by analytical gas chromatography. The deuterated compound was prepared from deuterated cyanuric acid by reaction with phosphoryl chloride and dimethylaniline [6]. Cyanuric acid was deuterated by

[1] R. T. BAILEY and D. STEELE, *Spectrochim. Acta* **23A**, 2989 (1967).

[2] J. SCHERER, *Spectrochim. Acta* **20**, 345 (1964).

[3] J. SCHERER, *Spectrochim. Acta* **23A**, 1489 (1967).

[4] D. A. LONG and D. STEELE, *Spectrochim. Acta* **19**, 1791 (1963).

[5] R. T. BAILEY and D. STEELE, *Spectrochim. Acta* **23A**, 2997 (1967).

[6] J. BADDILEY and A. TOPHAM, *J. Chem. Soc.* 678 (1944).

repeated exchange with  $D_2O$  but complete exchange was found difficult to attain.

A mass spectral analysis carried out by Mead of B.P., Sunbury, showed that the deuterated species (D) contained  $15 \pm 0.5\%$  of  $C_4N_2Cl_3H(H)$ . Details of instruments used are as described in Parts I and II [1, 5]. Spectra were run as melt and in solutions of  $CS_2$  and  $CCl_4$ . Over certain spectral regions infra-red spectra were also recorded in nitromethane, benzene and *cyclohexane*. To distinguish contributions to the spectrum of D from H the spectra were recorded with varying amounts of H in the reference beam. When the very strong  $1105\text{ cm}^{-1}$  band due to the H species was balanced out the residual spectrum was taken as that of D. Infra-red spectra are shown in Figs. 1 and 2. Frequencies are given in Table 1.

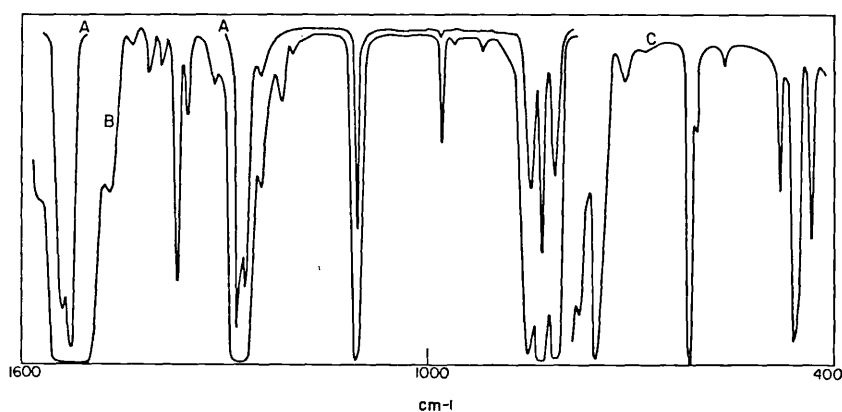


Fig. 1. Redrawn infra-red absorption spectrum of  $C_4N_2Cl_3H$  for range  $1600-400\text{ cm}^{-1}$ .

A solution  $0.013\text{ mm cell}$ .

B  $0.013\text{ mm cell}$ .

C  $0.05\text{ mm cell}$ .

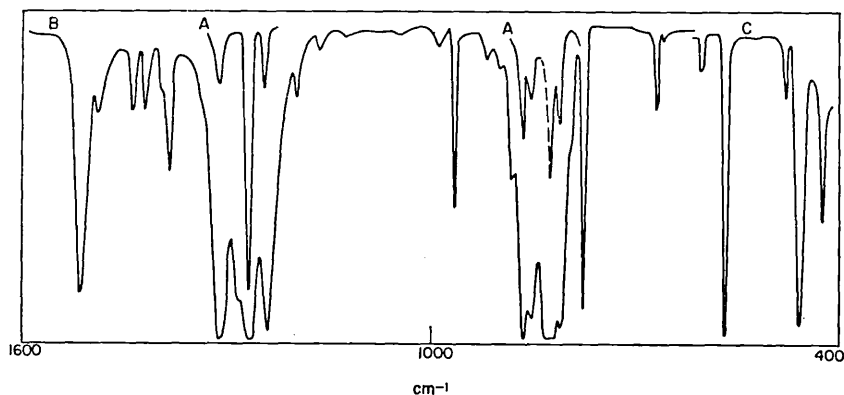


Fig. 2. Redrawn infra-red absorption spectrum of  $C_4N_2Cl_3D$  for range  $1600-400\text{ cm}^{-1}$ .

A solution  $0.013\text{ mm cell}$ .

B  $0.013\text{ mm cell}$ .

C  $0.05\text{ mm cell}$ .

Table 1. The observed Raman and infra-red frequencies of  $C_4N_2Cl_3H$  and  $C_4N_2Cl_3D$  and their assignments

$C_4N_2Cl_3H$		$C_4N_2Cl_3D$		Assignment	
Raman	Infra-red	Raman	Infra-red	Species	Mode
3112 mp	3108 s			$A_1$	CH stretch fund
3044 w	3043 m	3031 w	3036 m	$2 \times A_1$	$2 \times 1522$ (H) $2 \times 1513$ (D)
	2888 mw				
	2735 w		2710 mw		
	2714 mw				
	2640 w				
	2556 m		2506 m		
	2500 m		2475 m		
2387 w	2389 mw	2387 m	2387 w		
		2311 s,p	2313 s	$A_1$	CD stretch fund
	2296 m				
	2258 w				
			2233 w		
	2206 w		2205 w		
	1917 w		1910 w		
			1787 w		
			1670 w		
	1567 ms	1550 w			
	1539 vvs		1523 vvs	$B_2$	fundamental
1522 s	1528 xs			$A_1$	fundamental
		1513 s	1514 sh	$A_1$	fundamental
		1467 w	1476 w		
	1440 w		1442 w		
	1411 m		1422 w		
	1392 m	1392 vw	1388 m		
1366 w	1368 s			$B_2$	fundamental
	1352 m				
	1317 m	1312 vw	1314 s	$B_2$	fundamental
1277 m	1280 vs	1266 s	1269 vs	$A_1$	fundamental
1269 sh, m	1269 s		1242 s	$B_2$	fundamental
	1248 m				
1223 sh, w					
1210 m, p	1216 m	1212 s, p		$A_1$	fundamental
			1199 wm		
1193 w		1191 w			
			1167 w		
		1126 vw			
1103 w	1105 vs			$B_2$	fundamental
			1072 vw		
			1036 vw		
			991 w		
977 vs, p	990 w			$A_1$	fundamental
963 s, p	978 ms				
	965 m	964 vs, p	965 s	$A_1$	fundamental
			965 w		
918 vw	932 m			$B_1$	fundamental
			917 w		
		903 w	901 w		
			880 w		
		869 w	860 vs		
854 vw	849 vs			$B_2$	fundamental
830 w	833 vs			$B_2$	fundamental
	847 w			$A_2 + B_1$	614 + ~230
			849 s	$B_1$	fundamental
		819 m	818 vs	$B_2$	fundamental
		773 m	775 s	$A_2 + B_1$	565 + ~230
			806 s	$A_1$	fundamental
753 vw	813 vs			$B_1$	fundamental
	752 s				
	712 vw				
		682 w	667 m	$B_1$	fundamental
	614 s			$B_1$	fundamental

Table 1 (cont.)

$C_4N_2Cl_3H$		$C_4N_2Cl_3D$		Assignment	
Raman	Infra-red	Raman	Infra-red	Species	Mode
597 w	605 w	597 m	600 w	$B_1$	fundamental
	545 vw	561 w	565 s		
479 w	483 m	474 m	477 w	$B_2$	fundamental
456 m	462 s	454 s	457 s		
428 w	434 m	419 m	423 m		
414 sh, p		387 vs, p		$A_1$	fundamental
388 s, p		332 vw			
	314 w	282 vw		$A_1, B_2$	fundamental
202 vs	202 m	201 vs	200 m		
174 s	179 vs	167 s		$B_1$	fundamental
140 m	148 s	140 m			

## 3. CALCULATIONS

The method of setting up the secular equations and of deriving the vibrational frequencies and their eigenvectors was as described in Part I [1]. The force constants used were transferred from the papers by SCHERER [2, 3]. In this context, no distinction was made between the nitrogen and carbon atoms. Two sets of calculations were made. In the first (calc. A) a regular hexagonal geometry was assumed. In the second (calc. B) the molecular geometry was taken to be the same as for 2-amino 4,6 dichloropyrimidine [7] ( $\text{NCN} = 128^\circ$ ,  $\text{CNC} = 114^\circ$ ,  $\text{CCC} = 114^\circ$ ,  $r_{\text{CN}} = 1.32 \text{ \AA}$ ,  $r_{\text{CC}} = 1.36 \text{ \AA}$ ,  $r_{\text{C-Cl}} = 1.8 \text{ \AA}$ ). Computed frequencies are given in Tables 2 and 3. Species nomenclature is as used in Parts I and II and therefore the  $A_1$  and  $B_2$  labels apply to the in-plane modes.

## 4. ASSIGNMENTS

4.1 Assignment of fundamental frequencies expected above  $900 \text{ cm}^{-1}$ 

Polarised Raman bands allow positive identification of  $A_1$  fundamentals at 3112, 1210, 977/963, and  $388 \text{ cm}^{-1}$  in H and at 2311, 1212, 963 and  $387 \text{ cm}^{-1}$  in D. The average percentage discrepancies between observed and calculated frequencies are 2.6% for calculation A and 3.3% for calculation B. This gives an encouraging guide to the reliability of the calculations. Lack of further polarisation data and vapour phase band contours, necessitates considerable reliance on the calculations and observed isotopic H—D frequency shifts for further progress. The most striking fact about the computed frequencies is the insensitivity of the  $A_1$  frequencies to H, D substitution whilst four of the  $B_2$  modes show shifts in excess of  $20 \text{ cm}^{-1}$ . Three of these sensitive modes lie above  $1000 \text{ cm}^{-1}$  (the upper limit for any of the  $B_1$  modes with which they might be confused). This serves to identify two of these unambiguously as 1368 and  $1105 \text{ cm}^{-1}$  (H) and 1314 and  $860 \text{ cm}^{-1}$  (D). The calculations show that a further two ( $A_1$  and  $B_2$ ), fundamental frequencies have to be determined in the  $1500 \text{ cm}^{-1}$  region and two ( $A_1$  and  $B_2$ ) in the  $1300\text{--}1200 \text{ cm}^{-1}$

[7] C. J. B. CLEWS and W. COCHRAN, *Acta Cryst.* **1**, 4 (1948).

Table 2. The calculated and assigned in-plane frequencies of 2,4,6 tri-chloropyrimidine, its deuterio isomer and 1,3,5 tri-chlorobenzene (All frequencies in  $\text{cm}^{-1}$ )

$C_{2v}$ species	$C_4N_2Cl_3H$			$C_4N_2Cl_3D$		$C_6Cl_3H_3$ $D_{3h}$ species			
	Calc. A	Calc. B	Ass.	Calc. B	Ass.	Calc.	Ass.		
$A_1$	3070	3070	3112	2287	2311	3071	3084	$A_1'$	
						3069	3089	$E'$	
	1575	1539	1525	1524	1513	1632	1570	$E'$	
	1325	1250	1280	1243	1269	1436	1420	$E'$	
	1156	1136	1210	1136	1212	1159	1149	$A_1'$	
						1087	1098	$E'$	
	985	973	977/963	957	963	987	997	$A_1'$	
	790	790	813	787	806	791	816	$E'$	
	433	414	434	410	423	432	429	$E'$	
	375	366	388*	366	387	375	379	$A_1'$	
	185	187	179*	187	167*	184	191	$E'$	
	$B_2$						3069	3089	$E'$
		1609	1587	1539	1571	1522	1632	1570	$E'$
		1427	1423	1368	1357	1314	1436	1420	$E'$
1280		1240	1269	1240	1242	1359		$A_2'$	
			or 1248						
						1213		$A_2'$	
1129		1104	1105	873	860	1087	1098	$E'$	
780		787	840	773	818/775	791	816	$E'$	
465		413	462	413	458	446		$A_2'$	
428		400	388*	390		432	429	$E'$	
184		187	179*	186	167*	184	191	$E'$	

Calc. A made using regular hexagonal geometry.

Calc. B made using geometry described in text.

\* Double assignments.

Table 3. The calculated and assigned frequencies for the out-of-plane fundamentals of tri-chloropyrimidine and its deuterio isomer

Species	$C_4N_2Cl_3H$		$C_4N_2Cl_3D$	
	Calc.	Ass.	Calc.	Ass.
$B_1$	926	923	845	849
	753	752	684	667
	543	614	494	565
	214	202	208	201
	147	144	146	140
$A_2$	575		575	
	235	230*	235	230*

\* Estimated from Fermi resonance doublet.

region for both systems. Extremely strong infra-red absorption exists for H at 1539 and 1528  $\text{cm}^{-1}$ . A strong Raman line at 1522  $\text{cm}^{-1}$  favours identification of the lower frequency as due to the  $A_1$  mode. For D, an extremely strong band appears at 1529  $\text{cm}^{-1}$  with a shoulder at 1514  $\text{cm}^{-1}$  and one Raman band is at 1513  $\text{cm}^{-1}$ . The frequency shifts for the  $A_1$  and  $B_2$  species are computed to be 15 and 16  $\text{cm}^{-1}$  respectively and it would seem logical to assign the  $A_1$  frequency in D as 1513  $\text{cm}^{-1}$  and the  $B_2$  as 1523  $\text{cm}^{-1}$ . The observed frequency shifts, frequency range and strength of the corresponding Raman emission encourage assignment of the 1280

(H) and  $1269\text{ cm}^{-1}$  (D) bands to the remaining high frequency  $A_1$  fundamental. By elimination the  $B_2$  mode is correlated with the weaker, but still strong, absorption at  $1269\text{ cm}^{-1}$  (H) and  $1242\text{ cm}^{-1}$  (D). The frequency shift of  $27\text{ cm}^{-1}$  for the assigned bands is in poor agreement with the predicted shift of almost zero. An alternative interpretation is to assign these bands as Fermi resonance components of the  $A_1$  fundamental and the  $1248\text{ cm}^{-1}$  (m) infra-red band (H) to the  $B_2$  fundamental, the corresponding D band being masked by the  $A_1$  resonance doublet. On the present evidence it is not possible to decide between these.

#### 4.2 Assignment of fundamental frequencies expected below $900\text{ cm}^{-1}$

By virtue of its frequency range and the absence of any band of comparable strength within  $40\text{ cm}^{-1}$  in the spectrum of the D analogue, the  $\gamma_{\text{CH}}$  mode is identified at  $923\text{ cm}^{-1}$ . Support for this is found in the presence of a band at the expected frequency for its overtone. The  $\gamma_{\text{CD}}$  band should be located near  $840\text{ cm}^{-1}$ . In D, three other fundamentals are expected in the range  $900\text{--}780\text{ cm}^{-1}$ . One of these, the  $B_2\beta$  CD mode has been identified with the strong  $860\text{ cm}^{-1}$  absorption. In support of this we note that

1. The infra-red absorption at  $860\text{ cm}^{-1}$  (D) is far stronger than any in H between  $1000$  and  $860\text{ cm}^{-1}$ .

2. The strength of absorption is so far in excess of that of the  $\gamma_{\text{CH}}$  band and of that of the next highest frequency  $B_2$  mode of H, at  $752\text{ cm}^{-1}$ , that it is impossible that the absorption could be derived from these modes by any manner of mode mixing.

Having positively identified this  $B_2$  mode the  $\gamma_{\text{CD}}$  mode is recognised as responsible for the  $849\text{ cm}^{-1}$  absorption. The strength of the  $752\text{ cm}^{-1}$  band (H) and the absence of comparable absorption in the range  $760\text{--}700\text{ cm}^{-1}$  is sufficient to locate the second highest  $B_2$  fundamental at  $752\text{ cm}^{-1}$  (H) and  $667\text{ cm}^{-1}$  (D). This leaves three very strong unassigned bands near  $830\text{ cm}^{-1}$  in H and three near  $800\text{ cm}^{-1}$  in D to be identified with two fundamentals. Since it seems to the authors that one is forced to accept a resonance here then there must be at least one possible combination of fundamentals which will lead to the required resonance and explain the observed shifts. The number of possibilities at these low frequencies is very limited. Combination of the in-plane fundamentals amongst themselves could not explain the magnitude of the frequency shift between H and D. For symmetry reasons combinations of in-plane with out-of-plane modes is out. This reduces the possibilities to  $B_1 + B_1$  or  $B_1 + A_2$ . Now the  $A_2$  frequencies must be unchanged between H and D. With this in mind, only one possibility exists—the  $614\text{ (H) cm}^{-1} +$  lowest  $A_2$  and the  $565\text{ (D) cm}^{-1}$  and same  $A_2$  frequency. This necessitates that the frequency centres of the resonance pairs should show an isotope frequency shift of  $50\text{ cm}^{-1}$  and that the transitions involved should belong to the  $B_2$  species. In addition the  $A_1$  fundamental is expected to show an isotopic shift of  $5\text{ cm}^{-1}$ . These expectations are adequately satisfied by interpreting the  $A_1$  fundamentals at  $813\text{ cm}^{-1}$  (H) and  $806\text{ cm}^{-1}$  (D). In D the greater strength of the  $818\text{ cm}^{-1}$  component compared with the  $775\text{ cm}^{-1}$  component is to be expected in view of the fact that the shift in the combination frequencies is about  $15\text{ cm}^{-1}$  greater than the calculated  $B_2$  fundamental shift. From this resonance we also deduce that the lowest  $A_2$  fundamental (unobserved) is near  $230\text{ cm}^{-1}$ . Attempts were made to perturb the

resonance by solvent shifts and thereby confirm the above analysis, but were unsuccessful. The spectra were measured in *cyclohexane*, benzene, carbon disulphide and carbon tetrachloride.

Strength, range, and frequency shifts suffice to locate two more fundamentals—in H at  $462\text{ cm}^{-1}$  ( $B_2$ ) and  $614\text{ cm}^{-1}$  ( $B_1$ ) and in D at  $457\text{ cm}^{-1}$  ( $B_2$ ) and  $565\text{ cm}^{-1}$  ( $B_1$ ). Raman emission due to the highest  $A_2$  mode has not been observed. The lack of absorption between  $380\text{ cm}^{-1}$  and  $200\text{ cm}^{-1}$ , apart from a weak band at  $314\text{ cm}^{-1}$  detectable in the pure liquid at 2 mm thickness and the great strength of the absorption below and above this range strongly suggest absence of allowed fundamentals in this range. In addition we have already assigned a  $B_2$  fundamental at about  $460\text{ cm}^{-1}$ . Since the computations lead us to expect the four lowest  $A_1$  frequencies to be close to the corresponding  $B_2$  frequencies we tentatively propose that an  $A_1$  fundamental frequency is  $434\text{ cm}^{-1}$  (H),  $423\text{ cm}^{-1}$  (D) and that a  $B_2$  fundamental is partially responsible for the intense absorption at  $388\text{ cm}^{-1}$ . Finally we have three Raman/infra-red bands in the range  $210\text{--}140\text{ cm}^{-1}$  and four fundamentals to locate. If we accept that degeneracy of the lowest  $E'$  mode of trichlorobenzene is going to be little affected, being mainly a ring angle deformation mode, on going to the pyrimidine, then the assignments given in Tables 1–3 readily follow.

#### 5. COMPARISON WITH TRICHLOROBENZENE

The spectra of 1,3,5 trichlorobenzene have been studied by SCHERER *et al.* [8]. Calculation of the fundamental frequencies using Scherer's field for chlorobenzenes has not been reported. For this reason we have made these calculations (Table 2) and it can be seen that agreement with assignments is excellent. Correlation of the absorption spectra of trichlorobenzene and trichloropyrimidine is straightforward and supports the assignments made. As expected the extra  $E'$  CH deformation frequency, arising from the substitution of CH for N, identified at  $1420\text{ cm}^{-1}$ , causes the frequencies to move apart from those of the pyrimidine compound. The effect falls off to negligible proportions by  $1000\text{ cm}^{-1}$ .

[8] J. R. SCHERER, J. C. EVANS, W. W. MUELDER and J. OVEREND, *Spectrochim. Acta* **18**, 57 (1962).



## The force field for the out-of-plane vibrations of halogenated aromatic molecules

K. RADCLIFFE and D. STEELE

Department of Chemistry, Royal Holloway College, Englefield Green, Surrey

(Received 24 July 1968)

**Abstract**—The general quadratic force field for the out of plane vibrations of the series  $C_6H_6$ ,  $C_6H_5X$ ,  $p-C_6H_4X_2$  and their deuterated analogues ( $X = F, Cl, Br$ ) have been determined by perturbation procedures and by assuming transferability of the constants within a given X series. Agreement between the three sets of fields is excellent. Good agreement with the benzene fields proposed by Miller and Crawford, by Whiffen and by Scherer is also obtained. An alternative field for  $X = Br$  was found but is unacceptable by analogy with the  $X = F$  and  $Cl$  fields.

### INTRODUCTION

THE study to be described was initiated through a need for a set of reliable normal co-ordinates for the out of plane vibrations of mono- and di-substituted aromatic molecules. At the present time there is no data other than fundamental vibrational frequencies from which force fields for these molecules may be derived. Even with the use of isotopic vibrational frequencies to supplement those of the normal molecules the field will be severely under-determined. Two different methods are generally employed to overcome the indeterminacy of the force constants. The first is to assume a given force field model such as the Urey Bradley force field (UBFF), the Hybrid Orbital force field (HOFF) or a more arbitrary simplified harmonic field in which constants are held at given values. The second method, which on its own will usually still be inadequate to evaluate the most general harmonic force field, is the Overlay technique in which the force constants are assumed to be transferable between a set of structurally similar molecules. The UBFF and HOFF approximations are inapplicable to the out-of-plane vibrations of aromatic molecules and it is therefore necessary to apply the overlay approach. This has already been done for the complete range of chlorinated aromatic molecules of the type  $C_6H_xCl_{6-x}$  [1].

The vibrational assignments of some mono- and di-*para*-substituted aromatics have been examined in an accompanying paper [2] and the vibrational assignments preferred in that study were used throughout the work described here.

### METHOD OF COMPUTATION

Essentially the computations reported in this work were carried out following the procedure outlined by ALDOUS and MILLS [3, 4]. The vibrational problem was set up in symmetry co-ordinates but redundant co-ordinates were not eliminated. An exception here is for the  $D_{6h}$  species where the  $G$  and  $F$  matrices of WHIFFEN

[1] J. R. SCHERER, *Spectrochim. Acta* **23A**, 1489 (1967).

[2] P. N. GATES, K. RADCLIFFE and D. STEELE, *Spectrochim. Acta* **25A**, 507 (1969).

[3] J. ALDOUS and I. M. MILLS, *Spectrochim. Acta* **18**, 1073 (1962).

[4] J. ALDOUS and I. M. MILLS, *Spectrochim. Acta* **19**, 1567 (1963).

were used [13]. As a check on the symmetrization all the frequencies calculated by the above method were also evaluated using the method outlined by SCHACHTSCHNEIDER and SNYDER [5] and which does not involve the use of symmetry. The symmetry co-ordinates and symmetrized  $G$  and  $F$  matrices are available on request.

#### MOLECULAR GEOMETRY AND ATOMIC MASSES

Table 1 summarizes the values of the molecular parameters and atomic masses used in these calculations. Table 2 contains the internal co-ordinate definitions.

Table 1

C—H = 1.08 Å	C—C = 1.40 Å	C—F = 1.30 Å	C—Cl = 1.70 Å	C—Br = 1.865 Å
$m_{\text{H}} = 1.008$ a.m.u.	$m_{\text{C}} = 12.011$ a.m.u.	$m_{\text{F}} = 19.000$ a.m.u.		
$m_{\text{Cl}} = 35.457$ a.m.u. $m_{\text{Br}} = 79.916$ a.m.u. All angles assumed = 120°.				

#### WEIGHTING FACTORS

The weighting factor assigned to each experimental frequency varies between unity (complete confidence) and zero (complete uncertainty). The weight matrix  $W$  has diagonal elements proportional to  $(1/\lambda_{\text{obs}})^2$  since this type of weighting leads to a percentage fit to the observed frequencies rather than an absolute one.

#### OBSERVED DATA

The experimental frequencies used throughout this work were taken from the following sources: Benzene and hexadeuterobenzene [6];  $\text{C}_6\text{H}_5\text{F}$  and  $\text{C}_6\text{D}_5\text{F}$  [7];  $\text{C}_6\text{H}_5\text{Cl}$  and  $\text{C}_6\text{D}_5\text{Cl}$  [8];  $\text{C}_6\text{H}_5\text{Br}$  [9];  $\text{C}_6\text{D}_5\text{Br}$  [10];  $p\text{-C}_6\text{H}_4\text{X}_2$  and  $p\text{-C}_6\text{D}_4\text{X}_2$  [2, 11, 12].

None of the frequencies were corrected for anharmonicity. Experimental evidence seems to indicate this effect to be small in aromatic molecules of the type under consideration here.

All computations were carried out on the London University ATLAS computer, using autocode programs specially written for this work.

Table 2. Internal co-ordinates for the out-of-plane vibrations of aromatic molecules

$r\Delta\gamma_j$ : out of-plane bending of $\text{C}_j\text{—H}_j$ bond.
$R\Delta\phi_j$ : valency co-ordinate for twisting of both the carbon and hydrogen atoms about $\text{C}_j\text{—C}_{j+1}$ .
The factors $R$ (the CC equilibrium distance) and $r$ (the CH equilibrium distance) have been used to scale the co-ordinates.
$R = 1.40$ Å; $r_{\text{H}} = 1.08$ Å; $r_{\text{F}} = 1.30$ Å; $r_{\text{Cl}} = 1.70$ Å; $r_{\text{Br}} = 1.865$ Å.

- [5] J. H. SCHACHTSCHNEIDER and R. G. SNYDER, *Spectrochim. Acta* **19**, 117 (1963).  
 [6] S. BRODERSON and A. LANGSETH, *Kgl. Danske, Vidensk. Selskab. Mat. Fys. Skr.* **1**, No. 7 (1959).  
 [7] D. STEELE, E. R. LIPPINCOTT and J. XAVIER, *J. Chem. Phys.* **33**, 1242 (1965).  
 [8] T. R. NANNEY, R. T. BAILEY and E. R. LIPPINCOTT, *Spectrochim. Acta* **21**, 1495 (1965).  
 [9] D. H. WHIFFEN, *J. Chem. Soc.* 1350 (1956).  
 [10] T. R. BAILEY, E. R. LIPPINCOTT and J. C. HAMER, *Spectrochim. Acta* **22**, 737 (1966).  
 [11] A. STOJILJKOVIC and D. H. WHIFFEN, *Spectrochim. Acta* **12**, 47 (1958).  
 [12] P. R. GRIFFITHS and H. W. THOMPSON, *Proc. Roy. Soc.* **A298**, 51 (1967).  
 [13] D. H. WHIFFEN, *Phil. Trans. Roy. Soc.* **A248**, 131 (1955).

## RESULTS AND FORCE FIELD MODELS

The quadratic force field nomenclature for the out of plane vibrations is defined by:

$$\begin{aligned}
 2V = & \sum_i \gamma_X (r_{CX} \gamma_{X_i})^2 + 2 \sum_i \gamma \gamma_{XY}^o (r_{CX} \gamma_{X_i}) (r_{CY} \gamma_{Y_{i+1}}) \\
 & + 2 \sum_i \gamma \gamma_{XY}^m (r_{CX} \gamma_{X_i}) (r_{CY} \gamma_{Y_{i+2}}) + 2 \sum_i \gamma \gamma_{XY}^p (r_{CX} \gamma_{X_i}) (r_{CY} \gamma_{Y_{i+3}}) \\
 & + \sum_i \phi (R\phi_i)^2 + 2 \sum_i \phi \phi_o (R\phi_i) (R\phi_{i+1}) + 2 \sum_i \phi \phi_m (R\phi_i) (R\phi_{i+2}) \\
 & + 2 \sum_i \phi \phi_p (R\phi_i) (R\phi_{i+3}) + 2 \sum_i \gamma \phi_o^X (r_{CX} \gamma_{X_i}) (R\phi_{i-1} - R\phi_i) \\
 & + 2 \sum_i \gamma \phi_m^X (r_{CX} \gamma_{X_i}) (R\phi_{i-2} - R\phi_{i+1}) \\
 & + 2 \sum_i \gamma \phi_p^X (r_{CX} \gamma_{X_i}) (R\phi_{i-3} - R\phi_{i+2})
 \end{aligned}$$

The results of the various fields applied are given in Tables 3, 4. Initially a 12 parameter field was used to converge the calculations ( $\gamma \phi_m^X$ ,  $\gamma_{HX}^m$  and  $\gamma_{HX}^p$  were held at zero, and  $\gamma \phi_m^H$  was assumed to be zero throughout). Convergence was rapid in all cases and hence a 15 parameter field was then employed. (In the case of the runs containing hexafluorobenzene data inclusion of the  $\gamma_{XX}^o$  and  $\gamma \gamma_{XX}^m$  terms yielded a 17 parameter field.) The results of this field indicated that 5 of the force constants were essentially zero (within their statistical uncertainties). This led to an investigation of a 10 parameter field.

In the case of the fluorobenzenes two series of calculations were performed: one including data on hexafluorobenzene and another excluding this data.

In order to distinguish between  $\phi^{HX}$  and  $\phi^{HH}$  we defined  $\phi^{HX} = 0.5\phi^{HH} + 0.5\phi^{XX}$ .

## DISCUSSION

A number of authors have tackled the problem of determining an out-of-plane force field for benzene. MILLER and CRAWFORD [14] determined a complete, eight parameter, symmetry valence force field. (The completely general field, with eleven constants, is capable of reduction to one of the eight constants by means of internal relationships. Removal of explicit reference to the  $\phi \phi_m$ ,  $\phi \phi_p$  and  $\gamma \phi_p$  terms results in a force field containing eight parameters.) The results of MILLER and CRAWFORD, when transposed into valence force constants, formed the starting values of the work of KAKIUTI and SHIMANOUCI [15] who performed a least squares refinement on five valence force constants using the observed data for benzene and hexadeutero-benzene. SCHERER [1] has obtained an out of plane force field for the complete range of chlorobenzenes and compared his results with those of MILLER and CRAWFORD and KAKIUTI and SHIMANOUCI for the appropriate force constants. All the above authors used the delta co-ordinate rather than the phi co-ordinate suggested by BELL [16] and used by WHIFFEN [13] in benzene. We have worked throughout in

[14] F. A. MILLER and B. L. CRAWFORD JR., *J. Chem. Phys.* **14**, 282 (1946).

[15] Y. KAKIUTI and T. SHIMANOUCI, *J. Chem. Phys.* **25**, 1252 (1956).

[16] R. P. BELL, *Trans. Faraday Soc.* **41**, 293 (1945).

Table 3. Fifteen parameter force fields for the halogenobenzenes (mdyn/Å)

Force constant	Fluoro (+)	Fluoro (-)	Chloro	Bromo (1)	Bromo (2)
$\gamma_H$	0.2728 (0.0163)	0.2606 (0.0119)	0.2647 (0.0076)	0.2614 (0.0157)	0.2638 (0.0131)
$\gamma_X$	0.1996 (0.0206)	0.2126 (0.0170)	0.1226 (0.0049)	0.0845 (0.0076)	0.0922 (0.0073)
$\gamma\gamma_{HH}^o$	0.0166 (0.0059)	0.0132 (0.0039)	0.0123 (0.0024)	0.0127 (0.0050)	0.0132 (0.0041)
$\gamma\gamma_{HH}^m$	-0.0160 (0.0075)	-0.0112 (0.0053)	-0.0130 (0.0034)	-0.0109 (0.0072)	-0.0126 (0.0058)
$\gamma\gamma_{HH}^p$	-0.0149 (0.0084)	-0.0121 (0.0059)	-0.0115 (0.0038)	-0.0108 (0.0076)	-0.0135 (0.0065)
$\gamma\gamma_{HX}^o$	0.0145 (0.0110)	0.0166 (0.0093)	0.0154 (0.0037)	0.0157 (0.0081)	0.0139 (0.0070)
$\gamma\gamma_{HX}^m$	-0.0219 (0.0187)	-0.0041 (0.0165)	-0.0063 (0.0071)	-0.0020 (0.0112)	-0.0020 (0.0102)
$\gamma\gamma_{HX}^p$	-0.0075 (0.0386)	-0.0040 (0.0218)	0.0007 (0.0131)	0.0377 (0.0294)	0.0079 (0.0222)
$\gamma\gamma_{XX}^o$	0.0139 (0.0108)				
$\gamma\gamma_{XX}^m$	-0.0063 (0.0104)				
$\gamma\gamma_{XX}^p$	-0.0080 (0.0231)	0.0154 (0.0278)	0.0093 (0.0129)	0.0160 (0.0175)	0.0161 (0.0163)
$\phi_H$	0.0294 (0.0064)	0.0357 (0.0047)	0.0357 (0.0030)	0.0358 (0.0065)	0.0359 (0.0052)
$\phi_X$	0.0347 (0.0066)	0.0332 (0.0053)	0.0286 (0.0070)	0.0467 (0.0147)	0.0339 (0.0124)
$\phi\phi_o$	-0.0120 (0.0041)	-0.0072 (0.0029)	-0.0067 (0.0019)	-0.0067 (0.0041)	-0.0066 (0.0033)
$\gamma\phi_{oH}$	0.0135 (0.0025)	0.0123 (0.0018)	0.0125 (0.0012)	0.0125 (0.0024)	0.0126 (0.0020)
$\gamma\phi_{oX}$	-0.0006 (0.0057)	-0.0107 (0.0079)	-0.0034 (0.0049)	-0.0033 (0.0066)	-0.0047 (0.0062)
$\gamma\phi_{mX}$	0.0048 (0.0095)	-0.0067 (0.0086)	-0.0023 (0.0052)	-0.0070 (0.0089)	-0.0057 (0.0076)
$E'WE$	0.1664	0.0724	0.0319	0.1281	0.0870
$ \Delta\nu $ (cm <sup>-1</sup> )	15.0	10.9	5.0	10.5	8.0

Dispersions are in parenthesis.

Fluoro(+) relates to data including that of hexafluorobenzene.

Fluoro(-) relates to data excluding that of hexafluorobenzene.

phi co-ordinates and in order to compare our results with those of the previous authors we have used the relationships given by MILLER and CRAWFORD [14] and by LONG and STEELE [17] to convert all results to the same phi co-ordinate system and the same units of mdyn/Å. These results are given in Table 5. As can be seen from the Table the agreement of our results with those of WHIFFEN and SCHERER is excellent.

In Table 6 a comparison is made between our results for the chlorobenzenes and those of SCHERER. Again transformation into similar co-ordinate system and units has been effected. The results compare very favourably.

Tables 3 and 4 list the force constant values and dispersions obtained from both the 15 parameter and 10 parameter force field calculations. The results show that each of the force fields (excluding the fluoro run containing the hexafluorobenzene data) meets the requirement that the force constants of the benzene molecule,

[17] D. A. LONG and D. STEELE, *Spectrochim. Acta* **19**, 1791 (1963).

Table 4. Ten parameter force fields for the halogenobenzenes (mdyn/Å)

Force constant	Fluoro (+)	Fluoro (-)	Chloro	Bromo (1)	Bromo (2)
$\gamma_H$	0.2628 (0.0186)	0.2502 (0.0148)	0.2544 (0.0088)	0.2606 (0.0159)	0.2608 (0.0130)
$\gamma_X$	0.1876 (0.0094)	0.2095 (0.0119)	0.1203 (0.0045)	0.0913 (0.0068)	0.0932 (0.0058)
$\gamma\gamma_{HH}^o$	0.0157 (0.0065)	0.0127 (0.0047)	0.0124 (0.0027)	0.0134 (0.0050)	0.0135 (0.0042)
$\gamma\gamma_{HH}^m$	-0.0107 (0.0083)	-0.0062 (0.0066)	-0.0088 (0.0037)	-0.0116 (0.0067)	-0.0117 (0.0054)
$\gamma\gamma_{HH}^p$	-0.0101 (0.0092)	-0.0080 (0.0068)	0.0056 (0.0039)	-0.0098 (0.0073)	-0.0115 (0.0060)
$\gamma\gamma_{HX}^o$	0.0166 (0.0115)	0.0084 (0.0077)	0.0119 (0.0044)	0.0156 (0.0094)	0.0135 (0.0077)
$\phi_H$	0.0342 (0.0071)	0.0396 (0.0061)	0.0393 (0.0034)	0.0354 (0.0061)	0.0366 (0.0050)
$\phi_X$	0.0392 (0.0062)	0.0430 (0.0064)	0.0356 (0.0044)	0.0475 (0.0102)	0.0373 (0.0081)
$\phi\phi_o$	-0.0086 (0.0043)	-0.0048 (0.0037)	-0.0046 (0.0019)	-0.0068 (0.0036)	-0.0062 (0.0029)
$\gamma\phi_o^H$	0.0122 (0.0028)	0.0115 (0.0020)	0.0112 (0.0013)	0.0121 (0.0023)	0.0120 (0.0019)
$E'WE$	0.2254	0.1083	0.0474	0.1479	0.1033
$ \Delta\nu $ (cm <sup>-1</sup> )	16.8	14.5	7.5	10.8	9.3

Dispersions are in parenthesis.

Fluoro(+) relates to data including that of hexafluorobenzene.

Fluoro(-) relates to data excluding that of hexafluorobenzene.

Table 5. Benzene valence force constants in the phi co-ordinate system (mdyn/Å)

Force constant	WHIFFEN [13]*	MILLER† CRAWFORD	SHIMANOUCI [15]	SCHERER [1]	F	This work Cl	Br
$\gamma_H$ A †	0.270 (0.286)	0.277	0.226	0.268	0.261	0.265	0.261
$\phi_H$ B	0.029 (0.029)	0.028	0.045	0.033	0.036	0.036	0.036
$\gamma\gamma_{HH}^o$ $a_o$	0.011 (0.012)	0.068	0.061	0.063	0.013	0.012	0.013
$\gamma\gamma_{HH}^m$ $a_m$	-0.021 (-0.022)	-0.010		-0.007	-0.011	-0.013	-0.011
$\gamma\gamma_{HH}^p$ $a_p$	-0.016 (-0.017)	-0.019		-0.012	-0.012	-0.011	-0.011
$\phi\phi_o$ $b_o$	-0.010 (-0.010)	-0.011	-0.003	-0.008	-0.007	-0.007	-0.007
$\gamma\phi_o$ $c_o$	0.014 (0.014)	0.012	0.007	0.012	0.012	0.012	0.012
$\gamma\phi_m^H$ $c_m$	0 (0)	-0.0008		0.0008	—	—	—

\* The values in parenthesis are Whiffen's values using C—H = 1.05 Å.

† These values are modified by using presently accepted data [6, 19].

‡ Nomenclature due to MILLER and CRAWFORD [14].

obtained under the constraint of their transferability with the halogenated benzenes, should agree with the force constants obtained from benzene alone, and also provides a satisfactory frequency fit to some fortyeight or more observed fundamentals. Tables of computed frequencies and errors have been compiled and are available on request.

The fact that there is a close correspondence of the *ortho*, *meta* and *para*  $\gamma\gamma_{HH}$ ,  $\gamma\gamma_{HX}$  and  $\gamma\gamma_{XX}$  force constant values (where applicable) is extremely satisfactory.

The results of the 10 parameter force field calculations lead to error vectors ( $E'WE$ ) only slightly worse than with the 15 parameter field (Tables 3 and 4), indicating that in this particular case the 10 parameter field might be a useful approximation.

Table 6. Comparison of the valence force constants for the out-of-plane vibrations of chlorobenzenes (mdyn/Å)

Force constant	SCHERER [1] Delta	SCHERER [1] Phi	This work Phi
$\gamma_H$	0.384	0.268	0.265
$\gamma_{Cl}$	0.200	0.119	0.123
$\gamma\gamma_{HH}^o$	-0.062	0.063	0.012
$\gamma\gamma_{HH}^m$	0.003	-0.007	-0.013
$\gamma\gamma_{HH}^p$	-0.012	-0.012	-0.011
$\gamma\gamma_{HCl}^o$	-0.049	0.053*	0.015
$\gamma\gamma_{HCl}^m$	0.003	0.001*	-0.006
$\gamma\gamma_{HCl}^p$	-0.011	-0.011	0.001
$\gamma\gamma_{ClCl}^o$	-0.023	0.035	
$\gamma\gamma_{ClCl}^m$	0.003	-0.0003	
$\gamma\gamma_{ClCl}^p$	-0.005	-0.005	0.009
$\gamma\phi_{oH}$	-0.100	0.012	0.012
$\gamma\phi_{mH}$	0.023	0.0008	0 (assumed)
$\gamma\phi_{oCl}$	-0.077	-0.004	-0.003
$\gamma\phi_{mCl}$	0.022	0.019	-0.002
$\phi\phi_o$	0.033	-0.008	-0.007
$\phi_H$	0.132	0.033	0.036
$\phi_{Cl}$	0.177	0.044	0.029

\* Geometric mean parameters were used i.e.  $\rho$  value was taken as  $(\rho_H\rho_{Cl})^{1/2}$ .

#### Effect of hexafluorobenzene data

The inclusion of the hexafluorobenzene data tends to pull off the  $\gamma_H$  and  $\gamma_X$  force constant values (in particular) from the values obtained without this data, indicating that careful consideration must be exercised in applying the overlay technique to a wide range of compounds. Scherer has noticed this substituent dependence of the diagonal force constants.

The possibility cannot be ignored that the deleterious effect on the field of the inclusion of the hexafluorobenzene data may be due to erroneous frequency assignments. Only two of the six out-of-plane fundamentals are either infrared or Raman active. The other four were derived from combination bands.

#### Alternative solutions for the force field of the bromobenzenes

In the case of the bromobenzenes two alternative force fields were obtained and these are shown in Table 7.

Comparison of these fields with those of the fluoro- and chloro-benzenes indicates that solution (2) is to be preferred. The main differences between solutions (1) and (2) lie in the  $\phi_{Br}$  and  $\gamma\gamma_{HX}^p$  force constants. The values of these force constants in solution (2) are more in line with the values in the fluoro- and chloro-benzene fields than are the corresponding values in solution (1). Examination of the L matrices for the two solutions reveals that they differ in the mode descriptions of the 681 and 737  $\text{cm}^{-1}$  vibrations belonging to the  $B_2$  species of  $C_6H_5Br$ . This problem of alternative solutions to the inverse secular problem is a well known one and has been examined by, amongst others, TOMAN and PLIVA [18]. The alternative solutions arise from permutation of the 681 and 737  $\text{cm}^{-1}$  eigenvalues.

[18] S. TOMAN and J. PLIVA, *J. Mol. Spectry* **21**, 362 (1966).

Table 7

Force constant	Solution (1)	Solution (2)	Force constant	Solution (1)	Solution (2)
$\gamma_{\text{H}}$	0.261	0.264	$\phi_{\text{H}}$	0.036	0.036
$\gamma_{\text{Br}}$	0.084	0.092	$\phi\phi_{\text{o}}$	-0.007	-0.007
$\gamma\gamma_{\text{HH}}^{\text{o}}$	0.013	0.013	$\gamma\phi_{\text{o}}^{\text{H}}$	0.012	0.013
$\gamma\gamma_{\text{HH}}^{\text{m}}$	-0.011	-0.013	$\gamma\phi_{\text{o}}^{\text{Br}}$	-0.003	-0.006
$\gamma\gamma_{\text{HH}}^{\text{p}}$	-0.011	-0.014	$\gamma\gamma_{\text{HBr}}^{\text{m}}$	-0.002	-0.002
$\gamma\gamma_{\text{HBr}}^{\text{o}}$	0.016	0.014	$\gamma\gamma_{\text{HBr}}^{\text{p}}$	0.038	0.008
$\gamma\gamma_{\text{BrBr}}^{\text{o}}$	0.016	0.016	$\gamma\phi_{\text{m}}^{\text{Br}}$	-0.007	-0.006
$\phi_{\text{Br}}$	0.047	0.034	$E'WE$	0.1281	0.0870

Whilst we find it more convenient to work with internal co-ordinates all with the units of length, for angular displacements these are not necessarily the most instructive. Naive rehybridization arguments would suggest that the force required for unit angular displacement out of the ring plane would be, to a first approximation, independent of the substituent. Any changes would arise from  $\pi$  bonding or similar effects. The  $\gamma_{\text{x}}$  in mdyn  $\text{\AA}/\text{rad}^2$  are 0.303 (H), 0.359 (F), 0.350 (Cl) and 0.318 (Br). The higher values for fluorine and chlorine are of some interest but we shall restrict comment to the fact that the range is of the order of 20% compared with a factor of 3 in mdyn/ $\text{\AA}$ .

In view of the great difficulty in establishing reliable force fields the excellent agreement between the derived fields for the different halogen substituted aromatics is a most encouraging result. It suggests (a) that the force constant solution is the correct one and (b) that the out-of-plane force fields are indeed transferable.

*Acknowledgement*—One of us (K. R.) wishes to thank the Science Research Council for financial support in the form of a Postdoctoral Fellowship.

[19] B. P. STOICHEFF, *Can. J. Phys.* **32**, 339 (1954).

## The vibrational spectra of mono and *para* disubstituted halogenobenzenes

P. N. GATES, K. RADCLIFFE and D. STEELE

Department of Chemistry, Royal Holloway College, Englefield Green, Surrey

(Received 24 July 1968)

**Abstract**—The infrared and Raman spectra of *p*-dibromo- and *p*-difluorotetraduterobenzene have been measured and sets of assignments for the vibrational fundamentals are proposed. These are shown to be consistent with accepted assignments of related molecules by application of the product and inequality rules. Application of the product rule to the  $A_g$  species of *p*-dibromobenzene indicates that the assignment of Stojiljkovic and Whiffen is to be preferred to that of Shurvell, Dulaurens and Pestel. The vapour phase band contour of the band at  $816\text{ cm}^{-1}$  in *para*  $\text{C}_6\text{D}_4\text{Br}_2$  has been measured in a high temperature cell and shown to necessitate an assignment revision for *para*  $\text{C}_6\text{D}_4\text{Cl}_2$ .

### INTRODUCTION

A very considerable literature exists on the vibrational spectra of mono and *para* disubstituted aromatics [1–13] and a more restricted literature on their deuterated analogues [5, 13–15]. The interpretation of absolute intensity measurements requires a knowledge of the normal co-ordinates which in turn are dependent upon the force field. Reasonable force fields may only be determined if sufficient experimental data is available. We have studied the vibrational spectra of *p*-dibromo- and *p*-difluoro- tetraduterobenzene in order to supplement existing data with which to determine force fields for the halogenobenzenes [16].

### EXPERIMENTAL

The sample of *p*-dibromotetraduterobenzene was supplied by Anderman & Co. Ltd. with a quote of greater than 99% purity and was used without further purification. The sample of *p*-difluorotetraduterobenzene was prepared from *p*-difluorobenzene by the action of DCl and  $\text{AlCl}_3$  (as catalyst) following the procedure of BAK

- [1] D. H. WHIFFEN, *J. Chem. Soc.* 1350 (1956).
- [2] R. D. KROSS and V. A. FASSEL, *J. Am. Chem. Soc.* **77**, 5858 (1955).
- [3] E. K. PLYLER, H. C. ALLEN JR. and E. D. TIDWELL, *J. Res. Natl. Bur. Std.* **58**, 225 (1957).
- [4] A. STOJILJKOVIC and D. H. WHIFFEN, *Spectrochim. Acta* **12**, 47 (1958).
- [5] D. STEELE, E. R. LIPPINCOTT and J. XAVIER, *J. Chem. Phys.* **33**, 1242 (1960).
- [6] J. H. S. GREEN, *Spectrochim. Acta* **18**, 39 (1962).
- [7] J. R. SCHERER, *Spectrochim. Acta* **19**, 601 (1963).
- [8] J. R. SCHERER and J. C. EVANS, *Spectrochim. Acta* **19**, 1739 (1963).
- [9] J. R. SCHERER, *Spectrochim. Acta* **20**, 345 (1964).
- [10] H. F. SHURVELL, B. DULAURENS and P. PESTEL, *Spectrochim. Acta* **22**, 333 (1966).
- [11] P. R. GRIFFITHS and H. W. THOMPSON, *Proc. Roy. Soc.* **A298**, 51 (1967).
- [12] J. R. SCHERER, *Spectrochim. Acta* **23A**, 1489 (1967).
- [13] D. STEELE, W. KYNASTON and H. A. GEBBIE, *Spectrochim. Acta* **19**, 785 (1963).
- [14] T. R. NANNEY, R. T. BAILEY and E. R. LIPPINCOTT, *Spectrochim. Acta* **21**, 1495 (1965).
- [15] T. R. NANNEY, E. R. LIPPINCOTT and J. C. HAMER, *Spectrochim. Acta* **22**, 737 (1966).
- [16] K. RADCLIFFE and D. STEELE, *Spectrochim. Acta* **25A**, 597 (1969).



Table 1. Vibrational spectrum of paradifluorotetra deuterobenzene

Infrared liquid	Raman liquid	Assignment
163 s	169 w	$B_{3u}$ fundamental
348 s		$B_{2u}$
	366 m dp	$B_{2g}$
422 s		$B_{3u}$
	453 m p?	$A_g$
	600 w	$B_{2g}$
	614 m dp	$B_{1g}$ and $B_{3g}$ fundamentals
685 s		$B_{1u}$
695 w		
732 s	736 vw	$B_{3u}$
740 sh		
	780 s p	$A_g$ and $B_{2g}$ fundamentals
802 ms		$B_{2u}$
	828 } m p	$A_g$ fundamental in resonance
	867 }	with 2(422)?
859 s		$B_{1u}$
895 w		
	1008 s	$B_{3g}$
1103 w		
1130 s		$B_{1u}$
1140 m		
1202 m		
	1229 s p	$A_g$
	1242 w	
1287 w		$B_{2u}$
1328 w		$B_{2u}$
1360 w		
1373 w		
1390 w		
1435 vs	1442 vw	$B_{1u}$
1464 sh	1460 vw	
	1509 vw	
	1523 w	$B_{3g}$
1562 w		
	1595 w dp?	$A_g$
2277 w	2283 vw	$B_{1u}$
	2304 w dp	$B_{3g}$
	2313 ms p	$A_g$
2310 mw		$B_{2u}$

s: strong; m: medium; w: weak; v: very; p: polarised; dp: depolarised.  
All frequencies in  $\text{cm}^{-1}$ .

*et al.* [17] for related compounds. The reaction was followed by observing the infrared spectrum and the exchange stopped when bands attributed to  $\text{C}_6\text{HD}_3\text{F}_2$  were no longer being decreased significantly. Mass spectrometry indicated 93% purity (97% deuteration).

The far infrared spectra (below  $400 \text{ cm}^{-1}$ ) were recorded (as a saturated solution in benzene in the case of the bromo compound) in polythene cells, using either the far infrared vacuum grating spectrometer constructed in the department or a Grubb-Parsons Interferometer (below  $200 \text{ cm}^{-1}$ ).

Near infrared spectra were examined (as solutions in carbon disulphide or cyclohexane for the bromo compound) using Perkin-Elmer 337 and Unicam SP100 spectrometers.

The Raman spectrum of the fluoro compound was measured with a Hilger

[17] B. BAK, J. N. SCHOOLERY and Y. A. WILLIAMS, *J. Mol. Spectry* **2**, 525 (1958).

Table 2. Vibrational spectrum of *para*dibromotetradeuterobenzene

Infrared solution†	Raman solid	Assignment
164 m		$B_{2u}$ fundamental
	208 vvs	$A_g$
	264 s	$B_{2g}$
404 vvs	282 m	$B_{3g}$
404 vvs		$B_{1u}$
410 sh		$B_{3u}$
	602 s	$E_{2g}$
	630 mw	$B_{1g}$
	677 vvs	$A_g$
677 s		$B_{3u}$
	708 vw	
	786 vw	$B_{2g}$
788 w		$A_u$
816 s	822 vw	$B_{2u}$
837 w		$E_{1u}$
	857 } m	$A_g$ fundamental in resonance with
	866 } m	$264 + 602 = 866 (B_{2g} \times B_{2g}; A_g)$
	997 vw	$B_{3g}$
984 } 997 vs } 1016 vs }		$B_{1u}$ fundamental in resonance with
		$630 + 367 = 997 (A_u \times B_{1g}; B_{1u})$
		$602 + 410 = 1012 (B_{3u} \times B_{2g} =$
		$B_{1u})$
	1035 vs	$A_g$
1297 s		$B_{2u}$
1316 vw		
1350 vs		$B_{1u}$
1395 w		
	1531 m	$B_{3g}$
	1544 m	$A_g$
2280 sh		$B_{1u}$
2290 w	2296 vs	$A_g$ and $B_{3g}$ fundamentals
2305 w		$B_{2u}$

s: strong; m: medium; w: weak; v: very; p: polarised; dp: depolarised.

† solutions in carbon disulphide and cyclohexane.

All frequencies in  $\text{cm}^{-1}$ .

spectrometer using photographic detection and  $4358 \text{ \AA}$  excitation. The Raman spectrum of the bromo compound was obtained using the helium-neon laser excited Cary 81 spectrometer at Imperial College.

#### DISCUSSION

The symmetry of these molecules is  $D_{2h}(V_h)$  and the thirty normal vibrations belong to the following classes:

$$6A_g + 1B_{1g} + 3B_{2g} + 5B_{3g} + 2A_u + 5B_{1u} + 5B_{2u} + 3B_{3u}$$

where the  $z$  axis passes through the halogens and the  $x$  axis is taken perpendicular to the ring. All “ $g$ ” classes are Raman active and all the “ $u$ ” classes, except the  $A_u$ , are infrared active, the rule of mutual exclusion operating (at least in the gas phase).

#### ASSIGNMENTS

The observed infrared and Raman frequencies together with polarisation data and assignments are listed in Tables 1 and 2. No attempt has been made to account for all the combination tones. Spectra of *para*  $\text{C}_6\text{D}_4\text{Br}_2$  (redrawn) are shown in Fig. 1.

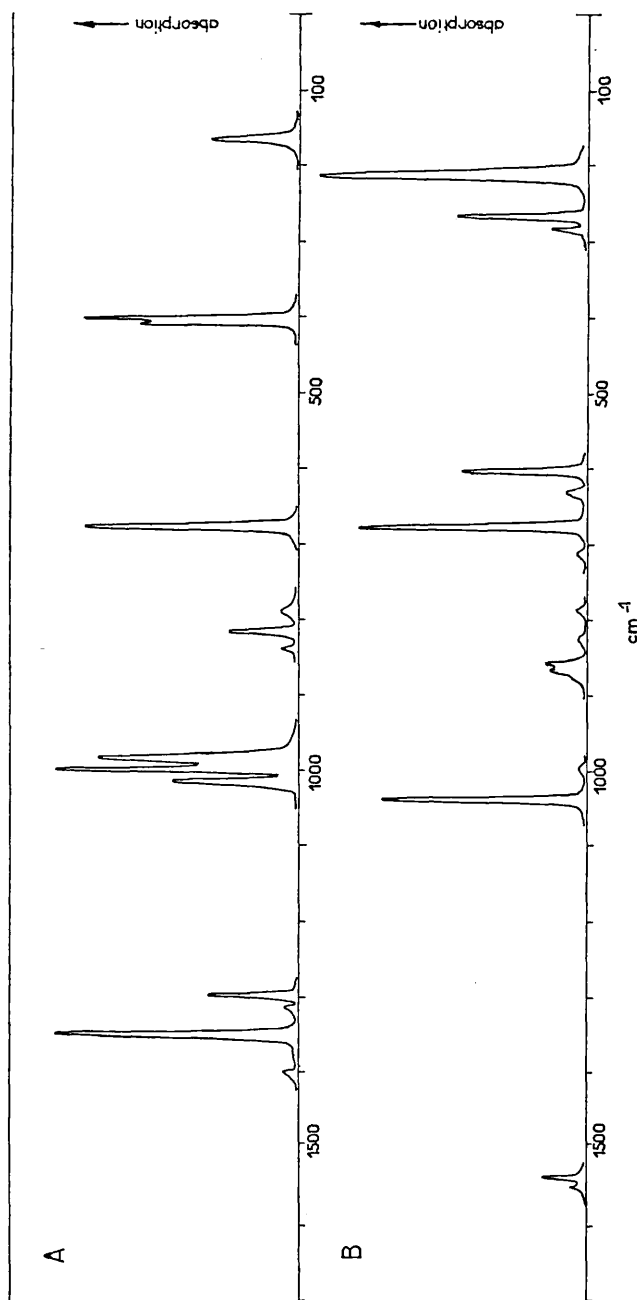


Fig. 1. Spectra of *para* C<sub>6</sub>D<sub>4</sub>Br<sub>2</sub>:  
(a) Infra-red of solution (solvent bands eliminated).  
(b) Raman of solid.

Table 3

Species	C <sub>6</sub> D <sub>4</sub> F <sub>2</sub>	C <sub>6</sub> D <sub>4</sub> Cl <sub>2</sub>	C <sub>6</sub> D <sub>4</sub> Br <sub>2</sub>	C <sub>6</sub> H <sub>4</sub> F <sub>2</sub>	C <sub>6</sub> H <sub>4</sub> Cl <sub>2</sub>	C <sub>6</sub> H <sub>4</sub> Br <sub>2</sub>
<i>B</i> <sub>1g</sub> R	614	632	630	800	815	815
	780	788	786	928	934	935
<i>B</i> <sub>2g</sub> R	600	599	602	692	687	685
	366	289	264	375	298	271
<i>A</i> <sub>u</sub> IR		780	788	943	951	950
		367		405	407	400
<i>B</i> <sub>3u</sub> IR	732	692	677	833	819	807
	422	417	410	509	485	473
	163	(118)	(103)	170	118	103
	2277	2291	2290	3065	3090	3050
<i>B</i> <sub>1u</sub> IR	1435	1365	1350	1511	1477	1468
	1130	1020	999†	1225	1090	1066
	859	840	837	1012	1015	1003
	685	531	404	737	550	429
	2310	2300	2305	3074	3090	3080
<i>B</i> <sub>2u</sub> IR	1328	1312	1297	1437	1394	1381
	1287	1208	[1289]	1285	1260/1221	1251
	802	815	816	1085	1107	1100
	348	226	164	350	226	173
	2313	2299	2296	3084	3070	3065
<i>A</i> <sub>g</sub> R	1595	1558	1544	1617	1574	1565
	1229	1074	1035	1245	1169	1170
	847*	867	861*	1142	1096	1064
	780	716	677	858	747	709
	453	328	208	451	328	214
<i>B</i> <sub>3g</sub> R	2304	2281	2296	3084	3065	3068
	1523	1531	1531	1617	1574	1570
	1008	1000	997	1285	1290	1289
	614	609	602	635	626	623
	[406]	330	282	430	350	307

All frequencies in cm<sup>-1</sup>.

\* Mean frequency of doublet.

[ ] = Determined from RT ratios—not observed.

( ) = Assumed values—not observed.

† = Mean frequency of triplet.

The assignments for *p*-difluoro- and *p*-dibromo-tetradeuterobenzene are compared with closely related molecules in Table 3.

As a final check on the assignments the inequality rule of STEELE and WHIFFEN [18] has been applied to the series C<sub>6</sub>D<sub>6</sub>-C<sub>6</sub>D<sub>5</sub>X-*para* C<sub>6</sub>D<sub>4</sub>X<sub>2</sub> (X = F, Cl, Br).

Table 4 lists the fundamentals of the above series for comparison. The Redlich-Teller product rule [19] has also been used as a check on the validity of the assignments. The Redlich-Teller (RT) ratios, both theoretical and experimental, are given in Table 5.

The assignments will now be considered, molecule by molecule and class by class.

#### *p*-Difluorotetradeuterobenzene

*A<sub>g</sub> class.* Vibrations of this class give rise to polarised Raman bands. On this basis the assignment of 780, 1229 and 2313 cm<sup>-1</sup> is certain. The two bands at 828/867 cm<sup>-1</sup> are both polarised and hence in resonance—the mean frequency is taken. The two remaining modes are assigned to the weak band at 1595 cm<sup>-1</sup>

[18] D. STEELE and D. H. WHIFFEN, *Trans. Faraday. Soc.* **55**, 369 (1959).

[19] G. HERZBERG, *Infrared and Raman Spectra of Polyatomic Molecules*, p. 231. Van Nostrand (1945).

Table 4

$C_6D_6$	$C_6D_5F$	$C_6D_4F_2$	$C_6D_5Cl$	$C_6D_4Cl_2$	$C_6D_5Br$	$C_6D_4Br_2$	$C_{2v}$	$D_{2h}$	
2294	2295	2277	2295	2291	2295	2290	$A_1$	$B_{1u}$	
2276	2275	2313	2275	2299	2275	2296		$A_g$	
2275	2270	1595	2270	1558	2270	1544		$A_g$	
2267	1578	1435	1563	1365	1551	1350		$B_{1u}$	
1553	1389	1229	1346	1074	1346	1035		$A_g$	
1330	1163	1130	1038	1020	1020	999†		$B_{1u}$	
970	959	847*	959	867	958	861*		$A_g$	
945	880	859	865	840	865	837		$B_{1u}$	
868	817	780	816	716	821*	677		$A_g$	
812	753	685	667	531	644	404		$B_{1u}$	
579	505	453	412	328	305	208	$A_g$		
2276	2276	2310	2275	2300	2280	2305	$B_2$	$B_{2u}$	
2267	2266	2304	2266	2281	2270	2296		$B_{3g}$	
1553	1564	1523	1543	1531	1541	1531		$B_{3g}$	
1330	1311	1328	1322	1312	1316	1297		$B_{2u}$	
1282	1281	1287	1260	1208	1278	[1255]		$B_{2u}$	
1055	1035	1008	1022	1000	1012	997		$B_{3g}$	
868	843	802	842	815	841	816		$B_{2u}$	
823	806	614	800	609	800	602		$B_{3g}$	
812	590	[406]	591	330	586	282		$B_{3g}$	
579	388	348	282	226	238	164		$B_{2u}$	
830	825	780	816	788	817	786	$B_1$	$B_{2g}$	
789	753	732	747	692	743	677		$B_{3u}$	
663	627	600	618	599	614	602		$B_{2g}$	
599	563	422	546	417	543	410		$B_{3u}$	
497	438	366	420	289	403	264		$B_{2g}$	
351	229	163	182	(118)	172	(103)		$B_{3u}$	
789	789		760	780	760	788		$A_2$	$A_u$
663	682	614	680	632	680	630			$B_{1g}$
351	350		350	367	350				$A_u$

All frequencies in  $cm^{-1}$ .

For explanation of various symbols see Table 3.

Table 5. Redlich-Teller product ratios

 $C_6H_4F_2/C_6D_4F_2$ 

Class	Theoretical	Experimental	Class	Theoretical	Experimental
$A_g$	1.998	2.019	$B_{2g}$	1.411	1.405
$A_u$	1.413		$B_{2u}$	1.981	1.953
$B_{1g}$	1.286	1.302	$B_{3g}$	1.985	1.985*
$B_{1u}$	1.981	1.946	$B_{3u}$	1.402	1.430

 $C_6H_4Br_2/C_6D_4Br_2$ 

Class	Theoretical	Experimental	Class	Theoretical	Experimental
$A_g$	1.998	2.035	$B_{2g}$	1.401	1.388
$A_u$	1.413		$B_{2u}$	1.964	1.964*
$B_{1g}$	1.286	1.293	$B_{3g}$	1.944	1.994
$B_{1u}$	1.964	1.966	$B_{3u}$	1.389	1.375

\* These values have been used to predict fundamental frequencies (see text).

(this fundamental must be above the  $1578\text{ cm}^{-1}$  in  $\text{C}_6\text{D}_5\text{F}$  and can only be thus assigned) and the weakly polarised band at  $453\text{ cm}^{-1}$  (approximate position indicated by the product rule).

*B<sub>1g</sub>* class. The RT product rule determines this frequency at  $620\text{ cm}^{-1}$ . The assignment of the  $614\text{ cm}^{-1}$  band to this mode is thus strongly indicated.

*B<sub>2g</sub>* class. The relative constancy of the two highest modes in the series  $\text{C}_6\text{H}_4\text{F}_2$ – $\text{C}_6\text{H}_4\text{Cl}_2$ – $\text{C}_6\text{H}_4\text{Br}_2$  indicates that these two modes will appear at approximately the same frequencies as in  $\text{C}_6\text{D}_4\text{Cl}_2$  i.e.  $599$  and  $788\text{ cm}^{-1}$ . Frequencies of  $600$  and  $780\text{ cm}^{-1}$  are thus assigned, the latter necessitating a double assignment (*A<sub>g</sub>*). The assignment of the  $\gamma_{\text{CF}}$  mode as  $366\text{ cm}^{-1}$  is necessitated by the corresponding assignment in  $\text{C}_6\text{H}_4\text{F}_2$ .

*B<sub>3g</sub>* class. The CD stretch is assigned to the weak  $2304\text{ cm}^{-1}$  band in keeping with the low intensity associated with such motions. The highest ring mode is expected near  $1540\text{ cm}^{-1}$  and is given the value of  $1523\text{ cm}^{-1}$ . The lack of movement of the higher frequencies in the series  $\text{C}_6\text{D}_6$ – $\text{C}_6\text{D}_5\text{F}$ – $\text{C}_6\text{D}_4\text{F}_2$  indicates the third mode to be near  $1020\text{ cm}^{-1}$ , hence the assignment as  $1008\text{ cm}^{-1}$ . The lowest ring mode (from the slight rise in the series  $\text{C}_6\text{H}_4\text{Br}_2$ – $\text{C}_6\text{H}_4\text{Cl}_2$ – $\text{C}_6\text{H}_4\text{F}_2$ ) is expected to occur just above  $609\text{ cm}^{-1}$ . The assignment of  $614\text{ cm}^{-1}$  (also assigned to the *B<sub>1g</sub>* class) is tentative. The  $\beta_{\text{CF}}$  mode must be near  $406\text{ cm}^{-1}$  from the RT product rule but is not apparently observed.

*A<sub>u</sub>* class. These frequencies are infrared inactive, though not infrequently appearing weakly in the infrared in similar compounds, in violation of the selection rules. The modes are almost constant in frequency in the series  $\text{C}_6\text{H}_4\text{F}_2$ – $\text{C}_6\text{H}_4\text{Cl}_2$ – $\text{C}_6\text{H}_4\text{Br}_2$ , indicating  $\sim 780$  and  $\sim 367\text{ cm}^{-1}$  as probable positions in the deuterio series. The position of the lower skeleton mode may also be approximated from  $\text{C}_6\text{D}_6$  since the mode itself does not involve movement of the substituents and hence its value should be close to that of  $351\text{ cm}^{-1}$  ( $\text{C}_6\text{D}_6$ ).

*B<sub>1u</sub>* class. The highest mode is assigned to the weaker of the infrared bands in the  $2300\text{ cm}^{-1}$  region [4]. The remaining modes of this class are assigned to the strong infrared bands at  $1435$ ,  $1130$ ,  $859$  and  $685\text{ cm}^{-1}$ , both on intensity considerations and application of the inequality rule.

*B<sub>2u</sub>* class. The stronger of the infrared bands in the  $2300\text{ cm}^{-1}$  region is assigned to the *B<sub>2u</sub>* CD stretch. The  $348\text{ cm}^{-1}$  band has previously been assigned to the  $\gamma_{\text{F}}B_{2u}$  mode by one of us [13], in line with the value of  $350\text{ cm}^{-1}$  for  $\text{C}_6\text{H}_4\text{F}_2$ . The three remaining modes (designated  $\nu_2$ ,  $\nu_3$  and  $\nu_4$ ) have ranges, determined by approximate application of the inequality rule to the series  $\text{C}_6\text{D}_6$ – $\text{C}_6\text{D}_5\text{F}$ – $\text{C}_6\text{D}_4\text{F}_2$ , of  $1311 > \nu_2 > 1281 > \nu_3 > 1055$ ;  $843 > \nu_4 > 823\text{ cm}^{-1}$ .

Five infrared bands appear in the  $\nu_2$  and  $\nu_3$  region:  $1287\text{ w}$ ,  $1328\text{ w}$ ,  $1360\text{ w}$ ,  $1373\text{ w}$  and  $1390\text{ m}$  ( $\text{cm}^{-1}$ ). The assignment of  $\nu_2 = 1328\text{ cm}^{-1}$  and  $\nu_3 = 1287\text{ cm}^{-1}$  is tentatively made, slight discrepancies in the inequality rule being invoked. In the  $\nu_4$  range two bands occur at  $803$  and  $859\text{ cm}^{-1}$ . The  $859\text{ cm}^{-1}$  band has already been assigned to *B<sub>1u</sub>* mode, leaving  $\nu_4 = 803\text{ cm}^{-1}$ . These assignments are confirmed by the vapour phase band contours (type *B* with *PR* separations of  $\sim 9\text{ cm}^{-1}$ ).

*B<sub>3u</sub>* class. The strong infrared band at  $732\text{ cm}^{-1}$  is clearly the *B<sub>3u</sub>* umbrella mode. The second mode of this class is assigned to the  $422\text{ cm}^{-1}$  band and is derived from the degenerate  $\text{C}_6\text{D}_6$  frequency at  $351\text{ cm}^{-1}$ , being made strongly infrared

active by mixing with the CF out of plane deformation. This CF out of plane deformation mode has previously been assigned the value  $163\text{ cm}^{-1}$  [13].

*p-Dibromotetradeuterobenzene*

*A<sub>g</sub> class.* The single intense band at  $2296\text{ cm}^{-1}$  in the Raman spectrum necessitates the assignment of the *A<sub>g</sub>* CD stretch to this frequency. The higher frequency component of the doublet at  $1531\text{--}1544\text{ cm}^{-1}$  is assigned to the *A<sub>g</sub>* CC stretching mode in parallel with the assignment of  $\text{C}_6\text{D}_4\text{Cl}_2$  by SCHERER [12]. A slight breakdown in the inequality rule is invoked since the frequency should lie between  $2270$  and  $1551\text{ cm}^{-1}$ . The assignment of the strong Raman band at  $1035\text{ cm}^{-1}$  to the  $\beta_{\text{CD}}$  mode is certain, both on its strength and position. The doublet at  $857\text{--}866\text{ cm}^{-1}$  is thought to arise from resonance between the *A<sub>g</sub>* fundamental (expected near  $860\text{ cm}^{-1}$ ) and the combination tone ( $264 + 602 = 866\text{ cm}^{-1}$ ) ( $B_{2g} \times B_{2g} = A_g$ ). The ring deformation mode is predicted by the inequality rule to lie between  $644\text{--}820\text{ cm}^{-1}$ . The very strong Raman line at  $677\text{ cm}^{-1}$  is so assigned, while the remaining mode is obviously the  $208\text{ cm}^{-1}$  band to be consistent with the value assigned to the same mode in  $\text{C}_6\text{H}_4\text{Br}_2$ .

*B<sub>1g</sub> class.* The Redlich–Teller product rule predicts the  $\gamma_{\text{CD}}$  mode to be at  $634\text{ cm}^{-1}$ . This is observed in the Raman at  $630\text{ cm}^{-1}$ .

*B<sub>2g</sub> class.* Exactly parallel arguments as proposed in the assignment of *p*-difluorotetradeuterobenzene strongly indicate the following assignments:  $786$ ,  $602$  and  $264\text{ cm}^{-1}$  for this class.

*B<sub>3g</sub> class.* According to WHIFFEN [4] the *B<sub>3g</sub>* CD stretch is likely to be the weaker of the two Raman lines in this region. Since only a single frequency at  $2296\text{ cm}^{-1}$  is observed it is presumed that the *A<sub>g</sub>* and *B<sub>3g</sub>* species overlies each other. The highest ring mode is assigned to the lower component of the  $1544\text{--}1531\text{ cm}^{-1}$  doublet, again in accord with SCHERER [12]. The relative constancy of the next two modes in the series  $\text{C}_6\text{H}_4\text{F}_2\text{--C}_6\text{H}_4\text{Cl}_2\text{--C}_6\text{H}_4\text{Br}_2$  and  $\text{C}_6\text{D}_4\text{F}_2\text{--C}_6\text{D}_4\text{Cl}_2$  clearly indicates the assignment of  $997$  and  $602\text{ cm}^{-1}$  to these modes. The Redlich–Teller product rule, along with a consideration of the above two series, locates the remaining frequency at  $282\text{ cm}^{-1}$ .

*A<sub>u</sub> class.* In accord with what has been said for the fluoro compound it is thought that the weak infrared band at  $788\text{ cm}^{-1}$  arises from the  $\gamma_{\text{CD}}$  motion. The other mode has not been located but its position should be close to the  $367\text{ cm}^{-1}$  in  $\text{C}_6\text{D}_4\text{Cl}_2$ .

*B<sub>1u</sub> class.* Two weak bands appear in the infrared spectrum in the CD stretch region:  $2290$  and  $2305\text{ cm}^{-1}$ . The lower frequency component is assigned to the *B<sub>1u</sub>* CD stretch. This assignment is somewhat arbitrary but examination of Table 3 for the relative magnitudes of the *B<sub>1u</sub>* and *B<sub>2u</sub>* CD stretching modes favours this assignment. The intense infrared bands at  $1350$ ,  $816$  and  $404\text{ cm}^{-1}$  are confidently assigned to the CC stretch, the  $\beta_{\text{CD}}$  and the CX stretching modes of this class. The remaining mode is expected near  $990\text{ cm}^{-1}$  but the infrared spectrum clearly shows an intense triplet at  $984$ ,  $997$  and  $1016\text{ cm}^{-1}$ . It is postulated that this is a Fermi triplet arising from the *B<sub>1u</sub>* fundamental itself (near  $990\text{ cm}^{-1}$ ) and the binary combinations ( $630 + 367 = 997\text{ cm}^{-1}$ ). ( $A_u \times B_{1g} = B_{1u}$ ) and ( $602 + 410 = 1012\text{ cm}^{-1}$ ) ( $B_{3u} \times B_{2g} = B_{1u}$ ).

*B<sub>2u</sub> class.* The higher frequency component of the absorption in the  $2300\text{ cm}^{-1}$

region is assigned to the  $B_{2u}$  CD stretch. The  $\beta_{CX}$  mode is confidently assigned to the  $164\text{ cm}^{-1}$  band, this value being in complete accord with its counterpart in  $C_6H_4Br_2$  [11]. The CC stretching mode of this class is assigned the value  $1297\text{ cm}^{-1}$ , its range being indicated as  $1316\text{--}1278\text{ cm}^{-1}$  according to the inequality rule and its counterpart in  $C_6H_4Br_2$  being of similar intensity. The assignment of  $B_{2u}$   $\beta_{CD}$  mode as  $816\text{ cm}^{-1}$  and the weak  $837\text{ cm}^{-1}$  absorption as  $B_{1u}$  is contrary to the assignments of *para*  $C_6D_4Cl_2$  by SCHERER but in line with the unequivocal assignments of *para*  $C_6D_4F_2$ . In an effort to confirm this reassignment the spectrum of *para*  $C_6D_4Br_2$  was measured in the vapour phase in a  $5\text{ cm}$  high-temperature/high-pressure cell which is to be described elsewhere [20]. The band at  $816\text{ cm}^{-1}$  turned out to be very weak in the vapour phase but at a temperature of about  $160^\circ\text{C}$  the band contour was clearly discernible as a type  $B$  with a  $PR$  maxima separation of  $9\text{ cm}^{-1}$ . As was predictable from the large moments of inertia about axes other than through the Br-Br axis type  $A$  bands showed no significant structure.

The remaining mode is predicted by the RT product rule to be near  $1289\text{ cm}^{-1}$  but is apparently unobserved. Interpolation within the series  $C_6D_4Cl_2\text{--}C_6D_4Br_2\text{--}C_6H_4Cl_2\text{--}C_6H_4Br_2$  cannot be made, since doubt still exists regarding the assignment of this mode in  $C_6H_4Cl_2$  [12].

$B_{3u}$  class. The strong infrared band at  $677\text{ cm}^{-1}$  is undoubtedly the umbrella mode. An intense band also appears in the Raman at this frequency, apparently in violation of the rule of mutual exclusion, but the strength of both bands strongly indicates this to be a frequency coincidence rather than a major breakdown of selection rules. Comparison of the series  $C_6H_4F_2\text{--}C_6H_4Cl_2\text{--}C_6H_4Br_2$  and  $C_6D_4F_2\text{--}C_6D_4Cl_2$  locate the intermediate mode of this class of  $410\text{ cm}^{-1}$ . The  $\gamma_{CX}$  mode is expected very near the value in  $C_6H_4Br_2$  i.e.  $103\text{ cm}^{-1}$ . No sign of a band in this region could be found despite the use of saturated solutions in benzene and the exact position of this mode is left open.

#### *Para-dibromobenzene assignment*

SHURVELL *et al.* [10] suggested some changes in the assignment of *p*-dibromobenzene given by STOJILJKOVIC and WHIFFEN [4] based upon the ultraviolet absorption spectrum. The points of difference between the two assignments may be seen from Table 6, which lists the  $A_g$  and  $B_{3g}$  frequencies of benzene and the halogenobenzenes.

The Redlich-Teller product ratios for the  $A_g$  and  $B_{3g}$  classes have been evaluated as:

$$A_g: \Pi\nu(H)/\Pi\nu(X) = (m_X/m_H)^{1/2}(f_{CH}/f_{CX})^{1/2}$$

and

$$B_{3g}: \Pi\nu(H)/\Pi\nu(X) = (m_X/m_H)^{1/2}(\beta_{CH}/\beta_{CX})^{1/2}(I_X^H/I_{XX})^{1/2}$$

where  $f_{CH} = E(f_{CX} = E^X)$  and  $\beta_{CH} = G(\beta_{CX} = G^X)$  see DUINKER [21].

The accompanying table lists the values of the force constants [21] used in the calculations, along with the moments of inertia perpendicular to the plane of the ring.

[20] B. SMETHURST, D. STEELE and W. WHEATLEY, to be published.

[21] J. C. DUINKER, Ph.D. thesis Amsterdam (1964).



Table 6

Benzene $A_{1g}, E_{2g}$	$C_6H_4F_2$ $A_g$	$C_6H_4Cl_2$	$C_6H_4Br_2$ (S + W)	$C_6H_4Br_2$ (S, D, P)	$C_6H_4I_2$
3073	3084	3072	3068	3068	3056
3055	1617	1573	1570	1570	1552
1600	1245	1169	1170	1067	1175
1177	1142	1106	1067	708	1044
993	858	747	708	623	680
607	451	330	218	218	157

All frequencies are in  $cm^{-1}$

$E_{2g}, A_{2g}$	$B_{3g}$				
3056	3084	3072	3068	3068	3056
1599	1617	1573	1570	1570	1552
1350	1285	1291	1289	1170	1292
1178	635	628	623	623	624
606	427	351	307	307	255

Table 7

X =	H	F	Cl	Br	I
$f_{CX}$	5.125	5.800	3.700	3.120	2.520 mdyn/Å
$\beta_{CX}$	0.881	1.030	0.573	0.321	0.250 mdyn/Å
$\beta_{CH}$	0.881	0.861	0.875	0.882	0.887 mdyn/Å
$I_X^x$	178.3	442.9	843.8	1876.6	3102.2 amu.Å <sup>2</sup>

Table 8

X	=	F	Cl	Br(S + W)	Br(SDP)	I
$A_g$ RT ratio	Theoretical	4.08	6.98	11.42	11.42	16.01
	Experimental	3.885	6.92	11.49	21.61	17.18
$B_{3g}$ RT ratio	Theoretical	2.52	3.37	4.55	4.55	5.06
	Experimental	2.71	3.42	3.98	4.37	4.83

The force constants are taken from force fields which reproduce all the frequencies of the halogenobenzenes to a high degree of precision.

The results of the calculations, shown in Table 8, strongly indicate that the WHIFFEN assignment is to be preferred.

It is appreciated that the above approximate RT rule would lead to exact agreement if all the force constants except the diagonal C—Br constant were unchanged in substituting two bromine atoms for hydrogen atoms in *para* positions in benzene and if correct diagonal constants are known. The first assumption is a reasonable one and should lead to little error. This implies that to fit the S,D,P assignment DUINKER's  $f_{CBr}$  force constant would have to be increased by a factor of four, i.e. to over 12 mdyn/Å. The assignment is therefore untenable.

*Acknowledgment*—One of us (K. R.) wishes to thank the Science Research Council for financial support in the form of a Postdoctoral Fellowship.

GALLEY W BB—13

Spectrochimica Acta  
1st Proof  
The Universities Press, Belfast2718  
MS pages 1-10Pergamon Press, Oxford  
Galley 1-3  
20.2.69

1

Spectrochimica Acta, Vol. ~~22~~, pp. ~~222~~ to ~~223~~. Pergamon Press 1969. Printed in Northern Ireland

## Some further observations on the vibrational spectrum of decafluorobiphenyl

D. STEELE

Royal Holloway College, University of London Englefield Green, Surrey

(Received 6 August 1968)

**Abstract**—The spectrum of decafluorobiphenyl below  $200\text{ cm}^{-1}$  has been remeasured using an interferometer. One strong new band is reported. The fundamentals have been computed on the basis of a planar  $D_{2h}$  model. Agreement with assigned frequencies is generally good. A few revisions of the assignments are suggested. The greatest remaining discrepancies of 10% are interpreted in terms of steric repulsion between the rings.

### 1. INTRODUCTION

IN a previous publication [1] STEELE *et al.* (SNL) discussed the vibrational spectrum of decafluorobiphenyl and assigned most of the fundamentals on the basis of Raman polarisation data, changes of infrared adsorption intensities between crystal and solution phases and comparison with known data on  $C_6F_5X$  systems. The data was interpreted to suggest that in the crystal perfluorobiphenyl was planar or almost planar, but in solution a degree of non-planarity was probable.

Additional deductions concerning the degree of interaction between the rings was impeded by lack of strong Raman and infrared absorption bands where fundamentals were expected. For this reason many assignments were very tentative. Two causes of this situation are to be noted. Firstly it has been noted many times by the author that C—F stretching modes give rise to very low intensity Raman bands. Secondly many of the modes in  $C_{12}F_{10}$  strongly resemble the  $C_6F_6$  modes from which they are derived—that is their frequencies and activities are similar. Hexafluorobenzene has  $D_{6h}$  symmetry and therefore many of the fundamentals are completely inactive in the infrared and Raman.

In the course of a study of some 2 substituted perfluorobiphenyls [2] occasion arose to compute the frequencies of  $C_{12}F_{10}$ . The results are reported in the present paper along with a reinvestigation of the far infrared spectrum of the compound.

### 2. EXPERIMENTAL

A spectrum of  $C_{12}F_{10}$  in  $CCl_4$  (concentrated solution of 2 mm thickness) was obtained over the range  $200\text{--}40\text{ cm}^{-1}$  using a Grubb Parsons/N.P.L. cube interferometer. The Fourier transformation (complex) of the interferogram is shown in Fig. 1 and corresponds to a resolution of  $2.5\text{ cm}^{-1}$ . Bands were observed at  $185\text{ cm}^{-1}$  (m) and  $1.6\text{ cm}^{-1}$  (s). The latter is reported for the first time.

[1] D. STEELE, T. R. NANNEY and E. R. LIPPINCOTT, *Spectrochim. Acta* **22**, 849 (1966).

[2] A. MASSEY and D. STEELE, to be published.

## 3. CALCULATIONS

In view of the results of SNL it seems adequate for the present purposes to assume a planar geometry with the rings as regular hexagons. The force field used for the in-plane vibrations was that of STEELE and WHIFFEN [3]. Its adequacy in predicting the frequencies of fluoro-aromatic systems is well established, e.g. [4, 5]. The inter-ring stretching constant was taken as 4.8 mdyn/Å and the force constant for the deformation of the angle between the inter-ring bond and the internal ring angle bisector was taken as 0.826 mdyn/Å. For the out-of-plane vibrations the field used

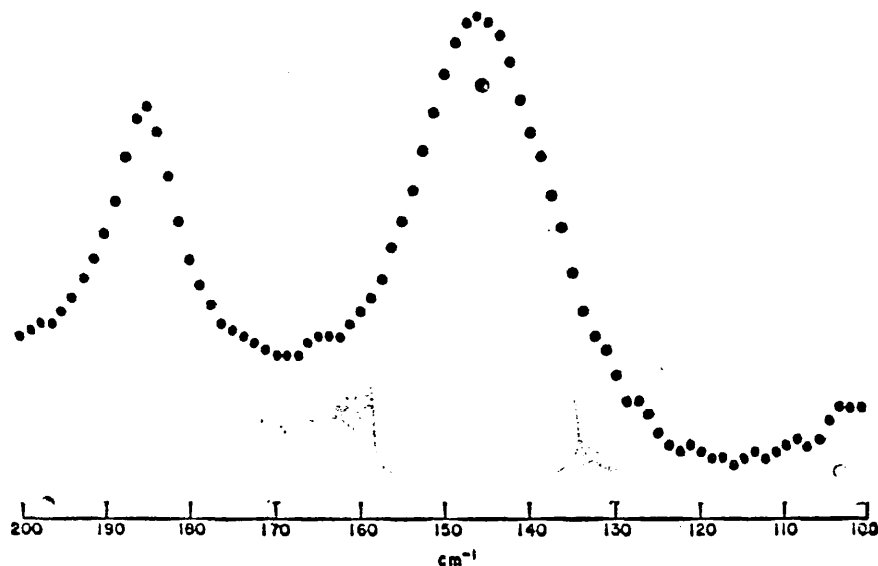


Fig. 1. Fourier transformation of interferogram of  $C_{12}F_{10}$  (solution) for frequency range 200–110  $\text{cm}^{-1}$ .

was one derived from a perturbation study of a series of fluoroaromatics [6] and is given in Table 1. The method of computation was as described in [4]. Results are given in Table 2. Some of the vibrational modes, details of which are referred to in this paper, are depicted in Fig. 2.

## 4. IN-PLANE FUNDAMENTALS

In the work of SNL it was demonstrated that the fundamentals could be classified adequately on the basis of molecular  $D_{2h}$  geometry. In the axis system adopted the in-plane vibrations classify as  $11a_g + 10b_{3g} + 10b_{1u} + 10b_{2u}$ .  $D_2$  geometry will result in coalescing of and consequential mode interaction between the classes  $a_g$  and  $a_u$ ,  $b_{1u}$  and  $b_{1g}$ ,  $b_{3g}$  and  $b_{3u}$  and  $b_{2g}$  and  $b_{2u}$ .

[3] D. STEELE and D. H. WHIFFEN, *Trans. Faraday Soc.* **56**, 5 (1960).

[4] R. T. BAILEY and D. STEELE, *Spectrochim. Acta*, **23A**, 2989 (1967).

[5] D. A. LONG and D. STEELE, *Spectrochim. Acta* **19**, 1947 (1963).

[6] K. RADCLIFFE and D. STEELE, *Spectrochim. Acta* **Ms2682** (1969).

Table 1. Out of plane force constants used in the calculations

Diagonal constants (mdyn/Å)	
$\gamma_F$	= 0.200
$\phi$	= 0.35
$\gamma_c$	= 0.14
Interaction constants	
$\gamma\gamma_{FF}^o$	= 0.014
$\gamma\gamma_{FF}^m$	= -0.006
$\gamma\gamma_{FF}^p$	= -0.008
$\gamma\phi_o$	= -0.0006
$\gamma\phi_m$	= 0.005
$\phi\phi$	= -0.009

Table 2. The computed and assigned frequencies for  $C_{12}F_{10}$  (frequencies in  $cm^{-1}$ )

Species	Calc.	Ass.*	Ass(SNL)	Species	Calc.	Ass.*	Ass.(SNL)		
$a_g$	1637	1661	1661	$b_{1u}$	1632	1656	1656		
	1531	1534	1534		1512	1530	1530		
	1420	1474	1474		1414	1374	1374		
	1366	1302	1302		1295	1272	1154		
	1160	1152	1152		1089	1038	1038		
	959	960	960		762	775	?		
	603	587	587		592	588	588		
	624	510	510		460	478	478		
	343	362	362		320	312	312		
	267	273	273		265	266	240		
	174	187	235						
	$b_{3g}$	1681	1661		1661	$b_{2u}$	1647	1650	1650
		1558	1533		1533		1515	1505	1505
		1268	1272		1272		1264	1294	1294
1171		1152	1092	1168	1078		1078		
1042		1003	1003	985	996		996		
739		678	678	653	728		728		
448		440	440	437	471		471		
306		344	344	290	344		344		
234		235	273	226	240		280		
177		187	190	54	?		183		
$b_{2g}$		800	?	653	$b_{1u}$		744	678	678
	663	653	?	599		618	618		
	411	386	386	339		344	344		
	225	235	235	222		183	240		
	194	187	187	166		146	183		
	106	?	156	49		?	?		
$b_{1g}$	626	?	?	$a_u$	627	?	?		
	392	411	411		394	?	?		
	135	156	156		135	?	?		
					16	?	?		

 $a_g$  species

Of the eleven fundamentals in this class the frequencies of six are unequivocally determined from Raman polarisation data. For these the average discrepancy between calculated and observed ( $\overline{\Delta\nu}$ ) is  $19.0\text{ cm}^{-1}$ . For the entire eleven  $a_g$  assignments of SNL  $\overline{\Delta\nu}$  is  $24.7\text{ cm}^{-1}$  with three maximum discrepancies of 64, 61 and  $56\text{ cm}^{-1}$ . Excluding the lowest fundamental frequency the average percentage error is only  $2.3\%$  with a maximum of  $5.2\%$ . Whilst the more tentative of the assignments

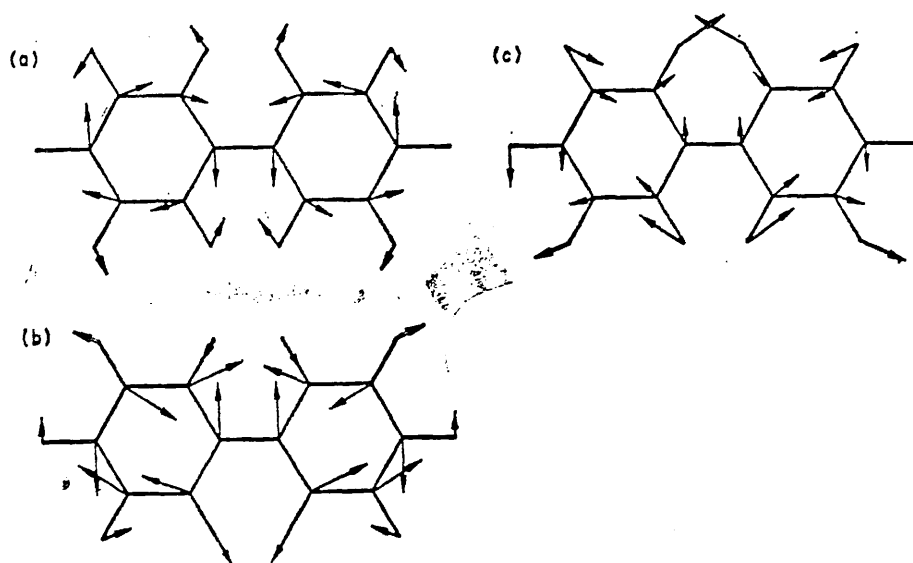


Fig. 2. The computed normal modes for the  $b_{2u}$  transitions at (a) 1168; (b) 653; and (c)  $54\text{ cm}^{-1}$  (calc. frequencies). The distortions are magnified by an arbitrary scale factor which is the same for (a) and (b) but four times smaller for (c).

corresponding to extremely weak Raman lines (e.g. 1152  $\nu\nu$  and 362  $\nu\nu$ ) must still remain uncertain these computations make it clear that the assigned frequencies based on the assumption of a pair of weakly interacting perfluorophenyl rings are close to the real frequencies. The sole reassignment suggested by the present work is to correlate the lowest  $a_g$  fundamental with the  $\nu\nu$  Raman line at  $187\text{ cm}^{-1}$ .

#### $b_{2u}$ species

Fundamentals of this species were identified by SNL through strong intensity changes in going from solidified melt to solution spectra. Of the ten fundamentals the seven with the highest frequencies would appear to be well established. For two of these the  $\Delta\nu$  is above  $35\text{ cm}^{-1}$   $\Delta\nu$  is in fact  $90\text{ cm}^{-1}$  and  $75\text{ cm}^{-1}$  for the  $1078$  and  $728\text{ cm}^{-1}$  modes respectively. In both of these cases the vibrational modes involve considerable changes in the  $22'$  carbon distances and in the corresponding fluorine distances (Fig. 2). This would indicate that the large  $\Delta\nu$  in these cases is due to an appreciable non-bonded interaction and possibly to neglect of a potential interaction term between the bonds in the two rings (arising from other than on-bonded interactions). The former seems highly probable in view of the very short distances between the  $22'$  fluorines. For the planar case it is calculated to be about  $1.6\text{ \AA}$  compared with the sum of the Van der Waal's atomic radii of  $2.7\text{ \AA}$ !!

One re-assignment clearly required is that for the lowest  $b_{2u}$  mode calculated to be at  $54\text{ cm}^{-1}$ . This frequency is very low for an in-plane vibration—and indeed it is much lower than any for  $\text{C}_6\text{F}_5\text{I}$  [7]. As shown in Fig. 2(a) it is primarily a ring buckling vibration. 85% of its energy arises from distortion of the angle between the

[7] D. A. LONG and D. STEELE, *Spectrochim. Acta* **19**, 1955 (1963).

bond axes of the two phenyl units. No trace of an absorption band could be found below  $100\text{ cm}^{-1}$ . However in 2H perfluorobiphenyl a band has been observed at  $\sim 60\text{ cm}^{-1}$  [2]. The only alternative explanation of the latter is as a torsion band but this is considered to be very unlikely.  $\overline{\Delta\nu}$  is relatively high at  $51\text{ cm}^{-1}$ . The reasons are probably those given above.

#### *b<sub>1u</sub> species*

The agreement is generally good. A single exception is the frequency calculated at  $1295\text{ cm}^{-1}$  and assigned at  $1154\text{ cm}^{-1}$ . A re-assignment to one of the weak infrared bands in the  $1200\text{--}1250\text{ cm}^{-1}$  range is obviously required, but in view of the weakness of these bands and the close relationship of the mode to the inactive *b<sub>2u</sub>* mode of  $\text{C}_6\text{F}_6$  at  $1253\text{ cm}^{-1}$  the choice must be somewhat arbitrary on the present evidence. The choice of the  $1272\text{ cm}^{-1}$  band is made on the grounds that it is the strongest band not assigned already to an ungerade vibration. On the same basis  $773\text{ cm}^{-1}$  is chosen as the previously unidentified fundamental. The lack of other fundamentals in this range makes this choice perhaps more reliable even though the absorption is very weak. It is to be noted that the slightly stronger  $750\text{ cm}^{-1}$  band has *b<sub>2u</sub>* characteristics (drastic reduction in strength in crystal) and is clearly a resonance component of the  $728\text{ cm}^{-1}$  fundamental.  $\overline{\Delta\nu}$  is  $18.4\text{ cm}^{-1}$  (1.8%).

#### *b<sub>3g</sub> species*

In view of the paucity of depolarised Raman lines of appreciable strength which could be easily identified as *b<sub>3g</sub>* fundamentals the value of  $\overline{\Delta\nu}$  of  $32.3\text{ cm}^{-1}$  is encouraging. Few of the assignments in this class can be considered to be on a very firm basis. Indeed in the case of the  $1092$  and  $678\text{ cm}^{-1}$  assignments no Raman bands were observed at all and the frequencies correspond to infrared bands. The justification for these lies in

(a) some of the modes are derived from inactive modes of  $\text{C}_6\text{F}_6$  and in modal form they are altered only a small amount.

(b) a degree of infrared activity will arise from mode mixing accompanying departures from planarity.

Two re-assignments are suggested. Firstly since the frequency computed at  $1171\text{ cm}^{-1}$  is close to that of the Raman active mode of  $\text{C}_6\text{F}_6$  at  $1155\text{ cm}^{-1}$  from which it is derived, it seems advisable to correlate it with the  $1152\text{ cm}^{-1}$  Raman line. The second lowest frequency is changed to  $235\text{ cm}^{-1}$ .  $\overline{\Delta\nu}$  is dropped to  $22.5\text{ cm}^{-1}$  by these two revisions.

### 5. OUT-OF-PLANE FUNDAMENTALS

Agreement with assigned frequencies is generally good. One result which was not anticipated was that the highest *b<sub>2g</sub>* mode is considerably above that of any out-of-plane mode of  $\text{C}_6\text{F}_6$ . No assignment of this mode is possible due to the complete lack of Raman bands between  $950$  and  $660\text{ cm}^{-1}$ . The observation of the low frequency band at  $146\text{ cm}^{-1}$  has led to a certain amount of re-assigning of the low frequency fundamentals of the *b<sub>2u</sub>* and *b<sub>3g</sub>* species. These follow from the calculations and require no further comment.  $\overline{\Delta\nu}$  is  $21\text{ cm}^{-1}$  for those assignments which it has been possible to suggest (11 of the 19 modes).

## 6. CONCLUSIONS

In accord with the observations of SNL it appears that the spectrum of  $C_{12}F_{10}$  can be adequately interpreted in terms of two weakly interacting perfluorophenyl rings in a planar- or near-planar configuration. The strongest evidence for this configuration (SNL) came from the observation that all infrared bands which were confidently correlated with the  $b_2$  modes of  $C_6F_5X$  systems showed a very marked decrease in intensity on crystallising a melt onto an alkali halide plate. Were the two rings at appreciable angles in-phase and out-of-phase coupling of the transition dipole vectors would lead to similar intensities of bands with transition dipole vectors at 90 degrees to one another. Thus the inference is that the dihedral angle is small. When one considers that for a planar system the 22' fluorine nuclei are less than 1.7 Å apart whilst the sum of their Van der Waal's Radii is 2.7 Å this result is surprising. It is also in contradiction to the results of dipole moment studies of 22' difluorobiphenyl and of NMR studies of decafluorobiphenyl itself. That these studies were of solutions may be significant but then no large frequency shifts occur on change of phase. The present study serves only to re-enforce the conclusions of the earlier vibrational study. Steric interactions between the rings are apparent from a comparison of observed and calculated frequencies. On the other hand it is unlikely that the frequencies—particularly the in-plane modes—will be much affected by small changes in dihedral angle. Reduction of the symmetry from  $D_{2h}$  to  $D_2$  results in coalescing of each of the in-plane symmetry species with an out-of-plane species. Clearly it will be only the low frequency modes which mix or for which the coupling conditions change. Even then from symmetry reasoning it follows that mixing between the in-plane and out-of-plane modes will be significant only if the carbon nuclei at the ring junctions move appreciably during the vibrations involved. It is assumed in the above arguments that changes in the force field with dihedral angle are insignificant.

In biphenyl itself no significant shifts between frequencies in the solid and in solution have been reported [8] despite known changes of dihedral angle. This serves to caution us not to draw too many conclusions from the success of the planar model in predicting observed spectra.

It would seem legitimate to conclude

- (a) that interactions between the rings are essentially Van der Waal's interactions and that no evidence of conjugation of the rings is evident. This parallels the conclusions of Zerbi and Sandroni for biphenyl [9].
- (b) that whilst evidence exists for planarity, or near planarity, in the solid no significant evidence for changes in dihedral angle with phase changes is yet forthcoming from vibrational spectroscopy.

[8] G. ZERBI and S. SANDRONI, *Spectrochim. Acta* **24A**, 483 (1968).

[9] G. ZERBI and S. SANDRONI, *Spectrochim. Acta* **24A**, 511 (1968).

Studies in Vibrational Absorption Intensities

Part 1. The Determination of Vibrational  
Transition Moments for Symmetric Top  
Molecules from P- and R-Branch Maxima.

by D. Steele and W. Wheatley

Department of Chemistry, Royal Holloway College,  
University of London, Englefield Green, Surrey.



Abstract

The vibrational transition moments of parallel and perpendicular vibrations of a number of oblate symmetric top molecules have been determined by comparison of calculated band shapes with experimental absorption coefficients at the P and R band maxima. The agreement between the values so derived and those obtained by integration over the entire band is very satisfactory.

## INTRODUCTION

In the approximation of the separability of vibrational and rotational wavefunctions, the probability of a single rovibrational transition is directly proportional to the vibrational transition moment multiplied by a rotational transition probability factor. If the intensity of a given fundamental transition and the rotational transition probability factor are known then it is possible to deduce the vibrational transition moment and hence a value of  $\delta\mu/\delta Q_i$  for the  $i$ -th vibration. For most molecules the allowed rovibrational transitions are so densely packed into the frequency spread of the fundamental band that only the overall infrared band contour can be obtained.

The computation of infrared band envelopes is now a familiar problem. Non-degenerate vibrations of symmetric top molecules have been treated by Gerhard and Dennison (1) and more recently Edgell and Moynihan (2) have included the effect of first order Coriolis interaction on the degenerate vibrations of symmetric top molecules. Whilst reference has been made to the possibility of determining vibrational transition moments from a comparison of experimental and calculated infrared band contours (3), there is as yet no published work of this type known to the authors. In view of the considerable difficulties in obtaining accurate and reproducible estimates of absolute infrared intensities, it is felt that this method may be useful and is well worth a detailed investigation. The results of such a study applied to the oblate symmetric top molecules  $C_6H_6$ ,  $C_6D_6$  and  $C_6F_6$  are presented in this paper.

The intensity of absorption arising from a given fundamental transition of energy  $h\nu$  is given by the Hönl-London expression (4)

$$a(\nu) = \bar{C} A_{J,K} \nu_{J,K} g_{J,K} e^{-F_{J,K} hc/kT} \langle \psi_{V'} | \mu | \psi_{V''} \rangle^2 \quad (1)$$

where  $g_{J,K}$  and  $F_{J,K}$  are the statistical weight and the rotational term value for the lower state,  $\langle \psi_{V'} | \mu | \psi_{V''} \rangle$  is the transition integral for the vibration and  $A_{J,K}$  is a term whose value depends on the rotational quantum numbers  $J$  and  $K$  and also on the selection rules for the transition.  $\bar{C}$  is a normalization factor which is a constant for *a given species* of any type of vibration (parallel or perpendicular) of a particular molecule. For symmetric top molecules the  $A_{J,K}$   $g_{J,K}$  values are as shown in equations (2)-(7)

parallel transitions:

$$J, |K| \rightarrow J + 1, |K| \quad (2 - \delta_{K,0}) \frac{(J + K + 1)(J - K + 1)}{J + 1} \quad (2)$$

$$J, |K| \rightarrow J, |K| \quad (2 - \delta_{K,0}) \frac{(2J + 1) K^2}{J(J + 1)} \quad (3)$$

$$J, |K| \rightarrow J - 1, |K| \quad (2 - \delta_{K,0}) \frac{(J + K)(J - K)}{J} \quad (4)$$

perpendicular transitions:

$$J, |K| \Rightarrow J + 1, |K| \pm 1 \quad \frac{(J \pm K + 1)(J \pm K + 2)}{J + 1} \quad (5)$$

$$J, |K| \rightarrow J, |K| \pm 1 \quad \frac{(2J + 1)(J \mp K)(J \pm K + 1)}{J(J + 1)} \quad (6)$$

$$J, |K| \rightarrow J - 1, |K| \pm 1 \quad \frac{(J \mp K)(J \mp K - 1)}{J} \quad (7)$$

in which  $J$  and  $K$  refer to the lower state and where  $\delta_{K,0}$  is the Kronecker delta ( $\delta_{K,0} = +1$  for  $K = 0$  and  $\delta_{K,0} = 0$  for  $K \neq 0$ ). For the  $0 \rightarrow 1$  vibrational transition, the transition integral becomes  $\langle 0 | \mu | 1 \rangle$  and the normalization factor may

be written

$$\bar{C} = \frac{8 \pi^3 N}{3 hc} \left[ \frac{\pi}{\left(\frac{hcB}{kT}\right)^3 \frac{C}{B}} \right]^{-\frac{1}{2}} \quad (8)$$

where N is the Avagadro number and B and C are rotational constants (cm.<sup>-1</sup>). In the case of oblate symmetric top molecules we use the recommended convention (5) (A = B = 2C).

The above expression for the normalisation factor was derived for both parallel and perpendicular transitions from the equality

$$\bar{C}'' \left( \sum_{JK} A_{JK} \sqrt{g_{JK}} e^{-F_{JK} hc/kT} \right) = \frac{8N\pi^3 g \nu_0}{3c} \quad (9)$$

by summing over J and K using (2) to (5) and the well known expression for the rotational partition function. The term in parentheses is the computer calculated sum. Substitution of this value into (9) and use of (8) served as a check on the adequacy of the range of summation over J and K. The R.H.S. of expression (9) is correct in as far as rotational quantisation may be neglected in deriving the relation between a band intensity and the vibrational transition moment. The correction term for both the parallel and perpendicular cases is (9)

$$1 + \frac{2Bc [1 + \exp(-h\nu_0/kT)]}{\nu[1 - \exp(-h\nu_0/kT)]}$$

and leads to a correction of less than 1% in the cases discussed. For this reason it has been neglected in eq. (8) and eq. (9).

The average absorption coefficient,  $\bar{a}(\nu)$ , within a frequency interval,  $\Delta\nu$ , and at a particular frequency,  $\nu$ , is related to the sum of the intensities due to transitions within that frequency range by (2).

$$\bar{a}(\nu) = \sum_{\nu-\frac{\Delta\nu}{2}}^{\nu+\frac{\Delta\nu}{2}} \frac{a(\nu)}{\Delta\nu} \quad (10)$$

Two conditions are required for satisfactory usage of equation (10). Firstly, the density of transitions within the chosen interval is sufficiently high for the edge effects arising from finite band widths to be negligible and secondly, that saturation of absorption over a given small frequency interval within the chosen interval does not occur. The former condition is certainly satisfied for heavy polyatomic molecules such as  $C_6H_6$ ,  $C_6D_6$  and  $C_6F_6$  and the latter situation does not, in fact, arise in infrared spectroscopy.

We have calculated the quantity  $\bar{C}_{A_{J,K}} S_{J,K} \nu_{J,K} e^{-F_{J,K} hc/kT}$  for selected infrared bands of  $C_6H_6$ ,  $C_6D_6$  and  $C_6F_6$  by direct summation on an electronic computer for  $J', J'' 0 \rightarrow 250$  and in frequency intervals of  $0.2 \text{ cm.}^{-1}$ . The parameters employed for  $C_6H_6$ ,  $C_6D_6$  and  $C_6F_6$  are listed in table 1.

The transition moment for the particular vibration has been determined from a comparison of the  $\alpha(\nu)$  values at the frequencies of the P- and R-branch maxima for the calculated and experimental band contours.

### RESULTS

The results are shown in table II. For the  $e_{1u}$  degenerate bands, the infrared band shapes are a function of the first order Coriolis coupling constant,  $\zeta_{11}$ . The  $\zeta_{11}$  value for the particular vibration must be determined before the transition moment can be derived from a comparison of the  $\alpha_{max}^P$  or  $\alpha_{max}^R$  values for the calculated and experimental bands. Some authors (6) have suggested that the frequency separation of the P- and R-branch maxima is sufficient criteria for the evaluation of reliable  $\zeta_{11}$  values. In the present work this procedure has proved somewhat less satisfactory than a detailed comparison of calculated and experimental band contours along the lines suggested by Edgell and Moynihan (2).

For the two lowest  $e_{1u}$  bands of both  $C_6H_6$  and  $C_6D_6$  the calculated and experimental band contours show good agreement with the values of  $\int_{ii}$  given in table 1. Only the lowest  $e_{1u}$  band of  $C_6F_6$  has been studied (see part II (10)). The remaining  $e_{1u}$  bands of  $C_6H_6$ ,  $C_6D_6$  and  $C_6F_6$  exhibit distorted band shapes as a result of Fermi resonance interactions and are therefore unsuitable for the present study.

The solitary  $a_{2u}$  mode of each molecule has also been studied. In the case of the  $a_{2u}$  mode of  $C_6D_6$  the interpretation of the experimental band is rendered complex due to the existence of sharp fine structure of uncertain origin.

A typical set of calculated and experimental band contours are shown in fig. 1 for the  $e_{1u}$  band of  $C_6H_6$  at  $1038\text{ cm.}^{-1}$ .

It is apparent from the results that, at least in the absence of higher order perturbations, accurate values of vibrational transition moments can be obtained from a comparison of  $\alpha_{\max}^P$  and  $\alpha_{\max}^R$  values for the calculated and experimental band contours.

TABLE I

Molecule	Symmetry Species	Frequency $\text{cm.}^{-1}$	$\alpha_{\max}^P$ (expt) $\times 10^{-19}$	$\alpha_{\max}^R$ (expt) $\text{mol.}^{-1}\text{cm.}^2$	Zeta Value $\int_{ii}$
$C_6H_6$	$e_{1u}$	1483	0.525	0.535	-0.45
	$e_{1u}$	1038	0.359	0.360	-0.55
	$a_{2u}$	673	4.420	4.600	-
$C_6D_6$	$e_{1u}$	1335	0.118	0.110	-0.40
	$e_{1u}$	814	0.357	0.316	-0.40
	$a_{2u}$	494	1.660	1.880	-
$C_6F_6$	$e_{1u}$	315	0.231	0.241	-0.60
	$a_{2u}$	215	0.231	0.262	-

Rotational Constants (A=B=2C)cm.<sup>-1</sup>

C<sub>6</sub>H<sub>6</sub> 0.188960

C<sub>6</sub>D<sub>6</sub> 0.156275

C<sub>6</sub>F<sub>6</sub> 0.034676

Values of  $\alpha(\nu)$  expt are obtained from:-

$$\alpha(\nu)_{\text{expt}} = \frac{22400}{N} \cdot \frac{760}{P} \cdot \frac{273+t}{273} \cdot \frac{2.303}{l} \cdot \log_{10} \frac{I_0}{I}$$

where N is the Avagadro number, p is the pressure of the vapour in mm Hg, t is the temperature in °C, l is the path length of the cell and  $\log_{10} \frac{I_0}{I}$  is the absorbance at a frequency  $\nu$ .

TABLE II

Molecule	Symmetry Species	Frequency cm. <sup>-1</sup>	$\left(\frac{\delta\mu}{\delta Q}\right)^{\text{INT}}$	$\left(\frac{\delta\mu}{\delta Q}\right)^{\text{P}}$	$\left(\frac{\delta\mu}{\delta Q}\right)^{\text{R}}$
	e <sub>1u</sub>	1483	± 0.39 <sup>a</sup>	± 0.38	± 0.39
C <sub>6</sub> H <sub>6</sub>	e <sub>1u</sub>	1038	± 0.32 <sup>a</sup>	± 0.33	± 0.32
	a <sub>2u</sub>	673	± 1.46 <sup>a</sup>	± 1.43	± 1.39
	e <sub>1u</sub>	1335	± 0.18 <sup>b</sup>	± 0.17	± 0.16
C <sub>6</sub> D <sub>6</sub>	e <sub>1u</sub>	814	± 0.31 <sup>b</sup>	± 0.30	± 0.27
	a <sub>2u</sub>	494	± 1.09 <sup>b</sup>	± 0.92	± 0.93
	e <sub>1u</sub>	315	± 0.17 <sup>c</sup>	± 0.17	± 0.17
C <sub>6</sub> F <sub>6</sub>	a <sub>2u</sub>	215	± 0.25 <sup>c</sup>	± 0.28	± 0.29

$\left(\frac{\delta\mu}{\delta Q}\right)^{\text{INT}}$ .

dipole gradient obtained from integrated band area.

$\left(\frac{\delta\mu}{\delta Q}\right)^{\text{P}}, \left(\frac{\delta\mu}{\delta Q}\right)^{\text{R}}$

dipole gradients obtained from comparison of  $\alpha(\nu)$  values at P- and R-branch maxima for calculated and experimental curves.

a data of Spedding and Whiffen (7)

b data of Dows and Fratt (8)

c data of Steele and Wheatley (10)

- 1 S.L. Gerhard and D.M. Dennison, Phys. Rev. 43, 197 (1933).
- 2 W.F. Edgell and R.E. Moynihan, J. Chem. Phys. 43, 1205 (1966).
- 3 W.F. Edgell and R.E. Moynihan, J. Chem. Phys., 27, 155 (1957).
- 4 a) H. Hönl and F. London, Z. Physik 33, 803 (1925).  
b) H. Hönl and F. London, Ann. d. Phys. 79, 273 (1926).  
c) F. Reiche and H. Rademaker, Z. Physik 39, 444 (1926)  
and 41, 453 (1927).
- 5 R.S. Mulliken, J. Chem. Phys., 23, 1997, (1955).
- 6 L.C. Hoskins, J. Chem. Phys., 45, 4594, (1966).
- 7 H. Spedding and D.H. Whiffen, Proc. Roy. Soc. (London)  
A238, 245 (1956).
- 8 D.A. Dows and A.L. Pratt, Spectrochim. Acta, 18, 433 (1962).
- 9 B.L. Crawford and H.L. Dinsmore, J. Chem. Phys., 18, 1682,  
(1950).
- 10 D. Steele and W. Wheatley - accompanying paper.



Studies in Vibrational Absorption Intensities

Part II Vibronic Effects in Hexafluorobenzene and Benzene

by D. Steele and W. Wheatley

Department of Chemistry, Royal Holloway College,  
University of London, Englefield Green, Surrey.

### Abstract

The absolute infra-red absorption intensities of the low frequency fundamentals of hexafluorobenzene have been measured - both by direct integration of extinction coefficients and by the P, R band maximum technique. An analysis of results in terms of the simple bond moment hypothesis and an electron rehybridisation moment accompanying the out of plane substituent deformation has lead to value of 0.3 D per radian for the latter. This is equal to the value for benzene. The <sup>in</sup><sub>λ</sub> sensitivity of both the C<sub>6</sub>F<sub>6</sub> and the C<sub>6</sub>H<sub>6</sub> results on the force fields, and the e<sub>1u</sub> first order Coriolis coupling constants in particular, is sufficiently low for the equality of the results to be significant.

Proofs to: Dr. D. Steele, Department of Chemistry,  
Royal Holloway College, Englefield Green, Surrey.

### Introduction

The use of the independent bond moment hypothesis (IBMH) to interpret the absolute intensities of infrared absorption bands generally results in different values of a derived bond parameter for the various symmetry species of the same molecule. Such discrepancies have often been explained by invoking the idea of a rehybridisation phenomena associated with certain modes. Thus Spedding and Whiffen [1] on the basis of the IBMH have derived an effective CH bond dipole of 0.6 D/rad. from the absolute absorption intensity of the  $a_{2u}$  mode of benzene and a value of 0.3 D/rad. from the intensities of the three normal vibrations of the  $e_{1u}$  species. In the motion described by the  $a_{2u}$  mode, the substituent moves out of the plane of the carbon skeleton with the result that the rehybridisation around the carbon nucleus will tend from a planar  $sp^2$  configuration to a non-planar  $sp^3$  configuration. This will produce an increase of electron density on the opposite side of the benzene ring to the substituent making the H end of the CH bond dipole appear more positive than that obtained from an in-plane motion of the substituent. There is strong evidence [2] [3] to suggest that the H atom is at the positive end of a CH bond dipole so that the larger value for the effective CH bond dipole as derived from the  $a_{2u}$  mode is consistent with this theory and would predict a rehybrid-

sation moment (RM) in benzene of 0.3 D/rad.

Kovner and Snegirev [4] refute such an interpretation on the grounds that the effective CH bond dipole cannot be different for the two motions. These workers ignore completely the rehybridisation phenomenon and prefer to explain the discrepancy which results from using the IBMH by introducing cross terms such as  $\delta\mu_i / \delta\beta_j$  into the theory. On this basis, the effective CH bond dipoles derived from the two motions are indeed the same and equal to 0.6 D/rad. This agrees with the value obtained by Spedding and Whiffen from the  $a_{2u}$  mode as indeed it must since no cross terms appear in the dipole derivative expressions for this mode.

It is the authors' belief that the rehybridisation phenomenon and associated vibronic effects are of importance and are certainly of more physical meaning than the cross terms in the dipole derivative expressions. Furthermore, we feel that these effects may be responsible for many of the inconsistencies which exist in the reported values of derived bond parameters and also for the discrepancies which frequently occur between intensity data for condensed and solution phases and the values obtained from vapour phase intensity data using dielectric theories. The work described in this paper was undertaken with the primary aim of justifying

the existence of a RM and to attach some meaning to its potential importance. Since the RM phenomenon only involves the electron cloud associated with the carbon nuclei, it is anticipated that the RM should be insensitive to the nature of the substituent on the aromatic ring. For vapour phase intensity studies in the infrared region a volatile compound of high symmetry is essential. Apart from benzene itself, hexafluorobenzene (HFB) is the only volatile aromatic molecule of  $D_{6h}$  symmetry and its remarkable similarity to benzene makes it a natural choice for this project. If an interpretation of the absolute infrared intensities of HFB using the IBMH is consistent with a RM of about 0.3 D/rad. then the inference is strong that the rehybridisation phenomenon is realistic and of significance.

HFB has four infrared active modes which have been assigned [5] to the three  $e_{1u}$  vibrations at 1531, 1006 (doublet) and 315  $\text{cm}^{-1}$  respectively and the  $a_{2u}$  vibration at 215  $\text{cm}^{-1}$ . The two high frequency modes have been previously studied by Steele and Whiffen [6] and one of these modes has also been studied by Person et al. [7]. The agreement between the absolute intensity data is excellent. Recently, Person et al. [7] have reported the absolute intensities for the two low frequency modes of HFB. The results are in poor agreement with those obtained in this work and,

in fact, a revised value for the absolute intensity of the  $315 \text{ cm.}^{-1}$  band has been quoted by Crawford et al. [8] which is in better agreement with ours.

### Experimental

The sample of HFB used in this work was a gift from Imperial Smelting Co. Ltd. Vapour phase chromatography of the sample and its infrared spectrum showed no trace of other components and the sample was used without further purification. B. pt.  $80.1^{\circ}\text{C}/760 \text{ mm.}$ , m.pt.  $5.5^{\circ}\text{C}$ .

The vapour phase intensities of the two low frequency fundamentals of HF3 were determined on an evacuated single beam grating spectrometer described elsewhere [9]. Linearity of the amplifier and detector system and uniformity of illumination over the slits has been verified by showing that the signal on the recorder is proportional to the square of the slit width as required for coupled entrance and exit slits to and from the monochromator. The spectral slit width was about  $1 \text{ cm.}^{-1}$ .

A 12 cm. gas cell with high density polythene (Rigidex) windows was used for sample containment. HF3 vapour was introduced into the evacuated cell in situ and nitrogen gas was introduced for pressure broadening to a total pressure of 1 atm. There was no evidence for intensity variation with

time and subsequent re-running of the background spectrum showed no traces of residual vapour. On this basis, possible absorption of the vapour by the polythene windows can be considered as being negligible.

A satisfactory Beer's law plot was obtained for the  $315 \text{ cm.}^{-1}$  band (fig. 1). In the case of the  $a_{2u}$  band at  $215 \text{ cm.}^{-1}$  the Beer's law plot was less satisfactory. Following Spedding and Whiffen [1], the contribution of the Q-branch to the  $215 \text{ cm.}^{-1}$  band was artificially separated from the P- and R-branches by taking frequency cut-offs at specific frequencies near minima. The separated P- and R-components gave a satisfactory Beer's law plot thus confirming that it is the sharp Q-branch which violates the Wilson-Wells conditions. The correct intensity of the Q-branch was obtained by extrapolating to zero pressure.

#### Band Shape Calculations

The object of the band shape calculations was twofold. Firstly, the force field for HFB is extremely ill-defined. Thus the quadratic force constant matrix for the  $e_{1u}$  symmetry species contains six independent terms - but there are only three experimental frequencies with which to evaluate these. In principle, the determination of first order Coriolis coupling constants from infrared band contours could furnish additional parameters. For HFB, only the  $e_{1u}$  mode at

315  $\text{cm.}^{-1}$  is expected to be free from Fermi resonance effects and the only second order Coriolis interaction which is likely to be of importance is that with the  $a_{2u}$  mode at 215  $\text{cm.}^{-1}$ . It will be shown later that this effect is unimportant in this instance. The first order Coriolis coupling constant associated with the 315  $\text{cm.}^{-1}$  mode furnishes an important test of the assumed force field.

The second object was to determine whether or not any apparent loss of Q-branch intensity had occurred in the 315 and 215  $\text{cm.}^{-1}$  experimental bands through inadequate pressure broadening. In addition, knowledge of the normalization factor for the theoretically computed band contours should allow the absolute intensity of an experimental band to be evaluated by fitting a convenient point on the computed band contour, such as the P- or R-branch maximum, to the experimental value as described in part 1 [10].

The experimental band shapes of the 315 and 215  $\text{cm.}^{-1}$  bands of HF3 show a marked asymmetry with ~5% difference in the intensities of the P- and R-branches. The low frequency P-branch is weaker for both bands. If the asymmetry had been caused by second order Coriolis coupling then the asymmetry of the  $e_{1u}$  band would have been the mirror image of that in the  $a_{2u}$  band [11]. To explain the asymmetry it is necessary to allow for differences between the ground and excited state rotational constants. Good agreement between the experimental



and computed band shapes was obtained with  $(B' - B'')/3'' = 0.0005$ . Figs. <sup>2</sup>3 and <sup>3</sup>4 show the computed and observed band contours of the  $315 \text{ cm.}^{-1}$  band for a series of zeta values and the influence of rotational constant changes. The band shape analysis leads to a Coriolis zeta value of  $-0.60 \pm 0.05$  for the  $315 \text{ cm.}^{-1}$  ( $e_{1u}$ ) band of HFB.

The experimental and computed band contours differ for two reasons. No account has been taken of 'hot bands' which are likely to be of importance at such low frequencies and also because the experimental bands were pressure broadened. Both factors lead almost solely to broadening of the Q-branch. We have separately estimated the intensity in the P, Q and R-branches of the experimental and computed bands. The ratios of the Q-branch to the combined P- and R-branch intensities are in good agreement and in the case of the  $215 \text{ cm.}^{-1}$  ( $a_{2u}$ ) band the ratio also agrees with that derived from the expression given by Gerhard and Dennison [12], where

$$\text{Fractional intensity in Q-branch} = \frac{[-\beta/1+\beta]^{\frac{1}{2}} - \sin^{-1}(-\beta)^{\frac{1}{2}}}{-\beta(-\beta/1 + \beta)^{\frac{1}{2}}}$$

$\beta = \frac{C}{B} - 1 = -\frac{1}{2}$  for disk-shaped molecules.

It must be concluded that any errors which might arise in the measured intensities due to inadequate pressure broadening are less than 5%.

The possibility of estimating integrated band intensities from computed band shapes has been examined in part 1 [10]. The absorption coefficient at a suitable frequency is computed in terms of the dipole derivative with respect to the normal coordinate associated with the particular vibration and is compared with the experimental value. Following this procedure, the dipole derivatives for the  $215 \text{ cm.}^{-1}$  ( $a_{2u}$ ) and  $315 \text{ cm.}^{-1}$  ( $e_{1u}$ ) vibrations were derived to be  $\pm 0.28 \times 10^{-10}$  (a.m.u.) $^{-\frac{1}{2}}$  D/Å and  $\pm 0.17 \times 10^{-10}$  (a.m.u.) $^{-\frac{1}{2}}$  D/Å respectively which are in excellent agreement with the values of  $\pm 0.25 \times 10^{-10}$  (a.m.u.) $^{-\frac{1}{2}}$  D/Å and  $\pm 0.17 \times 10^{-10}$  (a.m.u.) $^{-\frac{1}{2}}$  D/Å obtained from the integrated band areas.

#### The Force Field and The L Matrix

The force constant for the  $a_{2u}$  species is exactly defined within the quadratic approximation by the experimental frequency. For the  $e_{1u}$  class, Steele and Whiffen [13] derived a set of force constants based on assumptions which were chosen to minimize the interaction constants and to retain a field having the form of Whiffen's benzene force field [14]. Whilst these assumptions are now known to be ill chosen [15] there seems little point at present in deriving what must be an equally arbitrary field for  $C_6F_6$  based on a new set of assumptions. Fortunately we shall demonstrate that the

derived effective bond dipoles are, in this case, not very sensitive to changes in the force field. The F and L matrices are shown in table II, the force constants <sup>being</sup> ~~are~~ taken from Steele and Whiffen [13].

We have calculated the Coriolis zeta matrix for the  $e_{1u}$  species of  $C_6F_6$  using the expressions of Meal and Polo [16]. The zeta sum (trace) is equal to -1 [17]. The agreement between the calculated  $f_{20,20}$  value (-0.596) and the value of -0.60 obtained from the band shape analysis is well within the experimental uncertainty. The Jacobian elements of  $f_{20,20}$  with respect to the force constants have been calculated using the method described by Mills [18]. It is seen in table III that the sensitivity is primarily with respect to  $F_{18,18}$  and  $F_{18,20}$  whereas the frequency is dependent almost entirely on  $F_{18,18}$  and  $F_{18,19}$ .

To confirm the insensitivity of the  $\frac{\Delta \lambda_i}{\Delta J_\beta}$  to the field a new  $L$  matrix was computed corresponding to changes in  $J$  of  $J_{18,18}$  0.991  $\rightarrow$  1.03 and  $J_{18,20}$  0.197  $\rightarrow$  0.080 (values chosen to keep  $\lambda_{20}$  near observed value).

The new eigenvector matrix was

.4185, .3430, .1960
-.4601, -.1846, .0640
.3052, -.2067, .0043

These minor changes in the  $L$  matrix produced no significant changes in the derived dipole gradients. The corresponding change in  $f_{20,20}$  is only -0.022.

Interpretation of Intensities in Terms of Bond Parameters

Values for the dipole moment derivative with respect to the associated normal coordinate,  $\delta\mu/\delta Q_i$ , are obtained from the experimental band intensities using the expression

$$\Gamma_i = \frac{N\pi g_i}{3c^2\nu_0} \left( \frac{\delta\mu}{\delta Q_i} \right)^2$$

where  $N$  is Avagadro's number,  $g_i$  is the degeneracy factor (equal to 2 for  $e_{1u}$  modes and equal to 1 for the  $a_{2u}$  mode) and  $c$  is the velocity of light. The values of the dipole derivatives with respect to the symmetry coordinates,  $\delta\mu/\delta S_j$  are derived from the  $\delta\mu/\delta Q_i$  values using the coordinate transformation  $S = LQ$ . Table IV contains the possible solutions for  $\delta\mu/\delta S_j$  which are obtained from the various sign combinations of  $\delta\mu/\delta Q_i$ . To relate the  $\delta\mu/\delta S_j$  values to quantities which are directly related to bond properties we make use of the expressions derived by Spedding and Whiffen [1] for their interpretation of the intensities of benzene. Calculated values of the dipole moment derivatives with respect to CC stretching,  $\Delta R$ , CF stretching,  $\Delta r$ , CF deformation in the plane of the ring,  $\Delta\beta$ , and CF deformation out of the plane of the ring,  $\Delta\delta$ , are also given in table 4. Of the four possible solutions for the derived bond parameters in the  $e_{1u}$  species, only those obtained from the sign choice for

$\delta\mu/\delta Q$  of  $(\pm\pm\pm)$  and  $(\pm\pm\mp)$  can be regarded as probable. The solutions obtained from the sign choice  $(\pm\mp\mp)$  and  $(\pm\mp\pm)$  are completely unreasonable. We must now decide between the two more appropriate solutions, both of which give reasonable values for the effective bond dipoles. The solution obtained from the sign choice for  $\delta\mu/\delta Q$  of  $(\pm\pm\pm)$  gives a value for  $\delta\mu/\delta\beta$  which is greater than  $\delta\mu/\delta\gamma$  by an amount  $0.3D/\text{rad}$ . whereas the sign choice for  $\delta\mu/\delta Q$  of  $(\pm\pm\mp)$  shows  $\delta\mu/\delta\beta$  to be almost equal to  $\delta\mu/\delta\gamma$ . Thus the solution obtained from  $(\pm\pm\pm)$  yields a rehybridization moment of  $0.3D/\text{rad}$ . which is equal, but in the opposite direction, to that obtained for benzene. The solution obtained from  $(\pm\pm\mp)$  predicts an almost zero rehybridization moment. This solution can be rejected on the grounds that the relative signs of  $\delta\mu/\delta\beta$  and  $\delta\mu/\delta\Delta r$  are changed. Accepting that the fluorine atom is at the negative end of the CF dipole this would require the fluorine atom to become more positive on stretching which is contrary to general beliefs on this matter.

A rehybridization<sup>s</sup> moment<sup>m</sup> of the same order of magnitude as in the case of benzene is anticipated for hexafluorobenzene since such a moment will involve only the  $\pi$  electrons associated with the carbon nucleus. If we accept the available evidence [2][3] that in benzene the hydrogen atom is at the positive end of a moving CH dipole then it seems most likely that in HFB the fluorine atom is at the negative end of a

moving CF dipole. For out-of-plane deformation of a CH bond in benzene, rehybridization at the carbon atom takes place in the form of s-character being introduced into the  $p_z$  orbital. The effect is to make the hydrogen atom appear more positive and therefore the effective bond dipole for out-of-plane deformation is greater than for the in-plane motion. In the case of HFB the effect of rehybridization changes during out-of-plane deformation is also to make the fluorine atom appear more positive i.e. less negative so that we expect the effective CF bond dipole for out-of-plane deformation to be less than for the in-plane motion.

Our results show that an interpretation of the absolute infrared intensities of  $C_6F_6$ ,  $C_6H_6$  and  $C_6D_6$  using the IBMH is consistent with a rehybridization moment of 0.3D/rad. The inference is strong that the rehybridization phenomenon is indeed realistic and of significance.

In view of the rather large second dipole derivatives  $\partial^2 \mu / \partial \delta^2$  derived by Dunstan and Whiffen [19] for benzene it is necessary to consider the implications of higher terms in the dipole expansion on the rehybridization moment. Within the mechanical harmonic oscillator approximation, there is no contribution from these higher terms and it is well known that anharmonicities in aromatic compounds are low at least in CH bending modes. Boobyer [20] has examined the

effect of electrical and mechanical anharmonicities in CH stretching modes and it was concluded that the electrical anharmonic terms make little contribution to the fundamental intensities even though their numerical magnitude in  $D/\overset{\circ}{\text{A}}$  were often several times greater than the value of  $\delta\mu / \delta\Delta r$  in  $D/\overset{\circ}{\text{A}}$ . It appears then that it is legitimate to retain the approximation of electrical harmonicity.

The Rehybridization Moment in  $C_6H_6$  and  $C_6D_6$

In view of the changes in the force field of benzene which have been proposed since the work of Spedding and Whiffen [1] it is necessary to reconsider their intensity data in terms of the alternative fields [15][21]. The force field for the  $e_{1u}$  species is still very much ill-defined and all that can be achieved at present is to show that the various force fields lead to the same value for  $\delta\mu / \delta\beta$ . The results obtained by using the  $L(e_{1u})$  matrices of Whiffen [14] [22], Scherer [21] and Duinker and Mills [15] to interpret the absolute intensity data for  $C_6H_6$  [1] and  $C_6D_6$  [23] are shown in table V. It is seen that the differences in the values of  $\delta\mu / \delta\beta$  are quite insignificant. This result gives one good grounds to anticipate that future refinements to the force field of benzene will leave the present analysis unchanged.

Confirmation of the (+++) solution is obtained from a study of the deuterated benzenes. The (---) solution leads to drastically different  $\frac{\delta\mu}{\delta S_{20}}$  in  $C_6H_6$  and  $C_6D_6$  (reflected in  $\frac{\delta\mu}{\delta\Delta R}$  in table V) and to an unsatisfactory ratio for the intensities of the  $B_{2u}$  bands of p.  $C_6H_4D_2$  at 2278 and 1475  $cm^{-1}$ . This is true for all three fields. For example using the Duinker-Mills Field the intensity ratio for the two solutions are 1.77 and 0.97 respectively (observed 1.74). There appears to be no doubt then that the (+++) solution is indeed the correct one despite theoretical indications that  $\delta\mu/\delta\Delta R$  could be expected to be large [24].

Acknowledgements.

We thank the Hydrocarbon Research Group of the Institute of Petroleum who supported this research, Imperial Smelting Co. Ltd. who donated the sample of hexafluorobenzene used in this work and the University of London Central Research Fund who purchased the Golay Amplifier used in the experimental section.



Table I. The measured intensities of the vibrational transitions of hexafluorobenzene.

Symmetry Species	Frequency cm. <sup>-1</sup>	Integrated Intensity $\int$ , mol. <sup>-1</sup> cm. <sup>2</sup> x 10 <sup>-20</sup>	$\frac{\delta\mu}{\delta Q} \times 10^{-10}$ (a.m.u.) <sup>1/2</sup> D/R
	1530	5.93	± 2.543
e <sub>1u</sub>	1020 - 1002	6.70	± 2.197
	315	0.132	± 0.172
a <sub>2u</sub>	215	0.201	± 0.247

Table II. The force field and  $\mathcal{L}$  matrix for  $C_6F_6$

Force constants in Dynes/Å		The $\mathcal{L}$ Matrix (a.m.u.) <sup>-1/2</sup>			
$F_{18,18}$	0.991		$S_{18}$	$S_{19}$	$S_{20}$
$F_{18,19}$	0.1216	$Q_{18}$	.41759	.34223	.19930
$F_{18,20}$	0.197	$Q_{19}$	-.45913	-.18750	.06296
$F_{19,19}$	3.701	$Q_{20}$	.30618	-.20538	.00061
$F_{19,20}$	0.9984				
$F_{20,20}$	7.509				

$$S_{18} = \frac{1}{2r_0} (\Delta\beta_2 + \Delta\beta_3 - \Delta\beta_5 - \Delta\beta_6)$$

$$* S_{19} = \frac{1}{\sqrt{2}} (-\Delta R_1 + \Delta R_3 + \Delta R_4 - \Delta R_6)$$

$$S_{20} = \frac{1}{\sqrt{12}} (-2\Delta r_1 - \Delta r_2 + \Delta r_3 + 2\Delta r_4 + \Delta r_5 - \Delta r_6)$$

$$S_{11} = \frac{r_0}{\sqrt{6}} (\Delta\delta_1 + \Delta\delta_2 + \Delta\delta_3 + \Delta\delta_4 + \Delta\delta_5 + \Delta\delta_6).$$

\* Note that the unusual normalisation factor for  $S_{19}$  arises because the full set of symmetry co-ordinates includes

$$S_{19a} = \frac{1}{2} (-\Delta R_1 + \Delta R_3 + \Delta R_4 - \Delta R_6)$$

$$S_{21a} = \frac{R}{\sqrt{12}} (-2\alpha_1 - \alpha_2 + \alpha_3 + 2\alpha_4 + \alpha_5 - \alpha_6)$$

The  $E_{1u}$  redundancy condition can be written  $\frac{1}{\sqrt{2}}(S_{19} + S_{21}) = 0$ , so that a satisfactory symmetry co-ordinate orthogonal to above is  $\frac{1}{\sqrt{2}}(S_{19} - S_{21})$ .

Finally substituting  $S_{19} = -S_{21}$  the above  $S_{19}$  is arrived at. This last substitution may not, of course, be applied prior to evaluation of the symmetrised  $F$  matrix, which must show the correct  $\alpha$  dependence.

Table III. The zeta matrix of  $C_6F_6$  and its Jacobian

	$\zeta_{18}$	$\zeta_{19}$	$\zeta_{20}$
$Q_{18}$	-.8384	-.4815	-.2555
$Q_{19}$		.4345	.7612
$Q_{20}$			-.5961

$\zeta_i \zeta_j$	18,18	19,19	20,20
18,18	-.208	.369	-.161
18,19	-.315	-.335	.020
18,20	-.047	-.092	.139
19,19	-.095	.073	.022
19,20	-.053	.009	.044
20,20	.078	-.078	.0

Table IV. The derived dipole gradients of  $C_6F_6$ .

Force Field	Sign Choice for $\delta\mu/\delta Q$	$\frac{\delta\mu}{\delta S_{18}}$	$\frac{\delta\mu}{\delta S_{19}}$	$\frac{\delta\mu}{\delta S_{20}}$	$\frac{\delta\mu}{\delta \beta}$	$\frac{\delta\mu}{\delta \Delta r}$	$\frac{\delta\mu}{\delta \Delta R}$
Steele	+++ ---	$\pm 0.866$	$\pm 0.088$	$\mp 9.341$	$\pm 0.650$	$\mp 5.393$	$\mp 0.328$
	+- -+-	$\mp 0.373$	$\mp 1.467$	$\mp 9.984$	$\mp 0.278$	$\mp 5.768$	$\mp 1.026$
and Whiffen	+--+ -+-	$\mp 1.165$	$\pm 6.410$	$\pm 2.898$	$\mp 0.874$	$\pm 1.673$	$\pm 5.772$
	[13] +-- -+-	$\mp 2.404$	$\pm 4.856$	$\pm 2.255$	$\mp 1.804$	$\pm 1.302$	$\pm 5.074$

$$\frac{\delta\mu}{\delta S_{11}} = \pm 0.670 \quad \frac{\delta\mu}{\delta \delta} = \pm 0.351$$

Table V. The dipole gradients of  $C_6H_6$  and  $C_6D_6$  as derived using different force fields.

Force Field	Sign Choice for $\delta\mu/\delta Q$	$C_6H_6$			$C_6D_6$		
		$\delta\mu/\delta\beta$	$\delta\mu/\delta\Delta r$	$\delta\mu/\delta\Delta R$	$\delta\mu/\delta\beta$	$\delta\mu/\delta\Delta r$	$\delta\mu/\delta\Delta R$
Whiffen [14][22]	+++	+0.316	+0.465	+0.001	+0.318	+0.437	+0.028
	+++	+0.023	+0.397	-0.892	-0.166	+0.374	-0.722
	+++	-0.013	+0.533	+0.780	+0.192	+0.569	+0.472
	+++	-0.306	+0.466	-0.113	-0.293	+0.470	-0.223
Duinker and Mills [15]	+++	+0.318	+0.471	+0.070	+0.316	+0.468	-0.061
	+++	+0.045	+0.400	-0.868	-0.176	+0.373	-0.721
	+++	-0.036	+0.531	+0.767	+0.210	+0.568	+0.455
	+++	-0.309	+0.461	-0.171	-0.291	+0.473	-0.206
Scherer [21]	+++	+0.313	+0.460	-0.053	+0.318	+0.480	+0.006
	+++	+0.004	+0.396	-0.906	-0.158	+0.377	-0.719
	+++	+0.006	+0.534	+0.789	+0.181	+0.571	+0.491
	+++	-0.303	+0.470	-0.064	-0.295	+0.467	-0.234

References

1. H. Spedding and D.H. Whiffen, Proc. Roy. Soc. (London), A 238, 245, 1956.
2. R.P. Bell, H.W. Thompson and E.E. Vago, Proc. Roy. Soc. (London), A 192, 498, 1948.
3. A.R.H. Cole and A.J. Michell, Spectrochim. Acta., 20, 739, 1964.
4. M.A. Koyner and B.N. Snegirev, Optics and Spectroscopy, 9, 328, 1960.
5. D. Steele and D.H. Whiffen, Trans. Faraday Soc., 55, 369, 1959.
6. D. Steele and D.H. Whiffen, J. Chem. Phys., 29, 1194, 1958.
7. W.B. Person, D.A. Olsen and J.N. Fordenwalt, Spectrochim. Acta. 22, 1733, 1966.
8. T. Fujiyama and B. Crawford Jr., J. Phys. Chem., 72, 2174, 1968.
9. P.J. Hendra, R.D.G. Lane and B. Smethurst, J. Sci. Inst., 40, 457, 1963.
10. D. Steele and W. Wheatley, accompanying manuscript.

11. I.M. Mills, *Pure and Applied Chem.*, 11, 325, 1965.
12. S.L. Gerhard and D.M. Dennison, *Phys. Rev.*, 43, 197, 1933.
13. D. Steele, and D.H. Whiffen, *Trans. Faraday Soc.*, 56, 5, 1960.
14. D.H. Whiffen, *Phil. Trans. Roy. Soc. (London)*, A248, 131 1955.
15. J.C. Duinker and I.M. Mills, *Spectrochim. Acta*, 24A, 417, 1968.
16. J.H. Meal and S.R. Polo, *J. Chem. Phys.*, 24, 1126, 1956.
17. R.C. Lord and R.E. Merrifield, *J. Chem. Phys.*, 20, 1348, 1952.
18. I.M. Mills, *J. Mol. Spectry.*, 5, 334, 1960.
19. F.E. Dunstan and D.H. Whiffen, *J. Chem. Soc.*, 5221, 1960.
20. G.J. Boobyer, *Spectrochim. Acta*, 23A, 335, 1967.
21. J.R. Scherer, *Spectrochim. Acta*, 21, 321, 1965.
22. A.C. Albrecht, *J. Mol. Spectry*, 5, 236, 1960.
23. D.A. Dows and A.L. Pratt, *Spectrochim. Acta*, 18, 433, 1962.
24. T.L. Brown, *J. Chem. Phys.*, 43, 2780 (1965).

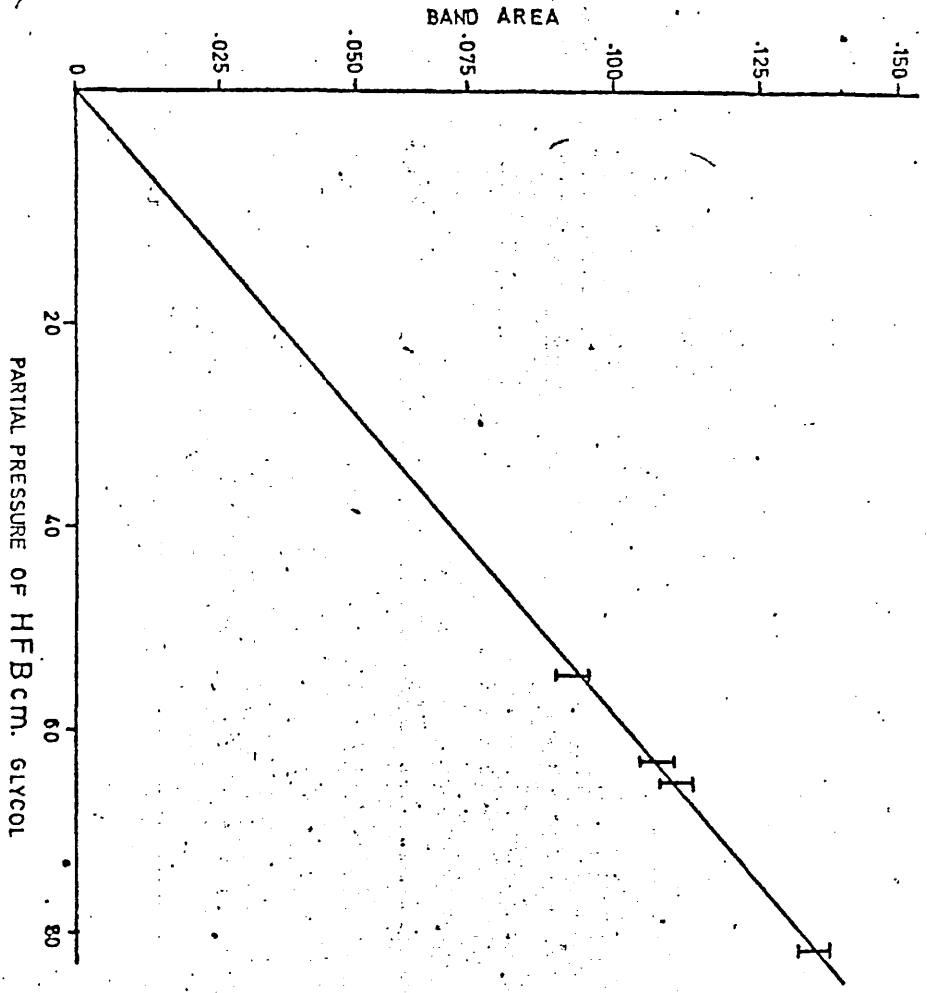
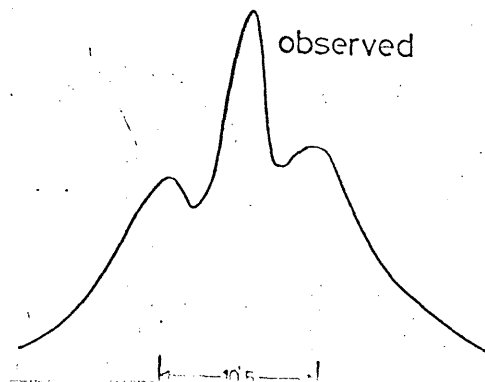
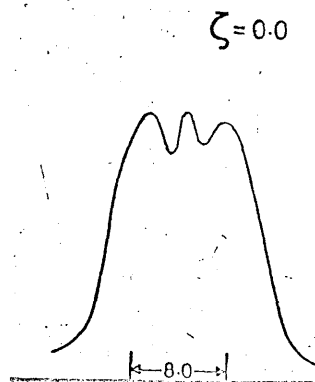
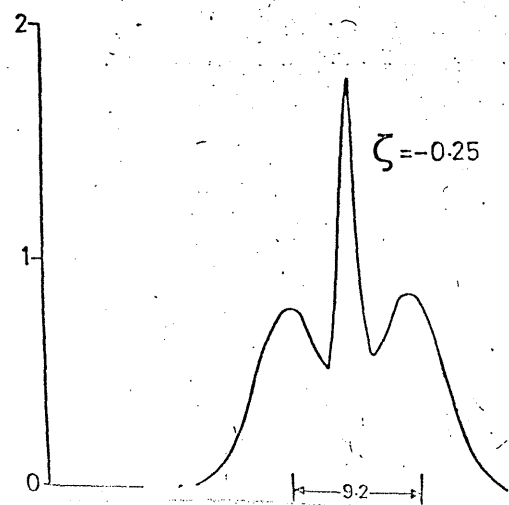
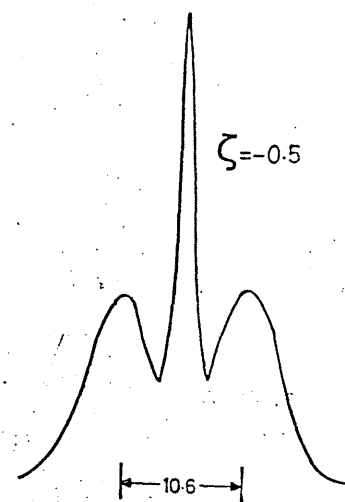
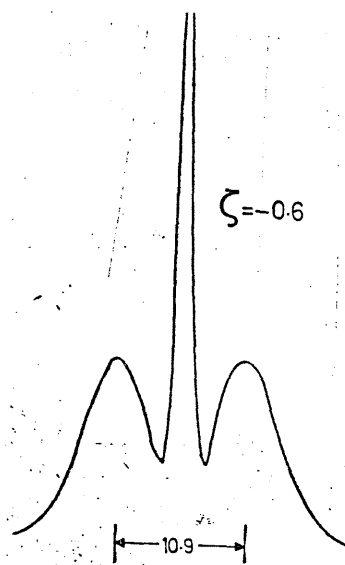
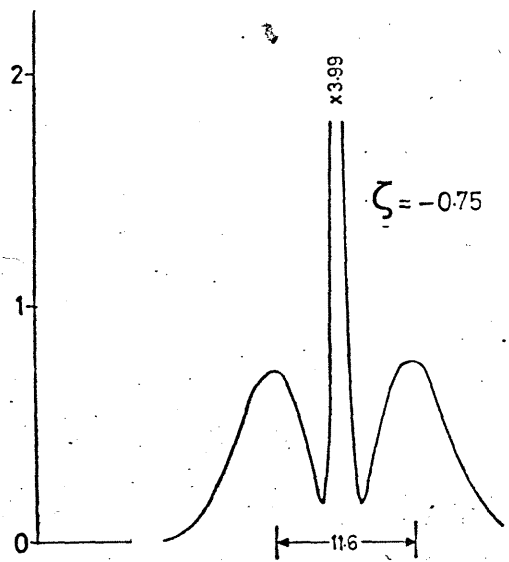


Fig. 1 Beer's Law Plot for E<sub>1u</sub> Band of HF B at 315 cm.<sup>-1</sup>





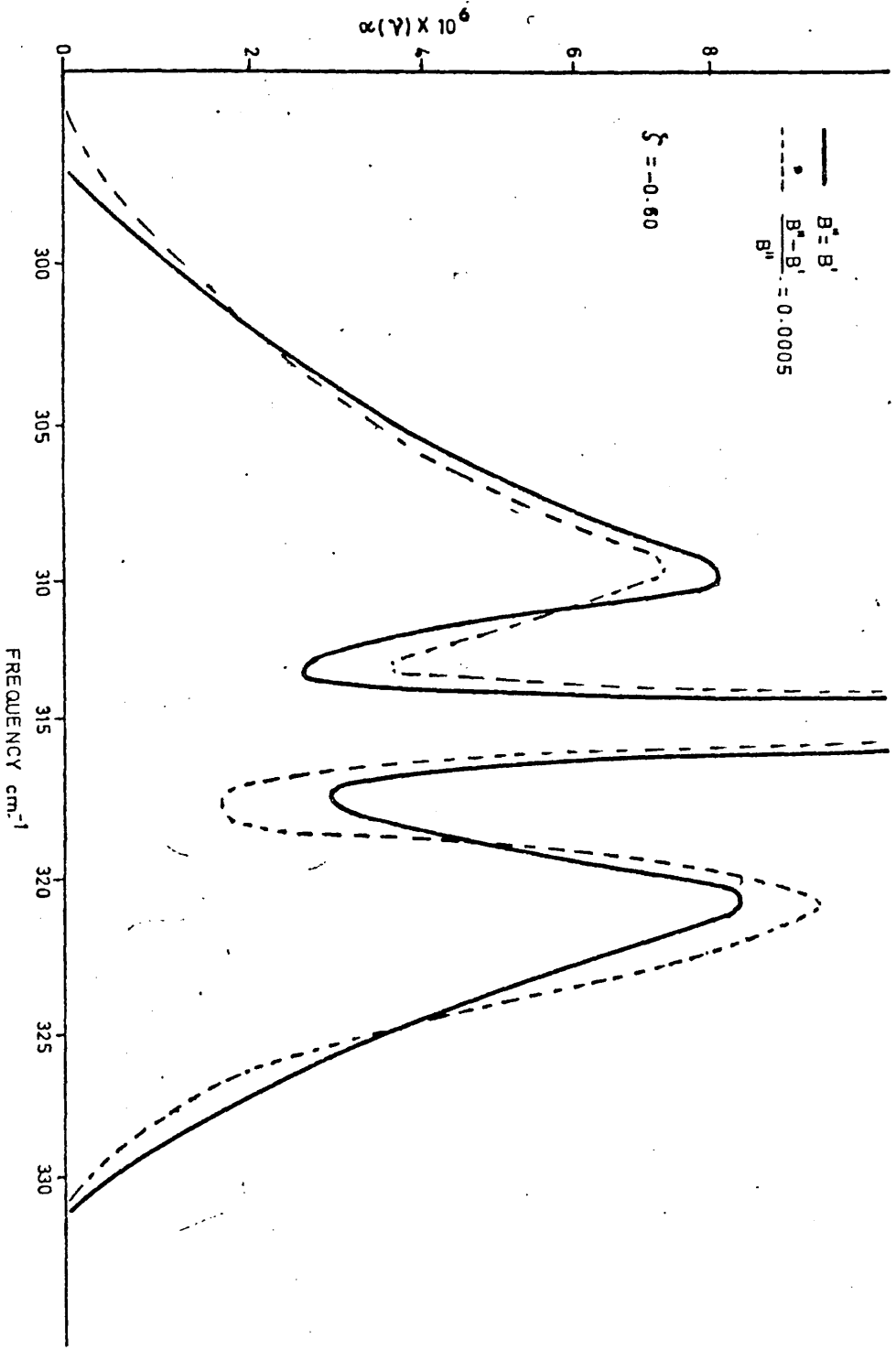


Fig 3 The Influence of Changes in Rotational Constant for the  $315\text{cm}^{-1}$  Band of HF B.

For these orientations the two molecules in the unit cell are magnetically equivalent.<sup>2</sup>

A typical ENDOR spectrum for succinic acid is shown in Fig. 1. Linewidths are in the range of 0.2 to 0.5 Mc. Linewidths in the EMR spectrum,<sup>2</sup> on the other hand, are in the range of 6 to 9 Mc. There are three pairs of strong lines in the upper two lines of the spectrum. Pairs  $a, a'$  and  $b, b'$  are due to the two  $\text{CH}_2$  protons while the pair  $c, c'$  is due to the CH proton. Pairs  $a, a'$  and  $b, b'$  vary over a range of less than 15% in frequency as the magnetic field is rotated relative to the crystal axis system while  $c, c'$  shows a much larger angular anisotropy.

The hyperfine splitting  $\Delta_i$  for proton  $i$  in the EMR spectrum of the free radical is related to the two ENDOR frequencies  $\nu_i$  and  $\nu_i'$  of that proton by

$$\Delta_i = \nu_i + \nu_i'. \quad (1)$$

The difference between  $\nu_i$  and  $\nu_i'$  is approximately twice the nuclear Zeeman frequency of 14 Mc. Splittings for the "forbidden"<sup>4</sup> ( $\Delta m_I = \pm 1$ ) hyperfine transitions are

$$\Delta_i = |\nu_i - \nu_i'|. \quad (2)$$

Preliminary calculations of  $\Delta_i$  based on ENDOR frequencies appear to be in general agreement with the values obtained from conventional EMR.<sup>2</sup>

In addition to the six lines mentioned above we note also a very intense line at 14.2 Mc surrounded by a number of weak satellites. This strong line is due to the depolarization of protons distant from the paramagnetic center.<sup>5</sup> The time required for recovery of the EMR signal after removal of the rf is of the order of 100 sec for the distant proton line while that for the intramolecular protons is 0.01 to 0.1 sec. This distant ENDOR appears to be very similar to the effect noted for distant aluminum nuclei in ruby.<sup>3</sup> The basic mechanism of the effect is that microwave power causes a dynamic polarization of distant nuclei which is removed by rf energy at the Larmor frequency of these nuclei. Satellite lines near the distant proton line correspond to hyperfine splittings of the unpaired electron by neighboring protons which are too small (less than 4 Mc) to be resolved in conventional EMR. Distant or depolarization ENDOR has also been observed in irradiated malonic acid.<sup>4</sup> This line shows the same relaxation characteristics as the distant ENDOR line in succinic acid.

Work is now in progress on the detailed calculation of the hyperfine tensors from ENDOR data.

<sup>1</sup> G. Feher, Phys. Rev. **103**, 500 (1956).

<sup>2</sup> C. Heller and H. M. McConnell, J. Chem. Phys. **32**, 1535 (1960).

<sup>3</sup> J. Lambe, N. Laurance, E. C. McIrvine, and R. W. Terhune, Phys. Rev. (to be published).

<sup>4</sup> H. M. McConnell, C. Heller, T. Cole, and R. W. Fessenden, J. Am. Chem. Soc. **82**, 766 (1960).

<sup>5</sup> A. Abragam and W. G. Proctor, Compt. rend. **246**, 2253 (1958).

## Comments and Errata

### Dissociation Energies of Diatomic Molecules\*

E. R. LIPPINCOTT, R. SCHROEDER,<sup>†</sup> AND D. STELL

Department of Chemistry, University of Maryland,  
College Park, Maryland

(Received December 14, 1960)

IN a discussion of dissociation energies of diatomic molecules G.R. Somayajulu<sup>1</sup> has used the relation

$$k_e r_e / D = \text{constant},$$

to relate the force constant  $k_e$ , dissociation energy and equilibrium distance  $r_e$ . He comments that a suitable potential function might be expected to lead to this relation but then states "It appears, however, the potential functions so far proposed do not lead to this result." We wish to point out that this relation may be derived from the previously proposed<sup>2</sup> function

$$V = D_e [1 - \exp(-n\Delta r^2/2r)] [1 + a f(r)],$$

where  $n = \text{constant}$  of Eq. (1),  $\Delta r = r - r_e$ ,  $a = \text{constant}$  and  $f(r)$  is a function such that  $f(r) = 0$  as  $r \rightarrow \infty$  and  $f(r) = \infty$  as  $r \rightarrow 0$ . Relation (1) has been used to relate and predict dissociation energies of diatomic molecules and bond energies of bonds in polyatomic molecules.<sup>2-4</sup> Somayajulu's results are in excellent agreement with our earlier calculations on diatomic molecules except where more recent data has been available. We also have used this relation to show that a value of 170 kcal/mole is favored for the heat of sublimation of graphite.<sup>4</sup> The main difference between use of this relation and that of Somayajulu is that we assumed a characteristic value for the constant  $n$  of Eq. (1) for different sequences of molecules, while we evaluated this constant from ionization potentials by means of an empirical rule.

It should be pointed out that relation (1) is not valid for excited states of diatomic molecules in that Somayajulu's sequence constants cannot be used without modification. We have derived some relations from consideration of the proposed function (2) which enable one to calculate dissociation energies of excited states from the equivalent of (1) through the use of  $r_e$  and vibrational frequencies for the excited states. Some results are given in Table I for  $\text{O}_2$  for which the relations are particularly good.

The working equation is

$$D_e(\text{ev}) = \frac{1.8387 \times 10^{-6} b^2 \mu \omega^4 r_e^{11/2} [1 - \frac{5}{4} a(x)]^2}{\omega_e^2 r_e^{-7/2}}$$

where  $a$  is the parameter  $a$  of Eq. (2),  $a(x)$  is the

is parameter for the ground state of the molecule, the reduced mass in atomic units,  $\omega_x$  and  $r_x$  refer to vibrational frequency and bond length of the ground state of the molecule in  $\text{cm}^{-1}$  and  $\text{A}$ , respectively.

TABLE I. Calculation of dissociation energies of excited states of  $\text{O}_2$  from  $\omega_e$  and  $r_e$ .

State	$\omega_e$	$r_e$	$D_e$ obs	$D_e$ calc
	1580.36 $\text{cm}^{-1}$	1.2074 $\text{A}$	5.220 eV	5.02 eV
	1509.3	1.2155	4.13	4.48
	1432.69	1.2267	3.58	3.55
	700.36	1.604	1.00	0.96
	650.49	1.597	0.67	0.69

and  $b$  is a constant defined by the form of  $f(r)$ .  $b$  is equal to 1.065 for all molecules excepting oxygen for which it takes the value 1.16. The parameter is given by

$$a = \frac{1}{6B_e^2/\alpha\omega + \frac{5}{4}} \quad (4)$$

parameter has been shown to be periodic within periodic table.<sup>5</sup> For an heteronuclear molecule the  $a$  is given satisfactorily as the mean of the  $a(x)$  for constituent elements.

It should be pointed out that the potential in (2) is not the only one which will allow a derivation of relation (1). Actually there are several forms of functions which give this relation but (2) is the only one which gives (1) and at the same time a usable correlation of anharmonicity, force constant, dissociation energy, and bond lengths.

This work has been supported in part by the Office of Ordnance Research, U. S. Army.

Present address: Department of Chemistry, Southwestern Louisiana University, Lafayette, Louisiana.

G. R. Somayajulu, *J. Chem. Phys.* **33**, 1541 (1960).

E. R. Lippincott, *J. Chem. Phys.* **21**, 2070 (1953); E. R. Lippincott and R. Schroeder, *ibid.* **23**, 1131 (1955); E. R. Lippincott, G. R. Somayajulu, and P. Caldwell, *ibid.* (to be published).

R. L. Bredt, *Collection Czechoslov. Chem. Commun.* **23**, 777, 46, 1852 (1958).

E. R. Lippincott and R. Schroeder, *J. Am. Chem. Soc.* **78**, 561 (1956).

G. R. Somayajulu and E. R. Lippincott (unpublished).

## Dissociation Energies of Diatomic Molecules\*

G. R. SOMAYAJULU

Department of Chemistry and Lawrence Radiation Laboratory,  
University of California, Berkeley 4, California

(Received January 9, 1961)

It is gratifying to note that Lippincott's function<sup>1</sup> which we have unfortunately overlooked) leads to

the relation

$$k_e r_e / D = n, \quad (1)$$

and at the same time satisfies the conditions desirable of a good potential function. Empirically, we have found<sup>2</sup> that  $n$  is approximately constant for sequences of similar diatoms in the ground state. Lippincott and Schroeder<sup>3</sup> use bond-dissociation energies of polyatomic molecules to conclude that  $n$  is constant for bonds of any type between two given atoms. Thus  $n$  should be constant for different types of bonds between similar atoms such as O, S, Se, and Te. It is found<sup>2</sup> that the first members of sequences of similar diatoms have different  $n$  values. Also the same value of  $n$  cannot be used for the ground state and excited electronic states. The relationship<sup>3</sup> between  $n$  and ionization potentials of the bonded atoms would seem more reasonable if valence-state ionization potentials were used. The resulting variation of  $n$  with valence state would explain the difference between the value of  $n$  for ground and excited states.

We may also point out that bond energy, bond length, and force constant are related<sup>4,5</sup> by the expression

$$k_e r_e^2 / E = \beta, \quad (2)$$

where  $E$  is the bond energy, and  $\beta$  is a constant for bonds of any type and of any order between two given atoms in their normal valence states. Relation (2) follows from the function<sup>6</sup>

$$U = ar^{-m} - br^{-n}, \quad (3)$$

and also from a number of other functions.<sup>7</sup>

The results which illustrate the validity of relation (3) for the S—S bonds have been presented in Table I.

TABLE I.

Bond	Molecule	$k_e$ (md/A)	$r_e$ (A)	$E$ (kcal/mole)	$\beta$
S=S	$\text{S}_2$	4.959	1.889	101.46	0.1744
S—S	$\text{H}_2\text{S}_2$	2.60	2.05	62.65	

The S—S bond energy of 62.65 kcal/mole was calculated from Eq. (3). A value of 63 kcal/mole for  $E(\text{S—S})$  may be obtained from the heats of atomization<sup>8</sup> of  $\text{H}_2\text{S}_n$ -type molecules and also from the heat of atomization<sup>9</sup> of gaseous  $\text{S}_8$ . Similar results confirming the validity of relation (2) have been obtained in a number of cases.

For bonds between two given atoms, relations (1) and (2) lead to the simple result that

$$Dr_e / E = \beta / n = \text{constant}. \quad (4)$$

It appears, however, that there are a few cases where the bond energies are approximately equal to bond dissociation energies. Obviously, in such cases relation

Reprinted from the JOURNAL OF CHEMICAL PHYSICS, Vol. 35, No. 1, 123-141, July, 1961  
 Printed in U. S. A.

## General Relation between Potential Energy and Internuclear Distance for Diatomic Molecules. III. Excited States

E. R. LIPPINCOTT, D. STELLE,\* AND P. CALDWELL†

Department of Chemistry, University of Maryland, College Park, Maryland

(Received November 21, 1960)

A previously proposed internuclear potential function has been used to calculate the dissociation energies for the excited states of a large number of diatomic molecules. From these results and the Wigner-Wintner rules the dissociation products are determined, and it is shown that in many cases it is possible to estimate independently, the dissociation energy of the ground state. The three- and five-parameter forms of the proposed function lead to nearly equal values for dissociation energies suggesting an equivalence of the two forms. This leads to a relation between the anharmonicity and the vibrational-rotational coupling constant which is slightly superior to the Pekeris relation. Equations derived from this relation are given relating the parameters  $a$  and  $b$  of the five-parameter functions to the anharmonicity or vibrational-rotational coupling constant. The parameter  $b$  and to a lesser extent  $a$  was found nearly constant for the excited states of all diatomic molecules.

### INTRODUCTION

IN a previous publication (1)<sup>1</sup> a relation between potential energy and internuclear distance was proposed. The relation had the form

$$V = D[1 - \exp(-n\Delta r^2/2r)] \times [1 + a^2(r)], \quad (1)$$

where  $D$  = dissociation energy referred to the bottom of the potential curve,  $\Delta r = r - r_e$ ,  $r_e$  = equilibrium bond distance,  $r$  = bond distance and  $a$  = constant. The parameter  $n$  is given by

$$n = k_e r_e^2 / D, \quad (2)$$

where  $k_e$  = force constant referred to zero displacement of the nuclei. When  $a$  is chosen zero the potential function Eq. (1) assumes a simple three-parameter form

$$V = D[1 - \exp(-n\Delta r^2/2r)]. \quad (3)$$

By expansion of  $V$  in a power series to the quartic term in  $\Delta r$ , followed by comparison of the corresponding terms with those expected for the solutions of the Schrödinger equation for an anharmonic oscillator, the following relations were obtained

$$D \text{ (ergs/molecule)} = k_e [(64\pi^2 c \mu \omega_e x_e)^2 / 3h - (1/r_e^2)], \quad (4a)$$

$$\omega_e x_e = 3h(n/r_e + 1/r_e^2) / 64\pi^2 c \mu, \quad (5a)$$

and

$$\alpha_e = 0. \quad (6a)$$

Or in terms of Varshni's<sup>2</sup> notation

$$G = 3[nr_e + 1] = 3[2\Delta + 1], \quad (5b)$$

$$F = 0, \quad (6b)$$

\* Post doctoral research fellow.

† Present address: National Bureau of Standards, Washington, D. C.

<sup>1</sup> E. R. Lippincott, J. Chem. Phys. **21**, 2070 (1953); E. R. Lippincott and R. Schroeder, *ibid.* **23**, 1131 (1955).

<sup>2</sup> Y. P. Varshni, Revs. Modern Phys. **29**, 664 (1957). Varshni has erroneously reported that  $\alpha_e$  is negative for the three-parameter function. He also reports an incorrect expression for the value of  $\alpha_e$  for the Linnert function (private communication).

where

$$F = \alpha_e \omega_e / 6B_e^2, \quad G = 8\pi c \mu \omega_e / B_e, \quad \Delta = k_e r_e^2 / 2D,$$

$\omega_e x_e$  = anharmonicity constant for zero displacement of the nuclei,  $\alpha_e$  = vibration-rotational coupling constant,  $\mu$  = reduced mass,  $c$  = velocity of light, and  $h$  = Planck's constant.

By using Eq. (4a) dissociation energies were calculated from bond lengths, force constants, and anharmonicity constants. The calculated values of  $D_e$  in general represented a marked improvement over the same  $D_e$  values calculated from the Morse function relation  $D_e = \omega_e^2 / 4\omega_e x_e$ , the resulting average percent deviations being of the order of 5 and 25%, respectively.<sup>1</sup> Independent empirical methods were given for evaluating the parameter  $n$  and with its use anharmonicity constants, as well as dissociation energies, were correlated or calculated more accurately than was previously possible.

The successful application of (3) to the properties of ground states of diatomic molecules suggested other applications. These included potential function models of hydrogen bonds<sup>3,4</sup> and empirical calculations of bond properties for bonds of polyatomic molecules using bond stretching force constants.<sup>3</sup> One disadvantage of (3) is that it predicts  $\alpha_e = 0$  for all diatomic molecules, corresponding to no interaction between vibrational and rotational motion. Although values of  $\alpha_e$  are small for the ground states of diatomic molecules, they are definitely not zero. This suggests that in (1)  $a \neq 0$ . Some theoretical justifications for this simple potential function are known since it may be derived from a semiempirical quantum-mechanical model of chemical binding.<sup>5</sup>

With  $a \neq 0$ , the internuclear potential function as-

<sup>3</sup> E. R. Lippincott and R. Schroeder, J. Chem. Phys. **23**, 1131 (1955); J. Am. Chem. Soc. **78**, 5171 (1956); J. Phys. Chem. **61**, 921 (1957).

<sup>4</sup> C. Rei 1, J. Chem. Phys. **30**, 182 (1959).

<sup>5</sup> E. R. Lippincott and M. O. Dayhoff, Spectrochim. Acta **16**, 807 (1960); E. R. Lippincott, J. Chem. Phys. **26**, 1678 (1957).

sumed a five-parameter form. The quantity  $f(r)$  was a function of  $r$  chosen such that  $f(r) = \infty$  when  $r=0$ , and  $f(r)=0$  when  $r=\infty$ . For large values of  $r$  the  $f(r)$  term was assumed to take the form of a Lennard-Jones 6-12 attractive potential, which is compatible with these conditions.

The general form was then

$$V = D_e [1 - \exp(-n\Delta r^2/2r)] \times \{1 - a(r_e/r)^6 \\ \times [1 - \exp(-b^2 n \Delta r^2 r^{12}/2r_e^{12})] + a(r_e/r)^{12} \\ \times [1 - \exp(-b^2 n \Delta r^2 r^{11}/2r_e^{12})]\}, \quad (7a)$$

where  $b = \text{constant}$ . For large values of  $r$  this equation assumes the form,

$$V = D_e [1 - \exp(-n\Delta r^2/2r)] \{1 + a[-(r_e/r)^6 \\ + (r_e/r)^{12}]\}.$$

Several other forms of  $V$  are possible which have the same expansion to the fourth power in  $\Delta r$  and consequently lead to the same relations between  $\omega_e$ ,  $B_e$ ,  $\alpha_e$ ,  $x_e \omega_e$ , and  $D_e$ . One of these which appears to reproduce experimental potential curves well, is

$$V = D_e [1 - \exp(-n\Delta r^2/2r)] \{1 - a(b^2 n/2r)^{1/2} \Delta r \\ \times \exp[-(b^2 n/2r)^{1/2} \Delta r]\}. \quad (7b)$$

This will be discussed in a later section.

The relations which may be derived from the use of (7) as an anharmonic oscillator in the Schrödinger equation are given below. These relations were used to obtain improved correlations and predictions of the five spectroscopic constants  $r_e$ ,  $k_e$ ,  $D_e$ ,  $\omega_e x_e$ , and  $\alpha_e$ . The internuclear potential function (7) has been used by Pliva<sup>6</sup> as the bond stretching part of a physically significant anharmonic potential function describing the motion of polyatomic molecules. With its use, he was able to correlate or predict accurately a number of the constants for the vibrational-rotational motion of triatomic molecules, including anharmonicity and vibrational rotational coupling constants. One important and convenient feature of (6) is that the parameters  $a$  and  $b$  were approximately constant for the ground states of the diatomic molecules studied, with values of  $b$  rarely deviating by more than 3% and values of  $a$  by more than 10%.

The purpose of this paper is to illustrate the function's application to the electronically excited states of diatomic molecules using both the three-parameter and five-parameter forms. Its usefulness in correlating and predicting bond properties will be discussed and some new relations given. In addition, the functions will be used to predict the states of separated atoms for diatomic molecules. Such an application can be useful in constructing energy level diagrams for diatomic

molecules when the states of the separated atoms are not known from other sources of information.

From a knowledge of the states of the separated atoms and approximate values of the dissociation energies of the excited states it is possible to estimate the dissociation energies of the ground states. In certain cases of considerable interest the derived value allows an unambiguous selection from previously proposed groups of values.

### SIMPLE THREE-PARAMETER FUNCTION

The use of the simple function and derived relations for calculating bond properties has been given in I and will not be repeated here. The working equation is (4a), and calculated dissociation energies have been obtained through the use of experimental  $k_e$ ,  $r_e$  and  $\omega_e x_e$  values. The results for a large number of excited states are given in Tables I, II, and III along with the experimental  $D_e$  values for a comparison. Table II contains calculations for salt like compounds, for which the model might be expected to be less reliable, and in Table III are given the dissociation energies for hydrogen containing molecules. The results for the ground states are included for the sake of completeness. The experimental  $D_e$  values are based on the assumption that the states for the separated atoms are known. Alternatively the predicted dissociation energy can be used to deduce the states of the separated atoms. The predicted or known separated atom states are given in column 9.

In reference 1 an independent empirical relation was given for the evaluation of  $n$  in terms of ionization potentials of the ground states of the separated atoms. From this relation and Eq. (2) it was possible to predict  $D_e$  from  $k_e$  and  $r_e$  values. Because the ionization potential of excited atoms differs from those of the ground state atoms, the values of  $n$  calculated for ground-state diatomic molecules are not necessarily valid for excited states of the same molecule and these  $n$  values cannot necessarily be used in Eq. (2) without appropriate modifications.

When reliable experimental data are available for comparison, the calculated  $D_e$  values agree well with the observed values.

### CALCULATIONS WITH THE FIVE-PARAMETER FUNCTIONS

The potential function, Eqs. (7), may be expanded in a power series of  $\Delta r/r_e$  giving<sup>7</sup>

$$V = D_e (nr_e/2) (\Delta r^2/r_e^2) \{1 - [1 + ab(nr_e/2)^{1/2}] (\Delta r/r_e) \\ + [1 - nr_e/3 + 3(ab/2)(nr_e/2)^{1/2} \\ + ab(nr_e/2)] (\Delta r/r_e)^2 + \dots\}. \quad (8)$$

Dunham has solved the problem of a nonrigid an-

<sup>6</sup> J. Pliva, Collection Czechoslov. Chem. Commun. **23**, 777, 1839, 1846, 1852 (1958).

TABLE I. Comparison of dissociation energies calculated from three- and five-parameter potential functions for excited states of diatomic molecules.

Molecule	State	Dissociation energy			Atomic excitation energy			Dissociation products	Ref.
		Obs <sup>a</sup>	S.F. <sup>b</sup>	5 par. F <sup>b,c</sup>	Te(ev)	Calc	Theoret		
B <sub>2</sub>	X <sup>3</sup> Σ <sub>g</sub> <sup>-</sup>	3.0±0.5	2.87	2.42	0			2 <sup>3</sup> P+2 <sup>3</sup> P	
	A <sup>3</sup> Σ <sub>u</sub> <sup>-</sup>	(10.0)	9.44	c.	3.790	10.2	10.8	3 <sup>3</sup> P+2 <sup>2</sup> D	
<sup>79</sup> Br <sup>81</sup> Br	X <sup>1</sup> Σ <sub>g</sub> <sup>+</sup>	1.971	2.33	1.75	0			4 <sup>2</sup> P+4 <sup>2</sup> P	
	B <sup>3</sup> Π <sub>ou</sub> <sup>+</sup>	(0.46)	0.354	c.	1.970	0.35	0.46	4 <sup>2</sup> P <sub>1</sub> +4 <sup>2</sup> P <sub>1</sub>	
C <sub>2</sub>	X <sup>3</sup> Π <sub>u</sub>	~5.6	5.66	5.44	0			2 <sup>3</sup> P+2 <sup>3</sup> P	
	A <sup>3</sup> Π <sub>g</sub>	(4.5)	4.71	3.50	2.393	1.4	1.26	2 <sup>3</sup> P+2 <sup>1</sup> D	
	B <sup>3</sup> Π <sub>g</sub>	(0.7)	0.73	0.47	4.969	0.1	0.0	2 <sup>3</sup> P+2 <sup>3</sup> P	
	a <sup>1</sup> Σ <sub>g</sub> <sup>+</sup>	(5.6)	5.96	5.16	-0.07	0.3	0.0	2 <sup>3</sup> P+2 <sup>3</sup> P	
	b <sup>1</sup> Π <sub>u</sub>	(4.6)	5.20	3.96	0.97	0.6	0.0	2 <sup>3</sup> P+2 <sup>3</sup> P	
	c <sup>1</sup> Π <sub>g</sub>	(5.3)	5.02	4.01	4.18	3.6	3.92	2 <sup>1</sup> D+2 <sup>1</sup> S	
	d <sup>1</sup> Σ <sub>u</sub> <sup>+</sup>		5.88	5.88	5.29	5.5	7.45?	2 <sup>3</sup> P+3 <sup>3</sup> P	?
CN	X <sup>2</sup> Σ <sup>+</sup>	8.3	8.00	7.49	0			2 <sup>3</sup> P+2 <sup>4</sup> S	
	A <sup>3</sup> Π <sub>i</sub>	(7.1)	6.25	6.00	1.146	-0.8	0.0	2 <sup>3</sup> P+2 <sup>4</sup> S	
	B <sup>2</sup> Σ <sup>+</sup>		8.00	4.58	3.192	2.9			
CO	X <sup>1</sup> Σ <sup>+</sup>	11.2	8.70	8.60	0			2 <sup>3</sup> P+2 <sup>3</sup> P	9
	A <sup>1</sup> Π	(3.1)	3.39	2.70	8.067	-0.2	0.0	2 <sup>3</sup> P+2 <sup>3</sup> P	
	a <sup>3</sup> Π <sup>+</sup>	(5.2)	5.08	4.83	6.036	0.0	0.0	2 <sup>3</sup> P+2 <sup>3</sup> P	
	a <sup>1</sup> Σ <sup>+</sup>	(4.3)	3.83	4.33	6.903	-0.3	0.0	2 <sup>3</sup> P+2 <sup>3</sup> P	
	d <sup>3</sup> Δ	(3.4)	4.21	c.	7.809	0.8	0.0	2 <sup>3</sup> P+2 <sup>3</sup> P	
	c <sup>2</sup> Σ <sup>-</sup>	(3.1)	3.05	6.23	8.098	0.0	0.0	2 <sup>3</sup> P+2 <sup>3</sup> P	10
(CO) <sup>+</sup>	X <sup>2</sup> Σ <sup>+</sup>	8.57	7.90	7.28	0				
	A <sup>3</sup> Π <sub>i</sub>		4.39	4.35	2.570	-1.6			
	B <sup>2</sup> Σ <sup>+</sup>		2.57	2.01	5.687	-0.2			
CP	X <sup>2</sup> Σ <sup>+</sup>	6±1	5.45	4.96	0			2 <sup>3</sup> P+3 <sup>4</sup> S	
	A <sup>3</sup> Π <sub>i</sub>	(~5)	4.54	c.	8.744	7.8	7.38	2 <sup>3</sup> P+3 <sup>4</sup> P	
					(8.548)				
	B <sup>2</sup> Σ <sup>+</sup>	(~2.4)	2.87	2.48	3.608	0.5	0.0	2 <sup>3</sup> P+3 <sup>4</sup> S	
CS	X <sup>1</sup> Σ <sup>+</sup>	7.2±1.0	6.25	6.18	0			2 <sup>3</sup> P+3 <sup>3</sup> P	11
	A <sup>1</sup> Π	(2.4)	2.67	2.84	4.824	0.3	0	2 <sup>3</sup> P+3 <sup>3</sup> P	
Cl <sub>2</sub>	X <sup>1</sup> Σ <sub>g</sub> <sup>+</sup>	2.51	(1.90)	c.	0			3 <sup>2</sup> P+3 <sup>2</sup> P	
	A <sup>3</sup> Π <sub>ou</sub> <sup>+</sup>	(0.24)	0.25	0.26	2.270	0.01	0	3 <sup>2</sup> P+3 <sup>2</sup> P	
(Cl <sub>2</sub> ) <sup>+</sup>	X <sup>3</sup> Π	4.4	3.46	c.	0			3 <sup>2</sup> P+3 <sup>3</sup> P	
	A <sup>3</sup> Π	(~1.82)	1.45	c.	2.578	0.0	0	3 <sup>2</sup> P+3 <sup>3</sup> P	
		(~1.85)	1.83		2.553				
ClF	X <sup>1</sup> Σ	2.62	1.51	1.02	0			3 <sup>2</sup> P+2 <sup>2</sup> P	
	A <sup>3</sup> Π <sub>o</sub> <sup>+</sup>	(0.27)	1.10	c.	2.350	~0.8	0	3 <sup>2</sup> P+2 <sup>2</sup> P	
GeO	X <sup>1</sup> Σ <sup>+</sup>	6.8±0.2	5.48	5.81	0			4 <sup>3</sup> P+2 <sup>3</sup> P	
	A <sup>1</sup> Σ <sup>+</sup>		2.41	3.62	4.681	0.2	0(0.07) (0.17)	4 <sup>3</sup> P+2 <sup>3</sup> P	
							0.88	4 <sup>1</sup> D+2 <sup>3</sup> P	
He <sub>2</sub>	X <sup>1</sup> Σ <sub>g</sub> <sup>+</sup>				0				
	a <sup>3</sup> Σ <sub>u</sub> <sup>+</sup>		1.69	2.10	...				
	e <sup>3</sup> Π <sub>g</sub>		4.76	2.08	...				
I <sub>2</sub>	X <sup>1</sup> Σ <sup>+</sup>	1.556	1.79	1.70	0			5 <sup>2</sup> P+5 <sup>2</sup> P	12
	B <sup>3</sup> Π <sub>ou</sub> <sup>+</sup>	(0.56)	0.46	0.40	1.939	0.8	0.94	5 <sup>2</sup> P <sub>1</sub> +5 <sup>2</sup> P <sub>1</sub>	
ICl	X <sup>1</sup> Σ <sup>+</sup>	2.178	2.35	2.13	0			5 <sup>2</sup> P+3 <sup>2</sup> P	
	A <sup>3</sup> Π <sub>i</sub>	(0.47)	0.53	0.36	1.704	0.0	0.0	5 <sup>2</sup> P+3 <sup>2</sup> P	
	B <sup>3</sup> Π <sub>o</sub> <sup>+</sup>	(0.02)	(0.10)	c.	2.149	0.0	0.0	5 <sup>2</sup> P+3 <sup>2</sup> P	
IO	X <sup>3</sup> Π <sub>1</sub>	1.9	2.59	2.57	0			5 <sup>2</sup> P+2 <sup>3</sup> P	13
	A <sup>3</sup> Π <sub>1</sub>	(1.19)	1.14	0.84	2.672	1.9	1.96	5 <sup>2</sup> P+2 <sup>1</sup> D	

TABLE I.—Continued.

Molecule	State	Dissociation energy			Atomic excitation energy			Dissociation products	Ref.
		Obs <sup>a</sup>	S.F. <sup>b</sup>	5 par. F <sup>b,c</sup>	Te(ev)	Calc	Theoret		
K <sub>2</sub>	X <sup>1</sup> Σ <sub>g</sub> <sup>+</sup>	0.520	0.60	0.47	0			4 <sup>2</sup> S+4 <sup>2</sup> S	
	B <sup>1</sup> Π <sub>u</sub>	(0.22)	0.35	0.26	1.906	1.7	1.61	4 <sup>2</sup> P+4 <sup>2</sup> S	
Li <sub>2</sub>	X <sup>1</sup> Σ <sub>g</sub> <sup>+</sup>	1.10±0.05	1.23	1.10	0			2 <sup>2</sup> S+2 <sup>2</sup> S	
	A <sup>1</sup> Σ <sub>u</sub> <sup>+</sup>	(1.2)	1.09	1.24	1.744	1.7	1.85	2 <sup>2</sup> S+2 <sup>2</sup> P	
	B <sup>1</sup> Π <sub>u</sub>	(0.4)	0.67	0.59	2.534	2.1	1.85	2 <sup>2</sup> S+2 <sup>2</sup> P	
N <sub>2</sub>	X <sup>1</sup> Σ <sub>g</sub> <sup>+</sup>	9.92	9.62	8.91	0			2 <sup>4</sup> S+2 <sup>4</sup> S	14, 15
	a <sup>1</sup> Π <sub>g</sub>	(6.1)	5.04	4.82	8.590	3.6	4.74	2 <sup>2</sup> D+2 <sup>2</sup> D	14
	q <sup>1</sup> Σ <sub>u</sub> <sup>+</sup>	(2.1)	(1.38)	(1.32)	13.72	(5.2)	5.93	2 <sup>2</sup> P+2 <sup>2</sup> D	
	a <sub>u</sub> ' ( <sup>1</sup> Σ <sub>u</sub> <sup>-</sup> )	(5.9)	4.23	3.47	8.740	3.0	4.74	2 <sup>2</sup> D+2 <sup>2</sup> D	16
	x <sup>1</sup> Σ <sub>g</sub> <sup>-</sup>	(5.8)	4.76	5.63	14.351	9.3	10.29	3 <sup>4</sup> P+2 <sup>4</sup> S	16
	A <sup>2</sup> Σ <sub>u</sub> <sup>+</sup>	(3.7)	3.71	2.73	6.224	0.0	0.0	2 <sup>4</sup> S+2 <sup>4</sup> S	
	B <sup>2</sup> Π <sub>g</sub>	(4.9)	5.05	4.62	7.392	2.5	2.37	2 <sup>4</sup> S+2 <sup>2</sup> D	
	C <sup>2</sup> Π <sub>u</sub>		5.87	5.11	11.05	7.0			
(N <sub>2</sub> ) <sup>+</sup>	X <sup>2</sup> Π <sub>g</sub> <sup>+</sup>	8.87	7.35	7.47	0			2 <sup>2</sup> P+2 <sup>4</sup> S	17
	B <sup>2</sup> Σ <sub>u</sub> <sup>+</sup>	(5.7)	6.08	4.44	3.156	0.3	0.0	2 <sup>2</sup> P+2 <sup>4</sup> S	
NO	X <sup>2</sup> Π <sub>1</sub>	~6.6	6.32	6.26	0			2 <sup>4</sup> S+2 <sup>2</sup> P	18
	A <sup>2</sup> Σ <sup>+</sup>	(7.7)	8.34	7.91	5.450	7.3	6.54	2 <sup>2</sup> D+2 <sup>1</sup> S	19
	B <sup>2</sup> Π <sub>r</sub>	(3.3)	3.50	3.42	5.692	2.6	2.37	2 <sup>2</sup> D+2 <sup>2</sup> P	
	E <sup>2</sup> Σ <sup>+</sup>	(8.2)	8.67	7.89	7.516	9.7	9.11	2 <sup>4</sup> S+3 <sup>5</sup> S	
	D <sup>2</sup> Σ <sup>+</sup>	(5.5)	5.67	4.40	5.449	4.6	4.33	2 <sup>2</sup> D+2 <sup>1</sup> D	19
	B <sup>2</sup> Δ	(2.7)	2.24	1.73	7.482	3.2	3.56	2 <sup>2</sup> P+2 <sup>2</sup> P	20
NO <sup>+</sup>	X <sup>1</sup> Σ <sup>+</sup>	10.6	8.42	9.09				2 <sup>2</sup> P+2 <sup>2</sup> P	19
	A <sup>1</sup> Π		2.65	2.04	9.106			or 2 <sup>4</sup> S+2 <sup>4</sup> S	19
Na <sub>2</sub>	X <sup>1</sup> Σ <sub>g</sub> <sup>+</sup>	0.75±0.03	0.88	0.72	0			3 <sup>2</sup> S+3 <sup>2</sup> S	
	A <sup>1</sup> Σ <sub>u</sub>	(1.0)	0.95	0.90	1.820	2.0	2.10	3 <sup>2</sup> S+3 <sup>2</sup> P	
	B <sup>1</sup> Π <sub>u</sub>	(0.3)	0.61	0.56	2.519	2.3	2.10	3 <sup>2</sup> S+3 <sup>2</sup> P	
O <sub>2</sub>	X <sup>3</sup> Σ <sub>g</sub> <sup>-</sup>	5.220	5.04	5.11	0			2 <sup>2</sup> P+2 <sup>2</sup> P	
	a <sup>1</sup> Δ <sub>g</sub>	(4.2)	4.29	4.39	0.981	0.0	0.0	2 <sup>2</sup> P+2 <sup>2</sup> P	
	b <sup>1</sup> Σ <sub>g</sub> <sup>+</sup>	(3.58)	3.55	3.41	1.636	0.0	0.0	2 <sup>2</sup> P+2 <sup>2</sup> P	
	B <sup>3</sup> Σ <sub>u</sub> <sup>-</sup>	(1.0)	1.48	1.18	6.174	2.5	1.96	2 <sup>2</sup> P+2 <sup>1</sup> D	
	<sup>1</sup> Σ <sub>u</sub> <sup>-</sup>	(0.68)	0.59	0.45	4.546	0.0	0.0	2 <sup>2</sup> P+2 <sup>2</sup> P	21
	<sup>3</sup> Σ <sub>u</sub> <sup>+</sup>		1.03	0.78					22
O <sub>2</sub> <sup>+</sup>	X <sup>2</sup> Π <sub>g</sub>	6.59	5.15	5.05	0			2 <sup>2</sup> P+2 <sup>4</sup> S	
	a <sup>1</sup> Π <sub>u</sub>	(2.6)	2.50	2.81	(3.955)	-0.1	0.0	2 <sup>2</sup> P+2 <sup>4</sup> S	
	A <sup>2</sup> Π <sub>u</sub>	(1.8)	1.45	1.25	4.809	-0.3	0.0	2 <sup>2</sup> P+2 <sup>4</sup> S	
	b <sup>4</sup> Σ <sub>g</sub> <sup>+</sup>	(2.5)	2.00	1.84	(6.011)	1.4	1.96	2 <sup>1</sup> D+2 <sup>4</sup> S	
P <sub>2</sub>	X <sup>1</sup> Σ <sub>g</sub> <sup>+</sup>	5.08	5.24	4.93	0			(3 <sup>2</sup> D+3 <sup>4</sup> D)	23
	B <sup>1</sup> Σ <sub>u</sub> <sup>+</sup>		2.07	1.78	5.819	2.8			23
	A <sup>1</sup> Π <sub>g</sub>	(2.6)	3.10	2.86	4.278	2.3	1.82	(3 <sup>2</sup> P+3 <sup>2</sup> P)	23
PN	X <sup>1</sup> Σ <sup>+</sup>	6.1±0.8	6.22	5.80	0			3 <sup>4</sup> S+2 <sup>4</sup> S	
	A <sup>1</sup> Π		4.07	4.39	4.935	2.9	2.37	3 <sup>4</sup> S+2 <sup>2</sup> D	
						3.56	3 <sup>4</sup> S+2 <sup>2</sup> P		
						2.31	3 <sup>2</sup> P+2 <sup>4</sup> S		
PO	X <sup>2</sup> Π <sub>r</sub>	5.4	5.65	5.20	0			3 <sup>4</sup> S+2 <sup>2</sup> P	
	A <sup>2</sup> Σ	(6.0)	6.12	3.97	5.009	5.7	5.57	3 <sup>2</sup> D+2 <sup>1</sup> S	



TABLE I.—Continued.

Molecule	State	Dissociation energy			Atomic excitation energy			Dissociation products	Ref.
		Obs <sup>a</sup>	S.F. <sup>b</sup>	5 par. F <sup>b,c</sup>	Te(ev)	Calc	Theoret		
S <sub>2</sub>	X <sup>3</sup> Σ <sub>g</sub> <sup>-</sup>	4.4	4.47	4.58	0			3 <sup>3</sup> P+3 <sup>3</sup> P	
	B <sup>3</sup> Σ <sub>u</sub> <sup>-</sup>	or 3.6 (1.6)	1.64	1.72	3.947	1.2	1.14	3 <sup>3</sup> P+3 <sup>1</sup> D	
SO	X <sup>3</sup> Σ <sup>-</sup>	5.22	5.02	5.61	0			3 <sup>3</sup> P+2 <sup>3</sup> P	
	B <sup>3</sup> Σ <sup>-</sup>		(0.68)	(2.28)	4.879	0.0	1.14 0.0	3 <sup>3</sup> P+2 <sup>3</sup> P 3 <sup>1</sup> D+2 <sup>3</sup> P	
Sc <sub>2</sub>	X <sup>1</sup> Σ <sub>g</sub> <sup>+</sup>	2.8±0.1	3.48	2.70	0			4 <sup>3</sup> P+4 <sup>3</sup> P	
	B ( <sup>1</sup> Σ <sub>u</sub> <sup>+</sup> )		0.70	0.47	3.228	1.1			
Si <sub>2</sub>	X <sup>3</sup> Σ <sub>g</sub> <sup>-</sup>	3.2	3.17	3.43				3 <sup>3</sup> P+3 <sup>3</sup> P	24
	D <sup>3</sup> Π <sub>g</sub>		2.99	2.83					
	H <sup>3</sup> Σ <sub>u</sub> <sup>-</sup>	(0.8)	0.89	0.68	2.984	0.7	0.77	3 <sup>3</sup> P+3 <sup>1</sup> D	
SiN	X <sup>2</sup> Σ <sup>+</sup>	4.5±0.4	4.91	4.63	0			3 <sup>3</sup> P+2 <sup>4</sup> S	
	B <sup>2</sup> Σ <sup>+</sup>	(1.5)	1.50	1.11	3.012	0.0	0.0	3 <sup>3</sup> P+2 <sup>4</sup> S	
SiO	X <sup>1</sup> Σ <sup>+</sup>	8.0±0.3	6.21	5.95	0			3 <sup>3</sup> P+2 <sup>3</sup> P	
	A <sup>1</sup> Π	(2.7)	2.85	3.35	5.310	0.1	0.0	3 <sup>3</sup> P+2 <sup>3</sup> P	
SiS	X <sup>1</sup> Σ <sup>+</sup>	6.35±0.1	5.34	5.54	0			3 <sup>3</sup> P+3 <sup>3</sup> P	25
	D <sup>1</sup> Π	(2.2)	2.67	c.	4.343	0.6	0.0	3 <sup>3</sup> P+3 <sup>3</sup> P	

<sup>a</sup> (G) = Gaydon (reference 45); (H) = Herzberg (reference 8).

<sup>b</sup> Values quoted in brackets are based on uncertain data.

<sup>c</sup> c = solution complex.

TABLE II. Comparison of dissociation energies calculated from three- and five-parameter potential functions for excited states of diatomic molecules.

Molecule	State	Dissociation energy			Atomic excitation energy			Dissociation products	Ref.
		Obs <sup>a</sup>	S.F.	5 par. F <sup>b</sup>	Te(ev)	Calc	Theoret		
AlBr	X <sup>1</sup> Σ <sup>+</sup>	4.3	2.72	5.44	0			3 <sup>2</sup> P+4 <sup>2</sup> P	
	A <sup>1</sup> Π		0.32	0.21	4.448	0.4	0.0(0.4)	3 <sup>2</sup> P+4 <sup>2</sup> P	
AlCl	X <sup>1</sup> Σ <sup>+</sup>	5.1	2.90	c.	0			3 <sup>2</sup> P+3 <sup>2</sup> P	
	A <sup>1</sup> Π		1.10	c.	4.742	0.7	0.0	3 <sup>2</sup> P+3 <sup>2</sup> P	
AlF	X <sup>1</sup> Σ <sup>+</sup>	6.8	3.33	6.01	0			3 <sup>2</sup> P+2 <sup>2</sup> P	26,27
	B <sup>1</sup> Σ <sup>+</sup>		2.41	1.74	6.724	2.3	3.13	4 <sup>2</sup> S+2 <sup>2</sup> P	
	A <sup>1</sup> Π		2.45	2.25	5.447	0.9	0.0	3 <sup>2</sup> P+2 <sup>2</sup> P	
	D <sup>1</sup> Δ		3.30	2.39	7.587	4.0	{4.00	3 <sup>2</sup> P+2 <sup>2</sup> P	
	C <sup>1</sup> Σ		4.13	4.08	7.158	4.0	{4.08	4 <sup>2</sup> P+2 <sup>2</sup> P	
AlO	X <sup>2</sup> Σ <sup>+</sup>	3.80 or 6.00	3.31	3.01	0			3 <sup>2</sup> P+2 <sup>3</sup> P	28
	A <sup>2</sup> Σ <sup>+</sup>		5.3	10.8	2.566	4.1	{4.00 4.08 4.17	3 <sup>2</sup> D+2 <sup>3</sup> P 4 <sup>2</sup> P+2 <sup>3</sup> P 3 <sup>2</sup> P+2 <sup>1</sup> S	
AlS	X <sup>2</sup> Σ <sup>+</sup>		2.745	2.33	0				29
	A <sup>2</sup> Σ <sup>+</sup>		4.46	7.43	2.904				
BBr	X <sup>1</sup> Σ <sup>+</sup>	4.1	3.26	2.94	0			2 <sup>2</sup> P+4 <sup>2</sup> P	
	A <sup>1</sup> Π		0.54	0.25	4.207	0.4	0.0	2 <sup>2</sup> P+4 <sup>2</sup> P	

TABLE II.—Continued.

Molecule	State	Dissociation energy			Atomic excitation energy			Dissociation products	Ref.
		Obs <sup>a</sup>	S.F.	5 par. F <sup>b</sup>	Te(ev)	Calc	Theoret		
BCl	X <sup>1</sup> Σ	5.1±0.4	5.09	4.16	0		0.0	2 <sup>2</sup> P+3 <sup>2</sup> P	
	A <sup>1</sup> Π		1.51	1.06	4.556	0.6	0.0	2 <sup>2</sup> P+3 <sup>2</sup> P	
BF	X <sup>1</sup> Σ <sup>+</sup>	8.5±0.5(G) 4.3(H)	4.24	3.85	0			2 <sup>2</sup> P+2 <sup>2</sup> P	30
	A <sup>1</sup> Π		2.62	1.99	6.341	1.2 or 4.6	0.0 or 4.94	2 <sup>2</sup> P+2 <sup>2</sup> P	30
	a <sup>3</sup> Π	4.59	c.					2 <sup>2</sup> P+3 <sup>2</sup> S	
	b <sup>3</sup> Σ	2.75	1.95						
BN	X <sup>3</sup> Π	4.0±0.5	4.57	c.	0			2 <sup>2</sup> P+2 <sup>4</sup> S	
	A <sup>3</sup> Π		2.82	2.14	3.456	~2	2.37	2 <sup>2</sup> P+2 <sup>2</sup> D	
BO	X <sup>2</sup> Σ <sup>+</sup>	9.1(H) 7.6±0.4(G)	7.45	7.24	0			2 <sup>2</sup> P+2 <sup>3</sup> P	
	A <sup>2</sup> Π <sub>i</sub>		3.48	5.56	2.97				
BaO	X <sup>1</sup> Σ	5.6	5.40	5.11	0		(1.15)	6 <sup>3</sup> D+2 <sup>3</sup> P	
	A <sup>1</sup> Σ		4.12	3.67	2.084	0.4	0.00	6 <sup>3</sup> D+2 <sup>3</sup> P	
BeF	X <sup>2</sup> Σ <sup>+</sup>	4±1	4.35	4.55	0			2 <sup>1</sup> S+2 <sup>2</sup> P	
	A <sup>2</sup> Π <sub>i</sub>		3.87	3.83	4.120	4.0	2.71	2 <sup>3</sup> P+2 <sup>2</sup> P	
BeO	X <sup>1</sup> Σ <sup>+</sup>	5.4	4.59	4.40	0			2 <sup>1</sup> S+2 <sup>3</sup> P	
	A <sup>1</sup> Π		3.85	4.57	1.166	0.0	0.0	2 <sup>1</sup> S+2 <sup>3</sup> P	
	B <sup>1</sup> Σ <sup>+</sup>		6.11	6.54	2.635	3.5	2.71	2 <sup>3</sup> P+2 <sup>3</sup> P	
	C <sup>1</sup> Σ		3.16	2.41	4.850	2.5	2.71	2 <sup>3</sup> P+2 <sup>3</sup> P	
CuF	X <sup>1</sup> Σ <sup>+</sup>	3.0	2.37	c.	0			4 <sup>2</sup> S+2 <sup>2</sup> P	
	B <sup>1</sup> Σ		2.57	c.	2.444	2.2	1.39(1.64)	4 <sup>2</sup> D+2 <sup>2</sup> P	
MgO	X <sup>1</sup> Σ	<4.0	2.89	2.58	0			2 <sup>1</sup> S+2 <sup>3</sup> P	
	A <sup>1</sup> Π		2.76	3.56	4.417	3.2	2.70	3 <sup>3</sup> P+2 <sup>3</sup> P	
	B <sup>1</sup> Σ		3.48	3.07	2.477	3.0	2.70	3 <sup>3</sup> P+2 <sup>3</sup> P	
PbS	X <sup>1</sup> Σ <sup>+</sup>	3.25±0.3	3.67	c.	0			6 <sup>3</sup> P+3 <sup>3</sup> P	
	A <sup>1</sup> Σ <sup>+</sup>		4.77	c.	2.337	3.9	3.8	6 <sup>1</sup> D+3 <sup>1</sup> D	
SnO	X <sup>1</sup> Σ <sup>+</sup>	5.7	4.37		0			5 <sup>3</sup> P+2 <sup>3</sup> P	
	D <sup>1</sup> Σ <sup>+</sup>		2.66		3.673	0.6	0.0	5 <sup>3</sup> P+2 <sup>3</sup> P	
SrO	X <sup>1</sup> Σ	5.0 or 3.6	2.56	1.87	0		(1.80)	5 <sup>3</sup> P+2 <sup>3</sup> P	
	A <sup>1</sup> Σ		4.80	3.77	1.350	1.1 or 2.5	2.50 0	5 <sup>3</sup> P+2 <sup>3</sup> P 5 <sup>1</sup> P+2 <sup>1</sup> D	
TiO	(X) <sup>3</sup> Π <sub>i</sub>	6.9±0.1	5.36	4.49	0			4 <sup>3</sup> F+2 <sup>3</sup> P	
	C <sup>3</sup> Π <sub>i</sub>		3.74	2.86	2.4	-0.8	0	4 <sup>3</sup> F+2 <sup>3</sup> P	
VO	(X <sup>2</sup> Δ)	6.3	5.02	c.	0			4 <sup>1</sup> F+2 <sup>3</sup> P	
	A <sup>(2</sup> Δ)		3.29	c.	2.170	-0.9	0	4 <sup>1</sup> F+2 <sup>3</sup> P	

<sup>a</sup> (G)=Gaydon (reference 45); (H)=Herzberg (reference 8).<sup>b</sup> c=solution complex.

TABLE III. Comparison of dissociation energies calculated from three- and five-parameter potential functions for excited states of diatomic molecules.

Molecule	State	Dissociation energy			Atomic excitation energy			Dissociation products	Ref.	
		Obs <sup>a</sup>	S.F.	5 par. F	Te(ev)	Calc	Theoret			
AgH	$X^1\Sigma^+$	2.6	2.28	<i>c.</i>	0			$5^2S+1^2S$		
	$A^1\Sigma^+$		0.76	0.54	3.714	1.9	0.0	$5^2S+1^2S$		
AlH	$X^1\Sigma^+$	3.0	2.46	2.76	0			$3^2P+1^2S$		
	$C^1\Sigma^+$		0.47	0.39	5.538	3.0	3.13	$4^2S+1^2S$		
	$A^1\Pi$		1.02	<i>c.</i>	2.909	0.9	0.0	$3^2P+1^2S$		
Al <sup>2</sup> H	$X^1\Sigma^+$	3.0	2.46	2.70	0			$3^2P+1^2S$		
	$A^1\Pi$		0.28	0.32	2.932	0.2	0.0	$3^2P+1^2S$		
AuH	$X^1\Sigma^+$	3.2	3.06	3.24	0			$6^2S+1^2S$		
	$A^1\Sigma^+$		1.23	1.03	3.430	1.4	0.0	$6^2S+1^2S$		
Au <sup>2</sup> H	$X^1\Sigma^+$	3.2	3.06	3.74	0			$6^2S+1^2S$		
	$A^1\Sigma^+$		0.99	0.80	3.427	0.9	0.0	$6^2S+1^2S$		
	$B^1\Sigma^+$		1.67	1.43	4.778	2.9	2.42(2.66)	$2^2D+1^2S$		
BH	$X^1\Sigma^+$	3.1±0.4	2.92	3.05	0			$2^2P+1^2S$		
	$A^1\Pi$		1.03	0.74	2.864	0.8	0.0	$2^2P+1^2S$		
	$B^1\Sigma^+$		2.22	2.78	6.488	5.6	5.91	$2^2D+1^2S$		
B <sup>2</sup> H	$X^1\Sigma^+$	3.1±0.4	3.00	3.19	0			$2^2P+1^2S$		
	$A^1\Pi$		1.66	1.39	2.869	1.4	0.0	$2^2P+1^2S$		
BaH	$X^2\Sigma^+$	1.8±0.1	2.169	1.93	0			$6^1S+1^2S$		
	$B^2\Sigma$		2.00	1.93	1.375	1.5	1.41	$6^1D+1^2S$		
	$E^2\Pi$			2.18	2.02	1.866	2.1	2.24	$6^3P+1^2S$	
				2.18	1.98	1.810			$6^1P+1^2S$	
				1.92	1.50	2.929	1.8	2.24	$6^3P+1^2S$	
						1.57				
BeH	$X^2\Sigma^+$	2.4±0.3	3.12	3.30	0			$2^1S+1^2S$		
	$A^2\Pi$		2.82	2.90	2.483	2.9	2.71	$2^3P+1^2S$		
(Be <sup>1</sup> H) <sup>+</sup>	$X^1\Sigma^+$	(3.3)	3.21	3.03	0			$2^2S+1^2S$		
	$A^1\Sigma^+$				4.887	5.8	3.95	$2^2P+1^2S$		
(Be <sup>2</sup> H) <sup>+</sup>	$X^1\Sigma^+$	(3.3)	3.22	3.12	0			$2^2S+1^2S$		
	$A^1\Sigma^+$		3.99	5.19	4.886	5.6	3.95	$2^2P+1^2S$		
BiH	$X(O^+)$	2.6±0.3	2.26	2.33	0			$6^4S+1^2S$		
	$A(I)$		2.10	1.98	0.6103	0.1	0.0	$6^4S+1^2S$		
	$B O^+$		1.71	1.68	2.636	1.7	1.42(1.91)	$6^3D+1^2S$		
Bi <sup>2</sup> H	$X(O^+)$	2.6±0.3	2.23	2.36	0			$6^4S+1^2S$		
	$B(O^+)$		1.48	1.18	2.636	1.5	1.42(1.91)	$6^2D+1^2S$		
CH	$X^2\Pi$	3.66	3.23	3.38	0			$2^3P+1^2S$		
	$A^2\Delta$		2.34	2.15	2.870	1.6	1.26	$2^1D+1^2S$		
	$B^2\Sigma^-$		0.407	0.317	3.217	0.0	0.0	$2^3P+1^2S$		
	$C^2\Sigma^+$		1.85	1.62	3.945	2.1	2.67	$2^1S+1^2S$		
(C <sup>1</sup> H) <sup>+</sup>	$X^1\Sigma^+$	3.47			0			$2^2P+1^2S$		
	$A^1\Pi$		0.800	0.795	2.993	0.3	0.0	$2^2P+1^2S$		
C <sup>2</sup> H	$X^2\Pi$	3.66	3.23	3.37	0			$2^3P+1^2S$		
	$A^2\Delta$		2.34	2.11	2.874	1.6	1.26	$2^1D+1^2S$		
	$B^2\Sigma^-$		0.38		3.222	0.0	0.0	$2^3P+1^2S$		
	$C^2\Sigma^+$		1.85	1.56	3.946	2.1	2.67	$2^1S+1^2S$		



TABLE III.—Continued.

Molecule	State	Dissociation energy				Atomic excitation energy			Dissociation products	Ref.
		Obs <sup>a</sup>	S.F.	5 par. F <sup>b,c</sup>	Te(ev)	Calc	Theoret			
<sup>2</sup> H <sub>2</sub>	X <sup>1</sup> Σ <sub>g</sub> <sup>+</sup>	4.746	4.29	4.79	0				1 <sup>2</sup> S+1 <sup>2</sup> S	31
	B <sup>1</sup> Σ <sub>g</sub> <sup>+</sup>		2.89	c.	11.368	9.6	10.15		2 <sup>2</sup> P+1 <sup>2</sup> S	
	C <sup>1</sup> Π <sub>g</sub>		2.11	2.25	12.408	9.8	10.15		2 <sup>2</sup> P+1 <sup>2</sup> S	
	E <sup>1</sup> Σ <sub>g</sub> <sup>+</sup>		(1.76)	(1.73)	12.413	9.6	10.15		2 <sup>2</sup> S+1 <sup>2</sup> S	
	I <sup>1</sup> Π <sub>g</sub>		1.76	1.69	14.015	11.0	12.04		3 <sup>2</sup> P+1 <sup>2</sup> S	
	a <sup>3</sup> Σ <sub>g</sub> <sup>+</sup>		2.80	3.65	12.017	10.1	10.15		2 <sup>2</sup> S+1 <sup>2</sup> S	
	e <sup>3</sup> Σ <sub>g</sub> <sup>+</sup>		1.92	2.19	13.358	10.5	10.15		2 <sup>2</sup> P+1 <sup>2</sup> S	
d <sup>3</sup> Π <sub>g</sub>		2.40	3.03	13.972	11.7	12.04		3 <sup>2</sup> P+1 <sup>2</sup> S		
<sup>2</sup> H <sub>2</sub>	X <sup>1</sup> Σ <sub>g</sub> <sup>+</sup>	4.746	4.18	4.69	0				1 <sup>2</sup> S+1 <sup>2</sup> S	
	a <sup>3</sup> Σ <sub>g</sub> <sup>+</sup>		2.74	3.29			10.15		2 <sup>2</sup> S+1 <sup>2</sup> S	
	d <sup>3</sup> Π <sub>g</sub>		2.39	3.04			12.04		2 <sup>2</sup> P+1 <sup>2</sup> S	
HF	X <sup>1</sup> Σ <sup>+</sup>	5.9	4.92	5.88	0				1 <sup>2</sup> S+2 <sup>2</sup> P	33
H <sup>79</sup> Br	X <sup>1</sup> Σ <sup>+</sup>	3.93	3.89	4.13	0				1 <sup>2</sup> S+4 <sup>2</sup> P	34
H <sup>81</sup> Br	X <sup>1</sup> Σ <sup>+</sup>	3.93	3.89	4.13	0				1 <sup>2</sup> S+4 <sup>2</sup> P	34
<sup>2</sup> H <sup>79</sup> Br	X <sup>1</sup> Σ <sup>+</sup>	3.93	3.87	4.085	0				1 <sup>2</sup> S+4 <sup>2</sup> P	34
<sup>2</sup> H <sup>81</sup> Br	X <sup>1</sup> Σ <sup>+</sup>	3.93	3.85	4.01	0				1 <sup>2</sup> S+4 <sup>2</sup> P	34
(HCl) <sup>+</sup>	X <sup>2</sup> Π <sub>i</sub>	4.7±0.2	3.34	3.50	0				1 <sup>2</sup> S+3 <sup>2</sup> P	
	A <sup>2</sup> Σ <sup>+</sup>		1.63	c.	3.550	0.4	0		1 <sup>2</sup> S+3 <sup>2</sup> P	
<sup>2</sup> H <sup>35</sup> Cl	X <sup>1</sup> Σ <sup>+</sup>	4.38	4.30	4.61					1 <sup>2</sup> S+3 <sup>2</sup> P	34
<sup>2</sup> H <sup>37</sup> Cl	X <sup>1</sup> Σ <sup>+</sup>	4.38	4.27	4.53					1 <sup>2</sup> S+3 <sup>2</sup> P	34
Hg <sup>1</sup> H	X <sup>2</sup> Σ <sup>+</sup>	0.372	0.553	0.399	0				6 <sup>1</sup> S+1 <sup>2</sup> S	
	A <sup>2</sup> Π <sub>i</sub>		(1.63)	(1.29)	3.047	~4.2		{(4.67) (5.46) 4.89	6 <sup>2</sup> P+1 <sup>2</sup> S	
	A <sup>2</sup> Π <sub>i</sub>		(2.53)	(3.22)	3.503	~5.6		{(4.67) (5.46) 4.89	6 <sup>2</sup> P+1 <sup>2</sup> S	
(HgH) <sup>+</sup>	X <sup>1</sup> Σ <sup>+</sup>	(2.4)	2.20	1.94	0				6 <sup>2</sup> S+1 <sup>2</sup> S	
	A <sup>1</sup> Σ <sup>+</sup>		1.50	1.29	5.494	4.7	6.38		6 <sup>2</sup> P+1 <sup>2</sup> S	
(Hg <sup>2</sup> H) <sup>+</sup>	X <sup>1</sup> Σ <sup>+</sup>	(2.4)	2.20	1.94	0				6 <sup>2</sup> S+1 <sup>2</sup> S	
	A <sup>1</sup> Σ <sup>+</sup>		1.49	1.28	5.493	4.6	6.38		6 <sup>2</sup> P+1 <sup>2</sup> S	
InH	X <sup>1</sup> Σ <sup>+</sup>	≤2.58	2.21	2.80	0				5 <sup>2</sup> P+1 <sup>2</sup> S	
	A <sup>1</sup> Σ <sup>+</sup>		0.84	0.37	2.018	0.3	0(0.27)		5 <sup>2</sup> P+1 <sup>2</sup> S	
	B <sup>1</sup> Π		0.51	0.37	2.097	0.0	0(0.27)		5 <sup>2</sup> P+1 <sup>2</sup> S	
K <sup>1</sup> H	X <sup>1</sup> Σ <sup>+</sup>	1.92	1.69	1.46	0				4 <sup>2</sup> S+1 <sup>2</sup> S	
	A <sup>1</sup> Σ <sup>+</sup>		(-0.29)		2.421					
K <sup>2</sup> H	X <sup>1</sup> Σ <sup>+</sup>	1.92	1.66	1.61	0				4 <sup>2</sup> S+1 <sup>2</sup> S	
	A <sup>1</sup> Σ <sup>+</sup>		-0.33		2.428					
Li <sup>1</sup> H	X <sup>1</sup> Σ <sup>+</sup>	2.6	2.25	2.45	0				2 <sup>2</sup> S+1 <sup>2</sup> S	
	A <sup>1</sup> Σ <sup>+</sup>		-0.04		3.287	~0.8	1.85		2 <sup>2</sup> P+1 <sup>2</sup> S	
	B <sup>1</sup> Π		0.026	0.039	4.327	1.8	1.85		2 <sup>2</sup> P+1 <sup>2</sup> S	
Li <sup>2</sup> H	X <sup>1</sup> Σ <sup>+</sup>	2.6	2.22	2.44	0				2 <sup>2</sup> S+1 <sup>2</sup> S	
	A <sup>1</sup> Σ <sup>+</sup>		-0.05		3.287	~0.8	1.85		2 <sup>2</sup> P+1 <sup>2</sup> S	
	B <sup>1</sup> Π		0.026	0.037	4.323	1.8	1.85		2 <sup>2</sup> P+1 <sup>2</sup> S	
Mg <sup>1</sup> H	X <sup>2</sup> Σ <sup>+</sup>	2.1±0.5	1.77	1.76	0				3 <sup>1</sup> S+1 <sup>2</sup> S	
	A <sup>2</sup> Π <sub>r</sub>		1.57	1.26	2.383	3.0	2.70		3 <sup>2</sup> P+1 <sup>2</sup> S	
	C <sup>2</sup> Π		1.31	3.61	5.098					

TABLE III.—Continued.

Molecule	State	Dissociation energy			Atomic excitation energy			Dissociation products	Ref.
		Obs <sup>a</sup>	S.F.	5 par. F <sup>b,c</sup>	Te(ev)	Calc	Theoret		
Mg <sup>2</sup> H	X <sup>2</sup> Σ <sup>+</sup>	2.1	1.81	1.63	0	2.30	2.70	3 <sup>1</sup> S+1 <sup>2</sup> S	
	A <sup>2</sup> Π <sub>r</sub>		1.91	1.66	2.383			3 <sup>2</sup> P+1 <sup>2</sup> S	
(Mg <sup>1</sup> H) <sup>+</sup>	X <sup>1</sup> Σ <sup>+</sup>	(2.2)	2.40	3.59	0	~8	8.86	3 <sup>2</sup> S+1 <sup>2</sup> S	
	A <sup>1</sup> Σ <sup>+</sup>		5.76	c.	4.451			3 <sup>2</sup> D+1 <sup>2</sup> S	
(Mg <sup>2</sup> H) <sup>+</sup>	X <sup>1</sup> Σ <sup>+</sup>	(2.2)	2.32	2.10	0	~8	8.86	3 <sup>2</sup> S+1 <sup>2</sup> S	
	A <sup>1</sup> Σ <sup>+</sup>		5.91		4.451			3 <sup>2</sup> D+1 <sup>2</sup> S	
MnH	X <sup>7</sup> Σ	<2.4	2.09	1.93	0			a <sup>6</sup> S+1 <sup>2</sup> S	36
Mn <sup>2</sup> H	X <sup>7</sup> Σ		2.21	1.95	0			a <sup>6</sup> S+1 <sup>2</sup> S	36
Na <sup>1</sup> H	X <sup>1</sup> Σ <sup>+</sup>	2.0	1.79	1.83	0			3 <sup>2</sup> S+1 <sup>2</sup> S	
	A <sup>1</sup> Σ <sup>+</sup>		-0.371		2.816				
OH	X <sup>2</sup> Π <sub>i</sub>	4.62	4.28	4.81	0	2.0	1.96	2 <sup>3</sup> P+1 <sup>2</sup> S	
	A <sup>2</sup> Σ <sup>+</sup>		2.66	2.66	4.052			2 <sup>1</sup> D+1 <sup>2</sup> S	
O <sup>2</sup> H	X <sup>2</sup> Π <sub>i</sub>	4.62	4.25	5.98	0	2.4	1.96	2 <sup>3</sup> P+1 <sup>2</sup> S	
	A <sup>2</sup> Σ <sup>+</sup>		2.58	2.74	4.447			2 <sup>1</sup> D+1 <sup>2</sup> S	
Pb <sup>1</sup> H	X <sup>2</sup> Π <sub>i</sub>	1.9±0.2(G) ≤1.59(H)	2.040	2.47	0			6 <sup>3</sup> P+1 <sup>2</sup> S	
	A <sup>2</sup> Σ		0.66	0.56	(2.181)	1.0	0(0.97)(1.32)	6 <sup>3</sup> P+1 <sup>2</sup> S	
	B <sup>2</sup> Σ		0.47	0.38	(2.235)	0.8	0(0.97)(1.32)	6 <sup>3</sup> P+1 <sup>2</sup> S	
Rb <sup>1</sup> H	X <sup>1</sup> Σ <sup>+</sup>	1.7±0.2	1.57	1.55	0			5 <sup>2</sup> S+1 <sup>2</sup> S	
	A <sup>1</sup> Σ <sup>+</sup>		-0.30		2.344				
SrH	X <sup>2</sup> Σ <sup>+</sup>	1.75±0.1	2.17	2.12	0			5 <sup>1</sup> S+1 <sup>2</sup> S	
	D <sup>2</sup> Σ <sup>+</sup>		1.63	1.22	2.584	2.5	2.69	5 <sup>1</sup> P+1 <sup>2</sup> S	
	C <sup>2</sup> Σ <sup>+</sup>		1.92	3.21	3.252	3.5	3.79	5 <sup>1</sup> D+1 <sup>2</sup> S	
Zn <sup>1</sup> H	X <sup>2</sup> Σ <sup>+</sup>	0.95	1.14	0.87	0			4 <sup>1</sup> S+1 <sup>2</sup> S	
	A <sup>2</sup> Π <sub>r</sub>		2.24	2.17	2.885	4.2	4.0	4 <sup>2</sup> P+1 <sup>2</sup> S	
	B <sup>2</sup> Σ <sup>+</sup>		(1.59)	(1.28)	3.420	4.0	4.0	4 <sup>2</sup> P+1 <sup>2</sup> S	
(Zn <sup>1</sup> H) <sup>+</sup>	X <sup>1+</sup>	2.9+0.4	2.36	2.35	0			4 <sup>2</sup> S+1 <sup>2</sup> S	
	A <sup>1+</sup>		3.37	3.57	5.789	6.2	6.0	4 <sup>2</sup> P+1 <sup>2</sup> S	
(Zn <sup>2</sup> H) <sup>+</sup>	X <sup>1+</sup>	2.9	3.36	c.	0			4 <sup>2</sup> S+1 <sup>2</sup> S	
	A <sup>1+</sup>		0.40	c.	5.789	6.2	6.0	4 <sup>2</sup> P+1 <sup>2</sup> S	

<sup>a</sup> (G)=Gaydon (reference 45); (H)=Herzberg (reference 8).

<sup>b</sup> Values quoted in brackets are based on uncertain data.

<sup>c</sup> c=Solution complex.

harmonic oscillator using the WBK method and the general potential<sup>7</sup>

$$V = a_0(\Delta r/r_c)^2 [1 + a_1(\Delta r/r_c) + a_2(\Delta r/r_c)^2 + \dots] \text{hc.} \quad (9)$$

The following values for  $a_0$ ,  $a_1$ , and  $a_2$  in Eq. (9) were

<sup>7</sup> J. L. Dunham, Phys. Rev. 41, 713, 721 (1932).

obtained from

$$a_0 = \omega_e^2/4B_e, \quad (10)$$

$$a_1 = -1 - \alpha_e \omega_e/6B_e^2 = -(1+F), \quad (11)$$

$$a_2 = (\frac{5}{4})a_1^2 - 2\omega_e x_e/3B_e = (\frac{5}{4})a_1^2 - G/12. \quad (12)$$

By comparing Eq. (8) with Eq. (9) and using Eqs.

(10), (11), and (12) one obtains the following relations

$$D_e = \omega_e^2 / 2nr_e B_e, \quad (13)$$

$$\alpha_e = (6abB_e^2 / \omega_e) (nr_e/2)^{1/2} \quad \text{or} \quad F = ab\Delta^{1/2}, \quad (14)$$

$$x_e \omega_e = \frac{3}{2} B_e \left\{ \frac{1}{4} + (nr_e/4) + ab(nr_e/2)^{1/2} + [(5a^2b^2/4) - ab^2](nr_e/2)^{1/2} \right\}. \quad (15)$$

Equation (13) is equivalent to (2). Equations (14) and (15) may be put in the form

$$2x_e \omega_e / 3B_e = \frac{1}{4} + (nr_e/4) + (\alpha_e \omega_e / 6B_e^2) + \frac{5}{4} (\alpha_e \omega_e / 6B_e^2)^2 - (nr_e/2)^{1/2} b \alpha_e \omega_e / 6B_e^2, \quad (16a)$$

or

$$G/12 = \frac{1}{4} + \Delta/2 + F + \frac{5}{4} F^2 - \Delta^{1/2} b F, \quad (16b)$$

or if one eliminates  $\Delta$

$$G = 12 \left[ \left( \frac{1}{4} + F \right) + 12F^2 \left[ \left( \frac{1}{2} a^2 b^2 \right) + \left( \frac{5}{4} \right) - (1/a) \right] \right].$$

Equation (16) has been used to calculate values of  $D_e$  from experimental values of  $k_e$ ,  $x_e \omega_e$ ,  $\alpha_e$ ,  $r_e$ , and  $b$ ;  $b$  was found to be constant within 3%. The value of  $b$  used in the calculations was 1.065. The calculated values of  $D_e$  are tabulated in Tables I-III and are compared with experimental values and with values for the dissociation energy calculated from the simple three-parameter function. In cases where the experimental values of  $x_e \omega_e$  and  $\alpha_e$  are well known the calculated values agree well with those calculated from the simple function. The agreement with experimental  $D_e$  values is good when these are well known from a knowledge of the excited states of the separated atoms. In most cases where the calculated value of  $D_e$  deviates markedly from that given by the simple functions, the experimental value of  $\alpha_e$  is not well known or is given with less than three significant figures. A small error in  $\alpha_e$  causes a relatively large error in  $D_e$  and it would appear that the lack of agreement between the two

calculated values of  $D_e$  is due in part to the uncertainty in  $\alpha_e$ . The experimental data for  $\omega_e$ ,  $B_e$ ,  $\omega_e x_e$ ,  $\alpha_e$ , and  $T_e$  have been taken from Herzberg<sup>8</sup> unless other references are quoted in column 10. The additional references<sup>9-39</sup> give more recent and, what has been assumed to be more accurate data. All dissociation energies, apart from that of  $C_2$ , have been taken from the second edition of Cottrell's book.<sup>40</sup>

The dissociation energies of the excited states are related to those of the ground states as in

$$T_e + D_e^* = D_e(X) + \Delta \text{ A.E.E.}, \quad (17)$$

where  $T_e$  is the electronic energy of the excited state,  $D_e^*$  is the dissociation energy for the excited state,  $D_e(X)$  is the dissociation energy for the ground state, and  $\Delta \text{ A.E.E.}$  is the difference between the atomic excitation energies in the two states (see Fig. 1). The electronic energy of the state is usually accurately known, and consequently the change in the atomic excitation energies can be evaluated from the calculated or observed dissociation energies. From the permitted dissociation products, and tables of atomic excitation

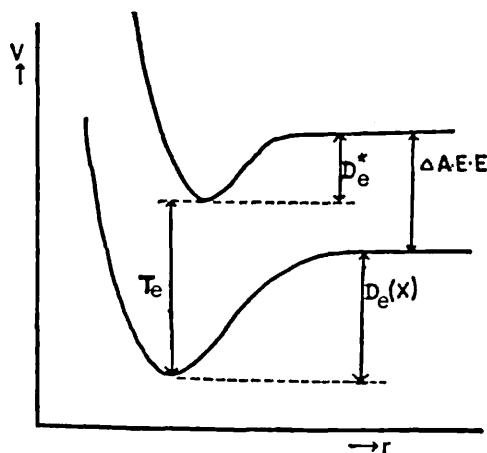


FIG. 1. Relation between dissociation energies of ground and excited states.  $T_e$  = electronic energy of the excited state,  $D_e^*$  = dissociation energy of the excited state,  $D_e(X)$  = dissociation energy of the ground state, and  $\Delta \text{ A.E.E.}$  = difference between the atomic excitation energies in the two states.

<sup>8</sup> G. Herzberg, *Spectra of Diatomic Molecules* (D. Van Nostrand Company, Inc., Princeton, New Jersey, 1950), pp. 502-581.

<sup>9</sup> D. H. Rank, A. H. Guenther, G. D. Saksena, J. N. Shearer, and T. A. Wiggins, *J. Opt. Soc. Am.* **47**, 686 (1957).

<sup>10</sup> G. Herzberg and T. J. Hugo, *Can. J. Phys.* **33**, 757 (1955).

<sup>11</sup> A. Lagerqvist, H. Westerlund, L. V. Wright, and R. F. Barrow, *Arkiv. Fysik* **14**, 387 (1959).

<sup>12</sup> R. D. Verma, *J. Chem. Phys.* **32**, 738 (1960).

<sup>13</sup> R. A. Durie, F. Legay, and D. A. Ramsey, *Can. J. Phys.* **38**, 444 (1960).

<sup>14</sup> A. Lofthus, *Can. J. Phys.* **34**, 780 (1956).

<sup>15</sup> B. P. Stoicheff, *Can. J. Phys.* **35**, 730 (1957).

<sup>16</sup> A. Lofthus, *J. Chem. Phys.* **25**, 494 (1956).

<sup>17</sup> P. G. Wilkinson, *Can. J. Phys.* **34**, 250 (1956).

<sup>18</sup> W. H. Fletcher and G. M. Begun, *J. Chem. Phys.* **27**, 579 (1957).

<sup>19</sup> E. Miescher, *Can. J. Phys.* **33**, 355 (1955).

<sup>20</sup> R. F. Barrow and E. Miescher, *Proc. Phys. Soc. (London)* **70A**, 219 (1957).

<sup>21</sup> G. Herzberg, *Can. J. Phys.* **31**, 57 (1953).

<sup>22</sup> G. Herzberg, *Can. J. Phys.* **30**, 185 (1952).

<sup>23</sup> A. E. Douglas and P. T. Rao, *Can. J. Phys.* **36**, 565 (1958).

<sup>24</sup> A. E. Douglas, *Can. J. Phys.* **33**, 801 (1955).

<sup>25</sup> G. Nilheden, *Arkiv Fysik* **10**, 19 (1956).

<sup>26</sup> S. M. Naudé and T. J. Hugo, *Can. J. Phys.* **31**, 1106 (1953).

<sup>27</sup> S. M. Naudé and T. J. Hugo, *Can. J. Phys.* **32**, 246 (1954).

<sup>28</sup> A. Lagerqvist, N. E. L. Nilsson, and R. F. Barrow, *Arkiv Fysik* **12**, 543 (1957).

<sup>29</sup> C. N. McKinney and K. K. Innes, *J. Mol. Spectroscopy* **3**, 235 (1959).

<sup>30</sup> R. Onaka, *J. Chem. Phys.* **27**, 374 (1957).

<sup>31</sup> B. P. Stoicheff, *Can. J. Phys.* **35**, 730 (1957).

<sup>32</sup> Y. Tanaka, *Sci. Papers Inst. Phys. Chem. Research (Tokyo)* **42**, 49 (1944).

<sup>33</sup> G. A. Kuipers, D. F. Smith, and A. H. Neilson, *J. Chem. Phys.* **25**, 275 (1956).

<sup>34</sup> H. M. Mould, W. C. Price, and G. R. Wilkinson, *Spectrochim. Acta.* **16**, 479 (1960).

<sup>35</sup> R. Velasco, *Can. J. Phys.* **35**, 1204 (1957).

<sup>36</sup> W. Hayes, P. D. McCarvill, and T. E. Neven, *Proc. Phys. Soc. (London)* **70A**, 904 (1957).

<sup>37</sup> D. F. Smith, M. Tidwell, and D. V. P. Williams, *Phys. Rev.* **79**, 1007 (1950).

<sup>38</sup> D. T. Smith, M. Tidwell, and D. V. P. Williams, *Phys. Rev.* **77**, 420 (1950).

<sup>39</sup> R. N. Dixon, *Can. J. Phys.* **37**, 1171 (1959).

<sup>40</sup> F. L. Cottrell, *The Strengths of Chemical Bonds* (Butterworths Scientific Publications Company, Ltd., London, 1958), 2nd ed.

TABLE IV.

Molecule	State	$\omega_e$	$B_e$	$\alpha_e$	$x_e\omega_e$ obs	$x_e\omega_e$ calc	$a$	$b$	Ref.
BF	$X^1\Sigma^+$	1402.13	1.5107	0.0165	11.84	10.24	0.543	0.987	30
BO	$X^2\Sigma^+$	1885.44	1.7803	0.01648	11.769	9.543	0.537	1.055	
	$A^2\Pi_i$	1260.70	1.4132	0.0196	11.157	12.490	0.577	1.130	
$^{79}\text{Br}^{81}\text{Br}$	$X^1\Sigma_g^+$	323.2	0.08091	0.000275	1.07	0.780	0.591	0.925	
	$B^2\Pi_{ou}^+$	169.71	0.0595	0.000625	1.913	2.1146	0.690	1.113	
$\text{C}_2$	$X^2\Pi_u$	1641.35	1.6326	0.01683	11.67	11.392	0.547	1.051	
	$A^2\Pi_j$	1788.22	1.7527	0.01608	16.44	10.744	0.529	0.851	
	$B^2\Pi_g$	1106.56	1.1922	0.0242	39.26	19.570	0.638	0.748	
	$a^1\Sigma_g^+$	1855.63	1.8205	0.01832	14.08	12.528	0.545	1.001	
	$b^1\Pi_u$	1608.33	1.6170	0.01720	12.14	11.584	0.550	1.039	
	$d^1\Sigma_u^+$	1829.57	1.8334	0.0204	13.97	13.995	0.559	1.066	
CO	$X^1\Sigma^+$	2169.829	1.9312	0.0175	13.295	13.197	0.542	1.061	9
	$A^1\Pi$	1515.61	1.6116	0.02229	17.2505	15.27	0.585	1.000	
	$a'^3\Sigma^+$	1230.65	1.345	0.0187	11.013	12.37	0.558	1.096	
	$a^3\Pi^+$	1739.25	1.6810	0.0193	14.47	14.05	0.570	1.049	
$\text{CO}^+$	$X^2\Sigma^+$	2214.24	1.9772	0.01896	15.164	14.44	0.552	1.065	10
	$A^2\Pi_i$	1562.06	1.5894	0.0194	13.532	13.48	0.571	1.063	
	$B^2\Sigma^+$	1734.18	1.7999	0.0302	27.927	23.44	0.6165	0.9733	
CP	$X^2\Sigma^+$	1239.67	0.7986	0.0059	6.86	6.36	0.566	1.03	
	$A^2\Pi_i$	1061.99	0.698	0.0077	6.035	9.59	0.622	1.354	
	$B^2\Sigma^+$	836.32	0.6829	0.0062	5.917	5.31	0.561	1.006	
CS	$X^1\Sigma^+$	1285.1	0.820044	0.005922	6.46	6.42	0.562	1.062	11
$\text{I}_2$	$X^1\Sigma_g^+$	214.52	0.03734	0.0001208	0.6127	0.600	0.636	1.054	12
ICl	$X^1\Sigma^+$	384.293	0.114154	0.000534	1.465	1.433	0.613	1.053	
	$A^2\Pi_i$	209.75	0.08389	0.0003828	1.947	0.664	0.503	0.612	
	$B^2\Pi_0^+$	(242)	0.090	0.0029	13	21.6	0.758	1.374	
IO	$X^2\Pi_1$	681.47	0.34026	0.002696	4.29	4.30	0.614	1.066	13
	$A^2\Pi_1$	514.57	0.27635	0.00273	5.52	4.37	0.634	0.945	
$\text{K}_2$	$X^1\Sigma_g^+$	92.64	0.05622	0.000219	0.354	0.224	0.459	0.832	
	$B^1\Pi_u$	75.00	0.04824	0.000235	0.3876	0.231	0.491	0.807	
$\text{Li}_2$	$X^1\Sigma_g^+$	351.435	0.67272	0.00704	2.592	2.287	0.425	0.994	
	$A^1\Sigma_u^+$	255.456	0.49749	0.00541	1.574	1.726	0.429	1.366	
	$B^1\Pi_u$	269.69	0.55723	0.00804	2.744	2.429	0.479	0.997	
$\text{N}_2$	$X^1\Sigma_g^+$	2358.07	1.99874	0.01709	14.188	13.46	0.542	1.036	14,15
	$a^1\Pi_g$	1693.70	1.6181	0.0183	13.825	13.46	0.569	1.050	14
	$B^2\Pi_g$	1735.42	1.6375	0.01794	15.198	13.71	0.570	1.035	
	$c^2\Pi_u$	2047.09	1.8247	0.01868	28.446	15.52	0.572	1.0131	
$\text{N}_2^+$	$X^2\Sigma_g^+$	2207.2	1.926	0.01743	16.14	13.45	0.547	0.97	17
NO	$X^2\Pi_1$	1904.03	1.7046	0.0178	13.97	13.91	0.567	1.062	18
	$A^2\Sigma^+$	2374.8	1.9972	0.01928	16.46	15.94	0.564	1.047	19
	$B^2\Delta$	1216.6	1.330	0.019	15.88	12.68	0.585	0.948	
	$B^2\Pi_1$	1036.96	1.076	0.0116	7.603	7.53	0.547	1.059	
	$E^2\Sigma^+$	2373.6	1.9863	0.0182	15.8(5)	14.89	0.556	1.030	
$\text{O}_2$	$X^2\Sigma_g^-$	1580.36	1.44566	0.01579	12.0730	12.17	0.570	1.070	
	$b^1\Sigma_g^+$	1432.687	1.400416	0.01817	13.9501	13.67	0.587	1.053	
	$a^1\Delta_g$	1509.3	1.4264	0.0171	12.(9)	13.05	0.581	1.071	



TABLE IV.—Continued.

Molecule	State	$\omega_e$	$B_e$	$\alpha_e$	$x_r\omega_e$ obs	$x_r\omega_e$ calc	$a$	$b$	Ref.
O <sub>2</sub> <sup>+</sup>	X <sup>3</sup> Π <sub>g</sub>	1876.4	1.6722	0.01984	16.53	16.37	0.588	1.060	
	a <sup>4</sup> Π <sub>u</sub>	1035.69	1.10466	0.01575	10.39	10.88	0.589	1.084	
	A <sup>2</sup> Π <sub>u</sub>	900	1.0617	0.01906	13.4	12.61	0.608	1.032	
	b <sup>4</sup> Σ <sub>g</sub> <sup>-</sup>	1196.77	1.28729	0.02206	17.09	16.36	0.615	1.041	
P <sub>2</sub>	X <sup>1</sup> Σ <sub>g</sub> <sup>+</sup>	780.89	0.30359	0.001477	2.820	2.73	0.579	1.046	23
	A <sup>1</sup> Σ <sub>u</sub> <sup>+</sup>	475.24	0.24166	0.00165	2.633	2.40	0.589	1.014	
S <sub>2</sub>	X <sup>3</sup> Σ <sub>g</sub> <sup>-</sup>	725.68	0.2956	0.00160	2.852	2.888	0.588	1.107	
	B <sup>3</sup> Σ <sub>u</sub> <sup>-</sup>	434.0	0.2219	0.0018	2.75	2.112	0.614	1.076	
SO	X <sup>3</sup> Σ <sup>-</sup>	1123.7	0.70894	0.005622	6.116	6.40	0.579	1.091	
Si <sub>2</sub>	X <sup>3</sup> Σ <sub>g</sub> <sup>-</sup>	506.72	0.2376	0.00135	1.97	2.04	0.573	1.085	24
	D <sup>3</sup> Π <sub>g</sub>	547.94	0.2596	0.00155	2.43	2.35	0.580	1.047	
	H <sup>3</sup> Σ <sub>u</sub> <sup>-</sup>	271.32	0.1699	0.00135	1.99	1.56	0.581	0.937	
SiN	X <sup>2</sup> Σ <sup>+</sup>	1151.68	0.7310	0.00567	6.561	6.35	0.574	1.047	
	B <sup>2</sup> Σ <sup>+</sup>	1031.01	0.7235	0.01037	16.743	13.48	0.647	0.954	
SiO	X <sup>1</sup> Σ <sup>+</sup>	1241.44	0.72729	0.00508	5.92	6.11	0.566	1.051	
	A <sup>1</sup> Π	852.71	0.63128	0.00695	6.44	7.25	0.596	1.113	

energies, the dissociation products of the excited states can then be deduced. Equation (18) assumes that the potential maxima are negligible. This is not generally true, but is a reasonable first approximation and appears to work very well except for certain hydrides. Where the maximum is not negligible, the effect will be to make  $\Delta$  A.E.E. too large. The dissociation products have been deduced for the various excited states and are given in column 9 of Tables I–III. In general no ambiguity in the products is possible as a result of the selection rules and widely separated energy states. When  $D_e(X)$  is uncertain and the dissociation products are known unambiguously, the calculated  $D_e^*$  can be used to deduce  $D_e(X)$ . Since the dissociation energies of many diatomic molecules are controversial or uncertain, it is important to look critically at this technique. Usually,  $T_e$  and  $\Delta$  A.E.E. will be accurately known. Consequently the uncertainty in  $D_e(X)$  will be equal to the uncertainty in  $D_e^*$  and in the potential maximum. This means that the uncertainty will be least when  $D_e^*$  is smallest. The effect of the potential maximum will be to overestimate  $D_e(X)$ . This technique will be applied to several cases of considerable interest.

It should be noted that  $a$  and  $b$  have nearly the same values respectively for all excited states of all molecules, which in turn are the same as those found valid for the ground states of diatomic molecules. The assigned values of  $a$  and of  $b$  enable one to calculate potential curves using the five-parameter functions and experimental values for  $k_e$ ,  $r_e$  and  $D_e$ . If values of  $D_e$  are not available predicted values may be obtained from experimental values of  $x_r\omega_e$  using Eq. (4a). This

method of computing potential curves will be enlarged upon below.

#### SOME ADDITIONAL RELATIONS

A comparison of  $D_e(S)$ , dissociation energy calculated from the simple function, with  $D_e(C)$ , dissociation energy calculated from the five-parameter function as tabulated in Table I shows that these two different internuclear potential functions give essentially the same results for  $D_e$  values where reliable data is available. This implies that an additional independent relation between the spectroscopic constants can be obtained by comparing the relations valid for the two functions.

By assuming that

$$D_e(S) = D_e(C),$$

and comparing Eq. (5b) with (16b) one obtains

$$\Delta = [1 + (\frac{5}{4})F]^2/b^2$$

or

$$D_e = (\frac{1}{2})kr_e^2b^2/[1 + (\frac{5}{4})F]^2 \quad (18)$$

and by resubstituting Eq. (5b)

$$G/3 = 1 + 2[1 + (\frac{5}{4})F]^2/b^2, \quad (19)$$

if one uses Eq. (14) with Eq. (16b) and eliminates  $nr_e/2 = \Delta$ , one obtains

$$F = a[1 + (\frac{5}{4})F]. \quad (20)$$

Equation (19) can be used to calculate values of  $x_r\omega_e$  from experimental values of  $\alpha_e$ ,  $\omega_e$ ,  $r_e$  and  $b$ . The known value of  $b$  is 1.065 within 3%. A number of these

TABLE V. Calculated values for  $x_e\omega_e$  and potential function parameters  $a$  and  $b$ .

Molecule	State	$\omega_e$	$B_e$	$\alpha_e$	$x_e\omega_e$ obs	$x_e\omega_e$ calc	$a$	$b$	Ref.
AlH	$X^1\Sigma^+$	1682.57	6.3962	0.188	29.145	31.23	0.5192	1.106	
	$C^1\Sigma^+$	1575.3	6.664	0.544	125.5	113.56	0.6406	1.012	
AuH	$X^1\Sigma^+$	2305.01	7.2401	0.2136	43.12	44.57	0.530	1.084	
	$A^1\Sigma^+$	1669.55	6.0069	0.249	55.06	48.18	0.565	0.993	
Au <sup>2</sup> H	$X^1\Sigma^+$	1634.98	3.6415	0.07614	21.655	22.40	0.529	1.084	
	$A^1\Sigma^+$	1195.24	3.036	0.103	34.813	29.86	0.588	0.983	
	$B^1\Sigma^+$	1165.4	2.961	0.079	21.85	21.01	0.549	1.043	
BaH	$X^2\Sigma^+$	1172	3.3823	0.0655	16	14.13	0.466	0.996	
	$B^2\Sigma$	1088	3.267	0.070	15	14.58	0.479	1.049	
	$E^2\Pi$	1231	3.486	0.074	17.5	16.43	0.489	1.030	
BeH	$X^2\Sigma^+$	2058.6	10.308	0.300	35.5	37.18	0.438	1.093	
	$A^2\Pi$	2087.7	10.470	0.329	39.8	40.72	0.454	1.078	
CH	$X^2\Pi$	2861.6	14.457	0.534	64.3	66.281	0.484	1.1319	
	$A^2\Delta$	2921.0	14.912	0.670	90.4	68.849	0.520	1.029	
	$B^2\Sigma^-$	2542.5	12.887	0.485	373.8	70.843	0.487	0.412	
	$C^2\Sigma^+$	2824.1	14.629	0.744	105.8	95.199	0.536	1.007	
CsH	$X^1\Sigma^+$	890.7	2.709	0.057	12.6	11.69	0.473	1.022	
	$A^1\Sigma^+$	204.0	1.126	-0.0185	-5.7	0.53			
HCl	$X^1\Sigma^+$	2989.74	10.5943	0.3042	52.05	55.78	0.502	1.052	
H <sup>79</sup> Br	$X^1\Sigma^+$	2649.22	8.4671	0.23226	44.077	46.70	0.514	1.085	34
HF	$X^1\Sigma^+$	4137.25	20.9456	0.7888	88.726	97.89	0.487	1.124	
LiH	$X^1\Sigma^+$	1405.65	7.5131	0.2132	23.200	24.852	0.424	1.1072	
	$B^1\Pi$	215.5	3.383	0.986	42.4	54.29	0.636	1.209	35
Li <sup>7</sup> H	$X^1\Sigma^+$	1055.12	4.2338	0.09198	13.228	14.26	0.424	1.1908	
	$B^1\Pi$	177.28	1.908	0.427	29.13	36.59	0.650	1.196	35
MnH	$X^7\Sigma$	1548.0	5.6841	0.1570	28.8	22.44	0.490	1.026	36
Mn <sup>2</sup> H	$X^7\Sigma$	1102.5	2.8956	0.0514	13.9	12.19	0.470	0.991	36
OH	$X^2\Pi_1$	3735.21	18.871	0.7138	82.81	88.838	0.487	1.1071	
	$A^2\Sigma^+$	3180.56	17.358	0.7868	94.93	92.071	0.522	1.0649	

calculations are reported in Tables IV and V. The calculated values agree well with the experimental  $x_e\omega_e$  values, the average percent error being approximately 5% for nonhydrides and 10% for hydrides in general. A particularly likeable feature of the  $x_e\omega_e$  calculated from (19) is that the agreement with the observed is better than 1% for the ground states of CS, O<sub>2</sub>, O<sub>2</sub><sup>+</sup>, CO, IO, and NO for which the data is accurate and well established. This promotes confidence in the validity of the relationship. These results in general are slightly better than one obtains using the Pekeris relation<sup>41</sup> (Morse function), particularly for hydrogen containing molecules.

It is interesting that the relation derived from the Morse function giving  $\alpha_e$  as a function of  $x_e\omega_e$  works so well, while the relation giving  $D_e$  as a function of

$x_e\omega_e$  ( $D_e = \omega_e^2/4x_e\omega_e$ ) is so poor, as is the relation giving  $D_e$  as a function of  $\alpha_e$ . This is well illustrated by Varshni<sup>2</sup> in plots of the experimental quantities  $G$  vs  $\Delta$  and  $F$  vs  $\Delta$  for a number of molecules followed by a comparison with curves expected from various potential functions. The curves for a Morse function deviate greatly from the experimental points, but in such a way that a plot of the  $G$  versus  $F$  would agree well with the experimental relationship. This illustrates the point that a potential function which relates some spectroscopic quantities well may relate others rather poorly.

Equation (18) can be used to calculate values of  $D_e$  from experimental values of  $\omega_e$ ,  $r_e$ , and  $\alpha_e$ . This would be particularly useful when one has no experimental data from which to obtain  $x_e\omega_e$  but does have microwave data giving  $\alpha_e$ . Our calculations indicate that Eq. (18) works well on most molecules. However,

<sup>41</sup> C. L. Pekeris, Phys. Rev. 45, 98 (1934).

TABLE VI. Calculation of  $D_e$  and  $x_e\omega_e$  from  $\alpha_e$ .

Molecule	State	$\omega_e$ cm <sup>-1</sup>	$B_e$ cm <sup>-1</sup>	$\alpha_e$ cm <sup>-1</sup>	$x_e\omega_e$ calc cm <sup>-1</sup>	$D_e$ calc ev	$D_e$ obs ev	Ref.
BrCl	$X^1\Sigma^+$	~430	0.152469	0.000745	1.658	2.68	2.31	37
BrF	$X^1\Sigma^+$	671	0.357143	0.005214	10.8	0.98	2.19 or 2.60	38
NH	$X^2\Sigma^-$	~3125	16.688	0.646	75.8	3.26	~3.8	39
	$A^2\Pi_i$	~3034	16.709	0.744	85.9	2.69	~1.4	

the value of  $D_e$  calculated for FBr does not agree with the experimental value, although the value of  $\alpha_e$  is reported to four significant figures. We have no explanation for this. It is perhaps significant that  $a$  evaluated using Eq. (19) is much larger than expected. Dissociation energies and anharmonicities have been evaluated for the ground states of NH and BrCl (Table VI). No anharmonicity values have been determined experimentally for these molecules. The dissociation energies are in accord with those quoted by Cottrell.<sup>40</sup>

Equation (20) can be used to calculate the parameter  $a$ . Since values for  $\alpha_e\omega_e/6B_e^2 = F$  vary from about 1 to 2.5,  $a$  cannot be constant. However it is seen from the calculated values of  $a$  given in Table IV, V, and VII that, except for elements in the first row of the periodic table,  $a$  has a value near 0.56. These values of  $a$  may be compared favorably with the values reported in I, calculated from Eq. (16) and experimental values for  $\alpha_e$ ,  $x_e\omega_e$ ,  $D_e$  and  $r_e$ . A more detailed analysis of  $a$  shows that it is periodic within the periodic table. This will be discussed in a future publication.<sup>42</sup> The parameter  $b$  may be conveniently evaluated from (19). For non-hydrides  $b$  is a good constant with a value of 1.065. The deviations from this value are rarely greater than 5% and it is tempting to conclude that where the calculated value deviates considerably from this value the data (in the majority of cases, probably  $\alpha_e$ ) is in error. The major discrepancies are for the  $A^3\Pi_0$  and  $B^3\Pi_0$  states of  $C_2$ ,  $A^3\Pi_i$ , and  $B^3\Pi_0^+$  states of  $ICl$  and the  $X^1\Sigma_g^+$  and  $B^1\Pi_u$  states of  $K_2$ . There appears to be no reason why these states should be different from the others for which such calculations have been carried out. The average value for  $b$  for the various electronic states of the isotopes of hydrogen is 1.158 with a mean deviation of 0.045. Since  $b$  was taken as 1.065 in evaluating  $x_e\omega_e$  from Eq. (19) this explains why the calculated anharmonicities for hydrogen are high in general. The anharmonicities have been recalculated for  $b=1.158$  and are reported in column 10 of Table VII.

#### DISCUSSION

The results in Tables I to VII show that the proposed internuclear potential functions, Eqs. (3) and (7), can be used to correlate and predict spectroscopic quantities for excited states of diatomic molecules as

well as for the ground states. Where reliable data are available calculated  $D_e(s)$  and  $D_e(c)$  values agree rather well. Since small changes in  $\alpha_e$  values produce large changes in calculated  $D_e(c)$  values, the simple function appears to be more reliable for calculating dissociation energies. This is illustrated by some recent data on the ground state of  $N_2$ . Lofthus's<sup>14</sup> data lowers  $x_e\omega_e$  from that given by Herzberg<sup>8</sup> by 1.7%, changing  $D_e(s)$  from 9.45 to 9.62 ev, whereas  $\alpha_e$  changed by about -9% (from 0.0187 to 0.0171) changing  $D_e(c)$  from 10.21 to 8.91 ev. The coincidence of  $D_e(s)$  and  $D_e(c)$  is further illustrated for ground states and excited states by calculations using recent data for  $CS$ ,<sup>11</sup>  $CO$ ,<sup>9</sup>  $O_2$ ,  $O_2^+$ ,  $IO$ ,<sup>13</sup>  $^{14}N^{16}O$ ,<sup>13</sup>  $^{15}N^{16}O$ ,<sup>13</sup> which all give  $D_e$  agreeing within 2%. Improved data usually gives better correlations or predictions for the functions, and the values for  $D_e(s)$  and  $D_e(c)$  usually converge. Examples are  $P_2(X^1\Sigma_g^+)$ ,<sup>23</sup>  $NO(X^2\Sigma^+)$ ,<sup>18</sup>  $H_2(1^1\Sigma_g^+)$ ,<sup>31</sup>  $N_2(a^1\Pi_g)$ ,<sup>14</sup>  $CO(X^1\Sigma^+)$ <sup>9</sup> and  $AlO(X^2\Sigma^+)$ .

However the  $B^1\Sigma_u^+$  states of  $^1H_2$ ,  $^1H^2H$  and  $^2H_2$  give very poor agreement between  $x_e\omega_e$  calculated and observed.<sup>8,32</sup> This may be due to the highly ionic character for this state or to an incorrect analysis. It is noted that the relationships hold reasonably well for HF, HCl, HBr, and HI.

The calculated  $\Delta$  A.E.E. for the  $^3\Pi_{0u}^+$  state of  $Br_2$  and  $I_2$  are consistent only with the dissociation products being  $^2P$  ground-state atoms, but with one of the atoms excited to a  $J$  value of one-half. This is in agreement with experimental findings and shows the sensitivity of the technique in favorable circumstances.

For many of the hydrides, especially for excited states, the calculated dissociation energies are much higher than is consistent with the known or preferred dissociation products. This suggests that the potential maxima for these cases are large.

One attractive feature of the five-parameter function is the remarkable constancy of  $b$  and to a lesser extent of  $a$  for all states of all molecules. Values of  $b$  and  $a$  are even more constant for the range of states of a given molecule. For hydrogen-containing molecules the values for  $a$  are usually lower than average. Pliva has shown that values of  $b$  and  $a$  are transferable to bonds of polyatomic molecules with some excellent results for spectroscopic constants of simple polyatomic molecules.<sup>6</sup>

It is interesting that the criteria that  $D_e(s) = D_e(c)$  gives a relation between  $x_e\omega_e$  and  $\alpha_e$  which is very

<sup>42</sup> D. Steele and E. R. Lippincott (to be published).

TABLE VII. Calculated values for  $x_e\omega_e$  and potential function parameters  $a$  and  $b$ .

Molecule	State	$\omega_e$	$B_e$	$\alpha_e$	$x_e\omega_e$ obs	$x_e\omega_e$ calc	$x_e\omega_e$ calc $b=1.158$	$a$	$b$	Ref.
$\text{H}_2$	$X^1\Sigma_g^+$	4400.39	60.8407	3.0177	120.815	145.66	126.71	0.344	1.192	31
	$B^1\Sigma_u^+$	1356.52	19.982	1.1077	22.857	49.55	43.06	0.352	1.762	32
	$C^1\Pi_u$	2442.72	31.340	1.626	(67.0)	82.10	71.25	0.365	1.201	
	$I^1\Pi_g$	2265.2	29.79	1.515	78.47	75.40	65.50	0.358	1.040	
	$c^3\Pi_u$	2465.0	31.07	1.425	61.4	75.15	65.35	0.345	1.203	
	$a^3\Sigma_g^+$	2664.83	34.216	1.671	71.65	85.52	74.31	0.355	1.184	
	$e^3\Sigma_u^+$	2195.8	27.30	1.515	65.80	77.47	67.10	0.385	1.171	
	$d^3\Pi_u$	2371.58	30.364	1.545	66.27	78.48	68.13	0.363	1.177	
	$K^3\Pi_u$	2336	29.40	1.58	(60)	80.44	69.73	0.376	1.268	
	$n^3\Pi_u$	2322	29.93	1.3	62.9	68.56	59.72	0.331	1.122	
$^1\text{H}^2\text{H}$	$X^1\Sigma_g^+$	3811.92	45.638	1.9500	90.711	108.86	94.68	0.347	1.066	31
	$C^1\Pi_u$	2139.1	23.64	0.938	66.55	56.63	48.25	0.343	0.730	
	$I^1\Pi_g$	1962.1	22.36	1.21	58.21	66.90	57.85	0.397	1.192	
	$a^3\Sigma_g^+$	2308.44	25.685	1.099	53.77	64.73	56.23	0.357	1.190	
	$e^3\Sigma_u^+$	1905.17	20.766	1.010	51.70	58.92	51.03	0.385	1.149	
	$d^3\Pi_u$	2054.59	22.810	1.020	49.74	59.57	51.70	0.364	1.186	
$^3\text{H}_2$	$X^1\Sigma_g^+$	3118.46	30.442	1.0623	64.10	72.69	63.04	0.347	1.16	31
	$C^1\Pi_u$	1735.85	15.665	0.5739	39.06	41.17	35.73	0.366	1.098	
	$E^1\Sigma_g^+$	1784.5	16.37	0.682	(48.1)	47.14	40.82	0.388	1.053	
	$I^1\Pi_g$	1600.1	14.739	0.526	39.42	37.36	32.45	0.358	1.032	
	$d^3\Pi_u$	1678.22	15.200	0.5520	32.94	39.56	33.60	0.391	1.268	
	$a^3\Sigma_g^+$	1885.84	17.109	0.606	35.96	34.62	37.88	0.360	1.195	
	$e^3\Sigma_u^+$	1556.64	13.856	0.541	34.51	38.76	33.58	0.382	1.140	
$^3\text{H}_2$	$X^1\Sigma_g^+$	2553.8	20.3243	0.59222	43.872	49.38	42.94	0.347	1.143	
	$a^3\Sigma_g^+$	1541.57	11.4374	0.3258	24.47	28.79	25.01	0.352	1.173	
	$d^3\Pi_u$	1372.11	10.150	0.3050	22.135	26.68	23.15	0.367	1.190	

similar to the Pekeris relation obtainable from the Morse function, but with slightly better results. In addition it offers a rapid method of calculating  $b$  and  $a$ , the values of which are essentially the same as calculated without this criteria.

#### DISSOCIATION ENERGIES OF SOME SPECIFIC MOLECULES

##### $D_e(\text{C}_2)$

The dissociation energy of carbon is uncertain. Cottrell lists it as 6.5 ev, but quotes a more recent examination of the evidence which gives 6.16 ev. Calculations from both the simple and five-parameter functions give a value near 5.6 ev. As explained in the introduction the dissociation energies calculated for the excited states can be used to deduce  $D_e(X)$ . The  $A^3\Pi_g$  and  $B^3\Pi_g$  states cannot both arise from the separate atom configurations  $2^3P+2^3P$ . Assuming that  $D_e(X)$  lies in the range 4 to 7 ev shows that the  $A^3\Pi_g$  arises from the  $3P+1D$  configuration.  $D_e^*$  for the  $B^3\Pi_g$  state is calculated to be only 0.7 ev. Allowing a 50% error in this value, this necessitates that  $D_e(X)$  is less than 6.0 ev and, assuming no potential maximum for the upper state, more than 5.4 ev (see Table VIII). This is in excellent agreement with the calculated value

of 5.6 ev. The dissociation energies of the  $A^3\Pi_g$  state as evaluated from the three- and five-parameter functions are in poor agreement. This is in accord with the low value of  $b$  calculated from Eq. (19).  $D_e$  from the simple function is again in good agreement with the assigned value of  $D_e(X)$ , thus suggesting that the value of  $\alpha_e$  for this state is in error.

The splitting of the singlet and triplet states is uncertain. Hicks<sup>43</sup> deduced that the  $1^1\Sigma_g^+$  state was 0.39 ev above the  $X^3\Pi_u$  state. According to a private communication from D. A. Ramsey to E. Clementi and K. S. Pitzer,<sup>44</sup> perturbations in the rotational spectrum of the  $3^3\Sigma_g^-$  state suggest that the  $1^1\Sigma_g^+$  state lies 0.07 ev below the  $3^3\Pi_u$  state. The difference between these values is too small compared with the uncertainty in the  $D_e^*$  of the singlet states for the present calculations to distinguish between them, though Ramsey's value is favored. As shown in Table VIII  $D_e(X)=4.9$  ev is definitely too low and  $D_e(X)=6.5$  ev is suggested to be too high, in confirmation of the deductions from the triplet states.

<sup>43</sup> W. T. Hicks, Spectroscopy of High Temperature Systems (thesis) UCRL-3696 (Feb. 1957).

<sup>44</sup> E. Clementi and K. S. Pitzer, J. Chem. Phys. **32**, 656 (1960); E. A. Balik and D. A. Ramsey, *ibid.* **31**, 1128 (1959).

TABLE VIII. Correlation of  $D_e(X)$  with dissociation products for  $C_2$ .

State	Te ev	$D_e$ ev	$\Delta A \cdot E \cdot E$ calc			Dissociation products	$\Delta A \cdot E \cdot E$
			$D_e(X)$ =6.5	$D_e(X)$ =5.6	$D_e(X)$ =4.9		
$X^3\Pi_u$	0	6.5 Cott. 5.6 calc 4.9 old.	0	0	0	$2^3P+2^3P$	0.0
$A^3\Pi_g$	2.39	4.7 (S) 3.5 (C)	0.6 -0.6	1.5 0.3	2.2 1.0	$2^3P+2^1D$	1.26
$B^3\Pi_g$	4.97	0.7	-0.8	0.1	0.7	$2^3P+2^3P$	0.0
$a^1\Sigma_g^+$	-0.07 0.39	6.0	-0.6 -0.1	0.3 0.8	1.0 1.5	$2^3P+2^3P$ $2^3P+2^3P$	0.0
$b^1\Pi_u$	0.97 1.43	5.2	-0.3 0.1	0.6 1.0	1.3 1.7	$2^3P+2^3P$ $2^3P+2^3P$	0.0
$c^1\Pi_g$	4.18 4.64	5.0	2.7 3.1	3.6 4.0	4.3 4.7	$2^1D+2^1S$ $2^3P+2^3S$	3.93 4.16
$d^1\Sigma_u^+$	5.29 5.73	5.9	4.7 5.1	5.6 6.0	6.3 6.7	? ?	

 $D_e(CO)$ 

The calculated dissociation energy favors the old value near 9 ev. However, the higher value of 11.1 ev now appears to be well established. The dissociation products of the excited states  $A^1\Pi$ ,  $a^3\Pi$ ,  $a'^3\Sigma^+$ , and  $C^3\Sigma^-$  are readily identified using  $D_e(X)=11.1$  ev as  $2^3P+2^3P$ . The agreement between the calculated and observed  $\Delta A.E.E.$  is very good indeed. However the data can also be explained, though much less satisfactorily using the low value of  $D_e$ . It would be expected that at least some of the excited states that have been studied arise from the  $2^3P$  atoms, thus it would seem that there is little doubt from this analysis that the high value is correct.

 $D(S_2)$ 

The spectroscopic data for the dissociation energy of  $S_2$  are consistent with any of the values 4.4, 3.6, or 3.3 ev. The individual values are favored by Gaydon, Herzberg and the N.B.S., respectively. Two thermochemical approaches to  $D(S_2)$  have been summarized by Cottrell. The first involving the heat of formation of SO favors 3.6 ev for  $D(S_2)$  and 5.15 ev for  $D(SO)$  (See below). The second approach involving the heat of formation of S-H leads to a preference for the highest value of  $D(S_2)$ . However the data on which the latter is based does not appear to be too reliable. The calculated dissociation energies using both the simple and five-parameter functions strongly favor the high value, 4.4 ev. This is confirmed by calculations on the  $B^3\Sigma_u^-$  state, the calculated dissociation energy indicating that the dissociation products are  $3^1D+3^3P$  and that the ground state dissociation energy is about 4.5 ev.

 $D_e(SO)$ 

A value of 5.15 ev is favored over 4.0 ev. Thermochemical data also favors the higher value (see Cottrell). Unfortunately the only data for excited states of this molecule, that for the  $B^3\Sigma^-$  state, is uncertain and leads to very poor agreement between  $D_e(s)$  and  $D_e(c)$ .

 $D(BF)$ 

Gaydon<sup>45</sup> gives  $D_e=8.5\pm 0.5$  ev whereas Herzberg suggests approximately 4.3 ev. The calculated value of  $D_e(s)$  is 3.1 ev and of  $D_e(c)=2.4$  ev suggesting strongly that the low value quoted by Herzberg is correct. The dissociation energy of the excited state  $A^1\Pi$  can be interpreted in terms of either value. The relative electronic energies of the singlet states are unfortunately unknown.

 $D_e(MnH)$ 

Calculations on MnH and MnD indicate that the value quoted by Cottrell for  $D_e$  of 2.4 ev (very uncertain) is of the right order of magnitude. The calculated value is about 2.1 ev.

## LIMITING FORMS OF POTENTIAL FUNCTIONS

A further discussion on the limiting forms of the five parameter function used for Eq. (1) is desirable since other information is available as to the form which an inter-nuclear potential function should assume as  $r \rightarrow \infty$  and as  $r \rightarrow 0$ .

<sup>45</sup> A. G. Gaydon, *Dissociation Energies* (Chapman and Hall, Ltd., London), 2nd ed.

For example for the  $r \rightarrow 0$  limit

$$V = (Z_a Z_b e^2 / r) + E_{ab} + \dots, \quad (21)$$

where  $Z_a$  and  $Z_b$  are the atomic numbers of atoms  $A$  and  $B$ , respectively, and  $E_{ab}$  is the energy of the state of the united atom formed.

Again, for  $r \rightarrow \infty$  and separated atom states without quadrupole moments ( $S$  states) one would expect a limiting form

$$V = A/r^n \quad (22)$$

with  $n=6$  and  $A$  is negative. On the other hand, for separated atomic states with quadrupoles one would expect  $n=5$  and  $A$  to be negative or positive.<sup>46</sup>

It would be desirable to incorporate some or all of these conditions in the form of  $f(r)$  of Eq. (1) provided that the proper relationships between the spectroscopic quantities  $r_e$ ,  $\omega_e$ ,  $D_e$ ,  $\alpha_e$  and  $x_e \omega_e$  are retained. The relationships between these quantities used here can be retained if the form for  $f(r)$ , on expansion to the second power in  $\Delta r$ , always has the form

$$f(r) = -(b^2 n r_e / 2)^{\frac{1}{2}} (\Delta r / r_e) + (b^2 n r_e / 2) (\Delta r / r_e)^2 + \dots \quad (23)$$

The correlation between the five spectroscopic parameters is extremely sensitive to the form of  $f(r)$  and seemingly minor but arbitrary changes in its form up to  $\Delta r^2$ , or to  $\Delta r^4$  in  $V(r)$ , cause large deviations among the relations for the spectroscopic quantities with the result that they cannot be used to predict unknown spectroscopic quantities from known quantities.

The form of (23) suggests that one form for  $f(r)$  would be a potential composed of two parts, one attractive and the other repulsive with the repulsive term the square of the attractive one. The repulsive term would be important for  $r < r_e$  but unimportant for  $r \gg r_e$ , while the attractive term would be important for  $r > r_e$  but not for  $r \ll r_e$ . Consideration of Eq. (1) and separated atom states without quadrupole moments suggests that one limiting form for  $f(r)$  would be a Lennard-Jones 6-12 potential. Accordingly  $f(r)$  was initially chosen to satisfy this condition. For molecular states which dissociate to atomic states with quadrupoles one could use a (5-10) potential. Since the  $A/r^5$  term would always be attractive, this suggests that for molecular states where the proposed function gives reliable correlation of spectroscopic quantities  $A$  must be negative for separated atom states with quadrupoles even though other considerations show that possibly  $A$  could be positive.

On the other hand, one can choose  $f(r)$  in other forms and still retain the terms given in (23) to  $\Delta r^2$ . One particularly useful form is

$$f(r) = -(b^2 n / 2r)^{\frac{1}{2}} \Delta r \times \exp[-(b^2 n / 2r_e)^{\frac{1}{2}} \Delta r]. \quad (24)$$

<sup>46</sup> J. O. Hirschfelder, C. E. Curtiss, and R. B. Bird, *Molecular Theory of Gases and Liquids* (John Wiley & Sons, Inc., New York 1954).

This particular form has the advantage of showing that a repulsive term in  $f(r)$  is not essential. It is also particularly easy to manipulate in calculations involving construction of potential curves and also seems to be more accurate than (7) when one makes a comparison with the experimental curves as constructed by the method of Klein-Rydberg-Rees as modified by Vanderslice *et al.*<sup>47</sup>

Although the conditions on  $f(r)$  seems to be highly specific, there is such flexibility left for its choice that one cannot choose between various suggested forms without additional considerations, the most important being an expansion to higher powers of  $\Delta r$  followed by correlation and prediction of additional spectroscopic parameters such as the second anharmonicity,  $y_e \omega_e$ , and the second-order vibration-rotation coupling constant,  $\gamma_e$ . Calculation of these quantities will be reported at a later date.

In conclusion it would seem that the five spectroscopic quantities,  $D_e$ ,  $\omega_e$ ,  $\omega_e x_e$ ,  $r_e$ , and  $\alpha_e$  do not give sufficient information concerning the limiting form of a potential function even though they can be adequately related provided that the function expands in a suitable manner up to the fourth power of  $\Delta r$ .

#### CONSTRUCTION OF POTENTIAL CURVES

When experimental data are available for a sufficiently large number of vibrational levels for a given diatomic molecule state the best method for construction of an internuclear potential curve is to use the Klein-Rydberg-Rees<sup>47</sup> method as modified by Vanderslice *et al.*<sup>48</sup> This method has the advantage that the resulting curve is based only on known experimental data for the vibrational levels and not on any assumed form for the potential function. This method has been applied to a number of diatomic molecules for both ground and excited states and for which the appropriate spectral data has been analyzed in detail.<sup>49</sup>

However, if one wished to construct the potential curve beyond the point for which there is information concerning the vibration levels these methods cannot be used and one must still use an empirical function. For this purpose most three-parameter functions are not sufficiently accurate. The Morse function is seriously off for values of  $R > R_e$  in that it predicts too much binding energy. The three-parameter function used here works reasonably well for values of  $R > R_e$ , particularly for large  $R$  but gives too much binding energy for  $R < R_e$ . In constructing empirical potential curves it would seem desirable to use a five-parameter function. One such function which can be readily used is the Hulbert-Hirschfelder function.<sup>50</sup> This function

<sup>47</sup> A. L. G. Rees, Proc. Phys. Soc. (London) **59**, 998 (1947).

<sup>48</sup> J. T. Vanderslice, E. A. Mason, W. G. Maisch, and E. R. Lippincott, J. Mol. Spectroscopy **3**, 17 (1959).

<sup>49</sup> J. T. Vanderslice, E. A. Mason, and E. R. Lippincott, J. Chem. Phys. **30**, 129 (1959); J. T. Vanderslice, E. A. Mason, and W. G. Maisch, *ibid.* **31**, 738 (1959); **32**, 515 (1960).

<sup>50</sup> H. M. Hulbert and J. O. Hirschfelder, J. Chem. Phys. **9**, 61 (1941).

has the convenience that its five parameters can readily be obtained from the five spectroscopic constants  $D_e$ ,  $R_e$ ,  $x_e\omega_e$ , and  $\alpha_e$ .

The five-parameter function, Eq. (7a), or the alternative proposed form, Eq. (7b) resulting from the substitution of Eq. (24) into Eq. (1), can be used equally well to construct potential curves from the appropriate spectroscopic constants. The latter form is superior to Eq. (7a) and yields potential curves agreeing well with experimental curves<sup>48,49</sup> over the complete range of  $r$ . The proposed function has the additional advantage that the constants  $b$  and  $a$  are reasonably transferable

from molecule to molecule, and thus curves can be constructed from experimental values of  $k_e$ ,  $r_e$  and  $D_e$  without other data. An additional advantage is that if an experimental  $D_e$  is not available from other information a reasonably accurate one may be computed from  $k_e$ ,  $r_e$  and either  $x_e\omega_e$ , or  $\alpha_e$  and used in the construction of the potential curve.

#### ACKNOWLEDGMENTS

The authors gratefully acknowledge financial support from the Office of Ordnance Research, U.S. Army, and assistance in the calculations by J. N. Finch.

## Construction of Reliable Internuclear Potential Curves from Equilibrium Bond Lengths and Vibrational Frequencies

D. STEELE AND E. R. LIPPINCOTT

Department of Chemistry, University of Maryland, College Park, Maryland

(Received March 13, 1961)

A method is presented for the construction of reliable internuclear potential curves using a previously proposed function and observed values of equilibrium bond lengths and vibrational frequencies. The function has the form

$$V = D_e \{1 - \exp[-(n\Delta r^2/2r)]\} \{1 + af(r)\}.$$

An explicit form is presented for the observed periodicity of the parameter  $a$  when referring to the ground states of diatomic molecules. This periodicity is shown to lead to relationships from which  $D_e$ ,  $\alpha_e$ , and  $x_e\omega_e$  can be calculated solely from  $\omega_e$  and  $r_e$ . An empirical relationship between the values of the parameter  $a$  in the ground and the excited states is presented from which

$D_e$ ,  $\alpha_e$ , and  $x_e\omega_e$  can be deduced for any nonionic excited state from  $\omega_e$  and  $r_e$  of that state. This latter relationship demonstrates that  $\omega_e r_e^2$  is not constant for all states of any molecule but is dependent in a predictable manner on the other spectroscopic constants. These relationships enable potential curves to be constructed solely from a knowledge of  $\omega_e$  and  $r_e$ . Calculated curves for the  $X^1\Sigma_g^+$  states of  $H_2$  and  $I_2$  and ground and excited states of  $N_2$  agree extremely well with experimental curves, deviating by no more than 2% of the dissociation energy. The agreement is very good for large values of  $r$  for  $H_2$  and  $I_2$ , which indicates that a general form exists for the interaction of bonding atoms at large distances.

THE construction of potential curves is of considerable value for the understanding of kinetics mechanisms, spectral phenomena, stellar structure, and many associated problems. In principle, such curves may be calculated *ab initio* from the Schrödinger equation. However, in practice, reliable curves cannot be obtained at present for anything more complicated than three-particle systems. They may be constructed for bound states of diatomic molecules from a knowledge of the experimental energy levels of the system by the method of Rydberg, Klein, and Rees as modified by Vanderslice and others<sup>1,2</sup> (hereafter referred to as the R.K.R.V. method). This method is a semiclassical one and consequently may give rise to errors for small changes in the bond lengths from the equilibrium values, that is, for small  $\Delta r$ . This has been checked<sup>3</sup> by comparison of the R.K.R.V. curve of  $H_2$  in the region of  $r_e$  with a calculated curve based on the Dunham method which is known to be reliable in this range. The results agreed to considerably better than 0.1%. This indicates that the curves obtained in the former manner may be taken as correct.

Unfortunately the curves obtainable by this method may be deduced only over the energy range for which energy levels are given by the spectroscopic data. Complete potential curves (that is, for all values of the interaction energy less than  $D_e$ ) are consequently known only for the ground states of  $H_2$  and  $I_2$ . In the vast majority of cases the experimental curves are known only for small internuclear displacements. A further disadvantage of the R.K.R.V. method is that spectroscopic constants, such as anharmonicity  $x_e\omega_e$ , the vibrational-rotational coupling constant  $\alpha_e$ , and higher terms cannot be deduced from limited experi-

mental data and hence the technique is of little value in predicting data. These considerations make empirical approaches to these problems of considerable value. In this paper it will be shown how an empirical approach can be used to obtain reliable potential curves for ground and excited states of diatomic molecules using very limited data, in particular, from the vibrational frequency  $\omega_e$  and the equilibrium bond length  $r_e$ . This implies that the anharmonic corrections can be deduced from the same limited data. Rules and equations are developed for doing the latter, which are then used to reduce the necessary amount of data required to plot curves using a previously proposed potential function.<sup>4</sup> Most empirical approaches require sufficient data to determine the first-order correction terms from the harmonic oscillator model, that is, the anharmonicity  $x_e\omega_e$  and the vibrational rotational coupling constant  $\alpha_e$ . Even when these are known the resulting curves are not usually of high accuracy.

The most successful approach to the potential problem is to assume a general analytical form for potential curves and to solve the Schrödinger equation using the general form for  $V(r)$ . Considerable simplification of this technique was effected by Dunham,<sup>5</sup> who solved the Schrödinger equation for a general power series expansion of  $V(r)$  and related the coefficients of  $\Delta r^n$  to the molecular constants. These relations may lead to useful correlations between the molecular constants for any given assumed form of  $V(r)$ . The earliest successful potential function was that of Morse,<sup>6</sup> which leads to a relation between  $\omega_e$ ,  $\omega_e x_e$ , and  $D_e$  from which either  $\omega_e x_e$  or  $D_e$  can be deduced from the other two constants with a reliability of about  $\pm 20\%$ . Many

<sup>1</sup> J. T. Vanderslice, E. A. Mason, and E. R. Lippincott, J. Chem. Phys. **30**, 129 (1959).

<sup>2</sup> J. T. Vanderslice, E. A. Mason, W. G. Maisch, and E. R. Lippincott, J. Chem. Phys. **33**, 614 (1960).

<sup>3</sup> J. T. Vanderslice, E. A. Mason, W. G. Maisch, and E. R. Lippincott, J. Mol. Spectroscopy **3**, 17 (1959).

<sup>4</sup> (a) E. R. Lippincott and R. Schroeder, J. Chem. Phys. **23**, 1131 (1955); J. Am. Chem. Soc. **78**, 5171 (1956); J. Phys. Chem. **61**, 921 (1957). (b) E. R. Lippincott and M. O. Dayhoff, Spectrochim. Acta **16**, 807 (1960); E. R. Lippincott, J. Chem. Phys. **26**, 1678 (1957).

<sup>5</sup> J. L. Dunham, Phys. Rev. **41**, 721 (1932).

<sup>6</sup> P. M. Morse, Phys. Rev. **34**, 57 (1929).



other general forms have been suggested, some involving only three parameters, others more. Those involving more than three parameters are generally of very limited value for the prediction of spectroscopic parameters since so many are necessary to define the function. One simple internuclear potential function which has been used very successfully in correlation and prediction studies<sup>4,7</sup> is

$$V(r) = D_e [1 - \exp(-n\Delta r^2/2r)] [1 + af(r)]. \quad (1)$$

$n$  is given by  $n = k_e r_e / D_e$ , where  $k_e$  is the force constant referred to zero displacement of the nuclei. In its simplest form  $a$  is taken as zero. This leads to reliable relationships between  $\omega_e$ ,  $x_e \omega_e$ , and  $D_e$  for ground and excited states of diatomic and polyatomic molecules. The relevant equations are

$$D_e (\text{ergs/molecule}) = k_e / [64\pi^2 c \mu \omega_e x_e / 3h - 1/r_e^2], \quad (2a)$$

$$\omega_e x_e = 3h(n/r_e + 1/r_e^2) / 64\pi^2 c \mu, \quad (3a)$$

and

$$\alpha_e = 0. \quad (4a)$$

In terms of Varshni's notation<sup>8</sup> (2a) and (4a) may be written

$$G = 3[2\Delta + 1] \quad (2b)$$

and

$$F = 0, \quad (4b)$$

where  $F = \alpha_e \omega_e / 6B_e^2$ ,  $G = 8x_e \omega_e / B_e$ ,  $\Delta = k_e r_e^2 / 2D_e$ .

However, Eq. (1) with  $a=0$  (hereafter designated S.F. or simple function) suffers from the disadvantages that it predicts  $\alpha_e$  equal to zero and that its limiting forms are unsatisfactory. On the other hand, it may be derived from a semiempirical delta-function model of chemical binding.<sup>4b</sup>

With  $a \neq 0$  the internuclear potential function assumes a five-parameter form. To reproduce potential curves of bound molecular states the quantity  $f(r)$  must be chosen such that  $V(r) = \infty$  when  $r=0$ , and  $V(r) = D_e$ , when  $r = \infty$ . For large values of  $r$ ,  $f(r)$  was originally assumed to take the form of a Lennard-Jones (6-12) attractive potential<sup>4</sup> which is compatible with these conditions. The general form was

$$V(r) = D_e [1 - \exp(-n\Delta r^2/2r)] \left\{ 1 - a(r_e/r)^6 \cdot \left[ 1 - \exp\left(-\frac{b^2 n \Delta r^2 r^{11}}{2r_e^{12}}\right) \right]^{\frac{1}{2}} + a \left(\frac{r_e}{r}\right)^{12} \cdot \left[ 1 - \exp\left(-\frac{b^2 n \Delta r^2 r^{11}}{2r_e^{12}}\right) \right] \right\}. \quad (5a)$$

This leads to the following relations:

$$D_e = \omega_e^2 / 2nr_e B_e, \quad (6)$$

$$\alpha_e = (6abB_e^2/\omega_e)(nr_e/2)^{\frac{1}{2}} \quad \text{or} \quad F = ab\Delta^{\frac{1}{2}}, \quad (7)$$

$$x_e \omega_e = \frac{3}{2} B_e \left[ \frac{1}{4} + \frac{1}{4} nr_e + ab \left(\frac{1}{2} nr_e\right)^{\frac{1}{2}} + \left(\frac{5}{4} a^2 b^2 - ab^2\right)^{\frac{1}{2}} nr_e \right], \quad (8)$$

or

$$\frac{1}{2} G = \frac{1}{2} + \frac{1}{2} \Delta + ab\Delta^{\frac{1}{2}} + \left(\frac{5}{4} a^2 b^2 - ab^2\right) \Delta.$$

Another proposed form for (1) which leads to the same relations between  $\omega_e$ ,  $r_e$ ,  $\alpha_e$ ,  $x_e \omega_e$ , and  $D_e$  (see below) is

$$V(r) = D_e \{ 1 - \exp[-(n\Delta r^2/2r)] \cdot \{ 1 - a(b^2 n/2r)^{\frac{1}{2}} \Delta r \exp[-(b^2 n/2r_e)^{\frac{1}{2}} \Delta r] \}. \quad (5b)$$

This will be shown to be superior to (5a). Eliminating  $a$  from (7) and (8) and using the experimental values for the spectroscopic constants,  $b$  is found to have a constant value of  $1.065 \pm 0.03$  for all states of all molecules with the exception of hydrogen, for which it is 1.16.<sup>7</sup> Equations (2) to (4) and (6) to (8) are based on the much used assumption that  $B_e^2/\omega_e^2$  is negligible in comparison with unity.<sup>5</sup> This is not strictly true for hydrogen and would appear to be a plausible reason for the value of  $b$  for this molecule being out of line with its value for other molecules. Combining Eqs. (6), (7), and (8) allows  $D_e$  to be calculated from experimental values of  $k_e$ ,  $x_e \omega_e$ ,  $\alpha_e$ ,  $r_e$ , and  $b$ . Where the data are reliable it has been shown that the dissociation energies calculated from the three- and five-parameter forms agree extremely well. This suggests an equivalence of the two forms. Comparing (2b) with (8) and eliminating  $\Delta$  using (2b) leads to

$$\frac{1}{3} G = 1 + 2[1 + \frac{5}{4} F]^2 / b^2. \quad (9)$$

Substituting  $b=1.065$  in (9) results in a relationship between  $\alpha_e$ ,  $\omega_e$ ,  $x_e \omega_e$ , and  $B_e$  only, which is very similar to the Pekeris relation (10)<sup>9</sup> obtained from the Morse function.

$$\frac{1}{8} G = (1 + F)^2 \quad (10)$$

Equation (9) is slightly superior to Eq. (10), particularly for hydrogen-containing molecules, and allows  $x_e \omega_e$  to be calculated with an average error of approximately 5%. For the ground states of CS, O<sub>2</sub>, O<sub>2</sub><sup>+</sup>, CO, IO, and NO for which the data are accurate and well established, the error is less than 1%. Solving (2b), (7), and (9) for  $a$  in terms of  $F$  one obtains

$$a = F / (1 + \frac{5}{4} F). \quad (11)$$

This allows the parameter  $a$  to be conveniently and rapidly evaluated from  $\alpha_e$ ,  $\omega_e$ , and  $B_e$  only. The results of such calculations show that for the ground states of homonuclear diatomic molecules  $a$  is periodic within the periodic table, rising from 0.344 for H<sub>2</sub> to 0.636 for

<sup>7</sup> E. R. Lippincott and D. Steele, J. Chem. Phys. (to be published).

<sup>8</sup> Y. P. Varshni, Revs. Modern Phys. **29**, 664 (1957).

<sup>9</sup> C. L. Pekeris, Phys. Rev. **45**, 98 (1934).

TABLE I. Calculation of ground-state data from periodic  $a$  rule. (a) homonuclear diatomics.<sup>a</sup>

Mol.	$a$ calc	$\omega_e$ (cm <sup>-1</sup> )	$r_e$ (Å)	$\alpha_e$ calc (cm <sup>-1</sup> )	$\alpha_e$ obs (cm <sup>-1</sup> )	$x_e\omega_e$ calc (cm <sup>-1</sup> )	$x_e\omega_e$ obs (cm <sup>-1</sup> )	$D_e$ calc (ev)	$D_e$ obs <sup>b</sup> (ev)
Li <sub>2</sub>	0.475	351.43	2.6725	0.00903	0.00704	2.946	2.592	1.065	1.10±0.05
Na <sub>2</sub>	0.495	159.23	3.0786	0.00117	0.00079	0.761	0.726	0.837	0.75±0.03
K <sub>2</sub>	0.515	92.64	3.923	0.000296	0.000219	0.314	0.354	0.681	0.520
B <sub>2</sub>	0.515	1051.3	1.589	0.0121	0.014	6.770	9.4	4.066	3.0±0.5
C <sub>2</sub> <sup>3</sup> Π	0.535	1641.35	1.3117	0.0157	0.01683	10.454	11.67	6.365	~5.6 6.1
C <sub>2</sub> <sup>1</sup> Σ	0.535	1855.63	1.2422	0.0173	0.01832	11.656	14.08	7.297	~5.6 6.1
Si <sub>2</sub>	0.555	506.72 <sup>c</sup>	2.252 <sup>c</sup>	0.00121	0.00135 <sup>c</sup>	1.762	1.97 <sup>c</sup>	3.564	3.2 <sup>c</sup>
N <sub>2</sub>	0.555	2358.07 <sup>d</sup>	1.0975 <sup>d</sup>	0.0184	0.01709 <sup>d</sup>	14.840	14.188 <sup>d</sup>	9.175	9.902 <sup>d,e</sup>
P <sub>2</sub>	0.575	780.89 <sup>f</sup>	1.8931 <sup>f</sup>	0.00145	0.001477 <sup>f</sup>	2.657	2.820 <sup>f</sup>	5.584	5.08 <sup>f</sup>
O <sub>2</sub>	0.575	1580.36	1.2074	0.0162	0.01579	12.625	12.0730	4.804	5.213
S <sub>2</sub>	0.595	725.68	1.889	0.00168	0.00160	3.094	2.852	4.114	4.4
Se <sub>2</sub>	0.605	391.77	2.157	0.000313	0.00027	1.144	1.06	3.536	2.8±0.1
Te <sub>2</sub>	0.615	251.	2.59	0.000099		0.502	0.55	3.008	2.3±0.2
F <sub>2</sub>	0.595	891.9	1.435	0.01234		9.280		2.131	1.6
Cl <sub>2</sub>	0.615	564.9	1.988	0.00168	0.0017	3.109	4.0	2.460	2.51
Br <sub>2</sub>	0.635	323.2	2.2836	0.00037	0.000275	1.265	1.07	1.931	1.971
I <sub>2</sub>	0.655	214.52	2.6666	0.000141	0.0001208	0.766	0.6127	1.423	1.556

<sup>a</sup> Unless additional references are listed the spectroscopic constants have been taken from G. Herzberg's *Spectra of Diatomic Molecules* (D. Van Nostrand Company, Inc., Princeton, New Jersey, 1950), pp. 502-581.

<sup>b</sup> Unless additional references are listed the observed dissociation energies are taken from a tabulation by A. G. Gaydon, *Dissociation Energies* (Chapman and Hall, Ltd., London, 1953), 2nd ed.

<sup>c</sup> A. E. Douglas, Can. J. Phys. 33, 801 (1955).

<sup>d</sup> A. Lofthus, Can. J. Phys. 34, 780 (1956).

<sup>e</sup> B. P. Stoicheff, Can. J. Phys. 35, 730 (1957).

<sup>f</sup> A. E. Douglas and P. T. Rao, Can. J. Phys. 36, 565 (1958).

I<sub>2</sub>. For heteronuclear molecules the  $a$  values are given satisfactorily by the mean value of the  $a$ 's of the constituent atoms with the sole exception of hydrides for which  $a(\text{H})$  is best taken as 0.376. Since the  $a$  values for the second column of the periodic table are unknown and those for the first column do not appear to be too reliable, it is not possible to give an unequivocal empirical form for  $a$  in terms of the position of the element within the periodic table. The present data are satisfactorily represented by

$$a(x) = 0.335 + 0.080\delta + 0.02[n_c + n_r], \quad (12)$$

where  $a(x)$  is the  $a$  value for the ground state,  $\delta$  is equal to unity for all molecules except hydrogen (hydrides) for which it is zero, and  $n_c$  and  $n_r$  are the column and row numbers of the element in the periodic table.

The above relationships allow  $D_e$ ,  $x_e\omega_e$ , and  $\alpha_e$  to be derived for the ground states of all diatomic molecules, apart from those involving transition atoms, solely from a knowledge of  $\omega_e$  and  $r_e$ . The appropriate equation for  $D_e$  is

$$D_e = \left(\frac{1}{2}b^2\right) k_e r_e^2 \left(1 - \frac{5}{4}a\right)^2. \quad (13)$$

The results of some such calculations are tabulated in Tables I-III, where they are compared with the experimental quantities. The average percent deviations are 10, 8, and 13% for  $\alpha_e$ ,  $x_e\omega_e$ , and  $D_e$ , respectively.

#### EXCITED STATES

The empirical equation (12) is valid only for the ground states of diatomic molecules. To extend these correlations to excited states it is necessary to find a relationship between  $\omega_e$ ,  $r_e$ , and  $a$  of the ground states and the corresponding parameters of the excited states. Birge<sup>10</sup> and Mecke<sup>11</sup> have shown that  $\omega_e r_e^2$  is a constant for the different electronic states of one and the same molecule. This suggests relationships of the form

$$a^* = \frac{4}{5} \left[ 1 - \frac{\omega^{(*)} r^{(*)y}}{\omega(x) r(x)^y} \left[ 1 - \frac{5}{4} a(x) \right] \right], \quad (14)$$

which were tried and found very successful with  $x=1$  and  $y=2$ . The result that the variations in  $a$  can be correlated with variations in  $\omega_e r_e^2$  indicates that, although the constancy of  $\omega_e r_e^2$  is a good approximation,

<sup>10</sup> R. T. Birge, Phys. Rev. 25, 240 (1925).

<sup>11</sup> R. Mecke, Z. Physik 31, 709 (1925).

TABLE II. Calculation of ground state data from periodic  $a$  rule. (b) heteronuclear.<sup>a</sup>

Mol.	$a$ calc	$\omega_e$ (cm <sup>-1</sup> )	$r_e$ (Å)	$\alpha_e$ calc (cm <sup>-1</sup> )	$\alpha_e$ obs (cm <sup>-1</sup> )	$x_e\omega_e$ calc (cm <sup>-1</sup> )	$x_e\omega_e$ obs (cm <sup>-1</sup> )	$D_e$ calc (ev)	$D_e$ obs <sup>b</sup> (ev)
BO	0.545	1885.44	1.2049	0.0172	0.01648	12.351	11.769	7.132	7.6±0.4
BN	0.535	1514.6	1.281	0.0178	0.025	10.666	12.3	5.310	4.0±0.5
CO	0.555	2169.83 <sup>c</sup>	1.1282 <sup>c</sup>	0.0187	0.0175 <sup>c</sup>	14.342	13.295 <sup>c</sup>	8.038	11.245 <sup>c</sup>
CP	0.555	1239.67	1.5621	0.00559	0.00597	5.924	6.86	6.345	6±1
CS	0.565	1285.1 <sup>d</sup>	1.5344 <sup>d</sup>	0.00604	0.00624 <sup>d</sup>	6.593	6.5 <sup>d</sup>	6.106	7.2±1.0 <sup>d</sup>
ICI	0.635	384.293	2.3207	0.000626	0.000534	1.8155	1.501	1.943	2.178
IO	0.615	681.47 <sup>e</sup>	1.8679 <sup>e</sup>	0.00271	0.002696 <sup>e</sup>	4.333	4.29 <sup>e</sup>	2.567	1.9±0.2 <sup>e</sup>
NO	0.565	1904.03 <sup>f</sup>	1.1508 <sup>f</sup>	0.0176	0.0178 <sup>f</sup>	13.701	13.97 <sup>f</sup>	6.452	6.609 <sup>f</sup>
PbS	0.605	428.14	2.3948	0.000391	0.000873	1.222	1.201	3.610	3.25±0.3
PN	0.565	1337.24	1.4910	0.00533	0.00557	6.313	6.983	6.900	6.1±0.8
PO	0.575	1230.64	1.4457	0.00578	0.0055	6.654	6.52	5.509	5.4
SiN	0.555	1151.68	1.5718	0.00504	0.00567	5.421	6.560	5.983	4.5±0.4
SiO	0.565	1241.44	1.509	0.00492	0.00508	5.846	5.92	6.428	8.0±0.3
SrO	0.565	653.5	1.921	0.00202	0.0020	2.724	4.0	3.837	5.0 or 3.6
SO	0.585	1123.73	1.4933	0.00584	0.00562	6.754	6.116	4.523	5.22

<sup>a</sup> See reference a, Table I.<sup>b</sup> See reference b, Table I.<sup>c</sup> D. H. Rank, A. H. Guenther, G. D. Saksena, T. N. Shearer, and T. A. Wiggins, *J. Opt. Soc. Am.* **47**, 686 (1957).<sup>d</sup> A. Lagerquist *et al.* *Arkiv. Fysik* **14**, 387 (1959).<sup>e</sup> R. A. Durie, F. Legay, and D. A. Ramsey, *Can. J. Phys.* **38**, 444 (1960).<sup>f</sup> W. H. Fletcher and G. M. Begun, *J. Chem. Phys.* **27**, 579 (1957).

small changes in this quantity can be simply related to changes in other molecular vibration-rotation parameters. The wide range of vibrational frequencies and bond lengths for hydrogen make it a very sensitive molecule for these correlations, and it was found that  $\omega_e r_e^2$  is not nearly constant and using these powers of  $\omega_e$  and  $r_e$  in (14) does not reproduce the  $a$ 's of excited states.

$\omega_e r_e^{7/4}$ , however, yields good correlations. Apart from hydrogen,  $\omega_e r_e^2$  can be used with little error. Equation (13) in conjunction with (14) does not always predict the molecular parameters with high accuracy, particularly  $D_e$ , but serves to indicate the approximate value of the dissociation energy, from which the dissociation products may be deduced and hence an

TABLE III. Calculation of ground state data from periodic  $a$  rule. (c) hydrides.<sup>a</sup>

Mol.	$a$ calc	$\omega_e$ (cm <sup>-1</sup> )	$r_e$ (Å)	$\alpha_e$ calc (cm <sup>-1</sup> )	$\alpha_e$ obs (cm <sup>-1</sup> )	$x_e\omega_e$ calc (cm <sup>-1</sup> )	$x_e\omega_e$ obs (cm <sup>-1</sup> )	$D_e$ calc (ev)	$D_e$ obs <sup>b</sup> (ev)
AlH	0.455	1682.57	1.64592	0.154	0.188	25.14	29.145	2.89	3.0
BaH	0.475	1172	2.2318	0.068	0.066	14.82	16	2.36	1.8±0.1
BeH	0.435	2058.6	1.3431	0.295	0.300	36.60	35.5	3.01	2.4±0.3
CH	0.455	2861.6	1.1198	0.462	0.534	56.83	64.3	3.70	3.66 <sup>a</sup>
CsH	0.465	890.7	2.494	0.055	0.057	11.23	12.6	1.81	1.8±0.3
HCl	0.495	2989.74	1.2744	0.292	0.304	52.17	52.05	4.31	4.38 <sup>a</sup>
HBr	0.505	2649.22 <sup>c</sup>	1.41468 <sup>c</sup>	0.222	0.232 <sup>c</sup>	42.14	44.077 <sup>c</sup>	3.97	3.93 <sup>c</sup>
HF	0.485	4137.25	0.91717	0.784	0.789	97.19	88.726	4.46	6.114 <sup>a</sup>
LiH	0.425	1405.65 <sup>d</sup>	1.59535 <sup>d</sup>	0.218	0.213 <sup>d</sup>	25.43	23.20 <sup>d</sup>	2.02	2.515 <sup>d</sup>
OH	0.475	3735.21	0.9706	0.669	0.714	82.70	82.81	4.29	4.624 <sup>a</sup>

<sup>a</sup> See reference a, Table I.<sup>b</sup> See reference b, Table I.<sup>c</sup> H. M. Mould, W. C. Price, G. R. Wilkinson, *Spectrochim. Acta.* **16**, 479 (1960).<sup>d</sup> R. Velasco, *Can. J. Phys.* **35**, 1204 (1957).

TABLE IV. Calculation of excited state data from empirical  $a$  rules.<sup>a</sup>

Mol.	State	$\omega_e$ (cm <sup>-1</sup> )	$r_e$ (Å)	$a$ calc	$\alpha$ calc (cm <sup>-1</sup> )	$\alpha$ obs (cm <sup>-1</sup> )	$x_e\omega_e$ calc (cm <sup>-1</sup> )	$x_e\omega_e$ obs (cm <sup>-1</sup> )	$D_e$ calc (ev)	$D_e$ obs <sup>b</sup> (ev)	Dissociation products
H <sub>2</sub>	$c \ ^3\Pi_u$	2465.0	1.0376	0.316	1.189	1.425	66.42	61.4	2.97	3.03	$2 \ ^2P+1 \ ^2S$
	$a \ ^3\Sigma_g^+$	2664.8	0.9887	0.319	1.450	1.671	77.28	71.65	3.12	3.01	$2 \ ^2S+1 \ ^2S$
	$e \ ^3\Sigma_u^+$	2195.8	1.1069	0.317	0.791	1.515	50.84	65.80	2.67	3.42	$3 \ ^2P+1 \ ^2S$
	$h \ ^3\Sigma_g^+$	2395.2	1.045	0.324	1.238	1.26	67.22	64.2	2.76	2.83	$3 \ ^2P+1 \ ^2S$
	$c \ ^1\Pi_u$	2442.72	1.0331	0.324	1.501	1.626	77.25	67.03	2.80	2.49	$2 \ ^2P+1 \ ^2S$
	$d \ ^3\Pi_u$	2371.58	1.0496	0.325	1.218	1.545	66.24	66.27	2.71	2.81	$3 \ ^2P+1 \ ^2S$
CH	$A \ ^2\Delta$	2921.0	1.1026	0.459	0.781	0.670	102.65	68.849	3.65	2.05	$2 \ ^1D+1 \ ^2S$
	$C \ ^2\Sigma^+$	2824.1	1.1132	0.465	0.668	0.744	83.34	95.199	3.36	2.39	$2 \ ^1S+1 \ ^2S$
Li <sub>2</sub>	$A \ ^1\Sigma_u^+$	255.46	3.108	0.458	0.00442	0.00541	1.439	1.574	0.84	1.2	$2 \ ^2S+2 \ ^2P$
	$B \ ^1\Pi_u$	269.69	2.936	0.487	0.0127	0.00804	4.24	2.744	0.70	0.4	$2 \ ^2S+2 \ ^2P$
C <sub>2</sub>	$A \ ^3\Pi_g$	1788.2	1.2660	0.545	0.0264	0.01608	21.09	16.44	6.52	4.5	$2 \ ^3P+2 \ ^1D$
	$B \ ^3\Pi_g$	1106.6	1.5350	0.579	0.0417	0.0242	48.00	39.26	2.76	0.7	$2 \ ^3P+2 \ ^3P$
	$a \ ^1\Sigma_g^+$	1855.6	1.2422	0.544	0.0204	0.01832	14.40	14.08	6.67	5.6	$2 \ ^3P+2 \ ^3P$
	$b \ ^1\Pi_u$	1608.3	1.3180	0.554	0.0195	0.01720	13.66	12.14	5.32	4.6	$2 \ ^3P+2 \ ^3P$
	$c \ ^1\Pi_g$	1809.1	1.2730	0.539	0.049	0.0180	20.14	15.81	7.06	5.3	$2 \ ^1D+2 \ ^1S$
CO	$A \ ^1\Pi$	1515.6	1.2351	0.563	0.0248	0.02229	17.83	17.2505	4.40	3.16	$2 \ ^3P+2 \ ^3P$
	$a' \ ^3\Sigma^+$	1230.7	1.3518	0.574	0.0143	0.0187	8.67	11.013	3.16	4.30	$2 \ ^3P+2 \ ^3P$
	$a \ ^3\Pi^+$	1739.3	1.2093	0.537	0.0195	0.0193	14.20	14.47	6.84	5.18	$2 \ ^3P+2 \ ^3P$
CS	$A \ ^1\Pi$	1072.3	1.5732	0.577	0.00996	0.005922	11.46	6.46	4.02	2.4	$2 \ ^3P+2 \ ^3P$
N <sub>2</sub>	$A \ ^3\Sigma_u^+$	1460.60	1.293	0.591	0.0187	0.01798	13.85	13.851	3.55	3.71	$2 \ ^4S+2 \ ^4S$
	$B \ ^3\Pi_g$	1734.42	1.212	0.578	0.0196	0.01794	14.94	15.198	4.97	4.90	$2 \ ^4S+2 \ ^2D$
	$^3\Delta_u$	1490	1.28	0.590	0.00959	...	6.116	...	3.66	4.74	$2 \ ^4S+2 \ ^2D$
	$a \ ^1\Pi_g$	1693.7 <sup>c</sup>	1.2197 <sup>c</sup>	0.581	0.0164	0.0183 <sup>c</sup>	11.60	13.83 <sup>c</sup>	4.67	6.07 <sup>c</sup>	$2 \ ^2D+2 \ ^2D$
	$a \ ^1\Sigma_u^-$	1530 <sup>d</sup>	1.270 <sup>d</sup>	0.587	0.0139	0.0164 <sup>d</sup>	9.497	12.0 <sup>d</sup>	3.92	5.92 <sup>d</sup>	$2 \ ^2D+2 \ ^2D$
	$y \ ^3\Sigma_u^-$	1522	1.276	0.587	0.0152	...	10.565	12.5	3.93	5.36	$2 \ ^4S+2 \ ^2P$
	$w \ ^1\Delta_u$	1548	1.263	0.587	0.0170	...	12.34	8±1	3.94	5.53	$2 \ ^2D+2 \ ^2D$
	$c \ ^3\Pi_u$	2047.09	1.148	0.563	0.0238	0.01868	20.26	28.446	4.09	4.92	$2 \ ^2P+2 \ ^2D$
	$E \ ^3\Sigma_g^+$	2184.5	1.12	0.556	0.0183	...	14.098	...	8.12	8.33	$2 \ ^4S+3s \ ^4P$
	$[\ ^1\Pi_u]$	2035.0	1.15	0.562	0.0161	...	11.879	...	7.08	8.64	$2 \ ^4S+sp^4 \ ^4P$
	$[\ ^1\Sigma_g^+]$	2215.0	1.12	0.553	0.0188	...	14.880	...	8.57	8.02	$2 \ ^4S+3s \ ^4P$
	$[\ ^3\Pi_u]$	1950.0	1.18	0.562	0.0166	...	12.661	...	6.84	7.4	$2 \ ^4S+3s \ ^4P$
	$p \ ^1\Sigma_u^+$	2217.0	1.12	0.553	0.0205	...	16.598	19	8.58	7.27	$2 \ ^4S+3s \ ^4P$
	$o \ ^1\Pi_u$	2020.0	1.19	0.550	0.0168	...	13.948	32.3	8.19	7.09	$2 \ ^4S+3s \ ^4P$
	$e \ ^1\Sigma_u^+$	2180.0	1.12	0.557	0.0171	...	12.880	...	8.04	8.40	$2 \ ^4S+4s \ ^4P$
	$x \ ^1\Sigma_g^-$	1910.0 <sup>d</sup>	1.168 <sup>d</sup>	0.571	0.0160	0.0225 <sup>d</sup>	11.888	20.7 <sup>d</sup>	5.96	7.41 <sup>d</sup>	$2 \ ^4S+3p \ ^4P$
	$y \ ^1\Pi_g$	1708.0 <sup>e</sup>	1.16 <sup>e</sup>	0.597	0.0197	...	12.70	...	3.69	5.65	$2 \ ^4S+3s \ ^4P$

Table IV (continued)

Mol.	State	$\omega_e$ (cm <sup>-1</sup> )	$r_e$ (Å)	$a$ calc	$\alpha$ calc (cm <sup>-1</sup> )	$\alpha$ obs (cm <sup>-1</sup> )	$x_e\omega_e$ calc (cm <sup>-1</sup> )	$x_e\omega_e$ obs (cm <sup>-1</sup> )	$D_e$ calc (ev)	$D_e$ obs <sup>b</sup> (ev)	Dissociation products
NO	$A^2\Sigma^+$	2374.8	1.0637	0.541	0.0211	0.01928	18.05	16.46	10.4	7.6	$2^2D+2^1S$
	$B^2\Pi_1$	1036.96	1.448	0.606	0.0121	0.0116	7.990	7.603	2.1	3.3	$2^2D+2^3P$
	$E^2\Sigma^+$	2373.6 <sup>a</sup>	1.0661 <sup>a</sup>	0.540	0.0199	0.0182 <sup>a</sup>	16.77	15.85 <sup>a</sup>	10.5	8.2 <sup>a</sup>	$2^4S+3^3S$
	$D^2\Sigma^+$	2323.90 <sup>f</sup>	1.0620 <sup>f</sup>	0.548	0.0256	...	23.38	23 <sup>f</sup>	9.4	5.5 <sup>f</sup>	$2^2D+2^1D$
					0.0166		12.84			or 10.3 or 3	$^5S+2^4S$
	$B^2\Delta$	1216.6	1.303	0.612	0.0196	0.019	13.26	15.88	2.2	2.7	$2^2P+2^3P$
O <sub>2</sub>	$a^1\Delta_g$	1509.3	1.2155	0.574	0.0171	0.0171	13.01	12.9	4.48	4.24	$2^3P+2^3P$
	$b^1\Sigma_g^+$	1432.69	1.2267	0.582	0.0183	0.01817	13.84	13.9501	3.55	3.58	$2^3P+2^3P$
	$B^3\Sigma_u^-$	700.36	1.604	0.629	0.0164	0.011	11.63	8.002	0.96	1.01	$2^3P+2^1D$
	$^1\Sigma_u^-$	650.49 <sup>g</sup>	1.597 <sup>g</sup>	0.643	0.0211	0.02055 <sup>g</sup>	15.051	17.036 <sup>g</sup>	0.69	0.67 <sup>g</sup>	$2^3P+2^3P$
O <sub>2</sub> <sup>+</sup>	$a^4\Pi_u$	1035.69	1.3813	0.610	0.0146	0.01575	9.812	10.39	1.93	2.64	$2^3P+2^4S$
	$A^3\Pi_u$	900	1.4089	0.629	0.0173	0.01906	10.986	13.4	1.23	1.78	$2^3P+2^4S$
	$b^4\Sigma_g^-$	1196.77	1.2795	0.608	0.0194	0.02206	13.574	17.09	2.25	2.54	$2^1D+2^4S$
IO	$A^2\Pi_1$	514.57	2.0723	0.656	0.00306	0.00273	5.228	5.52	1.09	1.2	$5^2P+2^1D$
K <sub>2</sub>	$B^1\Pi_u$	75.00	4.235	0.571	0.000495	0.000219	0.6153	0.354	0.336	0.22	$4^2P+4^2S$
S <sub>2</sub>	$B^3\Sigma_u^-$	434.0	2.180	0.637	0.00181	0.0018	2.826	2.75	1.24	1.6	$3^3P+3^1D$
Si <sub>2</sub>	$H^3\Sigma_u^-$	271.32	2.663	0.633	0.00148	0.00135	1.772	1.99	0.67	1.0	$3^3P+3^1D$
I <sub>2</sub>	$B^3\Pi_0^+$	128.0	3.016	0.687	0.000157	0.00017	0.6886	0.834	0.39	0.56	$5^3P_1+5^3P_1$

<sup>a</sup> See reference a, Table I.<sup>b</sup> See reference b, Table I.<sup>c</sup> A. Lofthus, Can. J. Phys. **34**, 780 (1956).<sup>d</sup> A. Lofthus, J. Chem. Phys. **25**, 494 (1956).<sup>e</sup> E. Miescher, Can. J. Phys. **33**, 355 (1955).<sup>f</sup> R. F. Barrows and E. Miescher, Proc. Phys. Soc. (London) **70A**, 219 (1957).<sup>g</sup> G. Herzberg, Can. J. Phys. **31**, 57 (1953).

accurate value of  $D_e$  determined. The corrected  $D_e$  can then be used to determine an improved  $a$ , then  $\alpha_e$  and  $x_e\omega_e$ . Calculated values of  $D_e$ ,  $\alpha_e$ , and  $x_e\omega_e$  are listed along with the observed values in Table IV. When the dissociation products are ionic, (1) is not valid and consequently none of the derived formulas are applicable. Generally, however, the ionic states can be recognized by their very low vibrational frequencies or negative anharmonicities. No known potential function is applicable to such states.

#### ALTERNATIVE FORMS FOR THE FIVE-PARAMETER FUNCTION

Expansion of the  $1+af(r)$  part of (5) as far as the second power of  $\Delta r$  leads to

$$1+af(r) = 1 - a \left\{ \left( \frac{b^2nr_e}{2} \right) \frac{\Delta r}{r_e} - \left( \frac{b^2nr_e}{2} \right) \left( \frac{\Delta r}{r_e} \right)^2 + \dots \right\}. \quad (15)$$

Higher powers of  $\Delta r/r_e$  do not affect the relations

between  $D_e$ ,  $B_e$ ,  $\omega_e$ ,  $\alpha_e$ , and  $x_e\omega_e$ . The function (5a), as has been previously pointed out,<sup>7</sup> is not the only function which will yield the above expansion and hence lead to Eqs. (6) to (8). Some of the alternative forms for  $1+af(r)$  are listed below

$$1+af(r) = 1 - a(b^2n/2r)^{\frac{1}{2}} \Delta r \exp[-(b^2n/2r)]^{\frac{1}{2}} \Delta r \quad (16a)$$

$$= 1 - a(b^2n/2r)^{\frac{1}{2}} \Delta r \exp[-(b^2n/2r_e)]^{\frac{1}{2}} \Delta r \quad (16b)$$

$$= 1 - a(b^2n/2r)^{\frac{1}{2}} \Delta r (r_e/r)^x \exp[-(b^2n/2r)]^{\frac{1}{2}} \Delta r. \quad (16c)$$

Others such as

$$1+af(r) = 1 - a(b^2n/2r)^{\frac{1}{2}} \Delta r$$

$$\times \{1 - \log_e[1 + (b^2n/2r)^{\frac{1}{2}} \Delta r]\}$$

do not go to the correct limits and need be considered no further. The test of the validity of the functions (16a) to (16c) is their ability to reproduce known

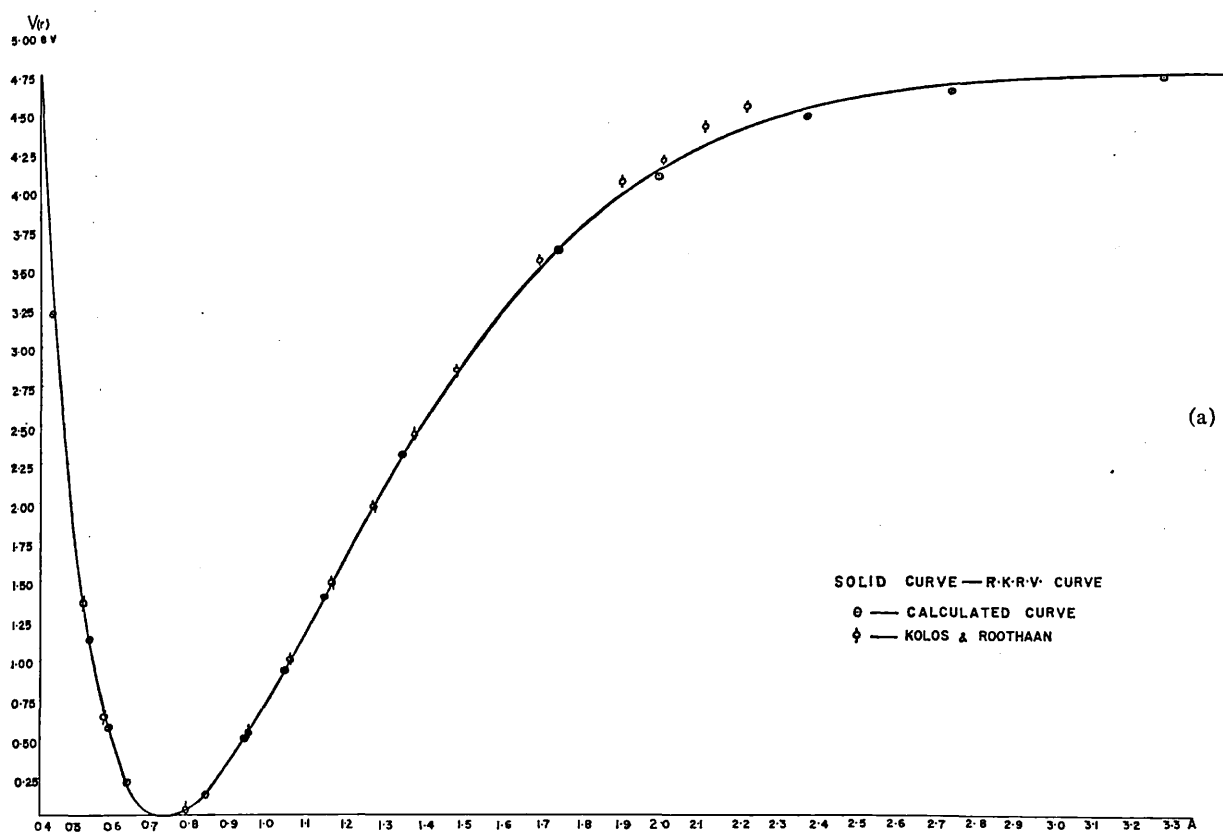
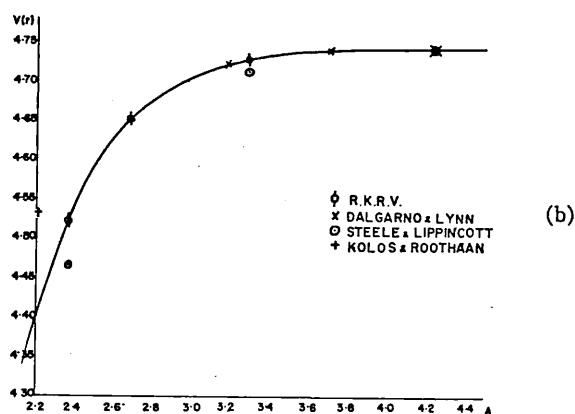


FIG. 1. (a) Potential energy curve of  $X^1\Sigma_g^+$  state of hydrogen.  
 (b)  $V(r)$  curve for  $X^1\Sigma_g^+$  state of  $H_2$  at large  $\Delta r$ .



potential curves and to allow higher-order vibration-rotation energy terms to be predicted. The latter will be discussed in a future publication. In the present paper the capability of the proposed functions to reproduce experimental curves, as given by the R.K.R.V. method, will be examined, and then formulas given in the previous section will be applied to constructing curves from limited data.

#### CONSTRUCTION OF POTENTIAL CURVES

Experimental curves are known for a considerable range of bond lengths for the following:  $X^3\Sigma_g^-$ ,  $^3\Delta_u$ ,

$^1\Sigma_u^-$ , and  $B^3\Sigma_u^-$  states of  $O_2^{12,2}$ ;  $X^2\Pi_i$ ,  $B^2\Pi$  of  $NO^{13}$ ;  $X^1\Sigma^+$  of  $HF^{14}$ ;  $X^1\Sigma_g^+$ ,  $A^3\Sigma_u^+$ ,  $B^3\Pi_g$ ,  $a^1\Pi_g$  states of  $N_2^1$ ;  $X^2\Pi_i$ , and  $A^2\Sigma^+$  states of  $OH^{15}$ ;  $X^1\Sigma_g^+$  state of  $H_2^2$  and  $X^1\Sigma_g^+$  state of  $I_2^{16}$ . The most complete curves are for the latter two molecules and consequently were

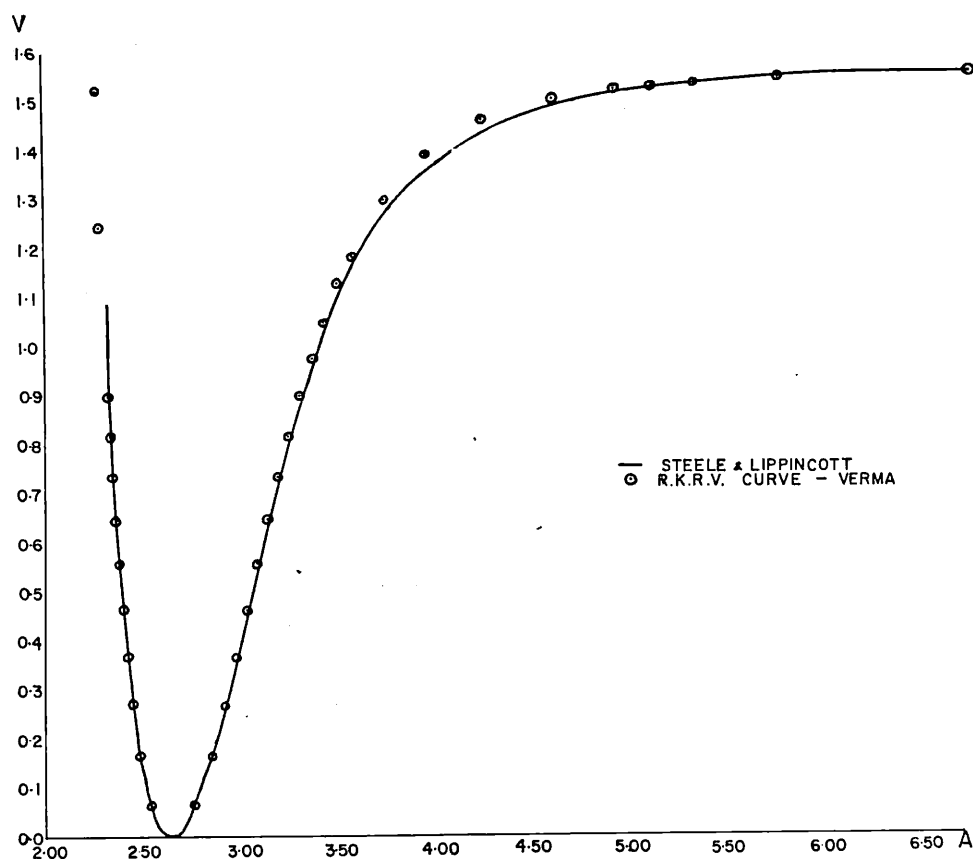
<sup>12</sup> J. T. Vanderslice, E. A. Mason, and W. G. Maisch, *J. Chem. Phys.* **32**, 515 (1960).

<sup>13</sup> J. T. Vanderslice, E. A. Mason, and W. G. Maisch, *J. Chem. Phys.* **31**, 738 (1959).

<sup>14</sup> R. J. Fallon, J. T. Vanderslice, and E. A. Mason, *J. Chem. Phys.* **32**, 698 (1960); **33**, 944 (1960).

<sup>15</sup> R. J. Fallon, I. Tobias, and J. T. Vanderslice, *J. Chem. Phys.* **34**, 167 (1961).

<sup>16</sup> R. D. Verma, *J. Chem. Phys.* **32**, 738 (1960).

FIG. 2. Potential energy curve of  $X^1\Sigma_g^+$  state of  $I_2$ .

— STEELE & LIPPINCOTT  
 ○ R.K.R.V. CURVE - VERMA

used first, along with that of the  $X^1\Sigma_g^+$  state of  $N_2$ , to test the proposed functions.  $V(r)$  as given by (5a) consistently gives potentials which are far too small for negative values of  $\Delta r$  and values somewhat too high for intermediate positive values of  $\Delta r$ . This is shown for  $N_2$  in Table V, where the potentials as given by (5a), (16a), and (16b) are compared with experimental values.<sup>1</sup> Equations (16a) and (16b) both yield potentials for the ground state of  $N_2$  which are never in error by more than 2% over the range of known values. Proceeding to  $H_2$  the potential curve of the

TABLE V. Potential energy of  $X^1\Sigma_g^+$  state of  $N_2$ .

$\Delta r$	$r_e = 1.0976 \text{ \AA}$		$\omega_e = 2358.07 \text{ cm}^{-1}$	
	$V(5a)$	$V(16a)$	$V(16b)$	$V[\text{R.K.R.V.}]$
-0.3	5.912 ev	14.708 ev	13.557 ev	
-0.2	2.590	4.907	4.792	4.96 ev
-0.1	0.675	0.931	0.929	0.935
0.1	0.572	0.560	0.568	0.57
0.2	1.895	1.794	1.810	1.77
0.4	5.278	4.542	4.716	4.59
0.6		6.559	6.996	
1.0	9.589	8.219	9.073	
2.0		9.311	9.861	

ground state has already been evaluated using (5)<sup>3</sup> and the results were similar to those of  $N_2$ . Clearly this function need no longer be considered. For large values of  $\Delta r$ , (16b) is much superior to (16a) (see Table VI). A comparison of observed curves with that calculated using (16b) is shown in Figs. 1 and 2. Good agreement for large values of  $\Delta r$  is also obtained for the  $X^1\Sigma_g^+$  state of iodine using (16b), though the potential curve is 2 to 3% low for values of  $\Delta r$ , for which  $V(r) \approx \frac{1}{2}D_e$  (Table VII). It should be noted that Verma's curve for  $v'' > 84$  is not completely reliable as it is based on an extrapolation procedure for estimating  $r_{\min}$ . This was necessary due to lack of data on  $B$ , and  $\alpha_v$ . Also Verma's Eqs. (17) and (18) are in error.<sup>2</sup> These results and the simplicity of (16b), as far as computing curves are concerned, have led the authors to adopt this form for the five-parameter function until more reasonably complete experimental potential curves are available on which to test the functions. A detailed comparison of the simple function, the complex function as defined by (16b) and functions proposed by other authors is now in progress.

#### CONSTRUCTION OF POTENTIAL CURVES FROM LIMITED DATA

As has already been shown, the parameter  $a$  can be estimated for any bound nonionic state of any diatomic molecule for which  $\omega_e$  and  $r_e$  are known. From this, an approximate value for the dissociation energy can be

TABLE VI. Potential energy curve of  $X^1\Sigma_g^+$  state of  $H_2$ .

$\Delta r$	$V$ (16a)	$V$ (16b)	$V$ [R.K.R.V.]	$V$ [Dunham and Lynn]
-0.3	3.4585 ev	3.2066 ev	3.50 ev	
-0.2	1.1437	1.1250	1.13	
-0.15	0.5654	0.5620	0.595	
-0.1	0.2232	0.2229	0.202	
0.1	0.1480	0.1481	0.147	
0.2	0.4895	0.4928	0.496	
0.3	0.9165	0.9271	0.905	
0.4	1.3679	1.3957	1.373	
0.6	2.2150	2.3022	2.260	
1.0	3.3854	3.6093	3.622	
1.2544	3.8093	4.0877	4.1309	
1.6331	4.1596	4.4665	4.5217	
2.0	4.3299	4.6267	4.670	
2.5418	4.4609	4.7136	4.7289	
3.49	4.5575	4.7430	...	4.744 ev
4.55	4.6193	4.47594	...	4.74595
$D_e=4.7462$ ev		$\omega_e=4400.39$ cm <sup>-1</sup>	$r_e=0.74173$ A	

obtained. Assuming that the dissociation energy of the ground state  $D_e(x)$  and the electronic excitation energy  $T_e$  are known, the atomic excitation energy  $\Delta'$  of the dissociation products of the excited state is then given by the relation.

$$T_e + D_e^* = D_e(x) + \Delta'. \quad (17)$$

This relation has been discussed in reference 7. Com-

TABLE VII. Potential energy curve of  $X^1\Sigma_g^+$  state of  $I_2$ .

$\Delta r$	$V$ (16b)	$V$ obs	
-0.3	0.7987 ev	0.759 ev	
-0.2	0.3012	0.291	
-0.1	0.0633	0.061	
0.1	0.0460	0.044	
0.2	0.1562	0.160	
0.4	0.4653	0.484	
0.6	0.7810	0.811	
1.0	1.2128	1.242	
2.0	1.4979	1.510	
2.895	1.5438	1.5406	
3.342	1.5512	1.5468	
3.854	1.5546	1.5508	
4.155	1.5556	1.5524	
$D_e=1.5570$ ev		$\omega_e=214.518$ cm <sup>-1</sup>	$r_e=2.668$ A

TABLE VIII. Potential curves of states of  $N_2$ .

State	$T_e$ (ev)	Dissociation products	$D_e$ (ev)	$a$	$V(-0.3)$	$V(-0.2)$	$V(-0.1)$	$V(0.1)$	$V(0.2)$	$V(0.4)$	$V(0.6)$	$V(1.0)$	$V(2.0)$	$V(3.0)$
$X^1\Sigma_g^+$	0	$2^4S+2^4S$	9.92	0.545	13.5172	4.7735	0.9258	0.5680	1.8080	4.7130	6.9928	9.0603	9.8591	13.5172
$A^3\Sigma_u^+$	6.209	$2^4S+2^4S$	3.71	0.586	5.1276	1.8178	0.3540	0.2172	0.6907	1.7967	2.6487	3.3957	3.6863	3.7079
$B^3\Pi_g$	7.392	$2^4S+2^2D$	4.90	0.580	7.4045	2.6104	0.5037	0.3040	0.9584	2.4577	3.5801	4.5229	4.8739	4.8986
$(^3\Delta_u)$	[7.552]	$[2^4S+2^2D]$	4.74	0.561	5.0575	1.8120	0.3607	0.2302	0.7484	2.0237	3.1033	4.2110	4.6944	4.7354
$\gamma^3\Sigma_u^-$	8.119	$2^4S+2^2P$	5.36	0.550	5.1613	1.8615	0.3722	0.2417	0.7926	2.1714	3.3819	4.6916	5.2994	5.3539
$\alpha^1\Pi_g$	8.590	$2^2D+2^2D$	6.07	0.550	6.5534	2.3452	0.4660	0.2977	0.9639	2.5966	3.9805	5.4000	6.0150	6.0644
$\alpha'^1\Sigma_u^-$	8.740	$2^2D+2^2D$	5.92	0.538	5.1927	1.8572	0.3745	0.2472	0.8135	2.2661	3.5849	5.0934	5.8403	5.9112
$W^1\Delta_u$	9.23	$2^2D+2^2D$	5.53	0.548	5.3235	1.9181	0.3837	0.2495	0.8163	2.2379	3.4858	4.8397	5.4566	5.5238
$C^3\Pi_u$	10.927	$2^2P+2^2D$	4.92	0.601	11.1996	3.9120	0.7236	0.3996	1.2249	2.9250	3.9652	4.6773	4.9087	4.9203
$E^3\Sigma_g^+$	11.88	$2^4S+3s^4P$	8.33	0.553	11.5852	4.0879	0.7930	0.4838	1.5391	3.999	5.9135	7.6315	8.2789	8.3258
$[^1\Pi_u]$	[12.16]	$2^4S+sp^4P$	8.64	0.537	9.5620	3.4146	0.6765	0.4271	1.3852	3.7264	5.6949	7.7059	8.5664	8.6322
$[^1\Sigma_g^+]$	[12.19]	$2^4S+s^2p^3s^4P$	8.02	0.561	12.1352	4.2694	0.8223	0.4945	1.5612	4.0052	5.8416	7.4059	7.9797	8.0179
$[^3\Pi_u]$	12.8	$2^4S+3s^4P$	7.4	0.552	8.9327	3.1776	0.6257	0.3903	1.2560	3.3354	5.0312	6.6756	7.3433	7.3947
$p'^1\Sigma_u^+$	12.94	$2^4S+3s^4P$	7.27	0.573	12.3961	4.3763	0.7548	0.4874	1.5304	3.8432	5.4903	6.7890	7.2465	7.2680
$O^1\Pi_u$	13.12	$2^4S+3s^4P$	7.09	0.568	9.8650	3.4885	0.6783	0.4145	1.3173	3.4430	5.0530	6.4949	7.0458	7.0862
$e^1\Sigma_g^+$	14.33	$2^4S+s^2p^4s^4P$	8.40	0.551	11.5035	4.0632	0.7827	0.4831	1.5375	4.0035	5.9354	7.6845	8.3489	8.3958
$x^1\Sigma_g^-$	14.35	$2^4S+s^2p^3p^4P$	7.41	0.545	8.4787	3.0252	0.5974	0.3758	1.2149	3.2490	4.9432	6.6385	7.3488	7.4031
$y^1\Pi_g$	(14.56)	$2^4S+s^2p^3s^4P$	5.65	0.549	6.8689	2.4430	0.4803	0.2997	0.9621	2.5509	3.8470	5.0985	5.6088	5.6459





of  $11.92 \text{ cm}^{-1}$  for  $x_e\omega_e$  and  $4.91 \text{ eV}$  for  $D_e$ . This is in excellent agreement with the dissociation energy based on the dissociation products being  $2^2\text{D}+2^2\text{D}$ .

The  $^5\Sigma_g^+$  state arising from ground state atoms is suggested<sup>20</sup> to have a bond length of about  $1.6 \text{ \AA}$  and a vibrational frequency of  $\sim 12 \text{ cm}^{-1}$ . These values lead to an impossibly low dissociation energy. Equating (13) and (14) and using the known  $D_e$  and the above value for  $r_e$  leads to  $\omega_e=469 \text{ cm}^{-1}$ . Clearly more reliable data are needed before an accurate curve can be constructed by this method.

The calculated potential curves agree well with the R.K.R.V. curves where these are available. For example, Eq. (16b) gives values of  $V(r)$  which are rarely more than 2% in error for the ground states of  $\text{I}_2$ ,  $\text{H}_2$ , and  $\text{N}_2$ . The discrepancy is somewhat larger for the  $C^3\Pi_u$  state. This is of interest as this state is strongly disturbed by another  $^3\Pi_u$  state, suggesting that the discrepancy is a consequence of this perturbation.

#### CONCLUSION

On the basis of the observed dependence of  $a$  on the position of the element in the periodic table for the function (1) in the form (5a) or (5b), the first-order anharmonic corrections to the potential  $x_e\omega_e$  and  $\alpha_e$  have been calculated from the vibrational frequencies and bond lengths. This allows the potential curves for the ground states to be evaluated. The potential function as defined by (5b), in conjunction with the simplification resulting from the above, lead to surprisingly accurate potential curves for ground states and excited states. Since in general the anharmonicity and/or the vibrational-rotational coupling constant are

not well known—if known at all—this technique should be of considerable value when other information is not available and a knowledge of potential curves is desirable.

Such curves are not readily calculated from first principles. The difficulty of calculating potential curves is well illustrated by the recent work of Kolos and Roothaan.<sup>21</sup> Using 50-term wave functions and a S.C.F. procedure, the potential curve was calculated for values of  $r$  from  $0.423$  to  $2.22 \text{ \AA}$ . For small internuclear displacements from equilibrium the calculated curve agrees extremely well with the experimental. However, for  $r > 1.6 \text{ \AA}$  the calculated curve deviates seriously from the R.K.R.V. curve (see Fig. 1). This is because the wave functions are a power series in  $r$ , and cannot behave properly for large values of  $r$ .

The excellent agreement between the calculated and experimental curves as defined by the R.K.R.V. method especially for hydrogen and iodine, even for large internuclear separations is indicative of the nature of the interatomic forces. The dissociation products for  $\text{I}_2$  are  $5^2P_{3/2}+5^2P_{3/2}$  while for  $\text{H}_2$  they are  $1^2S+1^2S$ . It is interesting that this agreement appears to hold for the states of separated atoms which have and do not have quadrupole moments since the long-range interaction potential is often believed to be different for the two cases. An improved R.K.R.V. curve for  $\text{I}_2$  at large internuclear separations would be of considerable value in this connection.

#### ACKNOWLEDGMENT

This work was supported in part by a grant from the U. S. Army Research Office.

<sup>21</sup> W. Kolos and C. C. J. Roothaan, *Revs. Modern Phys.* **32**, 219 (1960).

<sup>20</sup> C. M. Herzfeld and H. P. Broida, *Phys. Rev.* **101**, 606 (1956).

# Comparative Study of Empirical Internuclear Potential Functions\*

DEREK STEELE† AND ELLIS R. LIPPINCOTT

*Department of Chemistry, University of Maryland, College Park, Maryland*

AND

JOSEPH T. VANDERSLICE

*Institute for Molecular Physics, University of Maryland, College Park, Maryland*

## INTRODUCTION

KNOWLEDGE of internuclear potential curves is of fundamental importance in a wide variety of fields ranging from gas kinetics to stellar structure. In particular, the recent increased interest in astrophysical problems has emphasized the need for accurate potential curves governing the interaction of two atoms in either their ground or excited states, i.e., the potential curves for the different electronic states of diatomic molecules. The interaction potential arises, for various nuclear separations, from the change in interaction of all the charged particles in the system from those existing at infinite separations of one or more of the atoms from the remainder of the system. For a diatomic system, the energy levels are determined from<sup>1</sup>

$$(\hat{H}_n + \hat{H}_e)\Psi = E\Psi, \quad (1)$$

where  $\hat{H}_n$  and  $\hat{H}_e$  depend, respectively, on nuclear coordinates alone, and electronic coordinates alone and are given by

$$\hat{H}_n = -\sum_{\alpha} (\hbar^2/8\pi^2 M_{\alpha}) \nabla_{\alpha}^2 + \hat{V}_{nn}, \quad (2)$$

$$\hat{H}_e = -\sum_i (\hbar^2/8\pi^2 m) \nabla_i^2 + \hat{V}_{ne} + \hat{V}_{ee}, \quad (3)$$

where  $\hat{V}_{nn}$ ,  $\hat{V}_{ne}$ , and  $\hat{V}_{ee}$  are the internuclear, nuclear-electron, and electron-electron-potential operators, respectively.

If the Born-Oppenheimer approximation is valid  $\Psi = \psi_n \psi_e$  and

$$\hat{H}_e \psi_e = E_e \psi_e, \quad (4)$$

then,

$$(\hat{H}_n + E_e)\psi_n = E\psi_n. \quad (5)$$

Here,  $\psi_n$  depends only on the nuclear coordinates.  $E_e$  is the electronic energy which is a function of the internuclear distance  $r$ . According to Eq. (5), the potential-energy term appearing in the Hamiltonian for the nuclear motion is just the sum of  $E_e$  and  $V_{nn}$ . The problem of solving Eq. (4) for  $E_e$  is a highly complex

one, incapable of exact solution at the present stage of mathematical advancement, except for the simple, tripartite systems  $H_2^+$ , etc. The difficulties are well exemplified by the calculations of Kolos and Roothaan<sup>2</sup> on the  $X^1\Sigma_g^+$  and  $B^1\Sigma_u^+$  states of the hydrogen molecule. To calculate  $E_e$  for the  $X^1\Sigma_g^+$  state by a self-consistent-field procedure, 40- and 50-term wave functions were used. Excellent agreement with curves from experimental data was obtained at small displacements of the nuclei from the equilibrium position  $r_e$ . However, at bondlengths greater than 1.0 Å, deviations occurred despite the complexity of the wave function used.<sup>3</sup> The reason, in this case, is that the wave functions are of the polynomial type which requires more and more terms, for increasing  $r$ , to approach the correct asymptotic form. Their results on the  $B^1\Sigma_u^+$  state are not in as good agreement with the curve obtained from experimental data as in the case of the  $X^1\Sigma_g^+$  state, but here only a 34-term wave function was used. Actually, the Kolos and Roothaan curves are in remarkably good agreement with the curves based on experimental data near  $r=r_e$  and offer some hope that accurate calculated curves will soon be forthcoming for simple systems.

As the number of particles increases, however, the difficulties mount extremely quickly. At present, there does not seem to be much hope of obtaining accurate curves except for the simplest of systems. Furthermore, as the interacting atoms become more complicated, the number of electronic states arising from their interaction increases rapidly, thus compounding the difficulties.

Clearly, alternative procedures for obtaining potential curves are desirable, indeed essential at the present time. Potential curves for diatomic systems fall mainly into two categories, ones with appreciable minima (bound states) and ones which exhibit a very shallow minimum or none at all (repulsive states); we are concerned with the former. Three general methods exist for obtaining curves for the bound states of diatomic molecules. The first and perhaps most satis-

\* This research was supported in part by the Army Research Office, U. S. Army, and in part by the Office of Naval Research.

† Present address: University College of Swansea, Wales, United Kingdom.

<sup>1</sup> H. Eyring, J. Walter, and G. E. Kimball, *Quantum Chemistry* (John Wiley & Sons, Inc., New York, 1944), p. 190-192.

<sup>2</sup> W. Kolos and C. C. J. Roothaan, *Revs. Modern Phys.* **32**, 219 (1960).

<sup>3</sup> I. Tobias and J. T. Vanderslice, *J. Chem. Phys.* **35**, 1852 (1961).

factory of these is the calculation of the curve from the experimental energy levels using the method of Rydberg, Klein, and Rees (RKR).<sup>4-7</sup> This is a WKB method where one starts with the observed-energy levels  $E$  and from these calculates the maximum and minimum points of the vibration. Since this is a WKB method, one might expect this to be somewhat in error near  $r_e$ . However, the results near the minimum agree with the curve calculated by the Dunham procedure which is known to be accurate in this region.<sup>7</sup> Indeed, Jarman<sup>8</sup> has shown that the two are equivalent for the lower-vibrational-energy levels. One major disadvantage of the RKR method is that the potential curve can be constructed only in the region for which sufficient spectroscopic data exist. For this reason, other reliable techniques must be found.

The second general method is due to Dunham.<sup>9</sup> He used the WKB method to show that the energy levels have the form

$$E_{v,J} = \sum_{i,j} Y_{ij} (v + \frac{1}{2})^i J^j (J+1)^j, \quad (6)$$

where  $l$  and  $j$  are summation indices and  $v$  and  $J$  are the vibrational and rotational numbers, respectively, and where the  $Y_{ij}$  are coefficients which can be determined from the experimental rotational and vibrational levels. Here, the energy zero is taken at the minimum of the potential curve. If the potential is assumed to be of the form

$$V = a_0 \left( \frac{\Delta r}{r_e} \right)^2 \left[ 1 + a_1 \left( \frac{\Delta r}{r_e} \right) + a_2 \left( \frac{\Delta r}{r_e} \right)^2 + a_3 \left( \frac{\Delta r}{r_e} \right)^3 + \dots \right] + B_e J(J+1) \left[ 1 - 2 \frac{\Delta r}{r_e} + 3 \left( \frac{\Delta r}{r_e} \right)^2 - 4 \left( \frac{\Delta r}{r_e} \right)^3 + \dots \right], \quad (7)$$

where  $\Delta r = r - r_e$ , then the  $a_i$ 's can be related to the  $Y_{ij}$ 's. Since the  $Y_{ij}$ 's are determined from the experimental data, the potential function based on this data can be determined from Eq. (7). The most serious drawback of the Dunham method is that it diverges as the energy approaches the dissociation limit and, hence, must be used with care at the higher-vibrational levels.

The third general method is based on empirical potential functions. The assumption is made that all bonding-potential curves can be fitted to a certain form of algebraic expression when the parameters in the expression are evaluated from the known spectroscopic constants. Numerous attempts to find suitable functions have been made. The parameters of these proposed

functions can be related to the spectroscopic constants and also to the dissociation energy. For example, the vibrational frequency  $\omega_e$  and the dissociation energy  $D_e$  are given by the classical expressions

$$V''(r_e) = k_e = 4\pi^2 c^2 \omega_e^2 \mu \\ V(r_e) - V(\infty) = D_e \quad (8)$$

and these enable one to determine two parameters in the assumed-potential expression. By solving the Schrödinger equation with the assumed form for  $V(r)$ , the other parameters in the expression can be related to the higher-order spectroscopic constants. The whole procedure of relating the parameters in the assumed-potential expression is greatly simplified by expanding the assumed potential and putting it in the form given by Eq. (7). Then, the parameters are given directly in terms of the  $Y_{ij}$ 's as determined by the Dunham method.<sup>9</sup> However, since the fit of all potential curves to a given algebraic expression must be considered as approximate, the only useful parameters are the harmonic and the first-order correction terms. This limits the number of parameters in the function to five for them to be determinate. Therefore, if the potential function contains fewer than five parameters, internal relationships among the spectroscopic constants exist.

The performance of a given function in correlation of these spectroscopic constants may be used as a first criterion for reliability of the function. Varshni<sup>10</sup> has examined a selection of the better known three-parameter functions on this basis, expressing the results graphically by plotting  $G = (8\omega_e x_e / B_e)$  and  $F = (\alpha_e \omega_e / 6B_e^2)$  against  $\Delta = (k_e r_e^2 / 2D_e)$  and comparing with the experimental plots.

A far more stringent test of an empirical potential function lies in the comparison of the  $V(r)$  vs  $r$  dependence with the curves for the different states of different molecules as determined from either the RKR or the Dunham method. The only published work known to the authors in which this has been done is the original work of Rydberg<sup>4</sup> and the work of Vanderslice *et al.* on the ground state of the hydrogen molecule.<sup>7</sup>

In view of the considerable importance of the empirical functions in supplementing curves obtained from the RKR and Dunham methods, and in view of the fact that for many highly excited states of diatomic molecules, it is the only way at present of obtaining anywhere near reliable potential curves, a systematic and thorough comparison of a number of the better-known and more widely used functions is believed to be useful. Two criteria exist for testing the validity of a given expression, as indicated in the foregoing. The first is the testing of internal correlations resulting from the use of less than five parameters in a function. Although Varshni<sup>10</sup> has carried out fairly extensive comparisons of this nature, a quantitative reassessment in terms of average percent deviation is felt to be a

<sup>4</sup> R. Rydberg, *Z. Physik* **73**, 376 (1931); **80**, 514 (1933).

<sup>5</sup> O. Klein, *Z. Physik* **76**, 221 (1932).

<sup>6</sup> A. L. G. Rees, *Proc. Phys. Soc. (London)* **59**, 998 (1947).

<sup>7</sup> J. T. Vanderslice, E. A. Mason, W. G. Maisch, and E. R. Lippincott, *J. Mol. Spectroscopy* **3**, 17 (1959); **5**, 83 (1960).

<sup>8</sup> W. R. Jarman, *Can. J. Phys.* **38**, 217 (1960).

<sup>9</sup> J. L. Dunham, *Phys. Rev.* **41**, 713, 721 (1932).

<sup>10</sup> Y. P. Varshni, *Revs. Modern Phys.* **29**, 664 (1957).

very useful addition to the problem. This is a strict test of the validity of the function close to the equilibrium configuration, but good results here do not necessarily mean that the function accurately represents the potential at small or large internuclear distances.

The second criterion is a comparison of the calculated curves with those given by the RKR method. Although the basic procedure, as enunciated by Rydberg,<sup>4</sup> was published in 1931, no extensive comparisons have been made. The quantity of experimental data now available is considerable, thus allowing for such comparisons. This is a more thorough and satisfying test of the long-range validity of the function.

The choice of ground states and excited states of diatomic molecules for which a test of this second criterion may be carried out is of necessity limited to molecules to which the RKR method has been applied. The following 19 examples are used in this comparative study. These are: the  $X^1\Sigma_g^+$  state of  $H_2$ ;<sup>3</sup> the  $X^1\Sigma_g^+$  state of  $I_2$ ;<sup>11</sup> the  $X^1\Sigma_g^+$ ,  $A^3\Sigma_u^+$ ,  $a^1\Pi_g$ , and  $B^3\Pi_g$  states of  $N_2$ ;<sup>12</sup> the  $X^3\Sigma_g^-$ ,  $B^3\Sigma_u^-$ , and  $A^3\Sigma_u^+$  states of  $O_2$ ;<sup>13</sup> the  $X^1\Sigma^+$ ,  $d^3\Delta$ ,  $A^1\Pi$ ,  $e^3\Sigma^-$ , and  $a^3\Sigma^+$  states of  $CO$ ;<sup>14</sup> the  $X^2\Pi_{1/2}$  and  $B^2\Pi$  states of  $NO$ ;<sup>15</sup> the  $X^2\Pi_{1/2}$  and  $A^2\Sigma^+$  states of  $OH$ ;<sup>16</sup> and the  $X^1\Sigma^+$  states of  $HF$ .<sup>17</sup>

#### EMPIRICAL FUNCTIONS FOR COMPARATIVE STUDY

Since Varshni<sup>10</sup> has given a discussion of the different empirical potential functions as well as of the criteria which should be satisfied by the functions, we emphasize only a few salient points.

Most of the proposed potential functions have been given in closed analytical form and make use of three parameters. Four- and five-parameter functions have also been proposed which usually are extensions of known three-parameter functions. All parameters must be evaluated in terms of known spectroscopic constants. Three-parameter functions can be evaluated by the quantities: equilibrium-bond length  $r_e$ , vibrational frequency for zero displacement of the nuclei  $\omega_e$ , and bond-dissociation energy from the bottom of the potential curve  $D_e$ . The first two of these quantities are usually known if the state in question has been studied experimentally whereas the third  $D_e$  may or may not be well known, in which case a three-parameter function cannot be used to construct the potential curve unless a reasonably reliable method is available for predicting  $D_e$  from interrelations among the spectro-

scopic constants. This has been done with varying degrees of success for some of the proposed functions.

Five-parameter functions must be evaluated with the aid of two additional spectroscopic quantities. They usually are taken as the vibrational anharmonicity  $\omega_e x_e$  and the vibrational rotational-coupling constant  $\alpha_e$ . These quantities are usually not as well known for a given state as  $r_e$  and  $\omega_e$  and, unless a state has been extensively studied spectroscopically, they may be unknown or known only with rather doubtful accuracy.

For three-parameter functions, conditions (8) along with

$$(dV/dr)_{r_e} = 0 \quad (9)$$

are used with  $r_e$ ,  $\omega_e$ , and  $D_e$  to compute the three parameters. The higher derivatives  $(d^3V/dr^3)_{r_e}$  and  $(d^4V/dr^4)_{r_e}$  can then be used to predict or correlate the quantities  $\omega_e x_e$  and  $\alpha_e$ . For five-parameter functions, the higher derivatives must be used along with  $\omega_e x_e$  and  $\alpha_e$  to compute the parameters of the function.

In order to demonstrate the relation of the various spectroscopic constants used in describing the observed energy levels of a nonrigid, rotating, anharmonic oscillator to the parameters of any empirical function which may be expanded in a power series in  $(r-r_e)$ , it is sufficient to use the method of Dunham.<sup>9</sup> If  $B_e/\omega_e$  is sufficiently small, which is the usual case, with the possible exception of hydrides, the  $Y_{ij}$ 's in Eq. (6) are related to the experimentally determined, molecular constants as follows:

$$\begin{aligned} Y_{10} &= \omega_e & Y_{20} &= -\omega_e x_e & Y_{30} &= \omega_e y_e & Y_{40} &= \omega_e z_e \\ Y_{01} &= B_e & Y_{11} &= -\alpha_e & Y_{21} &= \gamma_e & & \\ Y_{02} &= -D_e & Y_{12} &= \beta_e & & & & \\ Y_{03} &= H_e & & & & & & \end{aligned} \quad (10)$$

Here, the experimentally determined, molecular levels are given by

$$\begin{aligned} E_{v,J} &= \omega_e(v + \frac{1}{2}) - \omega_e x_e(v + \frac{1}{2})^2 + \omega_e y_e(v + \frac{1}{2})^3 \\ &+ \omega_e z_e(v + \frac{1}{2})^4 + \dots + B_v J(J+1) - D_v J^2(J+1)^2 \\ &+ H_v J^3(J+1)^2 + \dots, \quad (11) \end{aligned}$$

with  $B_v = B_e - \alpha_e(v + \frac{1}{2}) + \gamma_e(v + \frac{1}{2})^2$  and  $B_e = h/8\pi^2 \mu r_e^2$ . Dunham's method shows that

$$\omega_e^2 = 4a_0 B_e \quad \text{or} \quad D_e = a_0/\Delta \quad (12)$$

$$\begin{aligned} \omega_e x_e &= (B_e/2)[3(a_2 - 5a_1^2/4)] \\ &\quad \text{or} \quad G = 12(a_2 - 5a_1^2/4) \quad (13) \end{aligned}$$

$$\begin{aligned} \omega_e y_e &= (B_e^2/2\omega_e)[10a_4 - 35a_1a_3 - 17(a_2^2/2) \\ &+ (225a_1^2a_2/4) - 705a_1^4/32] \quad (14) \end{aligned}$$

$$-\alpha_e = (B_e^2/\omega_e)[6(1+a_1)] \quad \text{or} \quad F = 1+a_1 \quad (15)$$

$$\begin{aligned} \gamma_e &= (6B_e^3/\omega_e^2)[5 + 10a_1 - 3a_2 + 5a_3 - 13a_1a_2 \\ &+ 15(a_1^2 + a_1^3)/2] \quad (16) \end{aligned}$$

$$D_e = (4B_e^3/\omega_e^2), \quad (17)$$

<sup>11</sup> R. D. Verma, J. Chem. Phys. **32**, 738 (1960).

<sup>12</sup> J. T. Vanderslice, E. A. Mason, and E. R. Lippincott, J. Chem. Phys. **30**, 129 (1959).

<sup>13</sup> J. T. Vanderslice, E. A. Mason, and W. G. Maisch, J. Chem. Phys. **32**, 515 (1960); **33**, 614 (1960).

<sup>14</sup> I. Tobias, R. J. Fallon, and J. T. Vanderslice, J. Chem. Phys. **33**, 1638 (1960).

<sup>15</sup> J. T. Vanderslice, E. A. Mason, and W. G. Maisch, J. Chem. Phys. **31**, 738 (1959).

<sup>16</sup> R. J. Fallon, I. Tobias, and J. T. Vanderslice, J. Chem. Phys. **34**, 167 (1961).

<sup>17</sup> R. J. Fallon, J. T. Vanderslice, and E. A. Mason, J. Chem. Phys. **32**, 698 (1960); **33**, 944 (1960).

TABLE I. Summary of information on various empirical, potential-energy expressions.<sup>a</sup>

Name of function	Expression for V	Relations between parameters and spectroscopic constants	Predicted expression for $\alpha_e$	Predicted expression for $\omega_e x_e$
Morse <sup>18</sup>	$D_e[1 - e^{-ax}]^2$ $x = (r - r_e)$	$a = (k_e/2D_e)^{1/2}$	$(6B_e^2/\omega_e)(\Delta^{\dagger} - 1)$	$\omega_e^2/4D_e$
Hulbert-Hirschfelder <sup>19, b</sup>	$D_e[(1 - e^{-ax})^2 + ca^2x^2e^{-2ax}(1 + abx)]$ $x = (r - r_e)$	$a = (k_e/2D_e)^{1/2}$ $b = 2 - \frac{1}{c} \left\{ \frac{1}{12} \frac{1}{a^2 r_e^2} \left[ \frac{5}{4} + \frac{5F^2}{2} + \frac{5F^2}{4} \frac{G}{12} \right] \right\}$ $c = 1 - (1/ar_e)(1 + F)$	...	...
Rosen-Morse <sup>20</sup>	$A \tanh(r/d) - C \operatorname{sech}^2(r/d)$	$\Delta = (r_e/d)^2 [1 + \tanh(r_e/d)]^2$ $A = -2C \tanh(r_e/d)$ $C = \frac{D_e}{[1 - \tanh(r_e/d)]^2}$ $d = (k_e/D_e)^{1/2}$	$\frac{6B_e^2}{\omega_e} \left[ \frac{2r_e}{d} \tanh\left(\frac{r_e}{d}\right) - 1 \right]$	$B_e \Delta [1 - e^{-2r_e/d} + e^{-4r_e/d}]$  $(11/12)B_e \Delta$
Rydberg <sup>4</sup>	$D_e[1 - (1 + dx)e^{-ax}]$ $x = (r - r_e)$	$a = (k_e/4D_e)^{1/2}$ $N = D_e/[1 - y^2]$ $M = Ny^4$	$(6B_e^2/\omega_e)[\frac{2}{3}(2\Delta)^{\dagger} - 1]$  $(6B_e^2/\omega_e)[\Delta^{\dagger} \coth \Delta^{\dagger} - 1]$	$B_e \Delta$
Pöschl-Teller <sup>21</sup>	$M \operatorname{cosh}^2(ar/2) - N \operatorname{sech}^2(ar/2)$	$y = \tanh(ar_e/2)$ $\Delta = m(m + 1 - nr_e)nr_e/[2(m - nr_e)]$ $a = D_e r_e^m [nr_e/(m - nr_e)]$ $b = maenr_e/nr_e^{m+1}$	$\frac{6B_e^2}{\omega_e} \left[ \frac{(m+1)(m-1) - (nr_e)^2 + 3nr_e}{3(m+1 - nr_e)} \right]$	$\frac{5B_e}{24} \left[ \frac{20 - (nr_e)^2}{4 - nr_e} \right]$ $-\frac{1}{8} B_e [120 - (nr_e)^2]/[4 - nr_e]$ $B_e \left\{ \frac{11(ar_e)^4 + 66(ar_e)^2}{+ 156(ar_e)^2 + 144(ar_e) + 36} \right\}$
Linnert <sup>22</sup>	$a/r^m - be^{-nr}$ $(m = 3)$	$a = [(1 + 2\Delta)^{\dagger} - 1]/r_e$ $b = D_e e^{nr_e} [1 + ar_e]$ $c = aD_e r_e^2 e^{nr_e}$	$\frac{2B_e^2}{\omega_e} \frac{(ar_e)[2(ar_e) + 3]}{[(ar_e) + 2]}$	$\frac{B_e}{8} \left\{ \frac{111}{8\Delta} - 12\Delta^{\dagger} + 66 - \frac{111}{\Delta^{\dagger}} + \frac{73}{\Delta} \right\}$
Frost-Musulin <sup>23</sup>	$e^{-nr}[c/r - b]$			
Varshni III <sup>10</sup>	$D_e \left\{ 1 - \frac{r_e}{r} \exp[-\beta(r^2 - r_e^2)] \right\}^2$	$\beta = (1/2r_e^2)[\Delta^{\dagger} - 1]$	$\frac{6B_e^2}{\omega_e \Delta^{\dagger}} [\Delta - 2\Delta^{\dagger} + 2]$	
Lippincott <sup>24-28</sup>	$D_e(1 - e^{-ax})\{1 - abx^{\dagger} \exp[-b(x_e^{\dagger}/r)]\}$ $r/r_e$ $b = 1.065$	$x = u(r - r_e)^2/2r$ $n = 2\Delta/r_e$ $a = (\frac{1}{8})(1 - \Delta^{\dagger}/b) \sqrt{\Delta^{\dagger}/2} b$	$(6B_e^2/\omega_e)ab\Delta^{\dagger}$	$\frac{B_e}{8} \left\{ \frac{3 + 12ab\Delta^{\dagger} + 6\Delta}{+ 15a^2b^2\Delta - 12ab^2\Delta} \right\}$

<sup>a</sup> The following definitions<sup>10</sup> are used in the table:  $\Delta = k_e r_e^3/2D_e$ ,  $F = \alpha_e r_e^2/6B_e^2$ ,  $G = 8\alpha_e r_e/B_e$ .  
<sup>b</sup> The reviewer has pointed out to us that the expression for the constant  $b$  given in the original Hulbert-Hirschfelder paper is in error. The correct one, given in this table, was used for the final calculations reported in this paper. [See H. M. Hulbert and J. O. Hirschfelder, J. Chem. Phys., 35, 1901 (L), (1961).]

TABLE II. Molecular constants used in calculations.<sup>a</sup>

Molecule	State	$\omega_e$ (cm <sup>-1</sup> )	$r_e$ (Å)	$B_e$ (cm <sup>-1</sup> )	$\omega_e x_e$ (cm <sup>-1</sup> )	$\alpha_e$ (cm <sup>-1</sup> )	$D_e$ (ev)
H <sub>2</sub>	X <sup>1</sup> Σ <sub>g</sub> <sup>+</sup>	4400.39	0.74173	60.8407	120.815	3.0177	4.7467
I <sub>2</sub>	X <sup>1</sup> Σ <sub>g</sub> <sup>+</sup>	214.518	2.668	0.03734	0.6127	1.208×10 <sup>-4</sup>	1.5571
N <sub>2</sub>	X <sup>1</sup> Σ <sub>g</sub> <sup>+</sup>	2358.07	1.0976	1.9987	14.188	0.0171	9.902
	A <sup>2</sup> Σ <sub>u</sub> <sup>+</sup>	1460.60	1.2867	1.4545	13.851	0.01798	3.690
	a <sup>1</sup> Π <sub>g</sub>	1693.7	1.2197	1.6181	13.825	0.0183	6.07
	B <sup>3</sup> Π <sub>g</sub>	1735.42	1.2128	1.6375	15.198	0.01794	4.90
	X <sup>2</sup> Σ <sub>g</sub> <sup>-</sup>	1580.36	1.20740	1.44566	12.0730	0.01579	5.2129
O <sub>2</sub>	B <sup>2</sup> Σ <sub>u</sub> <sup>-</sup>	700.36	1.604	0.819	8.0023	0.011	1.005
	A <sup>2</sup> Σ <sub>u</sub> <sup>+</sup>	801.0	1.5183	0.9142	13.81	0.0165	0.8239
	X <sup>1</sup> Σ <sup>+</sup>	2169.829	1.12822	1.9312	13.295	0.0175	11.245
	d <sup>3</sup> Δ	1137.79	1.3770	1.296	7.624	0.0171	3.516
	A <sup>1</sup> Π	1515.61	1.2351	1.6116	17.2505	0.02229	3.175
CO	e <sup>2</sup> Σ <sup>-</sup>	1093.99	1.3933	1.2663	9.578	0.0179	3.147
	a <sup>2</sup> Σ <sup>+</sup>	1230.65	1.3518	1.3453	11.0130	0.01872	4.324
	X <sup>2</sup> Π <sub>1/2</sub>	1904.03	1.1590	1.6809	13.97	0.0174	6.609
	B <sup>2</sup> Π	1036.96	1.4176	1.1226	7.603	0.0121	3.29
	X <sup>2</sup> Π <sub>1/2</sub>	3734.09	0.9705	18.867	82.665	0.708	4.624
OH	A <sup>2</sup> Σ <sup>+</sup>	3203.28	1.0117	17.358	113.85	0.7868	2.53
	X <sup>1</sup> Σ <sup>+</sup>	4137.25	0.91717	20.946	88.726	0.7888	6.114

<sup>a</sup> These constants are consistent with the data used in the calculation of the experimental-potential curves by the RKR method. The references to the original data are given in references (7), (11)–(17).

where, following Varshni,<sup>10</sup> we define

$$F = \alpha_e \omega_e / 6B_e^2, \quad G = 8\omega_e x_e / B_e \quad (18)$$

and  $\Delta = k_e r_e^2 / 2D_e$ . Additional relations are available relating higher-order terms.

By expanding any proposed function in a power series of the form of (7), one has a convenient method of relating the parameters of the function to the known spectroscopic constants. Also, it is convenient to use Eqs. (12) to (17) to evaluate any additional spectroscopic quantities not used in determining the parameters.

We have chosen nine empirical functions for this comparative study of internuclear potentials. Each function is evaluated for its ability to reproduce the potential curve as determined by the RKR method and for its ability to predict  $\omega_e x_e$  and  $\alpha_e$  or other spectroscopic quantities such as bond-dissociation energy. After careful consideration of all proposed functions known to us, we have selected the following for consideration: Morse<sup>18</sup>; Hulburt-Hirschfelder<sup>19</sup>; Rosen-Morse<sup>20</sup>; Rydberg<sup>4</sup>; Pöschl-Teller<sup>21</sup>; Linnett<sup>22</sup>; Frost-Musulin<sup>23</sup>; Varshni<sup>10</sup>; and Lippincott.<sup>24–28</sup> Several

factors affected this selection, including: known performance, form of the function, ability to correlate spectroscopic quantities, number of parameters, etc. The selection covers a sufficiently wide range of types so as to make an effective comparative study of empirical potential functions.

Table I summarizes the necessary information on these potential functions. The relations between the parameters and the spectroscopic constants were obtained from Eqs. (8) and (9). The predicted expressions for  $\alpha_e$  and  $\omega_e x_e$  for each potential function were obtained from Eqs. (12) to (17). The results in Table I agree with those of Varshni<sup>10</sup> except for the Linnett and Lippincott functions.<sup>29</sup>

Varshni<sup>10</sup> has proposed a number of functions for consideration as empirical internuclear potentials. We have used his III function in the comparison study here since it appears to be the best over-all function of those he proposed.<sup>10</sup>

The spectroscopic data needed for the evaluation of the parameters of the potential curves are given in Table II.

## RESULTS

The results of this comparative study are shown in Tables III to XXIV. Tables III to XXI show the comparison between the RKR and various empirical potential curves for all the molecular states considered. Tables XXII and XXIII give a comparison between the calculated and observed values of  $\omega_e x_e$  and  $\alpha_e$  for the various functions. Table XXIV gives a summary of the results showing the average percent errors from the experimental values for  $\omega_e x_e$  and  $\alpha_e$  and the average percent error for the quantity  $(|V - V_{\text{RKR}}|) / D_e$  for

<sup>29</sup> Varshni's expressions for  $\alpha_e$  in the case of the Linnett and Lippincott functions differ from the ones given above. Varshni (private communication) agrees that the above expressions are the correct ones. [See also Revs. Modern Phys. 31, 839 (1959)].

- <sup>18</sup> P. M. Morse, Phys. Rev. 34, 57 (1929).  
<sup>19</sup> H. M. Hulburt and J. O. Hirschfelder, J. Chem. Phys. 9, 61 (1941).  
<sup>20</sup> N. Rosen and P. M. Morse, Phys. Rev. 42, 210 (1932).  
<sup>21</sup> G. Pöschl and E. Teller, Z. Physik 83, 143 (1933).  
<sup>22</sup> J. W. Linnett, Trans. Faraday Soc. 36, 1123 (1940); 38, 1 (1942).  
<sup>23</sup> A. A. Frost and B. Musulin, J. Chem. Phys. 22, 1017 (1954); J. Am. Chem. Soc. 76, 2045 (1954).  
<sup>24</sup> E. R. Lippincott, J. Chem. Phys. 21, 2070 (1953).  
<sup>25</sup> E. R. Lippincott and R. Schroeder, J. Chem. Phys. 23, 1131 (1955); J. Am. Chem. Soc. 78, 5171 (1956); J. Phys. Chem. 61, 921 (1957).  
<sup>26</sup> E. R. Lippincott and M. O. Dayhoff, Spectrochim. Acta 16, 807 (1960); E. R. Lippincott, J. Chem. Phys. 26, 1678 (1957).  
<sup>27</sup> E. R. Lippincott, D. Steele, and P. Caldwell, J. Chem. Phys. 35, 123 (1961).  
<sup>28</sup> D. Steele and E. R. Lippincott, J. Chem. Phys. 35, 2065 (1961).

TABLE III. Results of potential-curve calculations for  $X^1\Sigma_g^+$  state of  $H_2$ .<sup>a</sup>

$r$ (A)	RKR (ev)	Morse	Hulburt-Hirschfelder	Rydberg	Pöschl-Teller	Linnett	Varshni	Rosen-Morse	Lippincott	Frost-Musulin
0.4109	4.729	3.868	4.652	3.680	4.854	6.918	5.787	3.189	4.187	4.946
0.4319	3.880	3.243	3.823	3.097	3.950	4.745	4.629	2.721	3.498	4.038
0.4597	2.935	2.533	2.913	2.435	2.982	3.930	3.421	2.172	2.716	3.054
0.5088	1.730	1.558	1.724	1.508	1.745	2.154	1.938	1.384	1.648	1.790
0.6337	0.269	0.259	0.268	0.256	0.269	0.291	0.279	0.248	0.264	0.272
0.8833	0.269	0.275	0.270	0.270	0.269	0.250	0.261	0.287	0.273	0.264
1.2186	1.730	1.734	1.724	1.790	1.687	1.450	1.608	1.869	1.757	1.608
1.5148	2.935	2.870	2.902	2.975	2.815	2.395	2.721	3.084	2.959	2.667
1.8524	3.880	3.715	3.782	3.838	3.672	3.183	3.628	3.924	3.846	3.500
2.3748	4.522	4.358	4.413	4.454	4.339	3.931	4.371	4.489	4.467	4.205
2.2835	4.729	4.679	4.690	4.712	4.676	4.491	4.712	4.714	4.714	4.626
4.23	4.745	4.736	4.737	4.743	4.735	4.673	4.745	4.743	4.743	4.722
6.35	4.747	4.747	4.747	4.747	4.747	4.744	4.747	4.747	4.747	4.747

<sup>a</sup> The energies given in Tables III-XXI are in ev.TABLE IV. Results of potential-curve calculations for  $X^1\Sigma_g^+$  state of  $I_2$ .

$r$ (A)	RKR (ev)	Morse	Hulburt-Hirschfelder	Rydberg	Pöschl-Teller	Linnett	Varshni	Rosen-Morse	Lippincott	Frost-Musulin
2.288	1.500-1.556	1.637	1.521	1.548	1.634	1.285	1.458	1.603	1.451	1.593
2.292	1.493	1.589	1.475	1.504	1.587	1.251	1.417	1.561	1.412	1.545
2.309	1.245	1.399	1.297	1.328	1.398	1.114	1.256	1.372	1.255	1.363
2.336	0.977	1.131	1.048	1.080	1.130	0.919	1.027	1.107	1.029	1.105
2.423	0.465	0.517	0.482	0.500	0.517	0.446	0.483	0.503	0.487	0.507
3.056	0.465	0.411	0.452	0.422	0.411	0.506	0.436	0.404	0.445	0.417
3.389	0.977	0.848	0.951	0.879	0.848	1.204	0.914	0.840	0.945	0.866
3.671	1.245	1.111	1.231	1.151	1.111	1.732	1.194	1.104	1.216	1.135
4.448	1.493	1.445	1.501	1.475	1.445	2.598	1.502	1.438	1.474	1.464
6.522	1.551	1.555	1.555	1.556	1.555	2.602	1.557	1.55	1.555	1.556
8.814	1.556	1.557	1.557	1.557	1.557	2.106	1.557	1.55	1.557	1.557

TABLE V. Results of potential-curve calculations for  $X^1\Sigma_g^+$  state of  $N_2$ .

$r$ (A)	RKR (ev)	Morse	Hulburt-Hirschfelder	Rydberg	Pöschl-Teller	Linnett	Varshni	Rosen-Morse	Lippincott	Frost-Musulin
0.896	5.021	5.128	4.925	4.926	5.166	5.181	4.801	4.950	4.854	5.207
0.919	3.865	3.764	3.624	3.634	3.784	3.791	3.551	3.673	3.597	3.809
0.942	2.618	2.673	2.582	2.595	2.685	2.684	2.543	2.618	2.576	2.704
0.983	1.280	1.290	1.256	1.263	1.294	1.289	1.244	1.272	1.258	1.302
1.027	0.435	0.433	0.426	0.427	0.434	0.431	0.424	0.432	0.426	0.429
1.185	0.435	0.434	0.443	0.439	0.435	0.436	0.445	0.432	0.444	0.430
1.261	1.280	1.252	1.297	1.277	1.251	1.267	1.305	1.267	1.303	1.245
1.358	2.618	2.510	2.639	2.580	2.507	2.573	2.662	2.559	2.678	2.503
1.447	3.865	3.675	3.893	3.795	3.671	3.811	3.941	3.740	3.988	3.668
1.528	5.021	4.656	4.949	4.820	4.651	4.883	5.025	4.742	5.102	4.653

TABLE VI. Results of potential-curve calculations for the  $A^3\Sigma_u^+$  state of  $N_2$ .

$r$ (A)	RKR (ev)	Morse	Hulburt-Hirschfelder	Rydberg	Pöschl-Teller	Linnett	Varshni	Rosen-Morse	Lippincott	Frost-Musulin
1.046	2.257	3.181	2.968	3.023	3.194	2.973	2.878	3.066	2.910	3.178
1.089	1.564	1.886	1.772	1.813	1.892	1.780	1.741	1.838	1.771	1.884
1.145	0.780	0.822	0.783	0.800	0.824	0.784	0.778	0.804	0.791	0.821
1.203	0.268	0.243	0.236	0.239	0.244	0.235	0.236	0.233	0.238	0.242
1.405	0.268	0.281	0.291	0.285	0.280	0.291	0.291	0.286	0.290	0.279
1.503	0.780	0.733	0.778	0.752	0.733	0.784	0.775	0.745	0.779	0.736
1.633	1.564	1.379	1.486	1.424	1.378	1.533	1.483	1.399	1.507	1.389
1.756	2.257	1.924	2.082	1.994	1.923	2.210	2.086	1.950	2.129	1.942



TABLE VII. Results of potential-curve calculations for  $a^1\Pi_g$  state of  $N_2$ .

$r$ (Å)	RKR (ev)	Morse	Hulburt-Hirschfelder	Rydberg	Pöschl-Teller	Linnett	Varshni	Rosen-Morse	Lippincott	Frost-Musulin
1.013	2.686	2.69	2.70	2.59	2.70	2.69	2.52	2.61	2.55	2.72
1.036	2.016	2.00	2.00	1.93	2.00	1.99	1.89	1.95	1.91	2.02
1.077	1.103	1.08	1.08	1.06	1.09	1.08	1.04	1.07	1.05	1.09
1.139	0.311	0.30	0.29	0.29	0.30	0.30	0.29	0.30	0.29	0.30
1.325	0.311	0.32	0.32	0.32	0.32	0.32	0.33	0.33	0.33	0.32
1.445	1.103	1.10	1.11	1.13	1.10	1.13	1.16	1.13	1.16	1.10
1.564	2.016	1.99	2.01	2.05	1.99	2.07	2.13	2.03	2.15	1.99
1.655	2.686	2.63	2.67	2.72	2.63	2.77	2.84	2.69	2.88	2.63

TABLE VIII. Results of potential-curve calculations for  $B^3\Pi_g$  state of  $N_2$ .

$r$ (Å)	RKR (ev)	Morse	Hulburt-Hirschfelder	Rydberg	Pöschl-Teller	Linnett	Varshni	Rosen-Morse	Lippincott	Frost-Musulin
0.983	3.500	4.05	3.65	3.85	4.07	3.84	3.67	3.89	3.72	4.06
1.006	2.738	3.05	2.78	2.92	3.06	2.91	2.80	2.94	2.85	3.05
1.037	1.880	2.01	1.85	1.94	2.01	1.92	1.87	1.95	1.90	2.00
1.082	0.932	0.97	0.92	0.95	0.97	0.94	0.92	0.95	0.94	0.97
1.132	0.319	0.32	0.31	0.31	0.32	0.32	0.31	0.32	0.31	0.32
1.316	0.319	0.31	0.32	0.32	0.31	0.32	0.32	0.32	0.32	0.31
1.409	0.932	0.88	0.93	0.90	0.88	0.93	0.93	0.90	0.93	0.88
1.531	1.880	1.71	1.84	1.77	1.71	1.87	1.84	1.74	1.87	1.72
1.644	2.738	2.42	2.61	2.51	2.42	2.73	2.62	2.46	2.67	2.44
1.760	3.500	3.02	3.25	3.14	3.02	3.49	3.28	3.06	3.34	3.05

TABLE IX. Results of potential-curve calculations for  $X^3\Sigma_g^-$  state of  $O_2$ .

$r$ (Å)	RKR (ev)	Morse	Hulburt-Hirschfelder	Rydberg	Pöschl-Teller	Linnett	Varshni	Rosen-Morse	Lippincott	Frost-Musulin
0.979	3.551	3.623	3.590	3.461	3.642	3.570	3.330	3.483	3.371	3.656
1.022	2.063	2.108	2.076	2.034	2.114	2.085	1.972	2.037	2.004	2.121
1.067	1.034	1.063	1.046	1.037	1.066	1.067	1.013	1.037	1.028	1.068
1.158	0.098	0.108	0.101	0.102	0.102	0.119	0.101	0.094	0.102	0.104
1.262	0.098	0.095	0.096	0.096	0.094	0.110	0.095	0.094	0.096	0.095
1.422	1.034	0.983	1.021	1.007	0.982	1.035	1.036	0.994	1.039	0.984
1.556	2.063	1.900	2.001	1.961	1.898	2.040	2.040	1.929	2.067	1.905
1.662	2.844	2.561	2.711	2.652	2.559	2.800	2.771	2.600	2.820	2.573
1.768	3.551	3.125	3.310	3.240	3.123	3.476	3.392	3.171	3.447	3.143

TABLE X. Results of potential-curve calculations for  $B^2\Sigma_u^-$  state of  $O_2$ .

$r$ (Å)	RKR (ev)	Morse	Hulburt-Hirschfelder	Rydberg	Pöschl-Teller	Linnett	Varshni	Rosen-Morse	Lippincott	Frost-Musulin
1.334	0.956	1.132	0.942	1.069	1.133	0.946	1.003	1.129	1.005	1.110
1.356	0.749	0.895	0.745	0.850	0.894	0.759	0.802	0.893	0.808	0.879
1.405	0.441	0.499	0.423	0.480	0.498	0.436	0.459	0.503	0.465	0.491
1.531	0.043	0.047	0.044	0.046	0.047	0.046	0.046	0.053	0.046	0.046
1.683	0.043	0.037	0.039	0.037	0.037	0.039	0.037	0.041	0.037	0.036
1.962	0.441	0.382	0.460	0.395	0.382	0.467	0.411	0.389	0.421	0.387
2.232	0.749	0.666	0.798	0.691	0.666	0.908	0.720	0.674	0.735	0.679
2.865	0.956	0.938	0.995	0.956	0.938	1.439	0.975	0.945	0.957	1.005

all points considered for all states of all molecules for each function, along with the same quantity for values of  $r > r_0$ .

Some functions show an average performance which is distinctly superior to others. The five-parameter Hulburt-Hirschfelder gives an average error of about 1.5% in  $(|V - V_{\text{RKR}}|)/D_0$ , while the better three-parameter functions give average errors of 2% to 3%

in this same quantity. However, no one function is best for all molecular states considered, nor can we predict *a priori* which function will give the more correct potential for a restricted range of  $r$ . Furthermore, it is easy to see from Tables III to XXI that no one function gives consistent positive or negative deviations from the experimental curves for a given value of  $r/r_0$ .

The empirical potentials give better average

TABLE XI. Results of potential-curve calculations for  $A^3\Sigma_u^+$  state of  $O_2$ .

$r$ (A)	RKR (ev)	Morse	Hulburt-Hirschfelder	Rydberg	Pöschl-Teller	Linnett	Varshni	Rosen-Morse	Lippincott	Frost-Musulin
1.300	0.783	0.985	0.824	0.929	0.987	0.751	0.872	0.972	0.863	0.954
1.318	0.629	0.775	0.650	0.735	0.777	0.604	0.695	0.763	0.692	0.753
1.350	0.409	0.485	0.413	0.465	0.487	0.394	0.445	0.479	0.446	0.474
1.410	0.145	0.158	0.141	0.154	0.158	0.139	0.150	0.153	0.151	0.156
1.668	0.145	0.130	0.146	0.133	0.131	0.153	0.136	0.130	0.138	0.132
1.823	0.409	0.341	0.404	0.353	0.341	0.462	0.366	0.337	0.378	0.348
1.984	0.629	0.518	0.612	0.538	0.518	0.790	0.559	0.513	0.575	0.530
2.247	0.783	0.690	0.770	0.711	0.690	1.206	0.732	0.688	0.728	0.704

TABLE XII. Results of potential-curve calculations for  $X^1\Sigma^+$  state of CO.

$r$ (A)	RKR (ev)	Morse	Hulburt-Hirschfelder	Rydberg	Pöschl-Teller	Linnett	Varshni	Rosen-Morse	Lippincott	Frost-Musulin
0.901	5.428	5.283	5.480	5.086	5.357	5.611	5.059	5.048	5.052	5.439
0.923	4.211	4.081	4.211	3.945	4.127	4.291	3.921	3.930	3.927	4.181
0.952	2.878	2.802	2.873	2.723	2.827	2.913	2.706	2.718	2.716	2.856
0.997	1.430	1.392	1.416	1.364	1.401	1.429	1.356	1.369	1.362	1.411
1.054	0.400	0.389	0.392	0.384	0.390	0.393	0.383	0.392	0.384	0.395
1.220	0.400	0.407	0.404	0.411	0.405	0.402	0.414	0.413	0.413	0.408
1.322	1.430	1.452	1.437	1.482	1.448	1.431	1.505	1.481	1.507	1.440
1.438	2.878	2.916	2.881	2.998	2.907	2.883	3.074	2.986	3.096	2.889
1.544	4.211	4.258	4.207	4.398	4.246	4.227	4.539	4.372	4.595	4.218
1.649	5.428	5.475	5.416	5.671	5.461	5.469	5.880	5.627	5.967	5.424

TABLE XIII. Results of potential-curve calculations for the  $d^3\Delta$  state of CO.

$r$ (A)	RKR (ev)	Morse	Hulburt-Hirschfelder	Rydberg	Pöschl-Teller	Linnett	Varshni	Rosen-Morse	Lippincott	Frost-Musulin
1.097	2.367	2.411	2.715	2.305	2.430	2.443	2.239	2.308	2.265	2.452
1.119	2.000	1.944	2.141	1.865	1.956	1.962	1.815	1.869	1.840	1.973
1.151	1.475	1.385	1.484	1.336	1.391	1.392	1.304	1.343	1.325	1.400
1.204	0.744	0.718	0.744	0.699	0.720	0.720	0.686	0.705	0.697	0.722
1.277	0.209	0.203	0.205	0.201	0.204	0.203	0.198	0.204	0.201	0.204
1.506	0.209	0.207	0.210	0.210	0.207	0.209	0.213	0.213	0.211	0.207
1.657	0.744	0.722	0.754	0.740	0.720	0.738	0.761	0.738	0.764	0.719
1.837	1.475	1.391	1.497	1.437	1.389	1.450	1.484	1.422	1.514	1.388
1.991	2.000	1.893	2.064	1.962	1.891	2.006	2.049	1.934	2.082	1.894
2.122	2.367	2.246	2.455	2.328	2.244	2.411	2.435	2.299	2.470	2.249

TABLE XIV. Results of potential-curve calculations for  $A^1\Pi$  state of CO.

$r$ (A)	RKR (ev)	Morse	Hulburt-Hirschfelder	Rydberg	Pöschl-Teller	Linnett	Varshni	Rosen-Morse	Lippincott	Frost-Musulin
1.003	2.742	3.276	2.939	3.101	3.285	2.952	2.927	3.227	2.950	3.257
1.021	2.275	2.625	2.369	2.497	2.630	2.384	2.370	2.593	2.399	2.608
1.050	1.591	1.782	1.627	1.709	1.784	1.636	1.635	1.764	1.662	1.773
1.085	0.967	1.045	0.970	1.012	1.045	0.972	0.977	1.041	0.994	1.043
1.148	0.276	0.288	0.276	0.283	0.289	0.275	0.277	0.286	0.280	0.289
1.348	0.276	0.265	0.277	0.269	0.266	0.279	0.275	0.258	0.274	0.266
1.484	0.967	0.887	0.966	0.913	0.888	0.988	0.946	0.884	0.957	0.895
1.599	1.591	1.412	1.537	1.461	1.412	1.642	1.525	1.415	1.558	1.428
1.744	2.275	1.957	2.124	2.029	1.956	2.383	2.123	1.967	2.165	1.982
1.867	2.742	2.303	2.475	2.385	2.303	2.894	2.490	2.314	2.515	2.333

percentage deviations from the RKR curves for  $r > r_e$ , as shown in the fourth row of Table XXIII where the better functions give an average error between 1 and 2% in dissociation energy. This is not unexpected since, for  $r > r_e$ , a small change in  $r$  gives a large change in  $V$ . There are not many states for which data are available

for a comparison of the function for large  $r$ , the region of importance in the calculations of macroscopic properties that depend on collision phenomena like the transport properties. Although there are not many examples in Tables III to XXI where the RKR curves are available for  $r \gg r_e$ , the indications are that the

TABLE XV. Results of potential-curve calculations for  $e^2\Sigma^-$  state of CO.

$r$ (Å)	RKR (ev)	Morse	Hulburt-Hirschfelder	Rydberg	Pöschl-Teller	Linnett	Varshni	Rosen-Morse	Lippincott	Frost-Musulin
1.124	2.014	2.031	2.172	1.944	2.046	2.031	1.882	1.956	1.902	2.059
1.147	1.616	1.609	1.697	1.546	1.618	1.604	1.501	1.559	1.520	1.625
1.176	1.182	1.169	1.216	1.130	1.174	1.163	1.100	1.138	1.116	1.179
1.217	0.710	0.699	0.715	0.681	0.701	0.694	0.666	0.681	0.675	0.705
1.292	0.201	0.194	0.195	0.191	0.194	0.194	0.189	0.189	0.191	0.195
1.527	0.201	0.203	0.205	0.206	0.203	0.205	0.209	0.195	0.208	0.204
1.681	0.710	0.688	0.706	0.706	0.687	0.709	0.730	0.689	0.730	0.688
1.806	1.182	1.114	1.158	1.150	1.113	1.167	1.194	1.124	1.208	1.114
1.924	1.616	1.486	1.557	1.539	1.485	1.582	1.606	1.505	1.631	1.489
2.042	2.014	1.810	1.905	1.877	1.809	1.954	1.963	1.834	1.994	1.815

TABLE XVI. Results of potential-curve calculations for  $a^2\Sigma^+$  state of CO.

$r$ (Å)	RKR (ev)	Morse	Hulburt-Hirschfelder	Rydberg	Pöschl-Teller	Linnett	Varshni	Rosen-Morse	Lippincott	Frost-Musulin
1.075	2.907	2.692	3.044	2.578	2.720	2.775	2.523	2.574	2.534	2.749
1.094	2.397	2.236	2.494	2.149	2.255	2.295	2.104	2.147	2.120	2.279
1.119	1.829	1.723	1.890	1.663	1.736	1.759	1.630	1.663	1.647	1.751
1.164	1.071	1.013	1.060	0.985	1.019	1.027	0.969	0.986	0.980	1.025
1.257	0.226	0.210	0.216	0.207	0.211	0.213	0.206	0.208	0.207	0.211
1.479	0.226	0.238	0.234	0.241	0.238	0.238	0.244	0.236	0.243	0.238
1.681	1.071	1.078	1.056	1.108	1.076	1.093	1.141	1.095	1.147	1.074
1.846	1.829	1.805	1.778	1.867	1.802	1.854	1.939	1.839	1.965	1.798
1.981	2.397	2.326	2.305	2.411	2.323	2.419	2.515	2.371	2.554	2.322
2.122	2.907	2.780	2.770	2.882	2.777	2.926	3.011	2.831	3.048	2.778

TABLE XVII. Results of potential-curve calculations for the  $X^2\Pi_1$  state of NO.

$r$ (Å)	RKR (ev)	Morse	Hulburt-Hirschfelder	Rydberg	Pöschl-Teller	Linnett	Varshni	Rosen-Morse	Lippincott	Frost-Musulin
0.929	4.582	5.116	5.031	4.876	5.149	5.018	4.689	4.907	4.734	5.166
0.949	3.774	4.015	3.937	3.847	4.035	3.934	3.712	3.868	3.767	4.049
0.982	2.485	2.586	2.530	2.496	2.596	2.535	2.422	2.505	2.392	2.599
1.026	1.246	1.282	1.257	1.251	1.286	1.260	1.223	1.258	1.242	1.289
1.113	0.118	0.120	0.119	0.119	0.118	0.117	0.118	0.111	0.118	0.121
1.210	0.118	0.113	0.114	0.114	0.111	0.112	0.115	0.113	0.112	0.112
1.360	1.246	1.188	1.232	1.217	1.187	1.233	1.251	1.198	1.252	1.189
1.486	2.485	2.319	2.440	2.394	2.316	2.469	2.488	2.340	2.518	2.324
1.623	3.774	3.427	3.626	3.552	3.424	3.743	3.713	3.472	3.776	3.442
1.725	4.582	4.109	4.342	4.260	4.106	4.563	4.459	4.156	4.525	4.131

TABLE XVIII. Results of potential-curve calculations for the  $B^2\Pi$  state of NO.

$r$ (Å)	RKR (ev)	Morse	Hulburt-Hirschfelder	Rydberg	Pöschl-Teller	Linnett	Varshni	Rosen-Morse	Lippincott	Frost-Musulin
1.130	2.184	2.32	2.22	2.21	2.33	2.33	2.15	2.22	2.17	2.35
1.188	1.258	1.29	1.24	1.25	1.30	1.29	1.22	1.25	1.23	1.31
1.239	0.681	0.70	0.67	0.68	0.70	0.70	0.66	0.68	0.67	0.70
1.356	0.064	0.064	0.063	0.064	0.065	0.064	0.063	0.064	0.063	0.063
1.488	0.064	0.063	0.064	0.064	0.063	0.064	0.064	0.064	0.064	0.062
1.690	0.681	0.63	0.67	0.65	0.63	0.65	0.67	0.64	0.67	0.63
1.831	1.258	1.12	1.21	1.16	1.12	1.17	1.20	1.14	1.21	1.12
1.962	1.793	1.54	1.67	1.60	1.54	1.63	1.66	1.57	1.69	1.54
2.068	2.184	1.84	2.00	1.91	1.84	1.97	1.99	1.88	2.03	1.84

percentage errors in the interaction energy  $V-D_e$  will be large in this region and that the various functions will retain, for the most part, the same relative performance.

The average percent errors for  $\alpha_e$  and  $\omega_e x_e$  shown in Table XXIV indicate that a good fit with the RKR

curves may sometimes mean a satisfactory prediction of  $\alpha_e$  and  $\omega_e x_e$ , but this is not general for all functions. For example, this seems to hold for the Linnett and Lippincott functions and to a lesser extent with the Rydberg function, but does not hold for the Varshni III function which gives good correlation with the RKR

TABLE XIX. Results of potential-curve calculations for  $X^2\Pi$ , state of OH.

$r$ (A)	RKR (ev)	Morse	Hulburt-Hirschfelder	Rydberg	Pöschl-Teller	Linnett	Varshni	Rosen-Morse	Lippincott	Frost-Musulin
0.702	3.478	3.348	3.550	3.194	3.479	3.931	3.352	3.065	3.182	3.579
0.731	2.580	2.477	2.590	2.377	2.553	2.831	2.469	2.299	2.379	2.618
0.777	1.495	1.442	1.482	1.397	1.473	1.589	1.432	1.364	1.403	1.501
0.831	0.672	0.657	0.666	0.643	0.666	0.699	0.651	0.633	0.646	0.674
1.179	0.672	0.668	0.674	0.682	0.664	0.641	0.685	0.682	0.691	0.657
1.329	1.495	1.452	1.482	1.497	1.444	1.379	1.518	1.500	1.541	1.423
1.538	2.580	2.449	2.523	2.538	2.438	2.332	2.601	2.537	2.649	2.398
1.760	3.478	3.235	3.337	3.351	3.224	3.115	3.455	3.337	3.493	3.179

TABLE XX. Results of potential-curve calculations for  $A^2\Sigma^+$  state of OH.

$r$ (A)	RKR (ev)	Morse	Hulburt-Hirschfelder	Rydberg	Pöschl-Teller	Linnett	Varshni	Rosen-Morse	Lippincott	Frost-Musulin
0.752	2.394	2.50	2.19	2.37	2.55	2.70	2.35	2.33	2.31	2.60
0.777	1.797	1.90	1.69	1.81	1.93	2.02	1.79	1.78	1.78	1.96
0.809	1.233	1.29	1.18	1.24	1.30	1.35	1.23	1.23	1.23	1.32
0.863	0.565	0.60	0.56	0.58	0.59	0.61	0.57	0.57	0.58	0.61
1.244	0.565	0.54	0.56	0.55	0.54	0.54	0.56	0.55	0.57	0.53
1.428	1.233	1.13	1.19	1.17	1.13	1.14	1.22	1.16	1.23	1.13
1.614	1.797	1.61	1.68	1.67	1.61	1.66	1.74	1.65	1.76	1.61
2.038	2.394	2.21	2.25	2.27	2.21	2.34	2.34	2.24	2.32	2.21

TABLE XXI. Results of potential-curve calculations for the  $X^1\Sigma^+$  state of HF.

$r$ (A)	RKR (ev)	Morse	Hulburt-Hirschfelder	Rydberg	Pöschl-Teller	Linnett	Varshni	Rosen-Morse	Lippincott	Frost-Musulin
0.623	5.987	5.190	6.015	4.935	5.530	6.578	5.471	4.616	4.930	5.724
0.639	5.079	4.462	5.104	4.258	4.724	5.539	4.667	4.004	4.267	4.879
0.662	3.951	3.549	3.988	3.404	3.722	4.285	3.678	3.225	3.423	3.838
0.716	2.092	1.938	2.100	1.877	1.999	2.210	1.974	1.804	1.893	2.045
0.786	0.745	0.699	0.729	0.685	0.710	0.751	0.703	0.666	0.690	0.721
1.115	0.745	0.772	0.755	0.788	0.766	0.730	0.783	0.795	0.794	0.755
1.317	2.092	2.116	2.074	2.184	2.099	1.962	2.188	2.208	2.240	2.055
1.633	3.951	3.873	3.848	4.015	3.852	3.609	4.086	4.033	4.167	3.767
1.922	5.079	4.870	4.876	5.030	4.855	4.618	5.154	5.026	5.180	4.770
2.555	5.987	5.796	5.811	5.894	5.791	5.695	5.982	5.870	5.935	5.749

TABLE XXII. Comparison of observed values of  $\omega_e x_e$  with calculated values for various functions.

Molecule	State	$\omega_e x_e$ (observed)	Morse	Rosen-Morse	Rydberg	Pöschl-Teller	Linnett	Frost-Musulin	Varshni	Lippincott
H <sub>2</sub>	$X^1\Sigma_g^+$	120.815	126.545	84.5915	116.00	126.545	197.73	148.78	178.49	117.71
I <sub>2</sub>	$X^1\Sigma_g^+$	0.6127	0.9165	0.9039	0.8402	0.9165	0.41521	0.87153	0.84863	0.7016
N <sub>2</sub>	$X^1\Sigma_g^+$	14.188	17.4126	15.8476	15.9616	17.4126	15.6394	17.389	17.748	13.810
	$A^2\Sigma_u^+$	13.851	17.9278	16.9588	16.4339	17.9278	13.2889	17.527	17.595	13.994
	$a^1\Pi_g$	13.825	14.6494	13.3998	13.4287	14.6494	12.9074	14.591	14.864	11.595
	$B^3\Pi_g$	15.198	19.0633	17.8997	17.4748	19.0633	14.626	18.690	18.814	14.913
O <sub>2</sub>	$X^3\Sigma_g^-$	12.0730	14.8517	13.7959	13.6141	14.8517	12.240	14.676	14.850	11.682
	$B^3\Sigma_u^-$	8.0023	15.1264	14.7357	13.8659	15.1264	8.5264	14.475	14.362	11.653
	$A^2\Sigma_u^+$	13.81	24.1387	23.861	22.1272	24.1387	10.310	18.293	22.476	18.453
CO	$X^1\Sigma^+$	13.295	12.9777	11.3698	11.8963	12.9777	13.099	13.227	13.684	10.458
	$d^3\Delta$	7.624	11.4141	10.4383	10.4630	11.4141	10.060	11.369	11.582	9.0343
	$A^1\Pi$	17.2505	22.4280	21.4432	20.5591	22.4280	15.393	21.762	21.758	17.429
	$e^2\Sigma^-$	9.578	11.7890	10.8218	10.8066	11.7890	10.240	11.654	11.922	9.3178
	$a^3\Sigma^+$	11.0130	10.8575	9.7597	9.9527	10.8575	10.115	10.904	11.172	8.6483
NO	$X^2\Pi_1$	13.97	17.0042	15.7364	15.5872	17.0042	14.242	16.827	17.059	13.394
	$B^2\Pi$	7.603	10.1253	9.3063	9.2816	10.1253	8.7464	10.057	10.277	7.9991
OH	$X^2\Pi_1$	82.665	93.4369	77.545	85.6508	93.4369	105.76	98.429	103.22	77.162
	$A^2\Sigma^+$	113.85	125.642	111.419	115.172	125.642	122.92	101.81	131.39	100.75
HF	$X^1\Sigma^+$	88.726	86.8172	69.418	79.5827	86.8172	104.49	91.293	98.993	72.974

TABLE XXIII. Comparison of observed values of  $\alpha_e$  with calculated values for various functions.

Mole- cule	State	$\alpha_e$ (observed)	Morse	Rosen- Morse	Rydberg	Pöschl- Teller	Linnett	Frost- Musulin	Varshni	Lippincott
H <sub>2</sub>	X <sup>1</sup> Σ <sub>g</sub> <sup>+</sup>	3.0177	2.2319	0.9074	1.8156	3.0936	5.4483	3.5831	4.1481	2.7053
I <sub>2</sub>	X <sup>1</sup> Σ <sub>g</sub> <sup>+</sup>	0.0001208	0.000154	0.00015	0.000143	0.000154	0.000092	0.001482	0.000131	0.0001334
N <sub>2</sub>	X <sup>1</sup> Σ <sub>g</sub> <sup>+</sup>	0.0171	0.01983	0.01846	0.01812	0.02000	0.01939	0.02020	0.01656	0.01743
	A <sup>3</sup> Σ <sub>u</sub> <sup>+</sup>	0.01798	0.02182	0.02099	0.02007	0.02187	0.01827	0.02161	0.01808	0.01904
O <sub>2</sub>	a <sup>1</sup> Π <sub>g</sub>	0.0183	0.01863	0.01742	0.01703	0.01876	0.01791	0.01890	0.01552	0.01635
	B <sup>3</sup> Π <sub>g</sub>	0.01794	0.02236	0.02141	0.02055	0.02243	0.01922	0.02222	0.01852	0.01953
	X <sup>3</sup> Σ <sub>g</sub> <sup>-</sup>	0.01579	0.01749	0.01658	0.01604	0.01758	0.01591	0.01756	0.01451	0.01532
	B <sup>3</sup> Σ <sub>g</sub> <sup>-</sup>	0.011	0.01894	0.01863	0.01753	0.01896	0.01308	0.01835	0.01587	0.01644
	A <sup>3</sup> Σ <sub>u</sub> <sup>+</sup>	0.0165	0.02590	0.02572	0.02406	0.02591	0.01496	0.02485	0.02208	0.0224
CO	X <sup>1</sup> Σ <sup>+</sup>	0.0175	0.01642	0.01471	0.01489	0.01672	0.01796	0.01724	0.01406	0.01452
	a <sup>3</sup> Δ	0.0170	0.01685	0.01575	0.01540	0.01697	0.015286	0.01709	0.01403	0.01479
	A <sup>1</sup> Π	0.02229	0.02807	0.02723	0.02588	0.02811	0.02222	0.02760	0.02330	0.02445
	e <sup>3</sup> Σ <sup>-</sup>	0.0179	0.01803	0.01692	0.01650	0.01815	0.01713	0.01825	0.01501	0.01582
	a <sup>3</sup> Σ <sup>+</sup>	0.01872	0.01624	0.01497	0.01481	0.01641	0.01641	0.01667	0.01363	0.01429
NO	X <sup>2</sup> Π <sub>1/2</sub>	0.01781	0.01976	0.01867	0.01810	0.01986	0.01821	0.01987	0.01640	0.01731
	B <sup>2</sup> Π	0.0116	0.013851	0.01300	0.01267	0.01394	0.01309	0.01400	0.01152	0.01215
OH	X <sup>2</sup> Π <sub>1/2</sub>	0.708	0.70089	0.5881	0.6281	0.7310	0.8806	0.7781	0.6429	0.6269
	A <sup>2</sup> Σ <sup>+</sup>	0.7868	0.9539	0.8657	0.8671	0.9681	1.01068	0.9920	0.8091	0.8422
HF	X <sup>1</sup> Σ <sup>+</sup>	0.7888	0.6590	0.5226	0.5850	0.7040	1.10725	0.7501	0.6478	0.5946

TABLE XXIV. Average error (%) for the quantities  $\omega_e x_e$ ,  $\alpha_e$ ,  $[|V_{\text{RKR}} - V|/D_e]_{\text{all}}$ , and  $[|V_{\text{RKR}} - V|/D_e]_{r > r_e}$  for various potential functions.

	Morse	Hulburt- Hirschfelder	Rosen- Morse	Rydberg	Pöschl- Teller	Linnett	Frost- Musulin	Varshni	Lippincott
$\omega_e x_e$	26.93	...	21.24	19.71	26.93	14.94	24.29	28.94	12.18
$\alpha_e$	19.67	...	22.33	17.45	18.47	15.55	23.55	15.57	13.80
$[ V_{\text{RKR}} - V /D_e]_{\text{all}}$	3.68	1.51	3.71	2.94	3.48	4.18	3.41	2.28	2.17
$[ V_{\text{RKR}} - V /D_e]_{r > r_e}$	3.20	1.44	2.80	2.27	3.28	5.07	3.30	1.68	1.44

curves but is the poorest of all functions in predicting  $\omega_e x_e$ . This latter function would then be a poor one to predict dissociation values using  $r_e$ ,  $\omega_e$ , and  $\omega_e x_e$ . On the other hand, a study of Tables III to XXI shows that a function which predicts good values of  $\omega_e x_e$  and  $\alpha_e$  does not necessarily show good agreement with the RKR results. This is particularly true of the Linnett function.

We can summarize as follows. The Hulburt-Hirschfelder curve, being a five-parameter function, gives the best average results and in general gives the best or near the best fit of the potential for all the cases studied. However, for values of  $r > r_e$ , the Lippincott function gives equally good results. The Morse-Rosen-Morse and the Pöschl-Teller give very similar results. The Linnett curve ( $m=3$ ) gives good predictions for  $\omega_e x_e$  and  $\alpha_e$  for many states, and, in general, gives a good representation of the RKR curves for these same states. Nevertheless, its average performance is the worst and in many cases it predicts maxima in a potential curve where none exist or are expected to exist. The Frost-Musulin potential does not give any appreciable improvement over the Morse curve, whereas the Rydberg potential is a distinct improvement. The Varshni III and Lippincott functions, the best of the three-parameter functions in fitting the RKR results, both give good predictions of  $\alpha_e$ . On the other hand, the

Lippincott function gives fairly reliable predictions of  $\omega_e x_e$  (or  $D_e$  from  $\omega_e x_e$ ), while the Varshni III function does not.

#### DISCUSSION

It is desirable to investigate the possibility that an empirical function can be proposed which will yield curves for any state of any molecule to an accuracy of less than 1% in bond-dissociation energy. There seem to be two justifiable approaches to this problem. One is to consider the expressions for  $E$  obtained from quantum-mechanical calculations of potential curves for various diatomic molecules. If these expressions were similar for the various states of different molecules, then presumably one could arrive at suitable potential forms which would have some basis in fact. Unfortunately, in order to obtain reliable values of  $E_e$  for even the simplest systems, one has to use 40- and 50-term wave functions<sup>2</sup> which yield very complicated expressions for  $E_e$ . There does not seem to be any chance of obtaining a suitable potential form from this approach.

A second approach is to consider the relatively simple expression for the vibrational- and rotational-energy levels of a diatomic molecule, Eq. (6). It is well known<sup>30</sup>

<sup>30</sup> G. Herzberg, *Spectra of Diatomic Molecules* (D. Van Nostrand Company, Inc., Princeton, New Jersey, 1950).

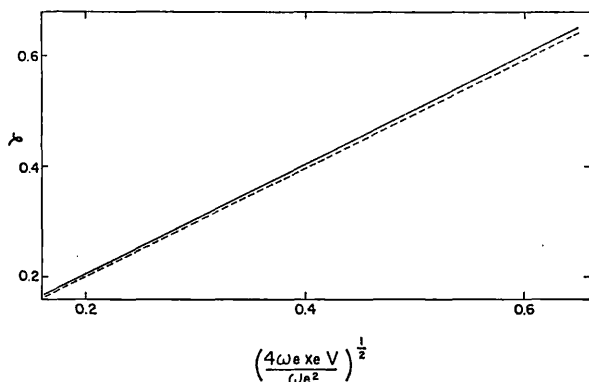


FIG. 1.  $\gamma = \tanh[(\omega_e x_e / B_e)^{1/2} (r_2 - r_1) / 2r_e]$  plotted against  $(4\omega_e x_e V / \omega_e^2)^{1/2}$ . The solid line corresponds to the  $X^1\Sigma_g^+$  state of  $N_2$ ; the dashed line corresponds to the  $a'^3\Sigma^+$  state of CO.

that, for many molecules, the first few terms in this equation are sufficient to fit the observed data within reasonable limits. The equation then reduces to the simple form

$$E_{vJ} = \omega_e(v + \frac{1}{2}) - \omega_e x_e(v + \frac{1}{2})^2 + B_e J(J+1) - \alpha_e J(J+1)(v + \frac{1}{2}). \quad (19)$$

In such a case, Rees<sup>6</sup> has shown that the potential

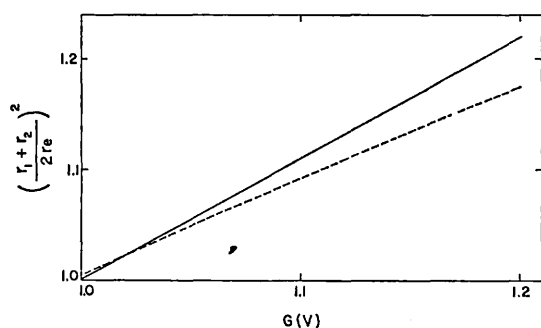


FIG. 2.  $[(r_1 + r_2) / 2r_e]^2$  vs  $G(V)$ . The solid line corresponds to the  $X^1\Sigma_g^+$  state of  $N_2$ ; the dashed line corresponds to the  $a'^3\Sigma^+$  state of CO.

curve can be obtained from the expressions

$$2f = (r_2 - r_1) = (B_e / \omega_e x_e)^{1/2} \ln W \quad (20)$$

$$2g = (1/r_1 - 1/r_2) = [1/B_e(\omega_e x_e)^3]^{1/2} (\omega_e / r_e)$$

$$\times \left[ \alpha_e (4\omega_e x_e V / \omega_e^2)^{1/2} + \left( 2 \frac{\omega_e x_e}{\omega_e} B_e - \alpha_e \right) \ln W \right] \quad (21)$$

$$W = (1 - 4\omega_e x_e V / \omega_e^2)^{1/2} / [1 - (4\omega_e x_e V / \omega_e^2)^{1/2}]. \quad (22)$$

Here,  $r_1$  and  $r_2$  are minimum and maximum points of the vibration. If  $\omega_e$ ,  $\omega_e x_e$ ,  $B_e$ ,  $\alpha_e$  are known, then  $r_1$  and  $r_2$  can be obtained for any  $V$  from the expression (20) and the following

$$(r_1 + r_2) / 2 = (f/g + f^2)^{1/2}. \quad (23)$$

Presumably, one could use Eqs. (20) and (23) as a

basis for an empirical potential curve for "well-behaved" molecular states whose energy levels are given by Eq. (19). First, let us put (20) in a more convenient form. By expanding the logarithms of the numerator and denominator of  $W$ , it is easy to show that  $\ln W = \tanh^{-1}(4\omega_e x_e V / \omega_e^2)$ , and, hence,

$$(4\omega_e x_e V / \omega_e^2)^{1/2} = \tanh(\omega_e x_e / B_e)^{1/2} (r_2 - r_1) / 2r_e. \quad (24)$$

Equation (23), which gives the average value of  $r$ , cannot be written in simpler form. It is possible to sidestep this problem by taking  $B_v$ , which is equal<sup>30</sup> to

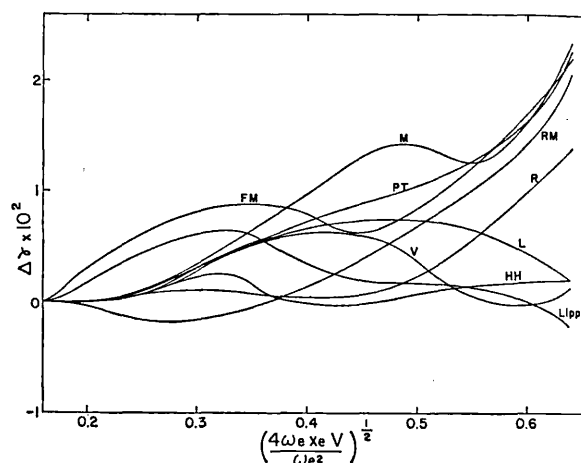


FIG. 3.  $\gamma - \gamma_{RKR}$  vs  $(4\omega_e x_e V / \omega_e^2)^{1/2}$  for the various potential functions. The meaning of the symbols is as follows:

M = Morse	L = Linnett
FM = Frost-Musulin	HH = Hulburt-Hirschfelder
RM = Rosen-Morse	V = Varshni
PT = Pöschl-Teller	Lipp = Lippincott
R = Rydberg	

$B_e r_e^2 / r^2$ , to be a measure of  $[(r_1 + r_2) / 2]^2$ . If this is so, then,

$$[(r_1 + r_2) / 2]^2 = B_e r_e^2 / B_v = B_e r_e^2 / [B_e - \alpha_e(v + \frac{1}{2})]. \quad (25)$$

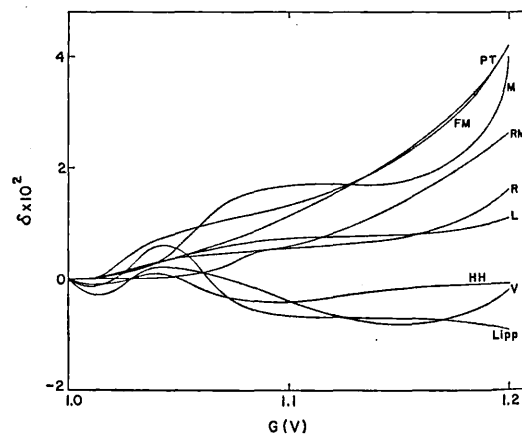


FIG. 4.  $\delta = [(r_1 + r_2) / 2r_e]^2 - [(r_1 + r_2) / 2r_e]_{RKR}^2$  vs  $G(V)$  for the various potential functions. Symbols are as in Fig. 3.

This can be written in terms of  $\omega_e$ ,  $\omega_e x_e$  and  $V$  to get

$$\left[ \frac{r_1+r_2}{2r_e} \right]^2 = 1 / \left[ 1 - (\alpha_e \omega_e / 2B_e \omega_e x_e) + \{ (\alpha_e \omega_e / 2B_e \omega_e x_e)^2 - \alpha_e^2 V / B_e^2 \omega_e x_e \}^{\frac{1}{2}} \right] = G(V). \quad (26)$$

Hence, for a molecule whose energy levels are given by Eq. (19), plots of

$$(4\omega_e x_e V / \omega_e^2)^{\frac{1}{2}} \text{ vs } \tanh(\omega_e x_e / B_e)^{\frac{1}{2}} (r_2 - r_1) / 2r_e$$

and

$$\left[ \frac{r_1+r_2}{2r_e} \right]^2 \text{ vs } G(V)$$

should be straight lines with a slope of unity. Figures 1 and 2 show such plots. The solid lines are the results for the ground state of  $N_2$  whose energy levels can be reasonably expressed by an expression of the form (19). The slopes, although close to unity, are not quite 1 since the  $\omega_e$ ,  $\omega_e x_e$ ,  $B_e$ , and  $\alpha_e$  used were determined from data at the lower-vibrational levels and not from the complete range of data.

It is now possible to compare the deviations of the proposed empirical potential functions from the experimental curves in a different manner. In Figs. 3 and 4 are plotted for each empirical function the differences of  $\tanh(\omega_e x_e / B_e)^{\frac{1}{2}} (r_2 - r_1) / 2r_e$  and  $\left[ \frac{r_1+r_2}{2r_e} \right]^2$  from the experimental values for the  $X^1\Sigma_g^+$  state of  $N_2$  as a function of  $(4\omega_e x_e V / \omega_e^2)^{\frac{1}{2}}$  and  $G(V)$ , respectively. In general, the various functions show the same relative deviations from the width of the potential bowl and the midpoint of the vibration as they show for errors in the quantities  $|V - V_{\text{RKR}}|$ ,  $\omega_e x_e$ , and  $\alpha_e$ . All of the proposed empirical functions considered predict too wide a bowl for the potential curve. The empirical curves generally give too large a value for the midpoint of the vibrations. The exceptions to this last point are the Varshni, Hulburt-Hirschfelder, and Lippincott functions. The Hulburt-Hirschfelder potential curve gives the best predictions of bowl width and midpoint of vibration. This is in agreement with the fact that this

potential gives the best reproduction of the RKR curves. The Varshni and Lippincott functions predict too large a bowl and too small a value for the midpoint. The deviations are relatively small, and the net result appears to be that these errors cancel somewhat so that these two functions give the next best average performance. For all others, the predicted bowl is too large and the midpoint is shifted to larger values, leading to poorer average performance.

The above conclusions are based, of course, only on the  $X^1\Sigma_g^+$  state of  $N_2$ . However similar results should follow for any state with energy levels represented by Eq. (19). It would seem that the least one could expect from any empirical function proposed in the future would be reliable predictions for "well-behaved" states like the ground states of  $N_2$ ,  $O_2$ ,  $I_2$ , and  $H_2$ .

It may be possible to generate reliable potential curves by using equations similar to (24) and (26). Since these are in reduced units, all well-behaved molecular states should give nearly the same plots as the ground states of  $N_2$  shown in Figs. 1 and 2. As a check, the  $a'^3\Sigma^+$  state of CO was chosen at random and similar plots were made. These are shown as the dashed lines in the figures. As one can see, particularly from Fig. 2, large errors could be made in the calculations of the potential curve for the  $a'^3\Sigma^+$  state of CO if the solid lines were chosen as the standard curves.

In summary then, the comparison of empirical potential functions given here indicates that the better 3-parameter functions can be expected to give potential curves with an average error of 2 to 3% in  $|V - V_{\text{RKR}}| / D_e$ , whereas the better 5-parameter functions should give average error of from 1 to 2%. It does not seem likely that any substantial improvement (errors of less than 1%) can be made by suggesting new functions which have no theoretical or experimental basis. The task of giving a satisfactory theoretical or experimental foundation for any empirical function appears difficult indeed.

On the dissociation products of  $C_2$ 

D. STEELE

Department of Chemistry, University College, Swansea†

(Received 11 August 1962)

**Abstract**—By fitting Lippincott potential curves to known potential curves the dissociation energies of the corresponding states can be estimated. These estimated values allow the states of the dissociated atoms to be determined. In certain cases it is found that the R.K.R.V. curves cannot be expressed by Lippincott potentials. When this is so, the deviations may be explained by regarding the true potential curve as perturbed by further electronic energy levels of the same symmetry. The states of the dissociated atoms of all known states of  $C_2$  have been deduced and the curves shown to be compatible with a ground-state dissociation energy of  $6.1 \pm 0.3$  eV.

THE potential function of LIPPINCOTT in the modified form [1, 2]

$$V(r) = D_e[1 - \exp(-n\Delta r^2/2r)][1 + a(b^2n/2r)^{1/2} \Delta r \exp\{-(b^2n/2r_e)^{1/2} \Delta r\}] \quad (1)$$

has been shown to reproduce, within reasonable limits, the known potential curves of a wide range of diatomic molecules [2]. The average discrepancy between the potential curves as evaluated using (1) and as evaluated by the method of RYDBERG *et al.* (R.K.R.V. method [3]) was 2.2 per cent of  $D_e$  over the known range of potential curves as given by the latter technique [4]. For  $r > r_e$  the discrepancy is considerably less, averaging 1.4 per cent.

The function is basically a five-parameter function. However, "b" is a good constant for all molecules (= 1.065) thus the parameters may be reduced to four— $D_e$ ,  $r_e$ ,  $n$  and  $a$ . These parameters are related to the vibrational frequency,  $\omega_e$ , the anharmonicity,  $\omega_e X_e$  and the vibrational rotational coupling constant,  $\alpha_e$ , by the equations (2–4)

$$n = \frac{k_e r_e}{D_e} \quad \text{where} \quad k_e = 4\pi^2 c^2 \omega_e^2 \mu \quad (2)$$

$$a = F/b \Delta^{1/2} \quad \text{where} \quad F = \alpha_e \omega_e / 6B_e^2 \quad (3)$$

and  $\Delta = k_e r_e^2 / 2D_e$

$$G = 12 \left[ \frac{1}{4} + F \right] + 12F^2 \left[ \frac{1}{2} a^2 b^2 + \frac{3}{4} - \frac{1}{a} \right]$$

where

$$G = 8\omega_e X_e / B_e \quad (4)$$

† Present address: Dept. of Chemistry, Royal Holloway College, Englefield Green, Surrey.

[1] E. R. LIPPINCOTT, *J. Chem. Phys.* **21**, 2070 (1953); E. R. LIPPINCOTT and R. SCHROEDER, *Ibid.* **23**, 1131 (1955).

[2] D. STEELE and E. R. LIPPINCOTT, *J. Chem. Phys.* **35**, 2065 (1961).

[3] J. T. VANDERSLICE, E. A. MASON, W. G. MAISCH and E. R. LIPPINCOTT, *J. Mol. Spect.* **3**, 17 (1959) and earlier references therein.

[4] D. STEELE, J. T. VANDERSLICE and E. R. LIPPINCOTT, *Revs. Mod. Phys.* **34**, 239 (1962).



$r_e$ ,  $D_e$ ,  $\mu$  and  $B_e$  have their usual meanings. By using (2) to (4) the potential curve can be calculated using four of the five experimentally determined constants,  $r_e$ ,  $\omega_e X_e$ ,  $\alpha_e$ ,  $\omega_e$  and  $D_e$ .

In a previous publication [2] additional relationships were derived by equating two forms of the Lippincott function. These forms, though they led to very different algebraic expressions for  $D_e$  gave essentially the same answers, especially where the spectroscopic data were known to be reliable. This led to (5) and (6)

$$a = F/(1 + \frac{5}{4}F) \quad (5)$$

$$G/3 = 1 + 2[1 + \frac{5}{4}F]^2/b^2 \quad (6)$$

These relationships effectively reduce (1) to a three-parameter function. The pleasing agreement between potential curves evaluated using this three-parameter form and the "true" R.K.R.V. curves suggests that a reasonable estimate of a dissociation energy may be deduced by fitting the potential curve of the corresponding state to the R.K.R.V. curve utilizing the appropriate  $r_e$  and  $\omega_e$  only. This can be utilized in two ways. Firstly, the ground-state dissociation energy,  $D_e$ , can be determined if the dissociation products of the state considered are known. Alternatively, knowing  $D_e$ , the atomic excitation energies of the separated atoms may be estimated. Comparison of the estimated sum of the excitation energies with those of allowed dissociation products may then establish the states of the separated atoms.

There has been considerable interest recently in the spectra and potential curves of  $C_2$  [5-9]. The evidence for the value of the ground-state dissociation energy of this molecule has been conflicting, and only recently has it been established as  $6.29 \pm 0.2$  eV [6] despite a considerable amount of spectroscopic data on the various excited states. In general the dissociation products of the excited states have not yet been established. Consequently there is ample justification for a further study of  $C_2$  using the technique described above.

The potential curves of several states of  $C_2$  have been evaluated by JARMAN [8] and by READ and VANDERSLICE [9]. The former work is restricted to the  $X^3\Pi_u$ ,  $A^3\Pi_g$ ,  $B^3\Pi_g$  and  $c^1\Pi_g$  states whereas the latter is for all nine states for which sufficient spectroscopic data has been established. The agreement between the two sets of results is excellent. Consequently all quoted "true potential energies" will refer to those taken from the more complete work.

This work was commenced before the publication of BREWER *et al.* [6] which seems to establish finally the dissociation energy as  $6.36 (\pm 0.2)$  eV above the potential minimum of the  $1^1\Sigma_g^+$  state, or  $6.29 (\pm 0.2)$  eV above the lowest of the  $3^1\Pi_u$  states. Potential curves were calculated for three values of  $D_e$  (6.2, 5.9 and 5.6 eV) in an effort to establish the correct value. The significance of these results will be

[5] E. A. BALLIK and D. A. RAMSAY, *J. Chem. Phys.* **31**, 1128 (1959).

[6] L. BREWER, W. T. HICKS and O. H. KRICKORIAN, *J. Chem. Phys.* **36**, 182 (1962).

[7] E. CLEMENTI and K. S. PITZER, *J. Chem. Phys.* **32**, 656 (1960).

[8] W. R. JARMAN, *Transition Probabilities of Molecular Band Systems XX*. The University of Western Ontario, Department of Physics Report, 1 July (1961).

[9] S. M. READ and J. T. VANDERSLICE, *J. Chem. Phys.* **36**, 2366 (1962).

discussed later. The source of values of  $\omega_e X_e$ ,  $r_e$  and  $\omega_e$  for each state is indicated at the foot of Table 1. For the excited-state calculations the dissociation energies were taken to be given by

$$D_e^* = D_e(X) + \Delta - T_e \quad (7)$$

where  $D_e^*$  and  $D_e(X)$  are the dissociation energies of the excited and ground states respectively,  $T_e$  is the electronic energy of the excited state and  $\Delta$  is the sum of the atomic excitation energies. Various plausible sets of dissociation products were considered for each state and the appropriate potential curve evaluated. Although it has now been established that the potential minimum of the  $a^1\Sigma_g^+$  state lies below that of the lowest  $^3\Pi_u$  [17], the latter is referred to as the  $X$  state throughout this publication to avoid confusion with previous work.

Initially the curves were evaluated using the four-parameter form of the function. As is evident in Table 1, the calculated potential curves for values of  $|r| < r_e/4$  are quite insensitive to the assumed values of  $D_e^*$ . This is understandable from a cursory examination of the power series expansion of (1) in terms of  $\Delta r$ .

$$\begin{aligned} V(r) &= D_e \left( \frac{nr_e}{2} \right) \frac{\Delta r^2}{r_e^2} \left\{ 1 - \left[ 1 + ab \left( \frac{nr_e}{2} \right)^{1/2} \right] \frac{\Delta r}{r_e} + \dots \right\} \\ &= \frac{\omega_e^2 \Delta r^2}{4B_e r_e^2} \left\{ 1 - \left[ 1 + \frac{F}{(hc)^{1/2}} \right] \frac{\Delta r}{r_e} + \dots \right\} \end{aligned} \quad (8)$$

using (2) and (3)

The agreement between the calculated curves and the R.K.R.V. curves is very satisfactory for the  $X^3\Pi_u$ ,  $b^1\Pi_u$  and  $a^1\Sigma_g^+$  states. For the  $c^1\Pi_g$  state the agreement is good for  $r < r_e$ , but very poor for  $r > 1.4 \text{ \AA}$ . At  $r = 1.62 \text{ \AA}$  the calculated potential is twice as great as the observed. It is difficult to believe that the variation of potential energy with inter-nuclear distance in this state is so radically different from the variation in the other states mentioned above. An alternative and much more acceptable explanation is that the associated molecular wave functions change in character due to resonance interaction with those of another state of the same symmetry. Such an interaction must result in a lower potential energy for the lower state, of which the  $c^1\Pi_g$  is an example. This hypothesis is supported by the fact that the vibrational and rotational levels cannot be described by simple power-series expansions in  $v$  and  $J$  [14].

In the three-parameter form of (1)  $n$  is not dependent on  $D_e$  and consequently the insensitivity of the calculated potential to the assumed value of  $D_e$  is removed. The parameters "a" can be evaluated in several ways. It has been shown previously [2] that the "a" of excited states ( $a^*$ ) are related to the ground state "a",  $a(x)$ , by empirical relationships

$$a^* = 0.8 \left[ 1 - \frac{(\omega_e r_e^{7/4})^*}{(\omega_e r_e^{7/4})_x} a(x) \right] \quad (9)$$

In the calculations to be described  $a(x)$  was taken to have the value given by equation (3) and the excited state "a" evaluated from  $a(x)$  by the use of (9). The uncertainty

Table 1. Calculations using four parameter form.

	$r$ (Å)	$V_r$ (eV)			$V_{R.K.R.V.}$
		$D_e(x) = 6.2$ eV	$=5.9$ eV	$=5.6$ eV	
$X^3\Pi_u$ ( $^3P + ^3P$ )	1.091	2.3287	2.3232	2.3170	2.3168
	1.208	0.3988	0.3939	0.3983	0.4011
	1.257	0.1000	0.0999	0.0997	0.1014
	1.374	0.0961	0.1016	0.1059	0.1014
	1.425	0.3042	0.3034	0.3037	0.3020
	1.479	0.5762	0.5763	0.5747	0.5973
	1.539	0.9889	0.9861	0.9833	0.9810
	1.592	1.3669	1.3612	1.3568	1.3532
	1.642	1.7405	1.7275	1.7167	1.7138
	1.726	2.3626	2.3412	2.3220	2.3168
$b^1\Pi_u$ ( $^3P + ^3P$ )	1.157	1.0458	1.0439	1.0421	1.0513
	1.203	0.4830	0.4825	0.4818	0.4891
	1.263	0.0969	0.0971	0.0972	0.0993
	1.381	0.0996	0.0993	0.0996	0.0993
	1.471	0.4909	0.4902	0.4893	0.4891
	1.505	0.6869	0.6852	0.6832	0.6795
	1.563	1.0564	1.0516	1.0461	1.0513
$a^1\Sigma_g^+$ ( $^3P + ^3P$ )	1.134	0.5672	0.5667	0.5654	0.5642
	1.156	0.3405	0.3416	0.3415	0.3412
	1.190	0.1159	0.1161	0.1164	0.1146
	1.301	0.1157	0.1157	0.1173	0.1146
	1.349	0.3457	0.3454	0.3449	0.3412
	1.384	0.5669	0.5662	0.5654	0.5642
$c^1\Pi_g$ ( $^1S + ^1D$ )	1.103	1.2201	1.2180	1.2158	1.2013
	1.132	0.7475	0.7469	0.7460	0.7396
	1.202	0.1189	0.1184	0.1184	0.1116
	1.313	0.1091	0.1093	0.1093	0.1116
	1.365	0.3528	0.3526	0.3523	0.3303
	1.444	0.8863	0.8841	0.8818	0.7396
	1.621	2.3391	2.3159	2.2898	1.2013

(Assumed dissociation products)

Sources of spectroscopic data.  $X^3\Pi_u$ ,  $A^3\Pi_g$  Ref. [10];  $B^3\Pi_g$  Ref. [11];  $b^1\Pi_u$ ,  $a^1\Sigma_g^+$  Ref. [12];  $d^1\Sigma_u^+$  Ref. [13];  $c^1\Pi_g$  Ref. [14];  $e^1\Sigma_g^+$  Ref. [15];  $v^3\Sigma_g^-$  Ref. [16].[10] J. G. PHILLIPS, *Astrophys. J.* **108**, 434 (1948).[11] J. G. PHILLIPS, *Astrophys. J.* **110**, 73 (1949).[12] J. G. PHILLIPS, *Astrophys. J.* **107**, 389 (1948).[13] O. G. LANDSVERK, *Phys. Rev.* **56**, 769 (1939).[14] G. HERZBERG and R. B. SUTTON, *Can. J. Res.* **A18**, 74 (1940).[15] V. H. FREYMARK, *Ann. Phys. (Leipzig)* **8**, 221 (1951).[16] E. A. BALLIK and D. A. RAMSAY, *J. Chem. Phys.* **29**, 1418 (1958).[17] E. A. BALLIK and D. A. RAMSAY, *J. Chem. Phys.* **31**, 1128 (1959).

Table 2. Calculations using two-parameter forms

	$r$ (Å)	$V_r$ (eV)			$V_{R.K.R.V.}$
		$D_e(x) = 6.2 \text{ eV}$	$= 5.9 \text{ eV}$	$= 5.6 \text{ eV}$	
$X^3\Pi_u$ ( $^3P + ^3P$ )	1.091	2.473	2.353	2.233	
	1.374	0.108	0.103	0.098	0.1014
	1.445	0.431	0.410	0.389	0.4011
	1.539	1.050	0.999	0.948	0.9810
	1.592	1.448	1.372	1.303	1.353
	1.642	1.837	1.749	1.662	1.714
	1.726	2.488	2.368	2.247	2.317
$b^1\Pi_u$ ( $^3P + ^3P$ )	1.157	0.994	0.937	0.880	1.051
	1.203	0.459	0.432	0.406	0.489
	1.263	0.092	0.087	0.082	0.099
	1.381	0.094	0.089	0.084	0.099
	1.471	0.467	0.440	0.415	0.489
	1.505	0.654	0.617	0.579	0.680
	1.563	1.007	0.949	0.892	1.051
$A^3\Pi_g$ ( $^3P + ^3P$ )	1.074	1.263	1.164	1.064	2.001
	1.087	0.956	0.881	0.806	1.688
	1.125	0.544	0.501	0.458	0.951
$A^3\Pi_g$ ( $^3P + ^3P$ )	1.156	0.308	0.284	0.260	0.541
	1.212	0.065	0.060	0.055	0.110
	1.325	0.061	0.056	0.051	0.110
	1.412	0.313	0.289	0.264	0.541
	1.476	0.572	0.527	0.482	0.951
	1.537	0.849	0.782	0.715	1.335
	1.602	1.159	1.067	0.976	1.688
1.675	1.504	1.386	1.267	2.001	
$a^1\Sigma_g^+$ ( $^3P + ^3P$ )	1.134	0.502	0.476	0.454	0.564
	1.156	0.303	0.289	0.274	0.341
	1.190	0.130	0.098	0.093	0.115
	1.301	0.103	0.098	0.093	0.115
	1.349	0.307	0.294	0.280	0.341
1.384	0.502	0.478	0.454	0.564	

introduced into the calculated potential by calculating "a" in this manner is not expected to be greater than 2 per cent of the dissociation energy or 5 per cent of the potential energy as measured from the potential minimum if this is the greater.

Assuming that the  $X^3\Pi_u$ , the  $b^1\Pi_u$ ,  $a^1\Sigma_g^+$  and the  $Y^3\Sigma_g^-$  states all dissociate into only  $2p^2\ ^3P$ , or ground state, carbon atoms, good agreement between the calculated and the R.K.R.V. potential curves is obtained taking  $D_e$  as about 6 eV above the potential minimum of the  $X^3\Pi_u$  state. If the accuracy of the calculated potentials is taken as  $\pm 5$  per cent, the dissociation energy of the ground state is  $5.8 \pm 0.3$ ,  $6.4 \pm 0.3$ ,  $6.8 \pm 0.3$  and  $5.6 \pm 0.3$  eV, respectively, for the four states. Whilst the spread of the values is well outside of the quoted 5 per cent accuracy, there can be

little doubt as to the correctness of a value of the dissociation energy of close to 6 eV. The average value is 6.1 eV. Furthermore, since the next lowest energy state of the isolated carbon atom is 1.26 eV above the  $^3P$  state, assuming that these states dissociate into other than  $^3P$  atoms will lead to a marked divergence between calculated and true potential curves.

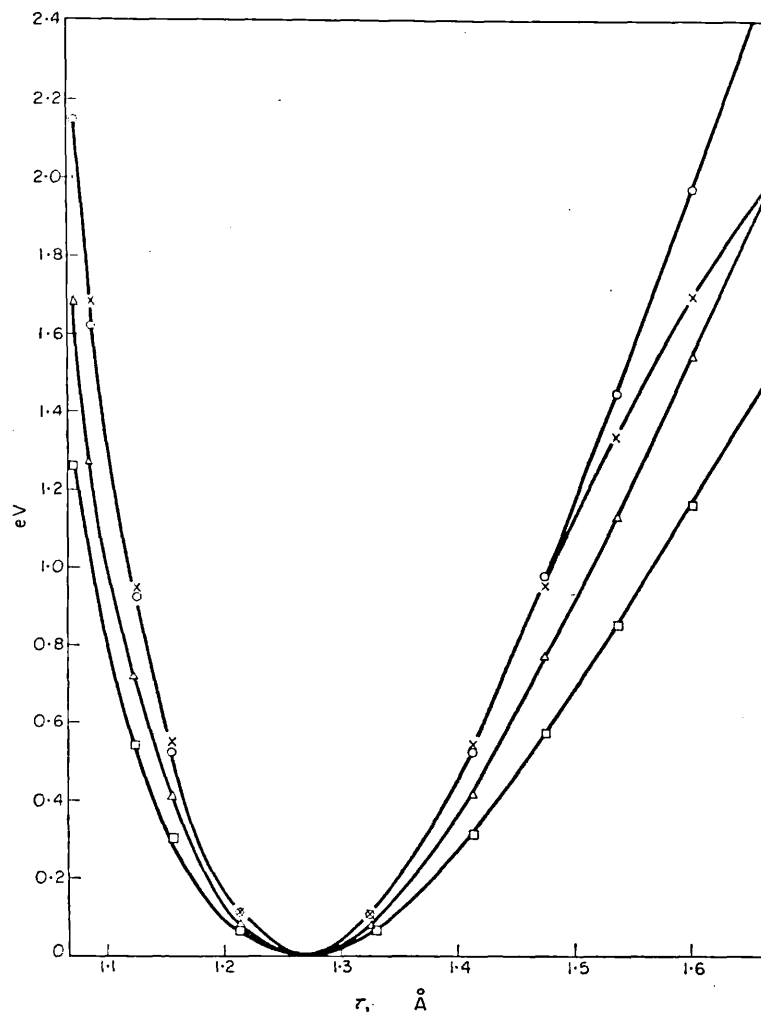
From the Wigner Witmer rules [18] the allowed dissociation products of lowest energy for a  $^1\Sigma_u^+$  state are  $2p^2\ ^1S + 2p^2\ ^1D$  and  $2p^2\ ^3P + 3s^3P$ . The sum of the excitation energies are 3.93 and 7.46 eV respectively. Consideration of each possibility in turn shows that the first pair is of too low an energy for the  $d\ ^1\Sigma_u^+$  state and that the latter products satisfactorily account for the observed potential curve. The calculated curve is somewhat above the R.K.R.V. curve. This may be due to mixing with one of the other  $^1\Sigma_u^+$  states and/or due to limitations in the simplified potential function. An alternative method of arriving at the preferred dissociation products is to deduce the value of the atomic excitation energies which gives agreement with the experimental curve. In this case it is 6.3, 6.1 and 6.1 eV for  $r = 1.297, 1.346$  and  $1.382\ \text{\AA}$ , respectively. The nearest possible values is 7.45 eV ( $2p^2\ ^3P + 3s^3P$ ).

None of the remaining four potential curves can be satisfactorily accounted for by any one assumed dissociation energy. This is shown for the  $A^3\Pi_g$  state in Fig. 1. In all of these cases neither could the vibrational nor the rotational terms be fitted to simple power-series expansions. Thus for the  $A^3\Pi_g$  state the first four vibrational terms and the first four rotational terms may be expressed as a linear function of  $v$ , but if one tries to include terms deduced from the tail bands, it is found that as many terms are needed in the expansion as there are constants to be expressed [10]. Such a marked change in the character of the binding with an increase in  $r$  as this implies, can be explained reasonably only if one assumes some form of perturbation such as is inherent in the non-crossing rule. This change in character as  $r$  increases will generally result in sudden departures to lower energy values since, in general one is dealing with the lower energy states. Another state must be raised simultaneously in energy, but no case is known where any data is available for this upper state.

Once the calculated curve deviates from the experimental, the true potential energy can be assumed to be intermediate between the calculated energies for two sets of allowed dissociation products. This approximation is valid only for small deviations from the initial curve due to changes in the hypothetical zero-order vibrational frequency and bond length for the modified wave function. As can be seen from Table 3 the isolated atom wave functions for the  $A^3\Pi_g$ ,  $B^3\Pi_g$ ,  $c^1\Pi_g$  and  $e^1\Sigma_g^+$  states are those of the  $2p^2\ ^3P + 2p^2\ ^1S$ ,  $2p^2\ ^3P + 2p^2\ ^1D$ ,  $2p^2\ ^1D + 2p^2\ ^1S$  and  $2p^2\ ^1S + 2p^2\ ^1S$  configurations, respectively, for small deviations from the equilibrium inter-nuclear distance.

It has been pointed out that there is little hope of finding a potential function which will reproduce known potential curves to better than 1 per cent of  $D_e$  on the average [4]. It is clear from the above that even such an accuracy cannot be possible generally for excited states due to changes in the isolated atom wave functions with changes in bond length. Rather, large deviations may well imply that there is a

[18] E. WIGNER and E. E. WITMER. *Z. Physik.* **51**, 859 (1928); G. HERZBERG *Spectra of Diatomic Molecules* pp. 315–322. Van Nostrand, New York.

Fig. 1. Potential curves of the  $A^3\Pi_u$  state

- × R.K.R.V.
- $^3P + ^3P$
- △  $^3P + ^1D$
- $^3P + ^1S$

perturbation to the electronic state under consideration. Furthermore, the values of higher order anharmonicities etc. existing in the literature are often meaningless as representing true anharmonicities and cannot, therefore, be used to extrapolate observed energy levels. BIRGE and SPOONER's extrapolation of the observed energy levels will, in such cases, give too low a value for the dissociation energy. Thus, assuming ground-state dissociation products for the  $A^3\Pi_u$  state an extrapolated dissociation energy of 5.42 eV above the potential minimum of the  $X^3\Pi_u$  state is obtained [19].

[19] G. HERZBERG, *Astrophys. J.* **89**, 290 (1939).

Table 3. Calculated potential curves of several states for various dissociation products assuming  $D_e(x) = 6.2$  eV

	$r$ (Å)	$(^3P + ^3P)$ (eV)	$(^3P + ^1D)$ (eV)	$(^3P + ^1S)$ (eV)	$V_{R.K.R.V.}$
$A\Pi^3_g$	1.074	1.263	1.682	2.150	2.001
	1.087	0.956	1.273	1.627	1.688
	1.125	0.544	0.724	0.926	0.951
	1.156	0.308	0.410	0.525	0.541
	1.212	0.065	0.087	0.111	0.110
	1.325	0.061	0.081	0.104	0.110
	1.412	0.313	0.417	0.533	0.541
	1.476	0.572	0.762	0.974	0.951
	1.537	0.849	1.130	1.445	1.335
	1.602	1.159	1.542	1.971	1.688
	1.675	1.504	2.002	2.559	2.001
		$(^3P + ^3P)$	$(^1D + ^1S)$		
$c^1\Pi_g$	1.103	0.350	1.031		1.201
	1.132	0.215	0.634		0.740
	1.202	0.034	0.101		0.112
	1.313	0.032	0.094		0.112
	1.365	0.104	0.306		0.330
	1.444	0.263	0.776		0.740
	1.545	0.513	1.511		1.078
	1.621	0.710	2.093		1.201
		$(^1D + ^1D)$	$(^1D + ^1S)$	$(^1S + ^1S)$	
$e^1\Sigma_g^+$	1.111	0.335	0.585	0.836	0.995
	1.133	0.226	0.395	0.565	0.666
	1.148	0.167	0.291	0.416	0.488
	1.200	0.037	0.064	0.091	0.102
	1.317	0.044	0.078	0.111	0.102
	1.421	0.239	0.417	0.596	0.488
	1.463	0.341	0.596	0.851	0.666
	1.545	0.557	0.973	1.390	0.995
		$(^3P + ^3P)$	$(^3P + ^1D)$		
$B^3\Pi_g$	1.365	0.238	0.482		0.544
	1.402	0.114	0.231		0.317
	1.469	0.029	0.059		0.067
	1.615	0.030	0.060		0.067
	1.686	0.100	0.202		0.196
	1.742	0.169	0.342		0.317
	1.791	0.237	0.480		0.433
	1.838	0.306	0.620		0.544

Table 3. (contd)

	$r$ (Å)	$(^1S + ^1D)$	$(^3P + 3s^3P)$	$V_{R.K.R.V.}$ (eV)
$d^1\Sigma_u^+$	1.130	0.361	0.623	0.556
	1.152	0.218	0.376	0.336
	1.186	0.074	0.127	0.113
	1.297	0.070	0.132	0.113
	1.346	0.232	0.401	0.336
	1.382	0.385	0.664	0.556
		$(^3P + ^3P)$ (eV)		
$Y^3\Sigma_g^-$	1.230	0.718		0.621
	1.249	0.515		0.447
	1.273	0.314		0.270
	1.311	0.100		0.098
	1.435	0.104		0.098
	1.489	0.311		0.270
	1.530	0.519		0.447
	1.565	0.722		0.621

## CONCLUSION

If it proves impossible to approximate an observed potential curve by the Lippincott function, it can be assumed that two or more potential curves of same symmetry would have crossed were it not for the repulsive interaction between them as expressed in the non-crossing rule. In such a case extrapolation of the observed energy levels results in too low a value for the dissociation energy of the state. Where it is possible to reproduce approximately the R.K.R.V. curve with a Lippincott curve the use of the three-parameter form leads to information on the dissociation energy of that state. From this value and a knowledge of the ground-state dissociation energy it is often possible to determine without ambiguity the states of the dissociated atoms.

*Acknowledgements*—I wish to express my gratitude to Professor J. T. VANDERSLICE for sending the results of his calculations on  $C_2$  prior to publication. Also, I gratefully acknowledge considerable assistance in the calculations by Miss K. LOGAN. This work was carried out during the tenure of an I.C.I. Fellowship.



As published in *J. Chemical Physics* 39 No 3. 564-572  
1 August 1963. 86 I

CALCULATIONS OF HIGHER ORDER SPECTROSCOPIC  
PARAMETERS USING EMPIRICAL POTENTIAL FUNCTIONS

by

Joel M. Stutman, Ellis R. Lippincott, and Derek Steele\*

Department of Chemistry  
University of Maryland  
College Park, Maryland

ABSTRACT

Empirical internuclear potential functions have been used to predict higher order spectroscopic parameters for ground and excited states of a representative sample of diatomic molecules. The parameters, viz., second order anharmonicities,  $\omega_e y_e$ , rotational-vibrational coupling constants,  $\gamma_e$ , and the first order vibrational corrections to the second order rotational constants,  $\beta_e$ , have been computed through the Dunham relations for the Hulburt-Hirschfelder, Varshni III, and Lippincott empirical internuclear potential functions. A table of Dunham-corrected equilibrium vibrational frequencies and equilibrium internuclear distances is given. The predicted values for the higher order spectroscopic parameters are compared with experimental values as found in the literature. Deviations of predicted from experimental values are discussed from different approaches. The empirical functions discussed should be useful in obtaining estimates of  $\omega_e y_e$ ,  $\gamma_e$ , and  $\beta_e$  when such values are not available because of limited experimental data.

\*Present Address: Department of Chemistry, Royal Holloway College, Englefield Green, Surrey, England

## I. INTRODUCTION

In a previous publication<sup>1</sup> (SLV) several internuclear potential functions were studied with respect to three criteria: their ability to predict a) first order vibrational-rotational coupling constants,  $\alpha_e$ 's, b) first order anharmonicities,  $\omega_e x_e$ 's and c) potential values which agree with observed values, at various internuclear separations, where the observed potential values were taken to be those obtained from the Rydberg-Klein-Rees-Vanderslice (RKR) method.<sup>2</sup> A number of these functions exhibited an average performance in fairly good agreement with known curves as given by the RKR method and predicted  $\omega_e x_e$ 's and  $\alpha_e$ 's which agreed well with experimental values.

This present work represents an extension of the above study. The main purpose of this paper is to determine the ability of the empirical internuclear potential functions to predict spectroscopic parameters such as second order anharmonicities,  $\omega_e y_e$ 's, rotational-vibrational coupling constants,  $\gamma_e$ 's, and first order vibrational corrections to the second order rotational constants,  $\beta_e$ 's.<sup>3</sup> In this publication, we have also compiled a table of Dunham<sup>3</sup> corrected equilibrium vibrational frequencies,  $\omega_e$ 's, and equilibrium internuclear distances,  $r_e$ 's, which may be of interest to some investigators. Several of the nine functions considered in the original paper have been eliminated from investigation in this work either because of their poor showing in

- 
1. D. Steele, E. R. Lippincott, and J. T. Vanderslice, Revs. Modern Phys. 34, 239 (1962).
  2. J. T. Vanderslice, E. A. Mason, W. G. Maisch, and E. R. Lippincott, J. Mol. Spectroscopy 3, 17 (1959); 5, 83 (1960).
  3. J. L. Dunham, Phys. Rev. 41, 713, 721 (1932).

the prediction of low-order constants, and/or their inaccurate curve representations, or because they predict a constant sign in one of the high order terms considered in this paper.

We use the method of Dunham<sup>3</sup> in order to demonstrate the relation of the various spectroscopic constants used in describing the observed energy levels of a rotating anharmonic vibrator to the parameters of any empirical internuclear potential function which can be expanded in a power series about  $(r-r_e)/r_e$ . Dunham used the WKB method to show that the energy levels will have the form

$$E_{vJ} = \sum_{l,j} Y_{lj} (v+1/2)^l J^j (J+1)^j \quad (1)$$

where  $l$  and  $j$  are summation indices and  $v$  and  $J$  are vibrational and rotational quantum numbers respectively, and where the  $Y_{lj}$ 's are coefficients which can be determined from the experimental molecular constants. Here, the energy zero has been taken to be at the minimum of the potential curve. If  $B_e/\omega_e$  is small, the  $Y_{lj}$ 's can be related to the band spectrum "constants" as indicated in Table I.

These symbols refer to the power series expansion for the molecular energy levels:

$$E_{vJ} = \omega_e (v+1/2) - \omega_e x_e (v+1/2)^2 + \omega_e y_e (v+1/2)^3 + \omega_e z_e (v+1/2)^4 + \dots + \quad (2)$$

$$B_v J(J+1) - D_v J^2(J+1)^2 + F_v J^3(J+1)^3 + \dots$$

where  $B_v = B_e - \alpha_e (v+1/2) + \beta_e (v+1/2)^2 + \dots$  (3)

and  $D_v = D_e + \beta_e (v+1/2) + \dots$  (4)

If the effective potential is assumed to have the form

$$V = a_0 \xi^2 \left( 1 + \sum_{i=1}^{\infty} a_i \xi^i \right) + B_e J(J+1) (1 - 2\xi + 3\xi^2 - 4\xi^3 + \dots) \quad (5)$$

where  $\xi = (r-r_e)/r_e$ , the  $a_i$ 's can be related to the  $Y_{lj}$ 's. Thus, if any given empirical potential function can be expanded in a power series about  $(r-r_e)/r_e$ , as assumed by Dunham, then one can arrive at expressions for the  $a_i$ 's in terms of the parameters of the particular empirical potential function employed. Thus all spectroscopic constants can theoretically be determined by the relationships given by Dunham, and they will be given in terms of parameters of the function used. In particular, in this study, we are interested in the prediction of  $\omega_e y_e$ ,  $r_e$ ,  $\beta_e$ , corrected  $\omega_e$ , and corrected  $r_e$ . These are given by the following equations in terms of  $a_i$ 's.

$$\omega_e y_e = (B_e^2/2\omega_e) (10a_4 - 35a_1 a_3 - 17a_2^2/2 + 225a_1^2 a_2/4 - 705a_1^4/32) \quad (6)$$

$$r_e = (6B_e^3/\omega_e^2) (5 + 10a_1 - 3a_2 + 5a_3 - 13a_1 a_2 + 15(a_1^2 + a_1^3)/2) \quad (7)$$

$$\beta_e = (12B_e^4/\omega_e^3) (19/2 + 9a_1 + 9a_1^2/2 - 4a_2) \quad (8)$$

$$r_e \text{ corr} = \left[ \frac{h \left\{ 1 + (B_e^2/2\omega_e^2) (15 + 14a_1 - 9a_2 + 15a_3 - 23a_1 a_2 + 21[a_1^2 + a_1^3]/2) \right\}}{8\pi^2 \mu B_e c} \right]^{1/2} \quad (9)$$

$$\omega_e \text{ corr} = \omega_e \left[ 1 + (B_e^2/4\omega_e^2) (25a_4 - 95a_1 a_3/2 - 67a_2^2/4 + 459a_1^2 a_2/8 - 1155a_1^4/64) \right]^{-1} \quad (10)$$

## II. FUNCTIONS CONSIDERED IN THIS INVESTIGATION

### Lippincott Function

This function has the form shown in Table II and can be used in a three or five parameter form. With  $a \neq 0$ , the function  $f(r)$  must satisfy the condition  $V(r) = \infty$  when  $r=0$  and  $V(r) = D_e$  when  $r=\infty$ . Several forms have been proposed for  $f(r)$ , the most useful of which is the one chosen for this comparative study and whose form is indicated in Table II. The five parameter function then has the form

$$V(r) = D_e (1 - e^{-x}) (1 - abx^{1/2} e^{-b(xr/r_e)^{1/2}}) \quad (11)$$

where  $x = n \Delta r^2 / 2r_e$ .

The parameters  $b_e$  and, to a lesser extent,  $a_e$  were found to be nearly constant for the states of all molecules in previous studies. This suggests that the five parameter function can be treated as a three parameter function for purposes of constructing potential curves and calculating spectroscopic quantities. Furthermore, it has been established<sup>4</sup> that both the five and three parameter forms predict essentially the same  $D_e$ . The assumption of this equivalence leads to relationships such as the one between  $\Delta$ 's which is being used in this study and represents the only difference between Lippincott I and Lippincott II, viz.,  $\Delta(I) = k_e r_e^2 / 2D_e$  and  $\Delta(II) = 4\omega_e x_e / 3B_e - 1/2$ . Expansion of the Lippincott function into Dunham form yields the coefficients shown in Table II. The results obtained from these two forms of the Lippincott function will be found in rows 1 and 2 respectively of Table III.

#### Hulburt-Hirschfelder Function<sup>5</sup>

This is a five parameter extension of the Morse function which has the advantage that the five major spectroscopic constants are fitted exactly. However, it has the disadvantage that no correlation checks among these five spectroscopic quantities are possible. The Hulburt-Hirschfelder function shows excellent correlation with the RKR curves as expected<sup>1</sup>. It was chosen for consideration here in order to determine whether  $\omega_e y_e$ ,  $\gamma_e$ , and  $\beta_e$  could be predicted if all five of the lower order spectroscopic constants were used. The form of the function and the forms of the Dunham coefficients are shown in Table II. The parameters predicted by this function are shown in row 3 of Table III.

---

4. E. R. Lippincott, D. Steele, and P. Caldwell, J. Chem. Phys. 35, 123 (1961).

5. H. M. Hulburt and J. O. Hirschfelder, J. Chem. Phys. 9, 61 (1941).

### Varshni III<sup>6</sup>

This is a three parameter function having the form shown in Table II. This function gives good performance with respect to agreement with the RKR curves and prediction of  $\alpha_e^{-1}$ . However the calculated values of  $\omega_e x_e$  are poor, being the worst for any function compared. The form of the  $a_i$ 's obtained from this function are also shown in Table II, and the calculated values of the higher order constants determined by this function are listed in Table III in row 4.

The remaining six empirical internuclear potential functions, which were investigated in the Steele-Lippincott-Vanderslice study,<sup>1</sup> will not be discussed here for reasons which are briefly stated below.

the Morse function: because it was not particularly suitable for the construction of potential curves, because it predicts zero values for  $\omega_e y_e$  for all diatomic states, and because it predicts  $\gamma_e$ 's which are always negative.

the Rosen-Morse function: because it yields no significant improvement over the Morse function with respect to both potential curve mappings and predictions of  $\omega_e x_e$ 's and  $\alpha_e$ 's.

the Poschl-Teller and Frost-Musulin functions: because the  $\omega_e x_e$ 's and  $\alpha_e$ 's predicted by these functions do not agree well with observed values, and because these functions give poor potential curve representations.

the Rydberg function: because it yields a consistently negative value for  $\omega_e y_e$ 's for all diatomic states.

the Linnert function: because it predicts false maxima in the potential curves of certain molecular states where none are observed or expected to exist.

---

<sup>6</sup> Y. P. Varshni, Revs. Modern Phys. 29, 664 (1957).

### III. DISCUSSION

In Table III, we have listed, for a representative sample of diatomic systems, the  $\omega_e y_e$ ,  $\gamma_e$ , and  $\beta_e$  values calculated from the empirical internuclear potential functions discussed. These calculated values are compared to experimental values available in the literature. It is evident that no great agreement exists between observed and calculated values. However, rather early in this study we realized that agreement to the "observed" spectroscopic constants would represent a very poor criterion on which to judge the predictions of the various potential functions, since, while the  $\omega_e$ ,  $\omega_e x_e$ ,  $\omega_e y_e$ , ..., values are in themselves quite accurate, they depend strongly on the method of data analysis, viz., on the number of terms used in the  $\Delta G(v+1/2)$  equation. In Table V we illustrate this inconvenient phenomenon from data on the  $X^1\Sigma_g^+$  state of  $^1\text{H}_2$  taken from the high resolution study of Herzberg and Howe,<sup>7</sup> in which were indicated six  $\Delta G''(v+1/2)$  equations. It can be seen that  $\omega_e$  has a range of 8 out of 4400  $\text{cm}^{-1}$  and  $\omega_e x_e$ , 7 out of 120  $\text{cm}^{-1}$ . However,  $\omega_e y_e$  varies from +1.24944 to +1.71223, not even appearing to vary in a consistent manner. The importance of this lies in the fact that these  $\Delta G''$ 's are measurable to six and a half significant figures but our spectroscopic "constants" seem reliable to a maximum of three for  $\omega_e$ . This illustrates the difficulty of extending these power series to a sufficient number of terms due to the possibilities of losing significant figures. However, one can have little confidence in the physical meaning of these higher order spectroscopic parameters which were obtained from low order power series equations even though they have maintained the proper accuracy with respect to significant figures. In a like manner, one should have little confidence in

---

7. G. Herzberg and L. L. Howe, Can. J. Phys. 37, 636 (1959).

parameters obtained from high order power series equations - say, from  $n=7, \dots, m$  where  $m$ =number of vibrational levels - since there is a loss of significant figures.

Thus it is necessary to emphasize that, if one insists on expanding the vibrational measurements in infinite power series, the series must indeed be infinite in order that the resulting numbers maintain their originally intended meaning. It is well known that this cannot be done in practice. It would be of considerable value in the future if an effort were made to obtain an expression for the vibrational energies in closed form.

Dunham's derivation of the eigenvalues of a rotating anharmonic oscillator involved assumptions incident upon the WKB method and also the assumption that the potential used could be expanded into a power series. It follows that the lower order spectroscopic constants  $\omega_e$ ,  $\omega_e x_e$ ,  $\omega_e y_e$ , are expressible in terms of the lower order  $a_i$ 's, viz.,  $a_1$ ,  $a_2$ ,  $a_3$  and  $a_4$ , (with small corrections involving  $a_5$  and  $a_6$ ). We have at our disposal some empirical potential functions, which fit observed potential curves very well. Thus, the  $a_i$ 's which are obtained from the empirical potential functions involve no approximations except those dependent on the RKR method, and the spectroscopic constants obtained from these  $a_i$ 's involve no approximations except those dependent on the Dunham method. Thus, to the extent that the empirical potential function's curve representation for a given molecular state is in agreement with the RKR curve, the spectroscopic constants obtained from this function for a given state should give a reasonable estimate for the values of such parameters. These estimates may perhaps be useful in cases where such parameters cannot be obtained experimentally due to unavailable or limited data.



$B_v$ ,  $D_v$ , and  $H_v$  are obtained by a graphical method, based on the assumption that all coefficients of  $(J+1/2)^n$  in the  $\Delta_2 F_v(J)/4(J+1/2)$  equations are zero for  $n > 4$ . Therefore, from plots of  $\Delta_2 F_v(J)/4(J+1/2)$  vs.  $(J+1/2)^2$  for all the vibrational levels,  $B_v$ ,  $D_v$ , and  $H_v$  are found as the intercept, slope, and curvature respectively. Then an equation is generated to express  $B_v$  in a power series in  $(v+1/2)$ . Using again the ground state of hydrogen for illustrative purposes, we see that Herzberg and Howe arrive at a four-term formula (developed from the first eight  $B_v$  values, in which  $\gamma_e = 0.06017 \text{ cm}^{-1}$ ), postulated as being an improvement over Stoicheff's<sup>8</sup> three-term formula (developed from the first four  $B_v$  values in which  $\gamma_e = 0.02855 \text{ cm}^{-1}$ ). This judgment is based on the small magnitudes of the residuals of the first five  $B_v$  values. In Table VI are compared  $B_e$ ,  $\alpha_e$ , and  $\gamma_e$  values obtained from three, four, five, and six term formulae using the first three, four, five, and six  $B_v$  values respectively in exact-fit equations.

Because of the inaccuracies inherent in graphical analysis of the rotational levels as well as the arbitrary power series cut-offs,  $\gamma_e$  values obtained from the above empirical potential functions again should be useful estimates of these quantities where insufficient data is available to determine them experimentally. Similar statements could be made for  $\beta_e$ , except the  $\beta_e$ 's obtained from the potential functions should be even more reliable than the other constants so obtained since they depend only on  $a_1$  and  $a_2$ .

It can be argued that relatively small errors in the assumed potential relative to the true (experimental) potential can give rise to errors of orders of magnitude in the coefficients,  $a_i$ 's, in the Dunham

---

8. B. P. Stoicheff, Can. J. Phys. 35, 730 (1957).

power series. An examination of Table III shows that the  $a_1$  and  $a_2$  values for the four functions generally agree reasonably well, the  $a_3$  values to within a factor of two, but the  $a_4$  values sometimes differ in sign. Since these comparisons can be made among the four functions whose curves depart from each other, as much as any of them depart from the RKR curve, it is not unreasonable to assume that the  $a_1$ ,  $a_2$ , and  $a_3$  values of the true (experimental) curves would be within the ranges given in Table III. Therefore  $\omega_e y_e$  which depends only on  $a_1$ ,  $a_2$ , and  $a_3$  should be quite reliable.

Although  $\omega_e y_e$  depends on  $a_4$ , this dependence is not as strong as its dependence on  $a_1$ ,  $a_2$ , and  $a_3$ , and one generally still is able to predict within an order of the magnitude the  $\omega_e y_e$  values.

One additional source of discrepancy between observed and calculated high order parameters may arise from interactions between states of the same symmetry whose potential curves would have crossed were it not for the mutual repulsion between these states expressed in the well-known non-crossing rule. These interactions will cause the original states to change in character as the bond lengths are altered. These changes are most pronounced in the vicinity of the bond length at which the two states, if they did not interact, would have had the same potential energy. Clearly, such changes in character, if localized in a limited range of  $v$  values, will cause the original  $\Delta G$  expansions in terms of powers of  $(v+1/2)$  to be no longer valid, if the coefficients are obtained from, for example, the first three or four levels. It has been shown that such cases can be recognized by divergences of the observed potential curves (RKR curves) from those given by the Lippincott function. In general empirical potential functions must conform to their general built-in shape, and are not able to reproduce the local humps and bumps caused by interacting non-crossing states even though the correct vibrational constants may be known.

Table IV contains a tabulation of corrected  $\omega_e$ 's and corrected  $r_e$ 's calculated from the Lippincott (I) function for some randomly selected molecular states. If any others are desired they may be calculated from equations (9) and (10) using the  $a_i$ 's in Table III.

We can say no more about the relative merit of the three potential functions tested except that the spectroscopic parameters obtained through the Lippincott and Hulburt-Hirschfelder functions should perhaps be received with more confidence than those obtained from Varshni III since the former give an overall performance in their potential curve representations which are superior to the latter.

TABLE I: Spectroscopic Parameters Represented by the  $Y_{lj}$ 's.

$j \backslash l$	0	1	2	3	4
0	-	$\omega_e$	$-\omega_e^x$	$\omega_e^y$	$\omega_e^z$
1	$B_e$	$-\alpha_e$	$\gamma_e$	$\delta_e$	
2	$-D_e$	$\beta_e^*$			
3	$F_e$				
4	$H_e$				

\* In the older spectroscopic convention all first order corrections were taken to be of opposite sign than the constant term e.g.,

$$G_v = \omega_e(v+1/2) - \omega_e^x(v+1/2)^2 + \dots; B_v = B_e - \alpha_e(v+1/2) + \dots; D_v = D_e - \beta_e(v+1/2) + \dots;$$

but modern convention maintains the same sign for  $D_e$  and  $\beta_e$ , i.e.

$$D_v = D_e + \beta_e(v+1/2) + \dots, \text{ so that the element at } 1,2 \text{ in Table I should}$$

$$\text{be } -\beta_e.$$

Table II: Form, Parameters, and Dunham Coefficients of the Potential Functions Considered.

	Lippincott	Hulburt-Hirschfelder	Varshni III
V(r)	$D_e(1 - \exp[-n r^2/2r])(1 + af(r))$	$D_e[(1 - \exp(-ax))^2 + ca^3 \exp(-2ax)(1 + abx)]$	$D_e \left[ \frac{(1-r_e)}{r} \exp(-\beta[r^2 - r_e^2]) \right]^2$
Special parameters	$f(r) = \exp(-x(r/r_e)^{1/2})$	$x = r - r_e$	$t = \beta r_e^2$
	$x = (b^2 n r^2/2r)^{1/2}$	$a = (k_e/2D_e)^{1/2}$	
	$*\Delta = k_e r_e^2/2D_e$ (I)	$cr = a \Delta^{1/2}/r_e$	
	$\Delta = (G-3)/6$ (II)	$b = 2 + [7/12 - (5/4 + 5/2F + 5 + 5/4F^2 - 16/3G)/a^2 r_e^2]/c$	
	$F = \zeta \omega_e^2/6B_e^2$	$c = 1 - (1+F)/ar_e$	
	$G = 8\omega_e^2 x_e/B_e$		
	$n = k_e r_e/D_e$		
	$b = \text{constant} = 1.065$		
$a_0$	$k_e r_e^2/2$	$k_e r_e^2/2$	$k_e r_e^2/2$
$a_1$	$-(1+F)$	$(c-1)ar_e$	$-[8t^3 + 8t^2 + 6t + 2]/\Delta$
$a_2$	$1 - \Delta/2 + 3F/2 + bF\Delta^{1/2}$	$(c[b-2] + 17/12)a^2 r_e^2$	$(28t^4/3 + 20t^3/3 + 9t^2 + 8t + 3)/\Delta$
$a_3$	$-1 - 15F/8 + \Delta - b^2 F\Delta/2 + F\Delta/2$	$(2c[1-b] - 1/4)a^3 r_e^3$	$-(8t^5 + 4t^4/3 + 22t^3/3 + 11t^2 + 10t + 4)/\Delta$
$a_4$	$1 + 35F/16 - 3\Delta/2 + \Delta^2/6 + 15bF\Delta^{1/2}/8$	$(2c[b-2/3 + 31/360])a^4 r_e^4$	$(248t^6/45 - 54t^5/15 + 14t^4/3 + 9t^3 + 13t^2 + 12t + 5)/\Delta$
	$-5F\Delta/4 + 3b^2 F\Delta/4 + Fb^3 \Delta^3/2/6 - Fb\Delta^3/2/2$		

\*See text and ref. 4.

Table III (continued)

Molecule	State	F	a <sub>1</sub>	a <sub>2</sub>	a <sub>3</sub>	a <sub>4</sub>	ω <sub>eye</sub>	obs	calc	δ <sup>e</sup>	obs	calc	δ <sup>e</sup>	obs	calc		
ICI <sup>(9)</sup>	A <sup>3</sup> Π <sub>i</sub>	4	-5.1974	14.4415	-26.8101	36.1069	-3.366-2	-7.069-3	-7.971-6	-7.971-6						1.709-9	
		1	-1.9112	1.9876	-1.1627	-1.6006	-5.8-3	-8.331-3	-8.0-5	-2.173-5	-2.173-5						2.8-8 4.451-8
		2	-1.9112	2.1391	-1.4919	-1.1578		-3.036-3		2.873-6	2.873-6						1.021-8
		3	-1.9112	1.9992	-2.0667	3.1637		-1.530-2		-8.481-5	-8.481-5						4.187-8
Li <sub>2</sub> <sup>(9)</sup>	A <sup>1</sup> Σ <sub>u</sub> <sup>+</sup>	4	-2.1538	2.9027	-3.4402	4.0649		-4.484-3	-1.943-5	-1.943-5						-3.513-8	
		1	-1.9306	2.5263	-2.3051	0.1064	1.8-3	7.094-3		4.504-5	4.504-5					-5.325-8	
		2	-1.9306	2.4506	-2.1315	-0.2345		4.985-3		3.593-5	3.593-5						-3.990-8
		3	-1.9306	2.5554	-3.0800	3.4155		7.363-5		8.402-6	8.402-6						-5.838-8
N <sub>2</sub> <sup>(13)</sup>	X <sup>1</sup> Σ <sub>g</sub> <sup>+</sup>	4	-1.9272	2.5794	-3.1989	3.8783		6.925-4	8.949-6	8.949-6						-6.389-8	
		1	-2.7721	4.8511	-4.9548	-6.5060	-2.0-2	4.247-2		9.175-5	9.175-5						9.2-9 -3.997-9
		2	-2.7721	4.8399	-4.9300	-6.5843		4.053-2		8.963-5	8.963-5						-3.342-9
		3	-2.7721	4.9098	-8.6497	16.4139		-4.973-2		-5.082-5	-5.082-5						-7.427-9
N <sub>2</sub> <sup>(9)</sup>	A <sup>3</sup> Σ <sub>u</sub> <sup>+</sup>	4	-2.6446	3.9447	-4.5615	5.0193		-2.549-2	-5.809-5	-5.809-5						+2.036-8	
		1	-2.5259	2.8186	-1.3294	-7.5216	-2.5-2	-1.033-1		-1.330-4	-1.330-4						6.964-8
		2	-2.5259	2.8219	-1.3362	-7.5189		-1.030-1		-1.324-4	-1.324-4						6.942-8
		3	-2.5259	1.5447	4.4894	-12.1087		-6.172-2		-2.078-4	-2.078-4						1.541-7
NO <sup>(9)</sup>	X <sup>2</sup> Π <sub>3/2</sub>	4	-3.0862	5.1775	-6.2455	6.5741		-4.362-2	-1.169-4	-1.169-4						6.419-8	
		1	-2.9437	5.4374	-5.7152	-9.1137	-1.2-3	4.945-2		1.020-4	1.020-4						3.676-9
		2	-2.9437	5.3861	-5.6036	-9.5017		3.978-2		9.172-5	9.172-5						6.691-9
		3	-2.9437	5.3677	-9.4653	18.4653		-5.599-2		-7.194-5	-7.194-5						7.773-9
4	-2.8121	4.3816	-5.1198	5.5162		-3.101-2		-7.511-5	-7.511-5						3.305-8		

Table III (continued)

Molecule	State	$\omega_{eye}$				$\delta_e$		$\beta_e$				
		$a_1$	$a_2$	$a_3$	$a_4$	obs	calc	obs	calc			
<sup>(9)</sup> NO	$B^2\Pi_r^+$	1	-2,7316	5,2461	-6,0924	-0,1606	9,67-2	8,780-2	+1,451-4	-3,595-8		
		2	-2,7316	4,6456	-4,6260	-6,4464		1,845-2	6,036-5	-1,294-9		
		3	-2,7316	4,6181	-5,3834	4,2216		3,235-2	2,783-5	2,918-10		
		4	-2,0892	2,7967	-3,3493	3,9899		-2,550-3	-5,047-6	-1,224-8		
<sup>(9)</sup> Na <sub>2</sub>	$X^1\Sigma_g^+$	1	-1,8760	1,2961	0,2148	-2,5962	-2,7-3	-3,190-3	-3,0-5	-7,087-6	5,0-9	5,565-9
		2	-1,8760	1,6635	-0,5593	-2,0406		-1,821-3	-3,594-6	-3,064-9		3,064-9
		3	-1,8760	1,2535	-0,3892	2,4126		-2,970-3	-1,053-5	-1,053-5		5,856-9
		4	-2,3960	3,3694	-3,9003	4,4511		-1,284-3	-3,263-6	-3,263-6		4,967-10
<sup>(9)</sup> O <sub>2</sub>	$X^3\Sigma_g^-$	1	-2,9900	5,5971	-5,9229	-9,9567	5,46-2	4,503-2	9,305-5	8,8-8	5,746-9	
		2	-2,9900	5,5797	-5,8852	-10,0938		4,204-2	8,989-5	8,989-5		6,670-9
		3	-2,9900	5,6093	-10,4540	21,5639		-5,678-2	-6,821-5	-6,821-5		5,093-9
		4	-2,8616	4,5179	-5,3030	5,6831		-2,913-2	-7,218-5	-7,218-5		3,351-8
<sup>(9)</sup> O <sub>2</sub>	$B^3\Sigma_u^-$	1	-2,9142	3,3745	-1,5884	-13,6501	-3,754-1	-1,783-1	-2,439-4		1,256-7	
		2	-2,9142	4,8240	-4,4961	-11,6003		-2,726-2	-1,783-6		3,447-8	
		3	-2,9142	4,1039	-13,8039	77,3073		-1,947-1	-4,833-4		7,974-8	
		4	-3,7723	7,5905	-10,3899	11,0991		-6,509-2	-2,088-4		1,449-7	
<sup>(14)</sup> AlH	$X^1\Sigma^+$	1	-2,2758	3,5316	-3,5662	-0,6055	2,389-1	5,069-1	1,61-3	4,836-3		-7,571-6
		2	-2,2758	3,3357	-3,1096	-1,7719		2,526-1	3,217-3		-4,277-6	
		3	-2,2758	3,4396	-4,4939	5,2926		6,662-2	9,163-4		-6,024-6	
		4	-2,0746	2,7741	-3,3309	3,9749		-4,900-2	-3,290-4		-3,781-6	

Table III (continued)

Molecule	State	$\omega_e \nu_e$				$\chi_e$				$\beta_e$		
		$a_1$	$a_2$	$a_3$	$a_4$	obs	calc	obs	calc	obs	calc	
${}^1\text{H}_2$ (7)	$X^1\Sigma_g^+$	1	-1.6091	1.8928	-1.8098	0.9553	7.242-1	2.168	6.017-2	1.361-1	-1.616-3	-1.743-3
		2	-1.6091	1.8754	-1.7739	0.8936		1.927		1.269-1		-1.608-3
		3	-1.6091	1.9129	-2.0735	1.9472		1.055		6.924-2		-1.899-3
		4	-1.8290	2.5498	-3.2866	4.0369		3.354		1.715-1		-4.072-3
${}^1\text{H}_2$ (7)	$B^1\Sigma_u^+$	1	-1.6947	2.3623	-2.6776	2.4761	8.7-1	2.719	1.452-1	1.217-1	-2.165-3	-1.755-3
		2	-1.6947	2.3540	-2.6492	2.3686		2.660		1.213-1		-1.729-3
		3	-1.6947	2.8736	-3.2172	2.4021		6.722		3.055-1		-3.330-3
		4	-2.1220	3.2362	-4.3531	5.4699		2.270		9.640-2		-1.757-3
${}^1\text{H}_2$ (9)	$a^3\Sigma_g^+$	1	-1.6339	1.9561	-1.8955	0.9936	9.2-1	1.260		7.348-2		-8.830-4
		2	-1.6339	1.9181	-1.8176	0.8582		9.648-1		6.326-2		-7.511-4
		3	-1.6339	1.9411	-2.0783	1.9338		6.436-1		3.330-2		-8.309-4
		4	-1.8501	2.5433	-3.2723	4.0167		1.667		8.000-2		-1.801-3
${}^1\text{H}_2$ (9)	$e^3\Sigma_u^+$	1	-1.7439	1.9624	-1.7316	0.2120	-4.33-1	-7.404-1		1.361-2		-2.263-4
		2	-1.7439	2.1806	-2.1624	0.8998		9.946-1		6.773-2		-7.757-4
		3	-1.7439	2.1948	-3.1466	4.5066		-2.759		-4.983-2		-8.113-4
		4	-1.9475	2.6015	-3.2096	3.8834		1.066-1		1.479-2		-8.601-4
${}^1\text{H}_2$ (9)	$d^3\Pi_u$	1	-1.6624	2.0709	-2.0814	1.1972	8.8-1	1.571		8.308-2		-1.001-3
		2	-1.6624	1.9813	-1.8970	0.8614		8.975-1		6.085-2		-7.273-4
		3	-1.6624	1.9993	-2.0853	1.8419		1.098		4.271-2		-7.823-4
		4	-1.8286	2.5543	-3.2961	4.0504		1.595		7.504-2		-1.627-3



Table III (continued)

Molecule	State	$\omega_e$				$\delta_e$						
		$a_1$	$a_2$	$a_3$	$a_4$	obs	calc	obs	calc			
$^9_2\text{H}_2$	$X^1\Sigma_g^+$	1	-1.5889	1.8297	-1.7159	0.8801	1.254	6.428-1	5.79-3	2.928-2	-1.18-4	-2.571-4
		2	-1.5889	1.7671	-1.5876	0.6717		3.576-1		2.123-2		-1.722-4
		3	-1.5889	1.7516	-1.6907	1.4344		3.800-1		7.495-3		-1.511-4
		4	-1.8289	2.5501	-3.2872	4.0379		1.185		4.275-2		-7.152-4
$^9_2\text{H}_2$	$B^1\Sigma_u^+$	1	-1.6798	2.3243	-2.6240	2.4199	4.1-1	9.207-1		2.952-2		-3.053-4
		2	-1.6798	2.3091	-2.5772	2.2584		8.850-1		2.917-2		-2.969-4
		3	-1.6798	2.7811	-3.0759	2.2831		2.222		7.134-2		-5.568-4
		4	-2.1212	3.2348	-4.3509	5.4670		8.090-1		2.434-2		-3.142-4
$^{15}\text{HF}$	$X^1\Sigma^+$	1	-2.2398	3.4487	-3.4918	-0.3054	5.334-1	2.165	8.73-3	2.759-3		-6.125-5
		2	-2.2398	3.2814	-3.0985	-1.3207		1.266		1.986-2		-3.943-5
		3	-2.2398	3.4466	-4.6884	5.6996		3.506-1		8.145-3		-6.098-5
		4	-2.0374	2.7186	-3.2876	3.9402		-1.426-1		-8.326-4		-3.365-5
$^{35}\text{Cl}$	$X^1\Sigma^+$	1	-2.3460	3.5634	-3.4081	-2.0644	3.6-2	1.898-1		1.462-3		-1.181-6
		2	-2.3460	3.5121	-3.2914	-2.3458		1.480-1		1.287-3		-9.606-7
		3	-2.3460	3.5859	-5.2186	7.6844		-1.256-1		-3.178-4		-1.277-6
		4	-2.2440	3.0647	-3.5903	4.1902		-7.262-2		-4.569-4		-3.159-7
$^{37}\text{Cl}$	$X^1\Sigma^+$	1	-2.3522	3.5970	-3.4652	-2.0160	6.3-2	2.041-1		1.519-3		-1.235-6
		2	-2.3522	3.5297	-3.3121	-2.3899		1.491-1		1.291-3		-9.486-7
		3	-2.3522	3.6033	-5.2010	7.5315		-1.117-1		-2.646-4		-1.262-6
		4	-2.2384	3.0541	-3.5801	4.1817		-7.071-2		-4.427-4		-3.357-7

Table III (continued)

Molecule	State	$\omega_{e^2}$				$\delta_e$		$\beta_e$		
		$a_1$	$a_2$	$a_3$	$a_4$	obs	calc	obs	calc	
$(\text{Hg}^2\text{H})^+$	$X^1\Sigma^+$	1	-2.5972	4.1931	-4.0381	-4.9709	6.0-1	8.559-2	7.470-4	-1.433-7
		2	-2.5972	4.0397	-3.7024	-5.7705		-1.015-2	4.238-4	1.578-7
		3	-2.5972	3.7766	-4.3735	5.4739		-1.289-1	-7.937-4	6.743-7
		4	-2.5449	3.7031	-4.2729	4.7689		-9.411-2	-5.797-4	4.553-7
$\text{Li}^{\textcircled{9}}\text{H}$	$X^1\Sigma^+$	1	-1.8849	2.4285	-2.2136	0.2662	1.633-1	2.760-1	4.800-3	-1.59-5
		2	-1.8849	2.3110	-1.9452	-0.2431		1.527-1	3.273-3	-9.919-6
		3	-1.8849	2.3822	-2.6309	2.6243		4.894-2	8.310-4	-1.384-5
		4	-1.9001	2.5535	-3.1907	3.8787		5.181-2	1.401-3	-2.159-5
$\text{Li}^{\textcircled{9}}\text{H}$	$A^1\Sigma^+$	1	-0.6149	-0.1245	0.6826	-0.9862	-4.185	-1.864-2	6.686-3	3.625-4
		2	-0.6149	5.9745	-12.5217	43.1305		-2.994-1	-8.028-2	-1.072-3
		3	-0.6149	7.3200	-10.2087	7.2621		-7.626	-3.557-2	-1.389-3
		4	-2.5175	3.9755	-5.4471	6.9246		-2.151-1	-3.321-3	-3.174-5
$\text{Mg}^{\textcircled{9}}\text{H}$	$X^2\Sigma^+$	1	-2.2284	3.3154	-3.2138	-0.8923	-1.5-1	3.373-1	3.696-3	1.0-5
		2	-2.2284	2.8741	-2.2247	-2.8899		-1.479-1	2.550-4	1.206-6
		3	-2.2284	2.5976	-1.3727	-1.0396		8.485-2	-1.288-3	5.752-6
		4	-2.0993	2.8127	-3.3626	4.0008		-5.587-2	-4.319-4	-3.340-6
$\text{Mg}^{\textcircled{9}}\text{H}$	$A^2\Pi_r$	1	-2.3249	3.5686	-3.4880	-1.5434	1.48	4.006-1	4.223-3	-5.745-6
		2	-2.3249	2.9050	-2.0253	-4.3248		-4.762-1	-1.635-3	5.346-6
		3	-2.3249	2.3614	0.5420	-6.0470		1.245-1	-2.706-3	1.443-5
		4	-2.1829	2.9534	-3.4859	4.1029		-9.566-2	-8.633-4	-2.158-6

Table III (continued)

Molecule	State	$\omega_e \nu_e$				$\nu_e$					
		$a_1$	$a_2$	$a_3$	$a_4$	obs	calc	obs	calc		
$1^1\text{H}$ NaH	$1^1\Sigma^+$	1	-2.1004	2.9210	-2.7035	-0.5930	1.60-1	1.934-1	2.604-3	-3.0-6	-5.310-6
		2	-2.1004	2.8030	-2.4349	-1.1470		9.776-2	1.820-3		-3.281-6
		3	-2.1004	2.8322	-3.3663	3.8264		-3.435-2	-2.098-4		-3.783-6
		4	-2.0439	2.7280	-3.2947	3.9458		-2.996-2	-1.632-4		-4.336-6
$1^1\text{H}$ NaH	$1^1\Sigma^+$	1	-0.6851	-0.2762	1.0546	-1.3639	-1.97-1	-5.307-3	8.797-4		2.171-5
		2	-0.6851	2.1729	-4.1662	8.1564		-2.756-2	-2.652-3		-1.075-5
		3	-0.6851	2.7132	-4.9989	4.9111		-3.081-1	-2.947-3		-1.791-5
		4	-2.0251	3.0497	-4.0745	5.0993		7.470-2	1.209-3		-8.186-6

a.  $D_e$  assumed 11.1 eVb.  $B_e$  assumed 1.076  $\text{cm}^{-1}$ 

9. G. Herzberg, Molecular Spectra and Molecular Structure I, D. Van Nostrand Co., Inc., New York, 1950.
10. D. H. Rank, A. H. Guenther, G. D. Saksena, J. N. Shearer, and T. A. Wiggins, J. Opt. Soc. Amer. 47, 686 (1957).
11. G. Herzberg and T. J. Hugo, Can. J. Phys. 33, 757 (1955).
12. L. Mathieson and A. L. G. Rees, J. Chem. Phys. 25, 753 (1956).
13. P. G. Wilkinson and N. B. Houk, J. Chem. Phys. 24, 528 (1956).
14. P. B. Zeeman and G. J. Ritter, Can. J. Phys. 32, 555 (1954).
15. G. A. Kuepers, D. F. Smith and A. H. Nielson, J. Chem. Phys. 25, 275 (1956).
16. B. H. Van Horne and C. D. Hause, J. Chem. Phys. 25, 56 (1956).

Table IV: Sample Collection of Dunham Corrected  $\omega_e$ 's and  $r_e$ 's

Molecule	State	$\omega_e$ obs	Corrected $\omega_e$	$r_e$ obs	Corrected $r_e$
C <sub>2</sub>	A <sup>3</sup> Π <sub>g</sub>	1788.22	1788.30	1.26600	1.26575
(CO) <sup>+</sup>	X <sup>2</sup> Σ <sup>+</sup>	2214.24	2214.30	1.11506	1.11481
I <sub>2</sub>	X <sup>1</sup> Σ <sup>+</sup>	214.251	214.251	2.66660	2.66483
Li <sub>2</sub>	X <sup>1</sup> Σ <sub>g</sub> <sup>+</sup>	351.44	351.44	2.67250	2.67183
N <sub>2</sub>	X <sup>1</sup> Σ <sub>g</sub> <sup>+</sup>	2357.78	2357.84	1.097100	1.09715
N <sub>2</sub>	C <sup>3</sup> Π <sub>u</sub>	2035.10	2035.23	1.14820	1.14794
NO	X <sup>2</sup> Π <sub>3/2</sub>	1903.68	1903.75	1.15080	1.15049
Na <sub>2</sub>	X <sup>1</sup> Σ <sub>g</sub> <sup>+</sup>	159.23	159.23	3.07860	3.07830
O <sub>2</sub>	X <sup>3</sup> Σ <sub>g</sub> <sup>-</sup>	1580.36	1580.42	1.207398	1.207068
O <sub>2</sub>	b <sup>1</sup> Σ <sub>g</sub> <sup>+</sup>	1432.69	1432.78	1.22675	1.22636
<sup>1</sup> H <sub>2</sub>	X <sup>1</sup> Σ <sub>g</sub> <sup>+</sup>	4400.39	4403.39	0.74158	0.73632
<sup>1</sup> H <sub>2</sub>	B <sup>1</sup> Σ <sub>g</sub> <sup>+</sup>	1358.94	1359.44	1.29253	1.27902
LiH	X <sup>1</sup> Σ <sup>+</sup>	1405.65	1405.88	1.59535	1.59303
Mg <sup>1</sup> H	A <sup>2</sup> Π <sub>r</sub>	1611.30	1611.18	1.67950	1.67792

TABLE V\*: Coefficients of  $(v+1/2)^n$  for  $x^1 \sum g^+$  State of  $H_2$  with Respect to the Number of Terms in the Power Series.

	$\omega_e$	$\omega_e x_e$	$\omega_e y_e$	$\omega_e z_e$
a	4400.39	120.815	0.72419	
b	4401.39	121.727	1.04515	-0.08904
c	4396.55	117.973	0.04339	0.08904
d	4399.46	119.605	0.18124	0.14939
e	4397.79	117.448	-1.24944	0.56462
f	4404.59	124.158	1.71223	0.09916

\*a refers to a three term equation; b, a four term; c, a five term; d, another five term; e, a six term equation; and f, a least squares four term equation of the first eight G values.

TABLE VI: Values for the Rotational Constants as a Function of the Number of Terms in the  $B_v$  Equation.

Number of Terms	$B_e$	$\alpha_e$	$\gamma_e$
3	60.8537	3.0483	0.0388 <sub>0</sub>
4	60.8643	3.0810 <sub>8</sub>	0.0644 <sub>5</sub>
5	60.868 <sub>7</sub>	3.0958 <sub>3</sub>	0.0788 <sub>7</sub>
6	60.8790	3.1326	0.1202 <sub>3</sub>

## CARBON-HYDROGEN STRETCHING VIBRATIONS IN FLUOROCYCLOHEXANES

D. STEELE and D. H. WHIFFEN

The Chemistry Department, The University, Edgbaston, Birmingham 15

(Received 11 October 1957)

**Abstract**—For perfluorocyclohexane derivatives in which not more than one fluorine at each carbon atom is replaced by a hydrogen atom, it is established that C-H groups with an axial hydrogen show infra-red absorption at  $2980\text{ cm}^{-1}$  and with equatorial hydrogen at  $2974\text{ cm}^{-1}$ . With 1H/2H-, 1H:2H/- and 1H:3H/-decafluorocyclohexane the frequencies are reduced somewhat. When the C-H groups are adjacent to a double bond the absorption is at  $2961\text{ cm}^{-1}$ , while olefinic C-H groups absorb near  $3095\text{ cm}^{-1}$  in the fluorocarbon series. The C-H absorption is at  $3102\text{ cm}^{-1}$  in pentafluorobenzene.

MANY perfluorocyclohexane derivatives have recently become available<sup>1-5</sup> for infra-red spectral investigation\* and when provided several of their structures were uncertain. In order to establish spectral correlations which might be useful in structure determination, it was decided to measure the carbon-hydrogen stretching frequencies near  $3000\text{ cm}^{-1}$  under high resolution to see if hydrogen atoms in the axial and equatorial positions could be differentiated.

### RESULTS

Table 1 shows the frequencies and approximate extinction coefficients in the gas phase. The boiling points are given to aid identification with the literature<sup>1-5</sup> where the preparation and the structure determinations are discussed. The second column of the table indicates the axial, *a*, equatorial, *e*, or olefinic, *o*, nature of the hydrogen atoms in the order quoted in the name. For the polyhydro compounds the numbering of the hydrogen atoms on one side of the cyclohexane ring are given in front of the solidus and the substituents *trans* to these, thereafter.

### DISCUSSION

For the saturated compounds at the head of Table 1 the carbon-hydrogen stretching frequency lies in the narrow range  $2968$  to  $2984\text{ cm}^{-1}$ , and it would seem that the variation between axial and equatorial substituents is much less than in the deuterated steroids<sup>7</sup> where the axial C-D links are found to absorb about  $40\text{ cm}^{-1}$  below the equatorial. Nevertheless a closer inspection shows that an isolated axial hydrogen,

\* The full spectra will be submitted to the Documentation of Molecular Spectroscopy punched card collection. Comparison of the spectra of dodecafluorocyclohexane and undecafluorocyclohexane confirm that the sample of the former used by Rowlinson and Thacker<sup>6</sup> contained some of the undecafluoro-body indicated by absorption at  $730$ ,  $830$  and  $943\text{ cm}^{-1}$  as these authors themselves suggest.

<sup>1</sup> R. P. Smith and J. C. Tatlow, *J. Chem. Soc.* 2505 (1957).

<sup>2</sup> D. E. M. Evans, J. A. Godsell, R. Stephens, J. C. Tatlow and E. H. Wiseman, *Tetrahedron* 2, 183 (1958).

<sup>3</sup> J. A. Godsell, M. Stacey and J. C. Tatlow, *Tetrahedron* 2, 193 (1958).

<sup>4</sup> G. B. Barlow, M. Stacey and J. C. Tatlow, *J. Chem. Soc.* 6090 (1955).

<sup>5</sup> R. Stephens and J. C. Tatlow, *Chem. & Ind.* 821 (1957).

<sup>6</sup> J. S. Rowlinson and R. Thacker, *Trans. Faraday Soc.* 53, 1, (1957).

<sup>7</sup> E. J. Corey, R. A. Sneen, M. G. Danaher, R. L. Young and R. L. Rutledge, *Chem. & Ind.* 1294 (1954).

TABLE I

Name		cm <sup>-1</sup>	$\epsilon$	Boiling point
Saturated				
Undecafluorocyclohexane	<i>a</i>	2979	8	63°C
1H/2H-decafluorocyclohexane	<i>a/a</i>	2977	12	70
1H:2H/- " " "	<i>a:e/</i>	2974, 2969	10, 6	91
1H:3H- " " "	<i>a/e</i>	2979, 2973	15, 3	78
1H:3H/- " " "	<i>a:a/</i>	2974	20	89
1H:4H- " " "	<i>a/a</i>	2980	15	78
1H:4H/- " " "	<i>a:e/</i>	2979, 2973	11, 11	86
1H/2H:4H-nonafluorocyclohexane	<i>a/a:a</i>	2983, 2974	5, 20	101
1H:4H/2H- " "	<i>a:e/a</i>	2984, 2979, 2973	9, 10, 9	93
1H:2H/4H- " "	<i>a:e/a</i>	2979, 2974	12, 10	107
1H:2H:4H/- " "	<i>e:a/a/</i>	2973, 2968	10, 8	136
1H:4H/2H:5H-octafluorocyclohexane	<i>a:e/a:e</i>	2979, 2974, 2970	10, 15, 8	118
*1CF <sub>3</sub> /4H-tridecafluoromethyl-cyclohexane	<i>/e</i>	2974	9	88 II <sup>a</sup>
*1CF <sub>3</sub> :4H/- " " "	<i>e/</i>	2981	11	88 I <sup>a</sup>
Mono-olefines				
1H-nonafluorocyclohexene	<i>o</i>	3104, 3073	7, 4	63
3H- " "	<i>x</i>	2961	8	69
4H- " "	( <i>a</i> )	2983	8	71
1H:2H-octafluorocyclohexene	<i>o:o</i>	3085	liq.	87
3H/4H- " "	<i>x/(a)</i>	2980, 2962	9, 7	86
3H:4H/- " "	<i>x:(a)/</i>	2979, 2960	7, 7	116
4H/5H- " "	( <i>a</i> )/( <i>o</i> )	2977, 2970	10, 8	90
4H:5H/- " "	( <i>a</i> ):( <i>e</i> )/	2979, 2975	8, 8	99
1H:5H- " "	<i>o:(a)</i>	3102, 3067, 2980	3, 6, 8	85
Polyenes				
1H-heptafluorocyclohexa-1:3-diene	<i>o</i>	3113, 3084	15, 4	72
2H- " "	<i>o</i>	3098	6	76
1H-heptafluorocyclohexa-1:4-diene	<i>o</i>	3097	8	67
*1H:4H-hexafluorocyclohexa-1:4-diene	<i>o:o</i>	3087	19	—
*1H:5H- " " "	<i>o:o</i>	3082	19	71
Pentafluorobenzene	<i>ar</i>	3102	4	89

*a* = axial, (*a*) = pseudoaxial, *e* = equatorial, (*e*) = pseudoequatorial, *o* = olefinic, *x* = adjacent to double bond, *ar* = aromatic.

\* These structures are not yet proved by chemical means, but are based on the methods of preparation and the infra-red spectra.

as in undecafluoro-, 1H/3H-, 1H:4H/- or 1H/4H-decafluorocyclohexane, absorbs at  $2980 \pm 2$  cm<sup>-1</sup> and that an isolated equatorial hydrogen absorbs at  $2974 \pm 2$  cm<sup>-1</sup>, as in the 1H/3H- and 1H:4H/-decafluorocyclohexanes. Indeed the identification between the *cis/trans* 1H:4H-isomers was originally made on the grounds that the first isomer obtained showed two overlapping bands and was therefore unlikely to be the *trans*-isomer which would be centrosymmetric and have only one infra-red active C-H stretch. This expectation was confirmed when the *trans*-isomer became available

and shown to have only one band: the identification has subsequently<sup>3</sup> been confirmed by dipole moment measurements. Based on the infra-red differentiation between axial and equatorial hydrogen atoms, it is possible to identify the isomers of 4H-tridecafluoromethylcyclohexane.<sup>4,8</sup> The bulky trifluoromethyl group in these compounds will ensure that the molecules adopt that conformation of the cyclohexane ring in which the  $-\text{CF}_3$  group is lying equatorially. A *trans*-hydrogen atom at position 4 must also be equatorial and would absorb at  $2974\text{ cm}^{-1}$  as observed for the isomer designated<sup>8</sup> II, whereas a *cis*-hydrogen at position 4 would be axial and the observed absorption at  $2981\text{ cm}^{-1}$  for isomer I is in accord with the predicted  $2980\text{ cm}^{-1}$  for this arrangement.

The frequencies given above for axial and equatorial hydrogens are shifted slightly when two hydrogens are on adjacent atoms in the ring or are both in axial positions on the same side of the plane of the ring. In the 1H/2H-compound one band is observed at  $2977\text{ cm}^{-1}$  which is only  $3\text{ cm}^{-1}$  from the expected position since both hydrogens are axial. This will be the out-of-phase C-H stretch, as the in-phase vibration will be almost inactive in the infra-red since the dipole moment change would, from symmetry considerations, be parallel to the twofold symmetry axis and consequently approximately perpendicular to the C-H bonds which are stretching. With 1H:2H/-decafluorocyclohexane the decrease in frequency is slightly greater and the bands are at  $2974$  and  $2969\text{ cm}^{-1}$ ; in this compound the hydrogens are closer together in space and it is perhaps a consequence of this that the frequencies move towards the hydrocarbon values. The hydrogens are also close in space in the 1H:3H/-compound in which they occupy axial positions on the same side of the ring plane and the frequency is again reduced about  $6\text{ cm}^{-1}$  to  $2974\text{ cm}^{-1}$ . In this case the single band observed will be the in-phase motion, since the out-of-phase motion must produce a dipole moment change perpendicular to the plane of symmetry and approximately perpendicular to the C-H bonds and so be very weak.

Experience with the 1H:2H:4H-nonafluorocyclohexanes suggests that their C-H stretching frequencies are governed by similar rules. Except when involved in 1H:2H/- or 1H:3H/-structures the C-H absorptions remain near  $2980\text{ cm}^{-1}$  when axial, and  $2974\text{ cm}^{-1}$  when equatorial, with a slight lowering for the 1H/2H-system. Again the characteristic frequency for the 1H:3H/-structures is  $2974\text{ cm}^{-1}$  when diaxial and the 1H:2H/-arrangement again gives a pair of bands near  $2974$  and  $2969\text{ cm}^{-1}$ . For example 1H/2H:4H-nonafluorocyclohexane (*a/a,a*) has absorption at  $2974\text{ cm}^{-1}$  attributable to the 1 : 3 diaxial structure of hydrogens on  $\text{C}_{(2)}$  and  $\text{C}_{(4)}$ ; this band is about double the intensity of that at  $2983\text{ cm}^{-1}$  which must be attributed to the isolated axial hydrogen on  $\text{C}_{(1)}$ .

In the fluorocyclohexene series there is seen from Table 1 to be a possibility of distinguishing hydrogen substitution at positions 4 and 5 from that at 3 and 6. The conformation will be the usual half chair form and the local arrangement at positions 4 and 5 is hardly to be distinguished from that in the cyclohexane series; the substituents are normally designated pseudo-axial and pseudo-equatorial. It is to be expected that the hydrogen atoms will prefer the pseudo-axial position and this is consistent with the frequency of  $2983\text{ cm}^{-1}$  in 4H-nonafluorocyclohexene. The three cyclohexene derivatives with the hydrogen at position 3 absorb at  $2960$ ,  $2961$  and  $2962\text{ cm}^{-1}$  respectively, and absorption at  $2961\text{ cm}^{-1}$  must be considered characteristic

<sup>8</sup> R. P. Smith, Ph.D. Thesis, University of Birmingham.



for substitution at this position. Indeed when first available the 3H:4H/- and 4H:5H/-octafluorocyclohexenes were merely known to be products of dehydrofluorination of 1H:2H/4H-nonafluorocyclohexane and these structures were suggested from the infra-red spectra and their confirmation by chemical methods consequently accelerated. In assigning structures the 3H-absorption in the cyclohexenes at  $2961\text{ cm}^{-1}$  was especially valuable.

Olefinic hydrogens appear to absorb in the range  $3070$  to  $3120\text{ cm}^{-1}$  according to the type of unsaturated system and the point of attachment thereto. There are insufficient examples to indicate the exact pattern to be expected except to comment that hydrogen attached to a 1:3-diene system absorbs at the upper end of this range and that in some cases the band was unexpectedly split, possibly by Fermi resonance. In the one case examined with hydrogens attached at both ends of a double bond, 1H:2H-octafluorocyclohexene, the absorption was too weak to measure accurately in the vapour.

In pentafluorobenzene the C-H stretching frequency at  $3102\text{ cm}^{-1}$  is slightly higher than the fundamental frequencies of 1:2:4:5-tetrafluorobenzene<sup>8,9</sup> at  $3097\text{ cm}^{-1}$  ( $A_g$ ) and  $3088\text{ cm}^{-1}$  ( $B_{1u}$ ).

It is clear that in all these compounds the presence of the fluorine raises the C-H stretching frequency by about  $70\text{ cm}^{-1}$  compared with the hydrocarbons. Taking average hydrocarbon frequencies<sup>10,11</sup> the comparison shown in Table 2 is obtained. The frequency shifts are probably electronic in origin.

TABLE 2

	Hydrocarbon	Fluorocarbon	Difference
Naphthenic C-H	$2890\text{ cm}^{-1}$	$2980\text{ cm}^{-1}$	$+90\text{ cm}^{-1}$
Olefinic C-H	$3020\text{ cm}^{-1}$	$3080\text{ cm}^{-1}$	$+60\text{ cm}^{-1}$
Aromatic C-H	$3040\text{ cm}^{-1}$	$3100\text{ cm}^{-1}$	$+60\text{ cm}^{-1}$

## EXPERIMENTAL

The compounds were measured in the gas phase in a 10 cm absorption cell using a 2500 l.p.i. N.P.L. replica grating of size 6 in.  $\times$  6 in. in the third order on the spectrometer previously described.<sup>12</sup> The frequencies are thought to be correct to  $\pm 2\text{ cm}^{-1}$  the chief error being that of locating the centre of the wide bands, especially when they overlap. The extinction coefficients<sup>11</sup>,  $\epsilon$ , are maximum values for non-overlapping bands and are approximate estimates of the separate intensities for overlapping bands; they are quoted to indicate relative intensities in each compound.

*Acknowledgements*—We wish to thank Dr. J. C. Tatlow and his co-workers Drs. D. E. M. Evans, J. A. Godsell, R. P. Smith, R. Stephens and Messrs. E. Nield and E. H. Wiseman for providing the compounds and for many discussions. We also wish to thank Professor M. Stacey for his interest in the work and Dr. L. A. Sayce for making the grating available. D. S. wishes to acknowledge the receipt of a University Appeal Scholarship.

<sup>8</sup> E. E. Ferguson, R. L. Hudson, J. R. Nielsen and D. C. Smith, *J. Chem. Phys.* **21**, 1464 (1953).

<sup>10</sup> L. J. Bellamy, *Infra-red Spectra of Complex Molecules*. Methuen, London (1954).

<sup>11</sup> R. N. Jones and C. Sandorfy, *Techniques of Organic Chemistry* p. 247, Vol. 9. Interscience, New York (1956).

<sup>12</sup> H. Spedding and D. H. Whiffen, *Proc. Roy. Soc. A* **238**, 245 (1956).

[Reprinted from the Journal of the American Chemical Society, 83, 2262 (1961).]  
 Copyright 1961 by the American Chemical Society and reprinted by permission of the copyright owner.

[CONTRIBUTION FROM THE DEPARTMENT OF CHEMISTRY, UNIVERSITY OF MARYLAND, COLLEGE PARK, MARYLAND]

## The Vibrational Spectra and Structure of Bis-cyclopentadienylmagnesium

BY ELLIS R. LIPPINCOTT, J. XAVIER<sup>1</sup> AND D. STEELE<sup>1</sup>

RECEIVED NOVEMBER 30, 1960

A study of the infrared and Raman spectra of bis-cyclopentadienylmagnesium in solution and in the solid state is reported. A comparison of the observed vibrational frequencies with those obtained for ferrocene indicate that the molecular geometry is best represented by a "sandwich" structure. An assignment of frequencies has been made which is quite similar to that reported for ferrocene and related compounds. The results are not in agreement with the early reports of an essentially ionic bonding in bis-cyclopentadienylmagnesium and are better explained by the presence of covalent ring-to-metal bonding, which is weaker than the metal to ring bonding in ferrocene.

### Introduction

The discovery of ferrocene has led to the synthesis and characterization of a large number of organo-metallic compounds.<sup>2-4</sup> Physicochemical investigations have reasonably well established the molecular structure and the type of chemical bonding in most of these substances. However, there still exist some doubts regarding the nature of the bonding in metal cyclopentadienyls and their derivatives.

A pentagonal antiprismatic structural configuration has been assigned to ferrocene and similar cyclopentadienyls. Weiss and Fischer<sup>5</sup> have shown that in the crystal form  $Mg(C_5H_5)_2$  has a "sandwich" configuration and proposed a rather weak covalent  $d^2sp^3$  hybridization overlapping the ionic electrostatic binding between the metal and cyclopentadienyl ions. However, based on magnetic, spectral and chemical investigations, Wilkinson, *et al.*,<sup>6</sup> conclude that the bonding in bis-cyclopentadienyl  $Mg(II)$  and  $Mn(II)$  is essentially ionic. According to these authors, two cyclopentadienide anions are expected on electrostatic grounds to align themselves on opposite sides of the cation with their planes parallel, the structure thus very closely resembling that of "sandwich bonded" molecules, such as ferrocene. The configuration in the case of the ionic molecules (*e.g.*,  $Mn(C_5H_5)_2$  or  $Mg(C_5H_5)_2$ ) is thus assumed to be due merely to the geometry resulting from charge distribution, whereas in the case of ferrocene-like

molecules, it is a requirement of the metal-to-ring covalent bonding. This postulation of difference in bond type has been prompted by notable differences in chemical properties, by conductivity measurements in liquid ammonia<sup>5</sup> and by mass spectra measurements and determination of appearance potentials.<sup>7</sup> The mass spectra do not provide confirmative evidence regarding the configuration. However, the stability of the parent compound is indicated by the stability of molecule-ions in the mass spectra. In the case of  $Mg$  and  $Mn$  cyclopentadienides, the parent molecule-ions  $C_{10}H_{10}M^+$  are relatively unstable, contributing only 20% to the total ion yield in contrast to the  $Fe$ ,  $Co$ ,  $Cr$ , etc., compounds, in which the molecule-ion contributes roughly 50% or more of the total ion yield. The instability of the molecule-ions in  $Mg$  and  $Mn$  compounds again is evidenced by the enhanced yields of  $C_5H_5M^+$  and  $M^+$  ions. These observations, along with the chemical properties of the compounds, such as metathetical reactions with ferrous chloride to form ferrocene, hydrolysis with water, etc., have led the previous workers<sup>5-7</sup> to reach the conclusion that the metal-to-ring bond in  $Mn$  and  $Mg$  cyclopentadienyls is of a quite different nature from that of the bonding in ferrocene-type molecules.

The concept of ionic bonding in  $Mg(C_5H_5)_2$  has been discussed by Cotton and Reynolds.<sup>8</sup> The analogy between the spectrum of  $Mg(C_5H_5)_2$ , especially in the C-H stretching region, and those of ferrocene and nickelocene indicate the sandwich structure in the free state. The existence of the ionic bonding in the magnesium compound has then been evaluated from a consideration of the molecular orbital overlap and on the basis of ionization potentials. Finally, they conclude that the magnesium compound does behave as though

- (1) Post-doctoral Research Fellows.
- (2) (a) M. Rausch, M. Vogel and H. Rosenberg, *J. Chem. Ed.*, **34**, 268 (1957); (b) E. O. Fischer, *Angew. Chem.*, 475 (1955).
- (3) P. L. Pauson, *Quart. Rev. (London)*, **9**, No. 4, 391 (1955).
- (4) "Advances in Inorganic Chemistry and Radiochemistry," Editors, H. J. Emeleus and A. G. Sharp, Vol. I, Academic Press, Inc., New York, N. Y., 1959, p. 55.
- (5) E. Weiss and E. O. Fischer, *Z. anorg. u. allgem. Chem.*, **278**, 219 (1955); E. O. Fischer and S. Schreiner, *Ber.*, **92**, 938 (1959).
- (6) G. Wilkinson, F. A. Cotton and J. M. Birmingham, *J. Inorg. Nuclear Chem.*, **2**, 95 (1956).

(7) L. Friedman, A. P. Irsa and G. Wilkinson, *J. Am. Chem. Soc.*, **77**, 3689 (1955).

(8) F. A. Cotton and L. T. Reynolds, *ibid.*, **80**, 269 (1958).

[CONTRIBUTION FROM THE DEPARTMENT OF CHEMISTRY, UNIVERSITY OF MARYLAND, COLLEGE PARK, MARYLAND]

## The Vibrational Spectra and Structure of Bis-cyclopentadienylmagnesium

BY ELLIS R. LIPPINCOTT, J. XAVIER<sup>1</sup> AND D. STEELE<sup>1</sup>

RECEIVED NOVEMBER 30, 1960

A study of the infrared and Raman spectra of bis-cyclopentadienylmagnesium in solution and in the solid state is reported. A comparison of the observed vibrational frequencies with those obtained for ferrocene indicate that the molecular geometry is best represented by a "sandwich" structure. An assignment of frequencies has been made which is quite similar to that reported for ferrocene and related compounds. The results are not in agreement with the early reports of an essentially ionic bonding in bis-cyclopentadienylmagnesium and are better explained by the presence of covalent ring-to-metal bonding, which is weaker than the metal to ring bonding in ferrocene.

### Introduction

The discovery of ferrocene has led to the synthesis and characterization of a large number of organo-metallic compounds.<sup>2-4</sup> Physicochemical investigations have reasonably well established the molecular structure and the type of chemical bonding in most of these substances. However, there still exist some doubts regarding the nature of the bonding in metal cyclopentadienyls and their derivatives.

A pentagonal antiprismatic structural configuration has been assigned to ferrocene and similar cyclopentadienyls. Weiss and Fischer<sup>5</sup> have shown that in the crystal form  $Mg(C_5H_5)_2$  has a "sandwich" configuration and proposed a rather weak covalent  $d^2sp^3$  hybridization overlapping the ionic electrostatic binding between the metal and cyclopentadienyl ions. However, based on magnetic, spectral and chemical investigations, Wilkinson, *et al.*,<sup>6</sup> conclude that the bonding in bis-cyclopentadienyl  $Mg(II)$  and  $Mn(II)$  is essentially ionic. According to these authors, two cyclopentadienide anions are expected on electrostatic grounds to align themselves on opposite sides of the cation with their planes parallel, the structure thus very closely resembling that of "sandwich bonded" molecules, such as ferrocene. The configuration in the case of the ionic molecules (*e.g.*,  $Mn(C_5H_5)_2$  or  $Mg(C_5H_5)_2$ ) is thus assumed to be due merely to the geometry resulting from charge distribution, whereas in the case of ferrocene-like

molecules, it is a requirement of the metal-to-ring covalent bonding. This postulation of difference in bond type has been prompted by notable differences in chemical properties, by conductivity measurements in liquid ammonia<sup>7</sup> and by mass spectra measurements and determination of appearance potentials.<sup>7</sup> The mass spectra do not provide confirmative evidence regarding the configuration. However, the stability of the parent compound is indicated by the stability of molecule-ions in the mass spectra. In the case of  $Mg$  and  $Mn$  cyclopentadienides, the parent molecule-ions  $C_{10}H_{10}M^+$  are relatively unstable, contributing only 20% to the total ion yield in contrast to the  $Fe$ ,  $Co$ ,  $Cr$ , etc., compounds, in which the molecule-ion contributes roughly 50% or more of the total ion yield. The instability of the molecule-ions in  $Mg$  and  $Mn$  compounds again is evidenced by the enhanced yields of  $C_5H_5M^+$  and  $M^+$  ions. These observations, along with the chemical properties of the compounds, such as metathetical reactions with ferrous chloride to form ferrocene, hydrolysis with water, etc., have led the previous workers<sup>5-7</sup> to reach the conclusion that the metal-to-ring bond in  $Mn$  and  $Mg$  cyclopentadienyls is of a quite different nature from that of the bonding in ferrocene-type molecules.

The concept of ionic bonding in  $Mg(C_5H_5)_2$  has been discussed by Cotton and Reynolds.<sup>8</sup> The analogy between the spectrum of  $Mg(C_5H_5)_2$ , especially in the C-H stretching region, and those of ferrocene and nickelocene indicate the sandwich structure in the free state. The existence of the ionic bonding in the magnesium compound has then been evaluated from a consideration of the molecular orbital overlap and on the basis of ionization potentials. Finally, they conclude that the magnesium compound does behave as though

(7) L. Friedman, A. P. Irsa and G. Wilkinson, *J. Am. Chem. Soc.*, **77**, 3689 (1955).

(8) F. A. Cotton and L. T. Reynolds, *ibid.*, **80**, 269 (1958).

(1) Post-doctoral Research Fellows.

(2) (a) M. Rausch, M. Vogel and H. Rosenberg, *J. Chem. Ed.*, **34**, 268 (1957); (b) E. O. Fischer, *Angew. Chem.*, 475 (1955).

(3) P. L. Pauson, *Quart. Rev. (London)*, **9**, No. 4, 391 (1955).

(4) "Advances in Inorganic Chemistry and Radiochemistry," Editors, H. J. Emeléus and A. G. Sharp, Vol. I, Academic Press, Inc., New York, N. Y., 1959, p. 55.

(5) E. Weiss and E. O. Fischer, *Z. anorg. u. allgem. Chem.*, **278**, 219 (1955); E. O. Fischer and S. Schreiner, *Ber.*, **92**, 938 (1959).

(6) G. Wilkinson, F. A. Cotton and J. M. Birmingham, *J. Inorg. Nuclear Chem.*, **2**, 95 (1956).

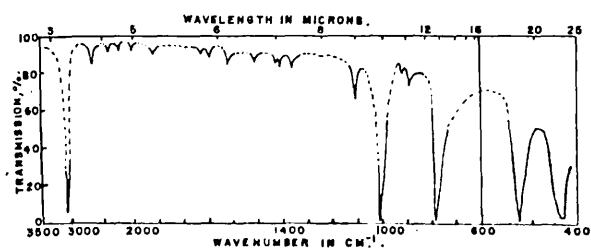


Fig. 1.—Infrared spectrum of  $\text{Mg}(\text{C}_5\text{H}_5)_2$  in benzene solution; concentration, approximately 1 M.

the net charge separation is appreciable, this leading to a tendency toward ionic dissociation.

The metal-to-ring bond energies calculated by subtracting ionization potentials of the free metal atom from the appearance potential of the corresponding ion from  $(\text{C}_5\text{H}_5)_2\text{M}$  also indicate weaker bonding in  $\text{Mg}(\text{C}_5\text{H}_5)_2$  and  $\text{Mn}(\text{C}_5\text{H}_5)_2$ .<sup>7</sup>

The structure of the so-called "ionic" metal-cyclopentadienyls thus seems to be an interesting problem. The present work was undertaken with the idea of gaining a better insight into the nature of the bonding between the metal and the cyclopentadienyl ring in  $\text{Mg}(\text{C}_5\text{H}_5)_2$ .

#### Experimental

Bis-cyclopentadienylmagnesium was prepared according to the method of Wilkinson, *et al.*<sup>5</sup> The cyclopentadienylmagnesium bromide was decomposed in vacuum ( $\sim 10^{-4}$  mm.) and the sublimate led through a glass-wool plug into a tube into which the solvent was later distilled. The apparatus was designed primarily to exclude air and moisture which would instantaneously decompose the product. By this method, the compound could be purified by a multiple sublimation process. The purity of the sample was established by melting point determination in a sealed tube (observed 176–179°) and also by the colorless solution obtained in benzene or cyclohexane. The final transfer of the solution to the Raman tube was cautiously made after sealing the ends and allowing the solution to flow slowly into the Raman tube, avoiding the transference of solid particles along with the solution. A near saturated solution (at room temperature) was thus sealed into the Raman tube. Benzene and cyclohexane were employed as solvents, the solubility being greater in the former solvent. The solvents were degassed before placing them in the tube containing the cyclopentadienylmagnesium.

Raman spectra were obtained by using a two-prism Huet spectrograph (aperture F/8) with a dispersion of 18 Å./mm. at 4358 Å. Excitation with both 4358 and 5461 Å. Hg was accomplished with a low pressure, water-cooled Toronto arc, using filters and photographic plates described earlier.<sup>9</sup> Infrared spectra were run on a Beckman IR4 automatic recording spectrophotometer. Cells of thickness 0.004 and 0.015 cm. were used for solutions, the openings having been sealed tightly with Teflon plugs and "Bi-Seal" self-bonding electrical tape (Bishop Manufacturing Corp. Cedar Grove, N. Y.) after insertion of the solutions. Spectra in the region 400–800  $\text{cm}^{-1}$  were studied with the same solutions using AgCl cells. The infrared spectra of the solid compound were taken using a diamond cell.<sup>10</sup> The cell was loaded inside a dry box containing an inert atmosphere. Medium pressure was applied between the diamonds. It was found that little decomposition occurred during the time of running of the spectra, as no appreciable change was observed in several consecutive spectra taken over a period of 2 to 3 hr.

The infrared spectra are reproduced in Figs. 1–3. The vibrational spectrum of cyclopentadienylmagnesium is

(9) E. R. Lippincott and R. D. Nelson, *Spectrochim. Acta*, **10**, 307 (1958).

(10) C. E. Weir, E. R. Lippincott, A. Van Valkenberg and E. N. Bunting, *J. Research Natl. Bur. Standards*, **A63**, 55 (1959); E. R. Lippincott, C. E. Weir and F. E. Welsh, *Anal. Chem.* (accepted for publication).

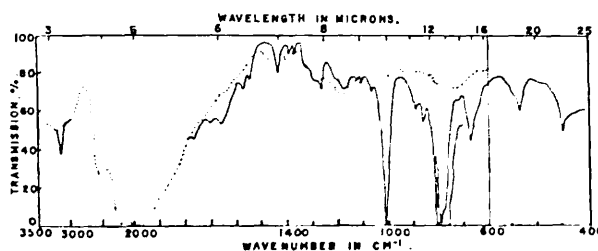


Fig. 2.———, infrared spectrum of  $\text{Mg}(\text{C}_5\text{H}_5)_2$  in solid state using diamond cell; ..... , spectrum of diamond cell.

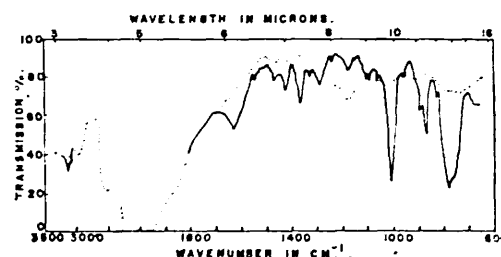


Fig. 3.———, infrared spectrum of  $\text{Mn}(\text{C}_5\text{H}_5)_2$  in solid state using diamond cell; ..... , spectrum of diamond cell.

listed in Table I, along with those of ferrocene and ruthenocene for comparison. The infrared spectra of cyclopentadienylmagnesium and -manganese in the solid state are given in Table II.

TABLE I

THE VIBRATIONAL SPECTRA OF  $\text{Mg}(\text{C}_5\text{H}_5)_2$ ,  $\text{Fe}(\text{C}_5\text{H}_5)_2^a$  AND  $\text{Ru}(\text{C}_5\text{H}_5)_2^a$

$\text{Mg}(\text{C}_5\text{H}_5)_2$		$\text{Fe}(\text{C}_5\text{H}_5)_2$		$\text{Ru}(\text{C}_5\text{H}_5)_2$	
Raman	Infrared (in solution)	Raman	Infrared	Raman	Infrared
191ms			170m		
229w		303m		330s	
		388w		402m	
	440ms		478s		446s
	526ms		492s		528w
752vw	783s		782w		763w
806vvw	890vw		811s	804w	806s
	915vvw		834w		835w
(1000)	1008s	1010w	1002s	996m	1002s
		1050w	1051w	1056m	1050m
1109ms	1108m	1105s	1108s	1112s	1104s
1163ms		1178m	1188w	1193w	
	1344vvw	1363vw	1356w		1360w
1410vvw	1420w	1408vw	1411s	1412m	1413m
	1425vw				
	1516vvw	1566vw			
	1610m				
	1625vw		1620m		1622m
			1650m		1651m
	1700vvw		1684m		1684m
	1736vvw		1720m		1727m
	1928vvw		1758m		1774m
	2050vvw				
	2395vvw				
(3080)	2600vvw	3085m		3089m	
3104s	3080s	3099s	3085s	3104s	3100m

<sup>a</sup> From ref. 9. s = strong; m = medium; w = weak; v = very.

The crystal spectra obtained using the diamond cell are in fairly good agreement with those run by the KBr disc

TABLE II  
 INFRARED SPECTRA OF  $Mg(C_5H_5)_2$  AND  $Mn(C_5H_5)_2$  IN SOLID STATE

KBr disc <sup>a</sup>	STATE		Mn(C <sub>5</sub> H <sub>5</sub> ) <sub>2</sub> Diamond pressure cell
	Mg(C <sub>5</sub> H <sub>5</sub> ) <sub>2</sub> Single crystal <sup>b</sup>		
441m		442m	
524m		527m	
663m		668m	
	700s		
758s	760s	764ms	748w
			765w
779vw		780s	780s
891		858w	830vw
		886vw	868ms
913			
959			960w
1004s	980ms	1008s	1008s
	1020w		1045vvw
1058		1060vvw	1062vw
1108	1100w	1106w	1095w
			1110w
		1176w	1158vw
			1176vw
1257	1250ms	1260w	1240w
1364	1345m	1368vw	1364m
	1395vw		
1428m	1430ms	1434m	1426m
	1480vw		1466w
1516	1540m	1540vw	1545vw
		1570vw	
1629	1605vw	1652vw	1634m
	1675vvw	1700vvw	
1751	1740w		
	1860vvw		
	1960vw		
2050	2070ms		
	2200ms		
(2249)	2270ms		
	2330vvw		
2373	2390vw		
	2460vw		
	2610vw		
2658	2640w		
	2730vw		
	2840vvw		
2913	3000w		
3063m	3060s	3100ms	3106ms
	3145w		

<sup>a</sup> From ref. 11. <sup>b</sup> From ref. 6 (approximate readings from the figure).

technique<sup>11</sup> as well as those obtained in solutions (Tables I and II). The deviation of the frequencies and intensities from those obtained by Wilkinson, *et al.*,<sup>6</sup> for a single-crystal spectrum is due to the interference of decomposition products. The spectra of bis-cyclopentadienylmagnesium (and manganese) run at long intervals of time using the diamond cell, also showed such deviations of frequencies and intensities, which were similar to those obtained by Wilkinson, *et al.*, on single-crystal spectra. The bis-cyclopentadienylmanganese(II) decomposed much more easily in the diamond cells than the corresponding magnesium compound. The increase in absorption intensities of bands at about 1008 1106 and 1420  $cm^{-1}$  during decomposition of the original compounds is observed readily and leaves little doubt that the spectrum reported for the single crystal contains large amounts of decomposed products.

**Assignment of Frequencies.**—A detailed account of the vibrational spectra of ferrocene, ruthenocene and nickelocene has been given by Lippincott and Nelson.<sup>9</sup> The fre-

(11) H. P. Fritz, *Chem. Ber.*, **92**, 780 (1959).

 TABLE III  
 FREQUENCY ASSIGNMENTS (FUNDAMENTAL MODES OF VIBRATION)<sup>a</sup>

Species	Pre- quency	Mg(C <sub>5</sub> H <sub>5</sub> ) <sub>2</sub>	Description	
A <sub>1g</sub> (Raman)	1	3104	Sym. CH stretching	
	2	806	Sym. CH bending (⊥)	
	3	1109	Sym. ring breathing	
	4	191	Sym. ring metal stretching	
A <sub>1u</sub> (inactive)	5	(1250) <sup>b</sup>	CH bending (  )	
	6	...	Internal rotation	
A <sub>2g</sub> (inactive)	7	(1200)	CH bending	
A <sub>2u</sub> (infrared)	8	3080	CH stretching	
	9	783	CH bending	
	10	1108	Antisym. ring breathing	
	11	526	Antisym. ring metal stretching	
	E <sub>1g</sub> (Raman)	12	(3085)	CH stretching
		13	(990)	CH bending (  )
		14	806	CH bending (⊥)
		15	1410	Sym. C-C stretch
		16	229	Sym. ring tilt
	E <sub>1u</sub> (infrared)		(186 calcd.)	
		17	(3100)	CH stretching
18		1008	CH bending (  )	
19		886 <sup>b</sup>	CH bending (⊥)	
20		1420	Antisym. C-C stretching	
21		440	Antisym. ring tilt	
E <sub>2g</sub> (Raman)	22	107	Ring metal ring bending	
		(calcd.)		
	23	(3085)	CH stretching	
	24	1163	CH bending (  )	
	25	(1050)	CH bending (⊥)	
	26	(1560)	C-C stretching	
	27	(885)	Ring distortion (  )	
	28	(570)	Ring distortion (⊥)	
	E <sub>2u</sub> (inactive)	29	(3100)	CH stretching
		30	(1170) <sup>b</sup>	CH bending
31		(1050) <sup>b</sup>	CH bending (⊥)	
32		(1560) <sup>b</sup>	C-C stretch	
33		(885) <sup>b</sup>	Ring deformation	
34		(570)	Ring deformation	

<sup>a</sup> Assignments not observed, but made in comparison to ferrocene and nickelocene.<sup>9</sup> <sup>b</sup> Observed in crystal spectra, using diamond cells.

quency assignments of the fundamental modes of vibration of  $Mg(C_5H_5)_2$  resemble closely the results obtained for ferrocene.

Assignments of fundamental modes are as shown in Table III. It is found that the arguments put forward in making the assignments of fundamental modes of ferrocene hold quite satisfactorily for  $Mg(C_5H_5)_2$ . An attempt is also made here to explain the appearance of non-fundamental bands (Table IV).

The selection rules for a D<sub>5d</sub> sandwich structure give A<sub>1g</sub>, E<sub>1g</sub> and E<sub>2g</sub> as Raman active species and A<sub>2u</sub> and E<sub>1u</sub> as infrared active species. A<sub>1u</sub>, A<sub>2g</sub> and E<sub>2u</sub> are inactive species. There are thus 15 Raman (4A<sub>1g</sub>, 5E<sub>1g</sub> and 6E<sub>2g</sub>) and 10 infrared (4A<sub>2u</sub> and 6E<sub>1u</sub>) fundamental vibrational frequencies predicted, though all are not observed. It is seen for ferrocene that certain fundamental modes of vibrations, which, on symmetry considerations, are forbidden in the infrared region, do appear in the spectrum of the solid.<sup>12</sup> This is also noticed in crystal spectra of  $Mg(C_5H_5)_2$  (see Table II).

A comparison of the spectra of ferrocene and ruthenocene with that of  $Mg(C_5H_5)_2$  reveals that the frequencies due to

(12) W. K. Winter, B. Curran, Jr., and S. E. Whitcomb, *Spectrochim. Acta*, **12**, 1085 (1959).

TABLE IV  
 ASSIGNMENT OF OBSERVED NON-FUNDAMENTAL FREQUENCIES

Frequency Raman	Explanation	Type
752	$\omega_4 + \omega_{23} = 191 + 570 = 761$	$A_{1g} \times E_{2g} = E_{2g}$
1345	$\omega_4 + \omega_{24} = 191 + 1163 = 1354$	$A_{1g} \times E_{2g} = E_{2g}$
Infrared		
1363	$\omega_{10} + \omega_4 = 1170 + 191 = 1361$	$E_{2u} \times A_{1g} = E_{2u}$
1425	$\omega_{16} + \omega_7 = 229 + 1200 = 1429$	$A_{2g} \times E_{1g} = E_{1g}$
	$\omega_{21} + \omega_{10} = 440 + 990 = 1430$	$E_{1u} \times E_{1g} = A_{1u} + A_{2u} + E_{2u}$
1516	$\omega_{18} + \omega_{11} = 990 + 526 = 1516$	$E_g \times A_{2u} = E_{1u}$
	$\omega_{18} + \omega_{23} = 1410 + 107 = 1517$	$E_{1g} \times E_{1u} = A_{1u} + A_{2u} + E_{2u}$
1540	$\omega_{10} + \omega_{21} = 1108 + 440 = 1548$	$A_{2u} \times E_{1u} = E_{1g}$
	$\omega_1 + \omega_{21} = 1109 + 440 = 1549$	$A_{1g} \times E_{1u} = E_{1u}$
1570	$\omega_{18} + \omega_{23} = 1008 + 570 = 1578$	$E_{1u} \times E_{2g} = E_{1u} + E_{2u}$
	$\omega_{11} + \omega_{23} = 526 + 1050 = 1576$	$A_{2u} + E_{2g} = E_{2u}$
1610	$2 \times \omega_{14} = 2 \times 806 = 1612$	$2E_{1g} = A_{1g} + E_{2g}$
1625	$\omega_7 + \omega_{11} = 1109 + 526 = 1635$	$A_{1g} \times A_{2u} = A_{2u}$
1700	$\omega_7 + \omega_{11} = 1200 + 526 = 1726$	$A_{2g} \times A_{2u} = A_{1u}$
1736	$\omega_4 + \omega_{23} = 191 + 1560 = 1751$	$A_{1g} \times E_{2g} = E_{2g}$
1928	$\omega_{10} + \omega_{23} = 886 + 1050 = 1936$	$E_{1u} \times E_{2g} = E_{1u} + E_{2u}$
2050	$\omega_{18} + \omega_{23} = 1008 + 1050 = 2058$	$E_{1u} \times E_{2g} = E_{1u} + E_{2u}$
2395	$\omega_{18} + \omega_{23} = 990 + 1420 = 2410$	$E_{1g} \times E_{1u} = A_{1u} + A_{2u} + E_{2u}$
2600	$\omega_7 + \omega_{18} = 1200 + 1410 = 2610$	$A_{2g} \times E_{1g} = E_{1g}$

vibrations within the rings are essentially the same, while the ring-metal-ring vibrations occur at different positions. The symmetric stretching frequency in ferrocene is at 303  $\text{cm}^{-1}$ , in ruthenocene at 330  $\text{cm}^{-1}$  in nickelocene (calculated to be) at 200  $\text{cm}^{-1}$  and in  $\text{Mg}(\text{C}_5\text{H}_5)_2$  at 191  $\text{cm}^{-1}$ . This would indicate a much weaker ring-metal bonding in  $\text{Mg}(\text{C}_5\text{H}_5)_2$ . A comparison of approximate force constants computed from this symmetric stretching mode indicates that the bond energy in  $\text{Mg}(\text{C}_5\text{H}_5)_2$  would be about half of that in ferrocene. Since the bonding is appreciably weaker, the ring modes may be expected to resemble more closely those for a free  $\text{C}_5\text{H}_5$  ring system. Consequently, some frequencies are expected to appear much more weakly in  $\text{Mg}(\text{C}_5\text{H}_5)_2$  than the corresponding ones in ferrocene, etc., when they are forbidden by selection rules for a free  $\text{C}_5\text{H}_5$  ring. This has been observed for the band at 1108  $\text{cm}^{-1}$ , which is unusually weak in  $\text{Mg}(\text{C}_5\text{H}_5)_2$ .

It is known that some of the frequencies due to the linear  $\text{XY}_2$  type modes are dependent on the mass of the metal atom and on the force constants. The assignment of the ring-metal antisymmetric stretching frequency of the magnesium compound has been made at 526  $\text{cm}^{-1}$ . This is the position expected for this frequency, when allowance is made for the mass of the Mg atom, from the unambiguous assignment of the totally symmetric stretching frequency at 191  $\text{cm}^{-1}$ . It should be noted that this particular band is at a higher frequency than the corresponding frequency in ferrocene, which is observed at 478  $\text{cm}^{-1}$ .

Certain deviations in the position and intensity of the bands have been noticed in the spectra of  $\text{Mg}(\text{C}_5\text{H}_5)_2$  and of ferrocene, though the two spectra fundamentally resemble each other. The frequency at 440  $\text{cm}^{-1}$  in the spectra of  $\text{Mg}(\text{C}_5\text{H}_5)_2$  is assigned to an antisymmetric ring tilt mode, while the corresponding value in ferrocene is 492  $\text{cm}^{-1}$ . Both bands are quite intense. However, the low value of this mode in the magnesium compound can be explained on the basis of a weak bonding in the molecule compared to that in ferrocene.

Another striking difference between the spectra of  $\text{Mg}(\text{C}_5\text{H}_5)_2$  and ferrocene is the low intensity of the 1420  $\text{cm}^{-1}$  band in the former, in contrast to the strong one at 1411  $\text{cm}^{-1}$  in ferrocene. It seems difficult to give a convincing explanation for this change in the intensity of the degenerate C-C stretching mode. However, it is observed that the intensity of the same band in the solid spectrum of  $\text{Mg}(\text{C}_5\text{H}_5)_2$  compares favorably with that of ferrocene. A solvent effect of this particular band presumably lowers the intensity in solution spectra.

Considerable evidence for the covalent nature of the bonding in bis-cyclopentadienylmagnesium can be found by a consideration of the intensity of the absorption band at 526  $\text{cm}^{-1}$ , the antisymmetric ring-metal stretching mode. The

absolute intensity  $A$  of an absorption band is given by the relation<sup>13</sup>

$$A = \frac{1}{Cl} \int \log_e \left( \frac{I_0}{I_\nu} \right) d\nu = \frac{N\pi}{3c} g \left( \frac{\delta\mu}{\delta Q} \right)^2$$

For practical purposes<sup>14</sup>

$$A = \frac{\pi}{2} \times \frac{1}{Cl} \log_e \left( \frac{I_0}{I_\nu} \right) \times \Delta\nu_{1/2}$$

where  $C$  = concentration of the solute in molecules per ml.

$c$  = velocity of light

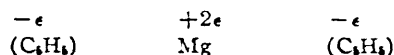
$l$  = cell length in cm.

$I_0$  and  $I_\nu$  are incident and transmitted intensities of monochromatic radiation of frequency  $\nu$

$\Delta\nu_{1/2}$  = half-intensity width of the absorption band

$g$  = degeneracy factor (= 1 in this case).

For the antisymmetric ring-metal stretching vibration it can be easily shown that  $\delta\mu/\delta r = 2e$ , assuming the ionic model



$e$  is equal to the electronic charge if the compound is considered to be fully ionic.

Then  $\delta\mu/\delta r = 9.604 \times 10^{-10}$  e.s.u. or 9.604 D./Å. Thus the absolute intensity on the theoretical basis should be  $A = 194 \times 10^{-7}$   $\text{cm}^{-2}$  molecules<sup>-1</sup> sec<sup>-1</sup>.

The observed intensity in molar benzene solution is found, using Ramsay's technique,<sup>14</sup> to be approximately  $2.9 \times 10^{-7}$ . This is lower than the intensity obtained on the above theoretical basis by a factor of 68. This corresponds to a value of 1.6 D./Å. for  $\delta\mu/\delta r$ . This may be compared with the experimental value for the strongly polar C-F bond ranging from 5-6 D./Å. The predominantly covalent nature of the ring-metal bonding is, therefore, evidenced by the low observed absorption intensity, compared with the theoretical for a simple triatomic system.

In support of this it is found that the peak intensity at equivalent concentration and cell thickness for the 526  $\text{cm}^{-1}$  antisymmetric ring-metal stretching band in  $\text{Mg}(\text{C}_5\text{H}_5)_2$  is equal to or slightly less than that for the peak intensity of the corresponding mode in ferrocene at 478  $\text{cm}^{-1}$ . The argument holds equally well if the 492  $\text{cm}^{-1}$  band in ferrocene is assigned to the antisymmetric ring-metal stretching mode. One would expect the peak intensity for the 526  $\text{cm}^{-1}$  band in  $\text{Mg}(\text{C}_5\text{H}_5)_2$  to be very much greater than that for the corresponding band in ferrocene, if the former molecule has appreciable ionic bonding.

(13) "Molecular Vibrations," E. B. Wilson, J. C. Decius and P. C. Cross, McGraw-Hill Book Co., Inc., New York, N. Y., 1955, pp. 163 ff.

(14) D. A. Ramsay, *J. Am. Chem. Soc.*, **74**, 72 (1952).

### Discussion

As has been shown, the intensity of the antisymmetric stretching mode is inconsistent with predominantly ionic character. For an essentially ionic system the model used to evaluate the intensity of this mode will be good though likely to lead to a slight overestimate of the intensity due to coupling of the vibration with the cyclopentadienyl modes. Unfortunately the model cannot be used to determine the extent of the ionic character since with covalent bonding rehybridizations seriously modify the transition moment. Thus the C-F bond in fluorocarbons has a dipole moment of about 1.3 D., whereas intensity studies have shown that the stretching gradient  $\delta\mu/\delta r_{CF}$  in fluoroaromatics is between 5 and 6 D./Å.<sup>15</sup>

The spectra as shown above are consistent with  $D_{3d}$  molecular symmetry. However, small deviations from this symmetry toward, for example,  $C_{2v}$  symmetry would be expected to have little effect on the observed spectra. The vibrational perturbations are likely to be small at the best, and the intensity changes resulting from a relaxation of the selection rules insufficient to avoid confusion with changes resulting from molecular interactions. For example, there is little change in the spectra of biphenyl in going from the solid phase ( $D_{2h}$  symmetry) to the solution phase (inter-ring angle  $\sim 30^\circ$ ) even though steric interactions and  $\pi$  conjugation undoubtedly are decreased.<sup>16</sup>

In summary, three factors indicate that Mg-

(15) D. Steele and D. H. Whiffen, *Trans. Faraday Soc.*, **56**, 177 (1960).

(16) D. Steele and E. R. Lippincott, in press.

( $C_5H_5$ )<sub>2</sub> should be considered as an essentially covalent compound, rather than ionic, with  $d^2sp^3$  hybridization to the Mg atom. The great similarity of the spectra of  $Mg(C_5H_5)_2$  in both solid and solution phases to that for ferrocene is in itself an argument for the covalent bonding in the magnesium compound. There are no features in the solution spectrum which would suggest that there has been a change in bonding from that of the solid form. Thus the same molecular units must be present in the solid phase as have been observed in solution.

The measured intensity of the antisymmetric ring-metal stretching in  $Mg(C_5H_5)_2$  is definitely inconsistent with the assumption of an ionic structure  $(C_5H_5)^-Mg^{++}(C_5H_5)^-$  or appreciable contribution from this structure.

The great solubility of the magnesium compound in benzene (about one g. in 5 ml. of benzene) and cyclohexane is another factor which may be taken as an additional evidence supporting the covalent nature of the molecule.

It may be concluded that the bis-cyclopentadienylmagnesium resembles the corresponding iron compound (ferrocene) in structure and in bonding. However, the much weaker ring-to-metal bond observed in the  $Mg(C_5H_5)_2$  may be considered responsible for the so-called "ionic" behavior of the compound, despite the fact that the bonding is essentially covalent in nature.

**Acknowledgments.**—The financial assistance from the Atomic Energy Commission and the National Science Foundation is gratefully acknowledged.

## Spectroscopic studies of compounds containing the —CN group—II. Vibrational spectra, assignments and configuration of sulphur dicyanide S(CN)<sub>2</sub>

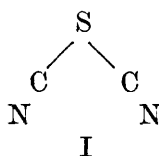
D. A. LONG and D. STEELE

Department of Chemistry, University College of Swansea

(Received 23 February 1963)

**Abstract**—The infrared and Raman spectra of sulphur dicyanide, S(CN)<sub>2</sub> are reported and shown to be in accord with C<sub>2v</sub> symmetry of the molecule. The ratio of the infrared intensities of the anti-symmetric and symmetric CN stretching modes is used to fix the CSC angle at 141 ± 5°. Assignments of the fundamentals are proposed.

THE compound sulphur dicyanide SC<sub>2</sub>N<sub>2</sub> has been known since 1828 when it was first reported by LASSAIGNE [1]. A variety of methods are now available for its preparation [2] and these and its properties [2, 3] are in accord with its formulation as S(CN)<sub>2</sub>, the dicyano derivative of sulphoxylic acid. It was suggested by GOEHRING [4] in 1943 that substantial differences in the reactivity of S(CN)<sub>2</sub> and SCl<sub>2</sub> might be due to major structural differences. The subsequent kinetic studies of KITCHING *et al.* [5] have shown that, in fact, the reaction rates can be satisfactorily accounted for in terms of the dicyanide structure. The only structural study of this molecule is that of ROGERS and GROSS [6] who measured the dipole moment and showed this to be consistent with a bent structure (I) in which the C—S—C angle is about 105°.



In this paper we report the infrared and Raman spectra of this compound and discuss them in relation to the molecular symmetry.

### EXPERIMENTAL

#### *Preparation of sulphur dicyanide*

20 g of silver cyanide was dispersed in 200 ml of warm carbon disulphide by vigorous stirring. 10 ml of sulphur dichloride was then added over a period of 15 min. Filtration gave a solution containing the bulk of the sulphur dicyanide.

The solid residues were treated with carbon disulphide to extract further sulphur dicyanide. Cooling of the combined carbon disulphide solutions gave crystals of the

[1] LASSAIGNE, *Ann. Chim. Phys.* **39**, 197 (1828).

[2] BELSTEIN, *Handbuch der Organische Chemie* Vol. 3, p. 180. Springer, Berlin (1921).

[3] H. E. WILLIAMS, *Cyanogen Compounds*. Arnold, London (1948).

[4] M. GOEHRING, *Ber. deut. chem. Ges.* **76B**, 742 (1943).

[5] W. KITCHING, R. H. SMITH and I. R. WILSON, *Australian J. Chem.* **15**, 211 (1962).

[6] M. T. ROGERS and K. J. GROSS, *J. Amer. Chem. Soc.* **74**, 5294 (1952).



dicyanide. Further purification was carried out by vacuum sublimation at room temperature.

Sulphur dicyanide obtained in this way forms colourless plate-like crystals m.p. 64–65°C. It is moderately soluble in water, very soluble in ether and soluble in warm carbon disulphide. The molecular weight, determined by depression of the freezing point of water was 79 [S(CN)<sub>2</sub> requires 84]. It is not markedly stable and at room temperature in the absence of air slowly forms a yellow compound of unknown composition. In the presence of air a compound with a red colour is formed. One sample

Table 1. Vibrational spectra and assignments for sulphur dicyanide. (Frequencies in cm<sup>-1</sup>.)

Infrared		Raman		Assignment
Solution	Solid	Solution	Solid	
			167 vw	
		223 w	218 w	$\nu_4(a_1)$ CSC deformation
		244 w		$\nu_8(a_2)$ SCN deformation (out-of-plane)
		294 vvw	290 w	$\nu_7(b_1)$ SCN deformation (in-plane)
		608 vvw		
663 vvs	673 vvs	652 vvw		$\nu_9(b_2)$ SCN deformation (out-of-plane)
684 vvs	691 vvs			$\nu_3(a_1)$ SCN deformation (in-plane)
	752 ms			$\nu_2(a_1)$ C—S stretch.
	838 m	837 vvw		$\nu_6(b_1)$ C—S stretch.
		918 vvw		684 + 223 = 907
	967 w			752 + 223 = 975
	1040 w			752 + 294 = 1046
			1272 vvw	752 + 294 + 223 = 1269
	1330 vw			
		1352 vw	1366 vvw	663 + 684 = 1347
		1459 vw		752 + 684 = 1436
			1526 vw	837 + 684 = 1521
			1664 vvw	2 × 838 = 1676
			1759 vvw	
		1851 vvw		} Ternary combination bands
		1880 vvw	1883 vvw	
	2028 vvw	2039 vvw	2025 vw	
	2132 m			
	2179 s			$\nu_5(b_1)$ CN stretch
	2190 m	2186 ms	2191 w	$\nu_1(a_1)$ CN stretch
	2208 w			} Ternary combination bands
	2232 vvw	2229 w	2221	
	2252 vvw			
	2286 vvw			
			2437 w	2190 + 244 = 2434
	2509 m	2492 w	2493 mw	2190 + 294 = 2484
	2688 m			2190 + 218 + 290 = 2698
	2874 d			2179 + 691 = 2870
	2976 m			2190 + 752 = 2942

w = weak, s = strong, d = diffuse, v = very, m = medium.

stored for some time in a sealed glass tube the top end of which was near the cooling coil of a refrigerator underwent a very slow sublimation. Large colourless crystals were formed at the top end of the tube. The crystals were purer than samples of sulphur dicyanide obtained in other ways. The melting point was  $69^{\circ}\text{C}$  and the stability was greater. For example a single crystal was stable for half an hour in the beam of an infra-red spectrometer whereas mulls or KBr disks of other samples discoloured more rapidly and soon became opaque to the beam.

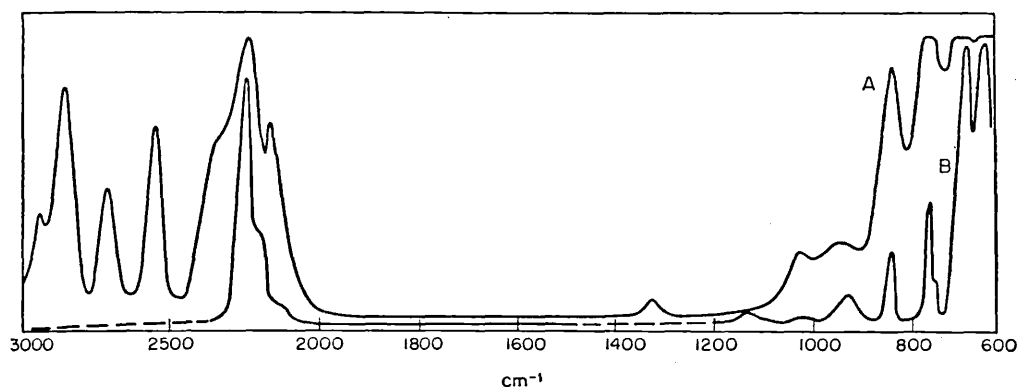


Fig. 1. Infrared spectra of sulphur dicyanide (low dispersion).  
A = single crystal, 1 mm thick, B = Nujol mull.

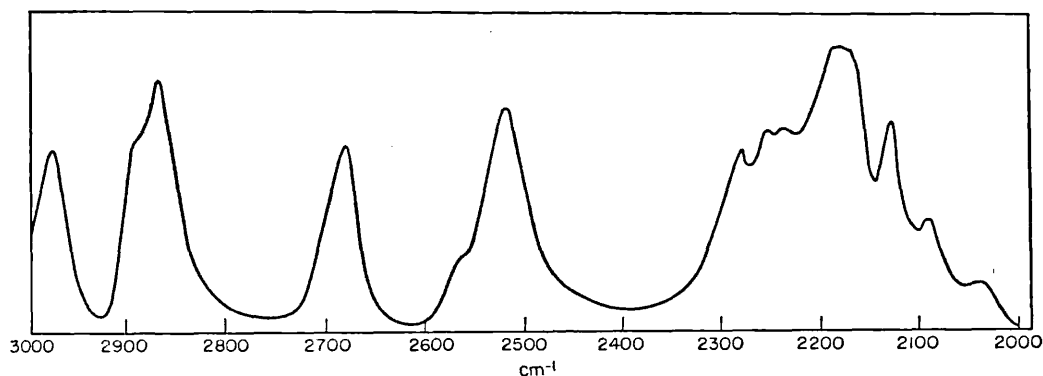


Fig. 2. Infrared spectrum of sulphur dicyanide, single crystal, 2000–3000  $\text{cm}^{-1}$ ,  
high dispersion.

### *Infrared spectra*

Infrared spectra were obtained in the range  $3200\text{--}670\text{ cm}^{-1}$  using the Perkin-Elmer Infra-cord and in the range  $3200\text{--}650\text{ cm}^{-1}$  using the Grubb-Parsons double beam grating spectrometer G.S.2. Most of the infrared spectra were obtained for solid sulphur dicyanide, in a Nujol mull, in a KBr disk or as a single crystal, but the infrared spectrum of a very dilute solution in ether was also obtained for the region  $650\text{--}770\text{ cm}^{-1}$ . The infrared frequencies with qualitative intensity estimations are included in Table 1. The infrared spectrum at low dispersion for the range  $3000\text{--}650$

$\text{cm}^{-1}$  is shown diagrammatically in Fig. 1. The region 3000–2000  $\text{cm}^{-1}$  is shown at much higher dispersion in Fig. 2. The infrared spectra of samples of sulphur dicyanide which had been kept for some time were also studied briefly. Initially, there appears in the CN stretching region another band which is broad and has its centre at approximately 2040  $\text{cm}^{-1}$ . In samples in which the yellow colour is well developed the infrared spectra show only one intense broad band at about 1280  $\text{cm}^{-1}$  presumably corresponding to a C=S stretching mode. The complete absence of CN stretching frequencies is noteworthy.

The Raman spectra of sulphur dicyanide, both in solution in ether (50% W/W) and as a crystalline solid, were obtained using methods described elsewhere [7]. The frequencies and qualitative intensities of the Raman lines are included in Table 1.

#### DISCUSSION AND ASSIGNMENTS

If the  $\text{S}(\text{CN})_2$  molecule had a linear structure it would belong to the point group  $D_{\infty h}$ . The activity and symmetry of the fundamental vibrations would then be:

$$2\Sigma_g^+(\text{R}) + 2\Sigma_u^-(\text{I.R.}) + 2\Pi_u(\text{I.R.}) + 1\Pi_g(\text{R})$$

The rule of mutual exclusion operates and thus the Raman spectrum should contain three fundamentals and the infrared spectrum four fundamentals none of these being coincident. If  $\text{S}(\text{CN})_2$  had the bent structure (I) it would belong to the point group  $C_{2v}$  and the corresponding classification of vibrations would be:

$$4a_1(\text{R and I.R.}) + 3b_1(\text{R and I.R.}) + 1a_2(\text{R}) + 1b_2(\text{R and I.R.})$$

All the modes except the  $a_2$  mode would then be active in both the infrared and Raman spectra. The presence of genuine coincidences between infrared and Raman frequencies would thus be positive evidence for  $C_{2v}$  symmetry. The absence of coincidences would suggest  $D_{\infty h}$  symmetry but the argument in this case would be less convincing since the lack of coincidence could arise because of experimental difficulties in observing weak lines.

The infrared spectra only go down to 650  $\text{cm}^{-1}$  and so a complete comparison of infrared and Raman spectra cannot be effected. It is nevertheless possible to distinguish between  $D_{\infty h}$  and  $C_{2v}$  symmetry by considering just the CN stretching frequencies. The infrared spectrum has two such frequencies, one at 2179  $\text{cm}^{-1}$  (strong) and one at 2190  $\text{cm}^{-1}$  (medium). The latter frequency is very close to the only strong sharp Raman line observed in this region at 2186  $\text{cm}^{-1}$  in solution or 2191  $\text{cm}^{-1}$  in the solid. As we are able to compare infrared and Raman frequencies for the solid this must be a genuine coincidence of fundamentals. Thus  $C_{2v}$  symmetry is established. For this symmetry the other infrared band should also have a Raman counterpart. It is presumably too weak to be observed but its absence does not invalidate our arguments. The strong infrared band at 2179  $\text{cm}^{-1}$  is assigned to the antisymmetric CN stretching mode  $\nu_5(b_1)$  and the CN frequency at about 2190  $\text{cm}^{-1}$  is assigned to the symmetric CN stretching mode  $\nu_1(a_1)$ .

The relative intensities of the two CN stretching modes in the infrared may be used to give a rough prediction of the CSC angle in  $\text{S}(\text{CN})_2$ . We shall make the following assumptions:

[7] D. A. LONG and W. O. GEORGE, *Trans. Faraday Soc.* **56**, 1570 (1960).

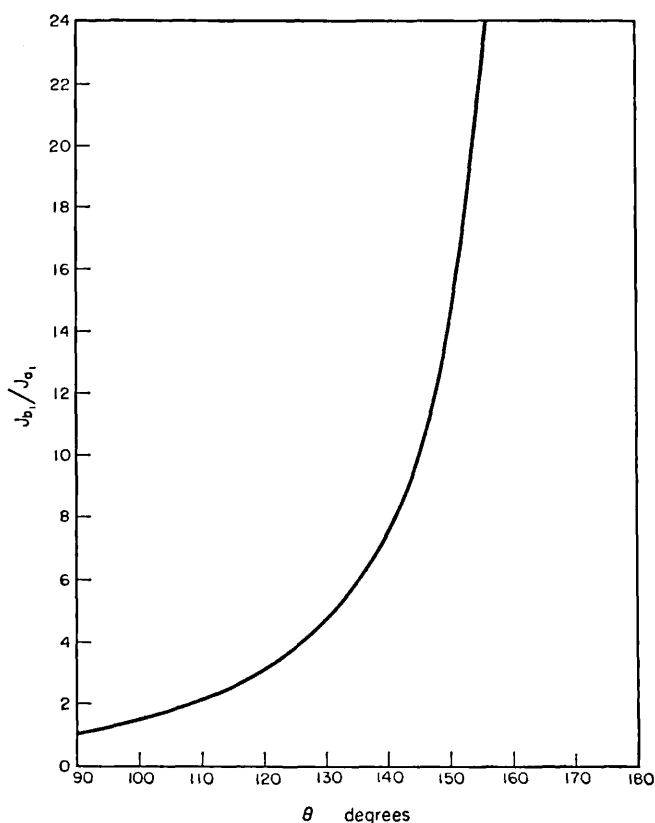


Fig. 3. Graph of  $\mathcal{I}_{b_1}/\mathcal{I}_{a_1}$  vs.  $\theta$

(a) That infrared intensities may be accounted for in terms of bond dipole derivatives.

(b) That there is negligible electric coupling between the two CN dipoles so that the CN bond dipole derivatives may be combined vectorially for the symmetric and anti-symmetric modes.

(c) That the CN stretching modes can be regarded as not coupled mechanically with other modes of the same class. The ratio of the intensity of the antisymmetric mode  $\mathcal{I}_{b_1}$  to the intensity of the symmetric mode  $\mathcal{I}_{a_1}$  is then given by:

$$\frac{\mathcal{I}_{b_1}}{\mathcal{I}_{a_1}} = \tan^2 \frac{\theta}{2}$$

where  $\theta$  is the C—S—C interbond angle. A graph of the ratio  $\mathcal{I}_{b_1}/\mathcal{I}_{a_1}$  against  $\theta$  is shown in Fig. 3. The intensity of a given infrared band is obtained by determining the area under that band in a plot of  $\log \{I_0/(I_0 - I)\}$  against frequency  $\nu$  where  $I_0$  is the incident intensity and  $I$  is the transmitted intensity. A plot of this kind for the frequency region 2150–2240  $\text{cm}^{-1}$  is shown in Fig. 4. The calculation of the areas under the bands is complicated by the incomplete resolution both of the  $\nu_1(a_1)$  and  $\nu_5(b_1)$  bands and of the  $\nu_5(b_1)$  band and a combination band at 2132  $\text{cm}^{-1}$ . The intensity ratio lies in the range 6.0–12.0, the large uncertainty reflecting the difficulty in

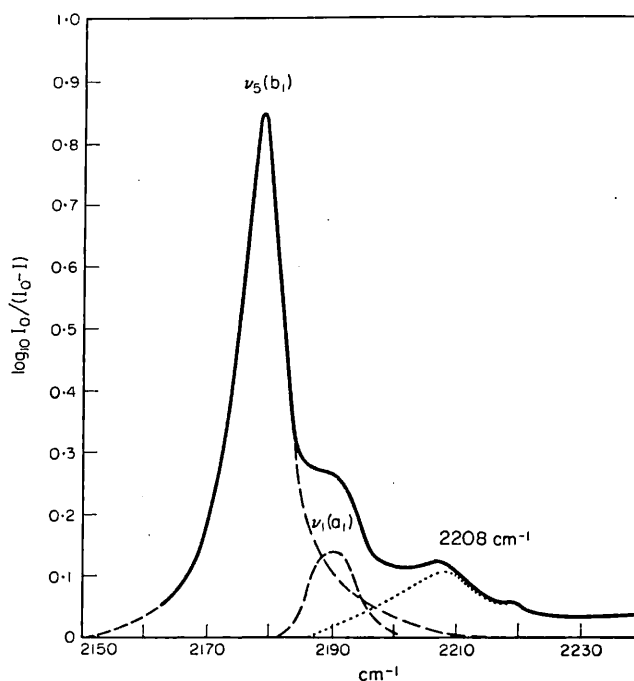


Fig. 4. Plot of  $\log_{10} I_0/(I_0 - I)$  vs.  $\nu(\text{cm}^{-1})$  for sulphur dicyanide, 2150–2240  $\text{cm}^{-1}$ .

assessing the areas of the two bands. Fig. 3 shows that even this relatively ill-defined ratio fixes the interbond angle in the range  $135^\circ$ – $146^\circ$ . This value is higher than the figure of  $105^\circ$  suggested by ROGERS and GROSS, but that depends on assumed bond dipole moments.

The remaining seven unassigned modes of vibration of sulphur dicyanide will consist of two C—S stretching modes ( $a_1$  and  $b_1$ ), one C—S—C angle deformation ( $a_1$ ) and four S—CN angle deformations, two in-plane ( $a_1$  and  $b_1$ ) and two out-of-plane ( $a_2$  and  $b_2$ ). The frequencies associated with all these modes will lie below  $1000 \text{ cm}^{-1}$  and we therefore look for prominent features in the infrared and Raman spectra in this lower-frequency region. The main low-frequency features of the infrared spectrum are two very strong bands at  $664$  and  $684 \text{ cm}^{-1}$  and two bands of medium strength at  $752$  and  $838 \text{ cm}^{-1}$ . Some of these bands have counterparts in the Raman spectrum but apart from these the most noteworthy feature of the Raman spectrum is the group of three lines at  $223$ ,  $224$  and  $294 \text{ cm}^{-1}$ . There are therefore seven observed bands of appropriate intensity and frequency to be allocated to the seven unassigned modes.

In dialkyl sulphides and disulphides the frequencies of C—S stretching modes have been found [8] to lie in the range  $630$ – $750 \text{ cm}^{-1}$  and this suggests either the pair of bands at  $663$  and  $684 \text{ cm}^{-1}$  or the pair at  $752$  and  $838 \text{ cm}^{-1}$  for the C—S modes.

The pair at the lower frequencies are too strong for the C—S stretching modes, particularly the symmetric C—S stretch and we have therefore associated the other pair of frequencies with these modes. The higher frequency,  $838 \text{ cm}^{-1}$  is assigned to

[8] D. W. SCOTT and J. P. McCULLOUGH, *J. Am. Chem. Soc.* **80**, 3554 (1958).

the  $b_1$  C—S stretch and the lower frequency,  $752\text{ cm}^{-1}$  to the  $a_1$  C—S stretch, in accord with the general pattern found for antisymmetric and symmetric modes.

In other dinitriles it has been found [9, 10] that the four nitrile deformations involve two frequencies around  $600\text{ cm}^{-1}$  and two below  $300\text{ cm}^{-1}$ . The two very strong infrared bands at  $663$  and  $684\text{ cm}^{-1}$  thus arise from two of the SCN deformations. The only other alternative would be to assign them to one SCN deformation and a combination or overtone band in Fermi resonance with it. No binary combination or first overtone can occur in this region since all the low-frequency fundamentals lie below  $290\text{ cm}^{-1}$ . We assign the lower frequency  $663\text{ cm}^{-1}$  to the  $b_2$  SCN out-of-plane deformation and  $684\text{ cm}^{-1}$  to the  $a_1$  SCN deformation.

The frequencies for the three remaining modes must now be selected from the three Raman frequencies,  $223$ ,  $244$  and  $294\text{ cm}^{-1}$ . The infrared spectrum contains a band at  $967\text{ cm}^{-1}$  which can be interpreted as a combination band  $752 + 223 = 975\text{ cm}^{-1}$ ; this precludes the assignment of  $223\text{ cm}^{-1}$  as the  $a_2$  mode. Similarly the presence of an infrared band at  $1040\text{ cm}^{-1}$  which can be interpreted as  $752 + 290 = 1042\text{ cm}^{-1}$  rules out  $290\text{ cm}^{-1}$  as the  $a_2$  mode. Thus  $244\text{ cm}^{-1}$  is the  $a_2$  fundamental. This argument is based on the assignment of  $752\text{ cm}^{-1}$  as the  $a_1$  C—S stretching mode. If however the assignment of the C—S stretching modes were reversed and  $837\text{ cm}^{-1}$  assigned as the  $a_1$  mode three binary combination infrared bands at  $975\text{ cm}^{-1}$  ( $752 + 223$ ),  $996\text{ cm}^{-1}$  ( $752 + 244$ ) and  $1046\text{ cm}^{-1}$  ( $752 + 294$ ) would be expected whereas only two bands at  $967$  and  $1040$  are observed. Further support for the assignment of  $244\text{ cm}^{-1}$  to the  $a_2$  fundamental is provided by the appearance in the Raman spectrum only of a line at  $2437\text{ cm}^{-1}$  which can be interpreted as  $2186(a_1) + 244(a_2) = 2430(a_2)$ .

In the dialkyl sulphides [8] the C—S—C angle deformation frequencies lie in the range  $187$ – $282\text{ cm}^{-1}$  and we have therefore assigned  $223\text{ cm}^{-1}$  to the  $a_1$  C—S—C deformation in  $\text{S}(\text{CN})_2$ . This leaves  $290\text{ cm}^{-1}$  as the antisymmetric  $b_1$  SCN deformation.

This assignment of the nine fundamentals leads to a satisfactory explanation of all the observed infrared bands and Raman lines as Table 1 shows.

*Acknowledgements*—We are indebted to the Royal Society, Imperial Chemical Industries (Ltd.) and the University College of Swansea for grants for the purchase of the spectroscopic equipment used in this work. One of us (D. S.) gratefully acknowledges the award of an I.C.I. Fellowship during the tenure of which this work was carried out.

[9] D. A. LONG and W. O. GEORGE. *Spectrochim. Acta* **19**, 1717 (1963).

[10] D. A. LONG and W. O. GEORGE. To be published.

## The vibrational spectra of diboron compounds—I.

### Infra-red spectra of diboron tetrafluoride

ARTHUR FINCH, I. HYAMS and D. STEELE  
Department of Chemistry, Royal Holloway College,  
Englefield Green, Surrey, England

(Received 28 September 1964)

**Abstract**—The infra-red spectrum of gaseous diborontetrafluoride has been measured from 4000 to 140  $\text{cm}^{-1}$ . The point group and modal distribution for freely rotating  $\text{B}_2\text{F}_4$  have been deduced using nuclear permutation methods. Failure to see an absorption band of the expected frequency and intensity for an “out-of-plane”  $\text{B BF}_2$   $\gamma$  mode is shown to be consistent with free rotation or almost free rotation.

WHILST a number of non-hydride compounds containing the B—B bond are known, the structures and spectra of few have been determined. Diboron tetrafluoride [1] ( $\text{B}_2\text{F}_4$ ) and diboron tetrachloride [2] ( $\text{B}_2\text{Cl}_4$ ) have been shown to be planar in the crystal phase whilst  $\text{B}_2\text{Cl}_4$  has the staggered configuration of  $Vd$  symmetry in the gas phase according to electron diffraction experiments [3]. The Raman and infrared spectra of the latter molecule support the electron diffraction conclusions [4] for the gas phase and lead to a barrier to rotation about the B—B bond of  $1700 \pm 600$  cal./mole. Recently the infra-red spectrum of  $\text{B}_2(\text{OH})_4$  has been reported [5]. The present communication is the first of a series of papers aimed at a better understanding of the molecular structures of compounds of the general formula  $\text{X}_2\text{B—BX}_2$ .

When this work was completed a private communication was received from GAYLES and SELF of Oregon State University who were kind enough to offer information of their work on this compound. They prepared the compound by a different route to that used by the present authors. The absence of several weak-to-moderate bands in their spectra as compared with our own indicates the greater purity of their sample. Apart from these bands the agreement between the spectra is good. They conclude from an examination of band shapes that the molecule has  $Vd$  symmetry. Free rotation about the B—B bond is discussed briefly but is not favoured since  $\text{CH}_2\text{F·BF}_2$  is believed to possess a significant potential barrier. It is the purpose of the present communication to show that anomalies in the observed spectral intensities probably arise from almost free rotation about the B—B bond.

### EXPERIMENTAL

Diboron tetrafluoride was prepared in high yield by the established procedure of Swarts fluorination of diboron tetrachloride [7]. The product was tensiometrically

- [1] L. TREFONAS and W. N. LIPSCOMB, *J. Chem. Phys.* **28**, 54 (1958).
- [2] M. ATOJI, W. N. LIPSCOMB and P. J. WHEATLEY, *J. Chem. Phys.* **23**, 1176 (1955).
- [3] K. HEDBERG, see Reference [4].
- [4] D. E. MANN and L. FANO, *J. Chem. Phys.* **26**, 1665 (1957).
- [5] NIKITIN, MAL'TSER and VINOGRADOVA, *Vestnik, Moskow Univ.* **3**, 14 (1963).
- [6] J. N. GAYLES and J. SELF, *J. Chem. Phys.* **40**, 3530 (1964).
- [7] A. FINCH and H. I. SCHLESINGER, *J. Am. Chem. Soc.* **80**, 3573 (1958).

homogeneous and apparently pure, but the vapour pressure of the liquid was lower than published values as shown below:

Vapour pressure (mm of Hg) of  $B_2F_4$  (a) solid, (b) liquid.

	(a)	(a)	(b)	(b)	(b)
Temperature °C:	-80.1	-63.5	-52.3	-49.6	-47.0
This work :	15	87	206	241	269
Reference [6] :	15	87.5	232	280	333

The spectra were recorded in 10 cm path cells with windows of KBr or rigidex polythene at pressures ranging from a few mm to 30 cm of Hg. A Unicam SP100 with SP130 grating accessories was used for the measurements at frequencies above 400  $cm^{-1}$  using spectral slit widths of 2  $cm^{-1}$  above 450  $cm^{-1}$ . Below 450  $cm^{-1}$  measurements were made on a far infra-red grating spectrometer constructed in the department and described adequately elsewhere [8]. The spectral slit widths employed were 2  $cm^{-1}$  at 400  $cm^{-1}$  and 3  $cm^{-1}$  at 320  $cm^{-1}$ . The observed frequencies are given in Table 1.

Table 1

Frequency ( $cm^{-1}$ )	Assignment
2821 v.w.	$2 \times 1415$
2755 w.	$2 \times 1372$
2570 v.w.	
2515 w-m	1372 + 1151
2085 w.	
2042 w.	1372 + 680
1822 w.	1151 + 680
1732 v.w.	
1688 w-m	1372 + 324
1548 w.	
1415 s.	$\nu BF(^{10}B^{11}B)$ ; $E(\Gamma_9)$ symmetry
1372 vs.	$\nu BF(^{11}B^{11}B)$ ; $E(\Gamma_9)$ symmetry
1275 w-m	
1157.5 } v.s.	$\nu BF B_2(\Gamma_3)$ symmetry
1151.5 }	
986-865 w-m	Impurity bands complex.
930 w-m	
821 w-m	
ca. 660 w. br.	B-BF <sub>2</sub> umbrella mode; $E(\Gamma_{10})$ symmetry
642; 621 m.	Impurity
548.5 }	
543 }	FBB deformation; $B_2(\Gamma_3)$ symmetry
541 }	
534 }	
461, 408 w.	Impurity
331, 324 m.	FBB deformation; $E(\Gamma_9)$ symmetry

The quantity of material available was insufficient to obtain a Raman spectrum of  $B_2F_4$  using conventional gas cells. An attempt was made in conjunction with Dr. BEATTIE of Kings College, London, to measure the spectrum of one atmosphere of  $B_2F_4$  in a conventional liquid cell using a Carey white spectrograph. Only one Raman band was observed at ca. 680  $cm^{-1}$ . This is clearly the fully symmetric B-B stretching vibration.

[8] P. J. HENDRA, R. D. G. LANE and B. SMETHURST, *J. Sci. Inst.* **40**, 457 (1963).



## INTERPRETATION

There are three possible structures for  $B_2F_2$ :

(a) A planar structure in which  $\tau$ , the angle between the  $BF_2$  planes, is  $0^\circ$  (symmetry  $Vh$ ).

(b)  $Vd$  structure in which case  $\tau = 90^\circ$ . In this case the molecule is a symmetric top.

(c) That in which there is free rotation about the B—B bond ((a) and (b)) would correspond to an energy barrier to rotation about the B—B bond much greater than  $kT$  whereas case (c) corresponds to an energy barrier considerably less than  $kT$ . In the intermediate case the structure (b) will prevail with the molecules able to undergo vibrations in a comparatively shallow potential trough arising from the potential barrier.

The lowest possible symmetry in case (c) is  $D_2$ , but the vibrational selection rules are those of a group of higher symmetry. This arises from the invariance of the potential energy to a reflection in a plane bisecting and perpendicular to the B—B bond for free rotation. It has been shown from a study of nuclear permutations [9] that the effective point group for a free rotor molecule need not necessarily be one of the regular point groups. Thus that for freely rotating ethane is deduced to be one of order 36 containing four non-degenerate, four doubly-degenerate, and one quadruply-degenerate representations. The study of the nuclear permutation group will be pursued in a later section. Kopelman has been reported [10, 11] as proposing that the proper point group for a freely rotating molecule should contain the groups of all instantaneous configurations as sub-groups. Both  $Oh$  and  $D\infty_h$  groups satisfy this criterion for  $B_2F_4$ . There is however evidence against this [11] and this method will not be pursued.

In the first instance the evidence for and against a fixed configuration will be discussed and then an attempt made to explain the inadequacies of the evidence in terms of free rotation.

## FREQUENCY CALCULATIONS

In the following the labelling of the molecular axes is as recommended by MULLIKEN [12] thus fixing the nomenclature of the symmetry classes as defined by HERZBERG. The resulting cartesian axes relative to the molecular framework are shown in Fig. 1 and the distribution of vibrational modes for  $Vh$  and  $Vd$  symmetry shown in Table 2.

CRAWFORD and WILSON have shown [13] that where a torsion or twist angle for a given molecule can be defined to be orthogonal to all other symmetry co-ordinates the vibrational problem can be solved independently of this torsion by simply dropping the appropriate row and column of the  $G$  and  $F$  matrices. In the following the torsion is ignored since the co-ordinates are readily defined to comply with this requirement.

[9] H. C. LONGUET-HIGGINS, *Mol. Physics*, **6**, 445 (1963).

[10] R. KOPELMAN, Ph.D. Thesis, Columbia University (1960).

[11] C. V. BERNEY, L. R. COUSINS and F. A. MILLER, *Spectrochim. Acta* **19**, 2019 (1963).

[12] R. S. MULLIKEN, *J. Chem. Phys.* **23**, 1997 (1955).

[13] B. L. CRAWFORD and E. B. WILSON, *J. Chem. Phys.* **9**, 323 (1941).

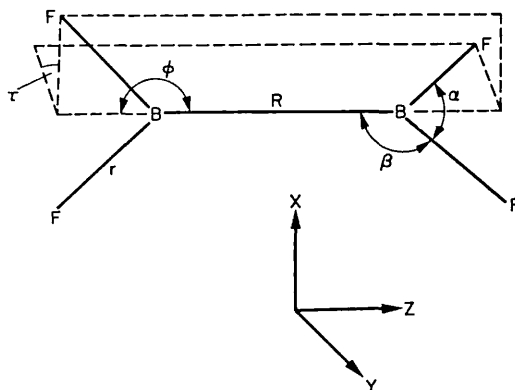


Fig. 1.

The  $G$  matrix terms for a molecule  $X_2Y_4$  have been tabulated by MANN and FANO [4] for the general case in which the angle between the two  $XY_2$  planes, is unspecified. Typographical errors occur in  $G$  9, 11 and  $G$  10, 11 which should both be of opposite signs. The force constants for the symmetry co-ordinates were determined as linear combinations of valence force constants by the matrix transformation.

$$\mathcal{F} = UFU^\dagger$$

where  $\mathcal{F}$  is the symmetry force constant matrix,  $F$  is the corresponding valence force constant matrix and  $U$  is the transformation matrix from valence to symmetry co-ordinates. The symmetry co-ordinates and the general  $\mathcal{F}$  terms are listed in Table 3.

As there are no structural data on  $B_2F_4$  in the gaseous phase, the geometrical parameters used were taken from the crystal data of TREFONAS and LIPSCOMB [1]. Assuming a  $120^\circ$  F—B—F angle the bond lengths in the crystal are  $1.67 \text{ \AA}$  for the B—B bond and  $1.32 \text{ \AA}$  for the B—F bond.

Table 2

(a) Symmetry $V_h \equiv D_{2h}$			
Class	No. of vibs.	Selection rules	i.r. band contours
$A_g$	3	$\alpha_{xx}, \alpha_{yy}, \alpha_{zz}$	—
$B_{1g}$	0	$\alpha_{xy}$	—
$B_{2g}$	1	$\alpha_{xz}$	—
$B_{3g}$	2	$\alpha_{yz}$	—
$A_u$	1 ( $\tau$ )	i.a.	—
$B_{1u}$	2	$T_z$	A (PR sep $13 \text{ cm}^{-1}$ )
$B_{2u}$	2	$T_y$	B (QQ sep $10 \text{ cm}^{-1}$ )
$B_{3u}$	1	$T_x$	C (PR sep $10 \text{ cm}^{-1}$ )
			very pronounced Q branch
(b) Symmetry $V_d \equiv D_{2d}$			
Class	No. of vibs.	Selection rules	i.r. band contours
$A_1$	3	$\alpha_{xx} + \alpha_{yy}, \alpha_{zz}$	—
$A_2$	1 ( $\tau$ )	i.a.	—
$B_1$	0	$\alpha_{xx} - \alpha_{yy}$	—
$B_2$	2	$T_z, \alpha_{xy}$	Type AQ sep $14 \text{ cm}^{-1}$
$E$	3	$(\alpha_{yz}, \alpha_{xz})$	Io/I total 0.2 Type AQ branch not very pronounced and broad.

Table 3

Force constant	Value BF <sub>3</sub> mdyn/Å	Value assumed mdyn/Å
$\mathcal{F}_{1,1} = f_R$	—	3.15
$\mathcal{F}_{1,2} = 2f_{Rr}$	—	0.0
$\mathcal{F}_{1,3} = 2.3^{-\frac{1}{2}}(f_{R\alpha} - f_{R\phi})$	—	0.0
$\mathcal{F}_{2,2} = \mathcal{F}_{4,4} = f_r + f_{rr}$	8.288	8.288
$\mathcal{F}_{2,3} = \mathcal{F}_{4,5} = 2.3^{-\frac{1}{2}}(f_{r\alpha} - f_{r\phi})$	—	0
$\mathcal{F}_{3,3} = \mathcal{F}_{5,5} = 3^{-1}(2f_\alpha + f_\phi - 4f_{\alpha\phi})$	$f_\alpha \cdot f_{\alpha\alpha} = 0.594$	0.594
$\mathcal{F}_{6,6} = \mathcal{F}_{9,9} = f_r - f_{rr}$	7.220	7.220
$\mathcal{F}_{6,7} = \mathcal{F}_{9,10} = f_{r\phi} - f_{r'\phi}$	$fr_\alpha \cdot fr'\alpha = 0.282$	0.282
$\mathcal{F}_{7,7} = \mathcal{F}_{10,10} = f_\phi$	$f_\alpha \cdot f_{\alpha\alpha} = 0.594$	0.594
$\mathcal{F}_{8,8} = \mathcal{F}_{11,11} = f_\gamma$	0.866	0.866

Terms involving  $\tau$ , and interactions involving  $\gamma$  assumed negligible.

An obvious source of values for the B—F force constants is the data of BF<sub>3</sub>. Force constants based on this data have been evaluated by several authors, e.g. [14, 15]. Due to symmetry restrictions the only constants which may be determined are as given in Table 3. In deriving  $F$  for B<sub>2</sub>F<sub>4</sub> it was assumed that the forces resisting deformation of the BBF angles are equal to those for the FBF angle. Since the restoring forces are principally determined by the electron configuration in the immediate vicinity of the central atom this ought to be a reasonable approximation. Likewise all interaction force constants involving  $\beta$  (see Fig. 1) are taken to be equal to their  $\alpha$  counterparts. The numerical values assumed are given in Table 3. The only value of a B—B stretching force constant in the literature is based on a Urey Bradley force field [4]. Based on this value a valence force constant of 3.0 mdyn/Å was assumed.

The calculated frequencies of "B<sub>2</sub>F<sub>4</sub> for  $\tau = 0^\circ$  and  $\tau = 90^\circ$  are given in Table 4.

The force constants for BF<sub>3</sub> are based on the harmonic vibrational frequencies, which all lie about 5% above the observed frequencies. To obtain a reasonable comparison between the calculated frequencies of B<sub>2</sub>F<sub>4</sub> and the observed it is necessary then to correct one or the other set for anharmonicity. It is reasonable

Table 4. Computed frequencies and intensities

Symmetry	Computed Freq.	Obs. Freq.	Intensities				
			$Vh$	$Vd$	Obs.*		
$Vh$	$Vd$	cm <sup>-1</sup>	cm <sup>-1</sup>	cm <sup>-1</sup>	( $\times 10^{-8}$ cm <sup>2</sup> mol <sup>-1</sup> sec <sup>-1</sup> ln)		
$B_{1u}$	$B_2$	1150	1150	1154	25	25	18.4
		557	557	543	5.5	5.5	1.8
	$E$	1431	1493	1372	24	20	15.3
$B_{2u}$ $B_{3u}$		789	1072	660?	3.3	6.7	0.1
		244	389	324	0.5	1.7	0.2

\* Arbitrary scale.

[14] W. R. HESLOP and J. W. LINNETT, *Trans. Faraday Soc.* **49**, 1266 (1953).

[15] D. C. MCKEAN, *J. Chem. Phys.* **24**, 1002 (1956).

to assume the same average anharmonicity for  $B_2F_4$  as for  $BF_3$  in which case the calculated frequencies must be reduced by 5%.

#### DISCUSSION OF EXPERIMENTAL RESULTS

The absence of authentic type *B* or type *C* bands makes a  $D_{2h}$  structure very unlikely for the gas. The only clearly resolved band contour—that of the  $541\text{ cm}^{-1}$  band places it unequivocally in the  $B_2$  class of the  $D_{2d}$  structure (or the  $B_{1u}$  class of the  $D_{2h}$  structure). Neither of the B—F stretching bands have the resolved band contours which are predicted utilising the formulae of GERHARD and DENNISON [16] and BADGER and ZUMWALT [17]. However this failure to resolve the band contour of high frequency modes is in the authors' experiences very common. Comparison with computations leads to the unambiguous assignment of the  $1372\text{ cm}^{-1}$  band to the *E* class and the  $1155\text{ cm}^{-1}$  band to the  $B_2$  class.

The infra-red active  $\hat{F}\hat{B}\hat{B}$  deformation is associated with the band at  $324\text{ cm}^{-1}$  though the observed intensity is low compared with that expected.

GAYLES and SELF consider the  $\gamma$  or out-of-plane B— $BF_2$  mode to be associated with a band at  $660\text{ cm}^{-1}$ . In our spectra this is overlapped by a doublet of moderate intensity which is presumably due to an impurity. A computation of the expected band intensities using the intensity parameters of  $BF_3$  derived by MCKEAN [18] indicates that this umbrella type mode band should be of comparable strength to the  $541\text{ cm}^{-1}$  band for both the *Vh* and *Vd* structures whereas it is less than  $\frac{1}{20}$ th of the intensity. The absolute gas pressures are only very approximately known due to the method of cell-filing employed (condensation in a cold finger within the cell), and consequently only relative intensities are significant. Computed and observed intensities are given in Table 4.

The observed combination bands have been discussed by GAYLES and SELF who have deduced the infra-red inactive frequencies, including the torsion frequency, from their assignments. Thus it is clear that the major unsatisfactory feature of an interpretation in terms of a rigid *Vd* molecule is the frequency and intensity of the  $\gamma$  bending mode. The assumption of a *Vh* structure affords better frequency agreement with expectation, but the expected intensity is still far too high and the band contours are irreconcilable.

#### FREE ROTATION

LONGUET-HIGGINS [7] defines the molecular symmetry group as the set of all feasible permutations, *P*, of positions and spins of identical nuclei and of all feasible  $PE^*$  where  $E^*$  is the inversion of all particle positions. Following this method of analysis the complete set of symmetry elements is *E*, (12), (34), (ab)(1324), (ab)(1423), (12)(34), (ab)(13)(24), (ab)(14)(23), and their products with  $E^*$ . 1, 2, 3 and 4 label the fluorine nuclei, *a* and *b* the boron nuclei and the brackets are conventional cyclic permutation brackets [18]. Tedious text-book techniques for determining

[16] S. L. GERHARD and D. M. DENNISON, *Phys. Rev.* **43**, 197 (1933).

[17] R. M. BADGER and L. R. ZUMWALT, *J. Chem. Phys.* **6**, 711 (1938).

[18] D. E. LITTLEWOOD, *The Theory of Group Characters*, Clarendon Press, Oxford (1950).

the irreducible representations of the appropriate group leads to the character Table 5 which is isomorphous with the  $D_{4h}$  point group.

Whilst this indicates the effective symmetry group for the vibrations it still remains to determine the distribution of the vibrations in the classes and their optical activities. The method used by the authors is an extension of the internal co-ordinate method for conventional point groups. Table 5 lists the characters  $\chi_i(R)$  where  $R$  is the internal co-ordinate and  $i$  the permutation. Then the number of vibrations associated with the internal co-ordinate  $R$  in species  $\Gamma$  is

$$n^\Gamma = 1/g \sum_i g_R \chi_i(R) \chi_i^\Gamma(R).$$

$\chi_i^\Gamma(R)$  is the character for permutation  $i$  in the irreducible representation  $\Gamma$ ,  $g_R$  is the degeneracy and  $g$  is the total number of permutations or the degree of the group. To determine the total number of vibrations in each irreducible representation it is necessary to remove the redundant symmetry co-ordinates. These were identified by inspection (Table 5).

The important result to be noted is that one pair of BF stretches and one pair of anti-symmetric in-plane angle bends form the symmetry co-ordinates for one degenerate class whilst the out-of-plane  $\gamma$  modes go into the other degenerate class. The full importance of this becomes apparent when the infra-red activities are considered. Unfortunately a complete treatment has not yet been worked out, but the implications are clear. The representation for the transition moment along the molecular B—B axis is  $\Gamma_3$ . This is most easily seen by noting the equivalent symmetry operations to the permutations (Table 5). In deducing these, the property is used that the two  $\text{BF}_2$  units can be freely rotated with respect to one another to bring the molecule back into its original configuration.  $C_1^{1,2}$  is a  $C_2$  rotation of the nuclear displacements associated with the  $\text{BF}_2$  unit carrying the fluorine labels 1 and 2.  $C_2^{\perp r}$  is a  $C_2$  rotation about an axis  $\perp^r$  to the B—B bond.

The transition moments  $\mu_x$  and  $\mu_y$  must form a degenerate pair but no clear method for deducing whether they belong to  $\Gamma_9$  or  $\Gamma_{10}$  has been worked out as yet. The authors' feeling is that they belong to  $\Gamma_9$ . However it is clear that the number of infra-red active fundamentals is less for a free rotor  $\text{B}_2\text{X}_4$  than for any fixed configuration.

#### DISCUSSION

The failure to observe a band of the expected strength for the  $\gamma$  type mode in the range 1000 to 600  $\text{cm}^{-1}$  may be due to free rotation about the B—B bond. In the case of a small potential barrier ( $< kT$ ) a fraction of the molecules ( $= \exp(-\Delta E/kT)$  where  $\Delta E$  is height of potential barrier) will be vibrating in the potential trough whilst the remainder will be undergoing free rotation. It is thus apparent that a weak  $\gamma$  mode and weak combination modes involving the torsion can be generally expected in an almost free rotor.

The shift of the infra-red active in-plane bend to lower frequencies resulting from condensation to the liquid phase reported by GAYLES and SELF is in accord with a free rotor structure in the gas phase as well as with a  $Vd$  type structure. In both cases removal of the degeneracy will lead to a splitting of the frequency components with the lower frequency becoming the ungerade component of the  $\gamma$  type



mode. The failure to see a B—BF<sub>2</sub> deformation band of expected intensity is therefore probably due to the fact that most of the molecules are undergoing free rotation. GAYLES and SELF have explained the long wavelength tails of the 657 and 325 cm<sup>-1</sup> bands by postulating the existence of a very low frequency torsion mode. This is also in accord with a low potential barrier.

*Acknowledgements*—Financial support from the Office of Naval Research, United States Navy and the European Research Office, U.S. Department of the Army is gratefully acknowledged. We are indebted to Dr. D. PETERS for helpful discussions.

C5

Offprinted from the *Transactions of The Faraday Society*,  
No. 504, Vol. 60, Part 12, December, 1964

VIBRATIONAL SPECTRA OF SOME HETROCYCLIC BORON COMPOUNDS  
PART 1.—COMPUTATIONS



# Vibrational Spectra of some Heterocyclic Boron Compounds

## Part 1.—Computations

BY ARTHUR FINCH AND D. STEELE

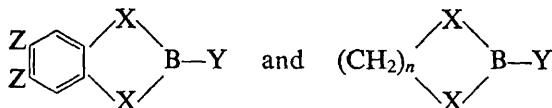
Moore Laboratory, Royal Holloway College (University of London),  
Englefield Green, Surrey

Received 29th May, 1964

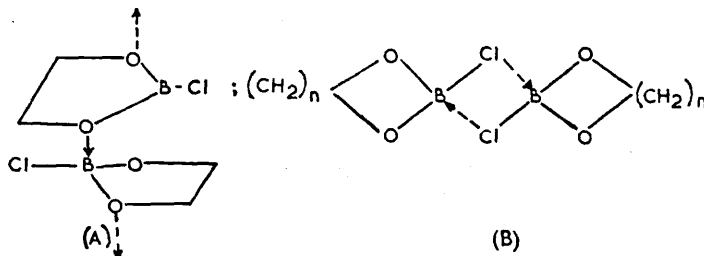
The fundamental vibrational frequencies and modes have been computed for some 5- and 6-membered cyclic boron compounds using a modified valence force field and treating  $\text{CH}_2$  units as point masses. The results are discussed in relation to previous assignments of BO, CO and B—Cl

vibrational bands in compounds containing the skeleton  $\text{C}_n \begin{array}{c} \diagup \text{O} \diagdown \\ \diagdown \text{B—Cl} \diagup \\ \diagup \text{O} \diagdown \end{array}$  and  $\text{C}_n \begin{array}{c} \diagup \text{O} \diagdown \\ \diagdown \text{B—phenyl} \diagup \\ \diagup \text{O} \diagdown \end{array}$ .

Heterocyclic boron compounds of the general formulae



have attracted considerable attention. In compounds of the first type in which  $\text{X} = \text{oxygen}$  and  $\text{Y} = \text{phenyl}$ , the antisymmetric BO and CO stretching modes were identified with two strong bands, at  $1326$  and  $1238 \text{ cm}^{-1}$ , respectively, which were insensitive to the exact structure of the aromatic moiety.<sup>1</sup> However, bands assigned to the symmetric vibrations were of variable strength and highly sensitive to the substituents. The BO assignments agree well with those given for the open chain  $(\text{RO})_2 \text{B-phenyl}$  systems.<sup>2</sup> The chemistry and some of the thermodynamic properties of compounds of the second type in which  $\text{X} = \text{oxygen}$ ,  $\text{Y} = \text{chlorine}$ , and  $n = 2$  or  $3$  [2-chloro-1,3,2-dioxaborolan (I), and -dioxaborinan (II), respectively] have been investigated.<sup>3, 4</sup> One feature is the varying degree of association of I, in liquid and solution phase,<sup>4</sup> resulting from relief of the ring strain inherent in the monomeric five-membered molecule. Association doubtless occurs as a result of a change in hybridization at the boron atom ( $sp^2 \rightarrow sp^3$ ). Boron-oxygen bridging, probably in a "stacking" arrangement such as (A), is presumably preferred to chlorine bridging as in (B):



Either form of bridging should in principle be reflected in a difference in vibrational spectrum between that of the monomeric, and that of the associated, molecule, since the change in structure will change the conditions for zero overall internal

momentum and, for chlorine bridging, the change in the B—Cl force constants will affect the appropriate observable frequencies.

The spectra of many molecules of the second class are known and some tentative assignments have been proposed.<sup>5, 6</sup> The attempt to identify characteristic B—Cl stretching bands in the spectra of compounds I and II was unsuccessful with compound I. This may be due in part to some B—Cl bridging, but the principal reason is the kinetic effect. The mass of the boron atom is so small compared with that of the chlorine atom that mixing of the B—Cl stretch with the O—B—O angle deformation and the symmetric O—B stretching co-ordinates is expected to be large. However, in the six-membered ring system, arguments have been given for assigning a band at 549 cm<sup>-1</sup> to the B—Cl stretching mode,<sup>5</sup> in accord with the analogous assignments of Lindemann and Wilson<sup>7</sup> at 696 cm<sup>-1</sup> in BF<sub>2</sub>Cl and of Lehmann, Onak and Shapiro<sup>8</sup> at 642 cm<sup>-1</sup> in (CH<sub>3</sub>O)<sub>2</sub>BCl. Gerrard and co-workers have preferred a B—Cl assignment close to 900 cm<sup>-1</sup>.<sup>9, 10</sup>

The approach to the above problems which is reported here was to compute the vibrational frequencies and modes of specific molecules, in particular compounds I and II and some related systems, using a modified valence force field transferred from related molecules and to compare calculated and observed transition frequencies.

#### COMPUTATIONS

##### MOLECULES OF GENERAL FORMULA C<sub>2</sub>Y<sub>2</sub>BX

The skeletons of (CH<sub>2</sub>)<sub>2</sub>O<sub>2</sub>BX molecules are essentially planar; thus the problem may be separated into the in-plane and out-of-plane motions if we treat the CH<sub>2</sub> unit as a point mass. The assumed geometry is that expected for 2-chloro 1,3-dioxaborolan, I, the principle molecule of interest, other systems being treated as isotopic homologues, and is shown in fig. 1a.

The vibrational problems were solved on the London University Mercury Computer as the eigenvalues and eigenvectors of the matrix  $\mathbf{D}^+\mathbf{F}\mathbf{D}$  where  $\mathbf{D}\mathbf{D}^+ = \mathbf{G}$  and  $\mathbf{G}$  and  $\mathbf{F}$  are the usual kinetic and potential matrices. The principal advantage of this technique is that redundancies in the symmetry co-ordinates are irrelevant, since the problem is transformed into cartesian. Further, the matrix  $\mathbf{D}^+\mathbf{F}\mathbf{D}$  is symmetric, thus permitting the use of fast programmes, such as Householders, to derive the eigenvalues and eigenvectors. The computer input consists of the  $\mathbf{F}$  matrix, a list of the atomic masses and the  $\mathbf{B}$  matrix. The  $\mathbf{B}$  matrix entries are trivial and given by the co-ordinate components of the Eliashevich-Wilson  $\mathbf{S}$  vectors.<sup>12</sup> For the O—B—Cl deformation the deformation co-ordinate was defined as the angle change between the B—Cl bond and the internal ring angle bisector.

The  $\mathbf{F}$  matrix requires comment. The force field is based on force constants for BCl<sub>3</sub>, H<sub>3</sub>BO<sub>3</sub> and aliphatic alcohols. The former molecule serves to determine  $f_{\text{BCl}}$  and  $f_{r\beta}$ . The force constants for B—O and O—B—O deformations were deduced from an analysis of the boric acid assignments of Hornig and Plumb<sup>13</sup> and Servoss and Clark<sup>14</sup> by ignoring the hydrogen atoms and assuming  $D_{3h}$  symmetry. For the symmetry co-ordinates,

$$S_1 = \frac{1}{\sqrt{3}}(\Delta r_1 + \Delta r_2 + \Delta r_3),$$

$$S_{2a} = \frac{1}{\sqrt{6}}(2\Delta r_1 - \Delta r_2 - \Delta r_3),$$

$$S_{3a} = \frac{r}{\sqrt{6}}(\theta_{12} + \theta_{31} - 2\theta_{23}),$$

where  $\Delta r_i$  is the stretching co-ordinate of the  $i$ th B—O bond and  $\theta_{ij}$  is the angular deformation of the angle between  $r_i$  and  $r_j$ , then

$$\begin{aligned} G_{11} &= 1/m_O, & F_{11} &= f_r + 2f_{rr'}, \\ G_{22} &= 1/m_O + 3/2m_B, & F_{22} &= f_r - f_{rr'}, \\ G_{33} &= 3/m_O + 9/2m_B, & F_{33} &= f_\theta - f_{\theta\theta'}, \\ G_{23} &= 3^{3/2}/2m_B, & F_{23} &= f_{r\theta} - f_{r\theta'} = 0 \text{ (assumed)} \end{aligned}$$

where  $f_{r\theta}$  refers to interaction between a stretching co-ordinate and one of its adjacent angles and  $f_{r\theta'}$  refers to non-adjacent interactions.

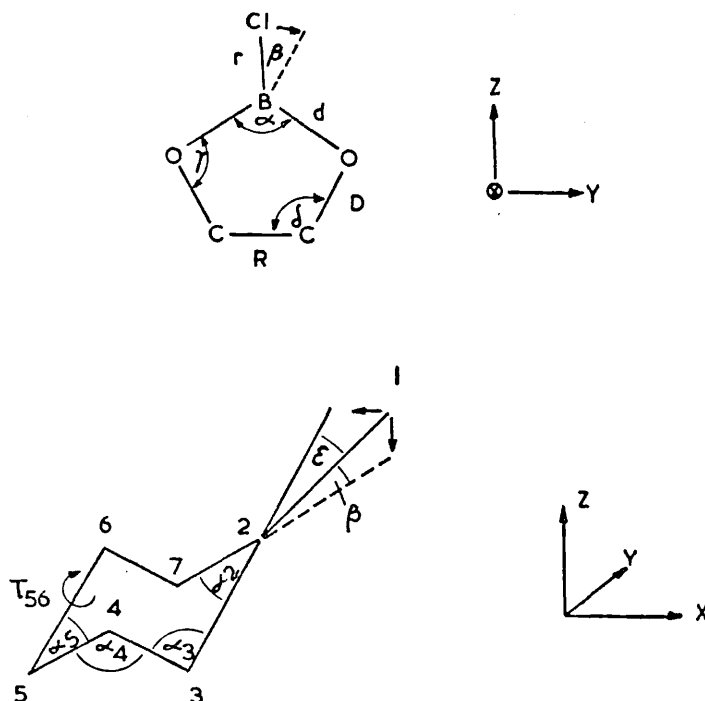


FIG. 1.—Internal co-ordinate definitions for compounds I and II.

For the  $a'$  class the B—O stretch is identified with the band at  $886 \text{ cm}^{-1}$ . In the  $e'$  class the BO stretch and the OBO deformations are at  $1430$  and  $544 \text{ cm}^{-1}$  respectively. This leads to the alternative sets of force constants

$$\begin{array}{ll} \text{(i)} & f_r = 5.62 \text{ mdynes/\AA}, & \text{(ii)} & 3.94 \text{ mdynes/\AA}, \\ & f_{rr} = 0.89 \text{ mdynes/\AA}, & & 1.74 \text{ mdynes/\AA}, \\ & r^2(f_\theta - f_{\theta\theta'}) = 0.74 \text{ mdynes/\AA}. & & 1.58 \text{ mdynes/\AA}. \end{array}$$

The first set is more satisfactory in that (i)  $f_{rr}/f_r$  is much less and (ii)  $f_\theta$  is more in line with the values for other  $\text{BX}_3$  compounds. The remaining problem is the choice of a magnitude for  $f_{\text{CCO}}$  for which no literature value could be found. Such angle force constants are expected to be determined principally by the central atom since the restoring forces arise from electron orbital deformations around this atom. A comparison of force constants for deformation XCY leads to a value of  $0.43 \text{ mdynes/\AA}$ . The complete list of force constants used is given in table 1. Whilst

TABLE 1

force constant value for co-ordinate	(mD/Å)
BCl	3.93
OB	5.62
OB/OB	0.89
BCl/OBO	-0.27
CO	5.4
CC	4.57
OBO $\times d$	0.74
BOC $\times D$	0.61
OCC $\times R$	0.43
CIBO $\times r$	0.46
torsions	0.04
Cl w.r.t. OBC $\times r$	0.414

such force constants must give only a poor approximation to the true force field the computed eigenvalues, or frequencies, are generally satisfactory—much more so than the eigenvectors. Even so the eigenvectors can be expected to give a good

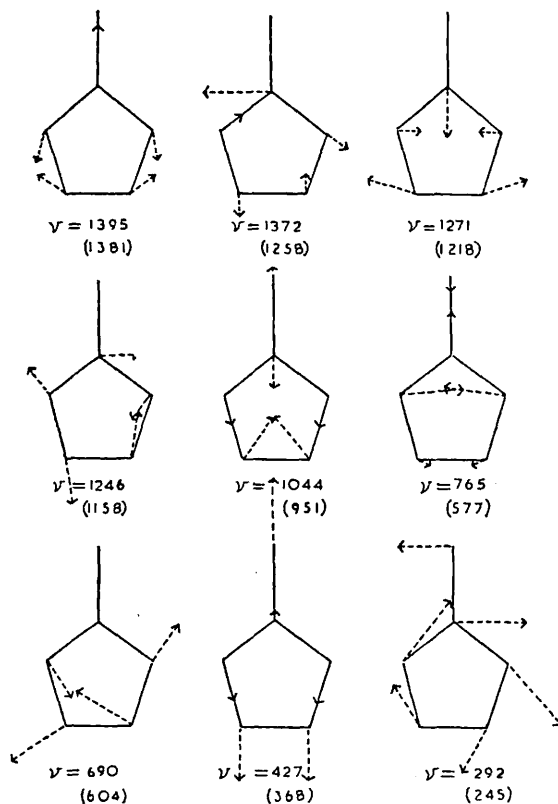


FIG. 2.—Normal co-ordinates for  $C_2O_2BCl(I)$  and  $C_2S_2BCl$  (frequencies of latter in parentheses).

qualitative picture of the vibrational modes, though they are unreliable for deducing dipole gradients from intensities.

The vibrational skeletal frequencies of  $C_2S_2BCl$  and  $C_2O_2BH$  were computed treating the systems as isotopic varieties of I. The computed frequencies for  $C_2O_2BCl$ ,

$C_2O_2BH$  and  $C_2S_2BCl$  are given in table 2 and the modes of  $C_2O_2BCl$  shown in fig. 2. The class designations follow from the recommendation of Mulliken.<sup>15</sup> The modes of  $C_2S_2BCl$  are similar to those of  $C_2O_2BCl$  and are indicated in fig. 2 by quoting the analogous  $C_2S_2BCl$  frequencies in parentheses.

TABLE 2.—COMPUTED AND OBSERVED FREQUENCIES ( $cm^{-1}$ )

$C_2O_2BCl$			$C_2S_2BCl$		$C_2O_2BH$		$C_3O_2BCl$	
calc.	sym.	obs.	calc.	sym.	calc.	sym.	calc.	sym.
1395	$a_1$	1475	1381	$a_1$	2677	$a_1$	1422	$a_1$
1372	$b_2$	1421	1258	$b_2$	1396	$b_2$	1324	$b_2$
1271	$a_1$	1320	1218	$a_1$	1348	$a_1$	1300	$b_2$
1246	$b_2$	1213	1158	$b_2$	1268	$b_2$	1266	$a_1$
1044	$a_1$	1051	951	$a_1$	1191	$a_1$	1134	$b_2$
765	$a_1$	719	604	$b_2$	990	$a_1$	1091	$a_1$
690	$b_2$	667	577	$a_1$	846	$b_2$	987	$a_1$
427	$a_1$		368	$a_1$	689	$b_2$	758	$a_1$
292	$b_2$		245	$b_2$	684	$a_1$	631	$a_1$
							508	$a_1$
							480	$b_2$
							390	$b_2$
							376	$a_1$
							226	$b_2$
							132	$a_1$

## 2-CHLORO-1,2,3 DIOXABORINAN

The  $F$  matrix is similar to that for the borolan except in that out-of-plane terms have to be introduced. However, the complexity of the  $B$  matrix warrants its description. Where internal co-ordinates are related by simple transformations of the type  $x_i^{Ra} \rightarrow \pm x_j^{Rb}$  the transformation coefficients alone are given for the second and further co-ordinates. The elements of the  $B$  matrix are the partial derivatives of the internal co-ordinates with respect to the cartesian co-ordinates, and are written down by inspection from the definitions of the internal co-ordinates in terms of the cartesian displacements  $X_i, Y_i, Z_i$ , of the  $i$ th atoms. These relationships are given below. The internal co-ordinates are as shown in fig. 1.

$$\Delta r_{12} = X_1 \sin \beta_2 + Z_1 \cos \beta_2 - Z_2 \cos \beta_2 - X_2 \sin \beta_2,$$

$$\Delta R_{23} = X_2 \cos \left( \frac{\alpha_2}{2} \right) \sin \beta_2 + y_2 \sin \left( \frac{\alpha_2}{2} \right) + Z_2 \cos \left( \frac{\alpha_2}{2} \right) \cos \beta_2,$$

$$- X_3 \cos \left( \frac{\alpha_2}{2} \right) \sin \beta_2 - y_3 \sin \left( \frac{\alpha_2}{2} \right) - Z_3 \cos \left( \frac{\alpha_2}{2} \right) \cos \beta_2,$$

$$\Delta R_{24} = +X_3 - X_4,$$

$$\Delta R_{45} \equiv \Delta R_{23} \quad \begin{array}{l} 2 \rightarrow 5 \quad X \rightarrow -X \\ 3 \rightarrow 4 \quad Y \rightarrow Y \\ \quad \quad \quad Z \rightarrow -Z, \end{array}$$

$$\Delta R_{56} \equiv \Delta R_{23} \quad \begin{array}{l} 2 \rightarrow 5 \quad X \rightarrow -X \\ 3 \rightarrow 6 \quad Y \rightarrow -Y \\ \quad \quad \quad Z \rightarrow -Z, \end{array}$$

$$\Delta R_{67} = -X_6 + X_7,$$

$$\Delta R_{72} \equiv \Delta R_{23} \quad \begin{array}{l} 2 \rightarrow 2 \quad X \rightarrow X \\ 3 \rightarrow 7 \quad Y \rightarrow -Y \\ \quad \quad \quad Z \rightarrow Z. \end{array}$$

$$\begin{aligned}
 R_{23}\Delta\alpha_2 = & -2X_2 \sin\left(\frac{\alpha_2}{2}\right) \sin\beta_2 - 2Z_2 \sin\left(\frac{\alpha_2}{2}\right) \cos\beta_2 + X_3 \sin\left(\frac{\alpha_2}{2}\right) \sin\beta_2 \\
 & - Y_3 \cos\left(\frac{\alpha_2}{2}\right) + Z_3 \sin\left(\frac{\alpha_2}{2}\right) \cos\beta_2 + X_7 \sin\left(\frac{\alpha_2}{2}\right) \sin\beta_2 \\
 & - Y_7 \cos\left(\frac{\alpha_2}{2}\right) + Z_7 \sin\left(\frac{\alpha_2}{2}\right) \cos\beta_2.
 \end{aligned}$$

$$\begin{aligned}
 R_{23}\Delta\alpha_3 = & X_2 \left[ \cos\left(\frac{\alpha_2}{2}\right) \cot\alpha_3 \sin\beta_2 + \operatorname{cosec}\alpha_3 \right] + Y_2 \cot\alpha_3 \sin\left(\frac{\alpha_2}{2}\right) \\
 & + Z_2 \cos\left(\frac{\alpha_2}{2}\right) \cot\alpha_3 \cos\beta_2 \\
 & + X_3 \left\{ \left( \frac{R_{23}}{R_{34}} \operatorname{cosec}\alpha_3 - \cot\alpha_3 \right) \cos\left(\frac{\alpha_2}{2}\right) \sin\beta_2 - \left( \operatorname{cosec}\alpha_3 - \frac{R_{23}}{R_{24}} \cot\alpha_3 \right) \right\} \\
 & + Y_3 \left\{ \left( \frac{R_{23}}{R_{34}} \operatorname{cosec}\alpha_3 - \cot\alpha_3 \right) \sin\left(\frac{\alpha_2}{2}\right) \right\} \\
 & + Z_3 \left\{ \left( \frac{R_{23}}{R_{34}} \operatorname{cosec}\alpha_3 - \cot\alpha_3 \right) \cos\left(\frac{\alpha_2}{2}\right) \cos\beta_2 \right\} \\
 & - X_4 \frac{R_{23}}{R_{34}} \left\{ \cot\alpha_3 + \cos\left(\frac{\alpha_2}{2}\right) \sin\beta_2 \operatorname{cosec}\alpha_3 \right\} - Y_4 \frac{R_{23}}{R_{34}} \sin\left(\frac{\alpha_2}{2}\right) \operatorname{cosec}\alpha_3 \\
 & - Z_4 \frac{R_{23}}{R_{34}} \cos\left(\frac{\alpha_2}{2}\right) \cos\beta_2 \operatorname{cosec}\alpha_3.
 \end{aligned}$$

$R_{45}\Delta\alpha_4 \equiv R_{23}\Delta\alpha_3$	2→5	$X \rightarrow -X$
	3→4	$Y \rightarrow Y$
	4→3	$Z \rightarrow -Z$
$R_{45}\Delta\alpha_5 \equiv R_{23}\Delta\alpha_2$	2→5	$X \rightarrow -X$
	3→4	$Y \rightarrow Y$
	7→6	$Z \rightarrow -Z$
$R_{56}\Delta\alpha_6 \equiv R_{23}\Delta\alpha_3$	2→5	$X \rightarrow -X$
	3→6	$Y \rightarrow -Y$
	4→7	$Z \rightarrow -Z$
$R_{27}\Delta\alpha_7 \equiv R_{23}\Delta\alpha_3$	2→2	$X \rightarrow X$
	3→7	$Y \rightarrow -Y$
	4→6	$Z \rightarrow Z$

$$\begin{aligned}
 r\Delta\gamma = & -X_1 \cos\beta_2 + Z_1 \sin\beta_2 - X_3 \frac{r}{R_{23}} \cos\beta_2 + Z_3 \frac{r}{R_{23}} \sin\beta_2 - X_7 \frac{r}{R_{23}} \cos\beta_2 \\
 & + Z_7 \frac{r}{R_{23}} \sin\beta_2 + X_2 \left( \cos\beta_2 + \frac{2r}{R_{23}} \cos\beta_2 \right) - Z_2 \sin\beta_2 \left( 1 + \frac{2r}{R_{23}} \right)
 \end{aligned}$$

$$\begin{aligned}
 r\Delta\beta = & Y_1 - X_3 \frac{r}{2R_{23}} \sin\beta_2 \sin\left(\frac{\alpha_2}{2}\right) + Y_3 \frac{r}{2R_{23}} \cos\left(\frac{\alpha_2}{2}\right) - Z_3 \frac{r}{2R_{23}} \cos\beta_2 \sin\left(\frac{\alpha_2}{2}\right) \\
 & + X_7 \frac{r}{2R_{23}} \sin\left(\frac{\alpha_2}{2}\right) \sin\beta_2 + Y_7 \frac{r}{2R_{23}} \cos\left(\frac{\alpha_2}{2}\right) + Z_7 \frac{r}{2R_{23}} \cos\beta_2 \sin\left(\frac{\alpha_2}{2}\right) \\
 & + Y_2 \left\{ 1 - \frac{r}{R_{23}} \cos\left(\frac{\alpha_2}{2}\right) \right\}.
 \end{aligned}$$

$$\begin{aligned}
 R_{23}\tau_{23} = & X_2 \cos \beta_2 \frac{(1 - \cos \alpha_2)}{\sin \alpha_2} - Y_2 \cot \alpha_3 \operatorname{cosec} \alpha_3 \cos \left(\frac{\alpha_2}{2}\right) \cos \beta_2 \\
 & + Z_2 \left( \cot \alpha_2 \sin \beta_2 + \cot \alpha_3 \sin \left(\frac{\alpha_2}{2}\right) - \operatorname{cosec} \alpha_2 \sin \beta_2 \right) \\
 & + X_3 \cot \alpha_2 \cos \beta_2 - Y_3 \left( \frac{R_{23}}{R_{34}} - \cos \alpha_3 \right) \operatorname{cosec}^2 \alpha_3 \cos \left(\frac{\alpha_2}{2}\right) \cos \beta_2 \\
 & + Z_3 \left( \frac{R_{23}}{R_{34}} \sin \left(\frac{\alpha_2}{2}\right) - \cot \alpha_3 \operatorname{cosec} \alpha_3 \sin \left(\frac{\alpha_2}{2}\right) - \cot \alpha_2 \sin \beta_2 \right) \\
 & + Y_4 \frac{R_{23}}{R_{34}} \operatorname{cosec}^2 \alpha_3 \cos \left(\frac{\alpha_2}{2}\right) \cos \beta_2 - Z_4 \frac{R_{23}}{R_{34}} \sin \left(\frac{\alpha_2}{2}\right) \operatorname{cosec}^2 \alpha_3 \\
 & - X_7 \cos \beta_2 \operatorname{cosec} \alpha_2 + Z_7 \sin \beta_2 \operatorname{cosec} \alpha_2.
 \end{aligned}$$

$$\begin{aligned}
 R_{34}\tau_{34} = & \frac{R_{34}}{R_{23}} \frac{\cos \left(\frac{\alpha_2}{2}\right) \cos \beta}{\sin \alpha_3} Y_2 + \frac{R_{34}}{R_{23}} \frac{\sin \left(\frac{\alpha_2}{2}\right)}{\sin^2 \alpha_3} Z_2 \\
 & + Y_3 \left\{ \frac{R_{34}}{R_{23}} \frac{\cos \left(\frac{\alpha_5}{2}\right) \cos \beta}{\sin^2 \alpha_3} - \frac{\cos \alpha_3 \cos \left(\frac{\alpha_5}{2}\right) \cos \beta}{\sin^2 \alpha_3} + \frac{\cos \alpha_4 \cos \left(\frac{\alpha_5}{2}\right) \cos \beta}{\sin^2 \alpha_4} \right\} \\
 & + \left\{ \frac{R_{34}}{R_{23}} \frac{\sin \left(\frac{\alpha_2}{2}\right)}{\sin^2 \alpha_3} + \frac{\cos \alpha_3 \sin \left(\frac{\alpha_2}{2}\right)}{\sin^2 \alpha_3} + \frac{\cos \alpha_4 \sin \left(\frac{\alpha_5}{2}\right)}{\sin^2 \alpha_4} \right\} Z_3 \\
 & + \left\{ \frac{R_{34}}{R_{45}} \frac{\cos \left(\frac{\alpha_5}{2}\right) \cos \beta}{\sin^2 \alpha_4} + \frac{\cos \alpha_4 \cos \left(\frac{\alpha_5}{2}\right) \cos \beta}{\sin^2 \alpha_4} - \frac{\cos \alpha_3 \cos \left(\frac{\alpha_2}{2}\right) \cos \beta}{\sin^2 \alpha_3} \right\} Y_4 \\
 & + \left\{ \frac{R_{34}}{R_{45}} \frac{\sin \left(\frac{\alpha_5}{2}\right)}{\sin^2 \alpha_4} + \frac{\cos \alpha_4 \sin \left(\frac{\alpha_5}{2}\right)}{\sin^2 \alpha_4} - \frac{\cos \alpha_3 \sin \left(\frac{\alpha_2}{2}\right)}{\sin^2 \alpha_3} \right\} Z_4 \\
 & - \frac{R_{34}}{R_{45}} \frac{\cos \left(\frac{\alpha_5}{2}\right) \cos \beta}{\sin^2 \alpha_4} Y_5 - \frac{R_{34}}{R_{45}} \frac{\sin \left(\frac{\alpha_5}{2}\right)}{\sin^2 \alpha_4} Z_5.
 \end{aligned}$$

$R_{45}\tau_{45} \equiv R_{23}\tau_{23}$	2→5	$X \rightarrow -X$
	3→4	$Y \rightarrow Y$
	4→3	$Z \rightarrow -Z$
	7→6,	
$R_{56}\tau_{56} \equiv R_{23}\tau_{23}$	2→5	$X \rightarrow X$
	3→6	$Y \rightarrow Y$
	4→7	$Z \rightarrow Z$
	7→4,	
$R_{67}\tau_{67} \equiv R_{34}\tau_{34}$	2→5	
	3→6	$Y \rightarrow Y$
	4→7	$Z \rightarrow Z$
	5→2,	
$R_{72}\tau_{72} \equiv R_{23}\tau_{23}$	2→2	$X \rightarrow -X$
	3→7	$Y \rightarrow Y$
	4→6	$Z \rightarrow -Z$
	7→3.	

The computed modes are shown in fig. 3, the  $XZ$  displacements being depicted as arrows from the nuclear positions of the atoms 1, 2, 3, 4 and 5. The designations

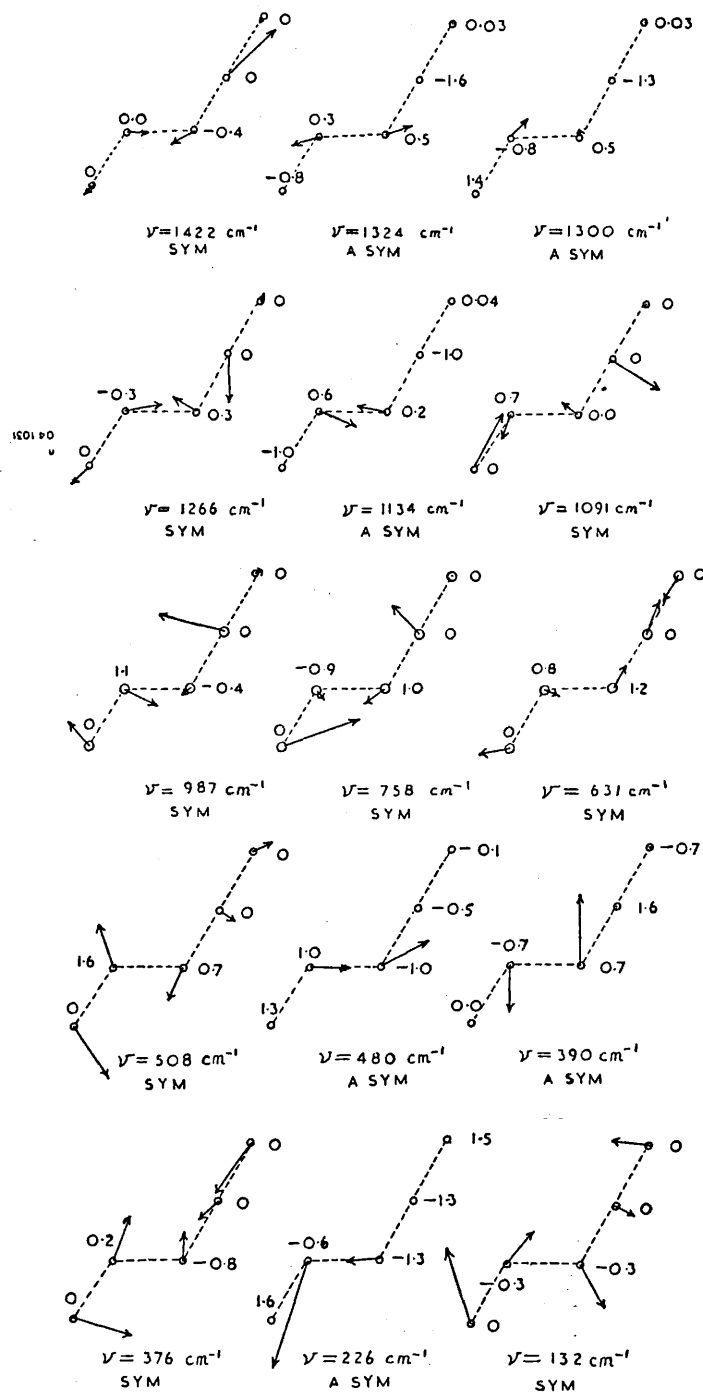


FIG. 3.—Normal co-ordinates for  $C_3O_2BCl(II)$ . Displacements shown for atoms 1 to 5. The other displacements follow from the symmetric or anti-symmetric behaviour of co-ordinates with respect to plane of symmetry.



symmetric and antisymmetric define the symmetry of the normal mode with respect to the plane of symmetry. Perpendicular displacements are quoted as  $[10^{\frac{5}{2}}/(v_j M_j)^{\frac{1}{2}}] Y_{ij}$ , where  $Y_{ij}$  is a term in the vector matrix of  $A$  such that  $YY^+ = E$ .  $M_j$  is the mass in a.u. corresponding to the  $j$ th co-ordinate.

## DISCUSSION

The agreement between calculated and observed bands for compound I indicates that the in-plane vibrations may be analyzed in terms of an isolated molecule model. Hence the known strong intermolecular association of this compound is not reflected in the vibrational spectrum, and it does not appear possible to differentiate between the various associative structures on this basis. Thus the existence of chlorine bridging (B, above) for example, may not be settled by attempts to distinguish a change in the vibrational frequency of the B—Cl mode between monomeric and polymeric species. An inspection of the modes shown in fig. 2 shows that mixing of the co-ordinates is very strong—especially in the symmetric class—and it is particularly difficult to assign the label B—Cl stretch to any one mode. An analysis of the potential energy distribution frequently assists in clarifying such a situation. The potential energy in a vibration  $i$  arising from any one force constant  $f_{jk}$  is  $l_{ij}l_{ik}f_{jk}$ . Since in general,  $f_{jj} \gg f_{jk}$ , a useful simplification is to consider only the diagonal force constants. In table 3, the potential energy distribution (p.e.d.)

is tabulated in the form  $\frac{(l_{ij})^2 f_{jj}}{\sum_k (l_{ik})^2 f_{kk}} \times 100$ . In this form it is apparent that the  $b_2$

vibrations may be classified according to mode type. More than 60 % of the potential energy in each case is associated with one type of deformation. However, the  $a_1$  vibrations are strongly mixed and any classification is artificial. The

TABLE 3

frequency	symmetry	% potential energy associated with force constant for							
		$r$	$d$	$D$	$R$	$d\alpha$	$D\gamma$	$R$	$r\beta$
1395 $\text{cm}^{-1}$	$a_1$	16	26	25	11	16	16	0	0
1372	$b_2$	0	76	10	0	0	2	7	4
1271	$a_1$	12	21	14	44	2	1	5	0
1246	$b_2$	0	15	67	0	0	2	11	5
1044	$a_1$	7	2	54	31	0	2	4	0
765	$a_1$	23	28	0	7	18	17	6	0
690	$b_2$	0	6	10	0	0	22	62	0
427	$a_1$	49	3	4	0	27	15	2	0
292	$b_2$	0	9	0	0	0	1	0	90

potential energy distribution indicates that the lowest  $a_1$  vibration is the best candidate as a B—Cl stretch. The reason that the p.e.d. shows this much more clearly than the diagrammatic representation of the modes is that the amplitude of the vibration is apparent in the diagrams and the energy associated with the deformation is proportional to the amplitude squared. Since the total energy is proportional to the frequency, the deformation amplitudes of the high frequency modes contribute a comparatively much smaller percentage of the energy to the mode than do the corresponding deformations of the low frequency modes to their vibrational energies. If, then, we do assign the lowest frequency vibration to the B—Cl mode it then becomes impossible to affix the symmetric ring angle deformation label to any single (observed) frequency. The best one can do is to say that the different

types of valence deformations contribute largely to certain vibrations in the following order of importance :

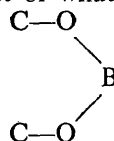
C—C stretch	1271, 1044 $\text{cm}^{-1}$ ,
C—O stretch	1044, 1395 $\text{cm}^{-1}$ ,
B—O stretch	765, 1395, 1271 $\text{cm}^{-1}$ ,
B—Cl stretch	427, 765, 1395, 1271 $\text{cm}^{-1}$ ,
OBO	427, 765, 1395 $\text{cm}^{-1}$ ,
BOC	765, 1395, 427 $\text{cm}^{-1}$ .

A striking fact apparent from this table—apart from the severity of the mixing—is that whenever the B—Cl stretch contributes largely to the p.e.d. so does the OBO angular deformation. Also, except for the lowest vibration the contribution of the B—O stretch parallels the contribution of the B—Cl stretch. These facts are exactly as expected from qualitative kinetic considerations.

The assignments proposed<sup>1</sup> for phenyl boronates are confirmed by the present work and, indeed, the agreement between the spectroscopic work and the calculations affords a vindication of the present model. As mentioned above, the anti-symmetric modes are pure individual co-ordinate deformation modes. The anti-symmetric BO stretching mode computed to be at 1372  $\text{cm}^{-1}$  in compound I is found at about  $1320 \pm 6 \text{ cm}^{-1}$  in the phenyl substituted analogues. The antisymmetric CO stretch computed to be at 1246  $\text{cm}^{-1}$  is found at  $1238 \pm 4 \text{ cm}^{-1}$  in the five-membered ring systems. However, the observed mass sensitivity of the symmetric modes is shown to arise from a strong coupling of the vibrations. That the coupling is far less in the antisymmetric modes is a natural consequence of the geometrical configuration which permits relatively independent displacements in the one case and not in the other.

An examination of fig. 3 shows that most of what has been said for I applies

to II. However, the non-planarity of the



system permits a smaller

degree of coupling between the individual vibrations except that coupling between CO and CC antisymmetric is greater. The mode at 631  $\text{cm}^{-1}$  is a "good" B—Cl stretching mode, but the symmetric vibrations near 1000  $\text{cm}^{-1}$  contain scarcely any contribution from this vibration. This confirms the B—Cl assignment given.<sup>5</sup>

<sup>1</sup> Butcher, Gerrard, Howarth, Mooney and Willis, *Spectrochim. Acta*, 1964, **20**, 79.

<sup>2</sup> Bellamy, Gerrard, Lappert and Williams, *J. Chem. Soc.*, 1958, 2412.

<sup>3</sup> Finch, Gardner and Pearn, *J. Chem. Soc.*, 1962, 1428.

<sup>4</sup> Finch and Gardner, *J. Inorg. Nucl. Chem.*, 1963, **25**, 927.

<sup>5</sup> Finch, Hendra and Pearn, *Spectrochim. Acta*, 1962, **18**, 51.

<sup>6</sup> Finch and Pearn, *Spectrochim. Acta*, 1963, **19**, 1621.

<sup>7</sup> Lindemann and Wilson, *J. Chem. Physics*, 1956, **24**, 242.

<sup>8</sup> Lehmann, Onak and Shapiro, *J. Chem. Physics*, 1959, **30**, 1219.

<sup>9</sup> Blau, Gerrard, Lappert, Mountfield and Pyszora, *J. Chem. Soc.*, 1960, 380.

<sup>10</sup> Butcher, Gerrard, Howarth, Mooney and Willis, *Spectrochim. Acta*, 1963, **19**, 905.

<sup>11</sup> Steele, *J. Mol. Spectr.*, in press.

<sup>12</sup> see Wilson, Decius and Cross, *Molecular Vibrations* (McGraw-Hill, London, 1955).

<sup>13</sup> Hornig and Plumb, *J. Chem. Physics*, 1957, **26**, 638.

<sup>14</sup> Servoss and Clark, *J. Chem. Physics*, 1957, **26**, 1175.

<sup>15</sup> Mulliken, *J. Chem. Physics*, 1955, **23**, 1997.

Offprinted from the *Transactions of the Faraday Society*,  
No. 506, Vol. 61, Part 2, February, 1965

## Far Infra-red Spectra of Boron Tri-bromide and Boron Tri-iodide

BY ARTHUR FINCH, I. J. HYAMS AND D. STEELE

Dept. of Chemistry, Royal Holloway College, University of London,  
Englefield Green, Surrey

Received 27th July, 1964

The far infra-red spectra of boron tri-bromide and boron tri-iodide have been measured. Previous assignments of the former compound have been confirmed, and for the latter compound one small change has been found necessary. Evidence for complexing with benzene is presented.

The vibrational spectra of the boron halides have been extensively investigated<sup>1-6</sup> with the principal aim of elucidating the force fields in this series of simple molecules.<sup>1-4, 7, 8</sup> Nevertheless the infra-red spectra of boron tri-bromide and boron tri-iodide have been measured only above 400  $\text{cm}^{-1}$ .<sup>1, 2</sup> The assignments for the former molecule are relatively firm, being based largely on the Raman spectrum.<sup>4-6</sup> However, some minor details remain to be clarified. For example, only the  $^{11}\text{B}$  isotope band has been observed for the umbrella motion ( $\nu_2$ ) and this but very weakly. Anderson, Lassetre and Yost failed to observe it at all, though they recorded its overtone frequency.<sup>4</sup> Boron tri-iodide is extremely difficult to maintain free of iodine and this precludes the measurement of its Raman spectrum using conventional mercury sources. The vibrational assignments of Wentink and Tiensuu<sup>1</sup> are based solely on the observation of the band due to the antisymmetric stretching fundamental ( $\nu_3$ ) and a number of very weak combination bands. The remaining fundamental bands are expected at frequencies which are below the accessible range in that investigation. Clearly a measurement of the far infra-red spectra of both these compounds is desirable.

### EXPERIMENTAL

Boron tri-bromide from L. Light & Co., Colnbrook, Bucks., was fractionally distilled and the portion boiling at 89.5° collected. Further purification was obtained by repeated vacuum distillation through a trap maintained at 5° into one at -79°, until the vapour pressure was 18.5 mm Hg at 0°.

Boron tri-iodide (3 N purity) from the above company, analyzed well for boron and iodine and was not further purified. (Found: B, 2.49; I, 96.6. Calc. for  $\text{BI}_3$ : B, 2.76; I, 97.2 %.) All manipulations were carried out in a dry, oxygen-free atmosphere of nitrogen.

The spectra were measured using a far infra-red grating spectrometer designed and constructed in this department and described in detail elsewhere.<sup>9</sup> Measurements were made over the range 430-100  $\text{cm}^{-1}$  on the pure boron tri-bromide (fig. 1a) and on solutions of boron tri-iodide in carbon disulphide and in benzene (fig. 1b and 1c).

### RESULTS AND DISCUSSION

#### BORON TRI-BROMIDE

The spectrum of boron tri-bromide is readily interpreted, as shown in table 1, on the expected  $D_{3h}$  nuclear symmetry. Four fundamentals are anticipated with

a class distribution of  $a_1'(R) + a_2''(I) + 2e'(I,R)$ . Activities are shown in parentheses. The observed isotope frequency ratio for the umbrella vibration agrees well with the theoretical (1.048, cf. 1.047). If the shoulder on the in-plane deformation band at  $151 \text{ cm}^{-1}$  is assumed to arise from isotope splitting a far too large Redlich-Teller

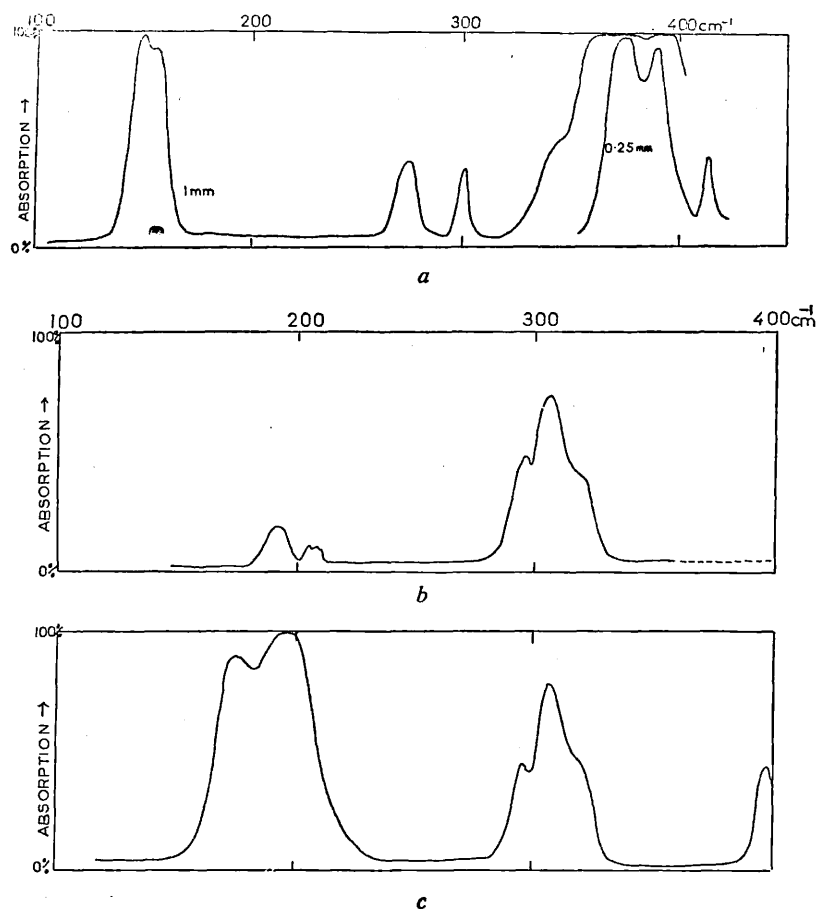


FIG. 1.—The far infra-red spectrum (redrawn) of (a) boron tri-bromide (pure liquid) 1 mm, 0.25 mm; (b) boron tri-iodide in CS (50% in 1 mm); (c) boron tri-iodide in  $\text{C}_6\text{H}_6$  (50% in 1 mm).

TABLE 1.—VIBRATIONAL SPECTRA OF  $\text{BBr}_3$  (LIQUID STATE FREQUENCIES)

i.r. <sup>a</sup> ( $\text{cm}^{-1}$ )	i.r. <sup>b</sup> ( $\text{cm}^{-1}$ )	Raman <sup>c</sup> ( $\text{cm}^{-1}$ )	assignments
n.m. } vvs	845	846	$\nu_3$ $^{10}\text{B}$ anti-symmetric stretch
n.m. }	802	800	$\nu_3$ $^{11}\text{B}$ " "
429 mw	430	—	$\nu_1 + \nu_4$
390 ms	n.m.	—	$\nu_2$ $^{10}\text{B}$ umbrella deformation
372 s	n.m.	372	$\nu_2$ $^{11}\text{B}$ " "
301 w	n.m.	—	$2 \times \nu_4(a+e')$
278 w	n.m.	279	$\nu_1$ symmetric stretch
155 ms sh	n.m.	—	$\nu_4 \rightarrow 2\nu_4$
151 s	n.m.	151	$\nu_4$ in-plane deformation

<sup>a</sup> this work.

<sup>b</sup> ref. 1: weak combination bands above  $430 \text{ cm}^{-1}$  not included.

<sup>c</sup> average data: ref. 4-6.

product ratio results when combining the data with the anti-symmetric stretch data. It must then be assumed that the observed shoulder is due to hot bands.

It is scarcely surprising that at the thicknesses employed the symmetric stretch transition results in a weak infra-red absorption. An accompanying band at  $301\text{ cm}^{-1}$  is presumably due to the first overtone of  $\nu_4$ . This has the symmetry  $a_1 + e'$  and may acquire some intensity by virtue of Fermi resonance with  $\nu_1$  though it is also active in its own right.

#### BORON TRI-IODIDE

The spectra were measured in solutions of carbon disulphide and benzene. In the frequency region above  $200\text{ cm}^{-1}$  the spectra agree well. No strong absorption appears in either case despite using concentrations of up to 4 parts of  $\text{BI}_3$  to 1 part of solvent in a 1 mm cell. This shows that the umbrella motion is far weaker than in  $\text{BBr}_3$  and would imply that the flow of electrons into the  $p_z$  orbital during the umbrella motion is just sufficient to compensate for the bond dipole movements. Only one component of the  $300\text{ cm}^{-1}$  complex can be explained as due to  $\nu_1 + \nu_4$  and it would appear necessary to assume that the  $\nu_2$  fundamental has in fact been observed and corresponds to the  $305\text{ cm}^{-1}$  band. The weak combination bands observed by Wentink and Tiensuu and explained by postulating  $\nu_2 = 336\text{ cm}^{-1}$  cannot all be conveniently reassigned. The  $717\text{ cm}^{-1}$  band is  $2\nu_2 + \nu_4$  in resonance with  $\nu_3$ ; but the  $806$  and  $772\text{ cm}^{-1}$  bands are not readily explained. The  $772\text{ cm}^{-1}$  band has in fact been observed in the present work as a weak shoulder on the fundamental band (at  $760\text{ cm}^{-1}$  in the liquid phase), but no trace of absorption at  $806\text{ cm}^{-1}$  could be seen in the liquid phase. Wentink and Tiensuu only noted this band in the vapour phase and therefore its existence must be suspect.

In the  $200\text{ cm}^{-1}$  region the benzene and carbon disulphide spectra are vastly different. That of  $\text{BI}_3$  in  $\text{CS}_2$  shows weak absorption at the expected position for the symmetric stretch. In benzene solution this band appears with considerable intensity though its frequency is little changed. This is as might be expected if  $\text{BI}_3$  is complexing to the benzene by some type of electron donation from the  $\pi$ -electron cloud to the vacant  $p_z$  orbital of the boron, thus destroying the planarity of the  $\text{BI}_3$ . The  $178\text{ cm}^{-1}$  band may be due to the first overtone of a somewhat reduced  $\nu_4$ .

Since the in-plane assignments for  $\text{BI}_3$  are unaltered by the present work the corresponding force constants derived in ref. 1, 7 and 8 remain unchanged. The corrected  $\nu_2$  frequency leads to a force constant for the umbrella motion of  $0.065\text{ md/\AA}$ . This value is to be compared with that of Wentink and Tiensuu of  $0.079\text{ md/\AA}$  ( $= k\Delta)/(3/2)$ . The value is still in line with those of the other boron halides.

TABLE 2.—VIBRATION SPECTRA OF  $\text{BI}_3$  (SOLUTION FREQUENCIES)

$\text{CS}_2$ ( $\text{cm}^{-1}$ )	$\text{C}_6\text{H}_6$ ( $\text{cm}^{-1}$ )	assignments
724 <sup>a</sup> vvs		$\nu_3$ <sup>10</sup> B
692 <sup>a</sup> vvs		$\nu_3$ <sup>11</sup> B
n.m.	396 w	$\nu_2 + \nu_4$
320 w	320 w	$\nu_2$ <sup>10</sup> B
305 m	306 m	$\nu_2$ <sup>11</sup> B
295 w	294 w	$\nu_1 + \nu_4$ ?
206 vw		$2 \times \nu_4$ <sup>10</sup> B or $\nu_2 - \nu_4$
202 vw		$2 \times \nu_4$ <sup>11</sup> B
189 w	196 s	$\nu_1$
	178 ms	$2 \times \nu_4$ ?

<sup>a</sup> ref. 1.

We gratefully acknowledge financial support from the European Research Office, U.S. Army, and the Office of Naval Research, U.S. European Research-Contracts Programme for research in the fields of boron chemistry and far infra-red spectroscopy respectively. The gratings used in the spectrometer are on loan from the National Physical Laboratory. We also wish to thank Mr. S. Ashdown who developed a technique of making vacuum-tight cells out of rigidex.

- 1 Wentink and Tiensuu, *J. Chem. Physics*, 1958, **28**, 826.
- 2 Lindemann and Wilson, *J. Chem. Physics*, 1956, **24**, 242.
- 3 earlier references quoted in ref. 1 and 2.
- 4 Anderson, Lassetre and Yost, *J. Chem. Physics*, 1936, **4**, 703.
- 5 Ananthakrishnan, *Proc. Indian Acad. Sci.*, 1936, **4**, 74.
- 6 Wagner, *Z. Physik Chem.*, 1943, **193**, 55.
- 7 Ladd, Orville-Thomas and Cox, *Spectrochim. Acta*, 1963, **19**, 1911.
- 8 Duncan, *J. Mol. Spectroscopy*, 1964, **13**, 283.
- 9 Hendra, Lane and Smethurst, *J. Sci. Inst.*, 1963, **40**, 457.

[Reprinted from the Journal of the American Chemical Society, **87**, 5346 (1965).]  
 Copyright 1965 by the American Chemical Society and reprinted by permission of the copyright owner.

## The Vibrational Spectra and Structure of Cyclooctatetraeneiron Tricarbonyl<sup>1</sup>

R. T. Bailey, E. R. Lippincott, and D. Steele

*Contribution from the Department of Chemistry, University of Maryland,  
 College Park, Maryland. Received May 28, 1965*

*The infrared (4000–110 cm.<sup>-1</sup>) and Raman (up to 1650 cm.<sup>-1</sup>) spectra of cyclooctatetraeneiron tricarbonyl are reported. The Raman spectra were excited by the rubidium resonance line at 7800 Å. obtained from a radiofrequency-powered rubidium plasma arc. The spectra indicated a low symmetry (C<sub>s</sub>) for the complex, with identical structures in the solid and solution states, and no free rotation between the hydrocarbon ring and the Fe(CO)<sub>3</sub> group. The results were also consistent with the presence of some π-electron delocalization in the uncoordinated part of the cyclooctatetraene ring system.*

### Introduction

Several structures based on a variety of physical and chemical evidence have been postulated for cyclooctatetraeneiron tricarbonyl, (COT)Fe(CO)<sub>3</sub>.<sup>2–6</sup> The pres-

ence of a single, sharp proton resonance in the nuclear magnetic resonance spectrum and the absence of a strong infrared absorption attributable to an olefinic C=C stretching vibration were widely interpreted as strong evidence for a planar cyclooctatetraene (COT) ring in the complex. Chemical evidence, indicating the absence of free olefinic double bonds, also influenced workers toward this conclusion. Two molecular orbital calculations, based upon a planar configuration of the COT ring claimed to have rationalized the bonding in the complex.<sup>5,6</sup> Recent X-ray diffraction data, however, clearly established that in the crystalline solid, at least, the Fe(CO)<sub>3</sub> group is bonded to the butadiene-like residue in the COT ring.<sup>7</sup> The structure is shown in Figure 1. The dihedral COT ring lies in two planes, the angle between which is 41°. The Fe(CO)<sub>3</sub> group is associated with only one pair of conjugated double bonds, with the remaining

(4) A. Nakamura and N. Hogihara, *Bull. Chem. Soc. Japan*, **32**, 880 (1959).

(5) D. A. Brown, *J. Inorg. Nucl. Chem.*, **10**, 39, 49 (1959).

(6) F. A. Cotton, *J. Chem. Soc.*, 400 (1960).

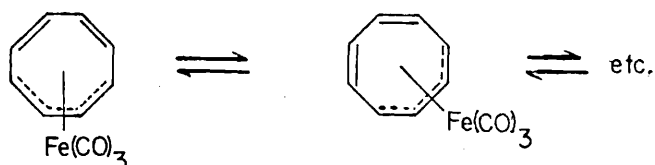
(7) (a) B. Dickens and W. N. Lipscomb, *J. Am. Chem. Soc.*, **83**, 4062 (1961); (b) *J. Chem. Phys.*, **37**, 2084 (1962).

(1) This work has been supported in part by the U. S. Atomic Energy Commission, the U. S. Public Health Service, and the Advanced Research Projects Agency, Department of Defense.

(2) T. A. Manuel and F. G. A. Stone, *Proc. Chem. Soc.*, 90 (1959); *J. Am. Chem. Soc.*, **82**, 336 (1960).

(3) M. D. Rausch and G. N. Schrauzer, *Chem. Ind. (London)*, 957 (1959).

pair forming a second plane and having relative positions very similar to those in butadiene. This structure, however, leaves unexplained the presence of the single sharp proton resonance in  $\text{CS}_2$  solution; such a structure should give rise to a more complicated n.m.r. spectrum. This anomaly can be resolved in one of three ways: by assuming a negligible relative chemical shift, a different geometry in the solid and solution states, or a dynamical effect. Dickens and Lipscomb<sup>7b</sup> concluded that a dynamical effect, resulting in the equivalence of all the protons in the COT ring, was the most plausible explanation. To accomplish this, the  $\text{Fe}(\text{CO})_3$  group is assumed to be rapidly rotating around the COT ring, *i.e.*



This mechanism has also been invoked to account for the single proton resonance observed in iron tricarbonyl complexes of the tropylium ion.<sup>8</sup>

In this work, the infrared and Raman spectra of  $(\text{COT})\text{Fe}(\text{CO})_3$  have been studied in an attempt to gain a better insight into the structure and chemical bonding involved in this compound. The Raman spectra were of particular interest in the  $\text{C}=\text{C}$  stretching region, where the infrared data were inconclusive, and also below  $250\text{ cm}^{-1}$ , where the low-lying fundamentals can be detected. Several partial infrared investigations have been reported,<sup>2,3,6</sup> and Fritz and Keller<sup>9,10</sup> measured the infrared spectra of the solid complex in KBr pellets from  $4000$  to  $250\text{ cm}^{-1}$ . No Raman data have previously been available for this compound since it is completely opaque to visible radiation.

### Experimental Section

$(\text{COT})\text{Fe}(\text{CO})_3$  was prepared by the photochemical reaction between COT and iron pentacarbonyl<sup>2,3</sup> and purified by recrystallization from *n*-hexane followed by vacuum sublimation. It was obtained as dark red crystals, m.p.  $94^\circ$ , stable in air and soluble in organic solvents to give dark red-brown solutions.

**Raman Spectra.** The Raman spectra were obtained on solutions of  $(\text{COT})\text{Fe}(\text{CO})_3$  in benzene and carbon disulfide. The spectra were excited in all cases by the rubidium resonance line at  $7800\text{ \AA}$ . isolated by two primary filter solutions. A saturated solution of  $\text{K}_2\text{Cr}_2\text{O}_7$  removed radiation below  $6000\text{ \AA}$ . while a  $0.25\text{ M}$  solution of  $\text{NdCl}_3$  in 6-mm. thickness effectively suppressed the intensity of the other Rb resonance line so that it did not excite Raman spectra. A radio-frequency-powered rubidium plasma discharge in a toroidal lamp provided the exciting radiation. Details of the plasma arcs and of their use in Raman spectroscopy have been published previously.<sup>11-15</sup> Photo-

(8) J. E. Mahler, D. A. K. Jones, and R. Pettit, *J. Am. Chem. Soc.*, **86**, 3589 (1964).

(9) H. P. Fritz and H. Keller, *Chem. Ber.*, **95**, 158 (1962).

(10) H. P. Fritz, *ibid.*, **95**, 820 (1962).

(11) F. X. Powell, O. Fletcher, and E. R. Lippincott, *Rev. Sci. Instr.*, **34**, 36 (1963).

(12) E. R. Lippincott, F. X. Powell, J. A. Creighton, and D. G. Jones, *Develop. Appl. Spectry.*, **3**, 106 (1964).

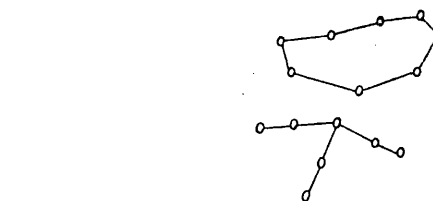


Figure 1. The structure of  $(\text{COT})\text{Fe}(\text{CO})_3$ .

graphic recording was employed using a Jarrell-Ash 75-000 F6.3 grating spectrograph. A plane grating ruled with 15,000 grooves/in. and blazed for  $7500\text{ \AA}$ . was used to give a dispersion of  $20\text{ \AA./mm.}$  in the first order. Hypersensitized Eastman Kodak 1-N photographic plates were used to record the spectra. With a slit width of  $200\text{ }\mu$ , exposure times of up to 30 hr. were required. The Raman spectra were not observed beyond  $1650\text{ cm}^{-1}$  owing to the rapid decrease in sensitivity of the photographic plates beyond  $9000\text{ \AA}$ . Polarization measurements were possible only for the strong lines due to the very long exposure times required. The plates were calibrated by means of a superimposed neon spectrum and measured using standard techniques. The strong Raman lines are estimated to be accurate to  $\pm 2\text{ cm}^{-1}$ , but for weak or diffuse features the error may be greater.

**Infrared Spectra.** The infrared spectra of  $(\text{COT})\text{Fe}(\text{CO})_3$  were recorded as solutions in  $\text{CS}_2$ ,  $\text{CCl}_4$ , and  $\text{C}_2\text{Cl}_4$  in the frequency range  $4000$ – $240\text{ cm}^{-1}$ , on a Perkin-Elmer 421 grating spectrometer equipped with low-frequency interchange, and in the range  $250$ – $110\text{ cm}^{-1}$  as a solution in benzene on a grating spectrometer designed and built at Royal Holloway College. The spectra of the solid complex were obtained in Nujol mulls and KBr pellets. The observed infrared and Raman spectra are listed in Table I.

In general, the infrared data are in reasonable agreement with those published by Fritz and Keller.<sup>9</sup> Some discrepancies were apparent but most of these can probably be ascribed to calibration errors; the strong band reported at  $1019\text{ cm}^{-1}$  was not, however, observed in this work.

### Discussion

The excellent agreement between the infrared spectra of  $(\text{COT})\text{Fe}(\text{CO})_3$  in the solid state and in solution is strong evidence for identical structures in both states. Thus one possible explanation of the single proton resonance observed in solution is eliminated. The assumption of a negligible relative chemical shift is also rendered unlikely by the appearance of two proton resonance frequencies in the disubstituted complex  $(\text{COT})\text{Fe}[(\text{CO})_3]_2$ , in which there is very little  $\pi$ -orbital overlap between the complexed portions of the COT ring. We are therefore led to the conclusion, reached previously by Dickens and Lipscomb,<sup>7b</sup> that tautomerism of the COT ring relative to the  $\text{Fe}(\text{CO})_3$  group is the most probable explanation of the single proton resonance. It should be noted, however, that the time scales required for n.m.r. equivalence and for equivalence in the vibrational spectra are totally dif-

(13) R. T. Bailey and E. R. Lippincott, *Spectrochim. Acta*, **20**, 1327 (1964).

(14) R. T. Bailey and E. R. Lippincott, *ibid.*, **21**, 389 (1965).



Table I. Observed Vibrational Spectra of (COT)Fe(CO)<sub>3</sub><sup>a</sup>

Infrared, cm. <sup>-1</sup>		Raman, cm. <sup>-1</sup>
Soln.	Solid	Soln.
3075 w		
3040 vs		
3022 s, sh		
~2925 w		
2879 w		
2061 vs	2062 vs	
1993 vs	1998 vs	
1976 vs	1982 vs	
1942 s	1947 w	
~1895 m		
1845 w		
1768 w		
1750 w		
1708 w		(1639)
1562 m		1563 m, p
1490 m		
1460 m		1460 s
1431 w		1431 m, p
1419 s	1418 w	(1406)
1401 vw		
1383 w		
1314 m	1313 w	1312 vw
1298 m	1299 w	1303 vw
1252 m	1256 vw	1255 w, br
1235 w, sh	1244 vw	1230 w, p
1177 m	1172 w	1180 m
	1150 vw	1147 m
1122 m	1125 w	1129 s
~1090 w		
1075 vw		(1080)
		1057 w
		1042 w
~1040 w, br		1024 vw, br
995 w, sh		
984 m	987 w	984 w
955 w	~945 w	951 m
922 m	918 w	924 m
898 s	898 m	889 w
864 s	868 m	875 w, br
846 m	845 w	849 w
		827 w
804 m	806 vw	
777 m	778 m	782 w
765 m, sh	765 w	766 w
743 m	741 vw	(730)
	715 vs	
707 vs	708 vs	716 vw
698 s, sh	698 vs	690 w, p
672 vw		
		643 vw
628 s, sh	627 s, sh	
607 vs	610 vs	607 s
597 vs, sh	597 vs	
561 vs	563 vs	563 m
537 vs	538 s	538 w
498 vs	498 s	498 w
485 s, sh		
461 vs	458 s	456 w
404 w	400 vw, sh	
	417 w	
389s	388m	391 m, vbr
362 w, sh	356 w, sh	
330 m	329 w, br	330 vs, br, p
	275 w	279 w
263 m	262 w	262 s, p
224 m		(238)
174 s		176 s
		137 m
		100 vs, vbr

<sup>a</sup> p, polarized; v, very; s, strong; m, medium; w, weak; sh, shoulder; br, broad. Values in parentheses indicate strong source lines which probably obscure Raman lines. N.M. designates no measurement.

ferent. Thus it does not necessarily follow that equivalence of the protons in the COT ring implies a high molecular symmetry with respect to the normal vibrational modes.

The vibrational spectra of the (COT)Fe(CO)<sub>3</sub> complex will now be considered in relation to its molecular structure. It is at once apparent from the large number of observed frequencies and coincidences between infrared and Raman bands that structures of high symmetry are precluded. Thus, structures having a planar COT ring and C<sub>8v</sub> symmetry are not consistent with the observed data.

The observed vibrational frequencies can be conveniently divided into three groups: (1) those belonging to the Fe(CO)<sub>3</sub> group, (2) those associated with COT ring modes, and (3) those arising from vibrations between the COT ring and the Fe(CO)<sub>3</sub> group. These three groups will be considered separately. Descriptive assignments of some of the observed frequencies are given in Table II.

Table II. Descriptive Assignments of Frequencies

Assign- ment, cm. <sup>-1</sup>	Descriptive assignment
3075	CH stretch
3040	
3022	
2061	CO stretch
1993	
1976	
1562	Sym. C=C stretch
1490	C=C stretch
1460	C=C stretch
1431	Ring deformation
1419	
1400	
to	CH deformation
1100	
750-500	
475-350	Fe-C-O angle bending
404	Fe-CO stretch
330	Ring tilt
137	Ring metal stretch
100	C-Fe-C angle bend

(1) *The Fe(CO)<sub>3</sub> Group.* Assuming identical structures in the solid and solution states, the highest possible symmetry for (COT)Fe(CO)<sub>3</sub> is C<sub>s</sub>. In many organometallic compounds containing metal-carbonyl groups M(CO)<sub>x</sub> bonded to an organic ring system, the observed spectroscopic data can be readily interpreted by considering only the local symmetry of the M(CO)<sub>3</sub> group and of the organic residue.<sup>15-17</sup> This approximation would<sup>16,17</sup> be valid only, however, if the M(CO)<sub>x</sub> group is rotating freely with respect to the ring system and there is no strong coupling between the vibrational modes of the two groups. On this basis, the Fe(CO)<sub>3</sub> group would belong to the C<sub>3v</sub> point group. The distribution of normal modes among

(15) R. T. Bailey and E. R. Lippincott, *J. Chem. Phys.*, **42**, 1121 (1965).

(16) F. A. Cotton in "Modern Coordination Chemistry," J. Lewis and R. G. Wilkins, Ed., Interscience Publishers, New York, N. Y., 1960, p. 301.

(17) F. A. Cotton, A. O. Liehr, and G. Wilkinson, *J. Inorg. Nucl. Chem.*, **1**, 175 (1955).

the various symmetry species for the  $C_{3v}$  point group is:  $4a_1 + a_2 + 5e$ . All species are infrared and Raman active except  $a_2$  which is Raman active only. The normal modes can be described approximately as follows: two C=O stretching ( $a_1 + e$ ), two Fe-CO stretching ( $a_1 + e$ ), four Fe-C-O angle bending ( $a_1 + a_2 + 2e$ ), and two C-Fe-C angle bending ( $a_1 + e$ ). Thus, two infrared-active C=O stretching vibrations would be expected, whereas, in fact, three frequencies at 2061, 1993, and 1976  $\text{cm}^{-1}$  are observed in the CO stretching region. This indicates a lower symmetry than  $C_{3v}$  (i.e.,  $C_s$ ) resulting in the splitting of the degenerate e-class CO stretching vibration. Thus, an asymmetric  $\text{Fe}(\text{CO})_3$  group not freely rotating in space is implied, contrary to the conclusions of Cotton.<sup>6</sup> This is supported by the X-ray data which show the  $\text{Fe}(\text{CO})_3$  to be slightly asymmetric.<sup>7b</sup> However, the vibrational data do not rule out a hindered or restricted rotation of the  $\text{Fe}(\text{CO})_3$  group. The reduction in symmetry will also result in a splitting of the other degenerate  $\text{Fe}(\text{CO})_3$  modes. In the case of the low-frequency modes, however, this may be too small to be observed under the present experimental conditions. A broadening of the degenerate modes should, however, be observed. The metal-carbonyl stretching frequencies are significantly lower than the corresponding modes in  $\text{Fe}(\text{CO})_5$  at 2117, 2034, and 2014  $\text{cm}^{-1}$ .<sup>18</sup> This is principally caused by back-donation from the filled d orbitals on the iron atom to vacant antibonding  $\pi$  orbitals on CO. This compensates for the formal negative charge imposed on the iron atom by coordination to the butadiene-like residue. There is also the possibility of some  $\pi$ -electron donation from bonding CO to vacant d orbitals on the metal atom, but this should be relatively small. This mechanism is consistent with the observed Fe-CO bond length which is about 0.17 Å shorter than the normal single bond distance.<sup>7b</sup> The assignment of the other  $\text{Fe}(\text{CO})_3$  modes is rendered rather difficult owing to overlapping with COT and ring-metal modes. Several C-H deformation and ring deformation modes of COT are found below 700  $\text{cm}^{-1}$ .<sup>19</sup> In general, M-C-O angle bending modes lie at higher frequencies than M-CO stretching modes, but they sometimes overlap.<sup>20</sup> In  $(\text{COT})\text{Fe}(\text{CO})_3$ , the M-C-O angle bending modes probably lie in the range 500–750  $\text{cm}^{-1}$  and the M-CO stretching modes in the range 350–475  $\text{cm}^{-1}$ . The M-CO stretching modes generally fall within a shorter frequency interval than M-C-O bending modes and in the neutral species rarely rise above 500  $\text{cm}^{-1}$ . The C-M-C angle bending modes generally are found near 100  $\text{cm}^{-1}$ . The frequencies at 176 and 100  $\text{cm}^{-1}$  probably belong to these modes. Since the 100- $\text{cm}^{-1}$  band is very broad, it is assigned to an unresolved splitting of the degenerate vibration. It is possible, however, that the COT-Fe-(CO)<sub>3</sub> bending modes will also occur in this region and overlap the C-Fe-C bending modes.

(2) *The COT Ring Modes.* Assuming  $C_s$  symmetry for the COT ring, eight infrared-active C-H stretching modes should be observed. Only two strong bands are found in the C-H stretching region in the infrared

(18) W. F. Edgell, W. E. Wilson, and R. Summitt, *Spectrochim. Acta*, **19**, 863 (1963).

(19) E. R. Lippincott, R. C. Lord, and R. S. McDonald, *J. Am. Chem. Soc.*, **73**, 3370 (1951).

(20) D. M. Adams, *J. Chem. Soc.*, 1771 (1964).

spectra of the complex. This implies a higher symmetry than  $C_s$  for the COT ring. Cyclooctatetraene has two strong bands in the C-H stretching region at 2955 and 3004  $\text{cm}^{-1}$ .<sup>19</sup> The corresponding frequencies in  $(\text{COT})\text{Fe}(\text{CO})_3$  are found at 3002 and 3040  $\text{cm}^{-1}$ , a shift toward the benzene frequencies at 3047, 3062, and 3099  $\text{cm}^{-1}$  implying an increase in aromatic character of the C-H stretching vibration. The strong infrared bands at 1609 and 1635  $\text{cm}^{-1}$  in cyclooctatetraene, characteristic of the stretching of conjugated double bonds, are not observed in the complex. The Raman data for  $(\text{COT})\text{Fe}(\text{CO})_3$  in this region are somewhat uncertain owing to the presence of a strong cesium resonance line at 1639  $\text{cm}^{-1}$ , but no Raman lines could be detected in this region. Manual and Stone<sup>2</sup> and Cotton<sup>6</sup> assigned the strong infrared band at 1416  $\text{cm}^{-1}$  to the C=C stretching vibration since no other strong bands were found in this region. This was cited as evidence for a planar regular octagonal structure for the COT ring. Fritz and Keller,<sup>9,10</sup> from infrared measurements on solid  $(\text{COT})\text{Fe}(\text{CO})_3$  in KBr, assigned a band at 1464  $\text{cm}^{-1}$  to the C=C stretching mode and frequencies at 1414 and 1372  $\text{cm}^{-1}$  to the C-H deformation modes.

In this work, bands at 1562, 1490, and 1460  $\text{cm}^{-1}$  were found in the solution spectra, and it is probable that these are attributable to C=C stretching modes. The highest frequency at 1562  $\text{cm}^{-1}$  is polarized in the Raman spectrum and may result from symmetric stretching of the conjugated double bonds in the uncomplexed portion of the COT ring. This band has a somewhat lower infrared intensity than is normally associated with bands derived from C=C stretching modes, but this may be due in part to the planarity of this part of the ring which has also acquired some aromatic character. Some delocalization in the uncomplexed portion of the COT ring would also explain the lower C=C stretching frequency observed, compared to free COT. The existence of partial delocalization over the dihedral form of the ring is supported by the calculation of overlap integrals between SCF carbon  $\pi$  orbitals.<sup>7b</sup> The calculated overlap integral of 0.25 between C-1 and C-3 indicates an appreciable  $\pi$ -orbital interaction between the complexed butadiene-like residue and the remainder of the ring. Furthermore, the free half of the ring is almost planar as required for maximum overlap. There is a continuous  $\pi$ -electron overlap of 0.16 or more around the dihedral COT ring.

The assignment of the bands at 1414 and 1372  $\text{cm}^{-1}$  to C-H deformation modes<sup>9,10</sup> seems questionable since the corresponding modes in COT are found at 1221 and 1202  $\text{cm}^{-1}$ .<sup>19</sup> The highest in-plane C-H deformations in ferrocene and benzene are found at 1178  $\text{cm}^{-1}$ . It appears probable that the frequencies found at 1431 and 1419  $\text{cm}^{-1}$  in this work are derived from ring deformation modes.

(3) *Ring Metal Modes.* The ring-metal modes will consist of a ring-metal stretch, a ring-tilt, COT-Fe(CO)<sub>3</sub> bending modes, and an internal rotation of the Fe(CO)<sub>3</sub> group relative to the COT ring. The latter mode should give rise to a fairly high frequency in view of the strength of the ring-metal bonding which is sufficient to distort the COT ring. The exact location of this frequency is, however, uncertain. The ring-metal

stretch, found at  $303\text{ cm}^{-1}$  in ferrocene,<sup>21</sup>  $298\text{ cm}^{-1}$  in  $\text{C}_6\text{H}_6\text{Cr}(\text{CO})_3$ ,<sup>22</sup> and  $279\text{ cm}^{-1}$  in  $(\text{C}_6\text{H}_6)_2\text{Cr}$ ,<sup>23</sup> is expected around  $300\text{ cm}^{-1}$ . This vibration would also involve a large change in polarizability and should, therefore, give rise to a strong Raman shift. The

(21) E. R. Lippincott and R. D. Nelson, *Spectrochim. Acta*, **10**, 307 (1958).

(22) H. P. Fritz and J. Manchot, *ibid.*, **18**, 171 (1962).

(23) H. P. Fritz, W. Lüttke, H. Stammreich, and R. Forneris, *ibid.*, **17**, 1068 (1961).

very strong polarized band at  $330\text{ cm}^{-1}$  is most likely derived from this mode. This line is, however, broad and so may overlap a COT mode. In ferrocene,  $\text{C}_6\text{H}_6\text{Cr}(\text{CO})_3$ , and  $(\text{C}_6\text{H}_6)\text{Cr}^{23}$  the ring-tilt is found at 388, 330, and  $333\text{ cm}^{-1}$ , respectively. The weak band at  $404\text{ cm}^{-1}$  may belong to this mode. The COT-Fe-(CO)<sub>3</sub> bending modes should be very low, below  $100\text{ cm}^{-1}$ , and were probably not observed in this work.

C8

Offprinted from the *Transactions of The Faraday Society*,  
No. 516, Vol. 61, Part 12, December, 1965

SPECTROSCOPIC EVIDENCE FOR COMPLEX FORMATION BETWEEN  
BENZENE AND BORON TRIHALIDES

# Spectroscopic Evidence for Complex Formation between Benzene and Boron Trihalides

BY ARTHUR FINCH, P. N. GATES AND D. STEELE

Dept. of Chemistry, Royal Holloway College, University of London,  
Englefield Green, Surrey

Received 18th June, 1965

Intensity measurements on the boron-halogen symmetric stretching frequency of boron tri-bromide + benzene and boron tri-iodide + benzene systems indicate the existence of 1 : 1 complexes. This is supported by  $^{11}\text{B}$  nuclear magnetic resonance spectra of boron tribromide + benzene systems; cryoscopic measurements gave inconclusive results.

The infra-red-inactive fundamental frequency  $\nu_1$  (symmetric stretching) of boron tri-iodide appears as a weak band in carbon disulphide solution but the intensity was observed to increase sharply when benzene was used as a solvent.<sup>1</sup> It was suggested that this might be due to weak complex formation through interaction of the  $\pi$ -electron system of benzene with the boron halide. The resulting increase in the  $p$ -character of the boron hybridization and the consequent non-planarity of the  $\text{BI}_3$  would allow the appearance of the symmetric stretching band. We have investigated the variation of intensity of this band (at  $196\text{ cm}^{-1}$ ) with the composition of the mixture and made a similar study of the boron tribromide + benzene system.  $^{11}\text{B}$  chemical shifts of the boron tribromide + benzene system supported the formation of a loose complex. Phase diagrams of the boron tribromide + benzene and boron tri-iodide + benzene systems were inconclusive.

## EXPERIMENTAL

Boron tribromide (L. Lights) was purified as described previously.<sup>1</sup> Boron tri-iodide (L. Lights) was recrystallized from benzene (found: B, 2.9; I, 96.4; calc. for  $\text{BI}_3$ : B, 2.8; I, 97.2 %). All transfer operations were carried out in an atmosphere of dry nitrogen. The far infra-red spectra were recorded on a grating spectrometer constructed in the department and described elsewhere.<sup>2</sup> A conventional liquid cell fitted with high-density polythene windows was used to contain the samples. Cell path lengths of 0.30-0.40 cm were employed.  $^{11}\text{B}$  chemical shifts (measured relative to pure boron tribromide) were obtained on a Perkin-Elmer nuclear magnetic resonance spectrometer operating at a frequency of 12.83 Mc/sec. Cryoscopic measurements were made using apparatus constructed in the department and described elsewhere.<sup>3</sup>

## RESULTS AND DISCUSSION

Plots of  $(\log(I_0/I))$  against composition (mole fraction of boron halide) for the boron tribromide + benzene and boron tri-iodide + benzene systems are shown in fig. 1. At lower concentrations of boron trihalide, a Beer law plot was obtained but the shape of the curve at higher concentrations strongly suggests complex formation. In both systems, the maximum value of  $(\log(I_0/I))$  was observed at a mole fraction of approximately 0.5. Fortunately, no shift in frequency between  $\nu_1$  for pure boron tribromide and the solutions in benzene was observed. Hence,

it is simple to compute the theoretical shape of the curve (assuming the formation of only a 1 : 1 species) from a knowledge of the initial slope and the value of  $\log(I_0/I)$  for pure boron tribromide. The computed part of the curve is shown as a dotted line in fig. 1. The observed deviation from the computed curve could be explained in terms of a dissociation of the type:

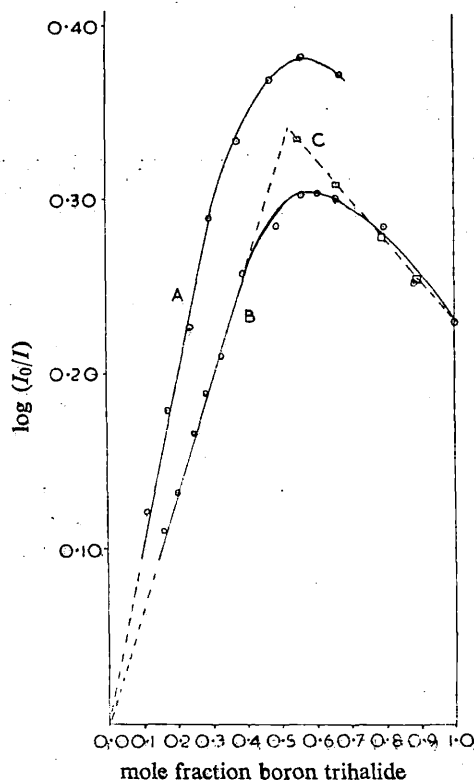
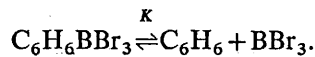


FIG. 1.— $\log(I_0/I)$  of symmetric stretching band against mole fraction of boron trihalide. A,  $\text{BI}_3$ +benzene in 0.30 cm cell; B,  $\text{BBr}_3$ +benzene in 0.40 cm cell; C, computed points curve for  $\text{BBr}_3$ +benzene system (calculated from the initial slope and  $\log(I_0/I)$  for pure  $\text{BBr}_3$ , assuming complete 1 : 1 association).

Equating activities with concentrations, a value for  $K$  can be obtained for the system from the relation

$$K = \frac{[ab]}{[a_0 - ab][b_0 - ab]}$$

where  $a_0$  and  $b_0$  are the concentrations of  $\text{BBr}_3$  and  $\text{C}_6\text{H}_6$ , based on the quantities used to prepare the system, and  $[ab]$  is the concentration of the species  $\text{C}_6\text{H}_6\text{BBr}_3$ .  $[ab]$  is then given by

$$[ab] = \frac{(\log(I_0/I))_{\text{obs.}} - E_a a_0 l}{(E_{ab} - E_a)l}$$

where  $(\log(I_0/I))_{\text{obs}}$  is the value of the optical density corresponding to the concentration  $a_0$ ,  $l$  is the path length of the cell,  $E_a$  is the extinction coefficient of pure  $\text{BBr}_3$  and  $E_{ab}$  is the extinction coefficient of the species  $\text{C}_6\text{H}_6\text{BBr}_3$ , obtained from the initial Beer law plot. The mean value obtained for  $K$  was  $4.8 \pm 0.8 \text{ mole}^{-1} \text{ l}$ .

A similar determination could not be made on the boron tri-iodide+benzene system as no value for the extinction coefficient of pure  $\text{BI}_3$  was obtained. Molar

ratios of  $\text{BI}_3$  greater than 0.70 were not achieved because of solubility limitations (e.g., a molar ratio of 0.67  $\text{BI}_3$  requires 8.9 g of  $\text{BI}_3$  to be dissolved in 1 ml of benzene). A Beer-law plot for  $\text{BI}_3$  in benzene gave an extinction coefficient of  $0.328 \text{ mole}^{-1} \text{ cm}^2$  (compared to  $0.156 \text{ mole}^{-1} \text{ cm}^2$  in the  $\text{BBr}_3$  benzene system). Making the reasonable assumption that the bond dipole of  $\text{B}-\text{Br}$  is greater than that of  $\text{B}-\text{I}$ , these values imply that there is a larger distortion of planarity in the boron tri-iodide. This implies that the donor acceptor interaction between benzene and the tri-iodide is the stronger of the two, in accord with previous results<sup>4,5</sup> on the acceptor properties of these two halides towards electron-pair donors.

The observed absorption intensity against concentration curve shows conclusively the existence of a 1:1 species. On the basis of absorption strength

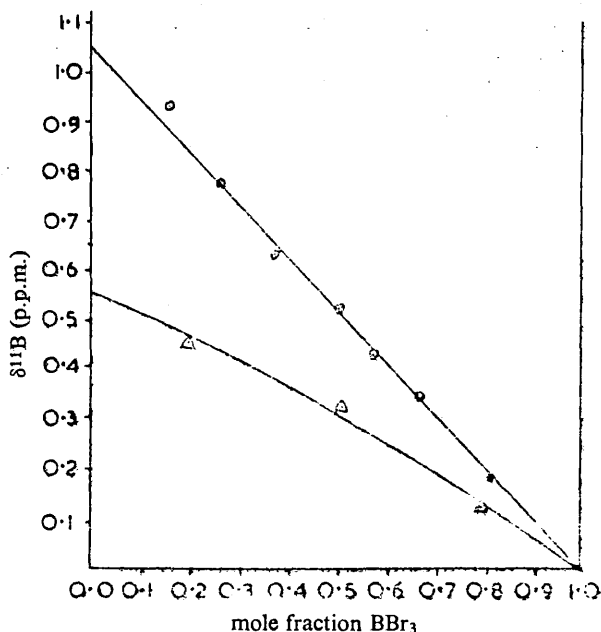


FIG. 2.— $^{11}\text{B}$  chemical shift,  $\delta^{11}\text{B}$ , against mole fraction  $\text{BBr}_3$ ; ○  $\text{BBr}_3 + \text{benzene}$ ; △  $\text{BBr}_3 + \text{cyclohexane}$ .

and the ability to fit the calculated curve to the observed using a dissociation constant for the 1:1 association, it would not appear that any 1:2 complex ( $\text{C}_6\text{H}_6 : 2\text{BBr}_3$ ) or  $[(\text{C}_6\text{H}_6)_2\text{BBr}_3]$  of more than a transient character exists.

It might be expected that any loss of planarity of the  $\text{BBr}_3$  molecules would be apparent from dipole moment measurements. A determination<sup>6</sup> of the dipole moment of  $\text{BBr}_3$  in benzene yielded a value of 0.194 e.s.u. Since very low values are unreliable it was inferred that the  $\text{BBr}_3$  was planar. However, in view of the present evidence, it is possible that this value may represent a real deviation from zero. Accordingly, further evidence was sought using cryoscopic and n.m.r. techniques.

In the phase diagram for the boron tribromide+benzene system only a single eutectic point at *ca.*  $-56^\circ$  was observed. In the boron tri-iodide+benzene system an eutectic at *ca.*  $-7^\circ$  was found; a slight discontinuity of the curve at a mole fraction of 0.5 indicated incongruity. However, no positive indication of complex formation could be inferred from these measurements.

Variation of the  $^{11}\text{B}$  chemical shifts (in p.p.m. relative to pure  $\text{BBr}_3$ ) with composition of the boron tribromide+benzene and boron tribromide+cyclohexane systems is shown in fig. 2. Separate signals for "free" and "complexed" boron tribromide were not observed, this being consistent with a rapid exchange between  $\text{BBr}_3$  and benzene molecules, thus giving rise to an average value for the chemical shift. This averaging may be used to estimate the lower limit to the mean lifetime  $\tau$  between exchanges. According to Gutowsky and Holm,<sup>7</sup>  $\tau \leq \sqrt{2/\pi\delta H}$  sec, where  $\delta H$  is expressed in c/sec. This leads to  $\tau < 0.035$  sec, but in view of the bulk solvent effect this is probably an over-estimate. It might be expected that a plot of chemical shift against composition would show a gradient change at 0.50 if a 1:1 species were formed. The monotonically increasing high-field shift with dilution in benzene suggests that the shifts arise mainly from a bulk solvent effect rather than from changes in the electron density at the boron atom. No gradient change (in the plot of chloroform proton shift against composition) was observed by Reeves and Schneider<sup>8</sup> for the chloroform+mesitylene system in which it was well-established that 1:1 complex formation occurs.

The  $^{11}\text{B}$  shifts at infinite dilution in benzene and cyclohexane are 1.05 and 0.55 p.p.m. respectively. (These are to be compared with a high-field shift of 45 p.p.m. observed<sup>5</sup> in the complex triethylamine+boron tribromide.) The increase of the chemical shift with dilution in cyclohexane can be accounted for entirely on the basis of the bulk diamagnetic susceptibility of the system. Measurement of the volume susceptibility of  $\text{BBr}_3$  gave a value of  $-0.900$  c.g.s. units and the observed shifts in cyclohexane vanish when a correction is made for this effect. However, the shifts in benzene solution cannot be wholly accounted for on this basis and there was still a residual high-field shift of 0.48 p.p.m. after the correction was made. This residual high-field shift strongly suggests that the principal orientation of boron is above and below the plane of the aromatic ring (where circulation of ring electrons causes a magnetic field which opposes the applied field). This is consistent with an interaction holding the molecules in this configuration. Such an interaction might well cause the loss of planarity of the  $\text{BBr}_3$  molecule, hence accounting for the variation in intensity of the symmetric stretching band. These results clearly eliminate the possibility of a hydrogen bonded complex (fig. 3)

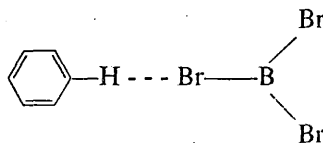


FIG. 3.

in which case the boron trihalide would experience an enhanced field from the  $\pi$ -electron circulation, with a consequent low-field shift.

Reeves and Schneider<sup>8</sup> have shown how chloroform proton shifts in chloroform+benzene systems can allow the average distance between the aromatic ring and the proton to be estimated. A similar calculation applied to the  $\text{BBr}_3 + \text{C}_6\text{H}_6$  system yields an average value for the boron-benzene distance of 4.7 Å. An attempt to carry out similar infra-red measurements on the mesitylene+boron tribromide failed due to a very strong absorption by mesitylene in the same region as the symmetric B-Br stretching frequency. The  $^{11}\text{B}$  shift at infinite dilution in mesitylene gave a higher value (1.20 p.p.m.) than in benzene which suggests that the average distance between the boron and the aromatic ring may be smaller.



We gratefully acknowledge financial support from the Office of Naval Research, U.S. European Research Contracts Programme. The gratings used in the spectrometer are on loan from the National Physical Laboratory. The Perkin-Elmer n.m.r. spectrometer was kindly made available by Dr. E. F. Mooney of Northern Polytechnic, London. Helpful discussions with Dr. K. A. McLauchlan are gratefully acknowledged.

<sup>1</sup> Finch, Hyams and Steele, *Trans. Faraday Soc.*, 1965, **61**, 203.

<sup>2</sup> Hendra, Lane and Smethurst, *J. Sci. Instr.*, 1963, **40**, 457.

<sup>3</sup> Finch, Gardner, Lane and Smethurst, *Lab. Practice*, 1965, **14**, 448.

<sup>4</sup> Cook, *Can. J. Chem.*, 1963, **41**, 522.

<sup>5</sup> Gates and Mooney, unpublished observation.

<sup>6</sup> Rollier, *Gazz. chim. ital.*, 1947, **77**, 372.

<sup>7</sup> Gutowsky and Holm, *J. Chem. Physics*, 1957, **25**, 1228.

<sup>8</sup> Reeves and Schneider, *Can. J. Chem.*, 1957, **35**, 251.

Offprinted from the *Transactions of The Faraday Society*,  
No. 516, Vol. 61, Part 12, December, 1965

VIBRATIONAL SPECTRA OF SOME HETEROCYCLIC TIN COMPOUNDS

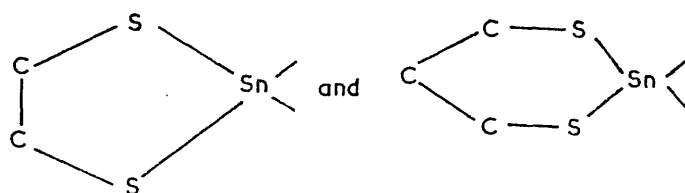
# Vibrational Spectra of some Heterocyclic Tin Compounds

BY ARTHUR FINCH \* R. C. POLLER † AND D. STEELE \*

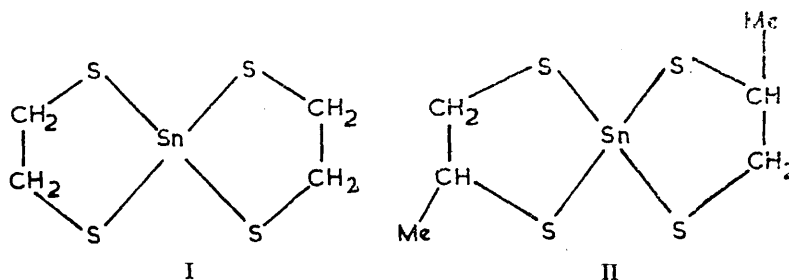
Received 23rd June, 1965

The infra-red spectra of some crystalline dithiastanna-cyclopentanes and cyclohexanes have been measured to  $110\text{ cm}^{-1}$ . Interpretation has been helped by computations of frequencies and modes of 1,4,6,9-tetrathia-5-stannaspiro [4,4] nonane(I) and of a model compound, the 3,7 dimethyl derivative(II). A correlation of ring C—C stretching frequencies with the number of adjacent C—C bonds is proposed. The antisymmetric C—S frequencies are found near  $920\text{ cm}^{-1}(s)$ , and the symmetric modes near  $850\text{ cm}^{-1}(s)$ . The methylated spiran absorbs *ca.*  $30\text{ cm}^{-1}$  lower. Tin-sulphur stretching vibrations are variable, ranging from  $392$  to  $330\text{ cm}^{-1}$  (symmetric) and  $363$  to  $267\text{ cm}^{-1}$  (antisymmetric).

In a recent paper<sup>1</sup> vibrational assignments for a number of 5- and 6-membered rings containing boron were made, and compared with experimental data. The availability of a series of 5- and 6-membered 1,3-dithia-2-stanna-cyclo-pentanes and -hexanes, of general skeletal formulae :



prompted the present investigation. The spiro-compounds I and II are of particular interest because of the uncertain stereochemistry of the strained spirocyclic system.



I, 1,4,6,9-tetrathia-5-stannaspiro [4,4] nonane.

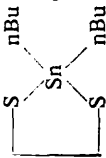
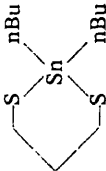
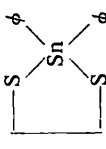
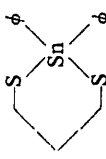
II, 3,7-dimethyl-1,4,6,9-tetrathia-5-stannaspiro [4,4] nonane.

Interpretation of the spectra of the 5-membered systems was attempted on the assumption of planar rings. This gives  $V_a$  symmetry for I; non-planarity of the rings will result in removal of the degeneracies and relaxation of the selection rules. To a good approximation the skeletal modes may be considered independently of the CH modes. In this approximation the skeletal vibrations of I have the group

\* Royal Holloway College, University of London, Englefield Green, Surrey.

† Queen Elizabeth College, Campden Hill Road, London, W.8.

TABLE I

II	Chemical Structures				Sn, nBu <sub>2</sub> Cl <sub>2</sub> (crystal)	φ SnBr <sub>3</sub>	assignments
							
1445 s	1462 s	1463 s	1480 s	1482 s	1468 s/1452 s	1575 s 1480 s	phenyl A <sub>1</sub> vCC n butyl CH <sub>3</sub> umbrella δCH <sub>3</sub>
1412 s	1419 s	1422 s	1433 s 1418 m 1382 w	1433 s 1423 s 1388 w		1434 ps	phenyl B <sub>1</sub> vCC δCH <sub>2</sub>
1372 s	1376 m 1361 w	1377 m	1334 m 1306 w-m	1338 m 1308 s	1381 s	1378 m	phenyl 2 × 686? δCH <sub>3</sub>
1302 s	1280 s	1306 s	1287 s 1264 w	1266 w		1332 s 1304 m	phenyl B <sub>1</sub> vCC phenyl νC—C CH <sub>2</sub> wag
1264 s	1246 s 1238 m	1273 w 1258 m	1251 w-m	1259 m			CH <sub>2</sub> wag νC—C νC—CH <sub>3</sub>
1222 s	1193 m	1197 m	1167 m 1118 m	1242 w	1180 s	1192 m 1162	CH <sub>2</sub> wag CH <sub>2</sub> wag phenyl βCH phenyl βCH } CH <sub>2</sub> twist νC—C n butyl vCC phenyl βCH
1176 m	1161 w 1114 w	1076 s	1072 s	1075 s	1079 s	1068 s	CH <sub>2</sub> rock
1099 s	1074 s	1050 w	1022 m-s	1023 m			CH <sub>3</sub> def.? phenyl βCH n butyl
1048 s	1050 w 1035 w	1050 w	1016 m-s	1016 s			
1028 m br.							



representations  $4A_1 + A_2 + 2B_1 + 4B_2 + 5E$ . The ring torsions, usually of low frequency and intensity, account for  $1A_2 + 1B_1 + 1E$ . Classes  $B_2$  and  $E$  are infra-red-active and classes  $A_1$ ,  $B_1$ ,  $B_2$  and  $E$  Raman-active. The dithia-stannacyclopentanes are of symmetry  $C_{2v}$  for two similar tin substituents and no ring substituents. In this case the classification is  $6A_1 + 4B_1 + 2B_2 + A_2$ , excluding the ring torsions. Computations of the skeletal frequencies of I and II have been carried out to facilitate assignments.

#### EXPERIMENTAL\*

1,4,6,9-Tetrathia-5-stannaspiro [4,4] nonane, m.p. 182-3°; 2,2-dibutyl-2-stanna-1,3-dithiacyclopentane, m.p. 59-60°; 2,2-diphenyl-2-stanna-1,3-dithiacyclopentane, m.p. 108-9°; 2,2-dibutyl-2-stanna-1,3-dithiacyclohexane, m.p. 63-64°; and 2,2-diphenyl-2-stanna-1,3-dithiacyclohexane, m.p. 103-4°, have already been reported.<sup>2a, b</sup>

3,7-Dimethyl-1,4,6,9-tetrathia-5-stannaspiro [4,4] nonane, m.p. 76-77° (found: C, 21.6; H, 3.7; Sn, 35.9;  $C_6H_{12}S_4Sn$  requires C, 21.7; H, 3.65; Sn, 35.9 %) was prepared by a similar method.<sup>2c</sup> The sharp melting point obtained for this compound indicated that only one of the three possible geometrical isomers was obtained.

Spectra were measured in KBr discs on a Unicam SP 100 with 130 grating accessories and in polythene discs<sup>3</sup> on a far infra-red spectrometer, details of which have been reported.<sup>4</sup> The observed frequencies are listed in table 1.

#### COMPUTATIONS

The eigenvalues and eigenvectors of the vibrational problem were evaluated from the secular equation in cartesian in the form  $\mathbf{D}^+\mathbf{F}\mathbf{D}\mathbf{Y} = \mathbf{Y}\mathbf{\Lambda}$  where  $\mathbf{D}\mathbf{D}^+ = \mathbf{G}$ , the inverse kinetic energy matrix,  $\mathbf{Y}$  is the eigenvector matrix in cartesian co-ordinates and  $\mathbf{\Lambda}$  is the eigenvalue matrix, the individual values of which are related to the frequencies by  $\lambda_i = 4\pi^2\nu^2c^2/N$ .  $\mathbf{D}$  is formed from the transformation matrix between internal and cartesian co-ordinates,  $\mathbf{B}$ , by post-multiplication by the diagonal matrix  $\mathbf{M}^{-1/2}$ , the diagonal elements of which are the inverses of the square roots of the atomic masses.

The problem was simplified in two ways. First, the hydrogen atoms were ignored, and secondly the torsion force constants were assumed to be zero. The latter assumption was made on the grounds that the contributions to the potential energy are very small and will have little effect on the calculated frequencies and modes. In any case it is difficult to estimate the value of these force constants due to lack of reliable values for other alicyclic systems.

The  $\mathbf{B}$  matrices will not be reproduced here as their evaluation is simple, and they are available on request. The geometrical parameters of the molecules are unknown but the following values are unlikely to be far from the true values:

$$\begin{array}{ll} r_{CS} = 1.82 \text{ \AA}, & \text{CCS} = 113^\circ, \\ r_{SnS} = 2.0 \text{ \AA}, & \text{SSnS} = 94^\circ 46', \\ r_{C-C}(\text{ring}) = 1.52 \text{ \AA}, & \text{CSSn} = 109^\circ 37', \\ r_{C-CH_3} = 1.54 \text{ \AA}, & \end{array}$$

The force constants were estimated from comparisons with related molecules. The values chosen were:

\* The authors thank Miss J. A. Spillman who kindly supplied some of the compounds used.

$$\begin{array}{ll}
 f_{CS} = 3.65 \text{ mdynes/\AA}, & r_{SSn}^2 f_{SSnS} = 0.06 \text{ mdynes/\AA}, \\
 f_{CS,CS} = 1.04 \text{ mdynes/\AA}, & r_{CC}^2 f_{CCS} = 0.28 \text{ mdynes/\AA}, \\
 f_{CC} = 4.58 \text{ mdynes/\AA}, & r_{CS}^2 f_{CSSn} = 0.2 \text{ mdynes/\AA}, \\
 f_{SnS} = 2.25 \text{ mdynes/\AA}, &
 \end{array}$$

The computed frequencies for I are:  $A_1$ , 1192, 716, 361 and 164  $\text{cm}^{-1}$ ;  $B_1$ , 1192, 716, 422 and 214  $\text{cm}^{-1}$ ;  $A_2$ , 108  $\text{cm}^{-1}$ ;  $E$ , 850, 450, 366 and 105  $\text{cm}^{-1}$ . Non-degenerate modes are shown in fig. 1. The form of the computer programme

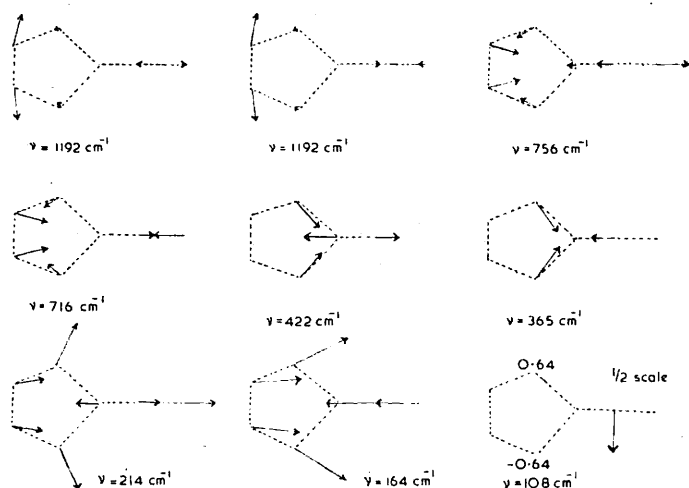


FIG. 1.—The arrows represent nuclear displacement amplitudes on an arbitrary magnified scale. For the 108  $\text{cm}^{-1}$  mode the displacement arrows have been drawn on half the scale used for the others. The numbers (0.64) used in drawing this mode are simply related to the arrows by noting that the displacement represented must equal the displacement represented by the corresponding arrows for the second ring.

prevents the degenerate eigenvectors being evaluated in the orthogonal form. However, the potential energy distribution is readily determined. This is given in table 2 for the degenerate vibrations. The available routines used for solving the

TABLE 2.—COMPUTED POTENTIAL ENERGY DISTRIBUTIONS FOR THE DEGENERATE VIBRATIONS OF I

frequency $\text{cm}^{-1}$	% potential energy distribution					
	SnS	CS	C—C	SSnS	SnSC	SCC
850	0	80	0	0	0	20
450	0	0	0	1	39	60
367	60	16	0	0	2	22
105	1	0	0	99	0	0

eigenvalue problem were inapplicable to matrices of order greater than 29. This prevented a complete solution of the skeletal vibration problem of the dimethyl derivative II. However, as the principal problem is to determine to what extent the methyl group interacts with the ring C—C and C—S vibrations, a satisfactory answer can be obtained by treating the molecule as if it were a substituted dithiastannacyclopentane. This is possible because of the negligible interaction between the C—C and C—S vibrations in the two rings (see fig. 1). Computed frequencies and potential energy distributions are given in table 3.

TABLE 3.—COMPUTED POTENTIAL ENERGY DISTRIBUTIONS FOR THE HIGHER FREQUENCY MODES OF II

frequency cm <sup>-1</sup>	% potential energy distribution							
	SnS	CS	C—C (ring)	C—CH <sub>3</sub>	SSnS	SnSC	SCC	CCCH <sub>3</sub> SCCH <sub>3</sub>
1288	0	18	45	31	0	1	3	0
1111	0	8	41	31	0	1	5	14
893	0	64	0	13	0	0	9	12
817	0	65	0	13	0	1	1	19
486	16	5	1	4	0	10	6	59
425	71	9	0	3	0	4	6	6
412	46	4	2	4	0	0	1	40
394	98	0	0	0	2	0	0	0

† lower frequencies

## VIBRATIONAL ASSIGNMENTS

COMPOUND I.—In addition to the skeletal frequencies, the frequencies of which have been computed (cf. previous section), the CH<sub>2</sub> units give rise to fundamental vibrations which have the group representations  $3A_1 + 3A_2 + 3B_1 + 3B_2 + 6E$ . However, interaction between the ethylenic units of the two rings will be very small and it is more useful to consider the vibrations involving the hydrogen atoms simply as if they belonged to a cis 1,2-disubstituted ethane. The vibrations now fall into the classification  $3A_1(r_{CH}, R, \delta) + 3B_1(r_{CH}, R, \delta) + 3B_2(r_{CH}, T, W) + 3A_2(r_{CH}, T, W)$ . The nature of the modes is shown in parentheses;  $r_{CH}, R, \delta, W, T$  represent CH stretching, CH<sub>2</sub> rock, CH<sub>2</sub> deformations, CH<sub>2</sub> wag and CH<sub>2</sub> twist motions respectively. The expected frequency ranges for these vibrations are *ca.* 2900 cm<sup>-1</sup> for stretching motions, 1430 cm<sup>-1</sup> for the deformations, 1330 cm<sup>-1</sup> for the wags, 1200–1150 cm<sup>-1</sup> for the twists and 950–850 cm<sup>-1</sup> for the rocking vibrations. These are based on comparison of spectra of 1:2 disubstituted ethanes in the gauche conformations. A comparison of calculated skeletal frequencies and expected CH<sub>2</sub> modes with the observed spectra leaves little scope for ambiguity in the assignment (see tables 1 and 4). The purity of the degenerate ring angle deformation at 442

TABLE 4.—COMPUTED AND ASSIGNED FREQUENCIES FOR THE MODES OF I

calc. skeletal frequency cm <sup>-1</sup>	approximate expected CH <sub>2</sub> frequency cm <sup>-1</sup>	obs. frequency cm <sup>-1</sup>	mode
	1430	1410	δCH <sub>2</sub>
	1330	1289/1283	CH <sub>2</sub> wag
1192 (B <sub>1</sub> )		1248	νC—C
	1170	1156/1122	CH <sub>2</sub> twist
	<i>ca.</i> 900	997	CH <sub>2</sub> rock
850 (E)		922	as. νC—S
716 (B <sub>1</sub> )		840	<i>s</i> νC—S
450 (E)		442	ring def.
422 (B <sub>1</sub> )		388	<i>s</i> νSn—S
366 (E)		327	as. νSn—S
214 (B <sub>1</sub> )		233	ring def.

cm<sup>-1</sup> is of interest. The lack of any contribution from the Sn—S stretching vibration suggests that it should remain constant in form and in frequency for 2,2-disubstituted dithia-cyclopentanes and cyclohexanes. The entirely satisfactory assignment on the basis of  $V_d$  symmetry is good evidence for the planarity, or near-planarity, of the individual rings.



COMPOUND II.—Introduction of the two methyl groups into compound I will have the principal effects of: (i) reducing symmetry and thus splitting the degenerate modes and also permitting activity of formerly infra-red inactive  $A_1$  modes; (ii) introducing methyl groups vibrations; (iii) coalescing pairs of methylene wags, deformations, and rocks; (iv) splitting of ring C—C modes through interaction with the C—CH<sub>3</sub> mode; (v) introducing modes due to methyl ring deformations which might interact with ring deformations.

The calculations reported in the computational section indicate that the new C—C frequencies should be 90 cm<sup>-1</sup> above and below the C—C frequency of I, and that the ring-methyl deformations do not interact appreciably with ring modes. The former fact would suggest that the C—C vibrations lie near 1340 and 1160 cm<sup>-1</sup>. The 1372 cm<sup>-1</sup> band, together with the 1445 cm<sup>-1</sup> band, must be correlated with the methyl group deformations. There remain bands at 1302(*s*), 1264(*s*), 1222(*s*), 1176(*m*) and 1099 cm<sup>-1</sup> (*s*). It is clear that interaction with the CH<sub>2</sub> modes is strong and any designation is artificial. However, on the basis of intensities and expected frequencies the bands at 1302 and 1099 cm<sup>-1</sup> are classified as the C—C modes. The remainder of the assignments above 800 cm<sup>-1</sup> follow. There can be little uncertainty about the C—S modes. This indicates that the strong bands at 694 and 597/540 cm<sup>-1</sup> which have no counterparts in I must arise from ring methyl deformations. Their computed frequencies are somewhat lower (486 and 412 cm<sup>-1</sup>).

As expected, the ring angle deformation is the same as that in I. Also the symmetric SnS stretch is the same. The presence of two strong bands at 363 and 341 cm<sup>-1</sup> shows that the methyl group has removed the degeneracy effectively enough to give an easily observable splitting.

DIPHENYL AND DIBUTYL COMPOUNDS.—Characteristic vibrations of the phenyl groups are readily identified from the tables of Randle and Whiffen,<sup>5</sup> and by comparison with the spectrum of phenyltin tribromide<sup>6</sup> (see table 1). The dibutyl frequencies can also be readily correlated with the frequencies of the *n*-butyl group in di-*n*-butyltin dichloride.<sup>7</sup> All the major spectral features above 600 cm<sup>-1</sup> can now be explained without difficulty. One tentative correlation of observed bands with ring size follows. Compound II and the cyclohexanes absorb strongly at 1308-1302 cm<sup>-1</sup> and also near 1260 cm<sup>-1</sup>. The pentanes absorb at 1286 and 1248, 1287 and 1252, and 1280 and 1246 cm<sup>-1</sup> respectively. This suggests that a chain of two carbon atoms with two sulphur attachments can be distinguished from a chain of three. Clearly much more data are necessary before this can be confirmed as a meaningful correlation.

The simplicity of the spectrum of di-*n*-butyltin dichloride, and its close similarity with that of the dibutyl cyclic tin compounds suggests that in both molecules the butyl groups are principally in the extended conformations. Both spectra differ markedly from, say, that of butylbromide.

We gratefully acknowledge partial financial support from the Office of Naval Research, U.S. European Research Contracts programme for research in far infra-red spectroscopy.

<sup>1</sup> Finch and Steele, *Trans Faraday Soc.*, 1964, 60, 2125.

<sup>2</sup> (a) Backer and Drenth, *Rec. trav. chim.*, 1951, 70, 559. (b) Poller, *Proc. Chem. Soc.*, 1963, 312. (c) Poller and Spillman, unpublished work.

<sup>3</sup> Smethurst and Steele, *Spectrochim. Acta*, 1964, 20, 242.

<sup>4</sup> Hendra, Lane and Smethurst, *J. Sci. Instr.*, 1960, 40, 457.

<sup>5</sup> Randle and Whiffen, *Molecular Spectroscopy* (Institute of Petroleum, London), 1955.

<sup>6</sup> Finch and Steele, unpublished work.

<sup>7</sup> Tobin, *J. Mol. Spectr.*, 1960, 5, 65.

Offprinted from the *Transactions of The Faraday Society*,  
No. 523, Vol. 62, Part 7, July, 1966

VIBRATIONAL SPECTRA OF SOME HETEROCYCLIC BORON  
COMPOUNDS

PART 2.—2-CHLORO- AND 2-PHENYL-1,3,2-DITHIOBOROLANS

# Vibrational Spectra of Some Heterocyclic Boron Compounds

## Part 2.—2-Chloro- and 2-Phenyl-1,3,2-Dithiaborolans

BY ARTHUR FINCH, J. PEARN AND D. STEELE

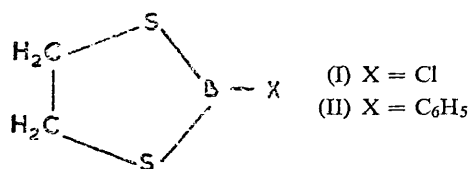
Dept. of Chemistry, Royal Holloway College, Englefield Green, Surrey

Received 28th September, 1965

The infra-red and Raman spectra of 2-chloro- and 2-phenyl-1,3,2-dithiaborolans have been measured. Evidence is presented for non-planarity ( $C_2$  symmetry) of the thiaborolan rings. A partial vibrational assignment, consistent with the computations of part 1 and with assignments of similar molecules, is proposed.

In part 1,<sup>1</sup> computations of vibrational frequencies and modes of 5- and 6-membered cyclic boron compounds were presented. In addition to the general frequency pattern it was demonstrated that severe mixing of B—Cl stretching modes with other vibrational modes occurred where this was permissible on symmetry grounds. The extent of mixing was such as to make the label B—Cl stretching vibration inappropriate for any real mode in these systems. Lack of experimental data other than liquid phase infra-red data made detailed comparisons between calculations and observations inappropriate.

In this paper experimental data are presented on the (I) 2-chloro- and (II) 2-phenyl-1,3,2-dithiaborolans. This system is characterized by considerable pyrolytic



stability.<sup>2a</sup> Molecular weight studies<sup>2b</sup> have shown that, unlike the oxygen analogues, there is no association in dilute benzene solution; assuming that this is also true in the pure phase, then the complications of the effects of dimerization and polymerization on the vibrational spectra are avoided. The 2-chloro-1,3,2-dioxaborolans and borinans proved too unstable for their Raman spectra to be obtained under normal conditions.

### EXPERIMENTAL

The infra-red spectra were run in the pure liquid phase on a Unicam SP 100 with grating accessories over the range 2000-400  $\text{cm}^{-1}$ , and at lower frequencies on a grating spectrometer designed and built in the department.<sup>3</sup> Raman spectra were recorded on a Cary 81 spectrograph utilizing slit widths of 8  $\text{cm}^{-1}$  and the mercury 4358 Å line for excitation. Polarization measurements were made using the method of Edsall and Wilson.<sup>4</sup> The observed values were corrected from calibration curves for the instrument determined using the true polarization ratios of carbon tetrachloride evaluated by Rank, Pfister and Grimm.<sup>5</sup> Observed spectra and frequencies are shown in tables 2 and 3 respectively.

Compounds were prepared by established procedures<sup>2a</sup> and manipulated in dry, oxygen-free enclosures. Satisfactory characterization was made by analysis and checking physical constants.

2-CHLORO-1,3,2-DITHIOBOROLAN.—B.p. 25-26°C/0.05 mm,  $n_D^{25} = 1.5776$  (lit. values, b.p. 24-25/0.1 mm,  $n_D^{25} = 1.5778$ ); found % Cl, 25.5; % B, 7.78;  $C_2H_4S_2BCl$  requires Cl, 25.6; B, 7.82.

2-PHENYL-1,3,2-DITHIOBOROLAN.—B.p. 90-92/0.05 mm,  $n_D^{25} = 1.6348$  (lit. values, b.p. 90-92/0.05 mm,  $n_D^{25} = 1.6346$ ); found B, 5.39;  $C_8H_9S_2B$  requires B, 5.56.

#### ASSIGNMENTS \*

It was assumed<sup>1</sup> that the 5-membered boron heterocyclic rings were planar. Following Mulliken<sup>6</sup> (recommendations 3 and 5a lead to *z*-axis as symmetry axis and *x*-axis as perpendicular to plane of molecular skeleton) the fundamental vibrational modes of I classify as

$$\begin{array}{ll} 5a_1 + 4b_2 + 2b_1 + a_2 & \text{(skeletal modes),} \\ + 3a_1 + 3b_2 + 3a_2 + 3b_1 & \text{(CH}_2\text{ modes).} \end{array}$$

Two possible structures of lower symmetry exist. First, if the skeleton exists in the envelope form the molecular symmetry is  $C_S$  and the  $a_1$  and  $b_1$  and the  $a_2$  and  $b_2$  classes coalesce. In the puckered ring configuration the symmetry is  $C_2$  and the  $a_1$  and  $a_2$  and the  $b_1$  and  $b_2$  classes coalesce.

TABLE 1.—POTENTIAL ENERGY DISTRIBUTION IN  $C_2S_2BCl$

	sym	B—Cl	B—S	C—S	CC	SBS	BSC	SCC	CBS
1381	$a_1$	26	22	5	21	16	9	1	0
1258	$b_2$	0	80	5	0	0	3	5	7
1218	$a_1$	15	14	12	49	5	0	4	0
1158	$b_2$	0	23	16	0	0	1	53	7
951	$a_1$	1	0	76	18	0	0	4	0
604	$b_2$	0	3	20	0	0	23	54	0
577	$a_1$	20	47	0	7	9	11	6	0
368	$a_1$	40	1	1	4	34	18	1	0
245	$b_2$	0	12	0	0	0	1	0	87

#### 2-CHLORO-1,3,2-DITHIABOROLAN (I)

There is a striking agreement between the frequencies and intensities of the bands above  $600\text{ cm}^{-1}$  of compound (I) and of the non-phenyl vibrations of the phenyl analogue (II). The only appreciable differences occur near  $950\text{ cm}^{-1}$ , the distribution of intensity amongst the components of the intense absorption complex being a little different in the two cases, and the frequencies of the chloro-compound being a little above those of the phenyl derivative. Corresponding Raman lines are strongly polarized. The band complex of the phenyl derivative is naturally assigned as due to the phenyl boron stretching mode by analogy with corresponding mass-sensitive bands of other phenyl derivatives.<sup>7</sup> Two arguments refute such a simple explanation. In the first case the computations presented in part I showed how considerably the B—Cl stretching mode mixed with other modes. Indeed, for the dioxa-analogue the band near  $1000\text{ cm}^{-1}$  was computed to have a relatively low B—Cl contribution. The mass changes inherent in substituting sulphur for oxygen could seriously affect the potential energy distribution, so this has been

\* The subsequent discussion relates only to frequencies below *ca.*  $2000\text{ cm}^{-1}$ .

computed for (I) (table 1). This indicates an even smaller B—Cl contribution. However, the cause of the mixing is the kinetic condition of momentum conservation more than the force field effects. The second argument is based on the spectra. It is difficult to estimate the effective mass of the phenyl ring but it ought to be less than that of the chlorine atom; first, the vibrational frequencies of the aromatic ring are close to the frequency of the band in question. Coupling of the modes will therefore occur rather than the phenyl unit vibrating as an entity. This indicates that the effective mass should probably be within twice that of an isolated carbon atom. Further, the B—Cl force constant is less than that of the B—C force constant in boron trimethyl.<sup>8</sup> This, in turn, should be less than that of the B-phenyl due to the  $\pi$  electron contributions to the bonding. This again will tend to reduce the "natural" B—Cl frequency as compared to the "natural" B-phenyl. The experimental evidence is that the frequency of the complex is higher for (I) than for (II). By the rule of mass effects<sup>9</sup> this indicates that the natural B-phenyl frequency lies above  $920\text{ cm}^{-1}$  and the natural B—Cl frequency lies below  $970\text{ cm}^{-1}$ . Mixing of modes then depresses the frequency of the intense complex in (II) but increases it in (I). It is believed that the principal contributing mode to both these complexes is the B—S stretching mode.

For a planar ring skeleton there are five  $a_1$  skeletal modes and two  $a_1$   $\text{CH}_2$  modes, a wag and a scissoring deformation. By analogy with the 1,2 disubstituted ethanes<sup>10</sup> the wag and scissoring modes are expected near  $1250$  and  $1430\text{ cm}^{-1}$ . The calculations of part I predict that the two highest skeletal modes are near  $1380$  and  $1220\text{ cm}^{-1}$ . These points show that the five strong polarized Raman bands at  $996$ ,  $948$ ,  $668$ ,  $477$  and  $338\text{ cm}^{-1}$  and the less strong  $841\text{ cm}^{-1}$  band are to be associated with the three remaining  $a_1$  fundamentals. The  $996$ ,  $948\text{ cm}^{-1}$  pair are readily explained as a fundamental in Fermi resonance with a combination band. The  $840\text{ cm}^{-1}$  band might be  $2 \times 420\text{ cm}^{-1}$ , though an alternative explanation is noted later. It seems unlikely that any of the other polarized bands arise from Fermi resonance and it is necessary to deduce that the skeleton is non-planar. The obvious mode possible for the additional band is the low-frequency rock. Other  $\text{CH}_2$  modes occur at too high frequencies to be responsible for the observed bands. The low-frequency rock belongs to the  $A$  class of gauche  $\text{XCH}_2\text{CH}_2\text{X}$  systems and is thus the out-of-phase mode. This would belong to the fully symmetric class of group  $C_2$  but not  $C_s$  showing that a thioborolan ring is puckered and does not have the "envelope" configuration. The  $B$ -class rock is to be expected between  $900$  and  $800\text{ cm}^{-1}$ . Strong infra-red absorption occurs at  $840\text{ cm}^{-1}$  but a Raman band with this frequency shift is polarized. For the  $B$  rock to be polarized the ring must assume the envelope configuration but this is inconsistent with the previous analysis leading to a puckered ring unless the C—S—B angles are non-equivalent. This seems unlikely. The polarization of the Raman band is consistent with it being the overtone of a  $420\text{ cm}^{-1}$  fundamental. The strength of the infra-red absorption may be due either to some acquired intensity for the  $1010$ - $920\text{ cm}^{-1}$  complex or from overlapping with the  $B$ -type rock.

In the trans and in the gauche 1,2 disubstituted ethanes, the  $\text{CH}_2$  scissoring deformations all occur in the range  $1460$  to  $1410\text{ cm}^{-1}$ . In the gauche halogeno ethanes, the  $A$  and  $B$  deformations are not resolved and the Raman bands are depolarized. The  $1430\text{ cm}^{-1}$  bands are consequently identified with these modes. Four ring modes and four twisting and wagging modes remain to be located at frequencies above  $1000\text{ cm}^{-1}$ . On the present evidence they cannot be identified with certainty. The assignment presented in table 2 is based on the results of the computations as given in part I on the basis of a planar ring structure and on the expected ranges for the  $\text{CH}_2$  modes based on the analogous frequencies of the

ethylene dihalides.<sup>8</sup> These lead to the following approximate anticipated frequencies: *A* modes (skeletal) 1380, 1220 (CH<sub>2</sub>), 1325 and 1200 cm<sup>-1</sup>; *B* modes (skeletal) 1260, 1160 (CH<sub>2</sub>), 1350-1250, 1250-1100 cm<sup>-1</sup>. Clearly it is possible to identify all the major unassigned bands with the skeletal modes alone or with the CH<sub>2</sub> modes alone. A comparison of intensities with those of the ethylene dihalides would favour slightly the asterisked assignments.

## 2-PHENYL-1,3,2-DITHIOBOROLAN (II)

A comparison of the observed spectra with those of phenyl boron dichloride leads to a classification of all absorption bands as phenyl vibrations or as alicyclic vibrations. The correspondence of frequencies and intensities is excellent throughout. We note the extreme weakness of the characteristic phenyl vibrations at 1500 cm<sup>-1</sup> which is due to an *a*<sub>1</sub> C—C stretching mode. This band is also very weak in the spectra of the corresponding borinan, but not in the -1,3,2-dioxaboroland and -borinans. It thus appears that this characteristic might

be diagnostic of the  $\begin{matrix} -S \\ \diagdown \\ B-\phi \\ \diagup \\ -S \end{matrix}$  grouping when used in conjunction with the presence of other characteristic phenyl vibrations. It is to be expected that the B— $\phi$  stretch will be near 1200 cm<sup>-1</sup> and it is certain that the very intense polarized Raman complex near this frequency is largely due to this mode probably interacting through Fermi resonance with the *a*<sub>1</sub> CH deformation. Of the remaining five mass-sensitive vibrations of the phenyl group<sup>7</sup> only three can be assigned with any degree of assurance. The *a*<sub>1</sub> vibration labelled *r* by Randle and Whiffen<sup>7</sup> and the low frequency vibration *x* have not been identified, but by comparison with other atomatics can be expected near 800 cm<sup>-1</sup> and near 200 cm<sup>-1</sup> respectively.

TABLE 2.—OBSERVED VIBRATIONAL FREQUENCIES OF 2-CHLORO-1,3,2-DITHIOBOROLAN AND THEIR ASSIGNMENTS

Raman		infra-red	ring modes assignments	CH <sub>2</sub> modes
1433 vs	dp	1428 s		<i>A, B</i> ( $\delta$ )
1360 w	(~0.1 <sub>5</sub> )	1378 m	<i>a</i> <sub>1</sub> (calc. 1381)	
1291 m	(0.4 <sub>1</sub> )	1282 s		<i>A</i> (W)
1262 mw	dp	1258 m	<i>b</i> <sub>2</sub> (calc. 1258) *	<i>B</i> (W)
1215 w	(~0.8)	1197 w		<i>A</i> (T) *
1173 s	(0.6 <sub>1</sub> )	1162 w	<i>a</i> <sub>1</sub> (calc. 1218) *	
1128 ms	dp	1118 m	<i>b</i> <sub>2</sub> (calc. 1158) *	<i>B</i> (T)
996 s	(0.7 <sub>3</sub> )	1010 vs	} <i>a</i> <sub>1</sub> (calc. 951) + (2 × 477) + (338 + 668)	
977 sh		970 vvs		
948 m	(0.1 <sub>9</sub> )	942 vvs		
		920 vs		
841 m	(0.6 <sub>0</sub> )	840 s-vs	2 × 420	<i>B</i> (R)
760 vw		755 w		
		669 w-m		
668 vvs	(0.2 <sub>7</sub> )	664 s	} <i>a</i> <sub>1</sub> (calc. 577) +	<i>A</i> (R)
477 vvs	(0.01 <sub>1</sub> )			
460 sh		457 w		
420 m	dp	410 m	<i>b</i> <sub>2</sub> (calc. 604)	
338 vs	(0.4 <sub>1</sub> )	326 m	<i>a</i> <sub>1</sub> (calc. 368)	
		294 vw		
220 s	dp		<i>b</i> <sub>2</sub> (calc. 245)	

\* preferred assignments

dp measured ratios 0.8-0.9

The non-aromatic bands above  $600\text{ cm}^{-1}$  are explained in a similar manner to their counterparts in the chloro-compound. The low-frequency spectra of the two ring compounds do not agree, showing that the low-frequency modes are much more sensitive to the ring substituent. This is as expected but renders assignments more difficult. As a result of the increased restoring force on the inter-ring bridging carbon atom as compared with that on the chlorine, and as a result of the higher mass of the chlorine atom, it is to be expected that the phenyl substituent frequencies will be appreciably higher than those of the chloro compound. In particular, it seems reasonable that the  $477\text{ cm}^{-1}$  band of the chloro derivatives should be increased to above  $600\text{ cm}^{-1}$  and it is proposed that the two intense polarized Raman lines at  $675$  and  $642\text{ cm}^{-1}$  are due to two  $a_1$  fundamentals in resonance. However, it is disconcerting to have a strong polarized Raman band at  $260\text{ cm}^{-1}$  which must be compared with the  $338\text{ cm}^{-1}$  band of  $\text{C}_2\text{S}_2\text{BCl}$ . Other low-frequency assignments are difficult to justify and are listed as tentative proposals.

TABLE 3.—OBSERVED VIBRATIONAL FREQUENCIES OF 2-PHENYL-1,3,2-DITHIOBOROLAN AND THEIR ASSIGNMENTS, TOGETHER WITH THE RELEVANT DATA FOR PHENYL BORON DICHLORIDE

$\text{S}-(\text{CH}_2)_2-\text{S}-\text{B}-\phi$ infra-red Raman		$\phi\text{BCl}_2$ infra-red	Raman	present in $\text{S}-(\text{CH}_2)_2-\text{S}-\text{B}-\text{Cl}$	assignment
1597 ms	1641 m 1600 vvs dp	1592 s			$\phi a_1 \nu_{\text{CC}}$ , $b_2 \nu_{\text{CC}}$
1495 vw	1548 w dp 1499 ms (0.57)	1488 w			$\phi a_1 \nu_{\text{CC}}$
1436 s 1427 m	1439 s dp	1433 ms		yes	$\phi b_2 \nu_{\text{CC}}$ Ac ring mixed
1336 w	1345 w				$a_1$ (1381)+ $\text{CH}_2$ def
1313 vw 1284 m	1289 ms	1311 w 1271 m		yes	Ac ring? or $\text{CH}_2$ twist
1263 ms	1261 sh			yes	Ac ring? or $\text{CH}_2$ twist
1248 m 1236 vs	1238 vvs (0.36)	1244 s 1233/1221 vs			$\phi a_1 \nu_{\text{B}-\phi}$
1188 w 1164 m.w 1114 w	1193 s (0.41) 1163 vs (0.66) 1117 m dp	1188 m.s 1160 v.w			$\phi a_1 \beta_{\text{CH}}$ $\phi b_2 \beta_{\text{CH}}$ Ac ring $b_2 \nu_{\text{CS}}$
1075 v.w 1034 vw 1002 m sharp 990 mw 955 ms	1074 m (0.41) 1036 vs (0.32) 1000 vs (0.4)	1001 m	1005		$\phi a_1 \beta_{\text{CH}}$ $\phi a_1 \nu$ ring
936 m 913 vs	957 w dp 908 w dp	968 m 953 s 920 vs		yes	Ac. ring $a_1$ $\nu_{\text{CS}}$

TABLE 3.—*contd.*

S—(CH <sub>2</sub> ) <sub>2</sub> —S—B— $\phi$		$\phi$ BCl <sub>2</sub>	present in		assignment
infra-red	Raman	infra-red	Raman	S—(CH <sub>2</sub> ) <sub>2</sub> —S—B—Cl	
904 vs		899 vs			$\nu_{CC} + \text{CH}_2$ rocks
842 ms	854 w 803 w dp	757 s 691 s			
751 s	758 m dp				$\phi b_1 \gamma_{CH}$
694 s				$\phi b_1 \gamma_{CH}$	
665 m	675 vs (0.67)	633 m	640 m	yes	$\phi b_1 \gamma \hat{\phi}_{Bring}$
632 s	642 vs (0.55)	618 w	626		
618 w	626 s dp	597 v.w			$\phi$ vib.
579 vw		565, 551 m			$\phi$ vib. $\gamma$
547 m	543 dp			yes	Ac $\delta_{CC}$
535 s					$\phi a_2 \phi_{CC}$
454 w	462 m dp	445 vw			Ac ring buckle
435	443 vs dp 407 w	402 w			Ac $a_1$ ring def.
392 m					
347 vw				234	
304 s				142	Ac torsion
268 s	260 s (0.41)				
	182 s				

## ABBREVIATIONS

Ac = acyclic,  $\phi$  = phenyl, vib. = vibration, s = strong, m = moderate, etc.

Numbers in parentheses refer to measured polarization ratios where these differ from 6/7. Due to experimental conditions, these values are not as reliable as for chloro analogue and little weight is to be attached to second significant figure.

- 1 Finch and Steele, *Trans. Faraday Soc.*, 1964, **60**, 2125.
- 2 (a) Finch and Pearn, *Tetrahedron*, 1964, **20**, 173. (b) Finch and Gardner, *J. Inorg. Nucl. Chem.*, 1963, **25**, 927.
- 3 Hendra, Lane and Smethurst, *J. Sci. Instr.*, 1963, **40**, 457.
- 4 Edsall and Wilson, *J. Chem. Physics*, 1938, **6**, 124.
- 5 Rank, Pfister and Grimm, *J. Opt. Soc. Amer.*, 1943, **33**, 31.
- 6 Mulliken, *J. Chem. Physics*, 1955, **23**, 1997.
- 7 Randle and Whiffen in *Report of the Molecular Spectroscopy Conference* (London, 1954) (Institute of Petroleum, 1955), p 111.
- 9 Ladd, Orville-Thomas and Cox, *Spectrochim. Acta*, 1963, **19**, 1911.
- 9 (i) Rayleigh's rule—see Wilson, Decius and Cross, *Molecular Vibrations* (McGraw-Hill, London, 1955), p. 190. (ii) Steele and Whiffen, *Trans. Faraday Soc.*, 1959, **55**, 369.
- 10 Brown and Sheppard, *Trans. Faraday Soc.*, 1952, **48**, 128.



Phosphorus Halide-Boron Halide Complexes. Part I. The Infrared  
Spectrum of  $\text{PI}_3\cdot\text{BI}_3$

By G. W. Chantry, Arthur Finch, P. N. Gates, and D. Steele

Reprinted from

JOURNAL  
OF  
THE CHEMICAL SOCIETY

---

SECTION A  
Inorganic, Physical, and Theoretical Chemistry

---

1966

## Phosphorus Halide-Boron Halide Complexes. Part I. The Infrared Spectrum of $PI_3 \cdot BI_3$

By G. W. Chantry, Arthur Finch, P. N. Gates, and D. Steele

The infrared spectrum of the complex  $PI_3 \cdot BI_3$  has been measured in the solid state between 30 and 1000  $cm^{-1}$ . Normal co-ordinate calculations show that the best fit to experimental data is obtained by assuming a force constant for the stretching of the P-B bond of 1.0 millidyne per Å. The P-B bond dissociation energy has been estimated to be ca. 16 kcal. mole $^{-1}$ .

PHOSPHORUS trihalides act either as Lewis acids or Lewis bases, and interesting examples of the latter are the complexes formed with boron halides. Although the stoichiometry of several of these adducts is now established, especially since the careful work of Holmes,<sup>1</sup> no quantitative description of the intermolecular bonding has been attempted. One of the objects of the present work is the derivation of such information through a study of the bonding in both thermochemical and spectroscopic terms. The adduct  $PI_3 \cdot BI_3$  was selected for initial investigation because (a) it may be assumed to exhibit the greatest (thermodynamic) stability, (b) no possibility of halogen-exchange exists,<sup>1,2</sup> and (c) recent work has established relevant ancillary physical data for the constituent molecules.<sup>3-5</sup> No energetic or detailed structural data are available.

Previous work on  $PI_3 \cdot BI_3$  is limited to a brief Note<sup>6</sup> describing its characterisation, and a very recent Paper<sup>7</sup> in which, *inter alia*, the infrared spectrum above 280  $cm^{-1}$  is reported. Since many of the fundamental vibrations lie below this region, we have investigated the spectrum down to 30  $cm^{-1}$  and attempted a detailed analysis of the results.

### EXPERIMENTAL

The adduct  $PI_3 \cdot BI_3$  was prepared as described previously.<sup>6,7</sup>

*Infrared Spectra.*—Solid-state spectra were recorded for Nujol mulls between silver chloride (400–1000  $cm^{-1}$ ) or high-density Polythene (30–400  $cm^{-1}$ ) plates. The region between 30 and 150  $cm^{-1}$  was covered using a Research and Industrial Instruments Co. interferometer, and that between 120 and 1000  $cm^{-1}$  with a far-infrared grating spectrometer

<sup>1</sup> R. R. Holmes, *J. Inorg. Nuclear Chem.*, 1960, **12**, 266.

<sup>2</sup> E. Wiberg and K. Schuster, *Z. anorg. Chem.*, 1933, **213**, 94.

<sup>3</sup> A. Finch, P. J. Gardner, and I. J. Hyams, *Trans. Faraday Soc.*, 1965, **61**, 649.

<sup>4</sup> A. Finch, I. J. Hyams, and D. Steele, *Trans. Faraday Soc.*, 1965, **61**, 203.

<sup>5</sup> A. Finch, P. J. Gardner, and I. H. Wood, *J. Chem. Soc.*, 1965, 746.

<sup>6</sup> R. F. Mitchell, J. Bruce, and A. Armington, *Inorg. Chem.*, 1964, **3**, 915.

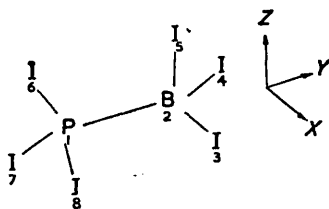
<sup>7</sup> A. H. Cowley and S. T. Cohen, *Inorg. Chem.*, 1965, **4**, 1200.

described elsewhere.<sup>8</sup> An interferometric spectrum in the region 100–400  $\text{cm}^{-1}$  confirmed in detail the spectrum obtained on the grating spectrometer in this region. For comparison with the spectrum of the complex, the spectrum of  $\text{PI}_3$  was measured in benzene and carbon disulphide over the range 400–120  $\text{cm}^{-1}$ . The observed bands, at 325s and 303m  $\text{cm}^{-1}$ , are in excellent agreement with earlier Raman data.<sup>9</sup>

## COMPUTATIONS

The procedure was to set up the B-matrix relating internal co-ordinates, R, to cartesian co-ordinates, q, in the sense  $R = Bq$ , and then to solve for the eigenvalues and eigenvectors of  $(BM^{-1})^+F(BM^{-1})$ , where F is the matrix of force constants for the internal co-ordinates, and  $M^{-1}$  is the diagonal matrix with non-zero entries equal to the square-roots of the reciprocals of the atomic masses. This is equivalent to solving the problem in cartesian co-ordinates, and has the advantage of rendering redundancies irrelevant.

Below are listed the unit vectors,  $e_{\alpha\beta}$ , from which the B-matrix elements are obtained by substituting into the appropriate equations.<sup>10</sup> The atoms are labelled as shown

FIGURE 1 Numbering of the atoms in  $\text{PI}_3\text{BI}_3$ 

in Figure 1. The P-B bond lies along the Y-axis with atoms 6, 1, 2, and 3 lying in the XY-plane.

Unit vectors,  $e_{\alpha\beta}$ 

$$\begin{aligned} e_{12} &= +Y \\ e_{23} &= +X \cos 19^\circ 28' + Y \sin 19^\circ 28' \\ e_{24} &= -X \cos 54^\circ 44' \cos 35^\circ 16' + Y \cos 54^\circ 44' \sin 35^\circ 16' \\ &\quad + Z \sin 54^\circ 44' \\ e_{25} &= -X \cos 54^\circ 44' \cos 35^\circ 16' + Y \cos 54^\circ 44' \sin 35^\circ 16' \\ &\quad - Z \sin 54^\circ 44' \\ e_{16} &= -X \cos 19^\circ 28' - Y \sin 19^\circ 28' \\ e_{17} &= +X \cos 54^\circ 44' \cos 35^\circ 16' - Y \cos 54^\circ 44' \sin 35^\circ 16' \\ &\quad - Z \sin 54^\circ 44' \\ e_{18} &= +X \cos 54^\circ 44' \cos 35^\circ 16' - Y \cos 54^\circ 44' \sin 35^\circ 16' \\ &\quad + Z \sin 54^\circ 44' \end{aligned}$$

The calculations were performed on the University of London Atlas Computer.

## RESULTS AND DISCUSSION

The infrared absorption spectrum of  $\text{PI}_3\text{BI}_3$  as a mull in Nujol is shown in Figure 2, and the bands are listed in Table 1. The frequencies previously listed<sup>7</sup> are essentially in agreement with our spectra where overlap occurs, with the exception of the highest frequency, which we observed at 647  $\text{cm}^{-1}$  (cf. 598  $\text{cm}^{-1}$ ).<sup>7</sup> The

<sup>8</sup> P. J. Hendra, R. D. G. Lane, and B. Smethurst, *J. Sci. Instr.*, 1963, **40**, 457.

<sup>9</sup> H. Stammreich, R. Forneris, and Y. Tavares, *J. Chem. Phys.*, 1956, **25**, 580.

<sup>10</sup> E. B. Wilson, J. C. Decius, and P. C. Cross, "Molecular Vibrations," McGraw-Hill, New York, 1955, p. 54.

bands observed in carbon disulphide solution by these workers appear to be due to dissociated  $\text{BI}_3$  and  $\text{PI}_3$ , as we did not observe them in the solid state.

Since one of the primary objects of these measurements was to obtain an estimate of the strength of the P-B bond (as measured by its stretching force constant), it was necessary to assume values of certain force constants, and then to compute sets of vibrational frequencies for a series of values of each of the more uncertain force constants. This procedure was necessary owing to a lack of isotopic data. Also, owing to lack of

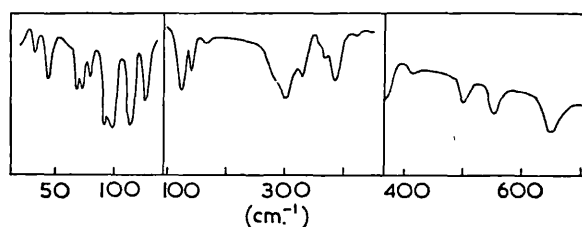
FIGURE 2 Infrared spectrum of  $\text{PI}_3\text{BI}_3$  in Nujol

TABLE 1

Infrared absorption bands of  $\text{PI}_3\text{BI}_3$ 

647s; 550m; 495m; 419w; 379s; 367w,sh; 327m; 303s; 285w; 165w; 128m; 117s; 97s, 94s,sh, and 92s; 84m, 78m, and 74m; 45m; 38m

w, weak; m, medium; s, strong; sh, shoulder.

Force field (millidynes  $\text{\AA}^{-1}$ )

Stretches	Stretch-stretch interaction
$f_{BP}$ (see Table 2)	$f_{BI/BP} = 0.10$
$f_{BI}$ (see Table 2)	$f_{BI/BI} = 0.41$
$f_{PI} = 1.21$	$f_{PI/PI} = 0.06$
	$f_{PI/BP} = 0.10$
Angle bends	Bend-bend interactions
$f_{IBI} = 0.12$	$f_{IBI/IBI} = -0.06$
$f_{IPI} = 0.18$	$f_{IPI/IPI} = 0.03$
$f_{IPB}$ } see Table 2	$f_{IPI/IPB} = 0.01$
	$f_{IBI/IPB} = 0.01$

structural data, assumptions were made as follows: (a) a staggered ethane-like configuration ( $C_{3v}$  symmetry) was assumed, with all angles tetrahedral, and (b) B-I and P-I bond lengths were taken as equal to the values in the parent compounds (2.10 and 2.47  $\text{\AA}$ , respectively);<sup>11,12</sup> the P-B bond length was taken to be 2.20  $\text{\AA}$  (estimated from the sum of the Pauling covalent radii). The P-I stretching and bending force constants were taken directly from the values for  $\text{PI}_3$ .<sup>9</sup> This part of the complex is expected to undergo relatively little change of geometry upon complex-formation, the bond angle being 102°<sup>12</sup> in  $\text{PI}_3$  itself. The change in the geometry of  $\text{BI}_3$  is more drastic, from planar ( $sp^2$ ) in  $\text{BI}_3$  to tetrahedral ( $sp^3$ ) in the complex. It has also been established<sup>13</sup> that the B-F bond in amine-boron trifluoride complexes is longer than in the parent  $\text{BF}_3$ , and that this is due to a decrease in double-bond character. Such an effect would be considerably smaller

<sup>11</sup> T. Wentinck and V. H. Tiensuu, *J. Chem. Phys.*, 1958, **28**, 826.

<sup>12</sup> S. M. Swingle, personal communication in P. W. Allen and L. E. Sutton, *Acta Cryst.*, 1950, **3**, 46.

<sup>13</sup> S. Geller and J. L. Hoard, *Acta Cryst.*, 1951, **4**, 399.

in  $\text{BI}_3$  complexes but may still be appreciable. Other recent spectroscopic studies<sup>14</sup> on amine-boron trihalide complexes showed that the antisymmetric B-X stretching frequency is reduced on complex-formation. Accordingly, the B-I stretching force constant has been given the value 1.50 millidynes per Å (as against 1.88 millidynes/Å for  $\text{BI}_3$  itself<sup>15</sup>). The greatest uncertainties in the force constants must lie in the P-B stretching and IPB and IBP angle bending values. Sets of frequencies have been computed for different combinations of these (assumed) force constants, and these are listed (together

favour the force field given in column 11. The good agreement obtained with this force field for the observed low-frequency bands (38 and 45  $\text{cm}^{-1}$ ) strongly suggests that these are fundamentals rather than lattice vibrations. However, several of the low-frequency bands show fine splitting under the high-resolution conditions used, and it seems very probable that these are due to crystal lattice effects.

The remaining observed bands, except for the 367w and 327m bands, are satisfactorily explained as binary combination bands. The bands at 367 and 327  $\text{cm}^{-1}$

TABLE 2

Computed fundamental frequencies ( $\text{cm}^{-1}$ ) and potential-energy distribution for $\text{PI}_3\text{BI}_3$														
$f_{\text{P-B}}$ (millidynes Å <sup>-1</sup> )	1	2	3	4	5	6	7	8	9	10	11	Obsd. Species	Potential-energy distribution (%)	
$f_{\text{B-I}}$	2.00	2.00	1.50	1.50	1.00	1.00	1.00	1.60	2.50	2.00	1.00			
$f_{\text{IPB}}$	1.50	1.88	1.88	1.88	1.88	1.88	1.70	1.70	1.88	1.20	1.50			
$f_{\text{IBP}}$	0.10	0.10	0.10	0.15	0.15	0.10	0.15	0.10	0.15	0.10	0.15			
	616	678	678	705	704	678	677	649	705	562	645	647	E 66 BI str, 10 BI def, 15 IBP def, 8 IPB def	
	708	721	647	662	583	566	575	656	801	699	566	550	A <sub>1</sub> 51 PB str, 21 BI str, 17 IBP def, 11 IBI def	
	367	368	368	377	377	368	375	368	377	364	374	379	E 8 BI str, 65 PI str, 16 IPI def, 7 IPB def	
	310	319	315	326	317	307	315	313	333	303	313	303	A <sub>1</sub> 12 PB str, 13 BI str, 20 PI str, 16 IPB def, 24 IPI def	
	147	150	149	151	148	145	146	147	155	143	144	128	A <sub>1</sub> 13 PB str, 28 BI str, 44 PI str, 9 IBP def	
	99	100	99	107	106	98	106	99	108	99	106	117	A <sub>1</sub> 26 PI str, 11 IBI def, 16 IPB def, 20 IBP def, 20 IPI def	
	92	96	96	99	99	96	97	94	99	87	94	95*	E 44 BI str, 13 PI str, 18 IBI def, 9 IPB def, 9 IBP def	
	86	86	86	87	87	86	87	86	87	86	87	84	E 19 PI str, 24 IBI def, 46 IPI def	
	65	66	66	72	72	66	72	66	72	65	72	76*	E 11 IBI def, 15 IPB def, 22 IBP def, 49 IPI def	
	37	37	37	45	45	37	45	37	45	37	45	45	E 58 IPB def, 42 IBP def	
	30	31	30	41	40	30	40	30	41	30	40	38	A <sub>1</sub> 8 PB str, 36 IBI def, 49 IBP def	

\* Average values; see Table 1.

with observed frequencies) in Table 2. It can be seen that the best fit to the experimental data was obtained using a force constant for the P-B bond stretching of 1.0 millidyne/Å (column 11). Most of the calculated frequencies agree well with the observed values for all the sets of force constants, and adjustments were necessary only to bring the two highest frequencies into agreement. It can be seen from Table 2 (column 10) that it is possible to produce a plausible fit to the observed data by using a very low value for  $f_{\text{B-I}}$  together with a value for  $f_{\text{P-B}}$  of 2.0 millidynes/Å. These values give rise to a frequency of 562  $\text{cm}^{-1}$  for the B-I antisymmetric stretch with the P-B stretch at 699  $\text{cm}^{-1}$ . However, the low value (1.20 millidynes/Å) required for  $f_{\text{B-I}}$  to produce this result seems improbable, and we

have been assigned as the ternary bands  $2 \times 128 + 95 = 351$  (E), and  $2 \times 95 + 128 = 318$  (A<sub>1</sub>, E). Fermi resonance with the adjacent E and A<sub>1</sub> fundamentals accounts for their appreciable intensity.

The vibrations have not been labelled in terms of specific distortions, as for many of the bands this would be quite meaningless. Included in Table 2 are the potential-energy distributions, which show the motions making the major contributions to each mode.

In general, force constants can only be used as a relative measure of bond strengths in a series of similar complexes. In the present situation we cannot make such comparisons, and an attempt to obtain an order of magnitude for the dissociation energy for the P-B bond has been made. In Figure 3 a plot of bond-dissociation

<sup>14</sup> R. L. Amster and R. C. Taylor, *Spectrochim. Acta*, 1964, 20, 1487.

<sup>15</sup> J. A. Ladd, W. J. Orville-Thomas, and B. C. Cox, *Spectrochim. Acta*, 1963, 19, 1911.

energy against the stretching force constant for several halogens, hydrogen halides, and other diatomic molecules

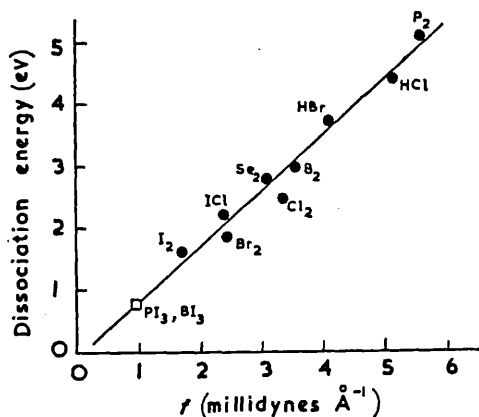
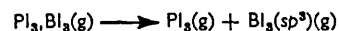


FIGURE 3 Plot of dissociation energy against force constant for various diatomic molecules

gives a roughly straight line. Extrapolation of this plot to 1.0 millidyne  $\text{\AA}^{-1}$  yields a value of 0.7 eV, or 16

kcal.  $\text{mole}^{-1}$ , for the dissociation energy of the P-B bond, as defined by the hypothetical process



Calorimetric (solution) measurements on this molecule are in progress; however, the instability of the compound renders it difficult to envisage any means by which relevant thermodynamic gas-phase data could be obtained. Hence, direct evaluation of the dissociation energy is probably not feasible, and the approximate value quoted above remains the only estimate to date. Later, a correlation between spectroscopic and thermochemical parameters of this and other members of the general class  $\text{PX}_3, \text{BX}_3$  will be attempted.

We thank Dr. K. K. Sen Gupta for a sample of  $\text{PI}_3, \text{BI}_3$ , and the U.S. Office of Naval Research for financial assistance. Part of this work was carried out in the research programme of the National Physical Laboratory.

ROYAL HOLLOWAY COLLEGE, ENGLEFIELD GREEN, SURREY.  
(G. W. C.) NATIONAL PHYSICAL LABORATORY,  
TEDDINGTON, MIDDLESEX.

[6/042 Received, January 13th, 1966]

## The vibrational spectrum of *ortho*-phosphoric acid in some non-aqueous solvents\*

R. J. LEVENE,† D. B. POWELL‡ and D. STEELES§

(Received 8 February 1966)

**Abstract**—The infra-red spectrum of *ortho*-phosphoric and deuterio *ortho*-phosphoric acids have been measured in acetonitrile, dioxan, acetone and tetrahydrofuran. The frequencies associated with the symmetric P—O and P=O stretching vibrations are observed to move apart from their observed frequencies in aqueous solutions. The observed data is shown to be consistent with accepted values of force constants for P=O and P—O bonds. There is uncertainty in the frequency of the lowest *e* fundamental.

THE PUBLISHED literature [1–7] on the infra-red and Raman spectra of *ortho*-phosphoric acid is entirely restricted to spectra measured either in the solid phase or in aqueous solution. X-ray studies [8] have shown that in the solid state the acid exists in the form of a “macro” molecule in which the individual PO<sub>4</sub> units are bound together by hydrogen bonds. Whilst the macro units are broken up in aqueous solution hydrogen bonding through the water molecules is still as strong, and as can be expected, considerable vibrational frequency shifts from those expected for isolated molecules are in evidence in the infra-red and Raman spectra. Previously little allowance has been made for this effect, except by CHAPMAN *et al.* [9], when discussing the observed spectrum.

Ideally one would study the infra-red spectra in dilute solution using a solvent such as carbon tetrachloride to break down the hydrogen bonding. Unfortunately orthophosphoric acid was found to be insoluble in carbon tetrachloride, tetrachlorethylene and similar solvents. It was soluble however in acetonitrile, dioxan, acetone and tetrahydrofuran and it appears from our results that the acid hydrogen bonds preferentially to the solvent. The observed vibrational frequency shifts for the orthophosphoric acid and its deuterio analogue indicate changes in the strength of the hydrogen bonding to the PO<sub>4</sub> groupings. The nuclear magnetic resonance spectra of the solutions confirm the changes in hydrogen bonding strengths.

\* Presented in part at the 8th European Congress on Molecular Spectroscopy, Copenhagen, August 1965.

† Department of Chemistry, Sir John Cass College, Jewry Street, London, E.C.3.

‡ School of Chemical Sciences, University of East Anglia, Wilberforce Road, Norwich.

§ Department of Chemistry, Royal Holloway College, Englefield Green, Surrey.

- [1] C. S. VENKATESWARAN, *Proc. Indian Acad. Sci.* **3A**, 25 (1936).
- [2] A. SIMON and F. FEHER, *Z. Anorg. Chem.* **230**, 289 (1937).
- [3] A. SIMON and G. SCHULZE, *Z. Anorg. Chem.* **242**, 313 (1939).
- [4] J. P. MATHIEU and J. JACQUES, *Compt. Rend.* **215**, 346 (1942).
- [5] N. R. RAO, *Indian J. Phys.* **17**, 357 (1944).
- [6] T. J. HANWICK and P. HOFFMANN, *J. Chem. Phys.* **17**, 1166 (1949).
- [7] A. C. CHAPMAN and L. E. THIRLWELL, *Spectrochim. Acta* **20**, 937 (1964).
- [8] S. FURBERG, *Acta. Chem. Scand.* **9**, 1557 (1955).
- [9] A. C. CHAPMAN, D. A. LONG and D. T. L. JONES, *Spectrochim. Acta* **21**, 633 (1965).

It would be expected that the OH stretching frequency would be affected most by hydrogen bonding, as it is in phenols and alcohols, and if the bonding were broken down, a shift to higher frequency would be expected. Spectra were obtained by compensating the absorption due to the solvent, but as all the solvents studied absorbed in the region of  $\nu\text{OH}$  no reliance could be placed on the spectra obtained.

It would also be expected that modes to which the P=O stretching contributes appreciably should be affected, since the hydrogen bond to this oxygen atom will cause an effective decrease in bond order. Thus, if the hydrogen bonding to the P=O is reduced by dissolving the acid in a non-polar solvent or by bonding preferentially to a different acceptor a shift in frequency is expected. DAASCH and SMITH [10] deduced from studies of the infra-red spectra of organophosphorus compounds that in these compounds the P=O stretching frequency is related to the electronegativities of the rest of the groups on the P atom. If hydrogen bonding were absent from phosphoric acid one would expect the  $\nu\text{P=O}$  to be near that of  $\nu\text{P=O}$  in trimethyl phosphate [10] ( $1275\text{ cm}^{-1}$ ) whereas CHAPMAN and THIRLWELL [7] show it occurs at  $1165\text{ cm}^{-1}$  in aqueous solution.

#### EXPERIMENTAL

Spectra in the region  $4000\text{--}650\text{ cm}^{-1}$  were obtained on a Hilger H 900 spectrometer and in the region  $1000\text{--}250\text{ cm}^{-1}$  on a Hilger H 800 spectrometer. Absorption due to solvents, where possible, was compensated using a variable path length cell with KBr windows and the spectrum of the aqueous acid was obtained between Irtrans flats. NMR spectra were obtained on an AEI RS2.

#### RESULTS AND DISCUSSION

Figures 1-3 show examples of some of the spectra obtained and Table 1 lists the frequencies due to phosphoric and deuterophosphoric acid in various solvents. The frequencies did not vary with the concentration of the acid over the concentration range studied. In comparison with the spectrum of the aqueous solution (Fig. 1) the most significant feature is the disappearance of the  $1165\text{ cm}^{-1}$  band and the appearance of a strong band around  $1240\text{ cm}^{-1}$ . We have assigned this frequency to the  $\nu\text{P=O}$  stretch. It is to be noticed that only this frequency is particularly sensitive to solvent effects, the frequency being highest in acetonitrile where the hydrogen bonding is expected to be least. This is confirmed by the NMR measurements (Table 2). A sharp rise in  $\tau$  values is observed in going from dioxan and acetone to acetonitrile. In the latter solvent the shift moves to high field with increasing dilution. These results are in accord with expectations from hydrogen bonding [11]. The absorption peak at about  $1000\text{ cm}^{-1}$ , assigned to the anti-symmetric P—O stretching mode of the  $E$  class, occurs at the same frequency in aqueous solution. We have assigned the  $876\text{ cm}^{-1}$  absorption peak to the symmetrical P—O stretch ( $A_1$  class). There are two vibrations around  $500\text{ cm}^{-1}$  which we have assigned to bending modes, but the  $E$  class bending mode which has been observed in the Raman spectra in aqueous solution was not observed in the infra-red

[10] L. W. DAASCH and D. C. SMITH, *Anal. Chem.* **23**, 853 (1951).

[11] J. A. POPLER, W. G. SCHNEIDER and H. J. BERNSTEIN, *High Resolution Nuclear Magnetic Resonance Spectroscopy*, Chap. 15, McGraw-Hill, New York (1959).

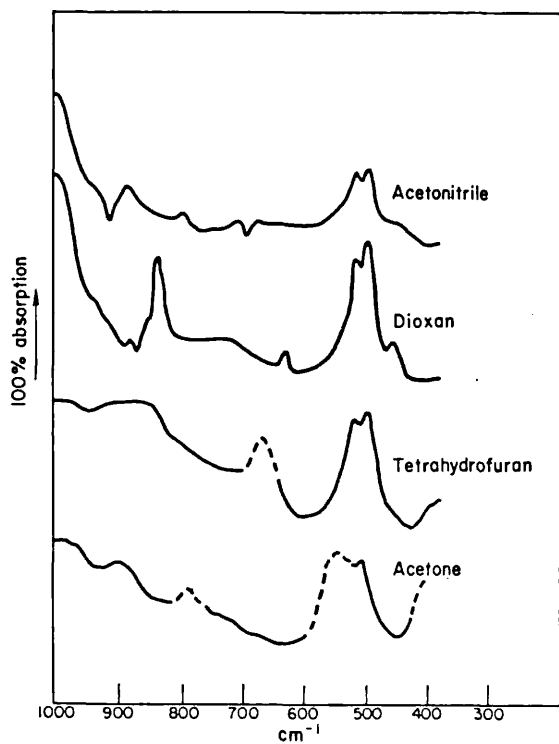
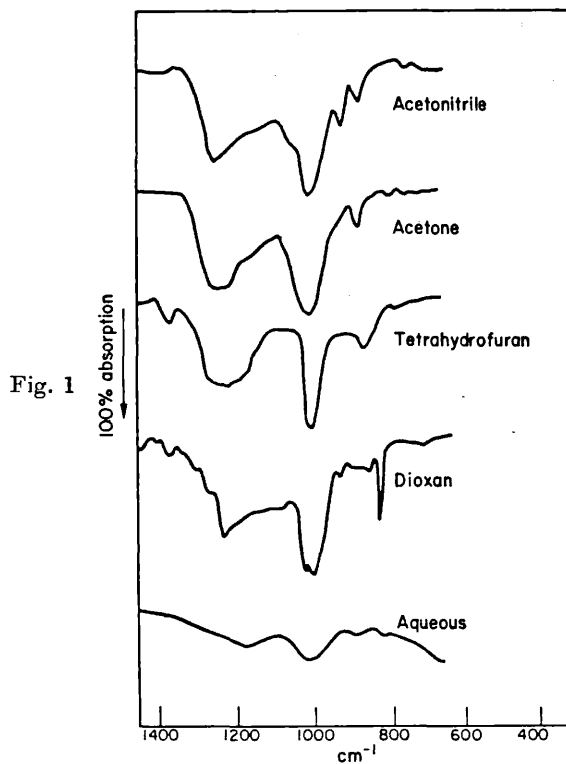


Fig. 2



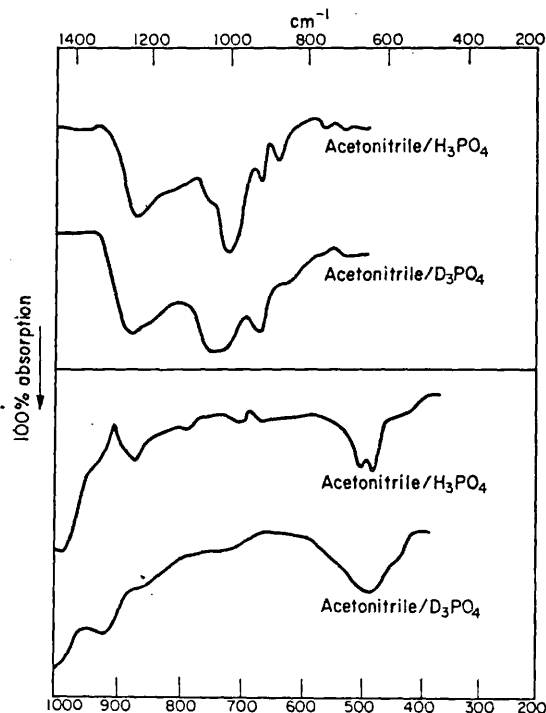


Fig. 3

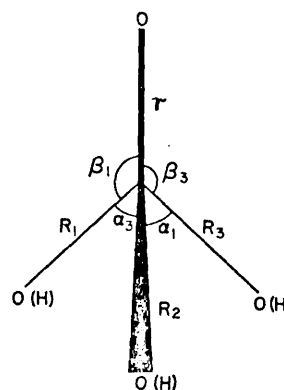


Fig. 4

Table 1. Calculated and observed frequencies of orthophosphoric acid (in  $\text{cm}^{-1}$ )

Calculated		Solvent						
Set 1	Set 2	Acetonitrile	Acetone	Tetrahydrofuran	Dioxan	Aqueous <sup>a</sup> Infra-red	Aqueous Raman	D <sub>3</sub> PO <sub>4</sub> in Acetonitrile
1287	1278	1242 s	1235 s	1220 s	1227 s	1165 vs	1190 wp	1240 s
791	836	876 m	880 m	870 m	— <sup>b</sup>	885 w	890 sp	850 sh
550	527	513 w	500 w	514 w	517 w	—	500 wp	500 wvb
911	1010	1000 vs	1002 vs	1000 vs	998 vs	1007 vs	1008 w	1000 vs
534	532	492 w	493 w	494 w	497 w	—	390 w	500 wvb
510	484	—	—	— <sup>c</sup>	—	—	345 w	—

Abbreviations: s. strong, vs. very strong, m. medium, w. weak, sh. shoulder, p. polarized, vb. very broad  
<sup>a</sup> Bands also observed in the infra-red at 1250 sh, 1070 w and in the Raman at 1060 wp. Assignments of these frequencies have been made by CHAPMAN and THIRLWELL [7].

<sup>b</sup> A very sharp band at 827  $\text{cm}^{-1}$  was observed, but due to very strong solvent absorption around 880  $\text{cm}^{-1}$  assignment of this frequency was not attempted.

<sup>c</sup> An absorption at 385  $\text{cm}^{-1}$  was observed at 50 per cent concentration of H<sub>3</sub>PO<sub>4</sub>.

Table 2. NMR Results proton chemical shifts

Solvent	$\tau$ values	
	conc. (1)	conc. (2)
Acetonitrile	+ 1.22	+ 1.99
Dioxan	- 0.11	
Acetone	- 0.15	

The concentration of orthophosphoric acid in (1) was twice that in (2).

Table 3

Force constant	Value in m.dyn/Å		Constraints
	Set 1	Set 2	
$f_r$ (P=O)	9.2	8.2	
$f_R$ (P—O)	4.31	4.9	$f_{r\beta} = f_{R\beta} = f_{R\alpha'}$
$f_{rR}$ Interaction	0.58	0.58	$f_{r\alpha} = f_{R\alpha} = f_{R\beta'} = 0$
$f_{RR}$ Interaction	0.67	0.8	
$f_\alpha$	0.9	0.9	
$f_\beta$ Interaction	0.9	0.9	
$f_{r\beta}$	—	0.2	

spectrum of the acid in the solvents used. A very weak absorption peak at  $385\text{ cm}^{-1}$  in tetrahydrofuran solution may be due to this vibration.

The frequencies were calculated using the Wilson  $G.F.$  matrix method; we calculated the  $G$ -matrix from first principles assuming a  $C_{3v}$  symmetry for the molecule (Fig. 4) and this was in agreement with the  $G$ -matrix calculated by LONG and THOMAS [12] for a molecule type  $MX_3Y$ . For our purposes we assumed the OH group to be a single unit of mass 17, as this simplifies the problem considerably and as we were not able anyway to observe the OH stretching frequency for reasons explained above. The values of the  $F$ -matrix elements that we took are tabulated in Table 3 and the problem was solved using symmetry co-ordinates by evaluating  $UGU^+$  and  $UFU^+$  using a  $U$ -matrix due to LONG [13] (Table 4). The computed frequencies are given in Table 1. From the equation  $\mathcal{L}^+\Delta\mathcal{F}\mathcal{L} = \Delta\lambda$  it was obvious from the coefficients of the  $\Delta f$ 's that certain frequencies were affected principally by varying certain force constants. Utilizing these principal terms a new set of force constants was chosen to try to improve the fit between observed and calculated frequencies. With this in mind the force constant  $f_{r\beta}$  was introduced into the problem. This is an angle bend/opposite bond stretch interaction force constant (the umbrella

Table 4

$U$ -Matrix										
	$R_1$	$R_2$	$R_3$	$r$	$R\alpha_1$	$R\alpha_2$	$R\alpha_3$	$R\beta_1$	$R\beta_2$	$R\beta_3$
$S_1$	—	—	—	1	—	—	—	—	—	—
$S_2$	$\frac{1}{\sqrt{3}}$	$\frac{1}{\sqrt{3}}$	$\frac{1}{\sqrt{3}}$	—	—	—	—	—	—	—
$S_3$	—	—	—	—	$\frac{-1}{\sqrt{6}}$	$\frac{-1}{\sqrt{6}}$	$\frac{-1}{\sqrt{6}}$	$\frac{-1}{\sqrt{6}}$	$\frac{-1}{\sqrt{6}}$	$\frac{-1}{\sqrt{6}}$
$S_4$	$\frac{2}{\sqrt{6}}$	$\frac{-1}{\sqrt{6}}$	$\frac{-1}{\sqrt{6}}$	—	—	—	—	—	—	—
$S_5$	—	—	—	—	$\frac{2}{\sqrt{6}}$	$\frac{-1}{\sqrt{6}}$	$\frac{-1}{\sqrt{6}}$	—	—	—
$S_6$	—	—	—	—	—	—	—	$\frac{2}{\sqrt{6}}$	$\frac{-1}{\sqrt{6}}$	$\frac{-1}{\sqrt{6}}$

[12] D. A. LONG and A. G. THOMAS, *Proc. Roy. Soc. (London)* **223A**, 130 (1954).[13] D. A. LONG, *Proc. Roy. Soc. (London)* **217A**, 203 (1953).

Table 5

$\Delta\lambda_1 =$	$0.084\Delta f_r - 0.043\Delta f_{rR} + 0.040\Delta f_{r\beta} + 0.016\Delta f_R + 0.032\Delta f_{RR} + 0.061\Delta f_\alpha + 0.061\Delta f_\beta$
$\Delta\lambda_2 =$	$0.008\Delta f_r - 0.023\Delta f_{rR} + 0.038\Delta f_{r\beta} + 0.052\Delta f_R + 0.102\Delta f_{RR} + 0.002\Delta f_\alpha + 0.002\Delta f_\beta$
$\Delta\lambda_3 =$	$0.003\Delta f_r - 0.003\Delta f_{rR} + 0.018\Delta f_{r\beta} + 0.002\Delta f_R + 0.004\Delta f_{RR} + 0.081\Delta f_\alpha + 0.081\Delta f_\beta$
$\Delta\lambda_4 =$	$0.364\Delta f_{r\beta} + 0.088\Delta f_R - 0.088\Delta f_{RR} + 0.101\Delta f_\alpha + 0.088\Delta f_\beta$
$\Delta\lambda_5 =$	$-0.006\Delta f_{r\beta} + 0.001\Delta f_R - 0.001\Delta f_{RR} + 0.119\Delta f_\alpha + 0.060\Delta f_\beta$
$\Delta\lambda_6 =$	$-0.110\Delta f_{r\beta} + 0.014\Delta f_R - 0.014\Delta f_{RR} + 0.032\Delta f_\alpha + 0.084\Delta f_\beta$

constant) and has been shown by ALDOUS and MILLS [14] to be very important in molecules of  $C_{3v}$  symmetry. With this new set an improved fit was obtained (Table 1), but with the sixth frequency still far from the value observed in the aqueous solution. To force a fit to this value would need unrealistic values of the force constants. The mode associated primarily with the P=O vibration is still calculated  $36\text{ cm}^{-1}$  high compared with its value in acetonitrile. However BELLAMY and co-workers [15] have shown that the P=O mode of  $(\text{CH}_3)_2\text{HPO}$  is very sensitive to solvent effects and is  $32\text{ cm}^{-1}$  lower in acetonitrile than in vapour phase ( $1257\text{ cm}^{-1}$  cf.  $1289\text{ cm}^{-1}$ ).

It appears possible from our observed and calculated frequencies that the sixth frequency might occur around  $500\text{ cm}^{-1}$  and may be accidentally coincident with one of the other vibrations near this frequency. The set of simultaneous equations obtained from the second set of force constant are listed in Table 5, indicating the dependence of the frequencies on the particular force constants.

The force constants we obtained, particularly the values of  $f_{\text{P=O}}$  and  $f_{\text{P-O}}$  ( $8.2$  and  $4.9\text{ m dyn/\AA}$ ), were in fair agreement with those calculated by CHAPMAN *et al.* [9] using Cruikshanks' method of relating force constants to bond order. The force constants are, of course, very approximate, but they show that in the phosphoric acids the P—O force constants are in reasonable agreement with those deduced previously for other systems containing P—O and P=O bonds. It is confirmed that the unusual values of CHAPMAN *et al.* deduced from data on aqueous solutions are due to hydrogen bonding destroying the distinction between the bonds.

*Acknowledgements*—We are grateful to Dr. R. F. M. WHITE of Sir John Cass College for measuring the NMR spectra and to the GLC for providing a research assistantship for one of us (R.J.L.).

[14] J. ALDOUS and I. M. MILLS, *Spectrochim. Acta* **19**, 1567 (1963).

[15] L. J. BELLAMY, C. P. CONDUIT, R. J. PACE and R. L. WILLIAMS, *Trans. Faraday Soc.* **55**, 1677 (1959).

Reprinted from JOURNAL OF MOLECULAR SPECTROSCOPY, Volume 16, No. 1, May, 1965  
Copyright © by Academic Press Inc. Printed in U.S.A.

JOURNAL OF MOLECULAR SPECTROSCOPY 16, 103-114 (1965)

## The Vibrational Spectra of Compounds Containing The Dimethylamino Grouping

### Part I. Dimethylamine and Tetrakis-dimethylamino Diboron

A. FINCH, I. J. HYAMS, AND D. STEELE

*Department of Chemistry, Royal Holloway College, University of London, London, England*

The vibrational frequencies and approximate modes of dimethylamine have been computed using the technique of King and Crawford. It is shown that the band at  $724\text{ cm}^{-1}$  is due to the symmetric—not the antisymmetric-NH deformation. The effect of increasing the mass of the amine hydrogen atom through the range 1 to 100 amu is explored and the results used to reinterpret the spectrum of tetra-kis dimethylamino diboron.

#### INTRODUCTION

When assigning the spectrum of a complex molecule it is important to take into consideration the degree of coupling between vibrations. In any particular case, say  $R-Y$ , certain vibrations of  $R$  will be highly sensitive to the effective mass of atom or group  $Y$ . It may occur that as the mass alters the frequency of these vibrations may or may not alter considerably. What is most important, however, is that a vibrational frequency that originally applied to an  $R-Y$  stretch may now refer to another stretching or even deformation vibration. A satisfactory answer may be had by solving the complete secular equation, though in large molecules this is often not practical. If a more approximate answer is sought the molecules may be considered as a framework to which groups of point mass are attached (1). This treatment certainly provides useful results but erroneous conclusions are often made when assigning those vibrations that are not isolated to the group or framework. Account of such vibrations may be taken by use of a method developed by King and Crawford (2) who have shown how  $\mathfrak{G}$  and  $\mathfrak{F}$  matrices may be reduced by factoring off modes which are characteristic of a group. The methyl group has been discussed in detail. Two of the C—H deformation modes and the C—H stretching vibrations are factored out leaving only two degenerate deformation modes and the C—X stretching vibration to be considered, X being the atom or group attached to the  $\text{CH}_3$ .

The following work is concerned with the dimethylamino group attached to an atom or group of varying mass. A comparison for each frequency of the potential energy distribution gives an immediate picture of how the type of vibration and

extent of coupling varies with the mass. The extent of the agreement between calculated frequencies of dimethylamine and the observed values will serve as a test both for the validity of the assignment and the usefulness of the model.

#### DISCUSSION

Spectroscopic and electron diffraction studies of ammonia, dimethylamine, and trimethylamine have indicated a pyramidal structure (1, 3-6). It would, therefore, seem reasonable to expect this structure to be retained for  $(\text{CH}_3)_2\text{N}-X$  derivatives so long as the N retains its trigonal form. The calculations have been based upon  $C_s$  symmetry (Figure 1), and even though, for steric reasons, the molecule may be slightly displaced from this configuration, the results are expected to suffer little alteration.

King and Crawford have shown that the four internal vibrations of the methyl group are little affected by the character of the molecular framework and can therefore be separated from the remainder of the vibrational problem. For methyls attached to aliphatic substituents these have the frequencies  $2932\text{ cm}^{-1}(A_1)$ ,  $3051\text{ cm}^{-1}(E)$ ,  $1451\text{ cm}^{-1}(E)$ , and  $1378\text{ cm}^{-1}(A_1)$ , if we employ the same force constants as do King and Crawford. The symmetries shown in parentheses assume  $C_{3v}$  molecular symmetry.

The inverse kinetic energy matrix in symmetry coordinates  $\mathcal{G}$  and the corresponding force constant matrix  $\mathcal{F}$ , were constructed from the following relationships:

$$\mathcal{F} = U F U^\dagger, \quad (1)$$

$$\mathcal{G} = U G U^\dagger, \quad (2)$$

where  $U$  is defined as

$$S = U R \quad (3)$$

and  $U^\dagger$  is the transpose of  $U$ .

$S$  is the matrix of symmetry coordinates and  $R$  the corresponding matrix for the internal coordinates.

$\mathcal{G}$  and  $\mathcal{F}$  are given in Tables I and II, respectively. The force constants listed in Table II were taken from the literature as were the molecular parameters in Fig. 1. By allowing  $X$  to take on the masses 1, 2, 5, 10, 20, and 100 most of the important substituents are covered. The effect of deviations of the N— $X$  force constant from the assumed N—H value will in general be small and predictable. Factorization of the characteristic methyl modes from the complete problem is effected by corrections to  $\mathcal{G}$  and  $\mathcal{F}$ . Following King and Crawford  $\mathcal{G}^+$  and  $\mathcal{F}^+$  will be used to represent  $\mathcal{G}$  and  $\mathcal{F}$  in reduced form. The relationship be-

TABLE I

$\mu_C + 2\frac{1}{3}\mu_N$	$-\frac{\sqrt{2}}{3}\mu_N$	$\frac{\sqrt{2}}{3}\mu_N(1-d/R)$	$-\frac{1}{3}\mu_N$	$\frac{1}{\sqrt{3}}\mu_N\sqrt{d}$	$\mu_N\sqrt{d}$
	$\mu_N + \mu_X$	$-\frac{1}{3}\mu_N$	$2\frac{\sqrt{2}}{3}\mu_N$	$-4\frac{\sqrt{2}}{3}\mu_N\sqrt{d}$	0
		$\mu_C + \mu_X \frac{d^2}{2R^2} + \mu_N(\frac{1}{6} + \frac{d}{3R} + \frac{d^2}{2R^2})$	$-\frac{1}{\sqrt{3}}\{4\mu_N(1-d/R) + 3\mu_C\}$	$\frac{1}{\sqrt{6}}\{2\mu_N(\sqrt{d} + \sqrt{R}) + \mu_C(1 + 3\sqrt{d}/\sqrt{2})\}$	$-\frac{1}{\sqrt{2}}\{2\mu_N(\frac{1}{6}R + \frac{5}{6}d) + \mu_C(1 + 3\sqrt{d})\}$
			$2\mu_C + \frac{8}{3}\mu_N$	$-\frac{1}{\sqrt{2}}\{4\mu_N\sqrt{d} + \mu_C(\frac{d}{\sqrt{2}} + 1)\}$	$-\frac{1}{\sqrt{2}}\{4\mu_N\sqrt{d} + \mu_C(\frac{d}{\sqrt{2}} + 1)\}$
				$\mu_H + \frac{11}{4}\mu_N\sqrt{d} + \mu_C(\frac{1}{6} + \frac{d}{R} + \frac{3d^2}{2R^2})$	$-\frac{1}{\sqrt{2}}\mu_N\sqrt{d} + \mu_H + \frac{9}{4}\mu_N\sqrt{d} + \mu_C(\frac{1}{6} + \frac{d}{R} + \frac{3d^2}{2R^2})$

A'

$\mu_C + \mu_N\frac{2}{3}$	$\sqrt{2}\mu_N(\frac{1}{3} + d/R)$	$-\frac{1}{\sqrt{3}}\mu_N\sqrt{d}$	$-\mu_N\sqrt{d}$		
	$\mu_C + \frac{3}{2}\mu_X \frac{d^2}{R^2} + \mu_N(\frac{1}{6} + \frac{d}{R} + \frac{3d^2}{R^2})$	$\frac{1}{\sqrt{6}}\{\mu_N(\sqrt{R} - \sqrt{d}) - \mu_C(1 + \frac{3d}{R})\}$	$\frac{1}{\sqrt{2}}\{\mu_N(\frac{d}{R} - \sqrt{R}) + \mu_C(1 + \frac{3d}{R})\}$		
		$\mu_H + \mu_N\sqrt{d} + \mu_C(\frac{1}{6} + \frac{d}{R} + \frac{3d^2}{2R^2})$	$\frac{\sqrt{2}}{4}\mu_N\sqrt{d}$		
			$\mu_H + \frac{3}{4}\mu_N\sqrt{d} + \mu_C(\frac{1}{6} + \frac{d}{R} + \frac{3d^2}{2R^2})$		

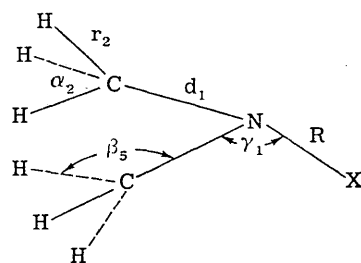
A''

TABLE II  
FORCE CONSTANT MATRICES AND SYMMETRY CO-ORDINATES

$\mathfrak{F}_{13.14} = f_d + f_{dd}$	$\mathfrak{F}_{15.15} = f_\gamma + f_{\gamma\gamma'}$	$f_\beta = 0.61 \text{ mdyn}/\text{\AA}$
$\mathfrak{F}_{13.14} = \sqrt{2}f_{dR}$	$\mathfrak{F}_{15.16} = \sqrt{2}f_{\gamma\gamma'}$	$f_d = 4.6 \text{ mdyn}/\text{\AA}$
$\mathfrak{F}_{13.15} = f_{d\gamma} + f_{d'\gamma}$	$\mathfrak{F}_{16.16} = f_{\gamma'}$	$f_R = 6.2 \text{ mdyn}/\text{\AA}$
$\mathfrak{F}_{13.16} = \sqrt{2}f_{d'\gamma}$	$\mathfrak{F}_{19.19} = f_d - f_{dd}$	$f_{dd} = 0.64 \text{ mdyn}/\text{\AA}$
$\mathfrak{F}_{14.14} = f_R$	$\mathfrak{F}_{19.20} = f_{d'\gamma} - f_{d\gamma}$	$f_{dR} = 0.1 \text{ mdyn}/\text{\AA}$
$\mathfrak{F}_{14.15} = \sqrt{2}f_{R\gamma}$	$\mathfrak{F}_{20.20} = f_\gamma - f_{\gamma\gamma}$	$f_\gamma = 0.45 \text{ mdyn}/\text{\AA}$
$\mathfrak{F}_{14.16} = f_R$		$f_{\gamma'} = 0.31 \text{ mdyn}/\text{\AA}$
$\mathfrak{F}_{17.17} = \mathfrak{F}_{18.18} = \mathfrak{F}_{21.21} = \mathfrak{F}_{22.22} = f_\beta - f_{\beta\beta}$		others zero

$S_{13} = (1/\sqrt{2})(\Delta d_1 + \Delta d_2)$
$S_{14} = \Delta R$
$S_{15} = (d/\sqrt{2})(\Delta\gamma_1 + \Delta\gamma_2)$
$S_{16} = d\Delta\gamma_3$
$S_{17} = (r/\sqrt{12})(2\Delta\beta_1 + \Delta\beta_2 + \Delta\beta_3 + 2\Delta\beta_4 + \Delta\beta_5 + \Delta\beta_6)$
$S_{18} = (r/2)(\Delta\beta_2 - \Delta\beta_3 - \Delta\beta_5 + \Delta\beta_6)$
$S_{19} = (1/\sqrt{2})(\Delta d_1 - \Delta d_2)$
$S_{20} = (d/\sqrt{2})(\Delta\gamma_1 - \Delta\gamma_2)$
$S_{21} = (r/\sqrt{12})(2\Delta\beta_1 + \Delta\beta_2 + \Delta\beta_3 - 2\Delta\beta_4 - \Delta\beta_5 - \Delta\beta_6)$
$S_{22} = (r/2)(\Delta\beta_2 - \Delta\beta_3 + \Delta\beta_5 - \Delta\beta_6)$



$$\begin{aligned}
 R &= 1.01 \text{\AA} & r &= 1.08 \text{\AA} \\
 d &= 1.46 \text{\AA} \\
 \alpha &= \beta = \gamma = 109^\circ 28'
 \end{aligned}$$

FIG. 1

tween  $\mathfrak{F}$  and  $\mathfrak{F}^+$  is particularly simple:

$$(\mathfrak{F}^+)_{14,14} = f_{N-X} - 0.06 = (\mathfrak{F})_{14,14} - 0.06,$$

$$(\mathfrak{F}^+)_{17,17} = (\mathfrak{F}^+)_{18,18} = (\mathfrak{F}^+)_{21,21} = (\mathfrak{F}^+)_{22,22}$$

$$= f_\beta - f_{\beta\beta} + 0.08 = (\mathfrak{F})_{17,17} + 0.08, \text{ etc.}$$

In  $\mathfrak{G}^+$  the corrections take the form of changes to the effective masses of the moving atoms. These changes are nonisotropic. Excluding the methyl rocking coordinate the correction changes the effective reciprocal carbon mass along the  $C_{3v}$  axis ( $\mu_C^z$ ) of the methyl group to  $0.0676 \text{ amu}^{-1}$  and along the perpendicular axes ( $\mu_C^{x,y}$ ) to  $0.0727 \text{ amu}^{-1}$ . For the methyl rocking modes  $\mu_C$  takes on the

$\mu_C^{z,u}$  value above and

$$\mu_H^+ = 0.7361 + 0.790a - 0.014a^2$$

where  $a$  is the ratio of the CH bond length to the C—N bond length. Off-diagonal  $\mathcal{G}^+$  elements are computed from Eqs. (20) and (33) in Reference 6.

The solution of the secular equation:

$$\mathcal{G}^+ \mathfrak{F}^+ \mathcal{L}^+ - \mathcal{L}^+ \Lambda^+ = 0$$

was achieved using a Ferranti Atlas computer.

The eigenvector matrix  $\mathcal{L}^+$  is related to the normal coordinate matrix  $Q^+$  and matrix  $S$  previously defined by

$$S = \mathcal{L}^+ Q^+ \quad \text{eigenvalues } \lambda_1 \cdots \lambda_n \quad (4)$$

$\Lambda^+$  is the diagonal matrix of the noncharacteristic eigenvalues.

In order to interpret a particular mode in terms of the familiar bond stretch or deformation vibration it was decided to follow the method used by Morino and Kuchitsu (7) by determining how the potential energy is distributed among the symmetry coordinates.

Table III lists the values for  $\mathcal{L}' \mathfrak{F} \mathcal{L}$  in percentage form. Since  $\mathfrak{F}^+$  is essentially diagonal only the terms  $(\mathfrak{F}^+)_{i,i} (\mathcal{L})_{i,n}^2$  have been evaluated.

#### RESULTS

It is immediately obvious from Table III that some frequencies will remain constant for any substitution. Two of the three methyl rocking modes in particular remain very pure and quite constant in frequency. In fact the  $A''$  rocking modes alter less than  $1 \text{ cm}^{-1}$  for an increase  $M_x$  from 5 to 100 amu. The anti-symmetric CN stretch also shows this marked independence of  $M_x$ . The small shifts which do occur are all in the sense expected for small kinetic interactions with the deformation mode and are in complete agreement with the interpolation rules. The lower frequency  $A'$  rock is extremely mass sensitive and for  $M_x > 5$  the mode is strongly mixed with CN and NX stretching modes. The higher frequency rock vibration is very constant in frequency, dropping monotonically from  $1226 \text{ cm}^{-1}$  for  $M_x = 1$  to  $1210 \text{ cm}^{-1}$  for  $M_x = 100$ . Rather surprisingly the principal mixing of the N—X stretch occurs with one of the  $\beta$  modes. For large masses the two vibrations become indistinguishable.

#### DIMETHYLAMINE

Comparison of these results for dimethylamine with a previous assignment (8) shows that little alteration is required (see Table IV). The  $A'$  band calculated at  $1226 \text{ cm}^{-1}$  is observed at  $1245 \text{ cm}^{-1}$  and is mainly a methyl deformation. The N—H stretch calculated at  $3349 \text{ cm}^{-1}$  is observed at  $3355 \text{ cm}^{-1}$ . The bands assigned to the  $A'$  and  $A''$  CN stretch and  $A'$  C<sub>2</sub>N deformation at 930, 1024, and



TABLE III  
DISTRIBUTION OF POTENTIAL ENERGY

Mass: 1 amu										
Vibration Freq. (cm <sup>-1</sup> ).....	3349	1227	1159	967	796.5	388	1390	1157	1048	982
CN	1	17	3	68	0	5	0	33	9	60
NX	99	0	0	0	0	0				
CNX	0	5	4	3	88	1	100	6	0	0
CNC	0	4	1	2	1	92				
HCN	0	1	88	9	2	1	0	1	68	25
HCN	0	73	3	18	8	2	0	60	23	15

Mass: 2 amu										
Vibration Freq. (cm <sup>-1</sup> ).....	2462	1220	1133	965	618	384	1162	1060	1010	981
CN	0	17	2	70	2	5	30	9	5	57
NX	98	1	2	0	0	0				
CNX	0	3	2	1	90	2	2	22	74	3
CNC	0	5	1	2	3	90				
HCN	2	0	91	7	2	0	5	67	7	28
HCN	0	74	2	21	3	3	63	1	15	12

Mass: 5 amu										
Vibration Freq. (cm <sup>-1</sup> ).....	1768	1215	1057	958	477	369.5	1160	1051	983	736
CN	2	14	0	74	5	4	31	9	60	0
NX	85	3	13	1	6	0				
CNX	1	3	0	0	71	17	0	0	0	100
CNC	1	5	0	2	16	75				
HCN	11	0	87	1	1	0	6	70	25	0
HCN	0	75	0	22	1	4	63	21	15	0

Mass: 10 amu										
Vibration Freq. (cm <sup>-1</sup> ).....	1528	1213	987	907	429	349	1160	1051	983	614
CN	5	12	29	40	1	3	31	9	60	0
NX	64	0	9	27	2	0				
CNX	1	3	0	0	50	46	0	0	0	100
CNC	2	4	0	1	46	47				
HCN	27	2	51	23	0	0	6	70	25	0
HCN	0	78	12	8	0	5	63	21	15	0

Mass: 20 amu										
Vibration Freq. (cm <sup>-1</sup> ).....	1432	1211	975	791	402	310	1160	1051	983	543
CN	8	11	51	17	2	1	31	9	60	0
NX	46	0	3	48	3	1				
CNX	1	3	0	2	17	77	0	0	0	100
CNC	3	4	1	0	77	16				
HCN	41	4	27	31	0	0	6	70	25	0
HCN	0	78	18	2	0	4	63	21	15	0

TABLE III—Continued

Mass: 100 amu										
Vibration Freq. ( $\text{cm}^{-1}$ )	1376	1210	972	643	379	234	1160	1050	983	478
CN	4	13	65	13	2	1	31	9	60	0
NX	31	6	1	49	5	11				
CNX	1	3	0	12	0	82	0	0	0	100
CNC	3	3	1	1	90	3				
HCN	49	5	17	24	0	0	6	70	25	0
HCN	1	70	16	1	2	3	63	21	15	0

TABLE IV  
DIMETHYLAMINE

	Fundamental frequencies		
	Observed in gas	Assignment	Calc.
	3355 $\text{cm}^{-1}$	$A'$ NH stretch	3349 $\text{cm}^{-1}$
	2967	$A''$ (1496 + 1466) or CH stretch	
	2912	$A''$ CH stretch	
	2855	$A'$ CH stretch	
	2802	$A'$ ( $2 \times 1404$ ) or CH stretch	
	1496	$A''$ $\text{CH}_3$ deformation	} 1451
	1466	$A'$ $\text{CH}_3$ deformation	
	1404	$A'$ $\text{CH}_3$ deformation	1378
	1245	$A'$ $\text{CH}_3$ deformation	1227
Splits into 1150 and 1178 $\text{cm}^{-1}$ in solid	1155	$A'$ and $A''$ $\text{CH}_3$ deformation	1159, 1157
Weak in infrared me- dium Raman	1078	$A''$ $\text{CH}_3$ deformation	1048
	1024	$A''$ CN stretch	982
	930	$A'$ CN stretch	967
Moves to 882 in solid	724	$A'$ N—H deformation	797
	397	$A'$ $\text{C}_2\text{N}$ deformation	388
	290	$\text{CH}_3$ twisting	
	250	$\text{CH}_3$ twisting	

397  $\text{cm}^{-1}$  agree well with the calculations. The band centered at 1155  $\text{cm}^{-1}$  appears to be complex. From the calculations it appears that two vibrations must be assigned to this band: the  $A'$  and  $A''$   $\text{CH}_3$  deformations that are calculated at 1159 and 1157  $\text{cm}^{-1}$ , respectively. In order to verify this, the low temperature work of Stewart (9) was repeated using a similar cell. To be certain that the sample of dimethylamine was in a crystalline form it was annealed by permitting the temperature to rise to about twenty or thirty degrees below the melting

point and then slowly cooled to  $-196^{\circ}$ . The process was repeated until the spectrum remained unchanged. The spectrum obtained agreed with that reported previously. The salient features of this work are as follows: (i) The band observed at  $1155\text{ cm}^{-1}$  in the gas splits into two in the solid, one at  $1150$  and the other at  $1175\text{ cm}^{-1}$ . The failure to observe splitting in other bands indicates that these components must result from the two vibrations previously mentioned and are not crystal splittings. (ii) The band at  $724\text{ cm}^{-1}$  in the gas moves to  $882\text{ cm}^{-1}$  in the solid. Such a large shift would be expected if, as appears quite reasonable, this band is an N—H deformation pushed to higher frequencies in the solid by hydrogen bonding. Previously (8) this band was assigned to the antisymmetric N—H deformation; however the calculations lead to an unequivocal assignment in the  $A'$  class. The  $A''$  N—H deformation mode is calculated at  $1390\text{ cm}^{-1}$  and is probably one of the bands in the  $1400\text{-cm}^{-1}$  region. It might well be the band observed at  $1430\text{ cm}^{-1}$  in the solid though it is difficult to understand why a shift equivalent to that for the  $A''$  band is not observed, and this peak could therefore equally well belong to one of the methyl deformation modes.

The only band not characteristic of the  $\text{CH}_3$  group which now remains to be assigned is the one calculated at  $1048\text{ cm}^{-1}$ . No band was observed in this region by Barcelo and Bellanto (8) but other workers have seen a weak absorption near here (10) and a band of medium intensity is observed in the Raman (11) at  $1078\text{ cm}^{-1}$ . This band is a methyl deformation vibration of the  $A''$  class. The selection rules lead one to expect this vibration to be both Raman and infrared active. It is difficult to see why this band does not appear more strongly in the infrared.

Apart from the low frequency  $\text{CH}_3$  twisting mode the remaining vibrations are characteristic of the methyl group. For standard  $\text{CH}_3X$  molecules they have been calculated at  $2932$  and  $3051\text{ cm}^{-1}$  for the symmetric and degenerate stretching vibrations, respectively (6) and at  $1378$  and  $1451$  for the methyl deformations which belong to the symmetric and degenerate classes, respectively. The deformation vibrations were observed as strong bands with peaks at  $1404$ ,  $1466$ , and  $1496\text{ cm}^{-1}$ . The low frequency band is probably the symmetric vibration and the two at higher frequencies are the components of the degenerate vibration split by the lower symmetry of dimethylamine. The discrepancies between the observed and calculated frequencies of the CN stretching vibrations were used to derive improved values of  $f_{\text{CN}}$  and  $f_{\text{CN/CN}}$ . This is justifiable on account of the high percentage purity of the modes (68 and 60%) and because the principal mixing is with  $\text{CH}_3$  modes for which the force constants are comparatively reliable. From  $\mathcal{L}'\Delta\mathcal{F}\mathcal{L} = \Delta\Lambda$ ,  $\Delta f_{\text{CN}}$  and  $\Delta f_{\text{CN/CN}}$  were derived to be  $0.05$  and  $0.61\text{ m dyn}/\text{\AA}$  leading to  $f_{\text{CN}} = 4.65\text{ m dyn}/\text{\AA}$  and  $f_{\text{CN/CN}} = 1.25\text{ m dyn}/\text{\AA}$ . This value of the interaction constant is somewhat higher than a previous estimate.

TETRAKIS (DIMETHYLAMINO) DIBORON  $B_2[N(CH_3)_2]_4$ 

This compound has been studied by Becher *et al.* (12) in the infrared and Raman. On steric grounds the overall symmetry is not expected to be above  $D_2$ , and comparison of the infrared and Raman indicates that the effective symmetry is not lower.

Varying degrees of approximation can be employed in interpreting the spectra of this molecule. Becher discusses the  $B_2N_4$  skeleton vibrations in some detail. This still leaves undecided the degree of coupling between the dimethylamino group and the skeleton. To determine the extent of this we may consider the spectra in the light of the previous calculations. The effective mass of the skeleton attached to the  $-N(CH_3)_2$  group must be greater than 11 amu but it is unlikely to exceed 20 amu. This would lead us to anticipate the fundamentals in the range

CH <sub>3</sub> rocking modes	$A'$ 1220–1200 $cm^{-1}$
CH <sub>3</sub> rocking modes	$A''$ ca. 1160 and ca. 1050 $cm^{-1}$
CH <sub>3</sub> umbrella mode	$A'$ and $A''$ 1378 $cm^{-1}$
CH <sub>2</sub> antisymmetric deformation	$A'$ and $A''$ 1450 $cm^{-1}$
CNC deformation	$A'$ 430–400 $cm^{-1}$
CNB deformation	$A'$ 350–310 $cm^{-1}$
CNB deformation	$A''$ 600–540 $cm^{-1}$
CH <sub>3</sub> rocking mode	$A'$ 1500–1400 $cm^{-1}$
CN stretch	$A'$ 990–970 $cm^{-1}$
NX stretch	$A'$ 900–790 $cm^{-1}$
CN stretch	$A''$ ca. 1000 $cm^{-1}$ .

That the B—N stretch and CH<sub>3</sub> rock are quite sensitive to mixing may be seen from Table III. This could well result in mixing between the CH<sub>3</sub> rocking modes of different dimethylamino groups. Table V lists the frequencies reported in Reference 12 slightly corrected to agree with measurements performed in the authors' laboratory.

Two intense polarized Raman lines occur at 586 and 1376  $cm^{-1}$ . The former must certainly arise from the B—B stretching vibration, but there are two contenders for the latter. These are the internal deformation of the CH<sub>3</sub> group that is predicted at 1378  $cm^{-1}$ , and the symmetric BN stretch as suggested in Reference 12. It is most probable that the band is due to the latter mode but with some contribution from the methyl vibration. In the infrared the band is found at 1367  $cm^{-1}$ . The two bands calculated near 420 and 330  $cm^{-1}$  are good examples of the coupling which may arise. Both contain 50% CNB and NC<sub>2</sub> deformation vibrations of the  $A'$  class of  $X-NMe_2$  for  $M_r = 10$ . If the dimethylamino groups in the diboron compound are vibrating almost independently of one another, which is reasonable, these vibrations will behave like a symmetric group vibration and appear as polarized lines in the Raman. Two polarized Raman lines are observed at 385 and 352  $cm^{-1}$ . If during this vibration the boron has an effec-

TABLE V  
 TETRAKIS (DIMETHYLAMINO) DIBORON FUNDAMENTAL FREQUENCIES

Raman	Infrared	Assignment
254 m	259 m	BN <sub>2</sub> deformation
	285 v.w.	NB <sub>2</sub> deformation
327 v.w.9	318 m	NB <sub>2</sub> deformation
362 w.p.		CNB deformation
385 m,p.	460 w	CNC deformation
	567 m	CNB deformation
586 s,p		B—B stretch
	608 m } 639 m }	BN <sub>2</sub> deformation and B out-of-plane
836 w	832 { 830 w-m } 839 w-m }	
895 m	892 m	NC stretch A''
937 m,p		NC stretch
	1049 m	CH <sub>3</sub> deformation
1066 m,dp.	1063 m	CH <sub>3</sub> deformation
	1101 w	Combination band?
1110 w	1117 s	BN antisymmetric stretch
	1128 w }	{ CN stretch ? or combination bands (2 × 567?)
1139 m,p	1140 w }	
	1186 m	CH <sub>3</sub> A'' deformation
	1216 s	CH <sub>3</sub> A' deformation
1342 m	1343 m	Coupled vibration involving B—N stretch?
1376 s,p	1367 s	Symmetric BN coupled with symmetric CH <sub>3</sub>
1414 s	1409 m	BN antisymmetric stretch
1447 s	1450 s }	CH <sub>3</sub> A' rocking deformation
	1502 s }	
2795 s	2798 s	CH stretch
2850 s	2862 s	CH stretch
2872 s	2870 s	CH stretch
2928 s	2890 s	CH stretch
	2900, 2923	CH stretch
2983 m	2978 s	(2 × 1502) or CH stretch

tive mass greater than 11 the 385-cm<sup>-1</sup> line will belong to the NC<sub>2</sub> and the 362 cm<sup>-1</sup> to the CNB deformation. Previously both were assigned to NC<sub>2</sub> deformations. Five or four more vibrations below 600 cm<sup>-1</sup> are now expected: two will be degenerate for V<sub>d</sub> symmetry, and the assumption of negligible coupling between dimethylamino groups is again assumed. The symmetric BN<sub>2</sub> deformation mode appears at 254 cm<sup>-1</sup> in the Raman and 259 cm<sup>-1</sup> in the infrared. The antisymmetric CNB deformation could be the 608- or 567-cm<sup>-1</sup> bands. Previous calculations, however, fix the 608-cm<sup>-1</sup> band as an antisymmetric BN<sub>2</sub> deformation (12). Although for most of the vibrations, the dimethylamino groups will be

independent, it is likely that there will be some coupling through the common boron atoms for the  $\text{NC}_2$  deformation and NC stretching modes. The extra vibration for the deformation mode is assigned to the infrared band at  $460\text{ cm}^{-1}$ . The extra CN stretching modes produced by the coupling probably will be weak and are assigned provisionally to the bands at  $892\text{ cm}^{-1}$  for the symmetric and  $1128\text{ cm}^{-1}$  for the antisymmetric. The degenerate  $\text{NB}_2$  deformation ( $V_d$  symmetry) will split for  $V$  or  $V_h$  symmetry and is assigned to the bands at  $285$  and  $318\text{ cm}^{-1}$ .

With the aid of Table III the band observed as a polarized Raman line of moderate intensity at  $973\text{ cm}^{-1}$  is assigned to the CN stretching vibration. Similarly, the band at  $1216\text{ cm}^{-1}$  is assigned to the  $A'$  and the  $1186$  and  $1066\text{ cm}^{-1}$  to the  $A''$  methyl deformation modes. The band observed at  $1409\text{ cm}^{-1}$  in the infrared which appears as an intense line in the Raman must be the antisymmetric B—N stretch.

Two further bands due to the  $-\text{N}(\text{CH}_3)_2$  moiety are expected near  $1000\text{ cm}^{-1}$ , the antisymmetric CN stretch computed to be near  $1000\text{ cm}^{-1}$  and the mixed BN stretch/ $\text{CH}_3$  rock mode computed as  $900$  to  $800\text{ cm}^{-1}$ . Both bands might be expected to have reasonable infrared intensity, and the former, in particular, would be expected to have a similar frequency in  $\text{B}[\text{N}(\text{CH}_3)_2]_3$ . The lack of infrared bands in the range  $1050$ – $900\text{ cm}^{-1}$  is surprising. It must be assumed that the  $892\text{-cm}^{-1}$  band is due to the antisymmetric CN stretch. A frequency higher than  $1100\text{ cm}^{-1}$  is unacceptable in view of the fact the mode is identified with a frequency of  $1024\text{ cm}^{-1}$  in  $(\text{CH}_3)_2\text{NH}$ . A re-investigation of the infrared spectra of tetrakis (dimethylamino) diboron was carried out and confirmed all details of spectra recorded by Becher. The lack of another candidate for the mixed CN/BN/ $\beta$  mode near  $900\text{ cm}^{-1}$  necessitates the assignment of the  $832\text{ cm}^{-1}$  band as this  $A'$  fundamental mode. (The infrared band was observed in this work to be a doublet with frequencies  $830$  and  $839\text{ cm}^{-1}$ .)

There remains only one antisymmetric B—N stretching vibration and two out-of-plane boron modes. The former is most likely the intense band observed at  $1117\text{ cm}^{-1}$  in the infrared. It appears as a weak band in the Raman and is also to be found in the spectrum of  $\text{B}[\text{N}(\text{CH}_3)_2]_3$ . The out-of-plane vibrations are probably the  $639$ - or  $608\text{-cm}^{-1}$  bands and the second component of the  $830\text{-cm}^{-1}$  doublet.

The only remaining band of any consequence which remains to be assigned is that at  $1343\text{ cm}^{-1}$  which is possibly a coupled vibration involving B—N stretching modes.

In conclusion it may be said that the assistance to be had from calculations of the type depicted is invaluable. The gross measure of agreement for dimethylamine certainly justifies the continued use of the model for more complicated molecules.

## ACKNOWLEDGMENTS

We gratefully acknowledge financial support from the European Research Office of the U. S. Army and the Office of Naval Research Contracts Program, for research in the fields of boron chemistry and far infrared spectroscopy, respectively.

RECEIVED October 28, 1964

## REFERENCES

1. HERZBERG, "Infra-red and Raman Spectra," Vol. II. Van Nostrand, Princeton, New Jersey, 1945.
2. W. T. KING AND B. CRAWFORD, *J. Mol. Spectry.* **5**, 421 (1960).
3. D. M. DENNISON, *Rev. Mod. Phys.* **12**, 175 (1940).
4. S. H. BAUER, *J. Am. Chem. Soc.*, **60**, 524 (1938).
5. V. SCHOMAKER according to P. W. ALLEN AND L. E. SUTTON, *Acta Cryst.* **3**, 46 (1950).
6. L. O. BROCKWAY AND H. O. JENKINS, *J. Am. Chem. Soc.* **58**, 2036 (1936).
7. Y. MORINO AND K. KUCHITSU, *J. Chem. Phys.* **20**, 1809 (1952).
8. J. R. BARCELO AND J. BELLANATO, *Spectrochim. Acta* **8**, 27 (1956).
9. J. E. STEWART, *Analyt. Chem.* **30**, 2073 (1958).
10. R. H. PIERSON, A. N. FLETCHER, AND E. S. GANTZ, *Analyt. Chem.* **28**, 1218 (1956).
11. J. BELLANATO, M. T. SARDINA, AND J. R. BARCELO, *Anales Real Soc. Espan. Fis. Quim. Madrid* **B51**, 271 (1955).
12. H. J. BECHER, W. SAWODNEY, H. NÖTH, AND W. MEISTER, *Z. Anorg. Allgem. Chem.* **314**, 226 (1962).

## THE IR SPECTRA OF THE $\text{CH}_3\text{CO}^+$ AND $\text{CD}_3\text{CO}^+$ IONS

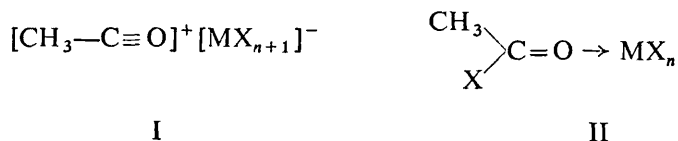
P. N. GATES AND D. STEELE

*Department of Chemistry, Royal Holloway College, University of London, Englefield Green, Surrey*

(Received November 14th, 1967)

### INTRODUCTION

The acetylium ion exists in systems such as (I) and is of interest (a) as an acetylating agent in Friedel–Crafts-type reactions and (b) because it is isoelectronic with methyl cyanide.



Previous IR studies<sup>1–3</sup> have been used to distinguish between the existence of such ions and donor–acceptor-type complexes (II) in systems of the type  $\text{CH}_3\text{COX—MX}_n$  (where X is a halogen and  $\text{MX}_n$  represents a Lewis acid). Cook<sup>4</sup> has examined several such systems and made tentative assignments for a number of the IR bands. In order to explain some of the bands in the solid-state spectra it was suggested that a simple system such as  $[\text{CH}_3\text{CO}]^+ [\text{MX}_{n+1}]^-$  did not exist, but rather, a more complex ion, possibly of the type  $[\text{CH}_3\text{—C}\equiv\text{O}\cdots\text{MX}_n]^+ \text{X}^-$ . However, recently<sup>5</sup> an X-ray analysis of the  $\text{CH}_3\text{COF—SbF}_5$  system has shown that the units  $\text{CH}_3\text{CO}^+$  and  $\text{SbF}_6^-$  are present in the crystal lattice. The C–C–O chain was found to be linear with a C–C bond length of 1.38 Å. This compares with a value of 1.46 Å in the isoelectronic methyl cyanide which represents a considerable shortening of the bond. The C–O bond length is 1.15 Å which compares with 1.13 Å in carbon monoxide.

The purpose of the present investigation was to compare the spectra of methyl cyanide and the acetylium ion and to assess the effect of the extra nuclear charge on the force field, and hence the spectrum, of the acetylium ion. However, in view of the uncertainty in the structures of the acetyl halide–metal halide complexes it was first of all necessary to prove that the acetylium ion exists as such in the system antimony pentachloride–acetyl chloride which was chosen for this investigation.



## EXPERIMENTAL

*Preparation of complexes*

$[\text{CH}_3\text{CO}]^+[\text{SbCl}_6]^-$  was prepared by the addition of  $\text{SbCl}_5$  to  $\text{CH}_3\text{COCl}$  (in 1:1 mole ratio) in  $\text{CCl}_4$  at room temperature, followed by filtration and drying of the white precipitate. All operations were carried out in an atmosphere of dry nitrogen. (Found: C, 6.32; H, 0.87; Cl, 55.3%.  $\text{CH}_3\text{CO} \cdot \text{SbCl}_6$  requires: C, 6.37; H, 0.80; Cl, 56.3%).  $[\text{CD}_3\text{CO}]^+[\text{SbCl}_6]^-$  was prepared in an exactly analogous manner (Found: C, 6.38; D, 1.68; Cl, 55.5%.  $\text{CD}_3\text{CO} \cdot \text{SbCl}_6$  requires: C, 6.31; D, 1.59; Cl, 55.8%).

*IR and Raman spectra*

IR spectra in the region  $4000\text{--}400\text{ cm}^{-1}$  were recorded as mulls in Nujol and hexachlorobutadiene contained between NaCl or KBr plates on Perkin-Elmer 337 and Unicam SP100 spectrometers. Spectra in the region below  $400\text{ cm}^{-1}$  were obtained as mulls in Nujol contained between polythene plates using a grating spectrometer constructed in the Department<sup>6</sup>. A low-frequency Raman spectrum on the solid material was obtained on a Cary-81 Raman spectrometer using Hg-4358 Å radiation and an inverted cone for sample containment.

## RESULTS AND ASSIGNMENTS

The IR spectra of the complexes are shown in Fig. 1 and the band positions and assignments listed in Table 1. The corresponding bands in  $\text{CH}_3\text{CN}$  and  $\text{CD}_3\text{CN}$  are also listed for comparison.

TABLE 1

IR SPECTRA AND ASSIGNMENTS FOR THE  $\text{CH}_3\text{CO}^+$  AND  $\text{CD}_3\text{CO}^+$  IONS

Frequency ( $\text{cm}^{-1}$ )				Species	Assignment
$\text{CH}_3\text{CO}^+$	$\text{CH}_3\text{CN}^7$	$\text{CD}_3\text{CO}^+$	$\text{CD}_3\text{CN}^8$		
2940 (s)	3009	2209 (s)	2270	<i>E</i>	$\text{CH}_3$ asym. stretching
2870 (s)	2920	2049 (s)*	2106	$A_1$	$\text{CH}_3$ sym. stretching
2295 (s)	2267	2297 (s)	2267	$A_1$	$\text{--C}\equiv\text{O}$ stretching
1360 (w)	1454	980 (w)	1052	<i>E</i>	$\text{CH}_3$ asym. deformation
		920 (w)			
1319 (s)	1389	1056 (s)	1115	$A_1$	$\text{CH}_3$ sym. deformation
1001 (s)	1041	834 (s)	850	<i>E</i>	$\text{CH}_3$ rocking
950 sh	920	834 (s)**	833	$A_1$	C-C stretching
540 (w)		540 (w)			
390 (m)	362	370 (m)	335	<i>E</i>	CCO deformation

s = strong; m = medium; w = weak; sh = shoulder.

\* see text.

\*\*this band has a double assignment (see text).

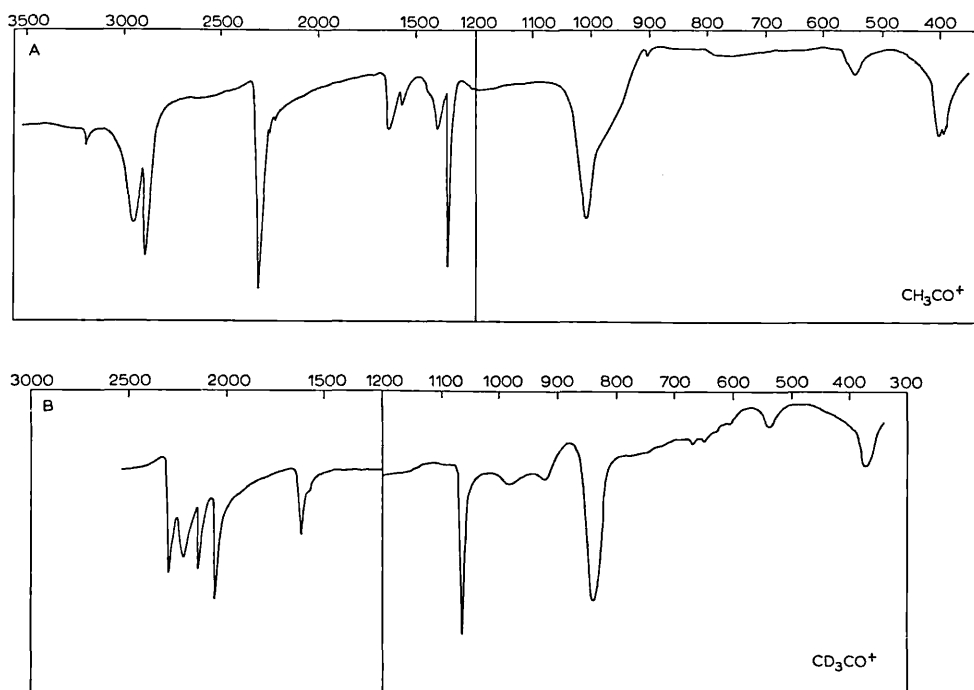


Fig. 1. IR spectra of  $\text{CH}_3\text{CO}^+$  and  $\text{CD}_3\text{CO}^+$  ions in nujol and hexachlorobutadiene mulls (re-drawn with bands due to the mulling agents removed).

The IR spectrum which we have observed is substantially in agreement with that of Cook<sup>4</sup> who measured the spectrum of the  $\text{CH}_3\text{COCl-SbCl}_5$  system down to  $650\text{ cm}^{-1}$ . There are, however, several bands listed in the latter work which we did not observe, in particular, those at  $1709\text{ cm}^{-1}$  and  $1139\text{ cm}^{-1}$ . However, both these bands appeared in a spectrum of a sample which was allowed to remain between the plates for about 1 hour and which had partially decomposed. A weak absorption appeared in our spectra at  $1615\text{ cm}^{-1}$ . This is not readily explained as arising from the acetylium ion and it seems possible that this may be due to a small amount of donor-acceptor complex (II). This is supported by the invariance of this frequency on substituting deuterium for hydrogen.

The existence of the complex primarily in the ionic form (I) is strongly suggested by our Raman spectrum of the solids which both contained three lines at  $334$ ,  $287$  and  $169\text{ cm}^{-1}$ . This agrees well with those previously observed<sup>9</sup> at  $329$ ,  $280$  and  $170\text{ cm}^{-1}$  for the  $\text{SbCl}_6^-$  ion and appears to rule out the possibility of a complex of the type  $[\text{CH}_3\text{CO}\cdots\text{SbCl}_5]^+\text{Cl}^-$ . This is in accord with the X-ray evidence<sup>5</sup> where no association between acetylium ions and  $\text{SbF}_6^-$  ions, other than ionic crystal packing was observed.

Turning to the acetylium ion we would expect 12 fundamental vibrational modes. On the basis of  $C_{3v}$  symmetry this should comprise  $4A_1 + 4E$  modes, all

of which should be active in both the IR and Raman spectra.

Since the acetylium ion and methyl cyanide are isoelectronic with similar nuclear masses, we might expect a close correspondence between the fundamental frequencies for the two systems. In spite of some discrepancies the similarity in absorption patterns in the two cases is sufficiently marked to allow most of the bands to be assigned with some confidence.

The bands due to CH, CD and CO stretching modes are unambiguously identified in Table 1. In the case of  $\text{CD}_3\text{CO}^+$  a fourth band is observed in the region  $2000\text{--}2300\text{ cm}^{-1}$  where only 3 bands are expected. However, the overtone of the CD deformation is expected near  $2112\text{ cm}^{-1}$  ( $2 \times 1056$ ). Fermi resonance between this overtone level and the  $A_1$  C–D stretching fundamental level might well be anticipated to be strong since both associated vibrations involve the same nuclei. The band at  $2133\text{ cm}^{-1}$  shows an upward shift of  $22\text{ cm}^{-1}$  from the expected position of the overtone and we might expect a similar depression in the second resonance component. This would place the undisturbed fundamental (C–D symmetric stretch) at  $(2049 + 22) = 2071\text{ cm}^{-1}$ .

The  $\text{CH}_3$  and  $\text{CD}_3$  symmetric deformation modes at  $1319$  and  $1056\text{ cm}^{-1}$  respectively are readily identified by their sharpness and strength. The CCO deformation ( $E$  class) gives rise to an absorption at  $390\text{ cm}^{-1}$  in  $\text{CH}_3\text{CO}^+$  and  $370\text{ cm}^{-1}$  in  $\text{CD}_3\text{CO}^+$ . The similar shapes and frequencies of the bands at  $1001\text{ cm}^{-1}$  in the acetylium ion and at  $1041\text{ cm}^{-1}$  in methyl cyanide leaves little doubt as to the identical origin of the two bands ( $E$ -class methyl rocking). It is to be expected that the ratios of the frequencies of the methyl to the methyl- $\text{D}_3$  rocking modes will be very close in the two cases. Again, this unambiguously identifies the  $834\text{ cm}^{-1}$  band in  $\text{CD}_3\text{CO}^+$  as arising from the rocking mode (see Table 1).

Two modes remain to be identified. These are the  $E$ -class methyl antisymmetric deformation and the C–C stretch ( $A_1$ ). No isolated strong bands remain to be correlated with these modes and their identification requires recourse to the Redlich–Teller product rule. The antisymmetric methyl deformation is to be expected on the high-frequency side of the symmetric deformation, and indeed there is a weak band at  $1360\text{ cm}^{-1}$  which is a reasonable candidate. Application of the Redlich–Teller product rule now predicts that the corresponding deuterio-frequency is at about  $940\text{ cm}^{-1}$ . Two weak bands occur at  $980$  and  $920\text{ cm}^{-1}$ . The latter is preferred on the above basis. By analogy with methyl cyanide the  $A_1$  C–C stretching mode should lie between  $1000$  and  $900\text{ cm}^{-1}$  and should be sharp. No sharp band is observed but a strong shoulder at  $950\text{ cm}^{-1}$  on the methyl rocking band requires explanation. Fermi resonance is not a possibility due to a lack of lower-frequency fundamentals, so that assignment to the C–C stretch seems inevitable. The Redlich–Teller product rule now predicts that the analogous mode in  $\text{CD}_3\text{CO}^+$  lies near  $834\text{ cm}^{-1}$ , thus necessitating a double assignment to this band. This accounts for the failure to observe the transition as an independent band.

It is clear from Cook's results that there is a large variation in the C-H stretching frequencies among the acetylium ions in the different acyl halide-Lewis acid systems. It seems probable that these might arise from crystal lattice interactions.

#### *Frequency and force constant calculations*

The object of the calculations performed pertaining to the acetylium ion were twofold. It was hoped that they would show that the present assignments were reasonable, and then from a perturbation analysis it was anticipated that an approximate set of force constants would be derived which would give some insight into the character of the bonding.

The secular equations were set up in symmetry co-ordinates. The choice of co-ordinates and the final algebraic form of the  $\mathcal{G}$  and  $\mathcal{F}$  matrices were consistent with those of Dowling et al.<sup>10</sup> (for  $\text{CH}_3\text{-C}\equiv\text{C-H}$ ). Tetrahedral angles were assumed for the methyl group, and the CH, CC and CO bond lengths were assumed to be 1.09, 1.38 and 1.13 Å respectively. An initial guess at a set of force constants was obtained by transferring the methyl constants of Snyder and Schachtschneider<sup>11</sup> along with values for  $f_{\text{C}\equiv\text{O}}$  and  $f_{\text{CCO}}$  of 20.0 and 0.28 mdynes Å<sup>-1</sup>. This set, as was anticipated, reproduced the experimental results badly. On refining the diagonal and 2 off-diagonal constants using standard perturbation procedures<sup>12</sup> the C-C and C≡O stretching modes were interchanged and convergence led to the absurd results that  $f_{\text{C-C}} = 20$  mdynes Å<sup>-1</sup> and  $f_{\text{C}\equiv\text{O}} = 6$  mdynes Å<sup>-1</sup>. The two constants were highly correlated and it was decided that the best approximation would probably be to retain the ratio  $f_{\text{C}\equiv\text{C}}/f_{\text{C-C}} = 20/5.8$ . In view of the fact that the results of Cook<sup>4</sup> showed that the stretching frequencies of acetylium complexes were very sensitive to the anion it was also considered that the CH modes should be given zero weighting and  $f_{\text{CH}}$  retained at 4.65 mdynes Å<sup>-1</sup>. Varying the remaining diagonal constants and the CC/HCC and CC/CO interaction constants led to the force constant and frequency set shown under calculation A (Tables 2 and 3). Apart from the CC/CO interaction constant the statistical dispersions on the constants are low. Indeed all the bending constants are well defined. The average weighted frequency fit, using the weighting parameters given in Table 3 and used in the perturbation calculation, was 15 cm<sup>-1</sup>. A 15 cm<sup>-1</sup> fit on any frequency is as good as one has a right to aim at in this instance with a restricted force field and data taken from the crystalline state in which the interionic interactions are likely to be strong. However two modes show unacceptably large deviations. These both belong to the *E* species of  $\text{CD}_3\text{CO}^+$ . In the first case the error on the 834 cm<sup>-1</sup> assignment is 53 cm<sup>-1</sup>. The 834 cm<sup>-1</sup> absorption band is doubly assigned to the *A*<sub>1</sub> and *E* species. However we believe this to be fairly reliable. The second case involves the highly questionable assignment of 920 cm<sup>-1</sup> (77 cm<sup>-1</sup> error, weighting 0.3). An examination of the  $\mathcal{L}$  matrices indi-

TABLE 2  
CALCULATED FORCE CONSTANTS (mdynes Å<sup>-1</sup>)

	Calculated		Diag. constants of CH <sub>3</sub> CN <sup>15</sup>
	A	B	
$f_{\text{HC}}$	(4.65)	(4.65)	4.94
$f_{\text{CC}}$	5.6 <sub>5</sub>	5.7	5.16
$f_{\text{CO}}$	19.5 ± 0.7	19.6 ± 0.5	18.1 (CN)
$r^2 f_{\text{HCH}}$	0.258 ± 0.005	0.282 ± 0.008	0.45
$r^2 f_{\text{HCC}}$	0.633 ± 0.015	0.600 ± 0.035	0.56
$r^2 c-c f_{\text{CCO}}$	0.153 ± 0.00006	0.153 ± 0.00005	0.29 (CCN)
CC/CO	0.3 <sub>8</sub> ± 0.5	(0.33)	
$r^2_{\text{HCH/HCH}}$	(-0.036)	(-0.036)	
$r^2_{\text{HCC/HCC}}$	(-0.01)	(-0.01)	
$r^2_{\text{HCH/HCC}}$	(-0.07)	-0.063 ± 0.000 <sub>4</sub>	
$r_{\text{CC/HCC}}$	0.336 ± 0.029	0.278 ± 0.022	

The values of those held constant are given in parentheses. Interaction constants between coordinates *a* and *b* are shown *a/b*. *r* is the CH bond length.

TABLE 3  
CALCULATED AND ASSIGNED FUNDAMENTAL FREQUENCIES OF CH<sub>3</sub>CO<sup>+</sup> AND CD<sub>3</sub>CO<sup>+</sup>

System and species	Frequencies (cm <sup>-1</sup> )			
	calc. A.	calc. B.	observed	weighting
CH <sub>3</sub> CO <sup>+</sup> (A <sub>1</sub> )	2843	2843	2870	0
	2295	2301	2295	1
	1288	1289	1319	1
	946	944	950	1
	(E)	2956	2956	2940
1396		1391	1360	1
995		1010	1001	1
382		382	390	1
CD <sub>3</sub> CO <sup>+</sup> (A <sub>1</sub> )	2298	2304	2297	1
	2046	2046	2049	1
	1070	1046	1056	1
	809	814	834	0.5
	(E)	2202	2203	2209
997		1000	920*	0.3
781		789	834	1
376		377	370	1

\* Preferred value now 980 cm<sup>-1</sup> (see text).

cated that these assignments might be sensitive to the HCH/HCC interaction constant. In another perturbation calculation this was allowed to vary and the ill-defined CC/CO constant was frozen. The sensitivity appeared as an immediate instability of the perturbation which required a fractional correction constant of 0.1 to be brought under control. Convergence was then smooth but the degree

of improvement was disappointing. Whilst further improvement could be obtained by allowing more constants to vary it is believed that the significance of the results would be too low to warrant it. The results of calculations A and B lead us to the following conclusions.

a) The failure of the perturbation to move the second-highest  $E$  mode of  $\text{CD}_3\text{CO}^+$  from about  $1000\text{ cm}^{-1}$  suggests that the  $980\text{ cm}^{-1}$  band is to be preferred to the  $920\text{ cm}^{-1}$  band. This new choice gives a slightly poorer Redlich-Teller product ratio but in view of the fact that the data refers to a highly ionic crystalline solid such a departure from the product ratio is probably insignificant.

b) The diagonal constants, especially the bending constants are reasonably well defined. The degree of reliability of these constants must be taken as appreciably greater than the statistical dispersions. However even with an error of three times the dispersion the bending constants for the HCC, HCH and CCO angles are  $0.27 \pm 0.02$ ,  $0.61 \pm 0.1$  and  $0.153 \pm 0.0002$  mdyne  $\text{\AA}^{-1}$ . The strong correlations between,  $f_{\text{C-C}}$ ,  $f_{\text{C=O}}$  and CC/CO make the first two rather less precise than originally anticipated and the CC/CO constant quite indeterminate.

c) The interaction constant CC/HCC is well determined and has a sign and value consistent with the expectations from the hybrid orbital force field of Mills<sup>13</sup>. According to this, its value (or more precisely that of CC/HCC-CC/HCH) is given by:

$$\text{CC/HCC} = \frac{\sqrt{6}}{r} \left( \frac{\partial R}{\partial \lambda} \right)_{\text{CX}} f_{\text{CC}}$$

The present values lead to  $\left( \frac{\partial R}{\partial \lambda} \right)_{\text{CX}} = 0.020$ . This value is very reasonable when compared with the values quoted by Mills.

d) The angle bending constants  $f_\alpha$  and  $f_\beta$  have derived values out of line with those of non-ionic molecules.  $f_\alpha$  usually has a value close to<sup>12</sup>  $0.48$  mdyne  $\text{\AA}^{-1}$ . Attempts to find an alternative solution with an  $f_\alpha$  more in line with that expected failed. In all cases convergence on the previous-quoted values occurred. The existence of an alternative solution cannot be discounted. It is intended to explore this more fully using the method of Needham and Overend<sup>14</sup>.

e) Comparison of the diagonal constants with those of methyl cyanide<sup>15</sup> clearly shows a greater resistance to deformation of the C-C and C $\equiv$ O bonds – and, if the present solution is correct, a marked weakening of the HCH angle deformation. In addition, the CCO angle deformation constant is considerably less than the CCN angle constant. The strengthening of the C-C bond is as expected since the C-C bond length is reduced from  $1.46\text{ \AA}$  to  $1.38\text{ \AA}$ . The accompanying weakening of CCX bending constant is much more surprising.

#### SUMMARY

The solid-state IR spectra of the complexes  $\text{CH}_3\text{COCl}\cdot\text{SbCl}_5$  and  $\text{CD}_3\text{COCl}\cdot$

SbCl<sub>5</sub> have been measured. Low-frequency Raman spectra show that the [SbCl<sub>6</sub>]<sup>-</sup> unit is present in both complexes, thus supporting the formulation as [CH<sub>3</sub>CO]<sup>+</sup> [SbCl<sub>6</sub>]<sup>-</sup>. The fundamental bands of the acetylium and the acetylium-D<sub>3</sub> ions have been assigned and compared with the isoelectronic methyl cyanide. Approximate force constants have been derived by standard perturbation procedures.

## REFERENCES

- 1 B. P. SUSZ AND J. J. WUHRMANN, *Helv. Chim. Acta*, 40 (1957) 722.
  - 2 B. P. SUSZ AND J. J. WUHRMANN, *Helv. Chim. Acta*, 40 (1957) 971.
  - 3 B. P. SUSZ AND D. CASSIMATIS, *Helv. Chim. Acta*, 44 (1961) 395.
  - 4 D. COOK, *Can. J. Chem.*, 40 (1962) 480.
  - 5 F. P. BOER, *J. Am. Chem. Soc.*, 88 (1966) 1572.
  - 6 P. J. HENDRA, R. D. G. LANE AND B. SMETHURST, *J. Sci. Instr.*, 40 (1963) 457.
  - 7 I. NAKAGAWA AND T. SHIMANOCHI, *Spectrochim. Acta*, 18 (1962) 513.
  - 8 J. C. EVANS AND H. J. BERNSTEIN, *Can. J. Chem.*, 33 (1955) 1746.
  - 9 I. R. BEATTIE, T. GILSON, K. LIVINGSTON, V. FAWCETT AND G. A. OZIN, *J. Chem. Soc.*, (A) (1967) 712.
  - 10 J. M. DOWLING, R. GOLD AND A. G. MEISTER, *J. Mol. Spectry.*, 1 (1957) 265.
  - 11 J. H. SCHACHTSCHNEIDER AND R. G. SNYDER, *Spectrochim. Acta*, 19 (1963) 117.
  - 12 J. ALDOUS AND I. M. MILLS, *Spectrochim. Acta*, 19 (1963) 1567.
  - 13 I. M. MILLS, *Spectrochim. Acta*, 19 (1963) 1585.
  - 14 C. D. NEEDHAM AND J. OVEREND, *Spectrochim. Acta*, 22 (1966) 1383.
  - 15 J. L. DUNCAN, *Spectrochim. Acta*, 20 (1964) 1197.
- J. Mol. Structure*. 1 (1967-68) 349-356

## A high-intensity red source for Raman spectroscopy

FRANCIS X. POWELL, ELLIS R. LIPPINCOTT and DEREK STEELE

Department of Chemistry, University of Maryland,  
College Park, Maryland

(Received 23 April 1961)

**Abstract**—The problem of excitation of Raman spectra of colored compounds is discussed. As a partial solution to this problem high-intensity cadmium and potassium lamps excited by radiofrequency radiation have been constructed. Spectra of carbon tetrachloride and azobenzene measured with such a cadmium lamp are shown and a brief discussion of the vibrational spectra of azobenzene presented.

MONOCHROMATIC red sources are of special interest in Raman spectroscopy since the blue and green lines of conventional mercury arcs are absorbed by compounds of only moderate coloration. Recent efforts [1–3] have shown that the yellow and red lines of helium and the yellow doublet of sodium are useful in obtaining Raman spectra of moderately colored compounds. The work of HAM and WALSH [2] is of special interest since as an alternative to a range of conventional discharge lamps, they used a series of annular electrodeless lamps which were powered by a microwave source. They illustrated the method with lamps which individually contained helium, mercury and sodium and showed that useful spectra could be obtained in short periods of time for He 5876 Å, Hg 4358 Å, Hg 5461 Å, and Na 5889–5896 Å excitation, respectively. MILLER and CARLSON [4] have used lamps of this design to achieve Raman spectra with the 7065 Å line of helium.

The red lines of helium at 7065–7281 Å are relatively weak and necessitate long exposure times. In addition, microwave-powered lamps appear to be limited by the necessity of using small dimensions for effective transfer of power. The resonance Raman effect is useful when a choice of exciting lines is available, and the application of optimum concentration techniques [5] can yield a maximum intensity for Raman scattering for substances which absorb wavelengths near the exciting line. However, these two methods are limited to special samples. Thus the problem of observing spectra for intensely colored substances such as azobenzene, azulene, etc., still remains.

As a partial solution to this problem we have constructed high-intensity cadmium and potassium arcs which are powered by a high-frequency (HF) generator. The technique used has had applications elsewhere [6–9], but not to Raman spectroscopy.

The excitation of cadmium and potassium, which yield strong lines at 6438 Å and 7664–7699 Å, respectively, was accomplished in a Pyrex annulus without the use of electrodes. The discharges are electromagnetic in nature and are readily

- [1] H. STAMMREICH, *Spectrochim. Acta* **8**, 41 (1956).
- [2] N. S. HAM and A. WALSH, *Spectrochim. Acta* **12**, 88 (1958).
- [3] F. T. KING and E. R. LIPPINCOTT, *J. Opt. Soc. Am.* **46**, 661 (1956).
- [4] F. A. MILLER and G. L. CARLSON, *Spectrochim. Acta* **16**, 6 (1960).
- [5] E. R. LIPPINCOTT, J. P. SIBILA and R. D. FISHER, *J. Opt. Soc. Am.* **49**, 83 (1959).
- [6] K. A. MACKINNON, *Phil. Mag.* **8**, 605 (1929).
- [7] A. T. FORRESTER, R. A. GUDMUNDSEN and P. O. JOHNSON, *J. Opt. Soc. Am.* **46**, 339 (1956).
- [8] E. J. JACOBSEN and G. R. HARRISON, *J. Opt. Soc. Am.* **39**, 1054 (1949).
- [9] W. F. MEGGERS and O. WESTFALL, *J. Research Natl. Bur. Standards* **44**, 447 (1950).



explained by analogy with elementary transformer theory: when a tube of gas at low pressure is inserted into a wire helix which is excited with radiofrequency energy, the gas will be partially ionized as a result of dielectric loss. If the excitation is great enough the ionization will be virtually complete and as a result the gas will approximate a shorted turn to the inducing coil. Dielectric loss is characterized by a weak glow and high load impedance as seen by the primary, while transformer action is characterized by a brilliant discharge and low load impedance as seen by the primary. Collisions within the gas serve to dissipate energy, and thus the gas serves as transformer secondary and load.

### Experimental

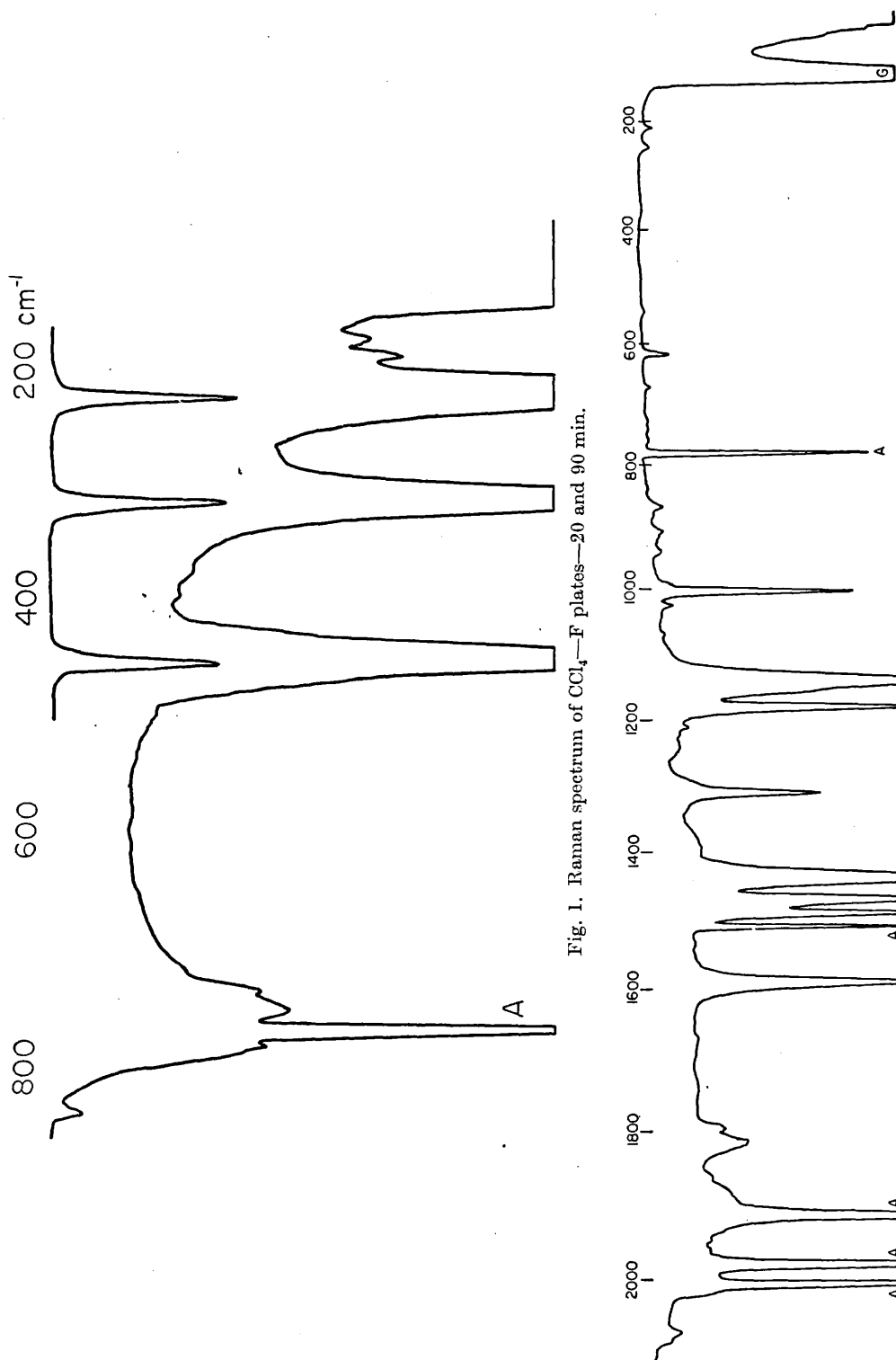
The annuli were constructed of Pyrex and are five inches long, 100 mm o.d. and 65 mm i.d. A 10-mm pump-out tube was welded to one end of an annulus. The outside of the annulus was covered with a sheet of wet asbestos paper which had been painted with a water slurry of magnesium oxide. When dry, the asbestos paper forms a hard, adherent heat insulator necessary for proper vaporization of the metal, and the magnesium oxide serves as an excellent reflector for the exciting radiation.

The load circuit is eighteen turns of  $\frac{1}{4}$ -in. copper tubing,  $\frac{1}{8}$ -in. between turns and 110 mm i.d. This is resonated with a 75- $\mu\mu\text{F}$  variable capacitor in parallel and is fed at the fifth turn by RG-11/U coax. The annulus is inside the copper coil during operation. This assembly is mounted on a  $\frac{1}{2}$ -in. thick transite platform which is directly over the spectrograph slit illumination system.

The exciter is a 150-W generator (3550 kc crystal, 6AG7-ECO, 6V6 push-push doubler and 807 push-pull output) used in the preliminary experiments. The plate transformer for the 807's is Variac controlled to give 20-35 W for an E.F. Johnson kilowatt amplifier which features two paralleled tetrodes (Eimac 4-400A) feeding a  $\pi$ -network output. This amplifier is not completely satisfactory as the 866 rectifiers need extra cooling to prevent arc-back and the plate transformer is overloaded during continuous (2-5 hr) duty at 1 kW.

Shielding is accomplished by enclosing all apparatus within a well grounded copper screen.

Initial operation of the lamps is accomplished in the following manner. Three grams of distilled metal are dropped through the pump out tube of an annulus. The annulus is then inserted into the load coil and the pump out tube connected to the vacuum line. When the pressure in the annulus has reached  $\sim 1 \times 10^{-6}$  mm Hg a heater is inserted in the annulus and the temperature slowly raised until the annulus is at 200-250°C for cadmium or 150-200°C for potassium. With the load capacitor set at minimum the amplifier and exciter are then switched on. If the vacuum is good and the temperature sufficiently high, the lamp will light spontaneously. The load capacitor is then increased until the lamp reaches maximum brightness, the amplifier plates re-tuned, and the pi network adjusted to 1 kW input to amplifier plates. After 5-20 min of operation, about half the metal will have distilled from the annulus, at which time the vacuum line is sealed off very close to the annulus. The lamp can be restarted by preheating to the proper temperature and then applying power.



All spectra have been taken on a JACO  $f/6.3$  grating spectrograph that has a dispersion of  $19 \text{ \AA}/\text{mm}$ , with the blaze at  $7500 \text{ \AA}$ . The photographic plates used were Eastman Kodak 103-aF for the range  $6400\text{--}7000 \text{ \AA}$ , 103-aU for  $7000\text{--}7500 \text{ \AA}$  and 1-N plates for the  $7500\text{--}8400$  range. Standard techniques were used in photographing and developing the spectra. The plates were not hypersensitized. The type of excitation, the type of photographic plate, and the concentration of sample were the factors which determined the time of exposure. Reference spectra were recorded below each Raman spectrum by means of a  $\frac{1}{4}W$  neon lamp. These reference spectra contain blue lines appearing in the second order of the spectrograph as well as some of the stronger lines of argon. Optical filtration was used to remove high-frequency lines from cadmium and potassium since they would appear in the Raman region as a result of diffraction in higher orders. An acidified solution of potassium dichromate was adequate as a filter for work with the  $6438 \text{ \AA}$  line of cadmium. However, a solution of phenol sulfonphthalein (phenol red), which was used for the  $7664\text{--}7699$  doublet of potassium, was equally satisfactory.

The sample tubes were  $10 \text{ mm}$  o.d. Pyrex and were filled to a height of about  $5 \text{ in.}$  by standard techniques. These tubes were then mounted in a water cooled filter jacket which was inserted into the annulus during operation.

### Performance

#### *Cadmium arcs*

With operation in excess of  $100 \text{ hr}$  the cadmium arc shows no apparent deterioration in either metal or glass. This arc is readily reignited when properly preheated. The spectrum of this arc contains only five relatively weak lines at wavelengths in the region of interest above the intense  $6438 \text{ \AA}$  line. Some interference from grating ghosts is present at  $\sim 150 \text{ cm}^{-1}$  to either side of the  $6438 \text{ \AA}$  line.

#### *Potassium arcs*

The potassium arc, although usable, shows an unusual amount of Stokes clutter. A sharp doublet at  $8183\text{--}8195 \text{ \AA}$  is attributed to sodium impurity, and the other lines are as yet unassigned. There is a considerable continuum that appears on the plates in the region close to the  $7664\text{--}7699$  doublet and also there are broad bands through the Stokes region. These can probably be reduced in intensity by control of the potassium pressure. Potassium arcs in Pyrex annuli deteriorate rapidly. The glass is rather severely etched by the action of the hot potassium and the color of the glass varies from light brown to almost black depending on the amount of usage. Lamps that have been in operation for  $15\text{--}20 \text{ hr}$  are difficult to reignite. We expect that silica annuli will be of considerable effect in reducing the amount of deterioration in these lamps. Further investigation of this possibility is in progress.\*

\* The use of silica has not improved the quality of this arc. Instructions for coating the Pyrex annuli were obtained from the Corning Glass Works, Corning, New York. The use of this coating (Corning K coat) has greatly extended the life of the potassium annuli. We are presently using such a coated annulus to investigate the Raman spectra of cyclo-octatetraene-iron tricarbonyl, azulene and other highly colored substances.

Table 1. Raman frequencies of azobenzene

Frequency ( $\text{cm}^{-1}$ )	Assignment*
209 w	N-ring def.
246 w	N-ring def.
614 w	$b_2 \alpha_{\text{CCC}}$
663 vw	—
719 vw	$b_1 \phi_{\text{CC}}$ (?)
860 w	—
898 vw	$b_1 \gamma_{\text{CH}}$
932 vw	—
1005 s	$a_1$ ring
1030 vw	$a_1 \beta_{\text{CH}}$
1144 vs	$b_2 \beta_{\text{CH}}$
1164 sh	—
1182	$a_1 \beta_{\text{CH}}$
1213 w	CN stretch
1263 vw	CN stretch (?)
1312 s	$b_2 \nu_{\text{CC}}$
1419 vs	N=N stretch ( <i>trans</i> )
1469 s	N=N stretch ( <i>cis</i> )
1492 m	$a_1 \nu_{\text{CC}}$
1593 s	$a_1$ and $b_2 \nu_{\text{CC}}$

\* The class designations are for isolated mono-substituted benzene rings and follow the recommendations of MULLIKEN [10].

### Spectra

Raman spectra have been recorded for iron pentacarbonyl, carbon tetrachloride, hexachloro-1:3-butadiene, *trans*-hexatriene and azobenzene. Two of these are illustrated in Figs. 1 and 2, which are densitometer tracings of the observed spectra. The Raman spectrum of azobenzene has not been previously observed and is tabulated in Table 1. A brief discussion is presented.

The Raman spectrum of molten azobenzene and of a solution of azobenzene in benzene were measured with the cadmium arc. The solution spectrum was also taken with the potassium annulus. As might be expected from the non-planar molecular configuration, the Raman as well as the infrared spectrum exhibits the characteristic features of mono-substituted benzene rings superimposed on the spectral bands associated with the *cis* and *trans* C—N=N—C groupings. The very strong Raman band at  $1419 \text{ cm}^{-1}$  clearly arises from the —N=N— stretching vibration of the *trans*-form. There is no trace of infrared absorption at this frequency. The *cis*-counterpart of this band is at  $1469 \text{ cm}^{-1}$ . By elimination of the bands known to be associated with the phenyl groups [11] the C—N stretch of one of the forms is seen to be at  $1213 \text{ cm}^{-1}$  and two of the N—C<sub>6</sub>H<sub>5</sub> deformation modes at 209 and  $246 \text{ cm}^{-1}$ . A more complete assignment will be undertaken when we have achieved the Raman spectrum of the solid material.

*Acknowledgements*—The authors would like to express their appreciation to Mr. OWEN FLETCHER who performed a valuable service in assembling electronic equipment, and to Mr. THOMAS KENNEY who assisted in the construction of apparatus. Financial assistance from the Atomic Energy Commission and National Science Foundation is gratefully acknowledged.

[10] R. MULLIKEN, *J. Chem. Phys.* **23**, 1997 (1955).

[11] R. R. RANDLE and D. H. WHIFFEN, *Report Mol. Spectroscopy Conf. Inst. Petroleum, London*, 1954 p. 111 (1955).

## The use of pressed polythene disks in infra-red spectroscopy

(Received 27 July 1963)

### INTRODUCTION

SEVERAL techniques have been developed for obtaining the infra-red absorption spectra of solids. These include mulling in paraffin (Nujol), melting on to transparent plates, attenuated total reflection, pressing between diamond and sapphire crystals and pressing in alkali halide disks. The only techniques suitable for the far infra-red are the nujol mull and the alkali halide disk techniques. The former does not permit quantitative intensity measurements and suffers from the disadvantage that it is difficult to obtain uniform dispersions. The alkali halide disk technique is frequency limited, involves dispersing the compound in an ionic medium which may have appreciable effects on the spectra, and presents difficulties in the exclusion of water.

The use of polythene disks has been mentioned in the literature in the past [1] but does not appear to have been widely used. The purpose of the present communication is to show that the technique has great promise—not only for far infra-red spectroscopy—but for special problems in the infra-red region generally. Its special advantages arise from the weakness of the absorption above  $750\text{ cm}^{-1}$ , the complete absence of absorption below  $700\text{ cm}^{-1}$ , the non ionic nature of the dispersant and the ease of exclusion of water.

### EXPERIMENTAL

Fine polythene powder as supplied by Gallenkamp for protective coatings (high density white polythene—cat. no. PP-560) is used as the dispersant. The compounds to be studied are finely powdered by the usual techniques, as, for example, in a vibration mill, and between 3 and 30 mg mixed in the mill with 150 mg of polythene. The disks are formed by applying heat and pressure to the mixture contained within a one inch diameter mould. It was found that the minimum effective temperature required to obtain homogeneous transparent disks was about  $120^\circ\text{C}$  at  $6\text{ tons/in}^2$  pressure. This minimum temperature seems relatively insensitive to pressure variations from about  $2\text{ tons/in}^2$  to the maximum obtainable with the apparatus of about  $8\text{ tons/in}^2$ . The use of lower temperatures gives brittle granular disks with consequential higher dispersion, but where lower temperatures are necessary due to instability these may be used in the low frequency ranges. It should be noted that the sample has to be ground prior to mixing with the polythene as the polythene powder has too great a cushioning effect in the mill.

The press used was a hydraulic specimen mounting press as supplied by Buehler Ltd. giving a maximum pressure of 5–6 tons on a  $\text{in}^2$  diameter mould (Analis Namur Press, catalogue number 1315 AB). This has been found to be ideal for the preparation of disks. The sample is heated *in situ* on the press by an electric mantle which completely encompasses the mould. Temperature is measured by a Weston all metal thermometer which passes down into the centre of the mould, thus giving reasonably accurate temperature recording. Pressure is applied as the sample approaches the plastic flow temperature. Cooling of the mould is increased by the use of a split brass heat sink as supplied with the instrument.

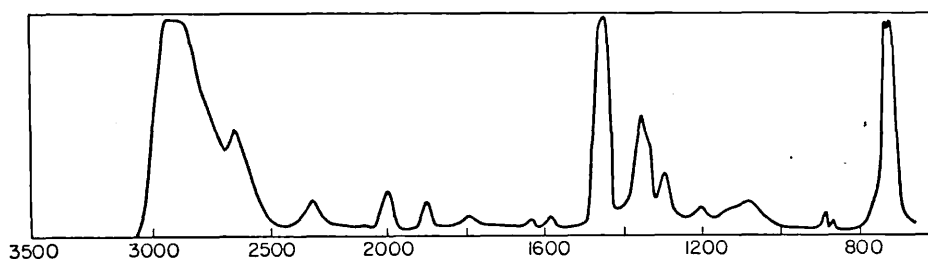


Fig. 1. Polythene disc, 0.006 in. thick.

## SPECTRA

The spectrum of a 0.006 in. thick disk shows only three strong absorption bands at 2850, 1450 and 720  $\text{cm}^{-1}$ . The effects of the remaining bands are easily eliminated by balancing with disks of appropriate thicknesses in double beam operation. The transmission of the disks away from absorption centres is 75 per cent.

Some representative spectra of compounds dispersed in polythene are shown in Figs. 2-4. FARMER has shown [2] that the spectra of phenols, carboxylic acids and simple alcohols in alkali halide disks are affected by adsorption of the samples on the alkali halide particles. These effects are eliminated in the above technique. The spectrum of benzoic acid (see Fig. 2)

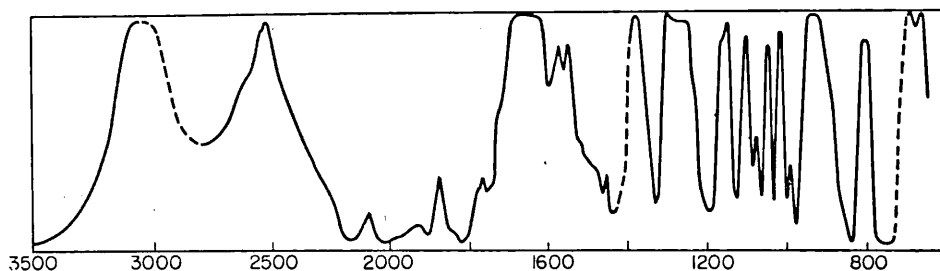


Fig. 2. Benzoic acid in polythene.

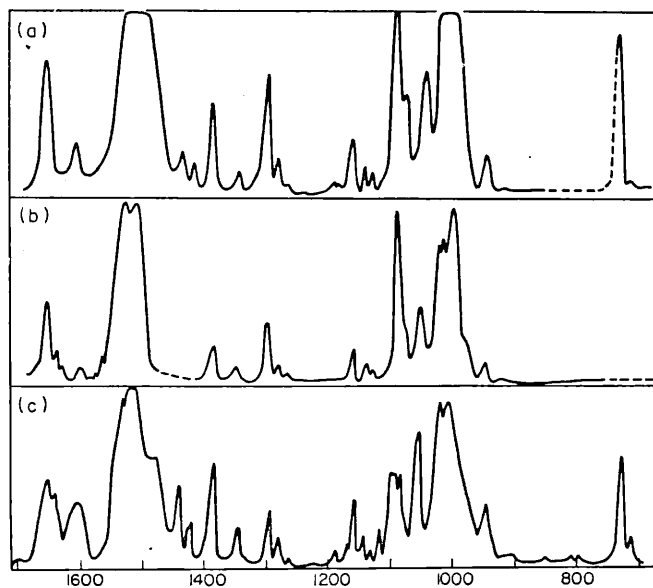


Fig. 3. Per-fluoro-biphenyl

- (a)  $\text{CCl}_4$  solution
- (b) Polythene disk
- (c) Solidified melt.

shows a strong shift in the O-H stretching frequency as compared with that of the acid in KBr discs, but it is in good agreement with that in Nujol mull.

That of perfluoro biphenyl (Fig. 3a) is compared with a solution spectrum and with that obtained by melting a sample between two salt plates and allowing to resolidify. The disk and solution spectra are identical whereas that of the solidified melt shows strong crystal orientation effects. This tendency of the solidified melt to give oriented crystals is a well-known, but often insufficiently appreciated, disadvantage of the technique.

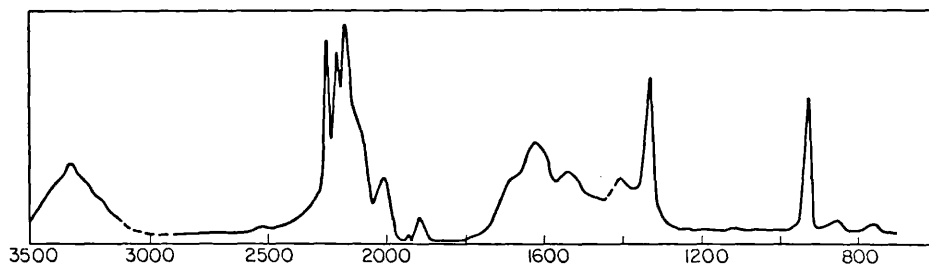


Fig. 4. Sodium dicyanamide in polythene disk.

Spectral changes have been observed in alkali halide disks of  $\alpha$  and  $\beta$ -D-glucose due to presence of traces of water. [3] In both cases the product was  $\alpha$ -D-glucose monohydrate. A polythene disk of  $\beta$ -D-glucose showed no evidence for having undergone a chemical change, even after exposure to laboratory conditions for several days.

Finally, the spectrum of an ionic salt, sodium dicyanamide, is shown in Fig. 4 as representative of a completely different class of compounds. The spectrum was identical in all respects to that obtained in KBr disks except in that moisture had been excluded.

The technique is now used routinely by the authors for far infra-red spectra and for handling moisture sensitive compounds or compounds which are liable to undergo halide exchange with the alkali halides. Its main limitation arising from the necessity of having to heat the disk mixture to 120°C has proved of little concern as few compounds are seriously affected at such temperatures.

*Acknowledgements*—We gratefully acknowledge a financial grant from the U.S. Navy for investigations on far infra-red spectroscopy. The  $\beta$ -D-glucose, the perfluoro-biphenyl and the sodium dicyanamide were gifts from Dr. H. WEIGEL, Professor J. C. TATLOW and Dr. D. A. LONG, respectively.

*Chemistry Department, Royal Holloway College,  
University of London,  
Englefield Green, Surrey*

B. SMETHURST  
D. STEELE

[1] H. YOSHINAGA and R. A. OETJEN, *J. Opt. Soc. Am.* **45**, 1085 (1955).

[2] V. C. FARMER, *Chem. & Ind. (London)* 586 (1955).

[3] S. A. BARKER, E. J. BOURNE, W. B. NEELY and D. H. WHIFFEN, *Chem. & Ind. (London)* 1418 (1954). S. A. BARKER, E. J. BOURNE, H. WEIGEL and D. H. WHIFFEN, *Chem. & Ind. (London)* 318 (1956).

Reprinted from August, 1966 issue of *Laboratory Practice*

## The Fabrication of Vacuum-tight High-density Polythene Cells

by S. Ashdown, T. F. Crowdy and D. Steele,  
Chemistry Department, Royal Holloway College, Englefield Green, Surrey

AT frequencies below  $200\text{ cm.}^{-1}$  (wavelengths greater than  $50\ \mu$ ) the only satisfactory transparent materials for cells are high-density polythene and polypropylene (Willis, Miller, Adams and Gebbie, 1963). A number of techniques for producing liquid cells for this far infra-red region are in common use. These include the

use of thin polythene bags held in shape by wire meshes, and sandwiching of spacers between polythene plates. The former technique is not all satisfactory for quantitative—or even semi-quantitative—intensity measurements, and it is the experience of many that the latter technique is frequently very troublesome when making measurements in a vacuum, as it is difficult to obtain

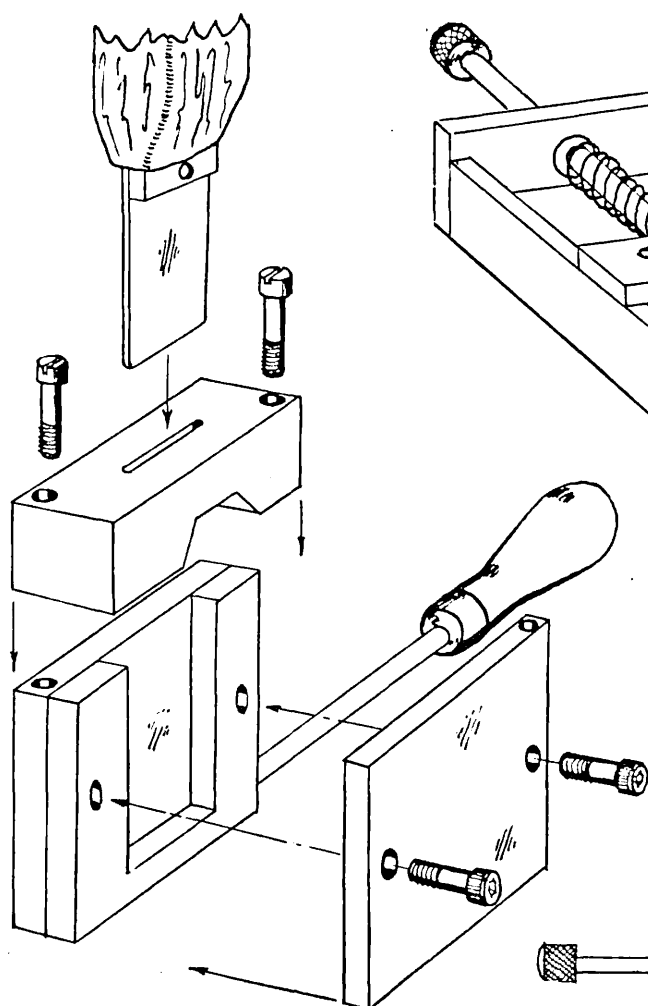


Fig. 1a. Expanded view of mould.

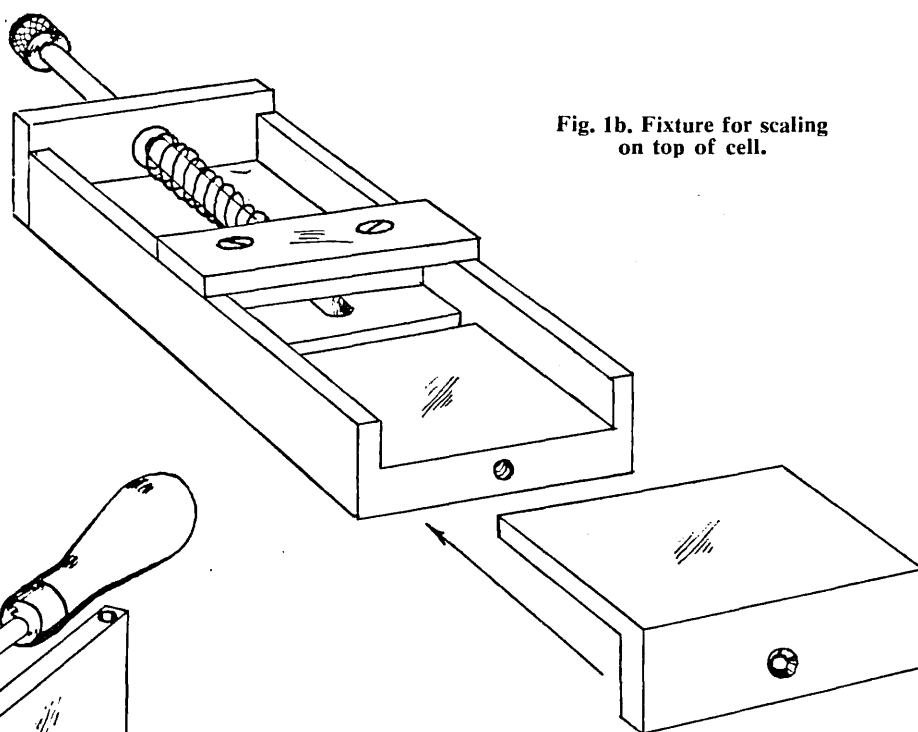


Fig. 1b. Fixture for scaling on top of cell.

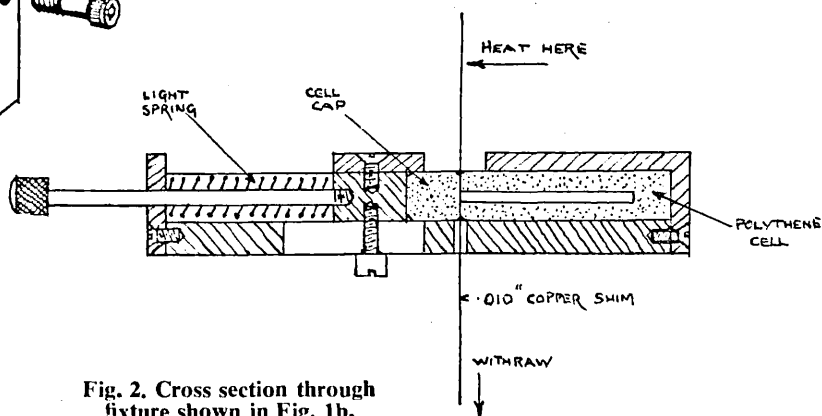


Fig. 2. Cross section through fixture shown in Fig. 1b.



vacuum-tight seals between the polythene plates and spacers.

We have developed a simple technique for fabricating cells out of single sheets of high-density polythene. These are fairly rigid, have a reasonable transmission and are reliably vacuum tight. In view of the current interest in far infra-red technology it seems worth describing the process. The basic procedure is to make a cavity of the required dimensions in a block of high-density polythene leaving an acceptable wall thickness ( $\sim 1$  mm.) on the transmitting surfaces. A cell is produced by sealing a polythene block on to the open end and drilling a sample loading aperture into it. It is our experience that the only way to make a satisfactory cavity is to extrude molten polythene from the block with the use of a metal blade. The apparatus we use for this is shown in Fig. 1a. A strip of polythene 1 in.  $\times$  1½ in.  $\times$  5 mm. (Iridon Ltd.) is loaded into the brass fixture and the asbestos guide block screwed down. The jig is heated over a burner till the polythene begins to become plastic (about 110°C) and the stainless steel sword, similarly heated, and lubricated with Nujol, forced down into the polythene. The extruded polythene is forced out through spacious vents in the asbestos. After rapid cooling the jig is dismantled and the blade withdrawn. The complete polythene block will have been melted and reformed during this process.

Two different procedures have been employed for sealing on the top of the cell. The earliest method was to heat the surfaces to be joined on a copper block until the polythene became transparent to a depth of approx. 1/20th in. and then the surfaces pressed together followed by pulling out slightly. As the clear plastic adheres to the block this tends to produce a messy looking,

though otherwise very satisfactory, joint. Smoothing off the joint is accomplished by the use of a hot blade.

An aesthetically more pleasing joint is obtained using the fixture shown in Fig. 1b. A narrow strip of polythene is placed in the top of the cavity to keep it in shape during the subsequent operations. The two parts to be joined are separated by a copper or steel blade which is heated by means of a gas flame. When the polythene has become transparent at the junction areas the blade is withdrawn with a shuttle type motion to avoid dragging the polythene with the blade. Under the pressure of the spring, which should not be too strong, the two parts join.

A hole drilled through the top plate serves for sample insertion, and can be satisfactorily sealed by use of a tapered piece of polythene rod. We have found polythene welding rod (Gallenkamp & Co. Cat. No. PP 792) ideal for this purpose.

A typical cell with 1¼ mm. cell walls had transmission of 56 per cent at 130  $\text{cm.}^{-1}$  dropping only slightly at 360  $\text{cm.}^{-1}$ . The cell walls may be made much thinner than this by using thinner polythene or thicker sword, and we can anticipate considerably increased transmissions if these are required. It is our custom to make these cells in batches but a single cell can be produced in about 30 min. and has a lifetime determined only by the materials used inside it.

ACKNOWLEDGEMENT.—*We gratefully acknowledge the assistance of W. Wheatley and R. Sutton in developing this technique.*

#### REFERENCE

Willis, H. A., Miller, R. G. J., Adams, D. M. and Gebbie, H. A. (1963). *Spectrochim. Acta.*, **19**, 1457.

R.H.C. 7  
LIBRARY

[Heavily obscured and illegible text]